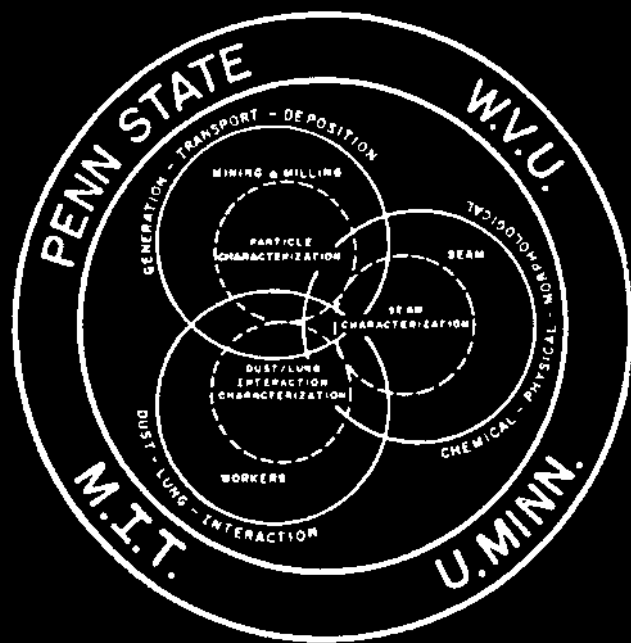


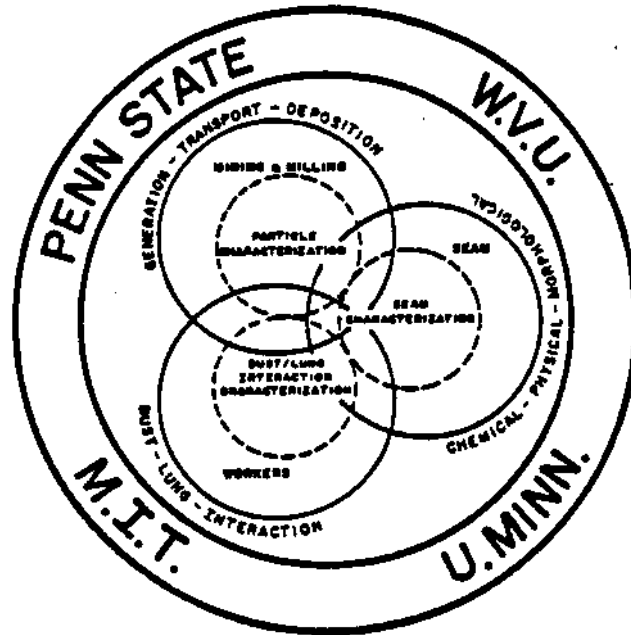
PUBLICATIONS 1988

Edited by
ROBERT L. FRANTZ
and
RAJA V. RAMANI



**GENERIC MINERAL
TECHNOLOGY CENTER
FOR RESPIRABLE DUST**

PUBLICATIONS 1988



GENERIC MINERAL TECHNOLOGY CENTER FOR RESPIRABLE DUST

The Pennsylvania State University
West Virginia University
University of Minnesota
Massachusetts Institute of Technology
Michigan Technological University

Submitted To
Office of Mineral Institutes
U.S. Bureau of Mines
Washington, D.C.

August 31, 1989

The views and conclusions contained in this document are those of the authors and should not be interpreted as necessarily representing the official policies or recommendations of the Interior Department's Bureau of Mines, the U.S. Government or of the Generic Mineral Technology Center for Respirable Dust. Reference to specific brands, equipment or trade names in this report is made to facilitate understanding and does not imply endorsement by the Bureau of Mines or the Dust Center.

PUBLICATIONS
PRODUCED IN
THE GENERIC MINERAL TECHNOLOGY CENTER
FOR RESPIRABLE DUST
IN THE YEAR
1988

Edited by
Robert L. Frantz
Raja V. Ramani

PENNSSTATE



WEST VIRGINIA UNIVERSITY



The views and conclusions contained in this document are those of the authors and should not be interpreted as necessarily representing the official policies or recommendations of the Interior Department's Bureau of Mines, the U.S. Government or of the Generic Mineral Technology Center for Respirable Dust. Reference to specific brands, equipment or trade names in this report is made to facilitate understanding and does not imply endorsement by the Bureau of Mines or the Dust Center.

PUBLICATIONS
PRODUCED IN
THE GENERIC MINERAL TECHNOLOGY CENTER
FOR RESPIRABLE DUST
IN THE YEAR
1988

Edited by
Robert L. Frantz
Raja V. Ramani

PENNSSTATE



WEST VIRGINIA UNIVERSITY



Volumes of the Respirable Dust Center

VOLUME 1	Status Report, 1984-1988
VOLUME 2	Report to the Committee on Mining and Mineral Resources Research, 1987
VOLUME 3	Publications, 1984
VOLUME 4	Publications, 1985
VOLUME 5	Publications, 1986
VOLUME 6	Publications, 1987
VOLUME 7	Respirable Dust Center Research Program Review
VOLUME 8	Publications, 1988
CONFERENCE PROCEEDINGS	Coal Mine Dust Conference West Virginia University Morgantown, West Virginia October 1984
CONFERENCE PROCEEDINGS	Respirable Dust in the Mineral Industries: Health Effects, Characterization and Control The Pennsylvania State University University Park, Pennsylvania October 1986

CONTENTS

	Page
Foreword	xi
National Plan	xii
Advisory Council Members	xiii
I. Control of Dust and Particulate Matter Generation	1
1. Estimating the Crush Zone Size Under a Cutting Tool in Coal	3
<i>R. Karl Zipf, Jr. and Z. T. Bieniawski, Department of Mineral Engineering, The Pennsylvania State University, University Park, PA. Published in the International Journal of Mining and Geological Engineering, 1988, 6, pp. 279-295. (PS-1)</i>	
2. Microscopic Studies of Fractures Generated Under Mixed Mode Loading	20
<i>R. Karl Zipf, Jr. and Z. T. Bieniawski, Department of Mineral Engineering, The Pennsylvania State University, University Park, PA. Published in the Proceedings of the 29th U.S. Rock Mechanics Symposium, 1988, A. A. Balkema, editor, pp. 151-158. (PS-1)</i>	
II. Dilution, Dispersion and Collection of Dust	29
3. Dust Flows in Mine Airways: A Comparison of Experimental Results and Mathematical Predictions	31
<i>R. Bhaskar and R. V. Ramani, Department of Mineral Engineering, The Pennsylvania State University, University Park, PA. Presented at SME-AIME Annual Meeting, Phoenix, AZ, January 1988. Preprint No. 88-191. (PS-2)</i>	
4. Experimental Studies on Dust Dispersion in Mine Airways	40
<i>R. Bhaskar¹, R. V. Ramani¹ and R. A. Jankowski², ¹Department of Mineral Engineering, The Pennsylvania State University and ²U.S. Bureau of Mines, Pittsburgh, PA. Published in Mining Engineering, March 1988, pp. 191-195. (PS-2)</i>	
5. On the Transport of Airborne Dust in Mine Airways	46
<i>R. V. Ramani and R. Bhaskar, Department of Mineral Engineering, The Pennsylvania State University, University Park, PA. Presented at the VIIth International Pneumoconioses Conference, Pittsburgh, PA, August 23-26, 1988, and published in the Proceedings (Abstract only). (PS-2)</i>	

	Page
6	47
<p>On the Relationship Between Quartz in the Coal Seam and Quartz in the Airborne Respirable Coal Dust</p> <p><i>R. V. Ramani, J. M. Mutmansky, R. Bhaskar, J. Qin and J. Organiscak</i>, Department of Mineral Engineering, The Pennsylvania State University and U.S. Bureau of Mines, Pittsburgh, PA. Presented at the Fourth International Mine Ventilation Congress, Brisbane, Australia, July 3-6, 1988 and published in the Proceedings, edited by A. D. S. Gillies, The Australasian Institute of Mining and Metallurgy, Melbourne, Australia. (PS-7)</p>	
<p>III. Characterization of Dust Particles 55</p>	
7.	57
<p>Characterization Problems in Comminution - An Overview</p> <p><i>R. Hogg</i>, Mineral Processing Section, Department of Mineral Engineering, The Pennsylvania State University, University Park, PA. Published in the <i>International Journal of Mineral Processing</i>, 22 (1988), pp. 22-40, Elsevier Science Publishers B. V., Amsterdam - Printed in the Netherlands. (PS-3)</p>	
8.	73
<p>A Rapid Method for Determination of Changes in Shape of Comminuted Particles Using a Laser Diffractometer</p> <p><i>L. G. Austin¹, O. Trass², T. F. Dumm¹ and V. R. Koka²</i>, ¹Mineral Processing Section, Department of Mineral Engineering, The Pennsylvania State University, University Park, PA. ²Department of Chemical Engineering, University of Toronto, Toronto (Canada). Published in <i>Particulate and Particle System Characterization</i>, 5, 1988, pp. 13-15. (PS-3)</p>	
9.	76
<p>Washability of Ultrafine Coal</p> <p><i>T. F. Dumm and R. Hogg</i>, Mineral Processing Section, Department of Mineral Engineering, The Pennsylvania State University. Presented at the SME Annual Meeting, Denver, CO, February 1987. SME preprint 87-136. (PS-3).</p>	
10.	84
<p>Potential Role of Silicon-Oxygen Radicals in Acute Lung Injury</p> <p><i>N. S. Dalal¹, X. Shi¹, V. Vallyathan²</i>, ¹Department of Chemistry, West Virginia University, Morgantown, WV and ²Division of Respirable Disease Studies, National Institute for Occupational Safety and Health, Morgantown, WV. Published in <i>Effects of Mineral Dusts on Cells</i>, edited by B. T. Mossman and T. Begin, NATO ASI Series, Vol. 000, Springer-Verlag (1988). (WV-10)</p>	
11.	92
<p>On the Mechanism of the Chromate Reduction by Glutathione: ESR Evidence for the Glutathionyl Radical and an Isolable Cr(V) Intermediate</p> <p><i>X. Shi and N. S. Dalal</i>, Department of Chemistry, West Virginia University. Published in <i>Biochemical and Biophysical Research Communications</i>, Vol. 156, No. 1, 1988, pp. 137-142. (WV-10)</p>	

CONTENTS

		Page
12.	Cytotoxicity and Spectroscopic Investigations of Organic Free Radicals in Fresh and Stale Coal Dusts <i>N. S. Dalal¹, B. Jafari¹, and V. Vallyathan²</i> , ¹ Department of Chemistry, West Virginia University and ² National Institute for Occupational Safety and Health, Morgantown, WV. Presented at the VIIth International Pneumoconioses Conference, Pittsburgh, PA, August 23-26, 1988, and published in the Proceedings (Abstract only). (WV-10)	98
13.	Generation of Free Radicals From Freshly Fractured Silica Dust: Potential Role in Acute Silica-Induced Lung Injury <i>V. Vallyathan¹, X. Shi², N. S. Dalal², W. Irr¹, and V. Castranova¹</i> , ¹ Division of Respiratory Disease Studies, National Institute for Occupational Safety and Health, Morgantown, WV and ² Department of Chemistry, West Virginia University. Published in the <u>American Review of Respirable Diseases</u> , 138, 1988, pp. 1213-1219. (WV-10)	99
14.	Detection of Hydroxyl Radicals in Aqueous Suspensions of Fresh Silica Dust and Its Implication to Lipid Peroxidation in Silicosis <i>N. S. Dalal¹, X. Shi¹ and V. Vallyathan²</i> , ¹ Department of Chemistry, West Virginia University and ² Division of Respiratory Disease Studies, National Institute for Occupational Safety and Health, Morgantown, WV. Presented at the VIIth International Pneumoconioses Conference, Pittsburgh, PA, August 23-26, 1988, published in the Proceedings. (WV-10)	106
15.	Suppression of Inhaled Particle Cytotoxicity by Pulmonary Surfactant and Re-toxication by Phospholipase: Distinguishing Properties of Quartz and Kaolin <i>W. E. Wallace, M. J. Keane, V. Vallyathan, P. Hathaway, E. D. Regad, V. Castranova and F. H. Y. Green</i> , West Virginia University and Appalachian Laboratory for Occupational Safety and Health, Division of Respiratory Disease Studies, National Institute for Occupational Safety and Health. Published in the <u>Ann. Occupational Hygiene</u> , Vol. 32, pp. 291-298, Supplement 1, 1988. Inhaled Particles VI, Pergamon Press, printed in Great Britain. (WV-12)	113
16.	Oxygenated Radical Formation by Fresh Quartz Dust in a Cell-Free Aqueous Medium and Its Inhibition by Scavengers <i>N. S. Dalal¹, X. Shi¹ and V. Vallyathan²</i> , ¹ Department of Chemistry, West Virginia University and ² The Division of Respiratory Disease Studies, National Institute for Occupational Safety and Health, Morgantown, WV. Published in <u>Effects of Mineral Dust on Cells</u> , NATO ASI Series, Vol. 000, edited by B. T. Mossman and R. Begin, Springer-Verlag, 1988. (WV-12)	121

	Page
<p>17. Mineral Surface-Specific Differences in the Adsorption and Enzymatic Removal of Surfactant and Their Correlation with Cytotoxicity <i>W. E. Wallace</i>^{1,2}, <i>M. J. Keane</i>¹, <i>P. S. Muke</i>¹, <i>C. A. Hill</i>², and <i>V. Vallyathan</i>², ¹West Virginia University and ²The Division of Respirable Disease Studies, National Institute for Occupational Safety and Health, Morgantown, WV. Published in Fourth International Workshop: Effects of Mineral Dusts on Cells, a NATO Advanced Research Workshop held September 21-23, 1988, Quebec, Canada. (WV-10)</p>	129
<p>18. ESR Evidence for the Hydroxyl Radical Formation in Aqueous Suspension of Quartz Particles and Its Possible Significance to Lipid Peroxidation in Silicosis <i>X. Shi</i> and <i>N. S. Dalal</i>, Department of Chemistry, West Virginia University. Published in the <i>Journal of Toxicology and Environmental Health</i>, 25, pp. 237-245, 1988. (WV-10)</p>	137
<p>19. Do Silicon-Based Radicals Play a Role in Quartz-Induced Hemolysis and Fibrogenicity? <i>N. S. Dalal</i>¹, <i>X. Shi</i>¹, and <i>V. Vallyathan</i>², ¹Department of Chemistry, West Virginia University and ²The Division of Respirable Disease Studies, National Institute for Occupational Safety and Health, Morgantown, WV. Presented at the VIIth International Pneumoconioses Conference, Pittsburgh, PA, August 23-26, 1988, and published in the Proceedings. (WV-10)</p>	146
<p>20. Respirable Particulate Surface Interactions with the Lecithin Component of Pulmonary Surfactant <i>M. J. Keane</i>¹, <i>W. E. Wallace</i>^{1,2}, <i>M. S. Seehra</i>², <i>C. A. Hill</i>², <i>P. S. Raghootama</i>², and <i>P. Muke</i>², ¹National Institute for Occupational Safety and Health and ²West Virginia University. Presented at the VIIth International Pneumoconioses Conference, Pittsburgh, PA, August 23-26, 1988, and published in the Proceedings. (WV-12)</p>	154
<p>21. Mineral Dust and Diesel Exhaust Aerosol Measurements in Underground Metal/Nonmetal Mines <i>B. K. Cantrell</i>¹ and <i>K. L. Rubow</i>², ¹U.S. Bureau of Mines, Twin Cities Research Center, Minneapolis, MN and ²Particle Technology Laboratory, Mechanical Engineering Department, University of Minnesota, Minneapolis, MN. Presented at the VIIth International Pneumoconioses Conference, Pittsburgh, PA, August 23-26, 1988 and published in the Proceedings (Abstract only). (MN-1)</p>	167
<p>22. Measurement of Coal Dust and Diesel Exhaust Aerosols in Underground Mines <i>K. L. Rubow</i>¹, <i>V. A. Marple</i>¹ and <i>B. K. Cantrell</i>², ¹University of Minnesota, Minneapolis, MN and ²U.S. Bureau of Mines, Minneapolis, MN. Presented at the VIIth International Pneumoconioses Conference, Pittsburgh, PA, August 23-26, 1988, and published in the Proceedings (Abstract only). (MN-1).</p>	168

CONTENTS

	Page
<p>23. Experimental and Theoretical Measurement of the Aerodynamic Diameter of Irregular Shaped Particles <i>V. A. Marple, K. L. Rubow and Z. Zhuqun</i>, Particle Technology Laboratory, University of Minnesota, Minneapolis, MN. Presented at the VIIth International Pneumoconioses Conference, Pittsburgh, PA, August 23-26, 1988, and published in the Proceedings (Abstract only). (MN-2)</p>	169
<p>24. Some Observations on Particulates Collected in Diesel and Non-Diesel Underground Coal Mines <i>J. M. Mutmansky and L. Xu</i>, Department of Mineral Engineering, The Pennsylvania State University. (PS-19)</p>	170
<p>25. Effect of Thermal Treatment on the Surface Characteristics and Hemolytic Activity of Respirable Size Silica Particles <i>B. L. Razzaboni¹, P. Bolsattis¹, W. E. Wallace² and M. J. Keane²</i>, ¹Energy Laboratory, Massachusetts Institute of Technology, Cambridge, MA and ²National Institute for Occupational Safety and Health, Morgantown, WV. Presented at the VIIth International Pneumoconioses Conference, Pittsburgh, PA, August 23-26, 1988, and published in the Proceedings (Abstract only). (MIT-2)</p>	196
<p>26. Alteration of Respirable Quartz Particle Cytotoxicity by Thermal Treatment in Aqueous Media <i>C. A. Hill¹, W. E. Wallace^{1,2}, M. J. Keane², S. J. Page³ and P. Bolsattis⁴</i>, ¹West Virginia University, ²National Institute for Occupational Safety and Health, Division of Respirable Disease Studies, ³U.S. Department of Interior, Bureau of Mines, ⁴Energy Laboratory, Massachusetts Institute of Technology. Presented at the VIIth International Pneumoconioses Conference, Pittsburgh, PA, August 23-26, 1988, and published in the Proceedings. (MIT-2)</p>	197
<p>IV. Interaction of Dust and Lungs</p>	209
<p>27. Factors That May Influence Interactions Between Mineral Dusts and Lung Cells <i>G. L. Bartlett and J. D. Barry</i>, Milton S. Hershey Medical Center, The Pennsylvania State University, Hershey, PA. Presented at the VIIth International Pneumoconioses Conference, Pittsburgh, PA, August 23-26, 1988, and published in the Proceedings (Abstract only). (PS-11)</p>	211
<p>28. Effect of Coal Dust on Mucin Production by the Rat Trachea <i>V. P. Bhavanandan</i>, Department of Biological Chemistry, The Milton Hershey Medical Center, The Pennsylvania State University, Hershey, PA. Presented at the VIIth International Pneumoconioses Conference, Pittsburgh, PA, August 23-26, 1988, and published in the Proceedings (Abstract only). (PS-11)</p>	212

	Page
<p>29. Acoustic Impedance Method for Detecting Lung Dysfunction <i>J. Sneckenberger and T. Whitmoyer, West Virginia University.</i> Presented at the VIIth International Pneumoconioses Conference, Pittsburgh, PA, August 23-26, 1988, and published in the Proceedings. (WV-14A)</p>	213
<p>30. Bronchoalveolar Lavage in Subjects Exposed to Occupational Dusts <i>G. Goodman, N. L. Lapp, V. Castranova, W. H. Pailles and D. Lewis,</i> West Virginia University Hospital and Division of Respirable Disease Studies, National Institute for Occupational Safety and Health, Morgantown, WV. Presented at the VIIth International Pneumoconioses Conference, Pittsburgh, PA, August 23-26, 1988, and published in the Proceedings (Abstract only). (WV-17)</p>	218
<p>31. Microcomputer Control of Particle Concentrations in a Cotton Dust Exposure System <i>T. B. Whitmoyer¹, J. E. Sneckenberger¹, D. G. Frazer², V. A. Robinson², A. Giza² and D. S. DeLong²,</i> ¹Department of Mechanical and Aerospace Engineering, West Virginia University and ²Physiology Laboratory, Investigations Branch, NIOSH, Morgantown, WV. Presented at the Winter Annual Meeting of the American Society of Mechanical Engineers, Chicago, IL, November 1988. Published in the Proceedings. (WV-14A)</p>	219
<p>32. Effects of Platelet Activating Factor on Various Physiological Parameters of Neutrophils, Alveolar Macrophages, and Alveolar Type II Cells <i>K. VanDyke¹, J. Rabovsky², D. J. Judy², W. H. Pailles², M. McPeck², N. A. Sapola² and V. Castranova^{2,3},</i> ¹Department of Pharmacology and Toxicology and ²Department of Physiology, West Virginia University and ³Division of Respirable Disease Studies, National Institute for Occupational Safety and Health, Morgantown, WV. Presented at the VIIth International Pneumoconioses Conference, Pittsburgh, PA, August 23-26, 1988, and published in the Proceedings. (WV-17)</p>	223
<p>33. Use of a Sensitive Electro-Optical Method to Quantify Superoxide Release from Single PAM Exposed to Dusts In Vitro or In Vivo: Some Current Experimental and Model Results <i>E. V. Cilento, K. A. DiGregorio and R. C. Lantz,</i> Department of Chemical Engineering and Anatomy, West Virginia University. Presented at the VIIth International Pneumoconioses Conference, Pittsburgh, PA, August 23-26, 1988, and published in the Proceedings (Abstract only). (WV-9)</p>	233
<p>34. A Kinetic Model of Superoxide Production from Single Pulmonary Alveolar Macrophages <i>K. A. DiGregorio, E. V. Cilento and R. C. Lantz,</i> Departments of Chemical Engineering and Anatomy, West Virginia University. Presented at the VIIth International Pneumoconioses Conference, Pittsburgh, PA, August 23-26, 1988, and published in the Proceedings (Abstract only). (WV-9)</p>	234

	Page
<p>35. Effects of Serum on Superoxide Release from Single Pulmonary Alveolar Macrophages <i>K. A. DiGregorio, E. V. Cilento and R. C. Lantz, Departments of Chemical Engineering and Anatomy, West Virginia University. Presented at the VIIth International Pneumoconioses Conference, Pittsburgh, PA, August 23-26, 1988, and published in the Proceedings (Abstract only). (WV-9)</i></p>	235
<p>V. Relationship of Mine Environment, Geology and Seam Characteristics to Dust Generation and Mobility</p>	
<p>36. An Analysis of the Mass-Size Distribution of Airborne Coal Mine Dust in Continuous Miner Sections <i>C. Lee and J. M. Mutmansky, Department of Mineral Engineering, The Pennsylvania State University. Published in the Journal of the Korean Institute of Mineral and Mining Engineers, Vol. 25, No. 2, pp. 109-117, 1988. (PS-5)</i></p>	239
<p>37. A Comparative Analysis of the Elemental Composition of Mining-Generated and Laboratory-Generated Coal Mine Dust <i>C. J. Johnson and C. J. Bise, Department of Mineral Engineering, The Pennsylvania State University. Presented at the VIIth International Pneumoconioses Conference, Pittsburgh, PA, August 23-26, 1988, and published in the Proceedings (Abstract only). (PS-5)</i></p>	243
<p>38. Seeking the "Rank Factor" in CWP Incidence: The Potential Role of Respirable Dust Particle Purity <i>R. L. Grayson, R. Andre and T. Simonyi, West Virginia University. Presented at the VIIth International Pneumoconioses Conference, Pittsburgh, PA, August 23-26, 1988, and published in the Proceedings (Abstract only) (WV-6A)</i></p>	244
<p>39. Mineral Content Variability of Coal Mine Dust by Coal Seam, Sampling Location, and Particle Size <i>T. J. Stobbe, H. Ktn and R. W. Plummer, Department of Industrial Engineering, West Virginia University. Presented at the VIIth International Pneumoconioses Conference, Pittsburgh, PA, August 23-26, 1988, and published in the Proceedings. (WV-6A)</i></p>	245
<p>40. Measurement of Airborne Diesel Particulate in a Coal Mine Using Laser Raman Spectroscopy <i>B. C. Cornilsen, J. H. Johnson, P. L. Loyselle and D. H. Carlson, Michigan Technological University. Presented at the VIIth International Pneumoconiosis Conference, Pittsburgh, PA, August 23-26, 1988, and published in the Proceedings. (MTU-1)</i></p>	255

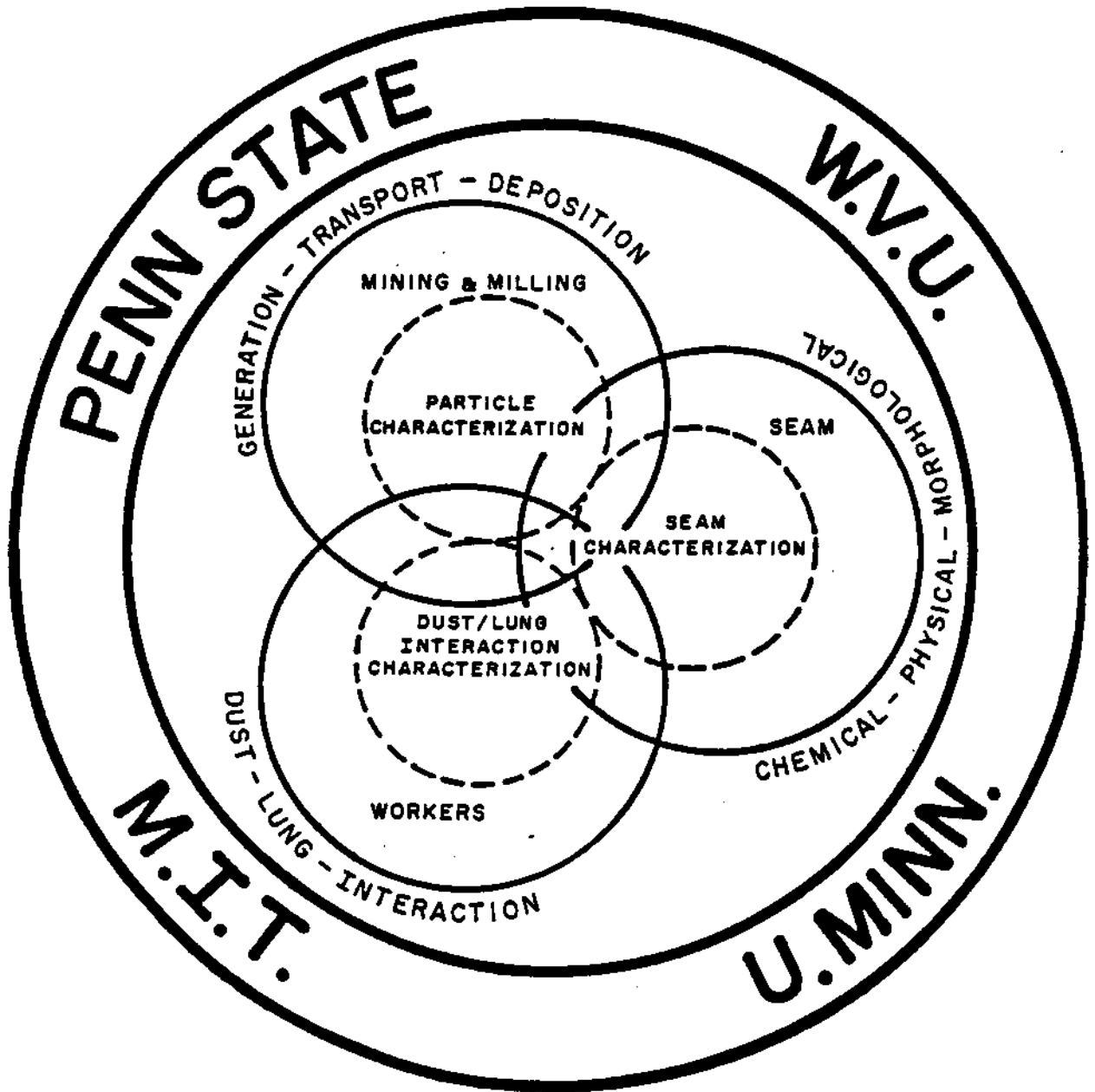
VI. Coordination

- 41. Air Quality in Mines: Progress and Prospects of Legal Control** **269**
R. V. Ramant, Department of Mineral Engineering, The Pennsylvania State University. Presented at the Fourth International Mine Ventilation Congress, organized by the Australasian Institute of Mining and Metallurgy, Brisbane, Australia, July 3-6, 1988, edited by A. D. S. Gillies. Published in the Proceedings. (PS-6)

INDEX **275**

Cumulative Author Index **277**

Cumulative Subject Index **281**



The Respirable Dust Center

FOREWORD

This volume contains publications resulting from respirable dust research performed in the Generic Mineral Technology Center for Respirable Dust by faculty, staff and graduate students at The Pennsylvania State University, West Virginia University, University of Minnesota, Massachusetts Institute of Technology and Michigan Technological University. These publications have appeared in scientific journals, proceedings of the national and international symposiums and at professional meetings in 1988. Complete citations of the publications can be found in the text. The Generic Mineral Technology Center for Respirable Dust is funded by the U.S. Bureau of Mines through the Mining and Mineral Resources Research Institute Program. The opinions and conclusions expressed in the papers are those of the authors alone and do not represent the opinions of the Generic Mineral Technology Center for Respirable Dust, the Mining and Mineral Resources Research Institute Program or the U.S. Bureau of Mines. Citation of manufacturers' names in the papers were made for general information purposes, and do not imply endorsement of the products by the authors.

All of the publications in this volume are on research that has been supported by the Department of the Interior's Mineral Institute program administered by the Bureau of Mines through the Generic Mineral Technology Center for Respirable Dust under allotment grant number G1135142 or G1175142.

In addition to these papers, the Center has organized a dust conference and an international symposium. In October 1984, a dust conference was held at West Virginia University, co-sponsored by the Generic Mineral Technology Center for Respirable dust, ACGIH, MSHA, NIOSH and USBM, the proceedings are available in the publication, 1984 Coal Mine Dust Conference, edited by Syd S. Peng, Morgantown, WV (Publication #PB86-169380). This publication is available from NTIS. An international symposium, Respirable Dust in the Mineral Industries: Health Effects, Characterization and Control, was held at The Pennsylvania State University in October 1986. Co-sponsored by the Generic Mineral Technology Center for Respirable Dust, ACGIH, MSHA, NIOSH, and USBM, the proceedings are available in the publication Respirable Dust in the Mineral Industries, edited by Robert L. Frantz and Raja V. Ramani, University Park, PA. This publication is available from ACGIH, ISBN: 0-936712-76-1 (Publication #3010).

The Generic Center maintains a reference center that serves as a clearinghouse for technical information for the generic area and supplies reports on generic center accomplishments.

The support from the United States Congress for the Generic Mineral Technology Center for Respirable Dust is gratefully acknowledged. We also acknowledge and appreciate the support and inputs from USBM, NIOSH, MSHA, the Research Advisory Council, and the Committee on Mining and Mineral Resources Research which have significantly contributed to the activities of the Generic Mineral Technology Center for Respirable Dust.

Respectfully submitted,

Robert L. Frantz
Co-Director, Generic Mineral
Technology Center for Respirable Dust
Co-Editor

R. V. Ramani
Co-Director, Generic Mineral
Technology Center for Respirable Dust
Co-Editor

THE RESPIRABLE DUST CENTER
Excerpted From The

**1988 UPDATE TO THE NATIONAL PLAN
FOR
RESEARCH IN MINING AND MINERAL RESEARCH**

Report to:


December 15, 1987

The Secretary of the Interior
The President of the United States
The President of the Senate
The Speaker of the House of Representatives

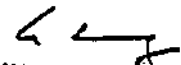
Section 9(e) of Public Law 98-409 of August 29, 1984, (98 Stat. 1536 et seq.) mandates that the Committee on Mining and Mineral Resources Research submit an annual update to the National Plan for Research in Mining and Mineral Resources: "Improving Research and Education in Mineral Science and Technology through Government-(Federal, State and Local), Industry, and University Cooperation."

Respirable Dust (centered at Pennsylvania State U. and West Virginia U., with affiliates at U. of Minnesota and Massachusetts Institute of Technology): brings together experts concerned with particles causing potentially disabling or fatal diseases, including pneumoconiosis ("black lung"), silicosis, and asbestosis, the latter of deep concern not just to workers in the mineral sector of the economy but also to the general populace.

SIGNED:




Carl V. Randolph
Mining Industry



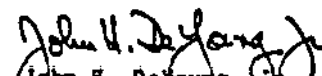
Win Aung
National Science
Foundation




Don L. Warner
University Administrator



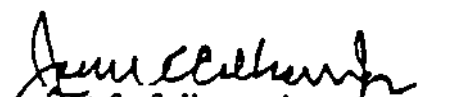
Walter R. Hibbard, Jr.
National Academy of
Sciences




John H. DeYoung, Jr.
U.S. Geological
Survey




Joseph N. Crowley
University Administrator



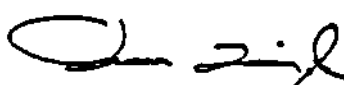
John C. Calhoun, Jr.
National Academy of Engineering



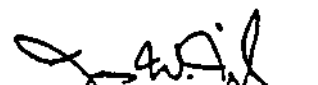
John D. Morgan
Bureau of Mines



Edward S. Frothing
Mining Industry



Orme Lewis, Jr.
Conservation Community
COCHAIR



James W. Ziegler
Asst. Secretary
Water & Science
U.S. Department of
the Interior
COCHAIR

Generic Mineral Technology Center For Respirable Dust

RESEARCH ADVISORY COUNCIL MEMBERS

Dr. John A. Breslin
Senior Staff Physical Scientist
U.S. Bureau of Mines
2401 E Street, N.W.
Columbia Plaza
Washington, D.C. 20241
(202) 634-1220

Dr. Ronald Munson
Director, Office of Mineral
Institutes - MS 1020
U.S. Department of the Interior
2401 E Street, N.W.
Washington, D.C. 20241
(202) 634-1328

Dr. Lewis Wade
Research Director
Twin Cities Research Center
U.S. Bureau of Mines
5629 Minnehaha Avenue, S.
Minneapolis, MN 55417
(612-725-4610)

Dr. John A. Campbell
Director, Engineering and
Technology Support
Kerr-McGee Corporation
P.O. Box 25861
Oklahoma City, OK 73125
(405) 270-3778

Mr. John Murphy
Research Director
Pittsburgh Research Center
U.S. Bureau of Mines
P.O. Box 18070
Pittsburgh, PA 15236
(412-675-6601)

Dr. James L. Weeks, C.I.H.
Deputy Administrator for
Occupational Health
United Mine Workers of
America
900 15th Street, N.W.
Washington, D.C. 20005
(202) 842-7300

Mr. Robert E. Glenn
Director, Division of Respiratory
Disease Studies - NIOSH
944 Chestnut Ridge Road
Morgantown, WV 26505
(304) 459-5978

Dr. Kandiah Sivarajah
State Toxicologist
Room 825--Health and Welfare
Building
Harrisburg, PA 17108
(717) 787-1708

Dr. Jerome Kleinerman
Department of Pathology
Cleveland Met. General Hospital
3395 Scranton Road
Cleveland, OH 44109
(216) 459-5978

Dr. Pramod Thakur
Research Group Leader
CONOCO, Inc.
R & D Division
Route #1, Box 119
Morgantown, WV 26505
(304) 983-2251

PAST RESEARCH ADVISORY COUNCIL MEMBERS

Mr. Darrel Auch
Senior Vice President
Northern West Virginia Region
Consolidation Coal Company
P.O. Box 1314
Morgantown, WV 26507
(304) 296-3461

Dr. Thomas Falke
President
Berwind Natural Resources
Company
Centre Square West
1500 Market Street
Philadelphia, PA 19102
(215) 563-2800

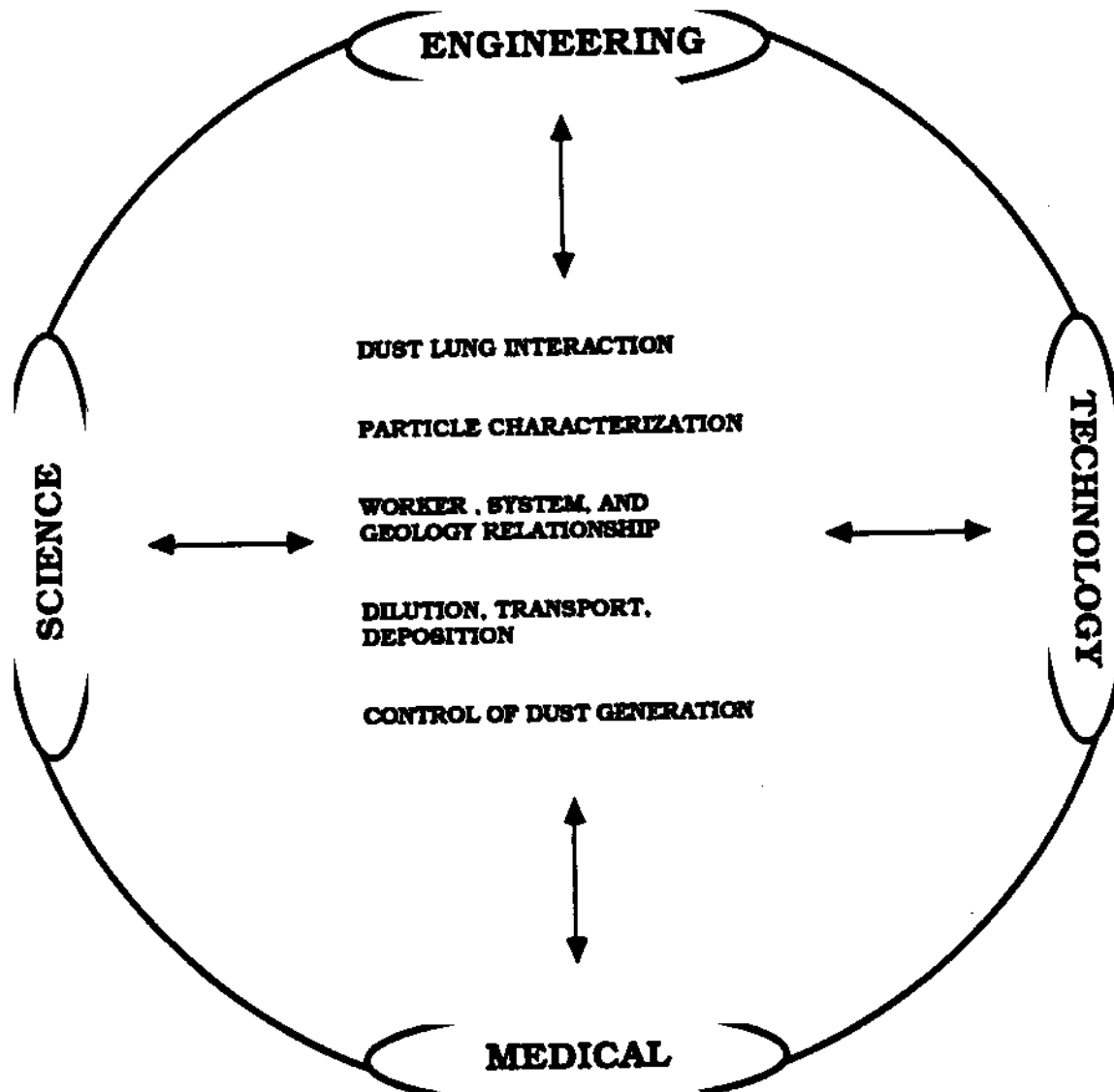
Mr. C. Wesley McDonald
Senior Vice President
(Mining)
Northern West Virginia
Region
Consolidation Coal Company
P.O. Box 1314
Morgantown, WV 26505
(304) 296-3461

Dr. J. Harrison Daniel
Program Manager, Mining
Research
Health and Safety
2401 E Street, N.W.
Washington, D.C. 20241
(202) 634-1253

Dr. Fred Kissell
Research Supervisor
Pittsburgh Safety Research Center
U.S. Bureau of Mines
4800 Forbes Avenue
Pittsburgh, PA 15213
(412) 675-6679

Dr. Donald Reid
Deputy Secretary for Public
Health Programs
Department of Health
Health and Welfare Building
P.O. Box 90
Harrisburg, PA 17108
(717) 783-8804

THE RESPIRABLE DUST CENTER



**Standardized protocols for Respirable Dust Research
in scientific, engineering, and medical areas.**

RESEARCH



CONTROL OF GENERATION

- Amount
- Fracture

**DILUTION,
TRANSPORT
AND
DEPOSITION**

- Concentration
- Size Consist
- Modeling

**MINE WORKER,
MINING SYSTEM,
SEAM GEOLOGY**

- Seam Sections
- Silica
- Trace Elements
- System Configuration
- Worker Location



- Coal Data Bank
- Mine Samples

**SUITE OF
GENERATED
RESPIRABLE
DUSTS**

- Anthracite
- Medium Volatile Bituminous
- High Volatile Bituminous
- Silica
- Fireclay
- Rock Dust



CHARACTERIZATION

- Size/Shape/Composition
- Surface/Functional Groups
- Particle Interaction

**DUST LUNG
INTERACTION**

- Medical/Cellular
- Medical/Animal
- Medical/Human
- Medical/Engineering

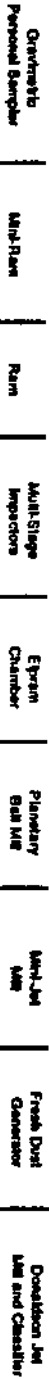


TRAINING

Train engineers, scientists, medical personnel, graduate students and undergraduate students in the interdisciplinary aspects of respirable dust.

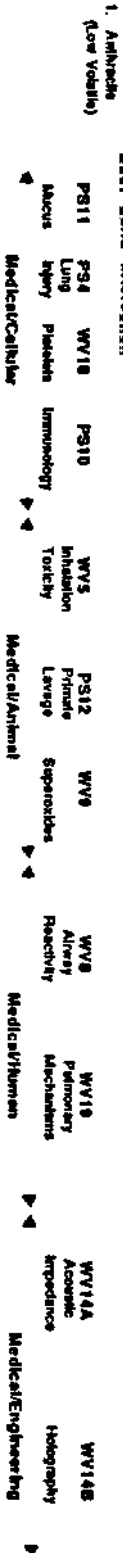
SAFETY AND DUST GENERATION METHODS

SUITE OF CHARACTERIZED DUST SAMPLES



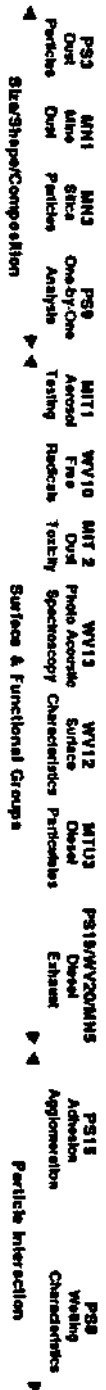
SUITE OF MEDICAL TESTS

1. Rats



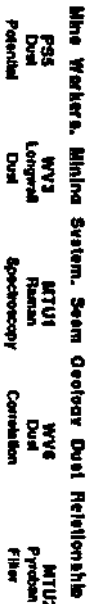
2. Humans (Medium Volume)

Particle Characterization



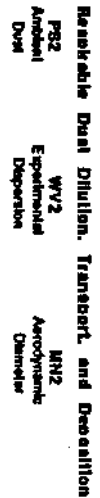
2. Guinea Pigs

3. Humans (High Volume)



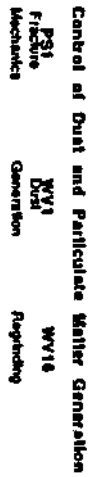
3. Dogs

4. Feeder



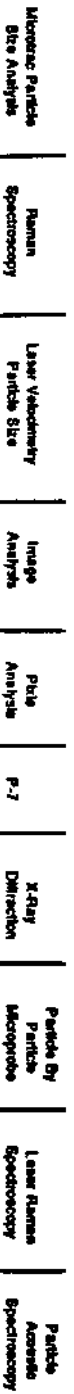
4. Non-Human Primates

5. Sites



5. Black Lung Patients

6. Products



6. Healthy People

The integration of scientific, engineering, and medical research findings into on-going projects.

The Generic Mineral Technology Center for Respirable Dust

SUITE OF CHARACTERIZED DUST SAMPLES	SAMPLING AND DUST GENERATION METHODS	SUITE OF MEDICAL TESTS
1. Anthracite (Low Volatile)	Dust/Lung Interaction	1. Rats
2. Bituminous (Medium Volatile)	Particle Characterization	2. Guinea Pigs
3. Bituminous (High Volatile)	Mine Workers Mining System Seam Geology Dust Relationship	3. Dogs
4. Fireclay	Respirable Dust Dilution Transport and Deposition	4. Non-Human Primates
5. Silica	Control of Dust Generation	5. Black Lung Patients
6. Rockdust		6. Healthy People

**SIZE, CHEMICAL AND
MINEROLOGICAL ANALYSIS**

STATEMENT OF GOAL

The primary goal of the Generic Mineral Technology Center for Respirable Dust is to reduce the incidence and severity of respirable dust disease through advancing the fundamental understanding of all aspects of respirable dust associated with mining and milling and the interaction of dust and lungs.

The holistic approach to standardized protocols and procedures.

I

**CONTROL OF DUST AND
PARTICULATE MATTER
GENERATION**

Estimating the Crush Zone Size Under a Cutting Tool in Coal

R. Karl Zipf, Jr. and Z.T. Bieniawski
Department of Mineral Engineering,
The Pennsylvania State University

Summary

As part of an effort to understand the mechanics of fine fragment formation in coal, which is important in studies of respirable dust due to mining, fracture toughness measurements and the strain energy density (SED) theory were applied to calculate the crush zone size under a cutting tool in coal. This zone is the major source of fine fragments in the 1 to 10 μm size range. The model used in these calculations is a boundary element program containing a failure criterion based on the SED theory. The boundary element program calculates linear elastic stresses at numerous points in the coal material ahead of a cutting bit. These stresses are then input to a subroutine called critical flaw length and orientation (CFLO) which uses the SED theory to determine the CFLO for a small crack at the boundary element stress computation point. The extent of crushing is based on earlier postulates about the role of inherent flaws in a fragmentation process. To form 1 to 10 μm fragments requires firstly a local stress strong enough to activate flaws with a characteristic length less than 1 to 10 μm and secondly, a flaw density sufficient to provide an average spacing between flaws also on the order of 1 to 10 μm . The locus of active 10 μm flaws represents the maximum possible extent of fine fragmentation in the 10 μm or less size range assuming that a sufficient inherent flaw density exists. The approach offers a first order approximation to the extent of crushing under a tool tip. The size and shape of the crush zone volume is affected by the attack angle and geometry of the tool.

Keywords: Coal dust; rock cutting tools; boundary element program; fragmentation; strain energy density.

Introduction

Fine fragment generation in the 1 to 10 μm size range under the action of a generic coal cutting tool may be explained on the basis of fracture mechanics which suggests two major sources of fine fragments: first in a crush zone near the tool tip and second by shear fracturing along major macrocrack surfaces (Zipf and Bieniawski, 1988a). In this paper, fracture toughness measurements and the strain energy density theory are used to calculate the crush zone size. This zone represents the major source of fine fragments in the 1 to 10 μm size range and understanding the mechanical factors controlling its size represents a first step toward using fracture mechanics to characterize the tendency of various coals to produce undesirable fine fragments.

Model description

The model used for these calculations consists of a boundary element program containing a failure criterion based on the strain energy density theory. In principle, the program is based on concepts advanced by Larchuk *et al.* (1985) for calculating the extent of crushing and material damage under a grinding tool acting on ceramics. The boundary element program provides linear elastic solutions for the stresses under a generic coal cutting tool. Stresses at numerous points in the coal material ahead of the bit are then input to a subroutine called critical flaw length and orientation (CFLO) which uses the strain energy density theory to determine the CFLO for a small crack at the boundary element stress computation point. Based on earlier postulates about the role of inherent flaws in a fragmentation process, the extent of material crushing in the 1 to 10 μm size range can be approximated. In order to form fragments in this size range, those postulates state first that the local stress field must activate flaws with a characteristic length less than 1 to 10 μm and second that the density of those 1 to 10 μm long inherent flaws is sufficient to provide an average spacing between flaws also in the order of 1 to 10 μm (Zipf, 1988; Zipf and Bieniawski, 1988a). Finally, the locus of active 10 μm flaws represents the maximum possible extent of fine fragmentation in the 10 μm or less size range again, assuming that a sufficient density of inherent flaws 10 μm or less in size exists.

Subroutine CFLO applies the strain energy density theory fully developed by Sih (1974) and Gdoutos (1984). Given the stress field in the neighbourhood of a point and a fracture criteria, it calculates the critical flaw length and crack growth direction for select initial flaw orientations. The output at each stress computation point is: 1, the given flaw orientation; 2, the calculated critical flaw length and 3, the calculated new crack growth direction. Details of the equations solved by this subroutine follow.

A crack of length $2a$ can be subjected to a purely normal stress as shown in Fig. 1a in which case the mode I stress intensity is given by $k_1 = S_n \sqrt{a}$. It can also be subjected to a purely tangential stress as shown in Fig. 1b where the mode II stress intensity is given by $k_2 = S_t \sqrt{a}$. The crack can also be inclined at some angle A in a uniaxial stress field S_y as shown in Fig. 1c. In this case, the crack is subjected to mixed mode loading and the stress intensity factors are $k_1 = S_y \sqrt{a} \cos A \cos A$ and $k_2 = S_y \sqrt{a} \cos A \sin A$ or equivalently $k_1 = S_y \sqrt{a} \sin B \sin B$ and $k_2 = S_y \sqrt{a} \sin B \cos B$. The most general loading case is shown in Fig. 1d where an inclined crack is subjected to a general loading. The stresses are first rotated into components normal and tangential to the crack plane with the following relations:

$$S_n = \frac{S_{yy} + S_{xx}}{2} + \frac{S_{yy} - S_{xx}}{2} \cos(2\alpha) - S_{xy} \sin(2\alpha)$$

$$S_t = \frac{S_{yy} - S_{xx}}{2} \sin(2\alpha) + S_{xy} \cos(2\alpha)$$

The stress intensity factors are then $k_1 = S_n \sqrt{a}$ and $k_2 = S_t \sqrt{a}$.

The strain energy density theory can now be applied to calculate first the crack extension angle for the flaw and second the critical flaw length that is just unstable in the given stress field. The strain energy density factor is defined as:

$$S = a_{11} k_1^2 + 2a_{12} k_1 k_2 + a_{22} k_2^2$$

ESTIMATING THE CRUSH ZONE SIZE

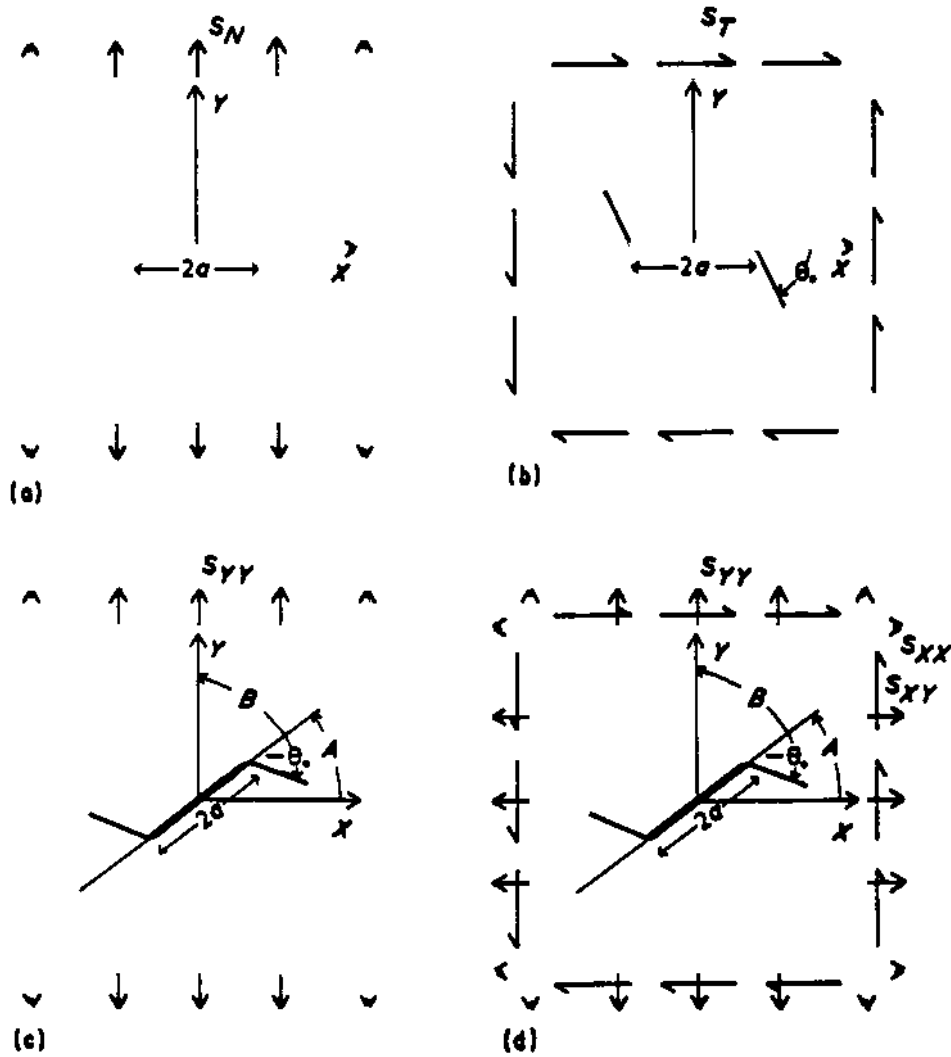


Fig. 1. Basic loading configurations and stress intensity factors for: (a) pure mode I loading, $k_1 = S_n \sqrt{a}$; (b) pure mode II loading, $k_2 = S_T \sqrt{a}$; (c) mixed mode loading in a uniaxial stress field, $k_1 = S_{yy} \sqrt{a} \sin B \sin B = S_{yy} \sqrt{a} \cos A \cos A$, $k_2 = S_{yy} \sqrt{a} \sin B \cos B = S_{yy} \sqrt{a} \cos A \sin A$; (d) mixed mode loading in a general stress field, $k_1 = S_n \sqrt{a}$, $K_2 = S_r \sqrt{a}$. S_n and S_r from stress transformation of S_{xx} , S_{yy} and S_{xy}

where a_{11} , a_{12} and a_{22} are the following functions of the crack extension angle, the shear modulus and the Poisson's Ratio:

$$\mu = \frac{E}{2(1+\nu)}$$

$$\kappa = 3 - 4\nu \text{ for plane strain}$$

$$\kappa = (3-\nu)/(1+\nu) \text{ for plane stress}$$

$$a_{11} = \frac{1}{16\mu} \{1 + \cos \theta\} \{\kappa - \cos \theta\}$$

$$a_{12} = \frac{1}{16\mu} \sin \theta \{2 \cos \theta - \kappa + 1\}$$

$$a_{22} = \frac{1}{16\mu} \{(\kappa + 1)(1 - \cos \theta) + (1 + \cos \theta)(3 \cos \theta - 1)\}$$

According to the hypotheses of the strain energy density theory, the crack extension angle is found by solving:

$$\frac{\partial S}{\partial \theta} = a'_{11}k_1^2 + 2a'_{12}k_1k_2 + a'_{22}k_2^2 = 0$$

subject to:

$$\frac{\partial^2 S}{\partial \theta^2} = a''_{11}k_1^2 + 2a''_{12}k_1k_2 + a''_{22}k_2^2 > 0$$

where the a' and a'' functions are:

$$a'_{11} = \frac{1}{16\mu} \{\sin 2\theta - (\kappa - 1)\sin \theta\}$$

$$a'_{12} = \frac{1}{16\mu} \{2 \cos 2\theta - (\kappa - 1)\cos \theta\}$$

$$a'_{22} = \frac{1}{16\mu} \{-3 \sin 2\theta + (\kappa - 1)\sin \theta\}$$

$$a''_{11} = \frac{1}{16\mu} \{2 \cos 2\theta - (\kappa - 1)\cos \theta\}$$

$$a''_{12} = \frac{1}{16\mu} \{-4 \sin 2\theta + (\kappa - 1)\sin \theta\}$$

$$a''_{22} = \frac{1}{16\mu} \{-6 \cos 2\theta + (\kappa - 1)\cos \theta\}$$

When the stress intensity expressions of k_1 and k_2 are substituted into the above expressions for the derivative of S , the crack length and the shear modulus divide out; thus, the crack extension angle is simply a function of the Poisson's Ratio and the normal to shear applied stress ratio. The applied stress ratio S_n/S_s depends solely on the initial crack angle B which can vary from -90 to $+90$ degrees.

The function $dS/d\theta$ always has four roots where $dS/d\theta=0$ in the interval from -180 to $+180$ degrees. Two of the roots can be immediately discarded because they do not satisfy the conditions that the second derivative of S is greater than 0 (i.e., S is at a local minimum). Finding the proper root from the remaining two depends on the signs of k_1 and k_2 and whether the local stress field is dominantly compressive or tensile.

ESTIMATING THE CRUSH ZONE SIZE

As shown in Fig. 2, four cases arise which correspond to different quadrants in a graph of k_1 versus k_2 . The crack inclination B is arbitrarily chosen as 45 degrees in this illustration and the approximate crack extension direction is also indicated in each diagram. In quadrant I, both k_1 and k_2 are positive so S_x and S_y are also positive. They can be resolved into a positive uniaxial tensile stress $+S_{yy}$ along the y axis. Similarly, in quadrant III, k_1 , k_2 and S_x , S_y are negative and the corresponding uniaxial stress is negative or compressional along the y axis. Quadrants II and IV correspond to an applied uniaxial stress along the x axis that is negative (compressional) or positive (tensile) respectively.

Knowing the quadrant to which k_1 and k_2 belong, places reliable bounds on the proper root of $dS/d\theta$. It is very easy to take advantage of these bounds when using a numerical root solver to find $dS/d\theta=0$ thus ensuring rapid convergence to the proper root.

Once the crack extension angle is determined with the root solving routine, solving for the critical flaw length in the given stress regime is very easy. It follows immediately from the definition of the strain energy density factor as:

$$a_{crit} = S_{cr} / (a_{11}S_x^2 + 2a_{12}S_x \cdot S_y + a_{22}S_y^2)$$

In the given stress regime, inherent flaws with a length less than a_{crit} remain stable whereas those with a length greater than a_{crit} propagate unstably in the crack extension angle direction determined earlier.

Subroutine CFLO

Programming the previous equations into subroutine CFLO and incorporating it into a boundary element program is straightforward. A flowchart for CFLO is shown in Fig. 3. CFLO is entered from the boundary element program immediately after stresses are determined at each user defined point. Stresses at the point are passed to CFLO in the call statement whereas the tested flaw orientation angles and the material properties including a critical strain energy density factor are passed in common. The program then enters the main do loop to perform critical flaw length computations for each test flaw orientation. The stresses are first transformed to the crack plane, and based on the signs of S_x and S_y , the approximate interval for the crack extension angle is found. Using this interval, subroutine ZEROIN computes the roots of $dS/d\theta=0$. ZEROIN is a root solver from Forsythe, Malcolm and Moler (1977). It begins with a bisection method to get close to the root and then finishes with a secant method. Once the crack extension angle is found, computation of the critical flaw length follows. Finally, the test flaw orientation, crack extension angle and critical flaw length are output prior to continuing with a new test orientation.

Subroutine CFLO is easily attached to a boundary element program such as TWOBI from Crouch and Starfield (1983) with minor modifications.

Calculations with CFLO

CFLO has been used to make preliminary calculations of the extent of crushing under a generic coal cutting tool using typical modulus and fracture toughness values determined from laboratory experimentation. Results are generally encouraging for this simplistic

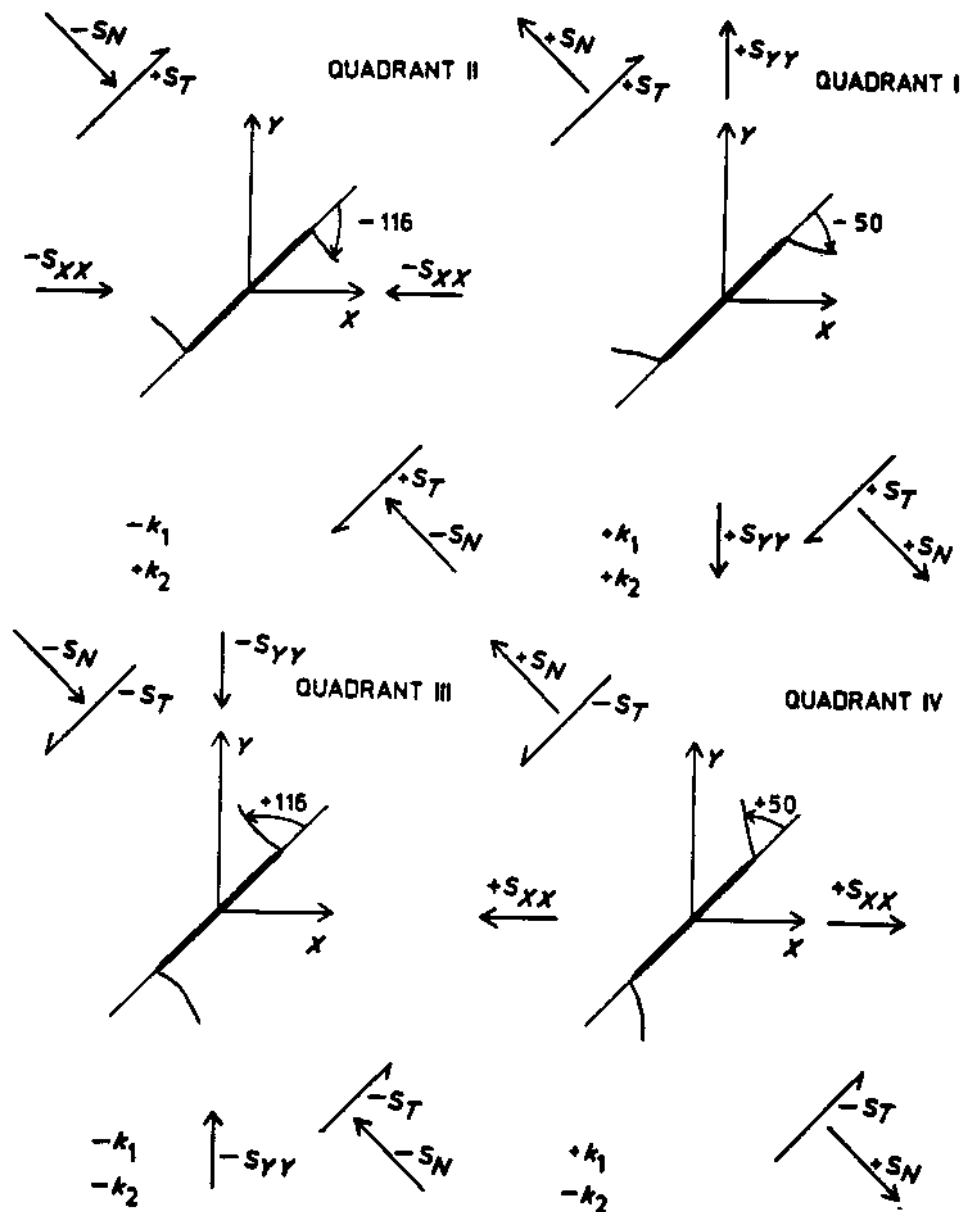


Fig. 2. Illustration of four separate cases for crack extension angle computations

computational procedure. Fig. 4 shows the boundary element models used in these computations along with the number of elements and stress computation points.

The boundary element models shown in Fig. 4 systematically altered the tool geometry from a narrow wedge with a 60° included angle through a 90° wedge to a 120° blunt wedge. The indentation width across the bit is arbitrarily fixed at 4 mm. Penetration depths then follow immediately as 3.5, 2.0 and 1.2 mm respectively. As a boundary condition at the bit/coal interface, a stress of 111MPa is applied which matches the 'average' bit stress

ESTIMATING THE CRUSH ZONE SIZE

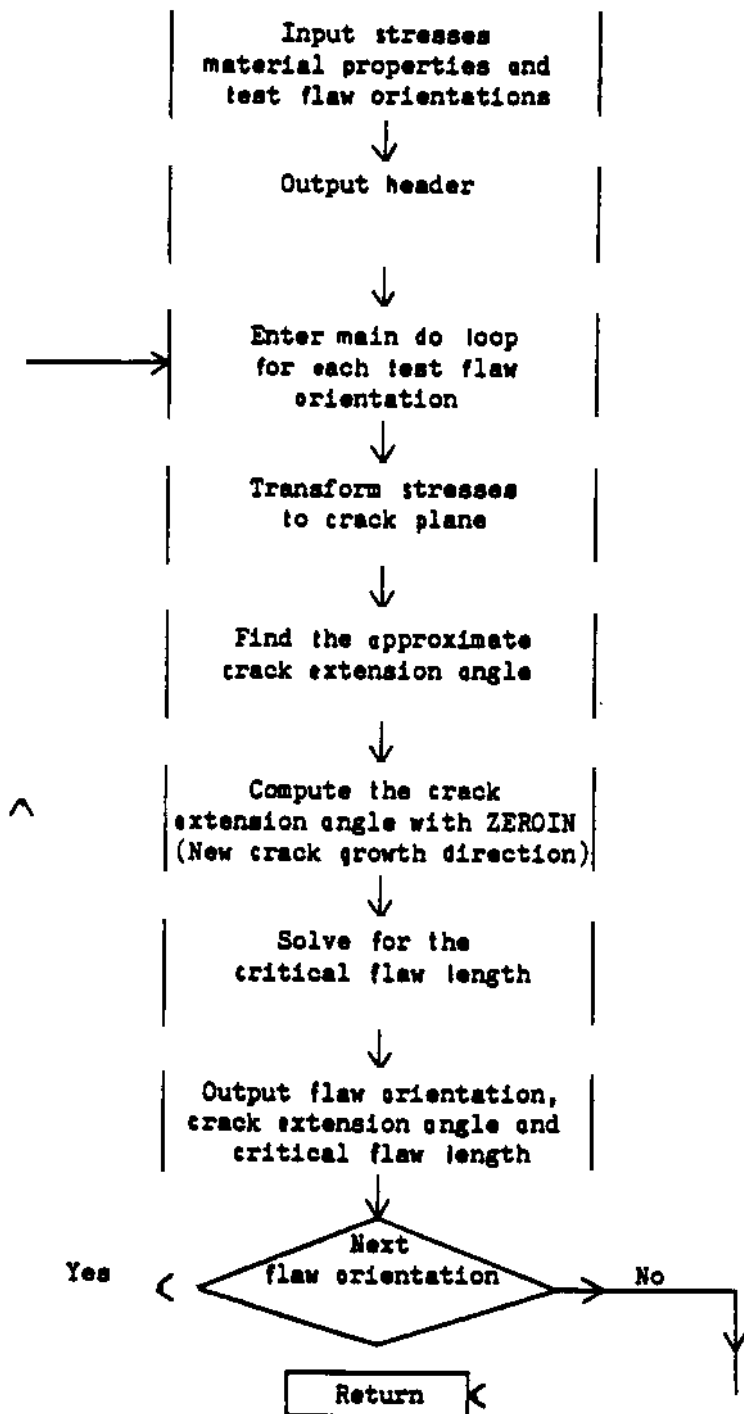


Fig. 3. Flowchart for subroutine CFLO which calculates critical flaw lengths and crack growth directions based on the given stress field, material properties and the strain energy density theory

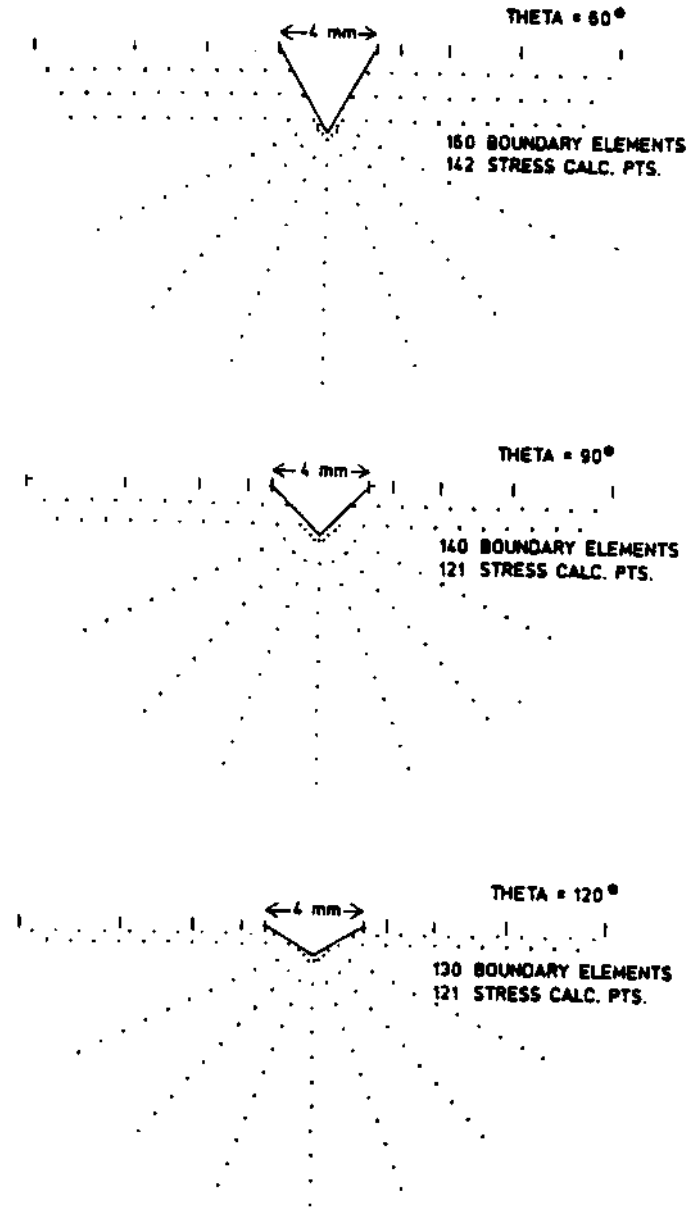


Fig. 4. Boundary elements models for three different tool geometries—the number of elements and stress computation points are indicated

estimated in earlier work by Zipf and Bieniawski (1988a) and Zipf (1988). To put this stress in perspective, the compressive strength of a 50 mm cube of Pittsburgh coal is typically around 20 MPa (3000 psi). This maximum stress is then rotated to approximately simulate various combinations of vertical and horizontal forces applied by the bit (i.e., the angle of attack). Stresses on the left and right sides of the bit/coal interface are given in Table 1. Average

ESTIMATING THE CRUSH ZONE SIZE

mechanical properties for the Pittsburgh coal are used in all 15 CFLO models. Young's Modulus is 2500 MPa; Poisson's Ratio is 0.400, and the critical strain energy density factor is 1 Nm^{-1} [Zipf, 1988; Zipf and Bieniawski, 1988b). Test flaw orientations range from -90 to $+90^\circ$ in 15° increments.

Table 1. Applied normal and shear stress on the left and right bit faces for the 15 CFLO models

Angle of Attack	Stress Orientation and Bit Face	60° bit stress MPa	90° bit stress MPa	120° bit stress MPa
0° (Vert.)	normal-left	-56	-50	-48
	shear-left	+32	+29	+28
	normal-right	-56	-50	-48
	shear-right	-32	-29	-28
15°	normal-left	-29	0	0
	shear-left	+17	0	0
	normal-right	-78	-96	-107
	shear-right	-79	-56	-29
30°	normal-left	0	0	0
	shear-left	0	0	0
	normal-right	-96	-107	-111
	shear-right	-56	-29	0
45°	normal-left	0	0	0
	shear-left	0	0	0
	normal-right	-107	-111	-107
	shear-right	-29	0	+29
60°	normal-left	0	0	0
	shear-left	0	0	0
	normal-right	-111	-107	-96
	shear-right	0	+29	+56

At each stress computation point, CFLO outputs each test flaw orientation and the computed crack extension angle and the critical flaw length in μm . From all the test flaw orientations, the smallest critical flaw length is selected and plotted at the appropriate stress computation point. Critical flaw lengths in the 1 to 5, 5 to 10, 10 to 100 and 100 to 1000 μm size range are displayed as zones in Fig. 5. The crush zone size under the tool tip is approximated as the locus where 10 μm or smaller flaws are active under the given loading conditions. This crush zone size is based on crucial assumptions concerning the role of inherent flaws in fragmentation processes. Again, to form 10 μm size fragments requires activation of flaws 10 μm or less in size with an average spacing also about 10 μm .

Promises and pitfalls with the CFLO approach

The crush zone size estimates shown in Fig. 5 must be considered tentative at best; nevertheless, they are extremely promising. First of all, the extent of crushing in the 1 to 10 μm size range certainly appears to be of the right magnitude. The calculations show that

THE RESPIRABLE DUST CENTER

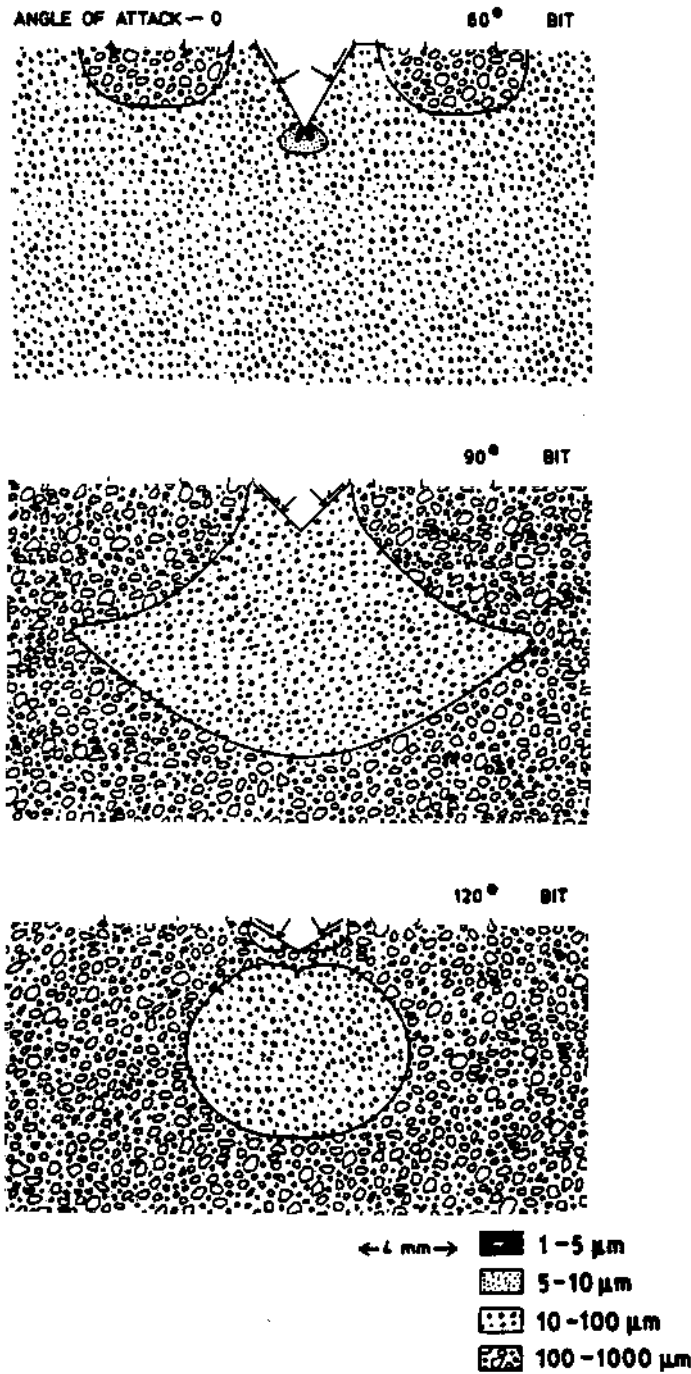


Fig. 5(a)

Fig. 5. Potential fragmentation under a tool tip: (a) angle of attack, 0°; (b) angle of attack, 15°; (c) angle of attack, 30°; (d) angle of attack, 45°; (e) angle of attack, 60°

ESTIMATING THE CRUSH ZONE SIZE

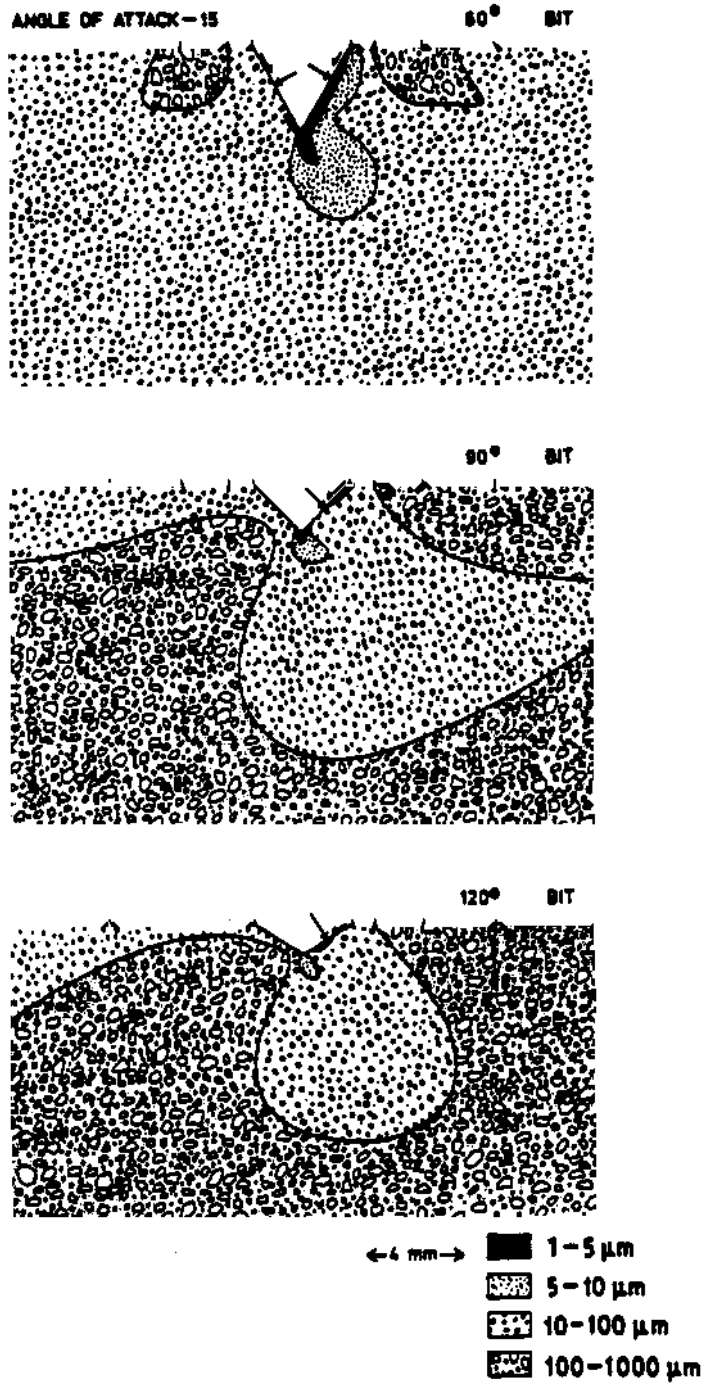


Fig. 5(b)

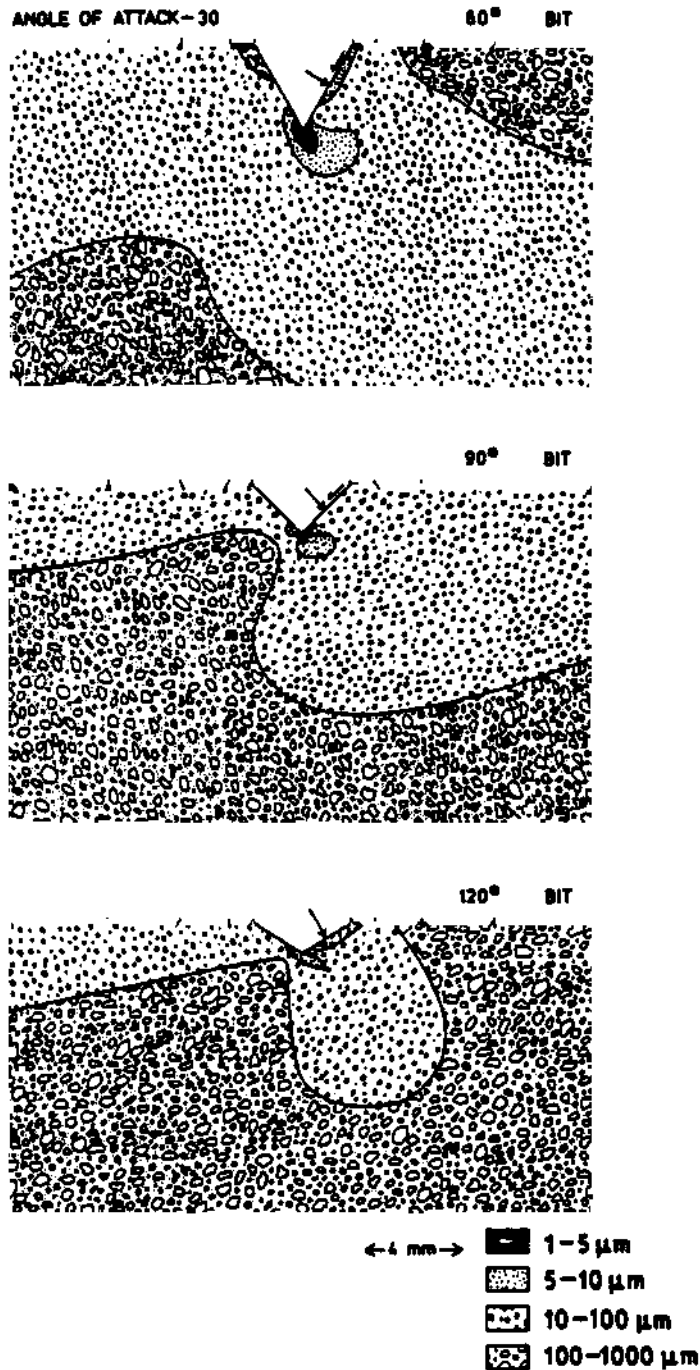


Fig. 5(c)

Fig. 5. Potential fragmentation under a tool tip: (a) angle of attack, 0°; (b) angle of attack, 15°; (c) angle of attack, 30°; (d) angle of attack, 45°; (e) angle of attack, 60°

ESTIMATING THE CRUSH ZONE SIZE

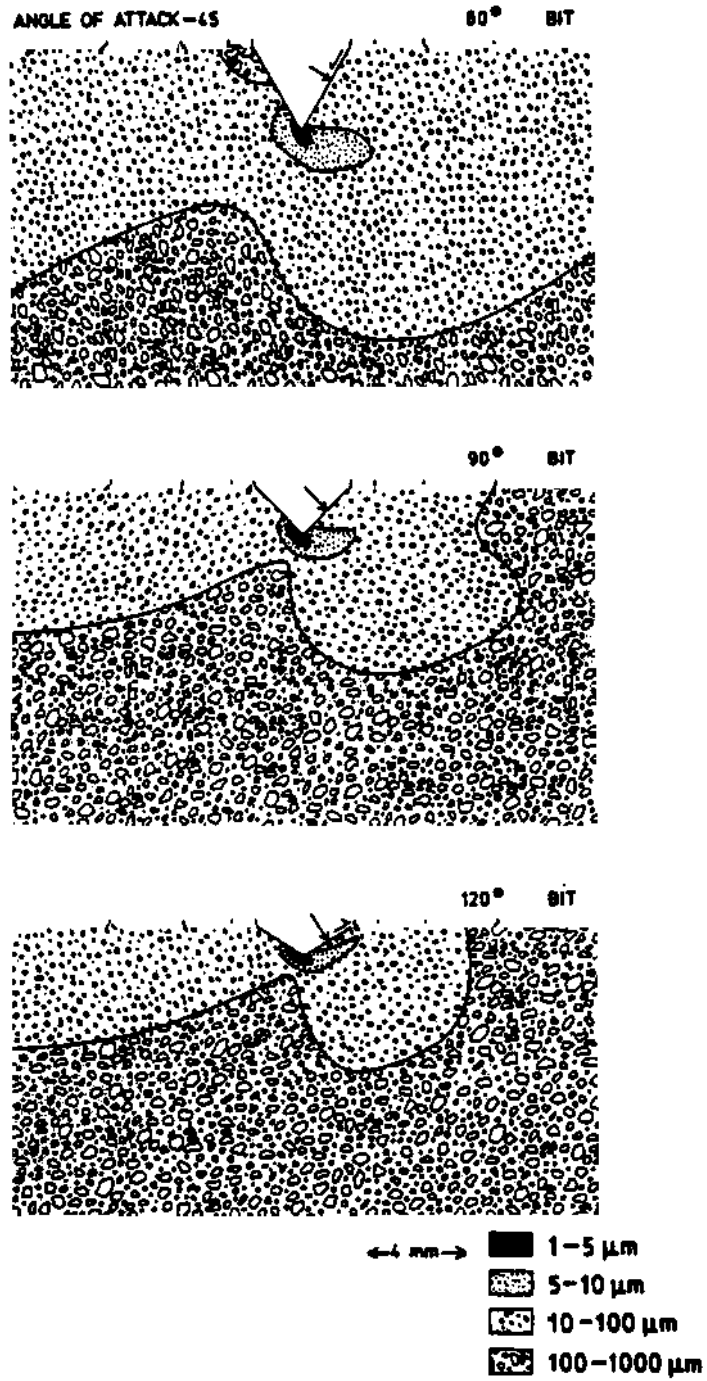


Fig. 5(d)

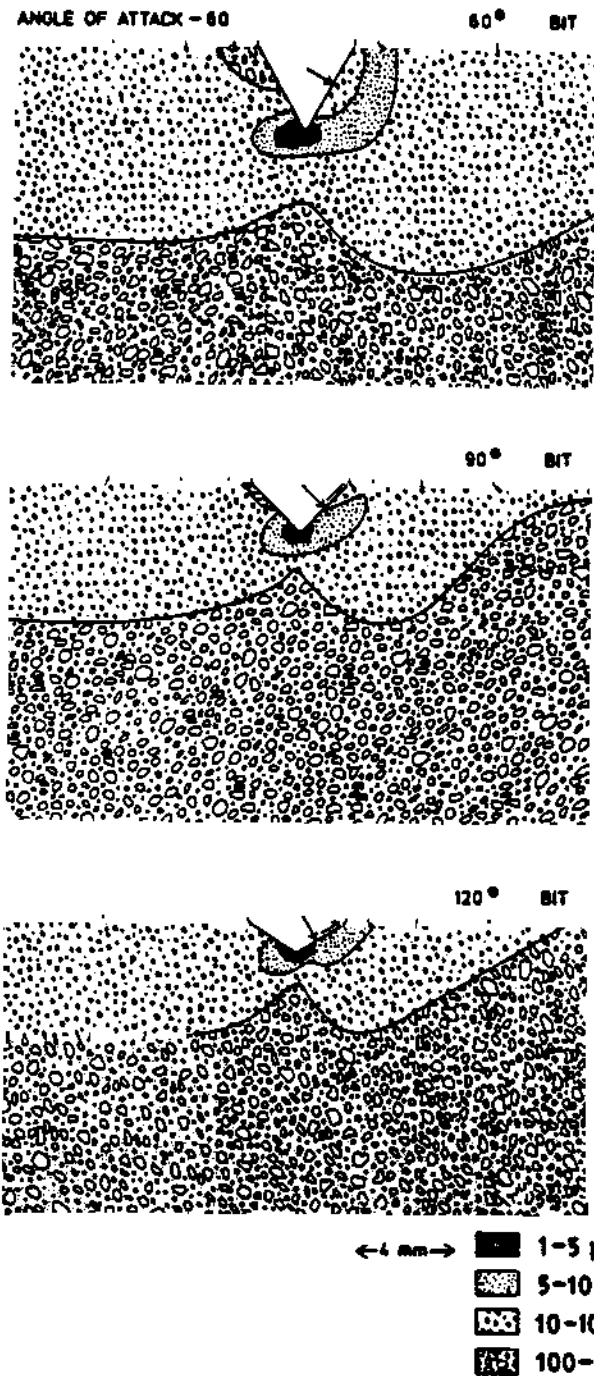


Fig. 5(e)
 Fig. 5. Potential fragmentation under a tool tip: (a) angle of attack, 0°; (b) angle of attack, 15°; (c) angle of attack, 30°; (d) angle of attack, 45°; (e) angle of attack, 60°

ESTIMATING THE CRUSH ZONE SIZE

the depth of crushing is on the order of 1 to 2 mm below the tool/coal interface which generally agrees with the depth of crushing suggested in full scale tests with actual cutting tools (Roepke *et al.*, 1976; Hanson and Roepke, 1979).

The calculations clearly show how the crush zone size is influenced by the angle of attack. As seen in Fig. 5, normal forces produce the least amount of undesirable crushing. Increasing the angle of attack, i.e., increasing the tangential force component, increases the amount of crushing under the tool tip. This numerical observation is also in good general agreement with the empirical findings (Roepke *et al.*, 1976; Evans and Pomeroy, 1966).

These calculations do not clearly indicate the effect of tool geometry on the extent of crushing. At present, they indicate that sharper tools produce more crushing than blunt tools which of course conflicts with all known observations. The performance of the tool geometries considered in these calculations are not directly comparable since the total bit forces are not the same for each tool. For this first modelling attempt with CFLO, the peak stress found from the earlier preliminary calculations is used at the bit interface. Tool width is also fixed; therefore, total bit forces for the 60° tool are greater than the 90° tool which is greater than the 120° tool. The more correct boundary condition is to keep the bit interface stresses and the total bit forces constant by adjusting the penetration depths somewhat; however, these calculations are reserved for further work.

The rather simple calculations by CFLO are not without their limitations. First, the analysis depends heavily on the nature of the bit/coal interface boundary condition. These analyses assume a stress type boundary condition; however, since the modulus constant between the bit and the coal is high, a displacement type boundary condition is probably better. The analysis also unrealistically assumes a smooth contact between the bit and the coal material. The actual contact area is more than likely to be highly irregular because of the rough fracture surfaces that the tool engages.

The CFLO approach makes the assumption that inherent flaws of a sufficient size and density exist in the material to serve as fracture initiation sites and produce the desired fragmentation. However, the size and density of those flaws must not significantly distort the global stress field induced in the material by the cutting tool. Global stresses are computed with a boundary element program at arbitrarily specified stress computation points. These stresses are assumed uniform over some small neighborhood of that point. The inherent flaws must be sufficiently small in size and density so that the computed global stresses are effectively seen as stresses at infinity by the flaw. In other words, the local stress field induced by the flaw itself must not significantly distort the global stress field in the neighborhood of the stress computation point. At fracture initiation, which is the only time when CFLO applies, this requirement can and must be met; however, as the flaws grow and begin to coalesce, such a requirement is inevitably violated.

The most serious problem with CFLO is in using a linear elastic continuum approach to a fragmentation related discontinuous phenomena. As the tool load increases, inherent flaws grow to create a discontinuous zone of fragmented material in the vicinity of the tool tip. The four step fine fragment formation model shows that this discontinuous zone will continue to propagate until a free surface is reached. Fine fragments exist close to the tool tip and grade into coarser fragments further away. The CFLO approach neglects the time dependent evolution of this discontinuous zone and its effect on the global stresses in the surrounding continuous zone. Of course, linear elasticity no longer applies in this fragmented discontinuous zone. This simple calculation procedure essentially assumes that the body

changes from continuous to discontinuous at one instant in time as opposed to an evolutionary change with increasing load.

Conclusion and possible related work

Despite the many difficulties associated with CFLO, the approach does offer a first order approximation to the extent of crushing under a generic coal cutting tool tip. It is based on a linear elastic analysis for the global stresses near a tool tip and a fracture mechanics analysis with the strain energy density theory of mixed mode fracture. The extent of crushing depends on activation of flaws below a certain critical size assuming that flaws of that size are present in sufficient density. As shown in Fig. 5 the CFLO approach can provide reasonable estimates of the crush zone size for typical cutting tools.

The approach may also offer useful insight in other related research. Howarth and Bridges (1988a, b) provided cross-sectional photomicrographs of the damage ahead of various percussive drill bits and indentation tools. Most striking in their work was how the grain structure (the microstructure or inherent flaw geometry) apparently controlled the fragmentation ahead of the tool. If suitable bit loads and material properties (K_{Ic}) are available, CFLO could model these experimental observations. Similarly, Cook *et al.* (1984) provided cross-sectional photomicrographs of microcrack development under a punch. They subsequently analysed their laboratory experiments using the finite element method and a Mohr-Coulomb failure criteria. Again, CFLO may provide useful insights into these experiments if the microstructure is known sufficiently. The observations by Friedman and Ford (1983) of cracking under a cutting tool might also be examined with an approach based on CFLO. Finally, CFLO may also assist in studies of the influence and behaviour of microcracks around a propagating macrocrack subjected to general mixed mode loading.

Acknowledgement

This research was supported under the Mineral Institutes Program by Grant No. G1135142/4201 from the US Bureau of Mines as part of the Generic Mineral Technology Center for Respirable Dust.

References

- Cook, N.G.W., Hood, M. and Tsai, F. (1984) Observations of crack growth in hard rock loaded by an indenter, *International Journal of Rock Mechanics and Mining Sciences & Geomechanics Abstracts*, 21 3, 97-107.
- Crouch, S.L. and Starfield, A.M. (1983) *Boundary Element Methods in Solid Mechanics*, George Allen & Unwin, London, 322 pp.
- Evans, I. and Pomeroy, C.D. (1966) *The Strength, Fracture and Workability of Coal*, Pergamon Press, New York, 277 pp.
- Forsythe, G.E., Malcolm, M.A. and Moler, C. B. (1977) *Computer Methods for Mathematical Computations*, Prentice-Hall, Englewood Cliffs, N.J., 259 pp.

ESTIMATING THE CRUSH ZONE SIZE

- Friedman, M. and Ford, L.M. (1983) Analysis of rock deformation and fractures induced by rock cutting tools used in coal mining, *Proceedings: 24th U.S. Symposium on Rock Mechanics*, Texas A&M University, pp. 713-723.
- Gdoutos, E.E. (1984) *Engineering Application of Fracture Mechanics, VII, Problems of Mixed Mode Crack Propagation*, Martinus Nijhoff Pub., Boston, 204 pp.
- Hanson, B.D. and Roepke, W.W. (1979) *Effect of Symmetric Bit Wear and Attack Angle on Airborne Respirable Dust and Energy Consumption*, USBM RI 8395, 24 pp.
- Howarth, D.F. and Bridge, E.J. (1988a) Microfracture beneath blunt disc cutters in rock, *International Journal of Rock Mechanics and Mining Sciences & Geomechanics Abstracts*, 25 1, 35-38.
- Howarth, D.F. and Bridge, E.J. (1988b) Observation of cracks at the bottom of percussion and diamond drill holes, *International Journal of Rock Mechanics and Mining Sciences & Geomechanics Abstracts*, 25 1, 39-44.
- Larchuk, T.J., Conway, J.C. and Kirchner, H.P. (1985) Crushing as a mechanism of material removal during abrasive machining, *Journal of the American Ceramics Society*, 68 4, 209-215.
- Roepke, W.W., Lindroth, D.P. and Myren, T.A. (1976) *Reduction of Dust and Energy During Coal Cutting Using Point Attack Bits*, USBM RI 8185, 56 pp.
- Sih, G.C. (1974) Strain energy density factor applied to mixed mode crack problems, *International Journal of Fracture*, 10 3, 305-321.
- Zipf, R.K. (1988) *The Mechanics of Fine Fragment Formation in Coal*, Ph.D. Dissertation, The Pennsylvania State University, 302 pp.
- Zipf, R.K. and Bieniawski, Z.T. (1988a) A Fundamental Study of Respirable Dust Generation in Coal, *Mining Science and Technology*, submitted for publication.
- Zipf, R.K. and Bieniawski, Z.T. (1988b) Mixed Mode Fracture Toughness Testing of Coal, *International Journal of Rock Mechanics and Mining Sciences and Geomechanics Abstracts*, submitted for publication.

Microscopic Studies of Fractures Generated Under Mixed Mode Loading

R. Karl Zipf, Jr. and Z.T. Bieniawski
Department of Mineral Engineering, The
Pennsylvania State University

ABSTRACT:

A set of fracture profile photomicrographs is presented for fractures generated under mixed mode loading of the Pittsburgh coal. The fractal dimension is used to characterize the irregularity of these profiles and a tentative relationship is presented between the fractal dimension and the fracture toughness. Surface roughness appears to depend solely on the stress intensity and no other dependence was observed with fracture loading mode, loading rate or specimen orientation. Observations of crack bifurcations in fracture profiles can indicate crack growth direction whereas direct surface observations generally cannot in materials such as rock and coal.

1 INTRODUCTION

The production of fine fragments of material as a result of some loading event occurs in many industrial processes. In crushing and grinding, the efficient production of fine fragments is the desired end result; however, in coal cutting, the production of fine fragments may lead to high levels of respirable dust in the immediate atmosphere with the danger of human lung diseases. Two of the most important sources of fragments in the 1 to 10 micron size range during a cutting process are 1) severe crushing in a zone near the loading tool and 2) subsequent shearing along major crack surfaces that form the larger fragments during material reduction. These and other sources of fine fragments generation are discussed by Roepke (1984) and Zipf and Bieniawski (1985). The physical character of the newly created major crack surfaces is believed to have a strong influence on the amount of fine fragment generation that occurs during subsequent shearing movement. When the major large fragments initially form, they are "locked" in place by the irregular character of the new fracture surface. Only after some relative motion has occurred between fragments are they actually liberated, and the net result is the formation of additional fine fragments. The fine fragmentation is not necessarily limited to the shearing of high points from the macrocrack surface since material remaining in the wake of the crack tip is damaged to a substantial depth below the actual crack surface.

STUDIES OF FRACTURES

2 OBJECTIVES

Quantitative observations of the macrocrack surfaces are required for better understanding of the shearing mechanism of fine fragment generation. Therefore, this study shall provide direct observations of fracture surfaces at a scale of 1 to 10 microns and will assess the influence of various mechanical and geometric properties on the fracture surface character.

3 MICROMECHANICS OF CRACK GROWTH AND CRACK BRANCHING

The failure process in brittle materials is generally considered a continuous process of microcrack nucleation, growth and coalescence into macroscopic faults followed by material disintegration. Costin (1987) traced the development of this concept and discussed evidence showing that microcracks originate from local stress concentrations arising from elastic mismatches along grain boundaries or from natural flaws and pores. The same process of nucleation, growth and coalescence of microcracks also describes the growth of a single macrocrack where the microcracks or so called "advance cracks" occur in a process zone around the macrocrack tip.

Ramulu and Kobayashi (1985) reviewed experimental evidence showing that this process generates the roughness of fracture surfaces and leads to the phenomena of crack branching. Advance cracks ahead of the main crack tip have been observed directly by Ravi-Chandar and Knauss (1984) with high speed photography of fracturing Homalite-100 specimens. They concluded that surface roughness on the main macrocrack results from the independent origins of the advance cracks which coalesce to form the main crack. In their bifurcation mechanism, crack branching occurs when one of these off axis microflaws connects with the main propagating crack tip. This same mechanism can also account for the formation of secondary cracks approximately parallel to the main crack if the propagating advance cracks do not link up with the main crack.

The influence of non-singular stresses on crack branching in conjunction with the microscopic observations has led to development of the two parameter branching criteria (Ramulu, Kobayashi and Kang, 1984; Streit and Finnie, 1980). These criteria retain higher order terms in the crack tip stress equations and postulate that branching occurs when $K > K_{TB}$ as a necessary condition and $r_o < r_c$ as a sufficient condition. Here, K_{TB} is the critical stress intensity for branching and r_c is a critical ratio with units of length. The value of r_o represents the ratio between the first and second terms of the crack tip stress series function and it also has a geometric interpretation as a description of the nearby microcracks.

This theoretical and experimental background suggests that the roughness of fracture surfaces generated in coal should show some dependence on the stress intensity and the microstructure. Subsequent experimental studies have sought to observe these possible relationships since the fracture surface character has a potential influence on the generation of extremely fine fragments through a macrocrack shearing mechanism.

4 EXPERIMENTAL STUDIES

Mixed mode fracture toughness tests have been conducted on a few different coals under a variety of fracture loading modes, loading rates and specimen orientations. The testing program and the operation of the testing system are described in Zipf and Bieniawski (1987). The testing rig is capable of applying mode I, mode II and mixed mode loads to a specimen through any of 7 rig positions. A schematic of the rig is shown in figure 1. On certain specimens, the fracture velocity was also determined with crack propagation gages as discussed in earlier work.

Aside from measuring critical fracture toughness and other mechanical parameters, the program generated a suite of new fracture surfaces under controlled loading modes, loading rates and orientations. The fracture surfaces were impregnated with a casting resin (styrene monomer and hardener) then carefully sectioned and polished for examination under a reflecting light microscope. Figure 2 shows a specimen sketch after fracturing and indicates the plane of sectioning. A series of photomicrographs beginning near the notch tip was completed at 500X magnification. Figures 3 and 4 show all sets of photomicrographs obtained.

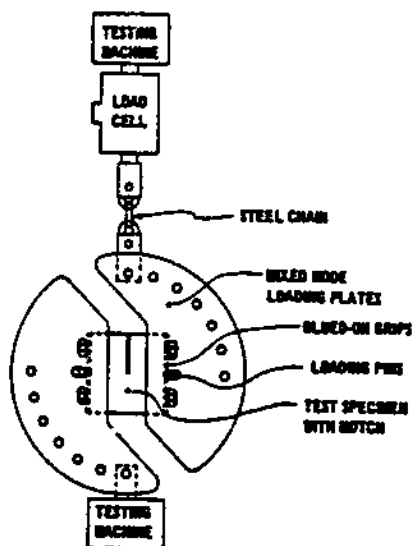


Figure 1. Schematic of mixed mode testing rig.

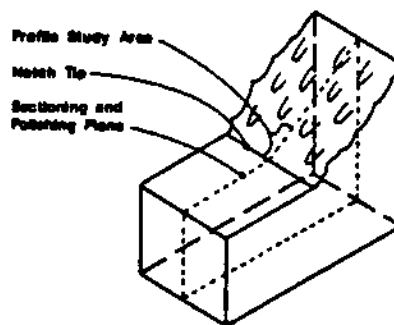


Figure 2. Schematic of fractured specimen showing sectioning and polishing plane.

Each set of photomicrographs has a specimen designation which indicates the type of coal tested, the orientation, the loading mode and the loading rate. All the tests shown are in the Pittsburgh coal (PT). The starter notch orientation is either parallel to the Bedding Plane (BP), the Face Cleat (FC), or the Butt Cleat (BC). Rig positions can vary from Hole 1 (H1) which is mode I through Hole 7 (H7) which is mode II or any mixed mode configuration in between. Last, loading rate is designated as either Slow (S), Middle (M) or Fast (F) corresponding to cross head displacement rates of 0.05, 0.5 and 5 mm/minute.

STUDIES OF FRACTURES

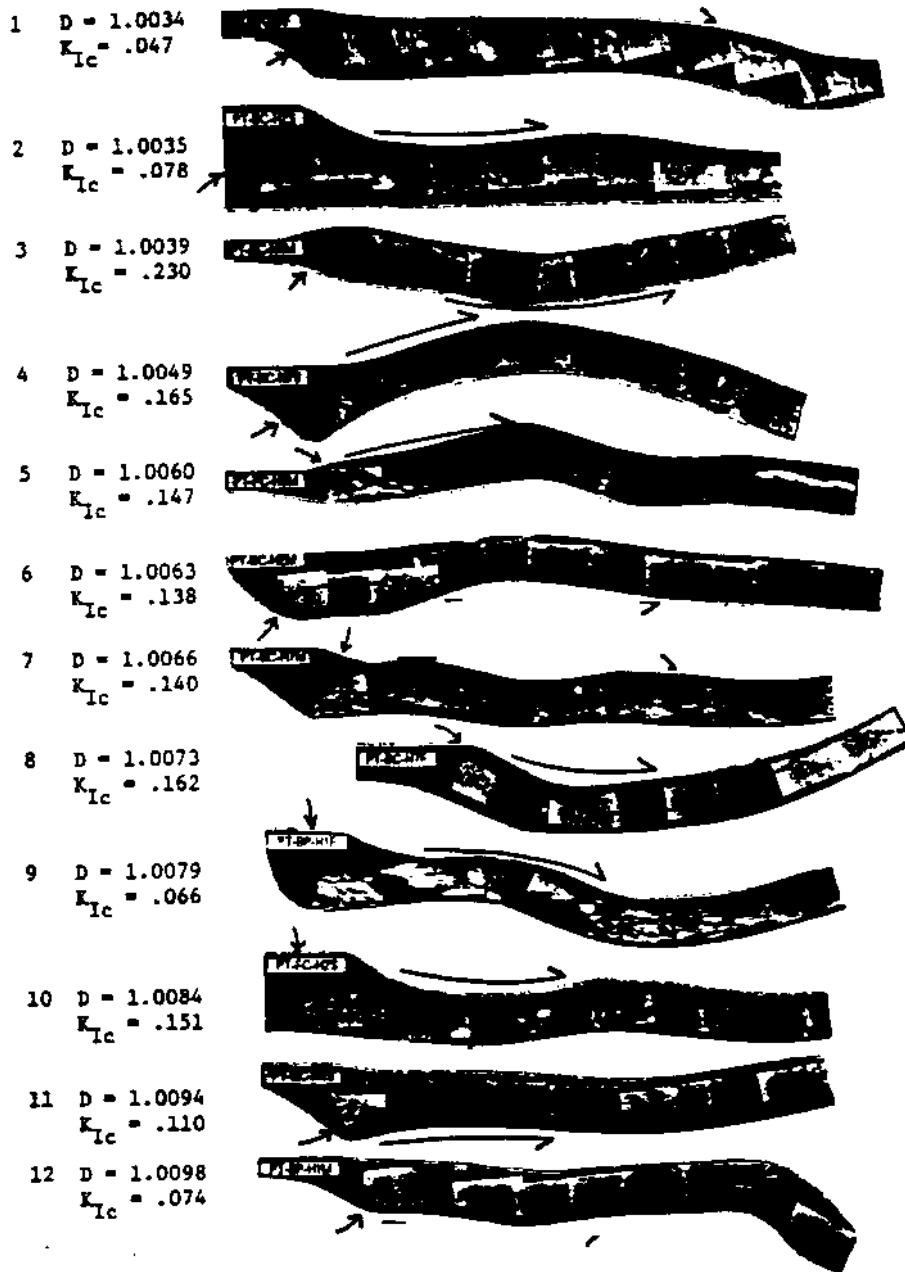


Figure 3. Photomicrograph sets 1 to 12 with specimen number, fractal dimension and fracture toughness. Crack initiation point and growth direction shown with arrows. Scale - 1 cm is approximately 200 microns.

The fractal dimension for these profiles was determined using the simple Richardson technique discussed in Mandelbrot (1982). The total length of a profile is given as $L = k S^{1-D}$ where L is the measured length, k is a constant, S is the scale length and D is the fractal dimension. Scale lengths of 12, 5, 2.5, 1 and 0.5 inches were used to measure L . The relationship between L and S as characterized by D was very good since the linear regression correlation coefficient always exceeded 0.95. The fractal dimension D therefore provides a repeatable, quantitative measure of fracture surface irregularity as was used earlier by Brown and Scholz (1985), Carr and Warriner (1987) and Turk, et al., (1987).

5 RESULTS

Measured fractal dimensions, fracture toughnesses and a few approximate fracture velocities are shown alongside each set of photomicrographs in figures 3 and 4. The profiles, numbered 1 through 23, are arranged in order of increasing fractal dimension which ranges from 1.0034 to 1.0274 while K_{Ic} ranges from 0.039 to 0.236 MPa \sqrt{m} . Next, a plot of fracture toughness versus fractal dimension (a measure of surface roughness) is shown in figure 5.

Initial inspection showed no readily apparent relationship between fracture toughness and fractal dimension. Furthermore, no meaningful relationship was discernible between fractal dimension and the loading mode, loading rate, specimen orientation or the few fracture velocities. However, the maceral composition of the coal did have considerable effect on the fracture surface character.

Most of the specimens dominantly contain the vitrinite group maceral collinite which is basically gray and structureless. Considerable amounts of the inertinite group maceral tentatively identified as fusinite are found in specimens 9, 16, 18, 20 and 23 where it appears as very light, fragmented or hackly shapes. Smaller portions of the exinite group maceral tentatively identified as sporinite are visible in specimens 5, 9, 10 and 21 where it appears as large black amorphous forms. In specimens 9, 16, 18, 20, 21 and 23 indicated with a + in figure 5, the macrocrack propagated mostly through inertinite and exinite group macerals and therefore should be expected to have a different fracture character than those fractures propagating mainly through a vitrinite group maceral. A linear regression calculation disregarding specimen 22 as an anomalous data point determined the best fit line through the vitrinite group data. That relation is also shown on figure 5.

6 DISCUSSION

The relationship between fracture toughness and fractal dimension which is used here as a measure of fracture surface roughness is in basic agreement with expectations, though at present, the supporting evidence is still considered tentative. Work is presently underway to extend the range of the relationship by studying an Anthracite coal which has a fracture toughness ranging from 0.3 to 0.5 MPa \sqrt{m} . The initial results for Pittsburgh coal are promising and generally agree with the fracture toughness-fractal dimension relationships reported by Mecholsky and Passoja, (1985) and Mecholsky, Mackin, and Passoja, (1986) for a wide

STUDIES OF FRACTURES

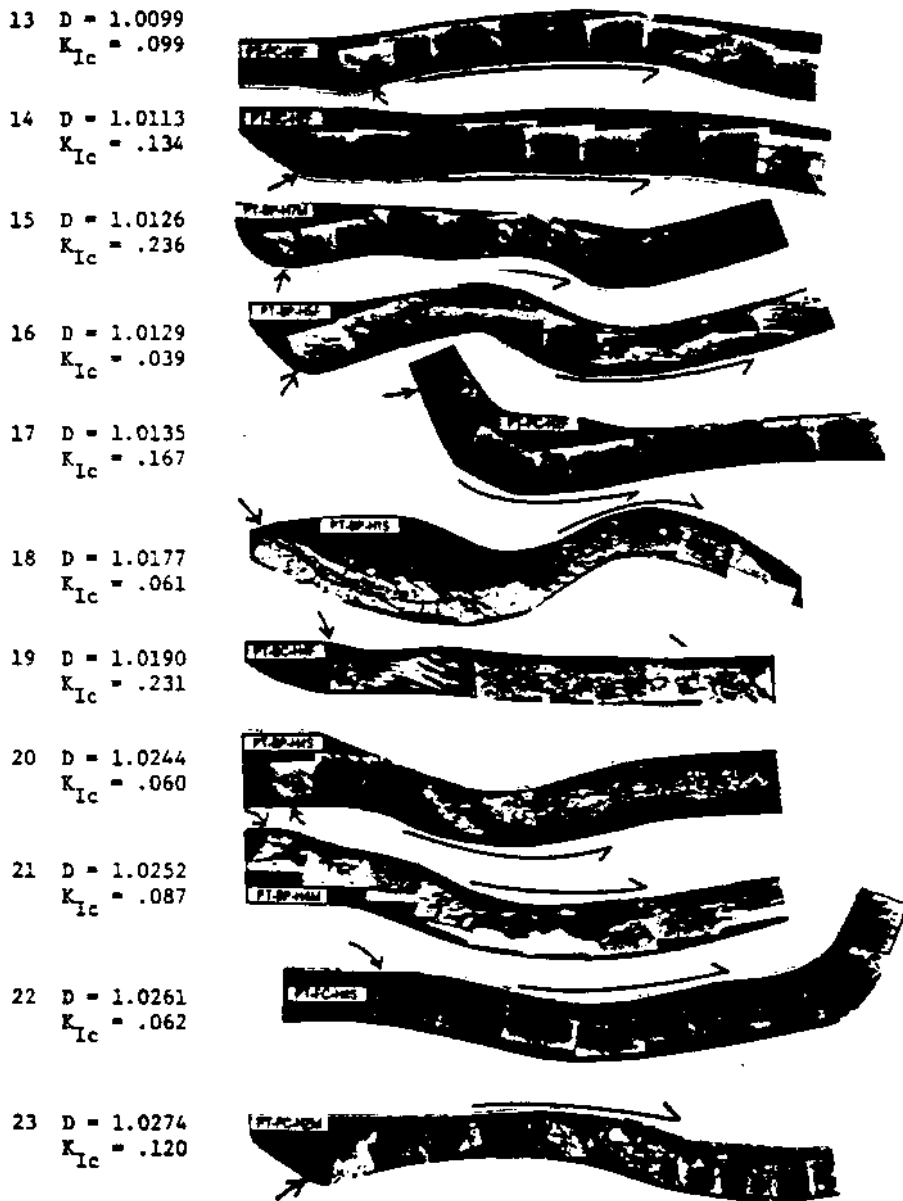


Figure 4. Photomicrograph sets 13 to 23 with specimen number, fractal dimension and fracture toughness. Crack initiation point and growth direction shown with arrows. Scale - 1 cm is approximately 200 microns.

THE RESPIRABLE DUST CENTER

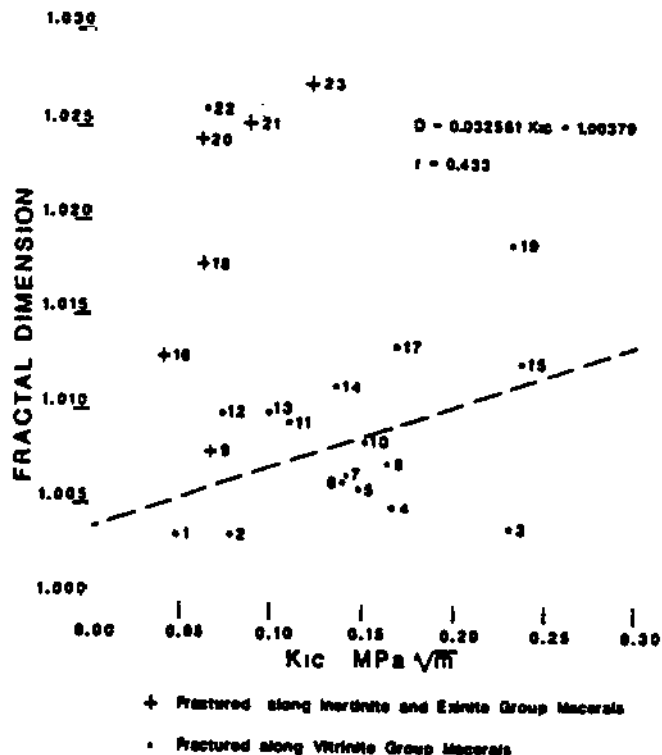


Figure 5. Fractal dimension versus fracture toughness for each numbered specimen in figures 3 and 4.

variety of ceramics. This relationship may provide the necessary understanding required for the shearing mechanism of fine fragment generation. No other significant relationships between fractal dimension and the fracture loading mode, loading rate and specimen orientation could be identified.

In further examinations of the photomicrographs, it is possible to discern the direction of propagation from the crack bifurcations. The acute angle formed at a crack branch will frequently point upstream, but it must be emphasized that this is not always the case and examination of numerous crack branches over a substantial length of fracture profile is required. Confusion can result when numerous secondary cracks are present which rejoin with the main crack. A few examples where these branches do indicate the direction of crack growth are found in specimens 6, 7, 12, 13, 21 and 22. Other examples where branching indicates the direction of crack growth are found in Freidman and Ford, (1963), and Ravi-Chandar and Knauss, (1984). Usually, it is the unsuccessful branching attempts that provide the best indication of direction. Deducing crack propagation direction from fracture profiles is not as convenient as simple fracture surface examination; however, with rock, it may be the only option.

7 REFERENCES

- Brown, S.R. and Scholz, C.H., (1985), "A Broad Bandwidth Study Of The Topography Of Natural Rock Surfaces", *J. Geophys. Res.*, V90 nB14, pp. 12575-12582.

STUDIES OF FRACTURES

- Carr, J.R. and Warriner, J.B., (1987), "Rock Mass Classification Using Fractal Dimension", Proceedings: 28th US Symposium on Rock Mechanics, A.A. Balkema, Boston, pp. 73-80.
- Costin, L.S., (1987), "Time-Dependent Deformation and Failure", Fracture Mechanics of Rock, ed. B.K. Atkinson, Academic Press, London, pp. 167-216.
- Freidman, M. and Ford, L.M., (1984), "Analysis of Rock Deformation and Fractures Induced by Rock Cutting Tools Used in Coal Mining", Proceedings: 24th U.S. Rock Mechanics Symposium, Texas A&M University, pp. 713-723.
- Mandelbrot, B.B., (1982), The Fractal Geometry of Nature, W.H. Freeman, New York, 468pp.
- Mecholsky, J.J. and Passoja, D.E., (1985), "Fractals And Brittle Fracture", Materials Research Society Extended Abstracts.
- Mecholsky, J.J., Mackin, T.J. and Passoja, D.E., (1986), "Crack Propagation In Brittle Materials As A Fractal Process", Materials Research Society Extended Abstracts.
- Ramulu, M., Kobayashi, A.S., and Kang, B.S.J., (1984), "Dynamic Crack Branching - A Photoelastic Evaluation", Fracture Mechanics: Fifteenth Symposium, ed. R.J. Sanford, ASTM STP 833, pp.130-148.
- Ramulu, M. and Kobayashi, A.S., (1985), "Mechanics of Crack Curving And Branching - A Dynamic Fracture Analysis", Int. J. Fract., V27, 1985, pp. 187-201.
- Ravi-Chandar, K and Knauss, W.G., (1984), "An Experimental Investigation Into Dynamic Fracture: II Microstructural Aspects", Int. J. Fract. V26, pp. 65-80.
- Roepke, W.W., (1984), "General Methods Of Primary Dust Control During Cutting", Mining Engineering.
- Streit, R. and Finnie, I., (1980), "An Experimental Investigation Of Crack Path Directional Stability", Experimental Mechanics, V20, n1, pp. 17-23.
- Turk, N., Greig, M.J., Dearman, W.R., and Amin, F.F., (1987), "Characterization Of Rock Joint Surfaces By Fractal Dimension", Proceedings: 28th US Symposium On Rock Mechanics, A.A. Balkema, Boston, pp. 1223-1236.
- Zipf, R.K. and Bieniawski, Z.T., (1986), "Mixed Mode Testing For Fracture Toughness Of Coal Based On Critical Energy Density", Proceedings: 27th US Symposium On Rock Mechanics, AIME, New York, pp. 16-23.
- Zipf R.K. and Bieniawski, Z.T., (1987), "Development Of A Mixed Mode Testing System For Geologic Materials", Proceedings of the International Conference on Fracture of Concrete and Rock, ed. S.P. Shah and S.E. Swartz, SEM, Bethel, CT., pp. 338-352.

II

**DILUTION, DISPERSION AND
COLLECTION IN MINE AIRWAYS**

Dust Flows in Mine Airways: A Comparison of Experimental Results and Mathematical Predictions

R. Bhaskar and R.V. Ramani
Department of Mineral Engineering,
The Pennsylvania State University

Abstract. The results of an experimental and theoretical research study into the spatial and temporal behavior of dust in mine airways is summarized in the paper. Experiments were performed in mine airways under both controlled and normal operating conditions. The controlled experiments included the documentation of the concentration and deposition patterns for two types of dust under three different velocities. Real-time dust concentration data were obtained using Real-time Aerosol Monitors (RAM-1) to determine the dispersion coefficient in a mine airway. On the theoretical front, a convection-diffusion model of the dust flow phenomenon in mine airways was developed considering dominant mechanisms affecting dust transport and deposition in mine airways. Mechanisms modeled include turbulent and gravitational deposition, coagulation, and dispersion.

In this paper, comparative analyses of results of the controlled experiments with the predictions of the mathematical model are presented. In addition to the overall validity, the adequacy of the individual components of the model, such as deposition in the total and respirable range, and dispersion are examined in light of the experimental observations.

The experimental data from controlled experiments compared more favorably with model predicted results for similar conditions as opposed to the comparative analysis results for in-mine experiments. Specifically, the model predictions for an 800-meter stretch of a mine airway reveal some significant differences from the behavior noticed in the mine. The deposition was lower than that predicted by the model. Consequently, concentrations were higher than those predicted by the model. The implications of these and other findings for further investigations are discussed in the paper.

INTRODUCTION

A review of literature reveals several theoretical and experimental studies relating to dust flow in mine airways. During the last three decades, several theoretical studies on the various mechanisms affecting dust behavior

have been reported (Dawes and Slack, 1954, Perales, 1958, Hwang et.al. 1972, and Courtney et.al. 1982). Experimental studies were performed by Bradshaw and Godbert (1954), Hall (1955), Hodgkinson (1957), Ford (1971) and Courtney et.al. (1982). The literature survey however, indicated the need for a concerted theoretical and experimental study to predict dust concentrations in mine atmospheres, incorporating recent findings in the mining and the aerosol sciences. The objective of a continuing research project in the Generic Mineral Technology Center for Respirable Dust (Ramani, 1983) is to aid in the control of dust in underground mines through an improved understanding of the behavior of dust clouds in mining environments.

The first phase of the research project involved the development of a mathematical model to predict dust concentrations in mine atmospheres. The second phase involved in-mine experimental studies on dust behavior in mine airways. The third phase involved the comparison of the mathematical model output with the in-mine experimental data for similar physical conditions. In this paper, the results of the work done in the third phase are presented in detail. For completeness, a brief description of the work performed in Phases I and II are also presented.

For the purpose of this paper, total dust includes all particles that are airborne. Respirable dust includes particles that are less than or equal to 5 microns. Deposition rate is calculated from the experimental data as the mass depositing per unit area, per unit time, per unit concentration $((\text{mg}/\text{m}^2/\text{sec})/(\text{mg}/\text{m}^3))$.

BACKGROUND

MATHEMATICAL MODEL

In phase I, a mathematical model was developed to study the dispersion and transport of dust in a mine airway. While mathematical models to study gaseous contaminants have been developed, the major difference between gaseous and particulate contaminants is the deposition

THE RESPIRABLE DUST CENTER

phenomenon. The deposition of particulate contaminants on surfaces is a function of several factors such as particle size, particle density, air viscosity and airflow rate. The model has incorporated the following mechanisms: diffusional deposition; convection-diffusion; sedimentation and coagulation. The diffusional deposition aspects of the model were based on studies in the aerosol sciences (Liu and Agarwal, 1974, Wood, 1981a, 1981b). Diffusion rates used in the model were obtained from studies into dispersion of contaminants in mine airways (Skobunov, 1973). Sedimentation was considered as a major mechanism of deposition on mine floors. Due to the non-linear nature of the sedimentation rate equation, the dust size distribution was discretized into several size classes and appropriate sedimentation equations were applied. With respect to coagulation a discretized form of the Smoluchowski equation (Chung, 1981) was used to determine addition and disappearance of particles from various size classes.

A detailed description of the model is presented in Bhaskar and Ramani (1986). Briefly, the transport and deposition of dust was modeled using a one-dimensional convection-diffusion equation of the form (Figure 1):

$$\frac{\partial c}{\partial t} = E \times \frac{\partial^2 c}{\partial x^2} - U \frac{\partial c}{\partial x} + \text{sources} - \text{sinks}$$

where,

- c - concentration of airborne dust
- t - time
- E - dispersion coefficient
- x^x - distance from source, and
- U - velocity of airflow.

The source term represents the dust generated during the cutting process, and is described by a step function. The particle size distribution of the source is discretized into small intervals by the model given (a) the

number of size classes desired, (b) the minimum and maximum particle diameter, (c) the median diameter and (d) standard deviation, to better simulate the mechanisms acting on the particle. Initial and boundary conditions appropriate to the case under study were selected and the equation was solved using finite difference techniques. The model was programmed for a computer-oriented solution. Due to the sparseness of the available experimental data to validate the model, preliminary validation of the model was restricted only to the model deposition component.

EXPERIMENTAL STUDIES

Concurrent with model development, a set of experiments were conducted in mine environments to better understand dust transport phenomena. The first set of experiments were designed so as to acquire data under varied but controlled experimental conditions. Specifically, experiments were conducted at three different velocities for each of two dust types for a total of six experiments.

Controlled Experiments: A long straight section of airway in the Lake Lynn Laboratory mine of the U.S. Bureau of Mines was selected for the experiments. The experimental design for data collection involved specifications of the methods of dispersing dust, the number of sampling points, the location of the sampling points and the method of sampling for determining airborne dust concentrations and floor depositions. A typical sampling plan is shown in Figure 2. Specifically, the following data were collected:

- * ambient dust concentration in the total, and the respirable size ranges;
- * deposition of dust in the total, and the respirable size ranges; and
- * cross-sectional sampling at several points, along with center-line sampling in the same sections.

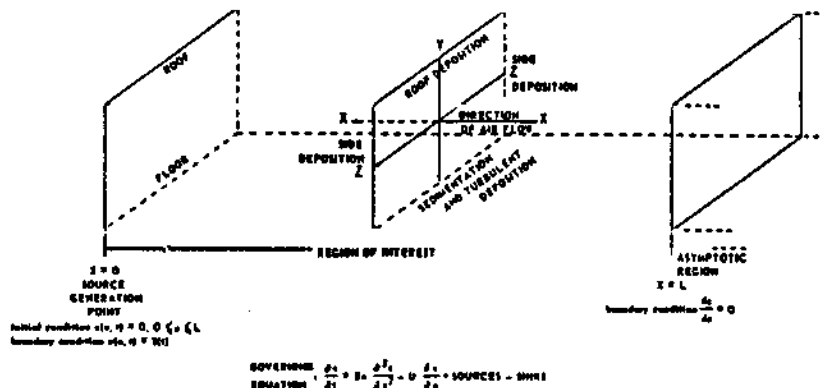


Figure 1. Schematic of Dust Flow in a Mine Airway.

DUST FLOWS IN MINE AIRWAYS

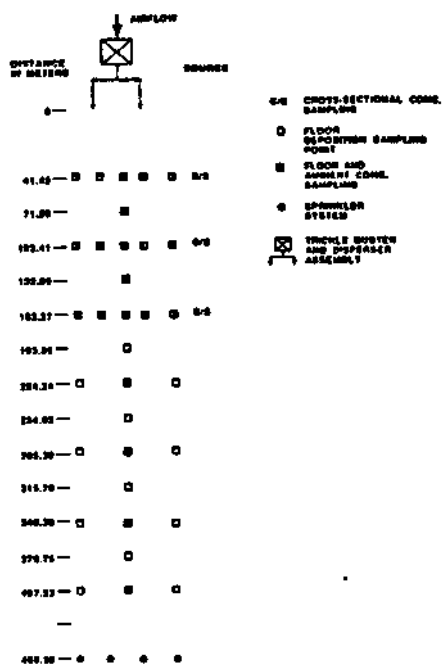


Figure 2. Ambient Concentration and Deposition Sampling Plan (Controlled Experiment 5)

The comprehensive set of data provided by these controlled experiments has enabled documentation of the behavior of dust clouds with respect to ambient concentration, deposition and size as a function of source dust characteristics and airflow conditions (Bhaskar, Ramani and Jankowski, 1986).

In-Mine Experiments: To relate the theoretical results with data from operating mines, two experiments were carried out in the return airway of working mine sections. The selection of site, data collection and analyses are similar to those outlined above for the controlled experiments. However, instantaneous concentration data were also collected using real-time aerosol monitors (RAM-1) connected to continuous data loggers (DL-331).

COMPARATIVE ANALYSES

A comparative analysis of the results obtained from the set of controlled experiments with the results of the simulation of the experimental conditions on the mathematical model was performed. Ambient concentration and floor deposition data were compared in the total and the respirable size ranges to identify areas where the model prediction and experimental observations were in agreement and where improvements to the model may be necessary. A similar but somewhat limited comparative analysis was performed for the in-mine experiments. In addition to the general comparison of the ambient concentrations and depositions, comparisons were also made between assumptions made in building certain model

components and the validity of the assumptions as revealed by the actual observations. Specifically, particle deposition rates, values of the dispersion coefficient and cross-sectional concentration of the dust were compared.

Input to Model

The inputs to the model were prepared based on the conditions under which the experiments were performed. The inputs include source dust characteristics, airway characteristics and airflow conditions.

Source Dust Characteristics: The characteristics inputted to the model are the density and the size distribution (mean size and standard deviation) of the source dust. The total amount of dust dispersed in the airway and the time duration of release were used to calculate the average release rate. Due to the high release rate of dust at the source points, a portion of the released dust settled beneath the source dispersal point before they were airborne. On the basis of the experimental data, this amount was estimated at eighteen percent. This fact is taken into account in calculating the release rate and duration of release for the model.

Mine Airway Characteristics: The inputs to the model are the height, width, length and the friction coefficient of the airway. The average of the height and width at thirteen equidistant locations along the airway was taken as the average height and width. The friction factor of the mine airway was determined from an altimeter survey.

Mine Airflow Parameters: Average velocity, temperature and viscosity of the air in the airway are required inputs to the model. The velocity and temperature were determined as the average of several measurements made during an experiment.

Experimental Conditions and Model Assumptions

Since the convection-diffusion model is only a simplified representation of the realworld dust transport phenomenon, several assumptions were made in deriving the model. Some of these assumptions were not fully satisfied in the experiments. There were also differences in the experimental conditions and the conditions incorporated in the model. In order to compare model predictions with experimental results, these differences have to be resolved. The following factors were considered important and accounted for.

- * The experimental data revealed that the average concentration over an airway cross-section is approximately 75% of the concentration in the center of the airway. The model assumes equal concentration over an airway cross-section. The experimental data used for comparison with the model output was obtained from the center of the airway. As such, the experimental centerline data was multiplied by a factor of 0.75, and then compared with the model output.
- * Floor deposition data from the experiments indicated maximum deposition in the center of the airway while decreasing deposition

towards the sides. The model assumes equal deposition over an airway cross-section. As such, prior to comparison, each experimental centerline deposition data was adjusted by a factor representing the ratio of the average deposition to center value for the station and experiment.

- * Every effort was made to ensure isokinetic sampling of dust. However, there were deviations from isokinetic sampling. The experimental data was adjusted to account for this deviation.
- * In the experiments, dust was dispersed at four points, one in the center of each of the four quadrants of the airway cross-section. This experimental procedure resulted in a less than complete mixing for some distance from the source. It was, however, seen that complete mixing of the dispersed dust with the air was achieved by the second station from the source. The model assumes an ideal dispersion, i.e., dust is released at an infinite number of points in the cross-section.
- * The comparison of in-mine experimental results with model predictions for similar conditions is difficult. Problems in developing model input arise from the fact that the source dust characteristics could not be adequately described. Therefore, in the input data preparation for the in-mine experiments, the first station located 30 meters from the source was used as the artificial source location. In addition, the mean size and size distribution of the dust collected at the first station are used to describe the source dust. The rest of the input data were prepared in the same manner as for the controlled experiments.

RESULTS

Ambient Concentration

The experimental results and corresponding model output for ambient total concentration are shown in Figures 3 and 4 for experiments employing the lowest 0.838 m/s (experiment 2), and highest velocity 1.855 m/s (experiment 4). The comparison for the lowest velocity experiment show good correlation between predictions and experimental data. The deviation between predicted values and experimental results are higher at the first measuring station. It appears that much of this is due to the fact that experimentally determined floor deposition rates per unit concentration are much higher than theoretically predicted deposition rates per unit concentration. The model predicted concentration is in better agreement with experimental data after the second station.

The predicted respirable concentration appear to be closer to the experimental value at the first few stations. As one moves away from the source, the deviations between predicted value and experimental data increase, with the model underpredicting the concentration.

The comparative analysis for experiment 4 is similar, where the predicted respirable

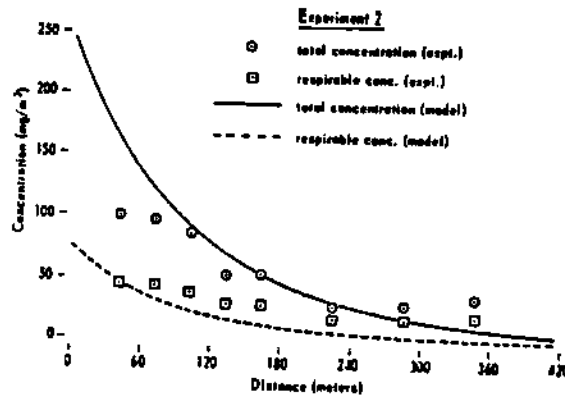


Figure 3. Comparison of Model Predicted Concentration With Experimental Data (Controlled Experiment 2)

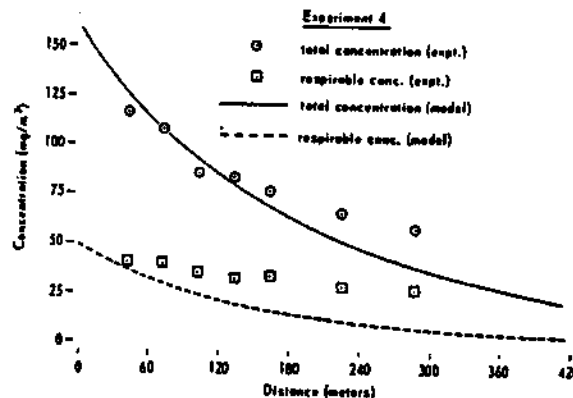


Figure 4. Comparison of Model Predicted Concentration With Experimental Data (Controlled Experiment 4)

concentration is lower than the experimental data, with the difference increasing with distance. The results of the analysis for other experiments are similar. However, there is no consistent underprediction or overprediction bias between the predicted concentration compared with experimental data.

The in-mine concentration data and model predicted concentration for similar conditions are presented in Figures 5 and 6. The ambient concentration at various stations are presented as a ratio of the concentration at station 2, since the data at station 1 was disrupted by high auxiliary fan velocity. There is some agreement between experimental data and model output for the first few stations. However, there is an increasing divergence between the two sets of data with increasing distance. In both the tests, the observed airborne concentration changes very little after 250 meters. The model however continues to predict a declining concentration, i.e., according to the model, the airborne dust cloud continues to be depleted of dust due to deposition.

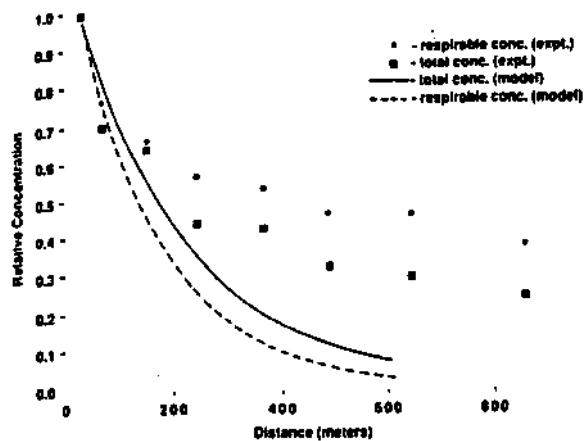


Figure 5. Comparison of Model Predicted Concentration With Experimental Data (In-mine Experiment 1)

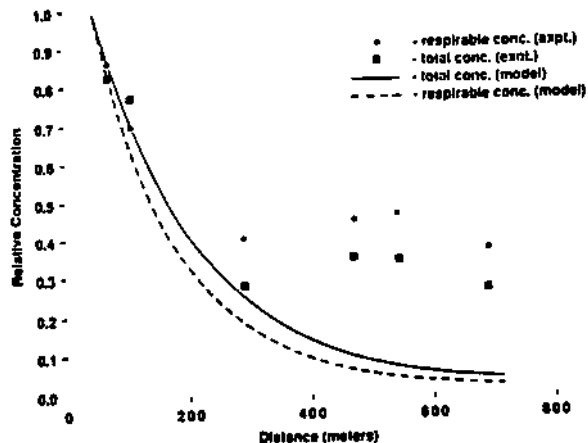


Figure 6. Comparison of Model Predicted Concentration With Experimental Data (In-mine Experiment 2)

Deposition

The floor deposition data is shown in Figures 7 and 8 for the experiments employing the lowest (0.838 m/s) (experiment 2) and highest (1.835 m/s) (experiment 4) velocities respectively. Superposed on these figures are the corresponding model predicted depositions. The data show good agreement between model predicted and experimental values of total deposition, especially at the first few stations. The respirable deposition also appears to be well predicted.

The predicted values appear to be better correlated with observed values at the lower velocity. However, the deposition data for experiment 4 show a consistent underprediction

of the total deposition by the model, when compared with the experimental data. The difference between the two values decreases with distance. The predictions for the respirable size range also appear to be lower than the experimental data. For the other four experiments, the differences between predicted and experimental values are more similar to those in experiment 2.

No deposition data could be collected for in-mine experiment 1 because of soggy floor conditions. Comparison of the observed and model predicted deposition data for in-mine experiment 2 (Figure 9) show that the model predicts a higher deposition rate than the experimental data in the first 300m and lower deposition rate after that. In fact, the experimental deposition data show a leveling off in deposition after about 300 m (1000 ft).

Deposition Rate

The deposition rate, calculated as the amount deposited per unit area, per unit time, at a station to the concentration at that station was determined for all the experiments. The average of the deposition rates at all stations for each size in each experiment calculated from the

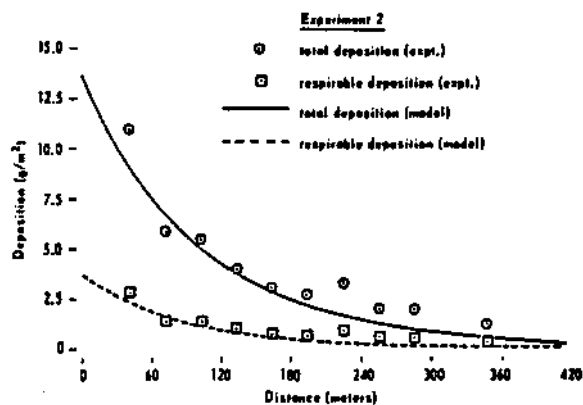


Figure 7. Comparison of Model Predicted Floor Deposition With Experimental Data (Controlled Experiment 2)

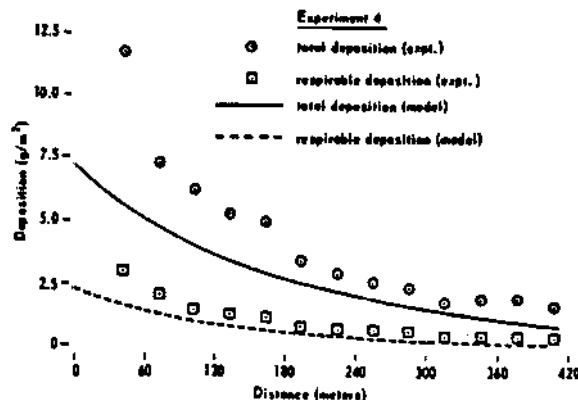


Figure 8. Comparison of Model Predicted Floor Deposition With Experimental Data (Controlled Experiment 4)

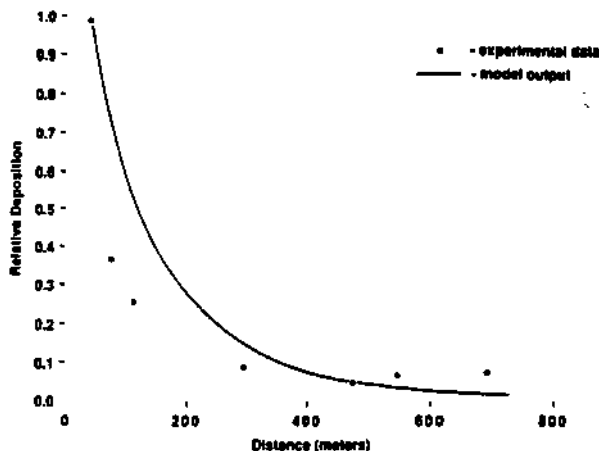


Figure 9. Comparison of Model Predicted With Experimental Data (In-mine Experiment 2)

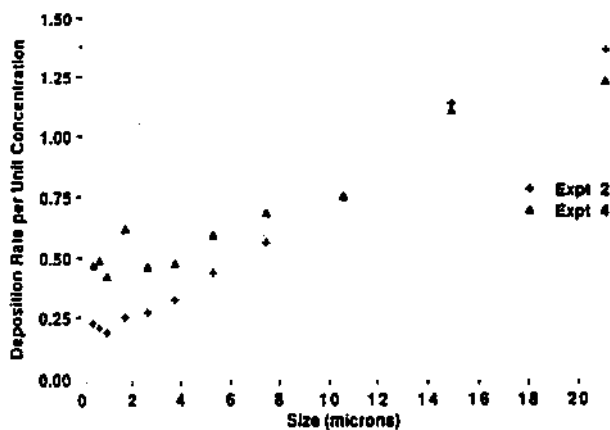


Figure 10. Deposition Rates for Various Particle Sizes

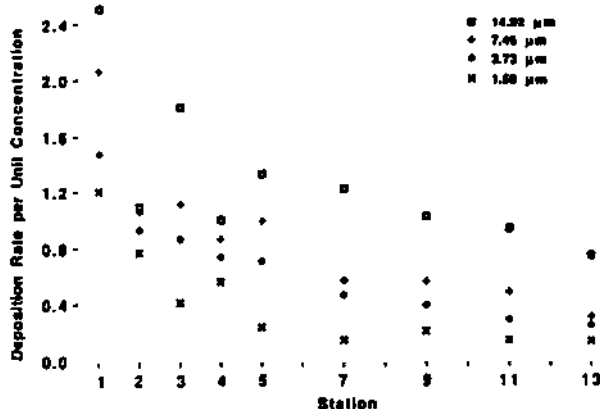


Figure 11. Variation in Deposition Rate With Distance From Source (Controlled Experiment 5)

model output is presented in Table 1. For experiments 1 and 2, which were conducted at low velocities of flow, the data show an increase in deposition rate up to 2.63 microns and is followed by a decrease in the 5.02 to 7.10 micron size interval indicating a possible transition from turbulent deposition to an increasingly gravity dominated one. At higher flow rates (experiment 3 and 4), the deposition rate shows a gradual decrease up to 7-10 micron range, and then shows an increase. Turbulent deposition mechanisms, in conjunction with sedimentation, may be causing this behavior. For the larger particle sizes, gravity dominates the deposition rate, with the 21.1 micron size class having the largest deposition rate. In the large size classes where gravity is the dominant deposition factor, the deposition rates for semi-anthracite and bituminous coal are in the same ratios as their specific gravities.

The effect of velocity on deposition rates in the various particle sizes is obvious in the smaller sizes where turbulent deposition is the dominant deposition mechanism. At low velocities (0.838 m/s), the deposition rate for semi-anthracite in the 0.63 micron class is 0.275 mg/m²/min while the rate goes up to 0.976 mg/m²/min for 1.525 m/s and to 1.187 mg/m²/min for 1.855 m/s. In contrast, for the largest size class (21.1 microns), the effect is negligible primarily because gravity induced deposition rate is independent of flow velocity. The deposition rate from experimental data was calculated for various particle size classes using the size distribution data. The results are presented in Table 2. The data show that, in general, the deposition rate decreases with the increase in size from 0.43 to 1.69 microns. Thereafter, the deposition rate increases with the increase in size. The model calculated deposition rate shows the minimum deposition rate occurring in the 5 to 7 micron range. The model predicted rates for the largest size, 21.1 microns, is lower than that obtained experimentally. The results for the lowest velocity (experiment 2) and the highest velocity (experiment 4) experiments are graphically presented in Figures 10. As expected, a steady increase in deposition rate with increase in particle size is noticed. However, particles less than 2 microns tend to behave differently from particles in other sizes. This probably occurs due to the increased action of coagulation or turbulent deposition. From Table 2, for experiments 1 and 5, it appears that 21.1 micron particles have a lower deposition rate than 14.92 micron particles. The data however is suspect, because only a small fraction of the dust (5%) is in the 21.1 micron range.

Experimental deposition rates for selected size class particles at various measuring stations along the airway are presented in Figure 11 for experiment 5. In general, the deposition rate is maximum at the first station, gradually decreasing with distance from the source. This occurs across all experiments and particle sizes. It must be noted that the size distribution of deposited dust is determined by a procedure which involves using an ultrasonic bath to deagglomerate the particles. In

DUST FLOWS IN MINE AIRWAYS

Table 1. Model Predicted Deposition Rates

Experiment No.	1	2	3	4	5	6
Particle Diameter (µm) (Projected Area)						
0.66	0.27	0.25	1.19	1.19	0.98	0.98
1.01	0.54	0.54	1.19	1.19	0.98	0.98
1.69	0.54	0.54	1.00	1.04	0.94	0.97
2.63	0.55	0.55	0.70	0.74	0.69	0.72
3.73	0.48	0.49	0.52	0.55	0.52	0.54
5.27	0.39	0.40	0.40	0.42	0.40	0.42
7.46	0.34	0.35	0.35	0.35	0.35	0.35
10.65	0.36	0.35	0.36	0.38	0.38	0.35
14.92	0.50	0.46	0.50	0.46	0.50	0.46
21.1	0.83	0.76	0.83	0.76	0.83	0.76

*Deposition in (mg/m²/min)/(mg/m³)

Table 2. Experimentally Determined Deposition Rates

Size (µm)	Deposition Rate					
	Exp. 1	Exp. 2	Exp. 3	Exp. 4	Exp. 5	Exp. 6
0.43	0.52	0.23	0.26	0.47	0.52	0.21
0.66	0.45	0.21	0.48	0.48	0.65	0.24
1.01	0.38	0.19	1.05	0.42	0.53	0.26
1.69	0.30	0.28	0.31	0.62	0.42	0.33
2.63	0.37	0.27	0.92	0.46	0.59	0.36
3.73	0.40	0.33	1.03	0.47	0.68	0.30
5.27	0.49	0.43	1.02	0.59	0.81	0.49
7.46	0.54	0.55	1.12	0.68	0.89	0.56
10.65	0.63	0.74	1.06	0.75	0.98	0.67
14.92	1.01	1.13	1.12	1.10	1.29	0.98
21.1	0.89	1.36	1.16	1.23	0.91	1.06

*Deposition rates are expressed as mg/m²/min per unit concentration (mg/m³).

practice, particles agglomerating to other particles will appear in a different and higher size range. Therefore, there can be a difference between the size distribution of the settling dust and the measured distribution. Since deposition rate decreases with distance from the source, and concentration decreases with distance, it may be that concentration and/or agglomeration is a major factor in affecting deposition by dynamically changing the size distribution during flow.

Cross-Sectional Concentration

During the experiments, the ambient concentration over the cross-section of the mine airway was measured at three equidistant stations along the airway. Twelve sampling points were established in a regular grid at each station. In addition, a sampling point was established at the center of the grid. The data show that, on the average, concentration of dust increases from the roof to the floor. Also, the equal-weighted average cross-sectional concentration using data from all the experiments is approximately 75% of the concentration in the center of the mine airway.

Dispersion Coefficient

Dispersion can have significant effects on the behavior of fine particles in air, especially deposition, for which reduction in dispersion increases the amount of dust deposited close to the source. Although the in-mine experiments were not designed for accurate determination of dispersion coefficient, these were calculated from the data. The experimental value varied from 11.79 to 45.06 m²/s for the same experiment. The experimental data are in the same order of magnitude as the model assumed value.

DISCUSSION

Two kinds of comparative analyses were performed with the experimental and model predicted data. In the first analyses, history matching of the concentration and deposition data was used to evaluate the appropriateness of

the model. However, due to the non-linear nature of some of the mechanisms incorporated in model components, limited comparisons of the experimental data and model performance on these components were made. The following conclusions are drawn from this study.

- (1) Deposition phenomenon, both in the total and respirable ranges, is well predicted by the model in almost all the controlled experiments especially at distances beyond 100 meters. This is probably due to the quality of deposition data collected in the experiments, as well as the adequacy of the deposition functions in the mathematical model. The data for stations close to the source tend to be distorted due to uneven mixing of dust. The model tends to compare well with experimental results collected at lower velocities than at higher air flow rates.
- (2) Concentration data comparison show that the model tends to predict better at lower flow velocities than at higher velocities. Also, total concentration appears to be better predicted than respirable concentration. The difference between the model predictions and experimental results for total concentration is primarily due to the differences between predicted and experimental respirable concentrations. If the respirable concentration were modeled more accurately then the model predictions for the overall size would have been better. Among the probable causes for this difference are (1) variation in deposition rate with concentration, (2) variation between model predicted and actual coagulation and (3) particle reentrainment. Particle reentrainment has not been included in the model.
- (3) The cross-sectional data collected from the experiments show that there exists a variation in dust

concentration in a mine airway cross-section. The concentration of dust increases from the roof to the floor. The average concentration of dust is approximately 75% of the concentration in the center of the airway.

- (4) From the experimental results, it appears that the deposition rate may be function of concentration. At higher concentrations near the source, the deposition rate is high, which results in large amounts of particles being deposited close to the source. The deposition rate tends to achieve a fairly uniform value away from the source. This behavior is noticed for all particle sizes.
- (5) The in-mine data show that respirable dust continues to be airborne for several hundred meters from the source. Therefore, while there is a rapid decrease of dust concentration near the source, the dust does not completely settle out even in the 900 meters of the airway and the concentration assumes an asymptotic form. In the model results, the concentration continues to show a decrease with distance.
- (6) No definite statement can be made about the value of the coefficient from the in-mine experiments due to both the very limited amount and coarseness of data. The dispersion coefficient calculation is sensitive to the concentration variation with time at a point, peak concentrations and flow velocity. The experimental values ranged from 11 to 45 m²/s while the model assumed value was approximately 60 m²/s.
- (7) The study is of practical importance when considering recirculation of mine air for ventilation purposes. The heavier particles in the recirculated air will deposit along the recirculation path, while the recirculated air may contain less dust in terms of mass but a higher percent of fines.

The comparative analyses have shown that, in general, the floor deposition part of the model is better correlated with experimental data, while the ambient concentration is better predicted at lower flow velocities. The analyses, however, indicate areas that need additional experimental and modeling studies. For example, experimental results at the first few stations may be subject to error due to inadequate mixing at the source. However, the divergence between the experimental and modeled respirable concentration data at distances further from the source maybe due to some phenomena which may not have been incorporated in the model. Clearly, the respirable portion of the model needs critical examination, especially at higher flow velocities.

ACKNOWLEDGEMENTS

The work reported here is a part of an ongoing research project in the Generic Mineral Technology Center for Respirable Dust at The Pennsylvania State University. The Center is supported by Grant No.G1135142 from the US Bureau of Mines. Support and assistance from USBM and The Pennsylvania State University are appreciated.

REFERENCES

- Bhaskar, R., R.V. Ramani and R.A. Jankowski, 1986, "Experimental Studies of Dust Dispersion in Mine Atmospheres", SME Preprint 86-140, accepted for Mining Engineering/SME Transactions, (In print).
- Bhaskar, R. and R.V. Ramani, 1986, "Behavior of Dust Clouds in Mine Airways", SME Transactions, Vol. 280, pp. 2051 - 2059.
- Bradshaw, F., and A.L. Godbert, 1954, "The Deposition of Dust in Return Airways," SMRE Research Report No. 92, 37 p.
- Chung, H.S., 1981, "Coagulation Processes for Fine Particles," Ph.D. Thesis, The Pennsylvania State University, University Park, Pa. 253 p.
- Courtney, W.C., Kost, J., and Colinet, J., 1982, "Dust Deposition in Coal Mines Airways," USBM Technical Progress Report TPR 116, 15p.
- Dawes, J.G., and Slack, A., 1954, "Deposition of Airborne Dust in a Wind Tunnel," SMRE Research Report No. 105, 41 p.
- Ford, V.H.W., 1971, "Experimental Investigations Into the Dispersion and Transport of Respirable Dust in Mechanized Coal Mining," Ph.D. Thesis, University of Newcastle upon Tyne, 233 p.
- Hall, D.A., 1955-56, "Factor Affecting Airborne Dust Concentrations with Special Reference to the Effect of Ventilation," Trans. Inst. of Min. Eng., Vol.115, pp. 245-269.
- Hodkinson, J.R., 1957-58, "The Mixing of Respirable Dust with the Mine Ventilation Studied by a Radio-active Tracer Technique," Trans. Inst. of Min. Engr. Vol. 117, pp. 223-244.
- Hwang, C.C., Geiger, G.E., and Radulovic, P., 1972, "Dust Concentration Simulator for Mine Ventilation Systems for Coal Mines," NTIS PB 213833, pp. 187-230.
- Liu, B.Y.H., and Agarwal, J.K., 1974, "Experimental Observation of Aerosol Deposition," Journal of Aerosol Science, Vol.5, No.2, pp. 145-155.

DUST FLOWS IN MINE AIRWAYS

- Pereles, E.C., 1958, "Theory of Dust Deposition from Turbulent Airstreams by Several Mechanisms," SMRE Research Report No.144, 34 p.
- Ramsni, R.V., 1983, "Prediction of Ambient Dust Concentration in Mine Atmospheres," a project proposal to The Generic Mineral Technology Center for Respirable Dust, The Pennsylvania State University, 4 p.
- Skobunov, V.V., 1973, "Turbulent Transport Coefficients for Mine Workings and Tunnels", Soviet Mining Science, Vol. 9, No. 4, pp. 402-412.
- Wood, N.B., 1981a, "The Mass Transfer of Particles and Acid Vapor to Cooled Surfaces," Journal of the Institute of Energy, June 1981, pp. 76-93.
- Wood, N.B., 1981b, "Calculation of Turbulent Deposition to Smooth and Rough Surfaces," Journal of Aerosol Science, Vol.12, No.3, pp. 275-290.

Experimental Studies on Dust Dispersion in Mine Airways

R. Bhaskar¹, R.V. Ramani¹, and R.A. Jankowski²

¹Department of Mineral Engineering, The Pennsylvania State University

²U.S. Bureau of Mines, Pittsburgh, Pa.

Abstract — *The spatial distribution of airborne dusts, deposition of dust in the airway, as well as the effect of airflow velocity and particle density on dust behavior in mine airways were studied in a set of experiments performed in a mine airway under controlled conditions. Considerable deposition of dust near the source was indicated. Pronounced effects due to velocity were observed in ambient dust concentration and deposition along the mine airway, both in the respirable and the total size ranges. Cross-sectional concentration measurements indicate an increase in concentration from the roof to the floor. The average cross-sectional concentration is about 75% of the concentration in the center of the airway.*

Introduction

A number of studies have been performed since the early 1950s on the behavior of dust in mine air (Bradshaw and Godbert, 1954; Dawes and Slack, 1954; Bradshaw et al., 1954; Hall, 1955-56; Reinhardt, 1971; Ford, 1971; Courtney et al., 1982). While the experimental data available from these studies are indeed useful in understanding dust cloud behavior in a specific situation, no generalized conclusions can be drawn because of the lack of data on parameters such as flow velocity, size distribution of the source dust, and particle density. These change from mine to mine or even within the same mine. The present study is aimed at providing a better understanding of the temporal and spatial behavior of dust particles in underground mine airways (National Academy of

Sciences, 1980). The characteristics studied encompassed airborne concentrations and floor deposition over the entire size range as well as the respirable size range. The experimental results in this paper are intended to complement a mathematical model developed to predict ambient concentration and deposition of airborne dust in mine airways (Bhaskar and Ramani, 1986).

Experimental design

The experiments were designed to simulate dust transportation and deposition in mines. They were performed in the D-drift at the Lake Lynn Laboratory of the US Bureau of Mines. Comprehensive description of this experimental mine can be found in Mattes et al. (1983). The drift has a cross section of 2.1 x 6.1 m (7 x 20 ft) and a length of 507 m (1663 ft). About 400 m (1312 ft) of the drift was used in the experiment. In all, 8 experiments were conducted, with each experiment

R. Bhaskar and R.V. Ramani, members SME, are research associate and professor of mining engineering, respectively, Department of Mineral Engineering, The Pennsylvania State University, University Park, PA. R.A. Jankowski, member SME is a physical scientist with the US Bureau of Mines, Pittsburgh, PA. SME preprint 86-140, SME-AIME Annual Meeting, New Orleans, LA, March 1986. Manuscript March 1986. Discussion of this paper must be submitted, in duplicate, prior to May 31, 1986.

DUST DISPERSION IN MINE AIRWAYS

differing from the others either in the type of dust dispersed or in the velocity of the air in the drift. The experiments are coded as follows:

	Dust Type	Velocity, m/s
Experiment 1	Semianthracite	0.838
Experiment 2	Bituminous	0.838
Experiment 3	Semianthracite	1.855
Experiment 4	Bituminous	1.855
Experiment 5	Semianthracite	1.525
Experiment 6	Bituminous	1.525

For each experiment, 10 to 13 measuring stations were set up, each 30.5 m (100 ft) apart (Fig. 1). The spacing between measuring stations was selected to utilize the maximum possible length of the drift for the experiment. The experiments were designed to provide data for studying:

- variations in ambient concentration (both total and respirable size range) along the length of a typical airway,
- variations in deposition of the dust (both total and respirable size range) along the airway,
- changes in the size distribution of the airborne dust as the cloud travels along the length of the airway,
- variations in dust concentration at various cross sections of an airway, and
- relationship between the average cross-sectional concentration and that in the center of the airway.

Sampling procedures

Sampling procedures were developed for collecting airborne concentration and floor deposition data.

Ambient concentration sampling

Two types of ambient concentration sampling were performed: sampling of air at the center of the airway and cross-sectional sampling. In each experiment, three measuring stations were selected for detailed cross-sectional sampling. At each cross section, 12 points following the equal area representation method were delineated, and personal gravimetric samplers were set up at these points (Fig. 2). These 12 sampling points were in addition to the sampling point in the center of the cross section.

Isokinetic sampling: To ensure isokinetic sampling under experimental conditions, specially shaped sharp-edged nozzles were designed and fabricated for use with conventional two-piece personal sampling units to reduce disturbance to the airflow at the point of sampling. By adjusting the pumping rate of the sampling unit, the velocity of the air through the nozzle was matched with the velocity in the airway. This procedure ensures that a representative sample of the mine air concentration is obtained in the cassette. Analysis of the data obtained from the experiments with the Belyeav and Levin (1974) corrections for isokinetic sampling indicated very little correction of gravimetric data for the size distribution of the dusts used in these experiments. If the experiments were performed in calm air, considerable correction would have been required.

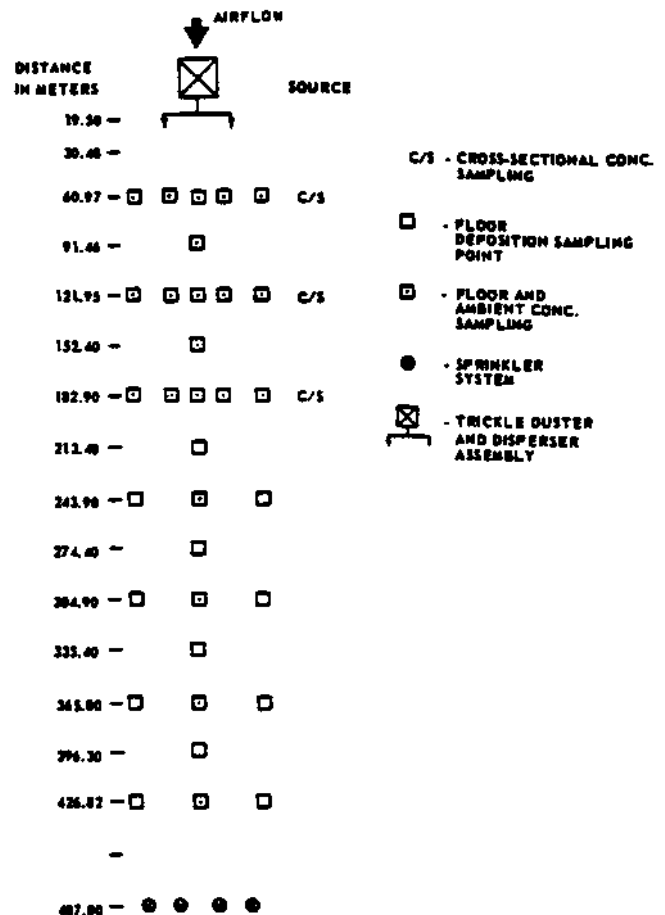


Fig. 1 — Schematic of the airway showing locations of the sampling points (experiment 6)

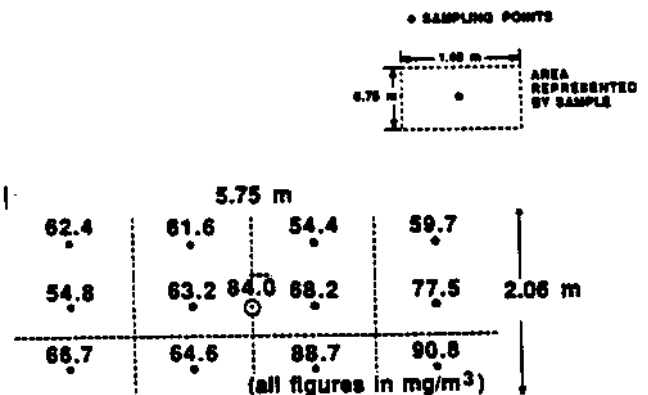


Fig. 2 — Cross-sectional ambient concentration sampling plan

To reduce the amount of dust deposited on the inner surface of the tube connecting the nozzle to the cassette, the tube was kept as short as possible. However, the tube was long enough to keep the sampling assembly from interfering with the airflow at the nozzle. The amount of dust deposited on the inner surface of the connector tube was determined and added to the filter weights.

*The use of specific brand names of products is for illustrative purposes only. This does not imply endorsement by the US Bureau of Mines or The Pennsylvania State University.

Filters: For this study, Nuclepore* filters were considered most suitable for sampling purposes, as the deposited dust would be subjected to gravimetric and size analyses. Compared to conventional filters, Nuclepore filters have a smooth surface, good control of pore sizes, and are nonhygroscopic. These filters also have a lower and more uniform weight but similar flow rate/pressure drop characteristics.

Pumps: Constant-volume flow pumps (MSA Fixt Flo and DuPont 2500 series) were used to ensure that pumping rate did not vary with filter loading.

Deposition

Deposition plates were placed at the measuring stations along the airway. To ensure that the amount deposited was comparable to that on the floor, flat plates without any lips were used. The absence of lips reduces the formation of eddies near the deposition sampling area. The flat plates were covered with "sharkskin" filter papers, which do not tear easily during sample handling. The rough texture and extremely light weight of the paper (about 2 g, or 0.07 oz, for a 29-cm, or 11-in., diam paper) make it ideally suited for gravimetric analysis.

Dust source

Dust generation

The dust was dispersed by a fluidized bed-type trickle duster through a specially designed system of 25-mm (1-in.) diam plastic tubes to four release points in a cross section. The location of the source in the airway (Fig. 1) was dictated by the need to ensure that at the point of release, the airflow is uniform, and that there is good mixing of dust with the air in the drift before the first sampling point.

Source dust

Two types of dusts (semianthracite and bituminous) were used in the experiments. The size distributions of the two source dusts (Table 1) show a significant proportion of respirable dust. The densities of the semianthracite and bituminous dusts were 1.567 and 1.4 g/m³, respectively.

Table 1 — Cumulative Size Distribution of Source Dust

Size* (microns)	Semianthracite (% finer)	Bituminous (% finer)
29.85	100.0	100.0
21.1	100.0	98.0
14.92	94.8	88.0
10.55	86.2	64.0
7.48	73.0	45.8
5.27	53.8	31.8
3.73	38.1	20.5
2.63	21.8	12.7
1.89	12.1	7.4
1.01	5.7	3.5
0.66	2.0	1.3
0.43	0.8	0.2
0.34	0.2	0.0

* Size analyses performed on Microtrac SPA.

Sample analysis

The cassettes from the personal gravimetric samplers and the deposition plates were processed at the dust laboratory at The Pennsylvania State University. The mass of dust was measured using a Mettler electronic microbalance. All size distributions were determined using an X-ray diffraction device (Microtrac small particle analyzer) capable of measuring dust in the 42.21- to 0.17-micron range.

Results

Several analyses were performed on the experimental data. The results of the following analyses are presented:

- ambient concentration characteristics of the dust cloud in the drift,
- deposition decay curves of the dust cloud,
- effect of velocity on ambient concentration and deposition patterns,
- cross-sectional sampling results, and
- variation in size distribution as the dust cloud traverses the drift and the relation between the velocity of airflow and size distribution of the dust at any point.

Ambient concentration

The ambient total concentration and ambient respirable concentration of dust along the length of the airway for experiments 1 and 6 are shown in Fig. 3. The respirable concentration is obtained from a size analysis of the total concentration dust. Particles less than 5.27 μm in projected area diameter are taken as respirable. This translates to slightly less than 5 μm aerodynamic diameter. In all the six experiments, ambient total concentrations decrease with distance faster than respirable concentrations, indicating longer residence times in the airflow for smaller particles. The rates of decrease in the concentrations, both total and respirable, are higher in the first 60 m (197 ft) than at greater distances from the source. Also, with distance, the total concentration curves tend toward the respirable concentration curves, showing that most of the larger particles are deposited in the initial portions of the airway.

Deposition

Depositions as a function of distance from the source for experiments 1 and 6 are shown in Fig. 4. As one moves away from the source, the total deposition curve approaches the respirable deposition curve, indicating a high proportion of respirable dust in the ambient air. At stations further from the source, both the curves assume an asymptotic form, indicating little change in deposition.

Effect of velocity on concentration and deposition patterns

The concentration and deposition results from experiments 2, 4, and 6 (bituminous dust at three different velocities) are presented in Figs. 5 and 6. The concentration data were normalized with respective

DUST DISPERSION IN MINE AIRWAYS

concentrations at the first point and expressed as a fraction of those at the first point. With the increase in velocity, the ambient concentration of total dust (Fig. 5) is more even along the airway, a trend that is also seen in the respirable size range (Fig. 6). At velocities of 1.525 and 1.855 m/s (5 and 6.1 fps), concentration curves approach a limit value after some distance from the source, indicating little deposition after that distance. In Figs. 5 and 6, this distance is about 290 m (950 ft). The effect of velocity on total and respirable dust deposition is shown in Figs. 7 and 8, respectively. Again, the curves tend to be flatter at higher velocities though the effects of velocity on depositions is not as dramatic as on ambient concentrations.

Cross-sectional sampling

Data from 18 cross-sectional concentration sampling setups (three cross-sectional sampling stations per experiment and six experiments) show that the average concentration across the cross section is 75% of the concentration at the center of the airway, with all the points in the cross section given equal weight. However, the concentration increases as one moves down from the roof to the floor. Specifically, for the consolidated data, the top third of the airway has a concentration 72% of that in the lower third. The concentration in the middle third of the airway is 89% of that in the lower third. An example of the cross-section data is shown in Fig. 2.

Variation in size distribution

The change in size distribution of the dust cloud as it traverses the airway is shown in Fig. 9. The data is from experiment 1. Similar analyses were performed for all the experiments. A distinct decrease in the larger-sized particles is indicated by a corresponding shift in the peaks for the 61-, 244-, and 366-m (200-, 800-, and 1200-ft) station ambient concentrations. The change in the shape of the curves in the smaller size range is less compared to that for the larger size. This complements the ambient concentration and deposition data, which show that smaller particles (respirable range) have a reduced rate of deposition.

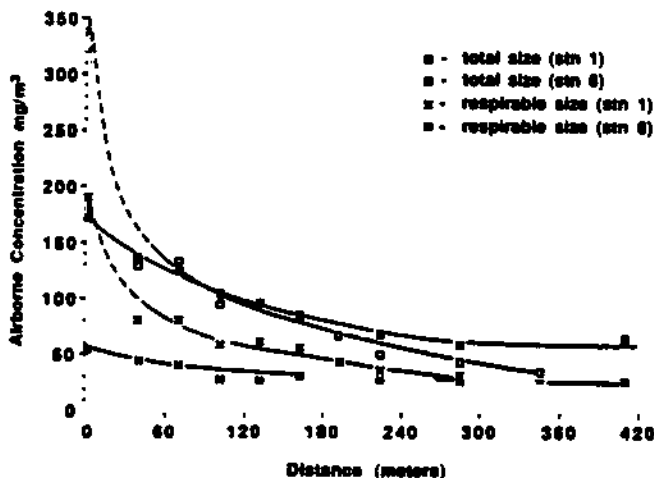


Fig. 3 — Concentration of airborne dust along airway

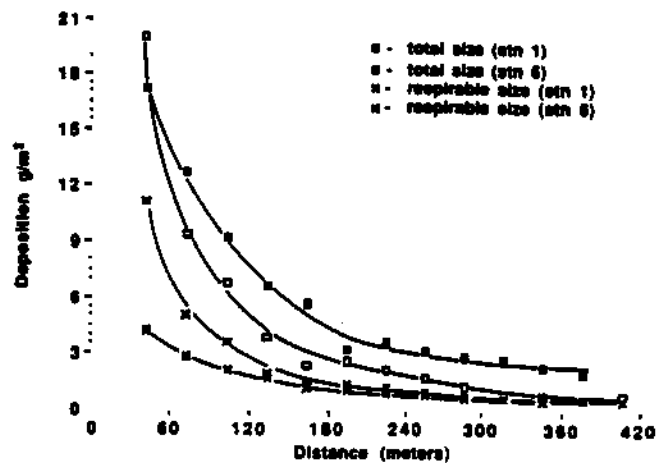


Fig. 4 — Deposition of airborne dust along airway

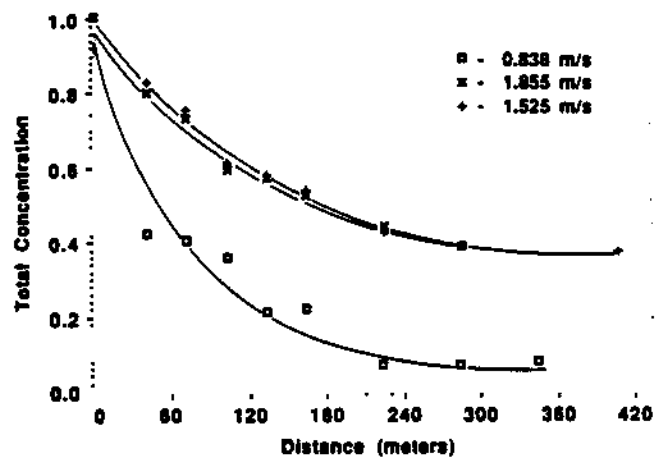


Fig. 5 — Effect of velocity on total airborne concentration (concentration normalized with respect to source concentration)

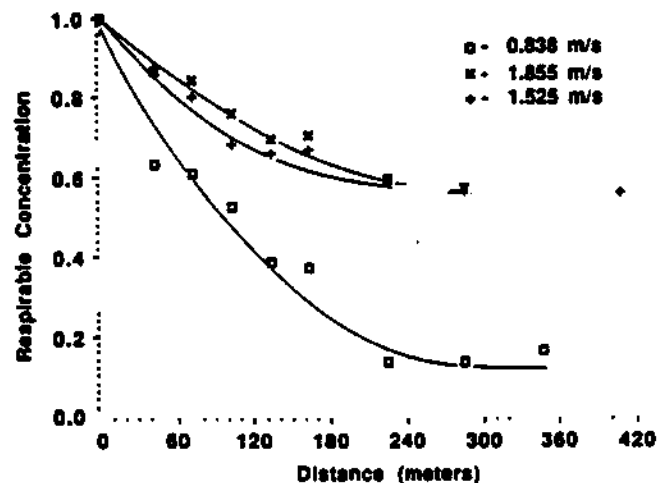


Fig. 6 — Effect of velocity on respirable airborne concentration (concentration normalized with respect to source concentration)

THE RESPIRABLE DUST CENTER

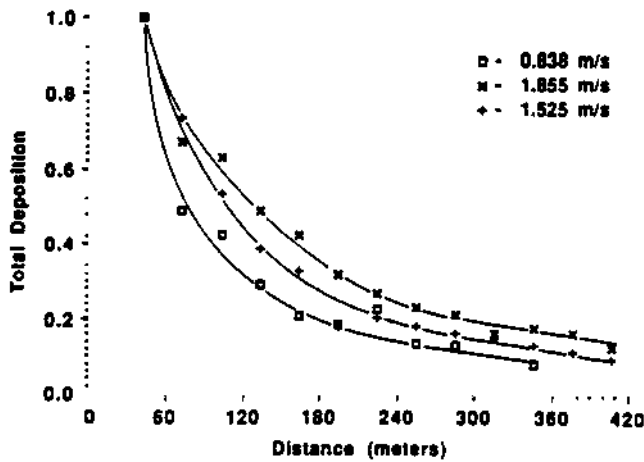


Fig. 7 — Effect of velocity on deposition (total size) (deposition normalized with respect to first sampling station)

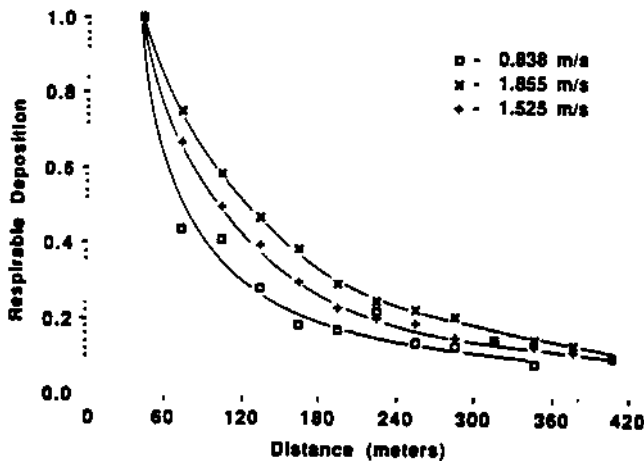


Fig. 8 — Effect of velocity on deposition (respirable size) (deposition normalized with respect to first sampling station)

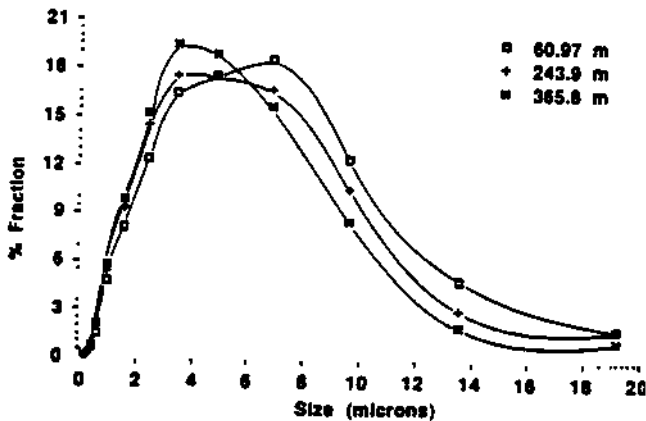


Fig. 9 — Change in size distribution of airborne dust with distance from source (experiment 1)

The size distributions of the dust clouds for 0.838, 1.855, and 1.525 m/s (2.75, 6, and 5 fps) measured at the 366-m (1200-ft) station are shown in Fig. 10. The data here is also from experiment 1. At the lower velocities a comparatively less amount of large-sized particles is found. As the velocity increases, larger particles are carried longer distances and, therefore, contribute to a higher concentration of large-sized particles down stream. Therefore, the peaks of the distributions tend to be flatter at high velocities. Again, the effect of velocity on the distribution for the smaller sizes is less noticeable.

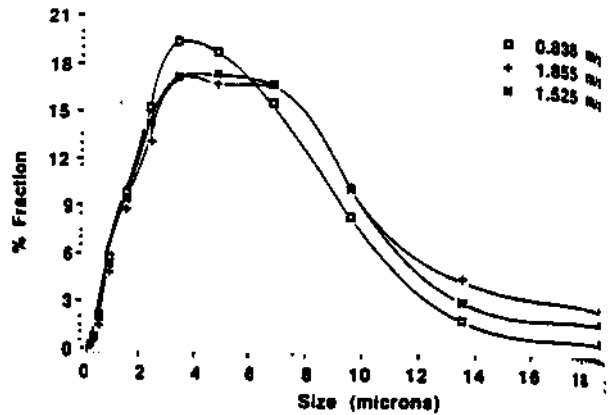


Fig. 10 — Size distribution at 365.8-m station at different velocities (experiment 1)

Discussion

The data from the ambient concentration-deposition experiments have enabled quantification of the spatial behavior of airborne dust clouds in mine airways — the decay patterns for ambient total concentration, ambient respirable concentration, and deposition. Experimental studies such as the one presented here are not without problems. For example, some deposition of extremely fine particles was noted on the sides of the airway. In some deposition plates, small pieces of falling roof rock caused distortion in values. Considering the fact that a large number of deposition data were collected, no systematic error contribution from the falling particles was noticed.

Errors in the ambient concentration data can result from variations in pump rate during the experiment as well as calibration, deviation from isokinetic sampling principles, and static charge effect during weighing. Pumps calibration errors of $\pm 10\%$ may occur. During the correction of concentration data for non-isokineticity, a correction of $+8\%$ to -11% was necessary for a few samples. However, no major errors were found in the concentration data, lending credence to the validity of the experimental design, sampling procedures, and sample analyses techniques. ■

Acknowledgments

The cooperation of the staff of the Ventilation Group, Pittsburgh Research Center, US Bureau of Mines, the staff at the Lake Lynn Laboratory, and the Department of Mineral Engineering is gratefully acknowledged.

The research reported in this paper was supported under the Mineral Institutes Program by Grant No. G1135142 from the Bureau of Mines, US Department of the Interior, as part of the Generic Mineral Technology Center for Respirable Dust at The Pennsylvania State University.

References

- Belyaev, S.P., and Levin, L.M., 1974, "Techniques for Collection of Representative Aerosol Samples," *Journal of Aerosol Sciences*, Vol. 5, No. 4, pp. 325-336.
- Bhaakar, R., and Ramani, R.V., 1966, "Behavior of Dust Clouds in Mine Airways," *Trans. SME-AIME*, Vol. 280, pp. 2051-2059.
- Bradshaw, F., and Godbert, A.L., 1954, "The Deposition of Dust in Return Airways," Research Report No. 92, SMRE, p. 37.
- Bradshaw, F., Godbert, A.L., and Leach, E., 1954, "The Deposition of Dust Conveyor Roads," Research Report No. 106, SMRE, p. 62.
- Courtney, W.G., Kost, J., and Colinet, J., 1962, "Dust Deposition in Coal Mine Airways," Technical Progress Report 116, US Bureau of Mines.
- Daws, J.G., and Slack, A., 1954, "Deposition of Airborne Dust in a Wind Tunnel," (Interim Report) Research Report No. 105, SMRE.
- Ford, V.H.W., 1971, "Experimental Investigations into the Dispersion and Transport of Respirable Dust in Mechanised Coal Mining," PhD Thesis, University of Newcastle Upon Tyne, June.
- Hall, D.A., 1955-56, "Factors Affecting Airborne Dust Concentrations with Special Reference to the Effect of Ventilation," *Trans. Institution of Mining Engineers*, Vol. 115, pp. 245-269.
- Mattes, R.H., Bacho, A., and Wade, L.W., 1963, "Lake Lynn Laboratory: Construction, Physical Description, Air Capability," *BulMines I.C.* 8811, p. 40.
- National Academy of Sciences, 1960, "Measurement and Control of Respirable Dust in Mines," Report of the Committee on Measurement and Control of Respirable Dust, NMAB 363, p. 405.
- Reinhardt, M., 1971, "Untersuchungen in Strecken über das Verhalten von Staub in Grubenwettern," *Gluckauf-Forschungshefte*, Vol. 33, No. 1, pp. 19-32 ("Studies in Mine Roads on the Behavior of Dust in Air Currents," NCS Translation, A.2945/AL).

On the Transport of Airborne Dust in Mine Airways

R.V. Ramani and R. Bhaskar
Department of Mineral Engineering, The
Pennsylvania State University

One of the primary means of control of health hazards from respirable contaminants in mine atmospheres is through design and operation of mines to meet mine health and safety regulations and recommended practices. A U.S. National Academy of Sciences study concluded that for significant progress in coal mine dust control, research should be directed more toward obtaining fundamental understanding of the origin, transport and characteristics of respirable coal mine dust. Theoretical and experimental studies on transport of dust in mine airways, particularly coordinated efforts to validate theory with practice, are scarce. Some empirical models, developed on the basis of experimental data, are available but these models cannot be applied to new conditions. The purpose of this paper is to present the results of theoretical and experimental studies on the transport and deposition of dust in mine airways. This study is a part of an on-going research project in the Generic Mineral Technology Center on Respirable Dust.

In the paper, the assumptions of the modeling phase of the project and the development of a convection-diffusion equation for dust transport in mine airways will be outlined. The important aspect of the modeling effort is the capture of the deposition phenomenon. The experiments performed under controlled conditions in a typical mine airway as well as under normal mine operating conditions will be discussed. The comparison of the model predictions with experimental results will be made to identify critical areas of agreements and deviations. The implications of the findings and areas for further research and development will be identified.

ind
lev
in
thi
sam
col
pro
ana
are

the
gen
mat
con
air
to
tha
tha
bre
tha

per
to
The
res
spe
dat
ref
--
pot

U.S
(C
71.
sta
cor
is
sta
sta

On the Relationship Between Quartz in the Coal Seam and Quartz in the Airborne Respirable Coal Dust

R.V. Ramani¹, J. M. Mutmanský¹, R. Bhaskar¹, J. Qin¹ and J. Organiscak²

¹Department of Mineral Engineering, The Pennsylvania State University

²U.S. Bureau of Mines, Pittsburgh, Pa.

ABSTRACT

The results of a two-year research study into the relationship between quartz dust levels in host material and in respirable dust in continuous mining sections are presented in this paper. The experimental design and sampling procedures for underground data collection are outlined. The sample analysis procedures for quartz determination, the analysis results and conclusions of the study are discussed.

The results of the study indicate that the quartz contents of the airborne dusts are generally higher than those in the host material and bulk samples; and the quartz content increases with decreasing size of the airborne dust. The source for quartz appears to be the roof and the floor materials rather than the coal seam itself. It also appears that the material containing quartz may be breaking into a different size distribution than coal.

INTRODUCTION

Without doubt, the potential for permanent and severe health damage exists due to respirable dust in the work environment. The attention directed at the reduction of respirable airborne dust to levels below those specified in the law and the achievements to date in meeting these standards are but a reflection of the recognition by many parties — government, industry, and labor — of this potential and the need to reduce it.

The ambient dust standard in underground U.S. coal mines (2 mg/m^3) has a qualifier (Code of Federal Regulations, Title 30, Part 71.101) to determine an applicable dust standard when a respirable dust sample contains more than 5% quartz. This standard is frequently referred to as the "reduced standard." The reasoning behind the reduced standard is the relative toxicity of the

quartz dust compared to that of pure coal dust. As the quartz levels in samples increase, the applicable standards become more stringent and maintaining the workings in compliance becomes increasingly difficult.

The number of underground work locations operating under the reduced standards has shown a dramatic increase since 1980 (Figure 1). For comparison purposes, there were no mining entities operating on reduced standards prior to 1977. The emergence of this problem, which affects the health and safety standards on one hand and creates severe compliance problems on the other, has been rapid.

The search for control of quartz dust exposure in underground coal mines raises several questions as to the origin, formation, entrainment, settling behavior and transport of quartz dust. The U.S. Bureau of Mines research program, in identifying the sources of quartz in continuous miner sections, has resulted in the development of more effective operational and maintenance procedures for the machines and the ventilation systems (Jankowski and Niewiadomski, 1987). However, the results of research studies point to the need for a clearer understanding and definition of the relationships between: (i) the natural conditions such as coal seam, roof and floor characteristics, quartz occurrences, and quartz breakage functions; (ii) the operational conditions such as machines, cut plans, face ventilation plans, dust control techniques, and quartz analysis procedures; and (iii) the amount of quartz in the dust samples (Kok et al., 1985; Taylor et al., 1986). The U.S. Bureau of Mines funded a study at Penn State entitled "Fundamental Studies on the Relationship Between Quartz Dust Levels in Host Material and Respirable Dust Generated During Mining" in September 1985 to further the understanding of the relationships between quartz in the airborne dust and that in the material being cut. The two specific objectives of this research project were to:

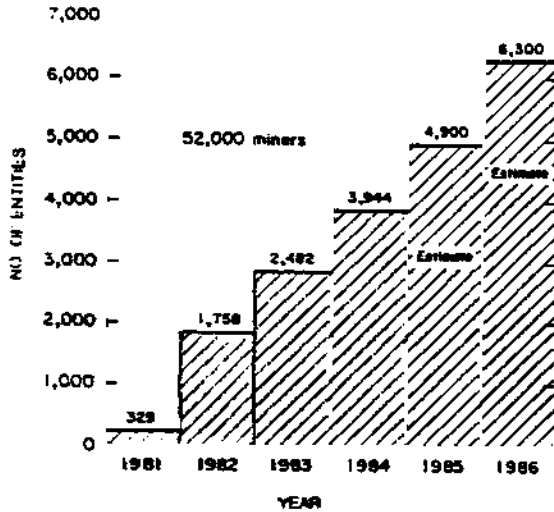


Figure 1. Number of entities placed on reduced dust standards, 1981-1986 (Ref. Jankowski et al., 1985).

- (i) study the relationship between quartz levels in the material being cut and those in the respirable dust, and
- (ii) study the relationship between types of material being cut, size consist of broken material and amount of respirable dust.

The results of the study with respect to the first objective are presented in this paper. More complete description of the study itself with complete documentation of the research design, experimental procedures and data and results can be found in the final report by Ramani et al. (1987).

EXPERIMENTAL DESIGN

This work was carried out in continuous miner development sections. There were three major tasks in the field work, viz:

- Task 1 - airborne coal mine dust sampling at several points in the mining section.
- Task 2 - channel sampling of the mining horizon at the mining face or locations close to the face.
- Task 3 - processing and sampling of ROM coal off the shuttle cars near the section feeder or feeder-breaker.

The sampling of the airborne dust is the most complicated of these tasks due to the larger number of sampling points required in the section. For better control over data and to enhance the ability to determine the relationship between the coal properties and the airborne dust properties, more extensive sampling near the continuous miner was performed during one carefully selected cut, hereafter called the selected cut. A generalized version of the sampling plan for airborne dust is illustrated in Figure 2.

Four mines were chosen for the field data collection. For each selected cut, the

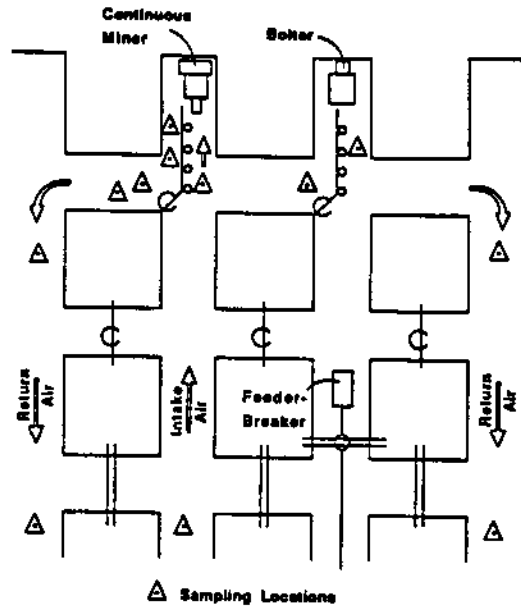


Figure 2. Generalized version of the airborne dust sampling plan.

following data were collected: (i) channel and chip samples at the working face to provide data on the quartz content in the coal and roof/floor strata; (ii) bulk (ROM) samples from the shuttle car/feeder-breaker discharge to provide data on (a) the size distribution of mined material, (b) the quartz content in each size fraction of the mined material, (c) the total quartz content in the mined material, (d) the Hardgrove Grindability Index (HGI) of the ROM material, (e) the fraction of the ROM material which can be identified as rock, and (f) the size distribution of the rock fraction in the ROM material; (iii) gravimetric samples (total airborne dust and respirable airborne dust) to provide data on the quartz content in the airborne total and respirable dust; and (iv) total airborne dust samples using multi-stage cascade impactors to provide data on (a) the quartz content in the various sized dusts and (b) the quartz content in total airborne dust. Some of the locations also had a Realtime Aerosol Monitor (RAM) fitted with data loggers to continuously monitor the dust concentration in the air stream. All of the instrument packages were hung from the roof bolts in the section or from telescopic poles at a position as close to the rib as possible.

Other necessary data collection activities such as ventilation plans and air quantity measurements were made for each sampling site. Time studies were performed using permissible tape recorders to correlate the RAM data with the specific activities of the continuous miner and shuttle cars. A summary of the sampling activities in the mine is shown in Table 1. The sampling plan for

QUARTZ DUST LEVELS

Table 1. Salient data on mines and sections sampled.

Mine	Number of Section	Location	Seams(s)	Shifts Sampled	Selected Cuts Sampled	Section Ventilation	Section Type	Section Dust Standard (mg/m ³)
A	1	PA	Upper Freeport	2	3	Brattice, Double-Split	Development	Miner: 2.0 Bolter: 2.0
B	1	OH	Pittsburgh	1	2	Tubing, Single-Split	Development	Miner: 2.0 Bolter: 1.7
B	2	OH	Pittsburgh	2	4	Tubing, Single-Split	Development	Miner: 2.0 Bolter: 1.2
C	1	UV	No. 2 Gas	2	4	Brattice, Single-Split	Development	Miner: 0.7 Bolter: 1.0
D	1	UV	Lower and Middle Eagle	2	2	Brattice, Single-Split	Pillar	Miner: 1.0 Bolter: 0.8

Mine C along with the cross-section cut are shown in Figures 3 and 4.

SAMPLE PROCESSING

The various steps in the processing of the collected samples are presented in Figure 5. Gravimetric samples, including total, respirable and oversize samples, were dried and weighed to determine the airborne dust concentration. Size analyses were performed on some of the samples for each selected cut. The samples were then ashed in a low-temperature asher and subject to an infrared scan to determine quartz peaks.

Impactor samples from the various stages were dried and weighed. The samples from stages 2 and 3, 4 and 5 and 6 through 8 were combined to obtain three reconstituted size classes for quartz analysis.

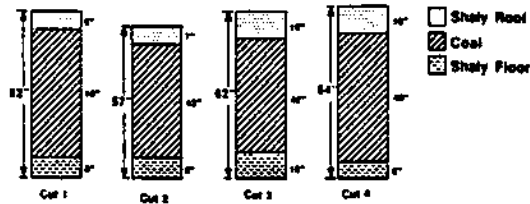


Figure 4. Cross-section of channel samples (Mine C).

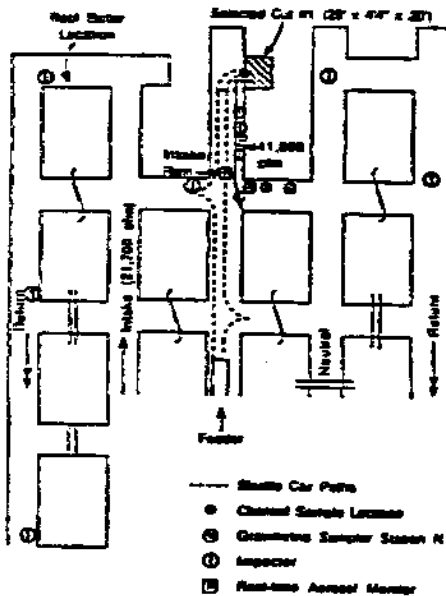


Figure 3. Section layout and sampling plan, Mine C, Cut 1.

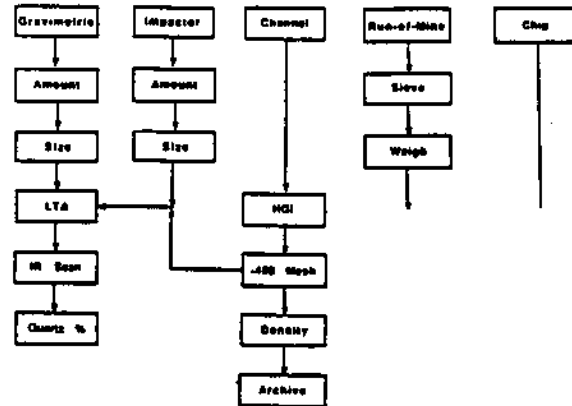


Figure 5. Samples processing procedure.

The channel samples from each horizon were crushed and ground to minus 400 mesh in a ball mill and quartz analyses performed. The ROM samples were screened (+4" (10 cm), -4" (10 cm) + 2" (5 cm), -2" (5 cm) + 1" (2.5 cm), -1" (2.5 cm)) and each individual size material weighed to determine the mass size distribution. The -1" (2.5 cm) material was further analyzed for size distribution to minus 400 mesh. The channel sample was reconstituted from the various size material. The sample was then crushed to minus 400 mesh before being subject to a quartz analysis. Chip samples were crushed and ground to

THE RESPIRABLE DUST CENTER

minus 400 mesh to determine their quartz content.

SILICA ANALYSES

Airborne dust samples

The airborne dust samples from the various samplers were analyzed for their quartz content using the P7 method (Anon., 1984). For the impactor samples, it was necessary to combine the collected dust masses from more than one stage (substrate) in order to increase the mass of dust and the mass of quartz to achieve the ranges suggested in the P7 analysis procedure.

Bulk samples

To avoid differences due to methods, the P7 procedure was used for bulk samples as well. For this purpose, channel, chip and ROM samples were ground to minus 400 mesh as follows:

- Step 1. Crush representative sample (say, 40 lbs (18 kg)) in a jaw and roll crusher to minus 10 mesh.
- Step 2. Riffle sample to a 2 lb (0.9 kg) representative sample.
- Step 3. Roll crush the 2 lbs (0.9 kg) of material further to produce 16 x 30 and minus 30 mesh material.
- Step 4. Recombine proportionally, samples of 16 x 30 and minus 30 mesh material to obtain a 20 to 40 gram sample which is then put into a ball mill and crushed to minus 400 mesh.
- Step 5. The uniform suspension of minus 400 mesh material can be obtained by mixing the minus 400 mesh material with coal dispersant in a beaker. After ultrasonic treatment, samples can be obtained by transferring the suspension and depositing on DM-450 filters.
- Step 6. Repeat the procedure of analyzing airborne dust.

Data management

To organize the large amounts of data, the data were saved as sequential records in computer files accessed by BASIC programs written for the IBM PC. This data can be listed, modified, supplemented or utilized for subsequent graphical and statistical analysis.

ANALYSIS OF RESULTS

Analysis of the quartz data

The quartz content in the channel samples, airborne dust and ROM coal for all the four mines are presented in Figures 6 through 9 and summarized in Table 2. Several

aspects of the data should be noted. An examination of the data shows that the quartz that the quartz is high mainly in the roof and floor. The quartz in the respirable dust is higher than that in the total dust for Mines A, C and D, while for

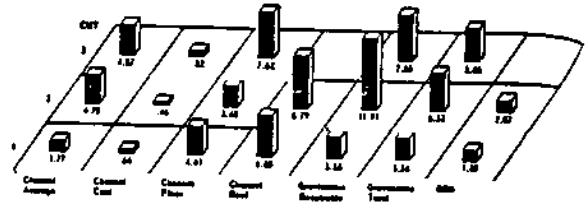


Figure 6. Quartz content in Mine A samples.

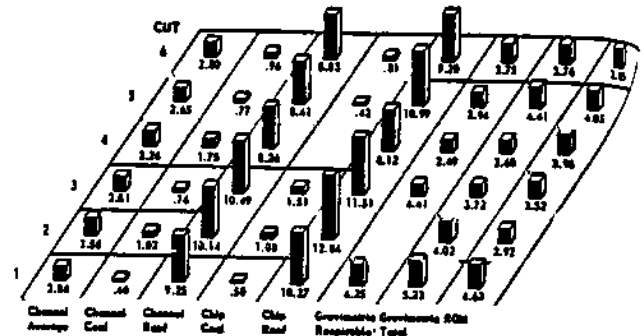


Figure 7. Quartz content in Mine B samples.

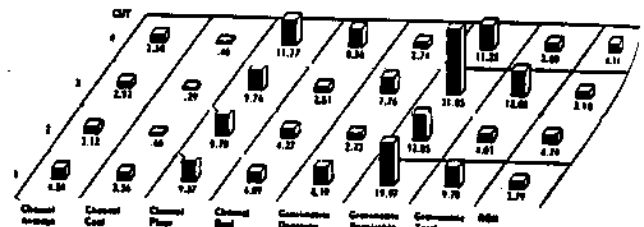


Figure 8. Quartz content in Mine C samples.

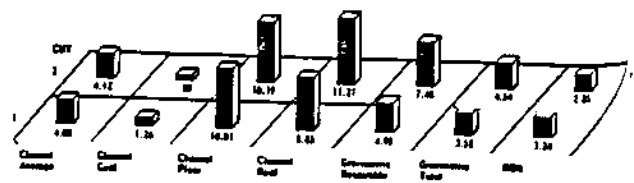


Figure 9. Quartz content in Mine D samples.

QUARTZ DUST LEVELS

Table 2. Average quartz content (%) in various samples.

Mine	Number of Selected Cut	Channel	Average Quartz Roof	Percent Floor	Coal	Respirable Airborne	Total Airborne	ROM
A*	3	3.8	7.8	5.3	0.64	7.7	5.11	1.98
B*	6	2.99	9.23	—	0.95	3.57	3.97	3.82
C	4	3.59	5.08	10.17	1.24	18.58	7.35	3.84
D**	2	4.06	10.03	10.1	1.07	6.23	4.06	3.09

+ - The major portion of the rock was cut separately and gobbled in cuts 2 and 3. ROM quartz is only from the coal seam and any remaining dilution.
 * - The face ventilation system practiced was tubing with auxiliary fan.
 ** - In cut 2 the channel sample and the machine cut were not in the same location. Also, the airborne samples could not be located close to the cut.

Mine B, it is lower than the quartz content in the total dust. For Mine A, the quartz contents of the roof and floor are an order of magnitude higher than the quartz content in the coal. The average quartz content in the channel sample for the three cuts is 3.8%, while the average quartz content in the ROM coal is only 1.98%. This is because the roof rock was cut separately for cuts 2 and 3 and gobbled. As a result, the quartz content shown in the ROM sample pertains only to that in the coal.

For Mine B, where the floor was not cut, this general trend is again apparent. The roof has, on the average, about ten times the quartz in the coal (0.95% for coal, 9.23% for roof). The average quartz content of the coal chip samples is 0.87% the quartz in the channel coal samples being comparable at 0.95%. The chip samples of the roof have an average quartz content of 10.48%, again comparable to 9.23% obtained for the channel samples. This mine used a tubing system for face ventilation. There appears to be a segregation of the airborne dust in the tube. For the six cuts, the average quartz content of the airborne respirable samples is 3.57%, while the gravimetric total airborne quartz has an average value of 4.0%. The average quartz content in the ROM coal is 3.82%, while the average channel quartz content is 3%.

The quartz data for Mine C (Figure 8), which was operating under reduced standards, show that the average quartz content in the floor material is 10.17%, twice the average quartz content in the roof (5.08%), while the average quartz content of the coal is 1.24%. The airborne gravimetric data show that the average quartz in the respirable sample is 18.58%, the corresponding value for total dust being 7.35%. One of the respirable samples (cut 3) has a quartz content of 31.05%. The average quartz in the channel sample is 3.59%, while the ROM coal has a comparable average of 3.84%.

The data for Mine D (Figure 9) show that the roof and floor have considerably more quartz than the coal. However, the gravi-

metric total airborne sample has an average of 4.06% quartz while the respirable data show a 6.23% quartz average. The ROM average quartz content is 3.09%. The channel sample yielded 4.06% quartz.

The quartz content in the chip and channel data for all the samples are presented in graphical form in Figure 10 and show good correlation between the quartz contents in the samples implying that, with care, chip samples can be taken in lieu of channel samples.

To further study the relationship between quartz in airborne dust and quartz in host material, a number of analyses were performed:

- (i) relationship between quartz in airborne dust and quartz in channel samples including composite channel sample and individual roof, coal and floor components;
- (ii) relationship between quartz in channel samples and quartz in run-of-mine samples; and
- (iii) relationship between quartz in various size fractions of the airborne dust and quartz in channel samples.

Results of the respirable dust analyses are presented here. In general, the results of the total dust analyses are similar to those obtained for respirable dust.

Scatter plots of the quartz in airborne respirable dust and quartz in the average channel sample (Figure 11) show that the quartz contents in the airborne dust are generally higher than that in the channel sample. The quartz content in the channel ranges from approximately 2 to 5 percent while the airborne respirable dust contains approximately 3 to 31 percent. As the quartz content in the channel sample increases, there is a considerable non-linear increase in the airborne quartz.

The airborne quartz concentration was plotted against the average quartz content in the roof and floor (Figure 12). The data points indicate a higher concentration of quartz in the respirable samples than in the corresponding combined roof and floor channel samples. Considering only the roof quartz

against airborne dust quartz content (Figure 13), the results are similar to the above case. Cuts 1 and 3 of Mine C have extremely large amounts of quartz in the airborne samples, which is not in line with that observed in other mines. In both these mines not only the proportion of the cut in the rock is higher but some floor was also taken. The floor contained high proportions of quartz.

Comparison of the quartz content in the ROM coal with the quartz in the channel samples (Figure 14) shows that the data points, in general, lie slightly above the line of perfect correlation indicating that ROM quartz content is slightly higher compared to channel quartz.

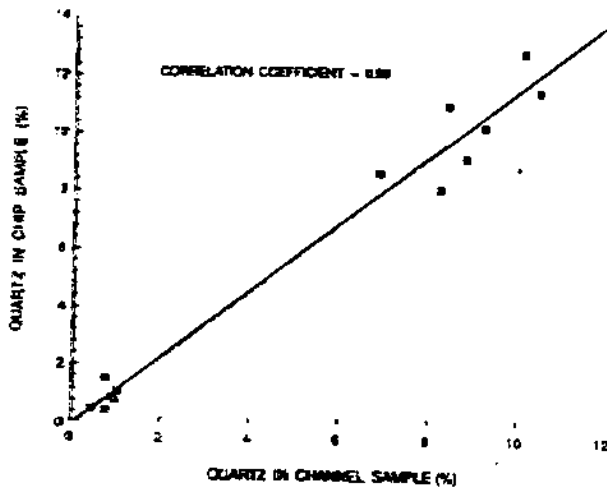


Figure 10. Correlation of quartz content in chip with quartz in channel samples.

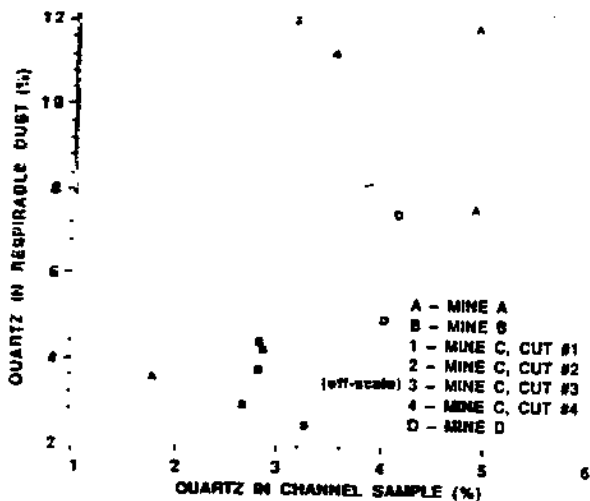


Figure 11. Plot of quartz in airborne respirable dust vs. quartz in channel sample.

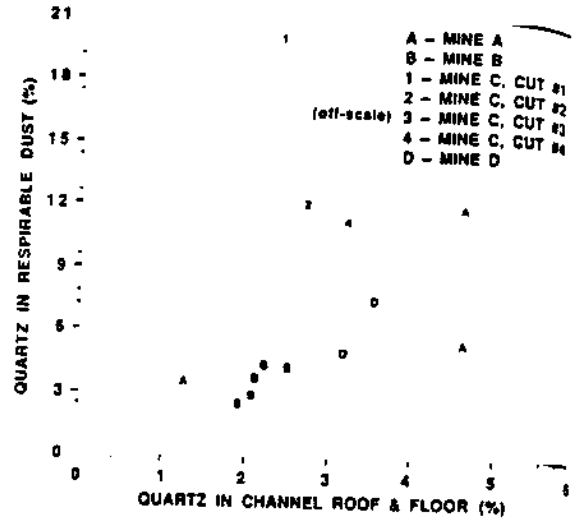


Figure 12. Plot of quartz in respirable dust vs. quartz in combined roof and floor channel samples.

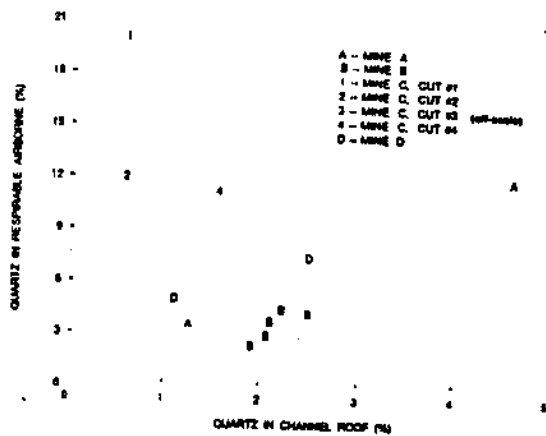


Figure 13. Plot of quartz in respirable dust with quartz in roof channel sample.

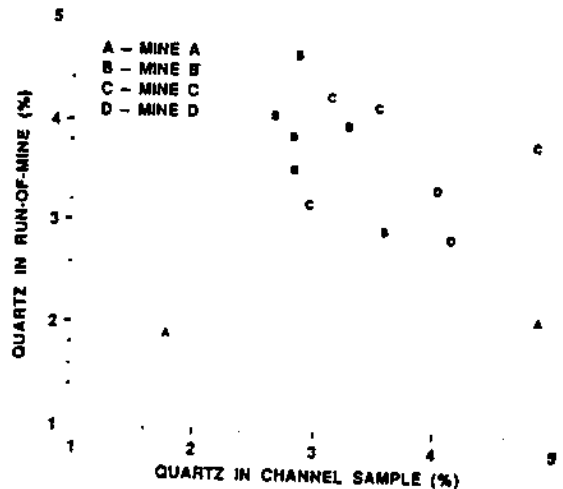


Figure 14. Plot of quartz content in ROM with quartz content in channel samples.

QUARTZ DUST LEVELS

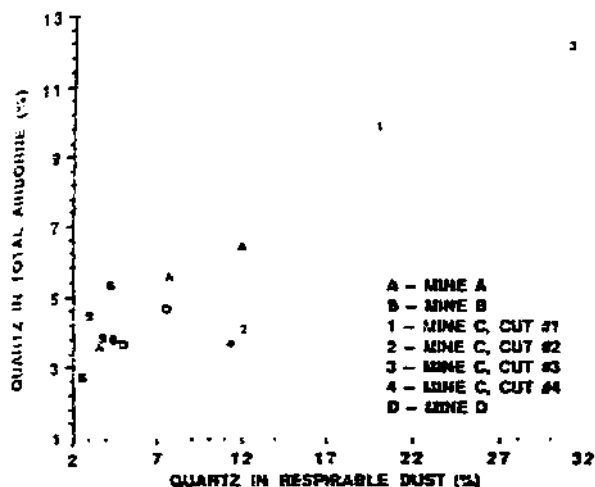


Figure 15. Plot of quartz in total airborne dust with quartz in airborne respirable dust.

The relationship between quartz in the total airborne dust, and quartz in respirable dust is shown in Figure 15. An increase in one leads to an increase in another. However, the quartz concentration in respirable dust is much higher than that in the total dust.

In summary, the gravimetric data indicate that quartz tends to be preferentially segregated into the airborne dust with more quartz being present in the respirable dust than in the total dust and that the source of much of the airborne quartz is roof and floor.

Impactor quartz analysis

Impactors were placed in a number of locations in each of the mines sampled. The locations analyzed in detail for this study were as follows:

- (i) **Face return:** this location represents the immediate return of the continuous miner. In mines using brattice for face ventilation, the impactor was placed close to the center of the cross-sectional area behind the return brattice. Where a tubing was used, the impactor was placed under the tubing about 3-5 ft from the end of the tubing where airborne dust generated by the continuous miner is assumed to exist.
- (ii) **Location 2X:** this location is two breakthroughs downwind of the continuous miner.
- (iii) **Location 4X:** this location is four breakthroughs downwind of the continuous miner.

The results were consistent from location to location even though the sample sizes for any size range were not large. The pattern for the samples taken at the different return locations for Mines B, C and D can be observed in Figures 16, 17 and 18, respectively.

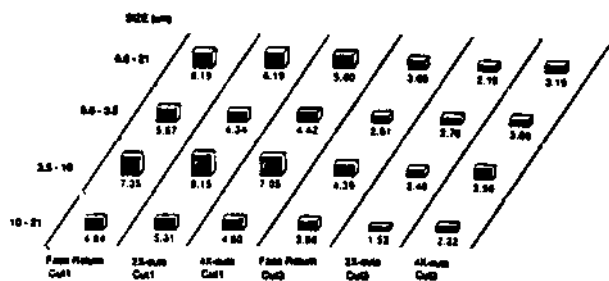


Figure 16. Quartz content in various dust particle sizes (Mine B).

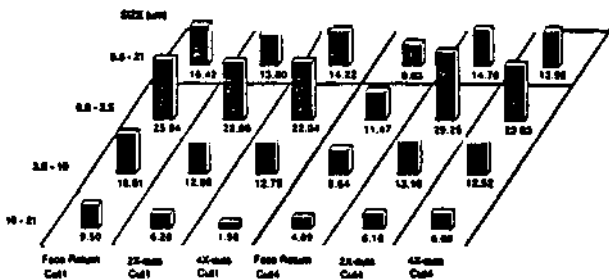


Figure 17. Quartz content in various dust particle sizes (Mine C).

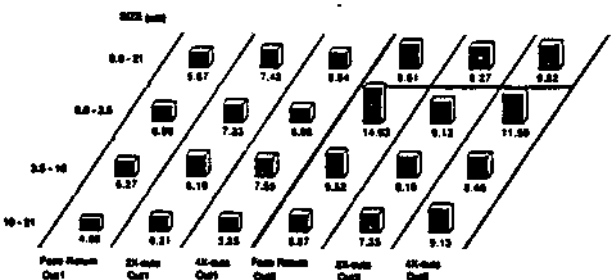


Figure 18. Quartz content in various dust particle sizes (Mine D).

The increase in quartz content with decrease in size is consistent in the results at the face return, the 2X and the 4X locations. A basic conclusion is that the percent quartz in airborne dust is greater in the fine size range than it is in the two larger size fractions, confirming gravimetric results.

CONCLUSIONS

This fundamental and experimental study has led to the following findings with respect

to quartz levels in the material being cut and those in airborne dust in continuous miner sections.

- (i) In the mines studied, the quartz contents of the roof and floor material are generally higher than those in the channel and ROM samples. Furthermore, the coal portion of the channel samples had smaller percentages of quartz compared to roof and floor.
- (ii) The gravimetric and impactor data reveal that the quartz contents in the respirable airborne dust are generally higher than the average quartz content in the channel or the ROM samples.
- (iii) Quartz level in the host material, expressed as weighted-average-quartz percent in a channel, does not show a strong relationship to quartz in airborne respirable (gravimetric samples).
- (iv) Quartz level in the roof and floor material, expressed as weighted-average-quartz percent, shows a strong relationship to quartz in airborne respirable dust (gravimetric samples).
- (v) Quartz level in the roof material, expressed as a percent, shows a stronger relationship to quartz in airborne respirable dust (gravimetric samples).
- (vi) Analysis of the quartz level in the airborne total dust shows that quartz content in the finest size range is higher than in the other size ranges (impactor samples).

A major conclusion of this study is that quartz in the airborne dust is more a function of quartz in roof and floor and the amount of roof and floor cut rather than the average quartz in the total material cut. Also, because quartz content is higher in the finer size ranges of the airborne dust, the manner in which high-quartz containing material breaks into fine particles and gets entrained may be different from that of other materials. Entrainment and quartz size distribution studies on samples of coal and rock separately may help explain any differences in breakage characteristics and entrainment propensity of the various sections of the material being mined.

ACKNOWLEDGEMENTS

The financial support of this research under Contract No. H0358031 by the U.S. Bureau of Mines is acknowledged. The cooperation and assistance extended to the project personnel by various mining companies is acknowledged and appreciated. Sincere thanks are extended to Dr. C. J. Bise and Dr. S. Chander, Department of Mineral Engineering and to the graduate students in the Mineral Engineering Department at Penn State for their assistance in field data collection and sample analysis.

REFERENCES

Anonymous, 1984. Infrared determination of quartz in respirable coal mine dust, Method No. P7, Mine Safety and Health Administration (Dust Division, Pittsburgh Health and Technology Center), 29 pp.

Jankowski, R. A., Nesbit, R. E. and Kissell, F. N., 1984. An update of the reduced standards problem and overview of improved control technology for respirable coal mine dust, in Mine Ventilation (Ed. P. Mousett-Jones), pp. 151-167 (Balkema, Rotterdam).

Jankowski, R. A. and Niewiadomski, G. E., 1987. Coal mine quartz dust control, an overview of current U.S. regulations and recent research results, in Coal Mining and Safety (Ed. C. I. Lee, H. T. Chon and T. Y. Kim), pp. 303-314 (Korean Institute of Mineral and Mining Engineers).

Kok, G. E., Adam, R. F. J. and Pimental, R. A., 1985. Control of respirable quartz on continuous mining sections, U.S. Bureau of Mines Contract J0338078, Ketron, Inc., November, 169 pp.

Ramani, R. V., Mutmansky, J. M., Bhaskar, R. and Qin, J., 1987. Fundamental studies on the relationship between quartz levels in the host material and the respirable dust generated during mining, Final report Volumes I and II to U.S. Bureau of Mines, Contract H0358031, The Pennsylvania State University, September, 269 pp.

Taylor, L. D., Thakur, P. C. and J. B. Reister, 1986. Control of respirable quartz on continuous mining sections, U.S. Bureau of Mines, Contract J0338077, Conoco, Inc., December, 67 pp.

III
CHARACTERIZATION
OF DUST PARTICLES

Characterization Problems in Comminution -- An Overview

R. Hogg

Mineral Processing Section, Department of Mineral Engineering,
The Pennsylvania State University

ABSTRACT

Hogg, R., 1988. Characterization problems in comminution — an overview. *Int. J. Miner. Process.*, 22: 25-40.

The problems of sampling particulate materials, and of characterizing the distributions of particle size and composition are reviewed. Requirements for sampling from comminution systems are discussed and a simple formula is presented for estimating the minimum sample size needed. The limitations and errors associated with the techniques available for particle size analysis are evaluated and guidelines are suggested for the selection of appropriate methods. The use of microscopic and macroscopic approaches to the characterization of particle composition are discussed.

INTRODUCTION

Comminution is a process of particle size reduction in which the goal is to produce a material with a specified particle size distribution from a coarser feed. In mineral processing applications, the product size distribution is often of secondary importance to the extent to which individual mineral grains can be liberated from one another. However, due to poor understanding of the nature of the liberation process and the lack of reliable procedures for characterizing it, the actual specification is normally in terms of particle size.

Particle size distribution can be regarded as the fundamental characteristic of a particulate system. The distributions of particle shape and composition among the various particle sizes present are often sufficient to define the bulk properties and behavior of the system. Description of the distributions of size, shape and composition of the different phases which may exist within individual particles is necessary to complete the picture and is especially important for predicting liberation etc., in comminution processes. It is quite obvious that the complete characterization of real particulate systems is a formidable, if not impossible task. Practical characterization procedures should involve evalua-

tion of those characteristics which are deemed to be important and which can be measured. In comminution systems, this should ideally include the particle size distribution, the size-by-size distributions of particle composition, and as much information as can be acquired on the internal composition and structure of individual particles. In most cases, of course, we fall far short of even this rather limited goal.

SAMPLING PARTICULATE MIXTURES

Virtually all particulate systems, especially those associated with comminution processes, are mixtures of particles of varying size, shape and composition. Sampling of such mixtures is the first step in any characterization procedure. There are two factors to be considered in any sampling scheme: the basis for sample selection, and the required sample size.

Sample selection

The ideal sampling procedure would involve the examination of individual particles one at a time on a random basis, such that at each step every particle in the population has an equal probability of being selected. This, of course, is very rarely practical, although the successive splitting procedures such as riffling and the cone-and-quarter technique can provide a reasonable approximation if properly applied. Simple grab sampling is seldom adequate unless the system is thoroughly mixed. However, a series of grab samples taken from different locations, or with intermediate mixing, may be sufficient and is often the only practical alternative for very large populations. If these are analyzed separately rather than combined into a simple analysis sample, information can be acquired on the heterogeneity of the mixture and on the extent of the sampling problems. Procedures for sampling from both batch and continuous flow systems have been discussed at length by Gy (1982).

Sample size

The discrete nature of particulate systems imposes constraints on the size of the sample which must be taken. For example, if a sample of ten particles were taken from a mixture containing 5% of one kind of particle, the best possible estimate of concentration (0 or 10%, corresponding to zero or one particle) would be in error by 100%. In other words, the sample must be large enough that each identifiable constituent can be expected to be present as a reasonable number of particles. Based on the statistics of random mixtures, it can be shown (Buslik, 1950; Stange, 1954, 1963; Poole et al., 1964; Harnby, 1967) that the expected variance of samples of mass M taken from a mixture

containing $i=1,2,3,\dots$ size classes and $j=1,2,3,\dots$ composition classes is given by:

$$\sigma^2 = \frac{f_{ij}(1-f_{ij})w_{ij} + f_{ij}^2(\bar{w} - w_{ij})}{M} \quad (1)$$

where f_{ij} is the mass fraction of the material which falls in size class i , and composition class j , w_{ij} is the corresponding mean particle mass, \bar{w} is the overall mean particle mass:

$$\bar{w} = \sum_i \sum_j f_{ij} w_{ij} \quad (2)$$

If the 95% confidence interval is approximated by two standard deviations on either side of the mean, the relative error ϵ , at the 95% confidence level, can be expressed as:

$$\epsilon = \frac{2\sigma}{f_{ij}} \quad (3)$$

Combination of eqs. 1 and 3 leads to the following simple expression for the minimum sample weight M_{ij} required to estimate the concentration of the ij component with relative error ϵ :

$$M_{ij} = \frac{4}{\epsilon^2} \left[\left(\frac{1}{f_{ij}} - 2 \right) w_{ij} + \bar{w} \right] \quad (4)$$

The required sample weight would be equal to the maximum value of M_{ij} . In practice, this will generally correspond to the coarsest size class and the composition class with the lowest concentration at that size. Note that eq. 4 also indicates a minimum sample size for any component in a given system i.e.:

$$M_{\min} = \frac{4\bar{w}}{\epsilon^2} \quad (5)$$

Thus, for systems containing some large particles (giving large \bar{w}) quite large samples may be needed for evaluation even of the very fine components. Eq. 4 can also be used to estimate the relative errors ϵ_{ij} which can be expected for a sample of mass M .

An example of the application of eq. 4 to sieving analysis of a system of quartz particles with a Rosin-Rammler distribution of sizes is given in Table I. In principle, the analysis can be extended indefinitely to coarser and coarser sizes simply by including the appropriate screens. However, the calculations show that, in order to obtain reliable information at these progressively coarser sizes, it is necessary to increase the sample size massively. While a 40 g sample is sufficient when all material coarser than 1 mm (18 mesh) is regarded as the top size, almost 6 tons would be needed to provide an accurate estimate of the

THE RESPIRABLE DUST CENTER

TABLE I

Sample size requirements for sieve analysis (quartz particles with a Rosin-Rammler size distribution with $k=1$ mm (18 US mesh) and $m=1$)

Coarsest screen used	Expected weight percent retained on coarsest screen, Q_m	Required sample weight for < 5% error in estimate of Q_m	100 g sample percent error in Q_m estimate	95% confidence range on Q_m
+18 US mesh	36.8	40 g	3.2	35.6-38.0
+14	24.3	130 g	5.7	22.9-25.7
+10	13.5	500 g	11	12.0-15.0
+7	5.9	2.5 kg	25	4.4-7.4
+5	1.8	18.4 kg	68	0.6-3.1
+3.5	0.35	230 kg	240	0.0-1.2
+5/16"	0.03	5.7 tons	1200	0.0-0.43

amount of +8 mm (5/16 inch) material in the distribution. It is clear that the 50-100 g samples commonly used in sieve analyses should be quite adequate for materials which are predominantly finer than about 1 mm. However, the sample size requirements can be severe for large particles — in the evaluation of crushers, autogenous grinding systems etc.

Sample size restrictions can also be very important in particle counting procedures, especially microscopy. An example is given in Table II for a fairly typical, sub-sieve, size distribution from a comminution process. In order to

TABLE II

Sample size for microscopy

Size range (μm)	Weight percent in size range	Required particle count for 10% error in top size
35 -50	29.3	200
25 -35	20.7	400
18 -25	14.6	800
12.5-18	10.4	1,800
8.8-12.5	7.3	3,200
6.3-8.8	5.2	6,400
4.4-6.3	3.7	13,000
3.1-4.4	2.6	26,000
2.2-3.1	1.8	50,000
1.6-2.2	1.3	100,000
1.1-1.6	0.9	200,000
0.8-1.1	0.6	400,000

Total count: 800,000 particles; sample size: 0.1 mg.

PROBLEMS IN COMMINATION

TABLE III

Size-specific gravity distribution of coal (after Sokaski et al., 1963). Values of f_{ij} (wt.%)

Specific gravity ρ_i	Size X_j							
	6" × 3"	3" × 1½"	1½" × ½"	½" × ¼"	¼" × 8 mesh	8 × 14 mesh	14 × 48 mesh	48 mesh × 0
1.3 float	4.44	5.73	16.30	8.75	9.75	4.91	5.58	2.32
1.3 × 1.4	1.62	2.09	5.63	3.26	3.05	0.94	0.77	0.33
1.4 × 1.5	0.64	0.68	1.40	0.84	0.93	0.32	0.25	0.12
1.5 × 1.6	0.43	0.46	0.86	0.34	0.43	0.17	0.16	0.08
1.6 × 1.7	0.21	0.26	0.49	0.17	0.22	0.09	0.08	0.04
1.7 × 1.8	0.13	0.18	0.37	0.11	0.16	0.06	0.06	0.04
1.8 sink	4.13	2.79	3.55	0.82	1.26	0.51	0.40	0.28
Total	11.6	12.2	28.6	14.3	15.8	7.0	7.3	3.2

Mean particle weight $\bar{w} = 143$ g.

obtain an estimate of the mass fraction in the coarsest size fraction (35–50 μm) with less than 10% error, it would be necessary to count about 200 of these particles. This would entail a total particle count of about 800,000. These numbers can be reduced substantially through the use of several magnifications but new errors are introduced in matching the counts at different levels.

The examples given in Tables I and II refer to the evaluation of particle size distribution only. Obviously, the problems are very much exacerbated for heterogeneous systems containing many different kinds of particles. The application to the evaluation of size-composition distributions is illustrated in Tables III and IV. Some published data (Sokaski et al., 1963) for the size-specific gravity distribution of coal are given in Table III. The sample weights, as calculated from eq. 4, which would be required to obtain the f_{ij} values of Table III to within $\pm 10\%$, are listed in Table IV. Strictly, the required sample size should be the maximum of these values, i.e. about 350 tons (for the 1.7 × 1.8 specific gravity fraction of the 6" × 3" particles). Obviously this would generally be impractical and it would be necessary to accept larger errors. For this particular system, in fact, an error of 100% in the smallest f_{ij} values ($\sim 0.1\%$) would not usually be considered serious. Consequently, in using this approach, it is normally necessary to make judgments as to what kinds of errors may or may not be acceptable.

PARTICLE SIZE ANALYSIS

In comminution systems, the particle size distribution of the product is the direct measure of process performance. Particle size information is needed for

THE RESPIRABLE DUST CENTER

TABLE IV

Minimum sample weights (kg) required for estimation of individual f_{ij} values with relative error < 10%

Specific gravity ρ_i	Size X_j							
	6"×3"	3"×1½"	1½"×½"	½"×¼"	¼"×8 mesh	8×14 mesh	14×48 mesh	48 mesh ×0
1.3 float	6,625	755	70	59	58	58	58	58
1.3×1.4	21,200	2,350	111	63	58	58	58	58
1.4×1.5	58,750	7,825	310	83	59	58	58	58
1.5×1.6	93,750	12,375	500	126	62	58	58	58
1.6×1.7	205,000	23,325	898	205	67	58	58	58
1.7×1.8	352,500	36,000	1238	298	71	58	58	58
1.8 sink	12,875	2,800	202	97	58	58	58	58

process evaluation, modeling (parameter estimation etc.) and control. In general, particle size distributions can be expressed in the form:

$Q(x)$ = relative quantity of material which is smaller than size x

Quantity can be represented by number of particles, volume, surface area etc. If density is constant, the volume and mass distributions are identical.

In principle, experimental determinations of particle size distributions involve two sets of measurements: quantity and size. In most practical procedures, however, x is assigned according to some specific criterion (sieve aperture, sedimentation time, etc.) and only Q is actually measured. Similarly, comminution processes generally operate on Q not x . Particles do not change in size; they are destroyed and new ones are created. (An exception to this generalization is found in the case of abrasive grinding, where a particle may retain its identity but be reduced in size.)

Errors in particle size analysis

Precision in the measurement of particle size distributions and in the description of comminution processes depends on how accurately Q can be measured. A typical example of the changes in particle size distribution during the course of a comminution process can be seen in Fig. 1. The family of curves shown is the result of a translation in the Q direction. This means that, in modeling the process, information obtained at short times (low Q) is used to predict the higher Q values at longer times. Ideally, this would require fixed relative errors in the Q measurement whereas the essentially linear response of most sizing techniques gives rise to fixed absolute errors, i.e. small measured Q values are subject to large relative error.

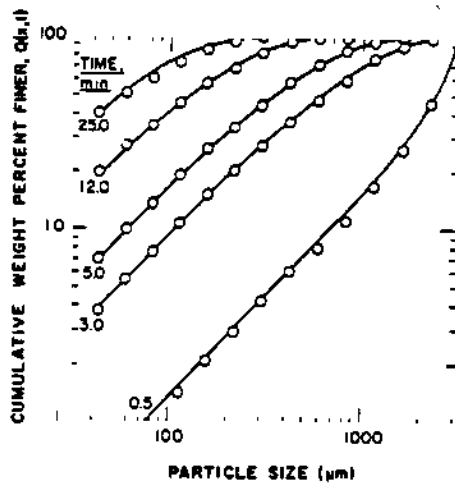


Fig. 1. Typical product size distributions in comminution.

Errors associated with the experimental determination of particle size distributions can be classified into three general types:

- (1) "Error-free" size (e.g. sieving, sedimentation). Since size is predetermined, errors can be assigned to Q .
- (2) Independent size and quantity (e.g. simple counting procedures). Ideally, the error should be in the size estimate, but there will often be missing or false counts.
- (3) Estimated size/inferred quantity (e.g. Coulter counter volume distribution). Individual particles are sized and the quantity is assigned based on the size estimate. This leads to inter-dependent errors in both Q and x .

These different kinds of errors can be partially responsible for apparent discrepancies among size distributions obtained by different techniques.

Size limitations

Essentially all particle sizing techniques have a limited range of applicability. Some common examples are shown in Table V. Both upper and lower limits can lead to problems in data evaluation and interpretation.

The upper limit is generally less serious than the lower limit since it can usually be circumvented by pre-classifying the sample at a smaller size. The classification must be very sharp, preferably by screening. This can present significant problems when the upper limit is less than about $30 \mu\text{m}$ (e.g. small aperture Coulter counter). The use of pre-classification requires careful evaluation of the correspondence of the definitions of size used in the size analysis and in the classifier.

TABLE V

Methods of particle size analysis

Method	Range of applicability	Limitations etc.	Examples of commercial equipment
Sieving (conventional) (micromesh)	> 30 μm > 5 μm	Blinding	Alpine jet sieve, Sonic sifter
Microscopy (optical)	> 1 μm	Lower limit of resolution at any magnification	Zeiss particle analyzer Quantimet B&L Omnicon, Lemont image analyzer
(SEM)	0.05-100 μm		
(TEM)	< 0.1 μm		
Sedimentation (gravity)	0.5-50 μm		Andreason pipet Micromeritics Sedigraph MSA-Whitby, LADAL Pipet & X-ray centrifuges, Joyce LoebI centrifuge, Photo Micron Sizer
(centrifugal)	0.01-20 μm		
Classification (liquid) (air)	> 10 μm > 1 μm		Warman cyclosizer Bahco, Haltain Infracizer, Roller separator, Donaldson Acucut classifier
Light scattering (photometry) (counters)	all sizes > 0.2 μm	Mean size only ^{a1} Lower detection limit	Brice-Phoenix Hiac/Royco, Spectrex
(Fraunhofer diffraction)	> 2 μm	Upper and lower detection limits	Microtrac, Malvern, granulometer
(Fraunhofer/right angle)	> 0.1 μm	Upper and lower detection limits	Microtrac (small particle analyzer)
(dynamic)	10 \AA -5 μm	Mean size ^{a1}	Coulter Model N4, Nicomp.
Electrical sensing	> 0.5 μm	Lower detection limit	Coulter Counter, Electrozone
Impactors	0.4-10 μm	Airborne particles	Andersen 2000
Acceleration	0.3-15 μm	Detection limits	TSI Aerodynamic particle sizer
Permeametry	0.1-50 μm	Mean size (surface area)	Blaine, Fisher sub-sieve sizer
Gas adsorption	< 20 μm	Surface area (incl. internal surface)	Quantasorb, Micromeritics

^{a1}Distribution can be estimated by curve fitting.

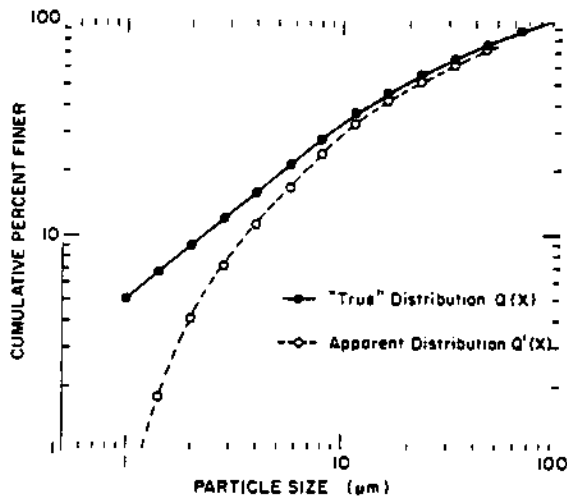


Fig. 2. The effect of a lower detection limit on a measured (apparent) size distribution.

The lower limit is generally the more serious of the two. Lower limits for different analytical procedures fall into two types:

(1) Measurement limits. Techniques with measurement limits give the quantity finer than the limit (x_0) and report the correct $Q(x)$ for $x > x_0$ but give no information for $x < x_0$. Sieving and incremental sedimentation are important examples of this class of methods.

(2) Detection limits. Particles smaller than the limit are ignored. The apparent size distribution is reported as:

$$Q'(x) = \begin{cases} \frac{Q(x) - Q(x_0)}{1 - Q(x_0)} & x \geq x_0 \\ 0 & x < x_0 \end{cases} \quad (6)$$

All methods which involve counting and sizing individual particles are subject to detection limits and give apparent distributions based on eq. 5 with $Q(x_0)$ unknown.

The effects of (lower) size limitations are illustrated in Fig. 2. Obviously, the measurement limit is to be preferred. Data obtained from techniques which involve detection limits should be questioned whenever significant quantities are reported at sizes close to the lower limit.

Methods of size analysis

Procedures for measuring $Q(x)$ also fall into two general types:

(1) Methods based on the collective response of the assemblage of particles, e.g. measurement of mass, scattering or absorption of radiation, etc. These are

generally subject only to measurement limits but there may be effective detection limits in specific applications (e.g. sedimentation balance, Microtrac).

(2) Methods based on the response of individual particles, e.g. microscopy, optical and electrical resistance counters. These methods are invariably subject to detection limits since there can always be some particle which is too small to "see". For microscopy, the detection limit can be extended indefinitely in principle, but there is usually some arbitrary cut-off in practice (limit of resolution of a particular instrument).

The collective response methods can give precise information on the volume (or area) distribution in the range between the upper and lower limits, even when there are particles outside of the range. However, transformation of the data to give the number distribution, for example, involves extrapolation beyond the lower limit and may be subject to serious error.

The individual response methods generally provide better estimates of the number distribution (albeit normalized, above the lower limit). In this case, transformation to the volume distribution is often suspect due to statistical problems at the coarse end. Individual response methods, especially automatic counters, are also subject to "coincidence" problems where two or more particles are counted and sized as one. This problem can be exacerbated by the presence of particles smaller than the detection limit. A device may respond to a group of particles even though the individuals are not detected. Coincidence of this kind would not be accounted for using the normal statistical criteria. To some extent, coincidence due to "undersize" particles may compensate for undetected material, but not in a realistic manner.

Definition of particle size

The definition of particle size, especially as a linear dimension, is unique only for simple shapes such as spheres and requires specification of the shape. Practical sizing methods typically resort to "equivalent sphere diameter" definitions where size is defined in terms of the response of a spherical particle. It follows that methods based on different kinds of measurements (settling velocity, light scattering etc.) use different definitions and give different results. Practical definitions can often be considered to involve combinations of:

d_v : volume diameter (diameter of a sphere with the same volume as the particle), and

d_a : projected area diameter (diameter of a sphere with the same projected area as the particle, in random orientation).

By considering size definitions in these terms, it is possible to obtain a qualitative picture of the relative magnitudes of the variations among methods. For example, electrical resistance methods such as the Coulter Counter, Elzone, etc. provide a direct estimate of d_v . Optical methods such as the Microtrac,

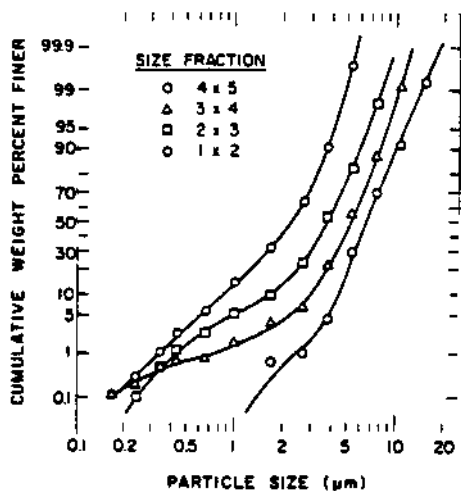


Fig. 3. Particle size distributions for air-classified narrow size fractions of Upper Freeport coal. Microtrac SPA measurements (after Dumm, 1986).

granulometer, etc., are based on d_n . Sedimentation methods yield the Stokes diameter d_{st} and:

$$d_{st} \sim \sqrt{\frac{d_v^3}{d_n}}$$

Where precise correlation of different methods is required, it is usually necessary to determine empirical conversion factors. Because particle shape can have a major influence on the definition of size, these conversion factors will generally be material dependent. If possible, several narrow size fractions of the material of interest should be prepared in the appropriate size range and direct measurements made on each. An example, for fine coal dust in the respirable size range, is given in Fig. 3 and Table VI, based on recent work by Dumm (1986). The fine coal was classified into four narrow fractions of nominal size 1×2, 2×3, 3×4 and 4×5 μm using a Donaldson Acucut classifier. The size distributions, determined using a Leeds and Northrop Microtrac small particle analyzer are shown in Fig. 3. Size analyses were also performed by sedimentation (LADAL pipet centrifuge), electrical sensing (Coulter, Model TA) and scanning electron microscopy in conjunction with a Zeiss, Model TG particle size analyzer. The observed mass (volume) median sizes are listed in Table VI. Conversion factors for each method, relative to sedimentation, are also given in Table VI. The results show the factors to be generally consistent, with no evidence for systematic variations with size. Similar measurements on a variety of coals and quartz with relatively broad size distributions (–10 μm)

TABLE VI

Correlation of methods for sub-sieve size analysis of classified coal dust

Size fraction	Mass median size \bar{x} (μm)				$\bar{x}/\bar{x}_{\text{Ladal}}$		
	Ladal centrifuge	Coulter Counter	Microtrac SPA	SEM	Coulter Counter	Microtrac SPA	SEM
4 × 5 μm	5.12	4.66	6.20	6.93	0.91	1.21	1.35
3 × 4	3.68	3.58	5.05	5.44	0.97	1.37	1.48
2 × 3	2.63	2.61	3.68	4.28	0.99	1.40	1.63
1.2	1.86	1.89	2.19	2.86	1.02	1.18	1.54
				Mean =	0.97	1.29	1.50
				Std. dev. =	0.05	0.11	0.12

could be correlated using essentially the same factors as for the narrow fractions (Dumm, 1986).

Choice of method

Sieving procedures are almost invariably used in laboratory evaluation of comminution processes. This is an obvious choice for many grinding systems, where most of the material is coarser than about 50 μm — a size range where sieving is generally the preferred method. Furthermore, the use of sieving methods allows the same procedures to be used in feed preparation as in the evaluation of performance, thus obviating the problems of different definitions of size.

In the case of fine grinding, it may be necessary to use sub-sieve sizing methods to extend the measurement range. Here, the choice of method becomes much less clear, and the selection will depend on availability and economic factors in addition to the actual merits of different procedures. Material factors can also be important: fine cement cannot be dispersed in water, for example. In general, the problems, errors, and limitations discussed above can be used as guidelines for the selection and application of fine-sizing techniques.

On-line sizing procedures are attractive for the control of comminution systems. Most sizing devices, however, are incapable of providing the instantaneous read-out desired for on-line measurement. Typical analysis times range from a few seconds (automatic particle counters) to more than 24 h (gravity sedimentation). Rapid-response instruments such as the Leeds and Northrup Microtrac device can provide data on an almost continuous basis and have been used, for example to monitor the grinding of taconite ores (Carr and Catz, 1976; Anonymous, 1977). A major problem appears to be the ability of the

equipment to withstand the adverse conditions (vibrations etc.) which commonly prevail in comminution plants.

The Armco-Autometrics particle size monitor has found considerable application, in the copper industry for example (Bassarear and McQuie, 1972). The basic device uses attenuation of ultra-sound to estimate slurry density and a single point on the size distribution. Alba and Herbst (1985) have extended the system to yield multi-point size distributions. Elimination of entrained air is critical to the successful use of these systems.

DISTRIBUTION OF PARTICLE COMPOSITION

The separation or liberation of individual mineral grains from composite particles is very commonly the primary purpose for carrying out comminution operations. Characterization is necessary to define the extent of liberation in a ground product and the potential for further liberation by additional grinding. The extent of liberation can be described using the set of size-composition distributions:

$q(x, c_i) dx dc_i$ = fractional quantity with size x to $x + dx$

and concentration c_i to $c_i + dc_i$ of mineral constituent i

In general, it would be necessary to specify one such distribution for each of the important mineral species present. In some cases, complex sulfide ores for example, several distributions may be required. Often, however, the distributions of one or two constituents would be sufficient. Further information on the distribution of mineral grains within individual particles, would be required for evaluation of liberation potential.

Image analysis techniques using optical and/or scanning electron microscopy are widely used for characterizing the distribution of particle composition. In principle, this approach can yield the size-composition distributions and also the distribution of grain structure within the particles. Major problems remain, however, in the transformation of data from two-dimensional images to give realistic volumetric concentrations etc. (Miller and Lin, 1985). Furthermore, the statistical problems discussed previously can cause data acquisition and interpretation to become prohibitively time-consuming even for modern image-analysis systems.

Macroscopic methods can also be used for determining size-composition distributions. This approach involves fractionation of the material on the basis of specific, composition-related properties such as density. For complete characterization of a system containing N constituents, $N-1$ such separations would be required. Thus for binary materials, the size-composition distribution can be obtained by gravity fractionation using heavy liquids followed by particle size analysis on the separate fractions as in Table III, for example.

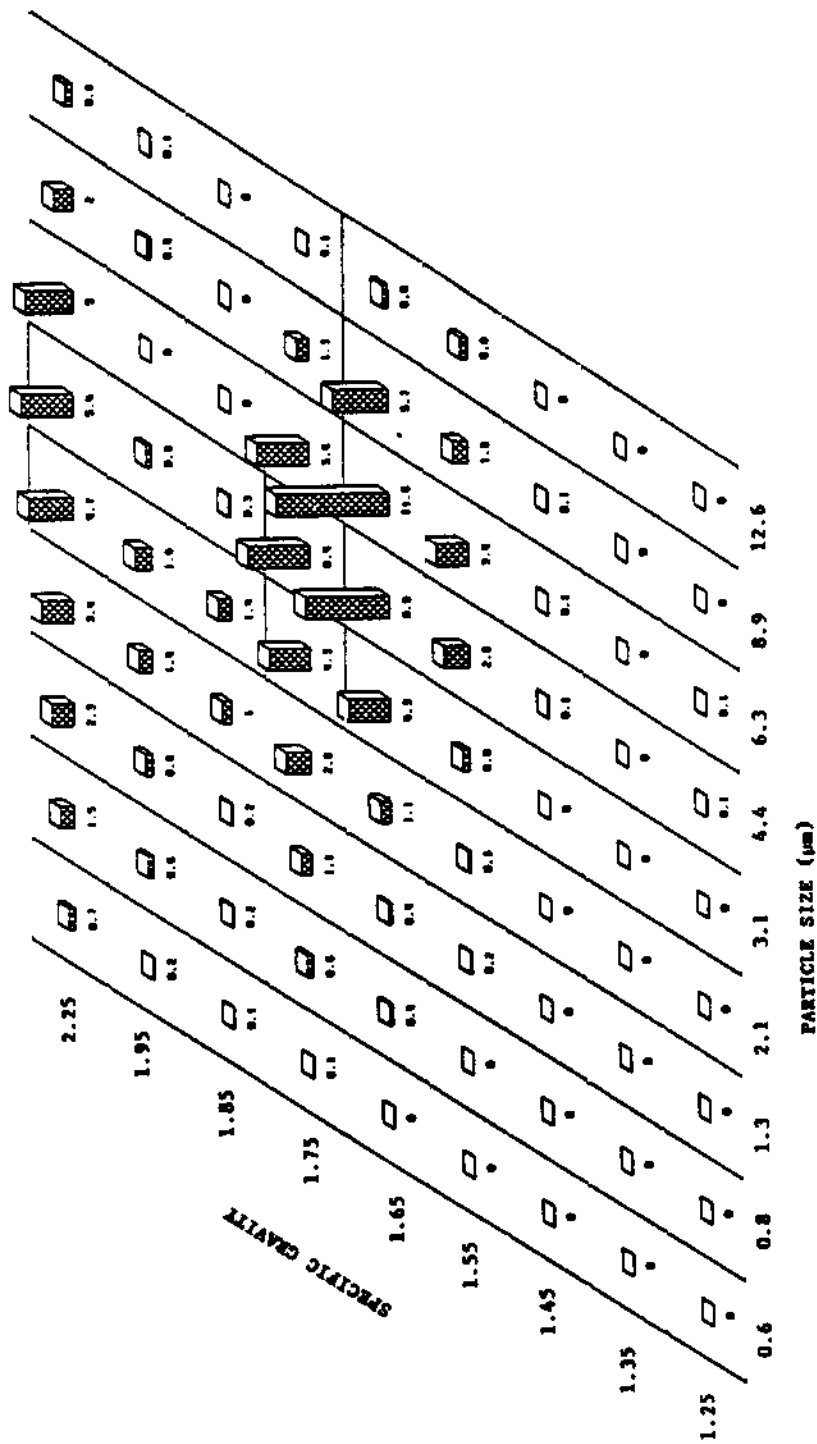


Fig. 4. Size-specific gravity distribution for anthracite coal dust (after Dumm, 1986).

Extension to ternary mixtures using, for example, high intensity magnetic separation in addition to gravity separation may be possible in some cases.

The macroscopic approach is widely used for evaluating the washability of coals. While most applications are to relatively coarse particles (+ 30 mesh), Dumm (1986) has successfully applied the technique to ultra-fine coal dust. An example showing the size-specific gravity distribution of an anthracite coal in the respirable size range ($-10 \mu\text{m}$) is given in Fig. 4. Fairly complete liberation of the organic matter (specific gravity ~ 1.6) from the mineral matter (specific gravity > 2.2) can be seen. In principle, the washability type of analysis can be applied to any mineral system using solutions of heavy metal (e.g. thorium) salts as the separation media. Macroscopic techniques, of course, yield essentially no information on the internal structure of particles and are of very limited value for predicting liberation during comminution.

In general, the microscopic methods provide the greatest amount of qualitative information but quantification is often questionable. The macroscopic approach, on the other hand, is more limited but is capable of significantly greater precision. A combination of qualitative/semi-quantitative image analysis with a washability-type analysis will usually provide the most complete picture of the size-composition characteristics of a complex particulate system. Microscopic analysis is probably necessary for forward prediction of liberation behavior; macroscopic analysis, especially in conjunction with a liberation model, will often be adequate for monitoring liberation as a function of grinding.

CONCLUSIONS

The selection of representative samples of appropriate size is a crucial first step in any characterization scheme. In the context of comminution systems, sample size requirements can become critical when large particles are present, as in coarse crushing or autogenous grinding, and in the use of microscopic methods for determining the distributions of particle size and/or composition. Specific guidelines are available which can be used to estimate minimum sample size requirements and to establish confidence limits on characterization data.

Product size distribution is obviously the most direct measure of performance in comminution systems. Available techniques for particle size analysis involve errors and are generally applicable only over limited ranges of size. In addition, different methods are based on different definitions of particle size. Careful consideration should be given to these factors in the choice of sizing methods to be used and in the interpretation of the resulting data. Errors, limitations etc., can be especially significant in the use of measured size distributions for estimating model parameters.

Particle size-composition distributions are important in the prediction and

evaluation of mineral liberation. Microscopic methods are excellent for qualitative evaluation of size-composition relationships but generally lack precision in quantitative use. Macroscopic methods yield less information but at greater precision. Combinations of the two probably represent the most useful approach to the analysis of mineral liberation.

REFERENCES

- Alba, J.F. and Herbst, J.A., 1985. Ultrasound absorption phenomena in slurries make possible the estimation of complete size distributions and solids concentrations. Paper presented at 16th Annual Meeting of the Fine Particle Society, Miami Beach, Fla.
- Anonymous, 1977. A laser that sizes up particles. *Business Week*, July 11, 1977.
- Bassarear, J.H. and McQuie, G.R., 1972. On-stream analysis of particle size. *Min. Congr. J.*, 58: 36-42.
- Buslik, D., 1950. Mixing and sampling with special reference to multi-sized granular material. *ASTM Bull.*, 165: 66-73.
- Carr, H.A. and Catz, S.J., 1976. Paper presented at the Joint ISA Mining and Metallurgy/CIM Symposium, Vancouver, B.C.
- Dumm, T.A., 1986. An evaluation of techniques for characterizing respirable coal dust. M.S. Thesis, The Pennsylvania State University, University Park, Pa.
- Gy, P., 1982. *Sampling of Particulate Materials, Theory and Practice*. Elsevier, New York, 2nd ed.
- Harnby, N., 1967. The estimation of the variance of samples withdrawn from a random mixture of multi-sized particles. *Chem. Eng.*, 214: CE270-271.
- Miller, J.D. and Lin, C.L., 1985. Treatment of polished section data for detailed liberation analysis. Paper presented at Engineering Foundation Conference: Recent Developments in Comminution, Hawaii, December 1985.
- Poole, K.R., Taylor, R.F. and Wall, G.P., 1964. Mixing of powders to fine-scale homogeneity: studies of batch mixing. *Trans. Inst. Chem. Eng.*, 42: T305-315.
- Sokaski, M., Jacobson, P.S. and Geer, M.R., 1963. Performance of Baum Jigs in treating Rocky Mountain coals. *U.S. Bur. Mines Rep. Invest.*, 6306: 29-30.
- Stange, K., 1954. Degree of mixing in a random mixture as the basis for evaluating mixing experiments. *Chem. Ing. Tech.*, 26: 331-337.
- Stange, K., 1963. Mixing quality in a random mixture of three or more components. *Chem. Ing. Tech.*, 35: 580-582.

A
S
D

L
1
M
Un
2
D

Ab

The
of g
frac
fun
ma:
of
seve

—

1

K
gr
th
qu
sc
in
sc
(A
gi
si
n
an

2

A
u
d
ir
g
s:

F

v
s
f
g
s
l

A Rapid Method for Determination of Changes in Shape of Comminuted Particles Using a Laser Diffractometer

L. G. Austin¹, O. Trass², T.F. Dumm¹ and V.R. Koka²

¹Mineral Processing Section, Mineral Engineering Department, The Pennsylvania State University

²Department of Chemical Engineering, University of Toronto, Toronto (Canada)

Abstract

The size distributions of carefully screened $\sqrt{2}$ size fractions of ground materials were determined using a Microtrac laser diffractometer. The size distributions were fitted to the empirical function $P(x) = 1/[1 + (x_{50}/x)^\lambda]$ where $P(x)$ is cumulative mass fraction less than Microtrac size, x . The standard deviation of λ for a 50 second test time was approximately 0.5, so that seventeen test times give a mean with an estimated error within

± 0.25 (95% confidence level). Values of λ were 5.44, 4.82, 4.40 for a coal ground under different conditions, indicating statistically different shape distributions; the average value for mica was 2.91 owing to the high aspect ratio of the particles. The ratio of x_{50} to the geometric mean sieve size was 1.2 for the coal and 0.70 for mica.

1 Introduction

Koka and Trass have presented evidence [1,2] that materials ground in the Szego mill [3] give different shapes depending on the milling conditions. The variations in shape were deduced qualitatively by viewing SEM photomicrographs of selected $\sqrt{2}$ screen fractions. This paper quantifies their observed differences in shape by using measurements of the size distributions of $\sqrt{2}$ screen fractions examined in a laser diffractometer [4] (Microtrac, Model 7991). The basic concept is that particles of a given "screen" size will give a wider distribution of "Microtrac" size when the particles are flaky with high aspect ratios, and a narrower distribution when the particles approach the cubical and spherical geometries.

2 Theory

Austin and Shah [5] have shown that coal screened within a $\sqrt{2}$ upper-to-lower sieve size range will give rise to a much wider distribution of Microtrac size. They found that the $\sqrt{2}$ screen interval of irregular fragments of comminuted coals or quartz gave Microtrac size distributions which could be described by the simple function

$$P(x) = \frac{1}{1 + (x_{50}/x)^\lambda} \quad (1)$$

where $P(x)$ is the cumulative mass fraction less than Microtrac size, x , as reported by the instrument; λ was found to be about five, and a mean shape factor, r , defined by x_{50} divided by the geometric mean screen size was in the range 1.2 to 1.3. Figure 1 shows typical results plotted in the form of $1/P(x)-1$ versus x on log-log scales. It is convenient to analyze results on this basis

because the size distribution is expressed in terms of the mean shape factor, r , and the distribution coefficient, λ , where a smaller value of λ means a distribution spread out over a greater range of sizes. Figure 1 shows that this function is a reasonable approximation for the major mass of the samples.

3 Experimental Technique

Samples of relatively strong material such as coal were received in $\sqrt{2}$ screen size fractions, which were then wet screened at 400 mesh to remove any fine material formed during transport. These samples were tested in the usual way in the Microtrac using 0.1% Calgon as dispersing agent, and 0.1% Aerosol OT as wetting agent, in concentrations of 0.50 g coal per liter of water, with a 50 second test time. Samples of comminuted mica were found to be fragile enough to break up on screening, so the samples were dispersed in water, allowed to settle for a few seconds and fine suspended particles decanted. The remaining slurry of screen-size material was then dispersed and tested in the Microtrac.

4 Results

The size distributions of each sample were run five times to enable statistical analysis to be performed. In addition, five separate tests using fresh samples were also performed for the coal ground under conditions A and B, as shown in Table 1. This data does not allow clear decisions to be made concerning statistical reliability because of wide variations in the estimates of standard deviations based on only five tests. Therefore, one

THE RESPIRABLE DUST CENTER

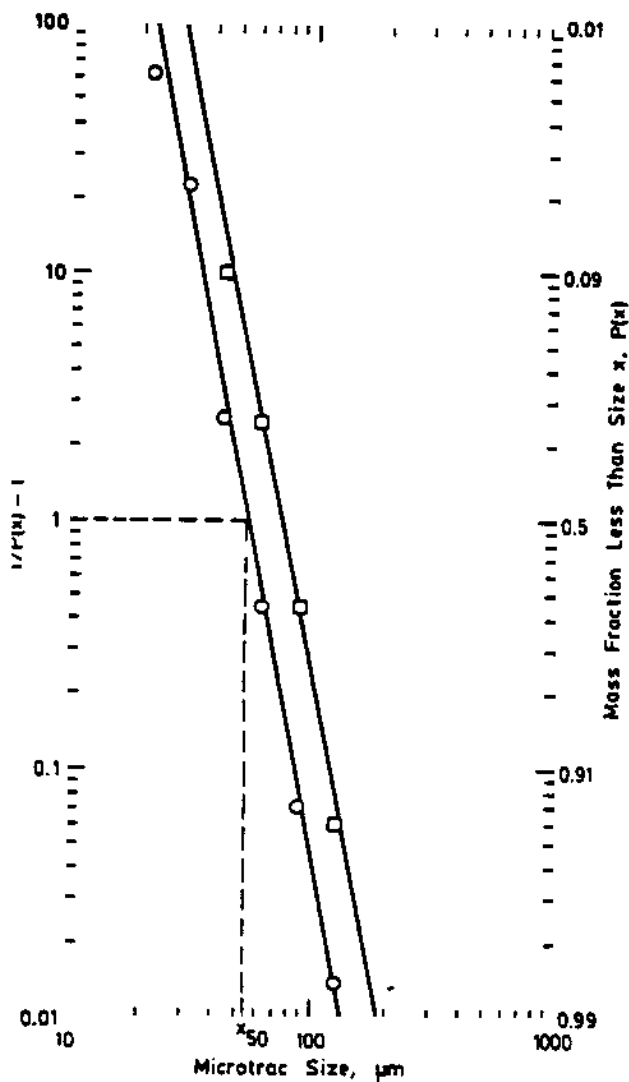


Fig. 1: Typical Microtrac size distributions for material in a 2 screen interval, plotted to fit $P(x) = 1/[1 + (x_{50}/x)^2]$ from [5]. \circ : coal, dry grinding, sieve size 38-53 μm . \square : coal, dry grinding, sieve size 53-75 μm .

sample was run repeatedly for seventeen tests to obtain a better estimate of standard deviation, giving the results shown in Table 2. To ensure consistency in data handling, the fit of Eq. (1) to the data for each test was performed by linear regression analysis using an unweighted least squares criterion.

The data of Table 2 show, as expected, that standard deviations about the mean are widely variable for each group of five tests taken from the population. The overall standard deviations based on the seventeen tests were 2.93 μm on x_{50} and 0.50 on λ for the coal of sieve size 53 \times 75 μm from dry grinding and 3.08 and 0.49, respectively, for the coal from slurry grinding.

The estimates of standard deviations based on the N tests give estimates of the error band on the means, to a 95% confidence level, of $\pm 2\sigma/\sqrt{N-1}$. For the results from only five tests (see Table 1), the values of σ for x_{50} and λ determined above, gave error bands of about $\pm 2.9 \mu\text{m}$ on x_{50} and ± 0.5 on λ , and hence, no statistically significant difference was present between tests A, B and C on either r or λ . As expected, there was a clear difference between these and tests D and E on mica. There was no statistically significant difference between the standard devia-

Table 1: Microtrac size analyses: average of 5 tests of 50 seconds duration.

Test sample (1,2)	Sieve size μm	Test operated five times				
		x_{50} μm	$\sigma_{x_{50}}$ μm	r	λ	σ_{λ}
A. Coal: dry grinding	38-53	53.7	0.58	1.20	4.98	0.31
	53-75	72.5	1.29	1.15	5.29	0.11
B. Coal: 25% in water slurry grinding	38-53	54.6	0.89	1.22	4.52	0.23
	53-75	74.8	1.50	1.19	4.56	0.20
C. Coal-Oil-Water grinding	38-53	55.4	0.89	1.24	4.71	0.27
	53-75	76.8	1.50	1.23	4.75	0.08
D. Mica: wet grinding	38-53	32.4	1.55	0.72	3.22	0.08
	53-75	42.3	1.88	0.67	2.79	0.20
E. Mica: dry grinding	38-53	31.2	0.65	0.70	3.11	0.17
	53-75	42.1	2.15	0.67	2.52	0.13

Five separate tests of 50 second duration

A. Coal: dry grinding	38-53	54.7	1.65	1.22	5.01	0.16
B. Coal: 25% in water slurry grinding	38-53	55.8	1.55	1.24	4.43	0.53

Table 2: Parameters for 50 second Microtrac tests repeated seventeen times.

A. Coal: dry grinding (53-75 μm)		B. Coal: 25% slurry grinding (53-75 μm)	
x_{50}	λ	x_{50}	λ
77.1	5.12	73.7	3.50
76.0	5.35	73.6	4.01
76.8	5.11	75.3	4.16
78.6	6.13	77.2	4.24
79.3	5.63	70.2	4.15
74.0	4.93	78.3	4.26
73.3	5.07	77.4	4.14
73.4	5.38	83.0	3.81
68.7	6.78	79.4	4.10
71.2	5.80	75.7	4.94
75.2	5.41	78.9	4.21
69.8	4.69	80.7	4.62
73.4	5.43	78.7	5.28
73.0	5.27	79.9	4.68
77.3	5.77	74.9	5.14
75.6	4.96	78.6	5.06
75.6	5.73	76.8	4.52
Mean	74.6	77.2	4.40

tions obtained from one test run five times or five separate tests each run one time.

In order to clarify the differences between the coal samples, the number of tests for each sample was increased to 17, reducing the 95% confidence levels on the mean λ to ± 0.25 for the 53-75 μm samples, giving the results in Table 3, A and B. Due to the close agreement of standard deviations between A and B, test C was just performed for a time of $17 \times 50 = 850$ seconds. The distribution of shapes is significantly wider (λ is smaller) for the 25% slurry ground coal than for the coal-oil-water ground coal than for the dry ground coal, in agreement with the qualitative

result:
are sh

Table 3
durati

Test se

A. Dr

B. 25

gr

C. Co

gr

100

Cumulative Weight Percent Less Than Size

Fig.
sieve
coal

Aus
hyd
per
ran
Ho
mo

results of *Trass* and *Koka* [1]. The calculated mean distributions are shown in Figure 2 in the form of Schuhmann plots.

Table 3: Microtrac size analyses: average of seventeen tests of 50 second duration.

Test sample	Sieve size μm	x_{50} μm	$\sigma_{x_{50}}$ μm	r	λ	σ_1
A. Dry grinding	53-75	74.6	2.93	1.18	5.44	0.50
B. 25% slurry grinding	53-75	77.2	3.08	1.22	4.40	0.49
C. Coal-oil-water grinding	53-75	76.0	—	1.21	4.82	—

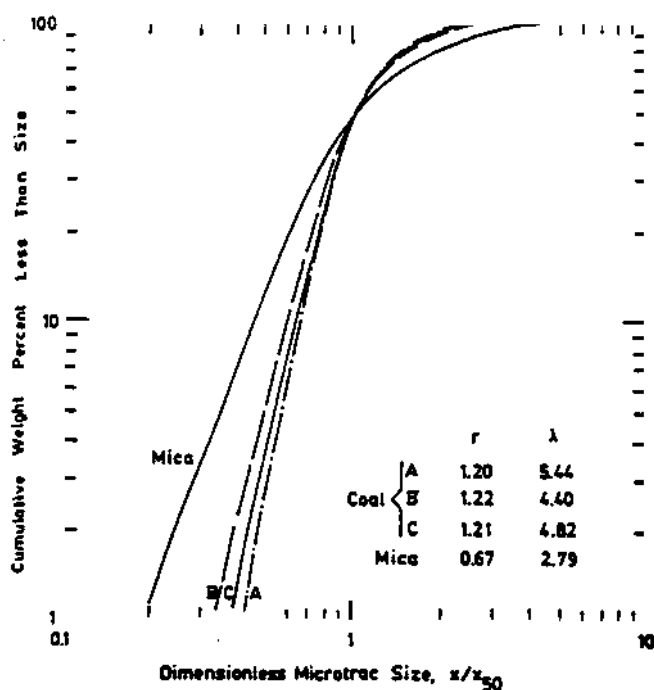


Fig. 2: Calculated average Microtrac size distributions for 53-75 μm sieve samples, averaged for seventeen test times of 50 second duration for coals and five test times of 50 second duration for wet-ground mica.

Austin, Gardner, and Walker [6] have shown that the mean hydrodynamic shape factor, ϕ , obtained from liquid permeability tests on packed beds of coal is a function of coal rank, for coals comminuted under identical conditions. However, the laser diffractometer measurement is simpler and more rapid to perform.

5 Conclusions

Differences in shape between 2 sieve size fractions of ground materials can be quantitatively expressed in terms of a mean shape factor, r , and the spread of the distribution, λ , as measured in a laser diffractometer. However, the standard deviation of the value of λ was 0.5 for a 50 second test time, in the Microtrac instrument, so that at least seventeen test times are necessary to give λ an accuracy within ± 0.25 . The instrument is easy to use, and running a measurement for a 15 minute test time presents no problem for strong materials that are not broken down by repeated passage through the circulating impellers. Future work will examine the variations of r and λ from a more fundamental viewpoint, but the technique can be used to obtain empirical shape factors which enable variation of shapes to be detected in a statistically reliable form.

6 Acknowledgements

Support for part of this work from the Natural Sciences and Engineering Research Council of Canada is gratefully acknowledged.

7 Symbols and Abbreviations

N	number of tests [—]
r	mean shape factor [—]
$P(x)$	cumulative mass fraction less than Microtrac size [—]
x	particle size [L]
x_{50}	median size of particle distribution [L]
ϕ	hydrodynamic shape factor [—]
σ	standard deviation [L, —]
λ	distribution coefficient [—]

8 References

- [1] *O. Trass, V. R. Koka, G. Papachristodoulou*: Particle Shapes Produced by Comminution in the Szego Mill: 1st World Congress Particle Technology, Part 2: Comminution. NMA Nürnberg Messe und Ausstellungen GmbH, 1986, pp. 501-514.
- [2] *V. R. Koka, O. Trass*: Analysis of the Kinetics of Coal Breakage by Wet Grinding in the Szego Mill. *Powder Technol.* 43 (1985) 287-294.
- [3] *E. A. J. Gandolfi, G. Papachristodoulou, O. Trass*: Preparation of Coal Slurry Fuels with the Szego Mill. *Powder Technol.* 40 (1984) 269-282.
- [4] Microtrac Operators Manual. Leeds & Northrup Corp., Largo, Florida.
- [5] *L. G. Austin, I. Shah*: A Method for Interconversion of Microtrac and Sieve Size Distributions. *Powder Technol.* 35 (1983) 271-278.
- [6] *L. G. Austin, R. P. Gardner, P. L. Walker, Jr.*: The Shape Factors of Coals Ground in a Standard Hardgrove Mill. *Fuel* 42 (1963) 319-323.

Washability of ultrafine coal

T.F. Dumm and R. Hogg

Abstract – With increasing interest in the physical cleaning of fine coal, there is a need for extension of the sink-float analysis procedure to finer sizes. Problems arise, however, in ensuring complete dispersion of the particles in the heavy liquids. A procedure has been developed in which surfactants are used as dispersing agents, and solids concentration is minimized (using a simple formula to estimate the minimum weight needed for statistical reliability). Using centrifuges to increase separation rates and subsieve particle size analysis of the specific gravity fractions, a complete size-specific gravity distribution can be obtained. Analyses have been performed on coal samples as fine as $-10\ \mu\text{m}$.

Introduction

Traditional gravity separation techniques such as jigging, heavy media and water-only cyclones, shaking tables, etc., have been used to remove impurities from coal ranging in size from about 15 cm (6 in.) to about 150 μm (100 mesh). The coal washability or float-and-sink technique is a well-established procedure for determining the optimum extent to which a coal can be cleaned by such physical separation methods. Because of the desire to recover even finer coal fractions by gravity separation techniques, there is a need to extend the coal washability analysis into the ultrafine range. The purpose of this paper is to describe some of the significant factors that influence fine particle specific gravity separation. Washability analyses have been performed on three ultrafine ($<10\ \mu\text{m}$) coal samples representing three general mining districts in Pennsylvania. Results of these analyses indicate that the washability technique can be successfully applied to ultrafine particles when proper care is taken.

Specific gravity fractionation

It is possible to characterize, to some extent, the mineral-organic associations in coal particles on a bulk basis using an analysis called float-and-sink, washability, or specific gravity fractionation. By choosing a liquid that has a specific gravity that is

intermediate between the range of specific gravities of the coal particles, a physical separation will occur when the coal powder is placed in the liquid. Particles with specific gravities less than the liquid will float, and particles with higher specific gravities will sink. The float and sink particles are collected, dried, and weighed to determine the fraction of coal powder greater and less than the liquid specific gravity. The sink fraction can then be redispersed in a liquid of higher specific gravity than the previous liquid, resulting in another float and sink fraction. This float material has specific gravities that range between those of the two liquids; the closer the liquids are in specific gravity, the narrower this range. By successively redispersing the sink particles in higher specific gravity fluids, or redispersing the float particles in lower specific gravity liquids, the coal powder can be separated into its specific gravity components.

Heavy organic liquids or solutions of zinc or calcium chloride are commonly used as the liquid medium. The salt solutions are the least expensive, but liquids heavier than about $1.9\ \text{g/cm}^3$ become too viscous for practical use unless more expensive salts, containing heavy metals such as thorium, are used. Organic liquids, such as mixtures of chlorine and bromine halogenated hydrocarbons, are generally more expensive than salt solutions, but offer a wider range of specific gravities (1.0 to $2.9\ \text{g/cm}^3$) with low viscosity. For most fine coal ($<75\ \mu\text{m}$) float-and-sink analyses, organic liquids are most desirable. The organic liquids used in this research are available commercially from American Chemsol Inc. under the trade name of Certigrav.

T.F. Dumm and R. Hogg, members SME, are graduate assistant and professor and section chairman, respectively, Mineral Processing Section, Department of Mineral Engineering, The Pennsylvania State University, University Park, PA. SME preprint 87-136, SME-AIME Annual Meeting, Denver, CO, February 1987. MMP paper 87-624. Manuscript February 1987. Discussion of this paper must be submitted, in duplicate, prior to April 30, 1988.

By separating the coal particles into size intervals before or after the liquid separation procedure, complete size-specific gravity units can be delineated from a sample of coal. The coal powder can then be characterized in terms of a two-dimensional, size-specific gravity matrix, or surface. Ash analyses performed on these units show how the inorganic material is distributed throughout the coal.

Separation rate

When the coal particles dispersed in a heavy liquid form distinct float and sink layers, with no particles in between, the separation is said to be complete. The time needed for particles to either float or sink can be calculated from Stokes' law knowing the particle densities. Particles with densities near to that of the heavy liquid, the "near-gravity" particles, may take a very long time to float or sink.

As can be seen from Table 1, the gravity settling of "near-gravity" particles (in this case, particles with densities within ± 0.01 g/cm³ of the liquid density) becomes extremely slow for particles less than about 150 μ m (100 mesh). Consequently, for ultrafine coal washability analyses, it is necessary to use centrifuges to increase particle settling rates.

Normally, a prior knowledge of the specific gravity distribution of a coal is not available. If a large portion of the coal consists of "near-gravity" particles, a complete separation may take an extremely long time. It is useful, therefore, to centrifuge for various lengths of time until the best separation is obtained.

Table 1 — Particle Separation Times

$\rho = 0.01$ g/cm³; $\mu = 0.01$ poise; settling distance = 3 cm.

Size	Settling Time	
	Gravity	Centrifugal*
4 mesh	0.2 sec	—
12 mesh	2 sec	—
30 mesh	15 sec	—
100 mesh	4 min	0.5 sec
200 mesh	16 min	2 sec
400 mesh	1.1 hrs	8 sec
10 μ m	15.3 hrs	1.7 min
5 μ m	2.5 days	7 min
1 μ m	2.1 months	2.6 hrs

* 26-cm-diam centrifuge at 2000 rpm.

Sample size

When a coal washability analysis is performed, it is common practice to fractionate the coal sample into size fractions, and then submit each size fraction to specific gravity separation. In order for these size and composition fractions to be representative of the bulk material, it is necessary that each fraction contain a sufficient number of individual particles.

The critical size-specific gravity unit for a distribution of coal is usually the coarse, top-size particles that comprise a minimum weight percent of a certain specific gravity. To determine the required weight of coal, M_{ij} , based on the critical unit, the following equation can be used (Hogg, 1935):

$$M_{ij} = \frac{4}{\epsilon^2} [(1/C_j f_{ij} - 2) W_{ij} + \bar{W}] \quad (1)$$

where C_j is the overall mass fraction of specific gravity constituent j , f_{ij} is the mass fraction of constituent j that falls in size class i , W_{ij} is the mean

particle weight for constituent j in size class i , \bar{W} is the overall mean particle weight of the distribution, using average density and size, and ϵ is the acceptable tolerance at the 95% confidence level.

Table 2 shows the minimum amount of the size fractions listed to be used in a washability analysis that would give results having a tolerance of 5% at the 95% confidence level. As can be seen, the amount of coal needed for large particles, i.e., those above 2.5 cm (1 in.), is significant. However, the amount needed for an accurate representation of the fine fractions below 150 μ m (100 mesh) is much less than 1 g. Commonly, for reasons dictated by subsequent analyses of the float and sink fractions for such things as ash and sulfur or by gravimetric detection limits, the minimum weight used in a specific gravity fractionation is about 5 to 10 g. However, for separating ultrafine particles, it is necessary to minimize particle-particle interactions during separation to ensure complete dispersion of the particles. It is useful, therefore, to minimize the solids concentration by using the calculated minimum sample weight.

Table 2 — Minimum Sample Requirements for Washability Analysis

Size	Recommended Amount
5 x 3 in.	10 tons
2 x 1 in.	2 tons
4 x 6 mesh	1.1 kg
12 x 16 mesh	49 g
20 x 30 mesh	5 g
70 x 100 mesh	0.14 g
200 mesh x 0	64 mg
400 mesh x 0	8 mg
10 μ m x 0	1.6 mg

Fractionation scheme

There are several ways in which the washability analysis can be performed. Usually, the coal to be tested is sieved into size intervals, and each size interval is fractionated by successively redispersing the sink fraction in higher specific gravity liquids. However, in the case of ultrafine coal, it is not usually practical to separate the coal powder into size fractions. In this case, the specific gravity fractionation can be done on the entire size distribution, and subsieve size analyses performed on the resulting specific gravity units. This method of float-and-sink analysis, using successive separations of a single sample, will be referred to as the incremental method.

Another method of fractionating the ultrafine material is to disperse the calculated minimum amount of powder into each heavy liquid where a separation is to be made. After separation has occurred in each vessel, the resulting float fractions will represent the cumulative fraction of the total coal that floats at that specific gravity. The incremental weight fraction of material, w_j , contained within each specific gravity unit can be determined from

$$w_j = W_j - W_{j-1} \quad (2)$$

where W_j and W_{j-1} are the cumulative fractions of coal floating in the j^{th} separation and the previously lower specific gravity $j-1$ separation, respectively. For the first float and last sink fraction of a series, $w_1 = W_1$. This float-and-sink method will be referred to as the cumulative method. The cumulative method is preferred when analyzing ultrafine particles because

they are only ever in contact with one specific gravity fluid and because small differences in specific gravity fractions can be determined without handling extremely small quantities of coal.

Size analysis

If a large portion of the ultrafine coal powder is less than 38 μm (400 mesh) in size, subsieve sizing techniques must be used. Appropriate methods include the electrical sensing zone (Coulter Counter), light obscuration (Hiac/Royco Model 4300), and light scattering (Microtrac Particle Analyzer) techniques.

Size analysis on the cumulative float fractions will also yield cumulative size information. The incremental mass fraction f_{ij} of particles of size i within each specific gravity unit j can be extracted from the size distributions f'_{ij} of the cumulative float fractions such that

$$f_{ij} = \frac{W_j f'_{ij} - W_{j-1} f'_{ij-1}}{\sum_{l=1}^n \sum_{m=1}^m (W_j f'_{lm} - W_{j-1} f'_{lm-1})} \quad (3)$$

where f'_{ij} is determined by using a suitable particle sizing technique. For the first float and last sink fraction of the series, $f_{ij} = f'_{ij} W_j$.

Ash analysis

Ash analysis can be performed on the incremental or cumulative float-and-sink fractions to determine the ash content of each specific gravity fraction. If the cumulative washability technique is used, the incremental ash content value, a_j , can be determined by dividing the incremental weight of ash, b_j , by the incremental weight of coal, w_j , such that

$$a_j = \frac{b_j}{w_j} = \frac{B_j - B_{j-1}}{W_j - W_{j-1}} \quad (4)$$

where B_j and B_{j-1} are the cumulative ash weights, and W_j and W_{j-1} are the cumulative total weights at the j th separation and next lowest specific gravity, respectively.

Since the particles are not physically separated into size classes within each specific gravity unit, ash analyses can only be done on the entire unit. Although this does not give results on how mineral matter is distributed with particle size within the coal, its association with the specific gravity distribution can still be made.

Experimental

Materials

Three coals were chosen from the Penn State Coal Data Base to represent three different ranks of coal from three different mining areas in Pennsylvania. These coals are designated PSOC 1192M, PSOC 1361P, and PSOC 867. All coal samples used were originally collected as channel samples so that the composition of the final product would be representative of the whole seam. Three coal powders were prepared by a special technique (Dumm, 1986) to produce standard respirable dusts, i.e., coal powders that were less than 10 μm in size and that had uniform composition within each sample. Table 3 lists some important information on each of the three coals.

Table 3 — Coals Used in the Study

Coal Designation	PSOC 1192M	PSOC 1361P	PSOC 867
Seam	Lower Kittanning	Upper Freeport	Primrose
Seam Location, County	Clearfield	Lawrence	Schuylkill
ASTM Rank	Med. Vol. Bit.	Hi. Vol. A. Bit.	Anthracite
% Low Temperature Ash	9.54	7.77	24.20

Float-and-sink analyses were performed on the standard respirable dusts to determine their size-specific gravity and low temperature ash-specific gravity distributions.

Size analysis of one of the coal powders revealed that the top-size interval of the coal contained 2.3% by weight between 10.55 and 14.92 μm. Assuming that 10% of these particles are mineral matter (density 2.65 g/cm³), the minimum amount of coal to be representative of the bulk sample of standard respirable dust was determined to be about 2 mg using Eq. 1.

To avoid measurement limitations while weighing the specific-gravity fractions, however, the minimum amount of standard respirable coal dust used in the float-and-sink procedure was increased to about 10 mg.

Particle dispersion

When an adequate amount of coal dust had been determined using Eq. 1, the coal dust was dispersed in the desired Certigrav liquid. When this was done with the standard respirable dusts, it was observed that a certain degree of agglomeration was occurring. After ultrasonic treatment failed to alleviate the problem, several dispersants were tried. Of the dispersants that were available, 100% solid (nonaqueous) Aerosol-OT, distributed through Fisher Scientific Co., was found to give the most stable dispersion.

To determine the required amount of Aerosol-OT needed in solution with Certigrav, a series of Aerosol-OT/Certigrav mixtures was prepared using 1.4 specific gravity Certigrav with varying concentrations of Aerosol-OT. A 10-mg sample of a 1:1 coal (PSOC 1192M)/clay mixture was dispersed in each solution in a special centrifuge tube. These suspensions were then centrifuged for various lengths of time after which the float and sink were separated. The ash content of the float fraction was determined for each mixture and plotted against Aerosol-OT concentration. The optimum concentration of Aerosol-OT is that needed to reduce the ash content of the float to a minimum level. This procedure was repeated for a higher specific gravity of 1.9. Figure 1 shows the results of this procedure for both specific gravity liquids. It can be seen that both float fractions reach a fairly constant ash content of about 10% at Aerosol-OT concentrations greater than 20 mg/mL or 2% by weight. For all subsequent float-and-sink analyses, Certigrav containing 2% by weight of 100% solid Aerosol-OT was used.

Heavy liquid separation

Approximately 10 mg of coal dust was dispersed into two 50-mL Teflon FEP centrifuge tubes, each containing 30 mL of the same specific gravity, prepared Certigrav. It is necessary to use the Teflon centrifuge tubes because this plastic is inert to the Certigrav; it is also durable, flexible, and translucent. The two tubes containing the dispersed particles were balanced and placed into opposing holders in a Dynac Model 0063 centrifuge. In a similar manner, two more coal samples were dispersed into tubes containing

P V T B
PERCENT TA IN FLOAT FRACTION
F O C I
f h c n c o c f l s i g b t e i r e w d a t h r m r l p i t r a r p C P

COAL WASHABILITY

another specific gravity Certigrav, balanced, and placed into the centrifuge. When the centrifuge, which is capable of holding four 50-mL centrifuge tubes, was full, the contents were centrifuged at about 2000 rpm (about 600 G) for a set period of time.

8 hours at specific gravity intervals of 1.3, 1.4, 1.5, 1.6, 1.7, 1.8, 1.9, and 2.0 showed that all separations were complete after 15 minutes of centrifuging except in the 1.3 specific gravity liquid. Table 4 shows that at least three hours of centrifuge time is necessary before the 1.3 specific gravity fraction attains complete separation. Although the maximum centrifuging time could vary with each coal, three-hour runs were used for all subsequent analyses.

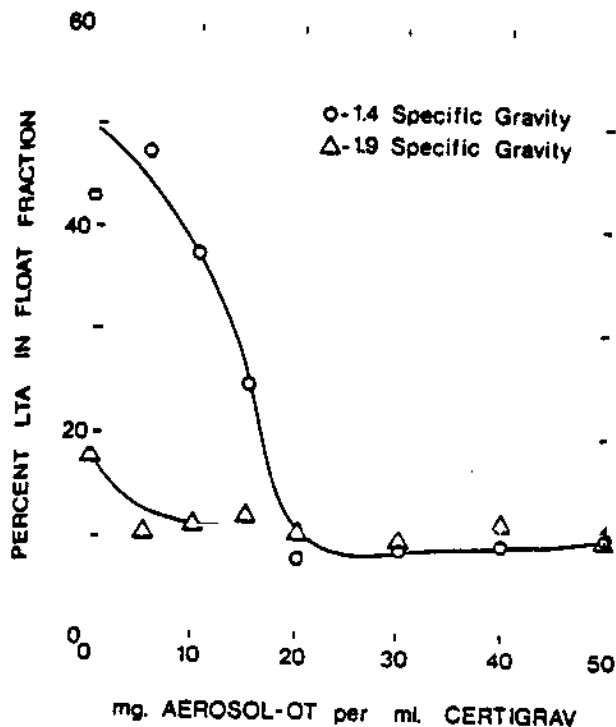


Fig. 1 — Percent ash in float fraction as a function of Aerosol-OT (100% solid) concentration in Certigrav from PSOC 1192M/clay mixture

Table 4 — Weight Percent of PSOC 1192M in Specific Gravity Intervals

Sp. Gr.	Centrifuge Time at 2000 rpm, Hours				
	1/4	1/2	1	2	3
1.3 Float	25.7	20.9	18.4	5.9	1.7
1.3 x 1.4	39.9	43.2	41.8	53.3	60.3
1.4 x 1.5	21.4	21.9	25.5	28.7	24.8
1.5 x 1.6	0.0	3.8	2.1	0.2	0.1
1.6 x 1.7	2.8	0.9	3.7	3.4	2.7
1.7 x 1.8	0.0	0.8	0.3	0.0	2.7
1.8 x 1.9	2.1	0.0	1.3	1.0	0.0
1.9 x 2.0	1.4	3.0	0.8	0.0	1.6
2.0 Sink	6.7	5.7	6.1	7.5	6.2

Size analysis

Size analyses were performed using the Microtrac Small Particle Analyzer (SPA), manufactured by Leeds and Northrup Inc., Largo, FL. The device determines particle size distributions of powders dispersed in a liquid from the forward and right angle scattering of light emitted from a helium-neon laser and a tungsten lamp. The size range determined by the apparatus is 42 to 0.12 μm .

Since there were two sets of float-and-sink data from each test (the two opposing tubes with the same specific gravity), one set was used for size analysis and the other for ash analysis. After all of the gravity fractions were weighed, size analyses were performed on the float fractions and final sink fraction of one set of fractionated coal dust using the Microtrac SPA. Each filter with deposited coal particles on it was put into a clean 30-mL beaker containing 20 mL of water with 0.2% Aerosol-OT and 0.1% sodium metaphosphate as wetting and dispersing agents. The beakers were then subjected to ultrasonic energy for as long as necessary (usually about three to seven minutes) until the coal particles were removed from the filter. Additional stirring and ultrasonic treatment after the filter was removed from the beaker and checking a drop of slurry under the optical microscope helped insure the particles were dispersed. The dispersed particles were analyzed for size by the Microtrac SPA (using a modified recirculator). Although it is possible to retrieve the particles from the Microtrac SPA after size analysis is performed, this was not done for the standard respirable dusts.

Having obtained a size analysis on the float and final sink fractions, Eq. 3 was used to determine the fraction of particles of size i contained in each specific gravity interval j . With this information, it is possible to develop a two-dimensional matrix describing the size-specific gravity distribution of the dust. It is also possible to report this information in terms of surface plots or block diagrams.

Ash analysis

The complementary set of fractionated coal dust samples was used for ash analysis using the low temperature ashing (LTA) technique.

When centrifuging was complete, the float and sink fractions were ready for separation. After a centrifuge tube was removed from the holder, the tube was carefully pinched at a predetermined level using a modified pair of Vice-grip clamps. The position of the clamp was such that 50% of the fluid was in each half of the tube after a tight seal was made. When the centrifuge tube had been crimped in the middle, the float material was poured onto a 25-mm, 0.4- μm pore size Nuclepore polyester membrane filter using a glass fiber backup filter. Nuclepore polyester membrane filters were used because they have very low tare weights, do not absorb ambient moisture, are inert to the Certigrav, and the deposited particles are easy to remove for subsequent size analysis.

The top half of the centrifuge tube was rinsed clean with ethyl acetate onto the filter, and the particles deposited on the filter were further rinsed to remove any residual Certigrav. The filter was removed from the filter holder and air-dried. The clamps were removed from the centrifuge tube, and the sink material was poured onto another Nuclepore filter, rinsed with ethyl acetate, and dried. This separation procedure was then repeated on the remaining centrifuge tubes. When all the tubes were emptied, another series of specific gravities was used, and the process was repeated.

Centrifuging time

Float-and-sink analyses of standard respirable dust PSOC 1192M at centrifuge times of 0.25, 0.5, 1, 2, and

THE RESPIRABLE DUST CENTER

The weights of the float and sink fractions were recorded, and each filter was placed in a 10-mL beaker. The beakers were then placed in the chamber of a Branson/IPC low temperature asher and ashed for about three hours. The LTA remaining in the beakers was redispersed and redeposited onto similar Nuclepore membrane filters. The LTA content was determined by weighing the filters and dividing by the original weight of coal.

Equation 4 was used to convert the cumulative low temperature ash content values into incremental ash content values.

Results

Table 5 lists the two sets of cumulative float data for PSOC 1192M. The raw data show that there is a small decrease in cumulative weight percent float for both sets of data at 1.8 specific gravity. Since all samples in each separation are considered identical, this decrease represents an error in either the 1.7 or the 1.8 specific gravity separation. These terms were corrected by replacing them with the average of the 1.7 and 1.8 cumulative float values. In both sets of data, the difference between the uncorrected and average values was less than 1% by weight. Whenever the difference between two cumulative values resulted in negative values in Eq. 2 to 4, the cumulative values were replaced with the average of the two.

Table 5 — Uncorrected and Corrected Data Sets of Specific Gravity Fractionation

Float	Cumulative Percent Float		Corrected Cumulative Percent Float	
	Set 1	Set 2	Set 1	Set 2
1.3	1.2	2.2	1.2	2.2
1.4	62.1	61.9	62.1	61.9
1.5	86.8	86.6	85.4	86.8
1.6	84.1	89.7	85.4	89.6
1.7	89.6	89.6	89.6	89.6
1.8	92.6	92.6	92.1	92.4
1.9	91.7	92.2	92.1	92.4
2.0	94.6	92.9	94.6	92.9

As can be seen from Table 5, the technique appears to give very reproducible results for sets that are centrifuged for the same amount of time.

The corrected cumulative float values of PSOC 1192M were used with Eq. 3 and the size distributions of each float fraction to obtain the size-specific gravity distribution of the coal. The results are given in Table 6

and illustrated graphically in Fig. 2. It can be seen from the table that the larger size intervals ($>2.63 \mu\text{m}$) contain more lower specific gravity particles than the smaller size intervals, which seem to contain more of the higher specific gravity particles. Size analysis of the float fractions indicates that the size distributions of the different specific gravity intervals are quite similar, with an average median size of $4.4 \mu\text{m}$; however, the 2.0 sink interval, with a median size of $2.91 \mu\text{m}$, is considerably finer than the float fractions. Table 6 and Fig. 2 show that the size-specific gravity distribution is distinctly bimodal. About 80% of the coal particles are less than 1.7 specific gravity, and in the size range 0.66 to $10.55 \mu\text{m}$, there are very few particles between 1.7 and 1.8 specific gravity. These results are consistent with what would be expected for a well-liberated coal.

The ash content of each specific gravity interval from the second set of data was calculated using Eq. 4 and normalized with respect to sample weight. Again, if the difference between two cumulative values resulted in a negative interval value, the cumulative values were replaced with the average of the two. Table 7 lists the ash content values of each specific gravity interval for PSOC 1192M. Cumulative ash values in Table 7 were determined by dividing the cumulative ash weights by 10,000 mg. The calculated ash was determined by adding the ash of the float and sink and dividing by the total weight of coal for each separation. The average of these values is to be compared to the total cumulative percent ash. The distribution of ash with respect to specific gravity is shown in Fig. 3.

From Table 7 and Fig. 3, it can be seen that 37% of the bulk composition of the coal dust above 1.8 specific gravity is inorganic matter, compared to just 4.2% of the bulk composition below this specific gravity. Again, these results are consistent with what would be expected for a well-liberated coal.

The size-specific gravity distribution of standard respirable coal dust PSOC 1361P is illustrated in Fig. 4. The distribution is quite similar to that for PSOC 1192M (Fig. 2) except that this coal contains substantially more of the very lightest fraction (1.3 float).

The distribution of ash content of the PSOC 1361P dust is given in Table 8. The overall cumulative percent ash value of 7.6 agrees well with the average value calculated from each separation.

The size-specific gravity distribution of PSOC 867 is shown in Fig. 5. It can be seen that this coal (anthracite) is significantly different from PSOC 1192M and 1361P, as would be expected. The composition of this coal is such that 67% is between specific gravities 1.9

Table 6 — Size-Specific Gravity Distribution of PSOC 1192M as a Percentage of the Total Coal

Size, μm	42.21	29.85	21.10	14.92	10.55	7.42	6.27	3.73	2.63	1.99	1.01	0.66	0.43	0.34	0.24	0.17
(% Total)	0.0	0.0	2.1	0.8	6.3	22.7	23.9	15.8	9.6	7.3	5.4	2.5	1.1	0.4	0.1	0.0
Sink/Float																
1.3	0.0	0.0	0.0	0.0	0.1	0.2	0.2	0.1	0.1	0.0	0.0	0.0	0.0	0.0	0.0	0.0
1.3 x 1.4	0.0	0.0	0.1	0.0	4.9	13.4	13.8	6.0	3.8	2.7	1.8	0.7	0.0	0.0	0.0	0.0
1.4 x 1.5	0.0	0.0	0.4	0.5	2.3	3.5	3.3	2.3	2.1	1.8	1.1	0.5	0.0	0.0	0.0	0.0
1.5 x 1.6	0.0	0.0	0.0	0.0	0.8	2.7	1.5	0.9	1.4	1.1	0.8	0.3	0.0	0.0	0.0	0.0
1.6 x 1.7	0.0	0.0	0.0	0.0	0.0	0.0	0.0	3.6	2.8	0.0	0.0	0.0	0.0	0.0	0.0	0.0
1.7 x 1.8	0.0	0.0	0.0	0.0	0.0	0.0	0.0	0.4	1.1	1.1	0.9	0.5	0.0	0.0	0.0	0.0
1.8 x 1.9	0.0	0.0	0.5	0.2	0.0	0.0	0.0	0.0	0.0	0.0	0.0	0.6	0.9	0.4	0.1	0.0
1.9 x 2.0	0.0	0.0	1.0	0.1	0.0	1.0	0.0	0.0	0.0	0.0	0.0	0.0	0.0	0.0	0.0	0.0
2.0	0.0	0.0	0.1	0.0	0.2	0.9	1.5	1.3	1.1	0.8	0.6	0.4	0.2	0.0	0.0	0.0

COAL WASHABILITY

and 1.5 having size of 1.0 to 14.9 μm . Only 1% by mass of this coal is less than 1.5 specific gravity compared to 70% for PSOC 1192M and 80% for PSOC 1361P. The size distribution determined from the 1.6 specific gravity fraction was assumed for the lower float fractions due to insufficient amounts of these materials for size

analysis. The float fraction size distributions tended from fairly coarse with median values of 5.9 μm at 1.6 specific gravity float to 4.8 μm at 2.0 specific gravity float. As with the other coals, the 2.0 specific gravity sink was substantially finer than the other fractions, having a median size of 3.8 μm .

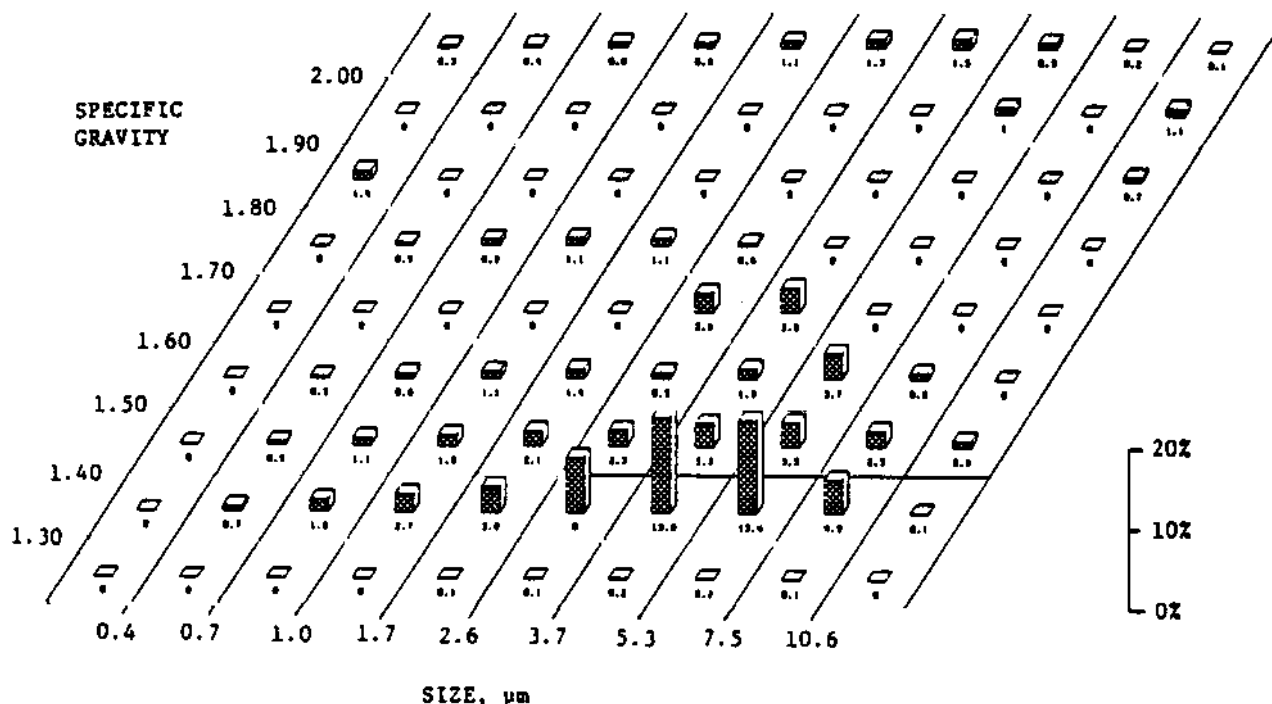


Fig. 2 — Size-specific gravity distribution of standard respirable dust PSOC 1192M as a percent of total coal

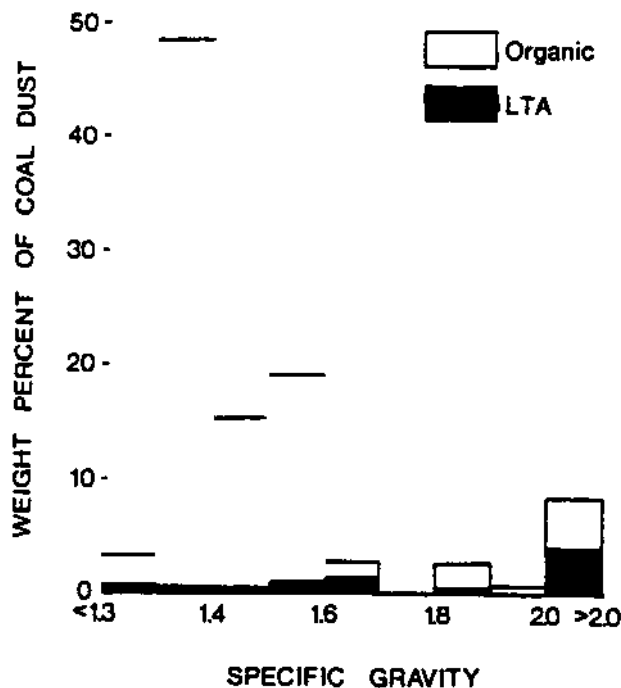


Fig. 3 — Low temperature ash-specific gravity distribution of standard respirable dust PSOC 1192M as a percent of total coal

Table 7 — Ash Analysis of PSOC 1192M Specific Gravity Fractions

Specific Gravity	Total WL in Interval, per 10 mg	WL Ash in Interval, per 10 mg	% Ash in Interval	Cumulative Ash Content	Calculated Ash of Float + Sink
1.3 Float	0.224	—	—	—	8.9
1.3 x 1.4	5.865	0.075	1.3	0.8	8.2
1.4 x 1.5	2.483	0.145	5.8	2.2	8.3
1.5 x 1.6	0.280	0.037	13.2	2.6	8.2
1.6 x 1.7	0.000	—	—	2.6	7.4
1.7 x 1.8	0.277	0.026	9.4	2.9	7.6
1.8 x 1.9	0.900	—	—	2.9	7.7
1.9 x 2.0	0.052	—	—	2.9	7.5
2.0 Sink	0.709	0.331	46.7	6.1	Avg. = 8.0
	10.000	0.781			

Table 8 — Ash Analysis of PSOC 1361P Specific Gravity Fractions

Specific Gravity	Total WL in Interval, per 10 mg	WL Ash in Interval, per 10 mg	% Ash in Interval	Cumulative Ash Content	Calculated Ash of Float + Sink
1.3 Float	2.032	0.055	2.7	0.6	6.2
1.3 x 1.4	1.578	0.000	0.0	0.6	7.8
1.4 x 1.5	4.390	0.100	2.3	1.6	7.9
1.5 x 1.6	0.618	0.013	2.1	1.7	7.8
1.6 x 1.7	0.474	0.043	9.1	2.1	7.9
1.7 x 1.8	0.078	—	—	2.1	7.5
1.8 x 1.9	0.151	—	—	2.1	7.6
1.9 x 2.0	0.014	—	—	2.1	7.8
2.0 Sink	0.688	0.508	75.8	7.2	Avg. = 7.8
	10.000	0.781			

THE RESPIRABLE DUST CENTER

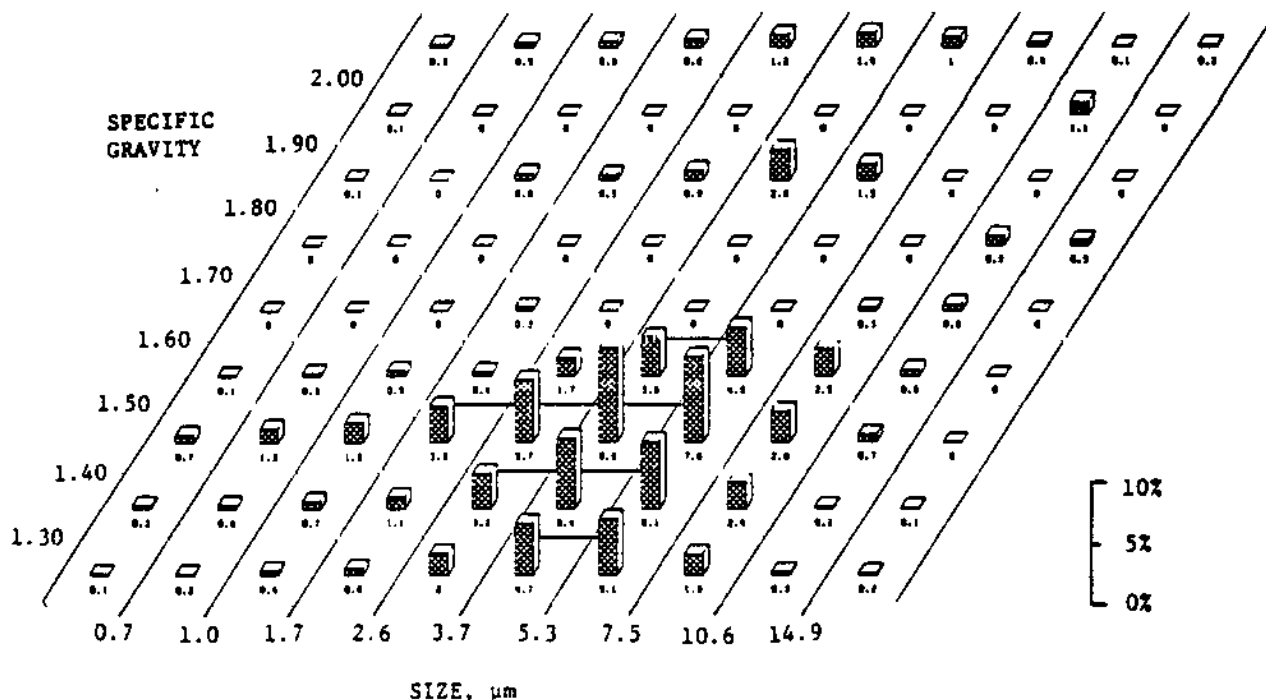


Fig. 4 — Size-specific gravity distribution of standard respirable dust PSOC 1361P as a percent of total coal

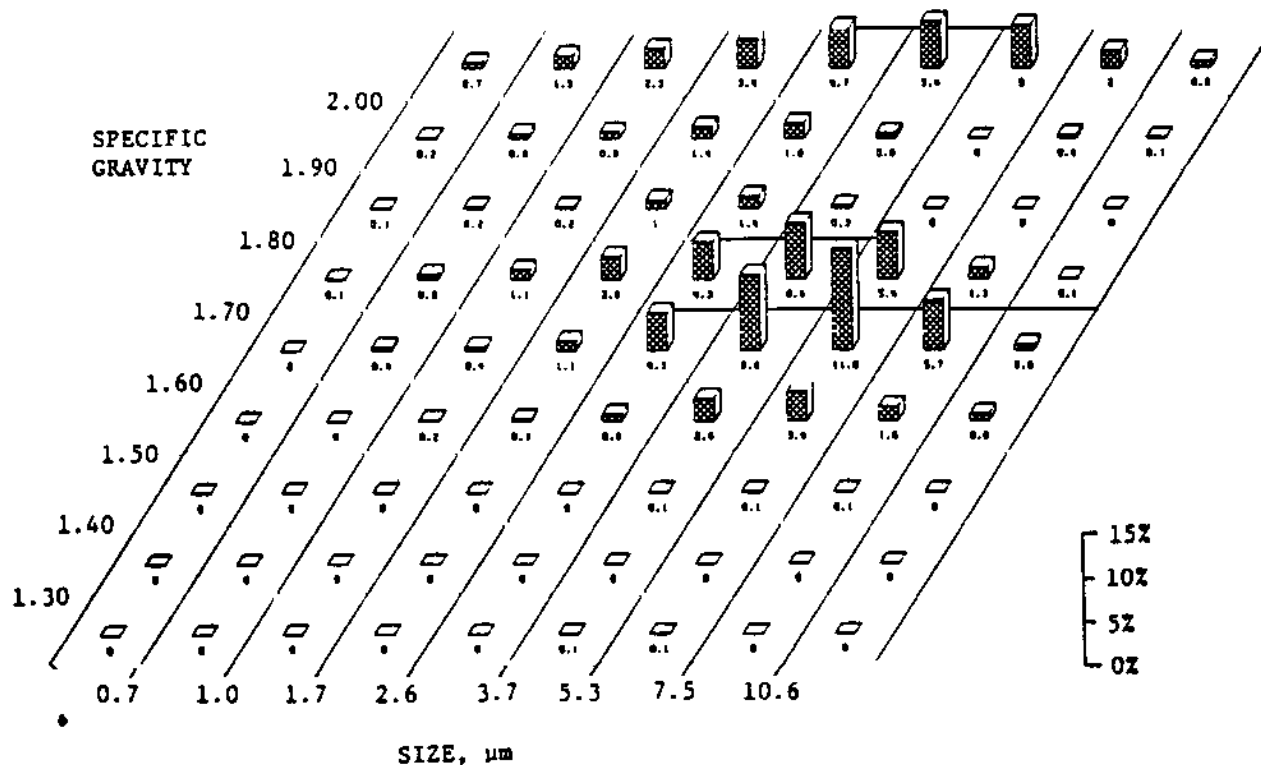


Fig. 5 — Size-specific gravity distribution of standard respirable dust PSOC 867 as a percent of total coal

Although the components of this coal have higher specific gravities than the previous standard respirable dusts, this technique still detects a distinct separation between organic and mineral matter at a specific gravity of 1.9, which again indicates that this is a well-liberated coal dust. Table 9 shows the ash associated with each specific gravity interval.

Errors

Because of the need to maintain extremely low solids concentrations in the heavy liquids in order to minimize particle agglomeration, it is clearly necessary to exercise great caution in performing these analyses to avoid weighing errors, losses during

COAL WASHABILITY

transfer, etc. It appears, however, that there may also be inherent errors in the fractionation process. Examination of Table 4 reveals that the quantity of material in the lightest fraction (1.3 float) decreases substantially with time over the three-hour centrifuging period. To some extent, this could be explained by the low settling rate of the near-gravity particles. However, calculated settling rates indicate that even particles of specific gravity 1.31 in the size range 1 to 10 μm , typical of this material (see Table 1), should have essentially all settled out in less than one hour.

Table 9 — Ash Analysis of PSOC 867
Specific Gravity Fractions

Specific Gravity	Total Wt. in Interval, per 10 mg	Wt. Ash in Interval, per 10 mg	% Ash in Interval	Cumulative Ash Content	Calculated Ash of Float + Sink
1.3 Float	0.023	—	—	—	22.9
1.3 x 1.4	0.022	—	—	—	21.5
1.4 x 1.5	0.042	—	—	—	23.0
1.5 x 1.6	1.006	0.080	8.0	0.8	16.1
1.6 x 1.7	3.413	1.034	1.0	1.1	21.4
1.7 x 1.8	2.174	0.054	2.5	1.7	19.3
1.8 x 1.9	0.240	0.093	38.8	2.8	21.6
1.9 x 2.0	0.000	—	—	2.8	21.4
2.0 Sink	3.080	1.849	60.0	21.1	Avg. = 20.9
	10.000	2.110			

An alternative explanation may be that the heavy liquids slowly penetrate into the porous coal particles, increasing their effective density with time. Such effects might not be observed in conventional sink-float analyses on +150- μm (+100-mesh) particles, where much greater penetration would be necessary before the change in apparent density would become noticeable and where the time of contact with the heavy liquid is normally much shorter. Slow penetration of porous coal particles by heavy liquids could also explain some apparently anomalous results reported by other investigators (US Dept. of Energy; Cho, 1986) who have observed a decrease in the relative amounts of the lightest fractions as the coal is ground progressively finer.

It is clear that further research is needed into the interaction of coal particles with the heavy liquids used for specific gravity fractionation. The apparent density of any porous solid in a fluid medium obviously

depends on the extent of penetration of the medium into the pores. For microporous materials such as most coals, where penetration rates may be quite low and dependent on wetting characteristics, etc., this raises questions not only with respect to the validity of float-and-sink data but also of the value of such data for predicting "washability."

Conclusions

The results of this investigation indicate that the float-and-sink procedure can indeed be extended to ultrafine particles provided steps are taken to ensure complete dispersion of the particles in the heavy liquids and sufficient time is allowed for separations to reach completion. Micron-size particles of near-gravity material may require very long separation times (hours) even in high-speed centrifuges. Appropriate measures to ensure dispersion of the particles include the use of surfactants such as Aerosol-OT to reduce particle-particle attraction and very low solids concentration to minimize interparticle collisions. Since statistical constraints are easily satisfied for very fine particles, sample size can be determined on the basis of the minimum quantity needed for reliable weighing of the fractions etc. The relative extent of heavy liquid penetration into the internal pores of the coal particle is an area where further research is clearly needed. ■

Acknowledgments

The work described in this paper was supported, in part, under The Mineral Institutes program by Grant No. G1135142 from the Bureau of Mines, US Department of the Interior, as part of the Generic Mineral Technology Center for Respirable Dust.

References

- Cho, H.C., 1986, "Liberation of Coal Macerals," MS Thesis, The Pennsylvania State University, University Park, PA.
- Dumh, T.F., 1986, "An Evaluation of Techniques for Characterizing Respirable Coal Dust," MS Thesis, The Pennsylvania State University, University Park, PA.
- Hogg, R., 1985, "Characterization Problems in Comminution — An Overview," Engineering Foundation Conference on Recent Developments in Comminution, Hawaii, December, to be published in *International Journal of Mineral Processing*, Vol. 22, 1988.
- US Department of Energy, Pittsburgh Energy Technology Center, private communication.

Potential Role of Silicon-Oxygen Radicals in Acute Lung Injury

N.S. Dalal¹, X. Shi¹ and V. Vallyathan²

¹Department of Chemistry, West Virginia University

²Division of Respiratory Disease Studies, National Institute for Occupational Safety and Health, Morgantown, WV

INTRODUCTION

This paper summarizes our recent investigations of the potential role of silicon-oxygen based free radical species in the biochemical mechanism of the lung injury caused by the inhalation of freshly fractured silica. The impetus for this study came from the following observations. Inhalation of crystalline silica is associated with the development of acute and chronic silicosis. Chronic silicosis is characterized by the development of sharply marked concentric fibrotic nodules in the lung. This occurs over a period of several decades with the development of progressive respiratory impairment. In contrast, acute silicosis is manifested by the filling of the alveoli with an amorphous lipoproteinaceous exudate within a short period after exposure, and rapid development of respiratory disability often leading to fatality. Most studies on the pathogenesis of silicosis have focused on the elucidation of cellular mechanisms of cell injury and the development of chronic silicosis. Because pulmonary responses to crystalline silica are distinctly different for the acute and chronic silicosis, we hypothesized that the acute response is associated with some unique properties of freshly formed silica particle surfaces, due to the formation of some reactive chemical species caused by the rupturing of the silicon-oxygen bonds. In occupations involving drilling, tunneling and sandblasting operations acute silicosis can be correlated with this unique surface reactivity of silica. The formation of reactive species was demonstrated, using electron spin resonance (ESR) spectroscopy (Dalal et

ESR, BIOCHEMICAL STUDIES OF QUARTZ

al., 1986; Fuibini et al., 1987; Hochstrasser and Antononi, 1972). Grinding of quartz crystals under ultra high vacuum (10^{-10} torr) leads to the formation of $\text{Si}\cdot$ and $\text{SiO}\cdot$ radicals and these radicals are quenched by exposure to air and other gases (Hochstrasser and Antononi, 1972). ESR signals have also been reported from micronized quartz samples that were evacuated at 413 K (Bolis et al., 1983). In order to find a more direct relationship of such radicals to acute silicosis, we made ESR measurements on quartz dusts freshly ground in ambient air and found that indeed grinding under ambient environment leads to the formation of the $\text{Si}\cdot$ and $\text{SiO}\cdot$ type of radicals which decay on storing the dusts in air or in biological buffers (Dalal et al., 1986; Vallyathan et al., 1988). The $\text{Si}\cdot$ and $\text{SiO}\cdot$ radical formation on grinding has also been reported by Fubini et al. (1987). In addition, we recently found that $\cdot\text{OH}$ radicals are generated in aqueous suspensions of freshly ground quartz (Dalal et al., 1988; Shi et al., 1988; Vallyathan et al., 1988). We have subsequently carried out detailed cytotoxicity and biological assays on freshly made as well as aged quartz dusts. As summarized below, the results provide new insight into the biochemical mechanism of acute silicosis.

MATERIALS AND METHODS

ESR spectra were obtained at X-band (-9.7 GHz) using a Bruker ER 200D ESR spectrometer, employing a self-tracking NMR gaussmeter and a microwave frequency counter. Crystalline quartz with particle sizes of 0.2 to 2.5 mm was obtained from the Generic Respirable Dust Technology Center, Pennsylvania State University, University Park, PA. Particles in the range of smaller than 25 microns were produced in an agate mortar ball machine grinder in air for 30 minutes and sieved through a 20-micron mesh filter before use. All chemicals and biochemicals used were obtained from Sigma, St. Louis, MO.

Alveolar macrophages were harvested from male pathogen-free Sprague-Dawley rats by bronchopulmonary lavage using a calcium- and magnesium- free Hank's balanced salts solution as described previously (Myrvia and Evans 1967). Microscopic estimates of purity indicated that 90 to 95% of the lavaged cells were alveolar macrophages (Phillips, 1973).

Silica-induced activation of respiratory burst in alveolar macrophages was monitored by measuring O_2^- and H_2O_2 release. O_2^- release was monitored by measuring the superoxide-dependent reduction of cytochrome c spectrophoto-

metrically at 550 nm using a Gilford Spectrophotometer (Model 300-N) (Sweeney et al., 1981). H_2O_2 release was monitored by measuring the change in fluorescence of scopoletin in the presence of horseradish peroxidase (Van Scott et al., 1984). Fluorescence was monitored at an excitation wavelength of 350 nm and an emission wavelength of 460 nm using a Perkin-Elmer Fluorescence Spectrophotometer (Model MPG-36) equipped with a stirrer and temperature controlled at 37°C.

The cytotoxic potential of fresh or aged silica was monitored by determining the effects of these dusts on cellular membrane integrity, i.e., hemolysis of red blood cells and release of cytosolic lactate dehydrogenase (LDH) from alveolar macrophages. Hemolytic activity of freshly ground or aged quartz particles was measured in a 2% suspension of sheep erythrocytes as the amount of hemoglobin released after incubation in the presence of quartz particles (Nolan et al., 1981). The LDH release was measured by incubating the alveolar macrophages (2×10^6) for different time intervals in a shaking water bath at 37°C in the presence of quartz particles. After incubation, cell suspensions were centrifuged and LDH released from the macrophages was estimated in the supernate (Wroblewski et al., 1955).

RESULTS

A. ESR Measurements on Freshly Ground Quartz

Figure 1 shows some typical ESR spectra of fresh quartz particles ground by an agate ball machine grinder in air. The measured g-values are $g_1 = 2.0017$ and $g_2 = 2.0007$. Such ESR spectra from quartz are characteristic of silicon-based radicals ($Si\cdot$, $SiO\cdot$) (Hochstrasser and Antonini, 1972; Dalal et al., 1986; Fubini et al., 1987; Vallyathan et al., 1988). It was found that these silicon-based radicals decay with a half-life of about 30 hours. We stress, however, that the decay kinetics followed "first order" only very approximately and that about 20% of the radicals were still detectable even after four weeks of storage in air. We note that the spectral resolution and lineshape depend somewhat on the grinding time and procedure as well as on temperature. Further studies are under progress to understand the details of these observations.

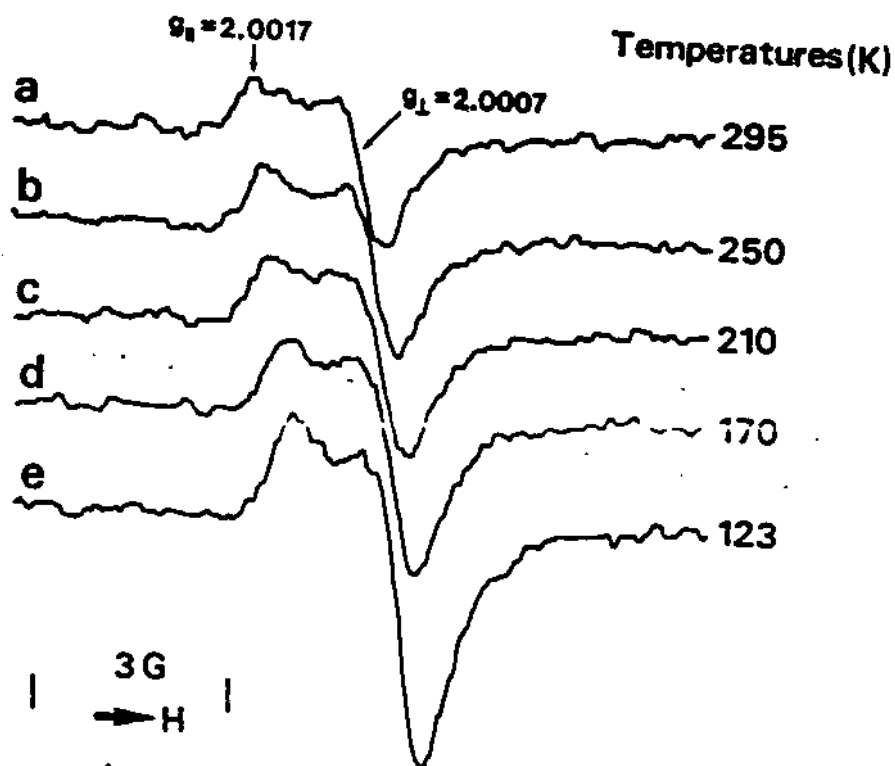


Figure 1. Typical ESR spectra from quartz dust freshly produced by an agate ball machine grinder in air. The spectra were recorded at different temperatures as indicated.

B. Activation of Alveolar Macrophages by Freshly Ground Quartz Particles

In order to investigate the possible role of silicon-based radicals and the oxygenated radicals generated upon reaction of freshly ground quartz particles with aqueous media (Dalal et al., 1988; Shi et al., 1988), we examined if freshly ground silica was a more potent stimulant of the respiratory burst in alveolar macrophages. The experiments consisted of measuring the O_2^- and H_2O_2 after *in vitro* exposure of alveolar macrophages to either fresh quartz particles or aged ones from the same stock. As shown in Figure 2, fresh quartz particle-induced O_2^- release decreased by 16% or 27% after storage in phosphate buffer for 24 or 96 hours, respectively. The fresh quartz particle-induced H_2O_2 release decreased by 65% after 24 hours of storage (Figure 3). From Figures 2 and 3, it may be noted that the half time for the decrease in the ability of fresh quartz particles to activate alveolar macrophages was approximately 22 hours, which was comparable with the half-life for the silicon-based radicals and the fresh quartz dust's ability to generate oxygenated radicals (Dalal et al., 1988; Shi et al., 1988).

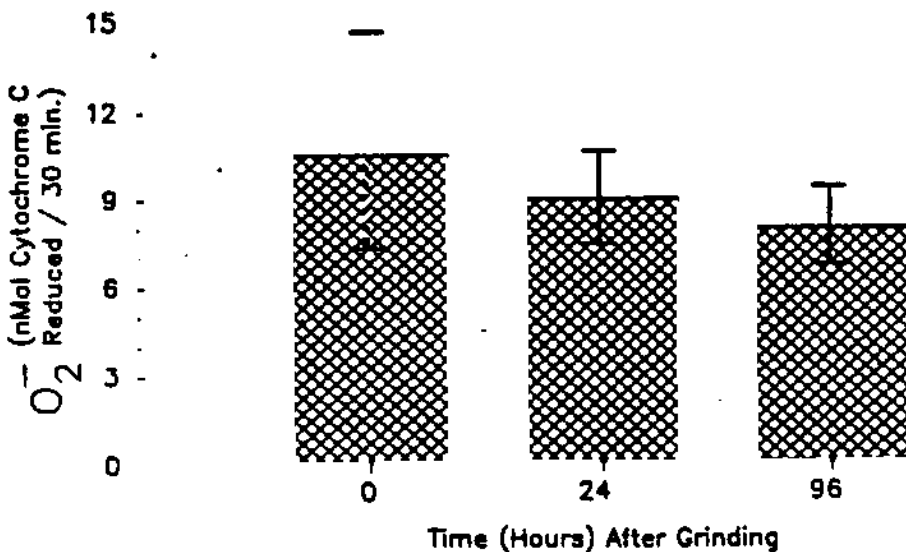


Figure 2. The effect of quartz particles on O₂⁻ release from alveolar macrophages.

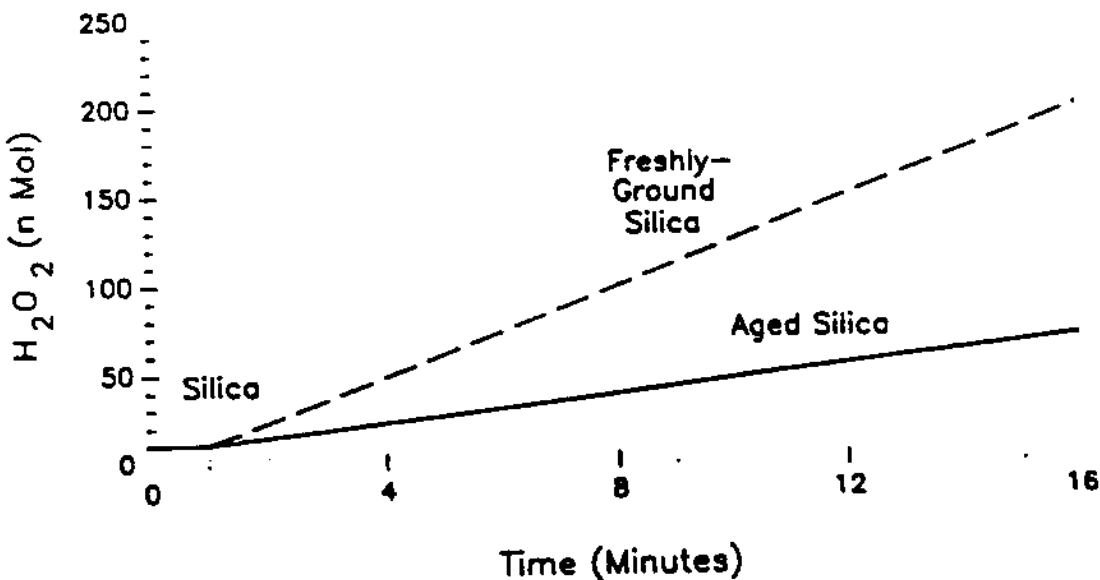


Figure 3. The effect of quartz particles on H₂O₂ release from alveolar macrophages.

C. Measurements of Cytotoxicity of Fresh Quartz Particles

Figure 4 shows that fresh quartz particles exhibit a greater disruptive effect on red blood cell membrane integrity than do particles stored in a phosphate buffer solution for several hours. Although there was a tendency for

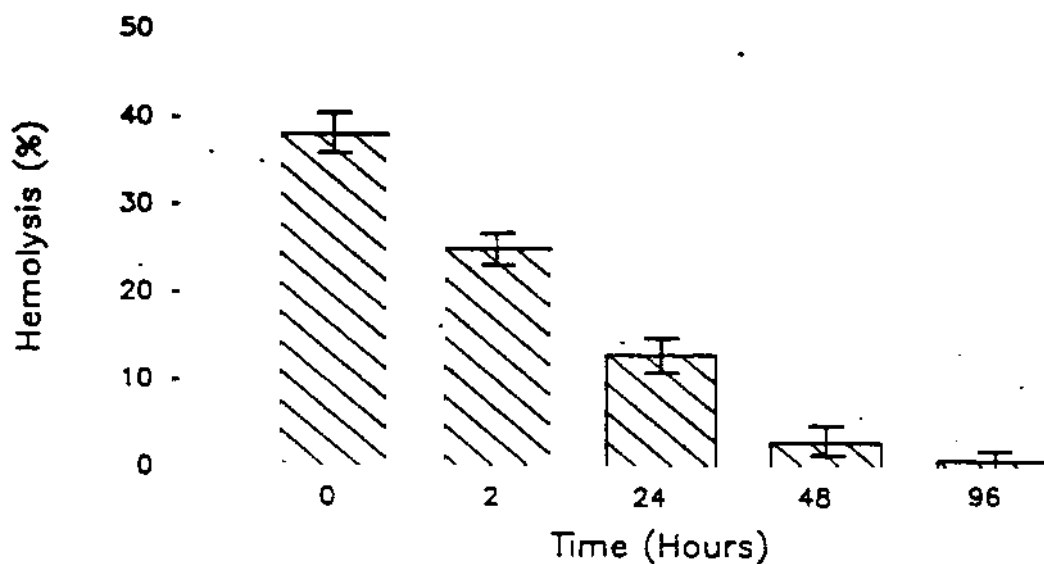


Figure 4. Hemolytic potential of quartz particles.

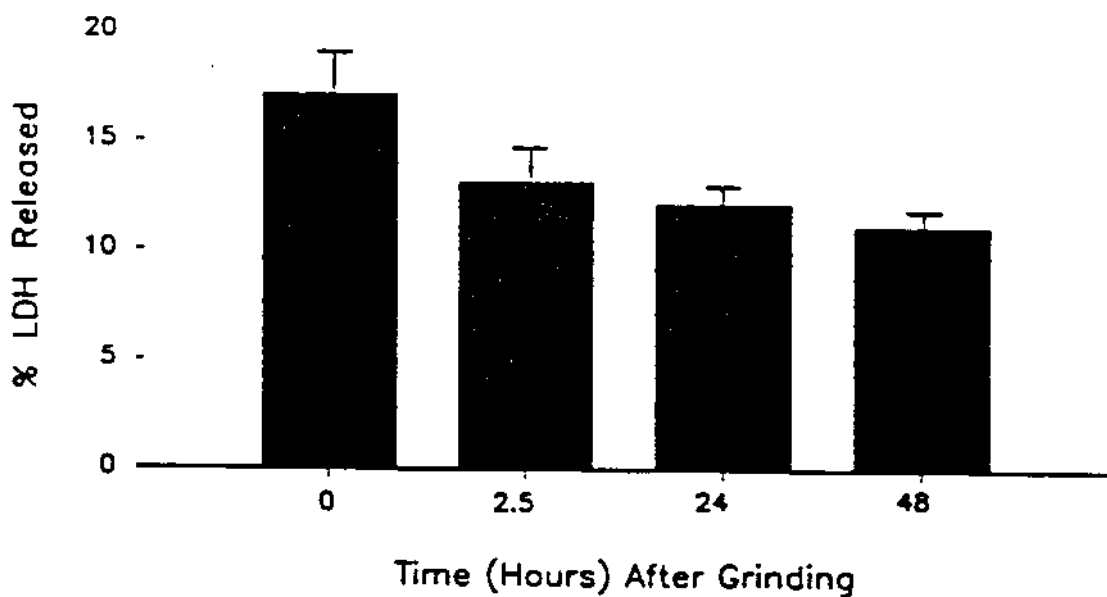


Figure 5. The effect of fresh ground quartz particles on release of cytosolic lactate dehydrogenase, LDH, from alveolar macrophages.

the fresh quartz particle-induced release of LDH to decline as silica aged, the differences were minimal (Figure 5) compared to hemolytic change.

DISCUSSION

Our results provide evidence that mechanical grinding of crystalline quartz under ambient laboratory conditions in air produces silicon-based radicals and

that these radicals decay with time (Dalal et al., 1986). In our preceding paper (Dalal et al., 1988) and elsewhere (Shi et al., 1988), we have reported that freshly ground quartz particles have the ability to generate oxygenated radicals and hypothesized that the silicon-based radicals and their associated oxygenated radicals might be involved in the initiation of the lipid peroxidation of the macrophage membrane, resulting into cell death (Dalal et al., 1988; Shi et al., 1988; Vallyathan et al., 1988). The results presented here show that fresh quartz particles are more biologically reactive than aged ones, i.e., fresh quartz particles induce a greater respiratory burst in alveolar macrophages. The generation of $\text{Si}\cdot$ and $\text{SiO}\cdot$ radicals and the formation of $\cdot\text{OH}$ radicals in suspensions of fresh silica dusts might partially explain the enhanced reactivity of fresh quartz particles and the pathogenesis of acute silicosis which results from the inhalation of fresh quartz. We also find that the ESR spectra obtained from quartz particles ground by an agate ball machine grinder (Figure 1) are different from those ground by hand using agate mortar and pestle as reported elsewhere (Dalal et al., 1986; Vallyathan et al., 1988). In this connection we point out that the method of reducing the particle size for quartz has been found to have a marked effect on the toxicity. For example, the toxicity was found to increase when quartz was ground in a mill than when crushed in a press (Rassk and Schilling, 1980; Robock and Klosterkötter, 1973). Further investigation of the effect of different ways of grinding on the free radical formation and its relevance to fresh quartz dust's fibrogenic and cytotoxic potentials is currently underway.

REFERENCES

- Bolis V, Fubini B, Venturello G (1983) Surface characterization of various silicas. A tentative correlation between the energy of adsorption sites and the different biological activities. *J Thermal Anal* 28:249-258.
- Dalal NS, Shi X, Vallyathan V (1988) Oxygenated radical formation by fresh quartz dust in a cell-free aqueous medium and its inhibition by scavengers. Paper in this volume.
- Dalal NS, Suryan MM, Jafari B, Shi X, Vallyathan V, Green FHY (1986) Electron spin resonance detection of reactive free radicals in fresh coal dust and quartz dust and its implications to pneumoconiosis and silicosis. In: *Respirable Dust in the Mineral Industries: Health Effects, Characterization, and Control* (Frantz R.L., and Ramani R.V., eds.), pp. 25-29. American Conference of Governmental Industrial Hygienists (ACGIH) Publication, ISBN 0-936712-76-7.
- Fubini B, Bolis V, Giamello E (1987) The surface chemistry of crushed quartz dust in relation to its pathogenicity. *Inorg Chim Acta* 138:193-197.
- Hochstrasser G, Antonini JF (1972) Surface states of pristine silica surfaces. *Surface Sci* 32:644-664.

ESR, BIOCHEMICAL STUDIES OF QUARTZ

Surface Sci 32:644-664.

- Myrvia QN, Evans DG (1967) Metabolic and immunologic activities of alveolar macrophage. *Arch Biochem. Biophys.* 14, 92-96.
- Nolan RP, Langer AM, Harington JS, Oster G, Selikoff IJ (1981) Quartz hemolysis as related to its surface functionalities. *Environ Res* 26:503-520.
- Phillips HJ. (1973) Dye exclusion tests for cell viability. In: *Tissue Culture Methods and Applications*, eds., Kruse PR, Patterson MD, pp. 406-408. Academic Press, New York.
- Raask E, Schilling CJ (1980) Research findings on the toxicity of quartz particles relevant to pulverized fuel ash. *Ann Occup Hyg* 23:147-157.
- Robock K, Klosterkötter W (1973) Specific toxicity of different silicon dioxide and silicate dust. *Staub* 33:60-63.
- Shi X, Dalal NS, Vallyathan V (1988) ESR evidence for the hydroxyl radical formation in aqueous suspension of quartz particles and its possible significance to lipid peroxidation in silicosis. *J Toxicol Environ Health* 25:237-245.
- Sweeney JD, Castranova V, Bowman L, Miles PR (1981) Factors which affect superoxide anion release from rat alveolar macrophages. *Exp Lung Res* 2: 85-96.
- Vallyathan V, Shi X, Dalal NS, Irr W, Castranova V (1988) Generation of free radicals from freshly fractured silica dust: potential role in acute silica-induced lung injury. *Am Rev Respir Dis* 138:1213-1219.
- Van Scott MR, Miles PR, Castranova V (1984) Direct measurement of hydrogen peroxide release from rat alveolar macrophages: artifactual effect of horseradish peroxidase. *Exp Lung Res* 6:103-104.
- Wroblewski F, LaDue JS (1955) Lactic dehydrogenase activity in blood. *Proc Soc Biol Med* 90:210-214.

Abstract: Electron spin resonance (ESR) measurements shows that grinding of quartz produces silicon-based radicals which decrease with aging in air. Biochemical measurements show that as compared to stale quartz freshly ground quartz particles cause a greater respiratory burst, i.e., enhanced secretions of superoxide anion and hydrogen peroxide from macrophage and a greater cytotoxicity effect on cellular integrity, i.e., an enhanced cytosolic lactate dehydrogenase release from macrophages and hemolytic potential. These results indicate a possible role of silicon related radicals in the biochemical mechanism of (acute) silicosis.

On the Mechanism of the Chromate Reduction by Glutathione: ESR Evidence for the Glutathionyl Radical and an Isolable Cr(V) Intermediate

X. Shi and N.S. Dalal

Department of Chemistry, West Virginia University

With a view of elucidating the role of glutathione (GSH) in the biochemical pathways of the chromate-exposure related carcinogenesis, we carried out electron spin resonance (ESR) spectroscopic investigations of the chromate-GSH redox reactions. The ESR measurements, employing spin-traps, provide evidence for the involvement of the glutathione (GS·) radical, as well as an isolable Cr(V)-glutathione intermediate. These results indicate a new mechanism for the reduction of chromate by GSH in *in vitro* cellular environment and help understand the (unexpected) increase in Cr(VI)-induced DNA strand breaks at elevated GSH levels.

We report here indirect electron spin resonance (ESR) evidence for the involvement of the glutathionyl (GS·) radical and direct evidence for a Cr(V) intermediate in the reactions of glutathione (GSH) with chromate for the first time. This work was undertaken to clarify the biochemical pathway of the reduction of chromate by GSH, since this reduction process is thought to be a critical step in the pathogenesis of the chromate-exposure related carcinogenesis¹. This follows from the literature reports which show that (a) Cr(VI) compounds have been proven to be carcinogens in laboratory animals as well as in human studies²⁻⁴, (b) Cr(VI) and not Cr(III) compounds are mutagenic⁵⁻⁷, (c) Cr(VI) and not Cr(III) compounds can penetrate cell membranes^{8,9}, (d) the final state of Cr(VI) in cellular reductions is Cr(III)¹, (e) by itself chromate (or Cr(VI)) cannot be directly mutagenic since Cr(VI) is known not to interact with isolated DNA under physiological conditions¹⁰, suggesting the significance of Cr(VI) reduction processes. One of the major reductants in cellular

CHROMATE REDUCTION BY GLUTATHIONE

environments is thought to be the GSH, both outside and inside the cells¹¹⁻¹³. Other evidence for the role of GSH in the chromate toxicity is seen from recent studies showing that exposure of hamster cells to non-toxic levels of added selenite increases the levels of GSH as well as the Cr(VI)-induced DNA strand breaks¹⁴, and that such DNA strand breaks in hepatocytes also change in direct proportion to their GSH content^{15,16}. These observations were interpreted as implying that the reduction of chromate by GSH to some reactive intermediate is an important step in the chromate carcinogenicity^{15,16}. The following reaction steps were suggested^{15,16}:

(A) Initial step:



(B) At high GSH levels:



(C) At low GSH levels:



where GSCrO_3^- is the glutathione-chromate-ester, GSSG the glutathione dimer, and $\text{GS}\cdot$ the glutathionyl radical. Thus far, however, in these reactions, the $\text{GS}\cdot$ radical has eluded spectroscopic detection, perhaps because of its high reactivity, whereas both positive^{17,18} as well as negative¹¹ evidence for Cr(V) formation has been reported. In the present undertaking, we have used the ESR spin-trap methodology to circumvent the anticipated high reactivity of $\text{GS}\cdot$ and find definitive evidence for the formation of this radical. In addition, we provide unequivocal evidence for the involvement of an intermediate species containing Cr(V).

MATERIALS AND METHODS: ESR spectra were obtained at X-band (-9.7 GHz) using a Bruker ER200D ESR spectrometer. The magnetic field was calibrated with a self-tracking NMR Gaussmeter (Bruker, Model ER035M) and the microwave frequency was measured with a Hewlett-Packard (Model 5340A) frequency counter. The spin probes, α -(4-pyridyl-1-oxide)-N-tert-butyl nitron (4-POBN) and 5,5-dimethyl-1-pyrroline-1-oxide (DMPO) were purchased from Aldrich, and used without further purification since very weak or no spin adduct signals were obtained

from the purchased sample when used alone. $K_2Cr_2O_7$ was purchased from Fisher. All experiments were done at room temperature.

RESULTS AND DISCUSSION: An aqueous solution of 0.1 M spin trap α -(4-pyridyl-1-oxide)-N-tert-butylnitron (4-POBN), either with chromate alone or GSH alone, did not give a detectable ESR spectrum. However, when chromate, GSH and 4-POBN were mixed, an ESR spectrum was observed which was a composite of the spin adduct signal (sharp doublets of triplets) and that of $Cr(V)^{17,18}$, the broad peak at $g = 1.995$ (Fig. 1 a-c). About ten minutes later, when the signal from $Cr(V)$ had decayed, a clear spectrum ($g = 2.0061$), consisting of only doublets of triplets was obtained (Fig. 1 f). This spectrum is assigned to the 4-POBN-GS adduct by its strong similarity to the spectrum reported earlier¹⁹ for the same adduct. The analysis of the spectrum in Fig. 1 f gave the nitrogen hyperfine coupling $a_N = 15.0$ G and proton hyperfine coupling $a_H = 2.3$ G, which compare well with those ($a_N = 15.13$ G and $a_H = 2.32$ G) reported earlier¹⁹.

Additional support for this identification was seen from ESR spectra using 5,5-dimethyl-1-pyrroline-1-oxide (DMPO). The spectrum obtained, Fig. 2 a, is composite of that of the spin adduct, a 1:2:2:1 quartet, and that of $Cr(V)$, as evidenced by the broad peak at $g = 1.995$. The analysis of the ESR spin adduct spectrum gave $a_N = 15.2$ G and $a_H = 15.9$ G. These values are very similar to those ($a_N = 15.4$ G and $a_H = 16.2$ G) reported^{20,21} earlier for the DMPO-GS spin adduct. The spin adduct spectrum shows rapid decay essentially as described^{20,21} previously.

An important observation in the spin-trap studies was that an increase in the amount of GSH caused an increase in the spin adduct ESR signal until the intensity leveled off at a molar ratio of about fifteen to one of GSH to $K_2Cr_2O_7$ (Fig. 1 a-c). No spin adduct ESR signal was detected for the molar ratio of less than one (Fig. 1 e). This observation is in contradiction to the steps (B) and (C) as outlined in equations (2) and (3) above.

Fig. 1 and Fig. 2 a-b provide direct evidence for the formation of a fairly long-lived $Cr(V)$ intermediate when the molar ratios of GSH to $K_2Cr_2O_7$ are higher than one. In agreement with earlier studies^{17,18}, different kinds of $Cr(V)$ complex are formed depending

on the reaction conditions (Fig. 1 a-d). We were able to isolate the $g = 1.995$ species with a yield of about 50 percent. A typical ESR spectrum for the powder is shown in Fig. 2 c. The measured g -values are $g_{\parallel} = 2.007$ and $g_{\perp} = 1.989$, with little variation with temperature from 115 K to 310 K. These values are typical of Cr(V) solids²². When the isolated Cr(V) intermediate was redissolved in water, its ESR spectrum was identical with that from the original solution.

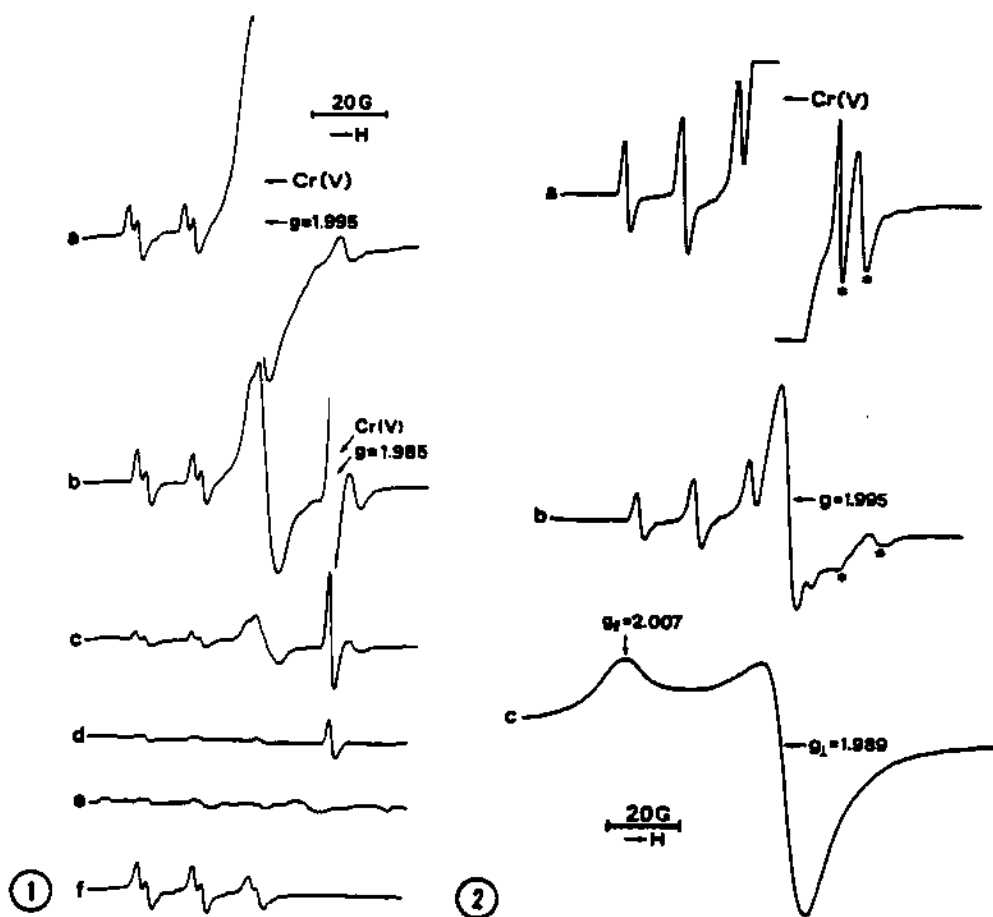


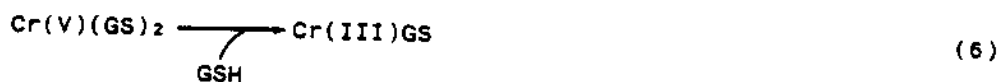
Fig. 1. ESR spectra recorded 2 minutes after mixing a 0.015 M solution of $K_2Cr_2O_7$ with the following concentrations of GSH: (a) 0.375 M, (b) 0.15 M, (c) 0.075 M, (d) 0.03 M, (e) 0.0075 M. The spectrum in (f), corresponding to $[GSH] = 0.575$ M, was taken after 10 minutes of the mixing, in order to obtain the spin adduct signal free of the Cr(V) signals. The concentration of spin trap used, 4-POBN, was 0.1 M.

Fig. 2. ESR spectra of chromate-glutathione mixtures: $[K_2Cr_2O_7] = 0.015$ M; $[glutathione] = 0.375$ M; $[DMPO] = 0.1$ M; (a) pH = 7.2; (b) pH = 4.0 M, recorded 2 minutes after mixing. (c) ESR spectrum of an isolated Cr(V) complex. The asterisks indicate minor Cr(V) species.

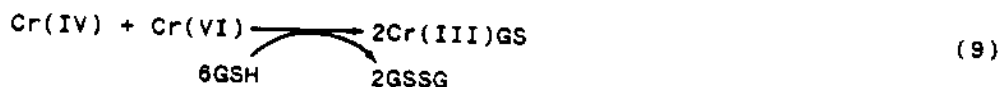
THE RESPIRABLE DUST CENTER

Using the isolated Cr(V) complex, as well as K_2CrO_4 , a known Cr(V) compound²², it was found that the Cr(V) intermediate also serves as an oxidant for the formation of $GS\cdot$, a result not discussed in any of the earlier studies of the chromate-GSH reaction^{1, 8-16}. We thus suggest the following alternative mechanisms for the chromate reduction:

(A) At high GSH levels:



(B) At low GSH levels:



The above results also help understand the recent reports^{15, 16} that increased levels of GSH in the cells result in increased DNA damage by Cr(VI). In the cellular environment the concentration of GSH is much higher than that of Cr(VI)¹⁰. Now this study shows that the simultaneous formation of $GS\cdot$ and Cr(V) takes place only at higher levels of GSH relative to Cr(VI). It thus appears that increased Cr(VI)-induced DNA strand breaks noted at higher GSH levels are related to the simultaneous formation of the $GS\cdot$ radicals and Cr(V) intermediates.

In conclusion, this work shows that both a long-lived, isolable, Cr(V) intermediate, and the $GS\cdot$ radical are formed in the reaction between chromate and GSH, but only at high levels of GSH relative to chromate ions, in disagreement with an earlier proposed mechanism^{15, 16}. Thus, a new mechanism has been suggested, which also provides a plausible explanation for the recent (unexpected) report of an increase in Cr(VI)-induced DNA strand breaks at increased GSH levels. Our success in isolating the Cr(V) complex opens up the

possibility of carrying out a detailed single crystal characterization of Cr(V)-(GSH)_n complexation, which may provide clues as to the mechanism of the chromate reduction by cellular thiols. Also a methodology for combating chromate-related carcinogenesis may be available as a results of these investigations.

REFERENCES

1. Connett, P.H., and Wetterhahn, K.E. (1983) *Struct. Bond.* 54, 93-124.
2. Enterline, P.E. (1974) *J. Occup. Med.* 16, 523-526.
3. Norseth, T. (1981) *Environ. Health Perspect.* 40, 121-130.
4. Doll, R. (1981) *Environ. Health Perspect.* 40, 11-20.
5. Leonard, A., and Lauwerys, R.R. (1980) *Mutat. Res.* 76, 227-239.
6. Bianchi, V., Celotti, L., Lanfranchi, G., Majone, F., Marin, G., Montaldi, A., Sponza, G., Tamino, G., Venier, P., Zantedeschi, A., and Levis, A.G. (1983) *Mutat. Res.* 117, 279-300.
7. Löfroth, G., and Ames, B.N. (1978) *Mutat. Res.* 53, 65-66.
8. Wetterhahn, J.K. (1981) *Environ. Health Perspect.* 40, 233-235.
9. Jennette, K.W. (1979) *Biol. Trace Element Res.* 1, 55-62.
10. Tsapakos, M.T., and Wetterhahn, K.E. (1983) *Chem.-Biol. Interact.* 46, 265-277.
11. Connett, P.H., and Wetterhahn, K.E. (1985) *J. Am. Chem. Soc.* 107, 4282-4288.
12. Connett, P.H., and Wetterhahn, K.E. (1986) *J. Am. Chem. Soc.* 108, 1842-1847.
13. Weigand, H.J., Ottenwälder, H., and Bolt, H.M. (1984) *Toxicology* 33, 341-348.
14. Sugiyama, M., Ando, A., Furuno, A., Furlong, N.B., Hidaka, T., and Ogura, R. (1987) *Cancer Lett.* 38, 1-7.
15. Wetterhahn, K.E., and Connett, P.H. (1984) *Trace Subst. Environ. Health* 18, 154-162.
16. Cupo, D.Y., and Wetterhahn, K.E. (1985) *Proc. Natl. Acad. Sci. USA* 82, 6755-6759.
17. O'Brein, P. (1985) *Inorg. Chim. Acta* 108, L19-20.
18. Goodgame, D.M.L., and Joy, A.M. (1986) *J. Inorg. Biochem.* 26, 219-224.
19. Niki, E., Tsuchiya, J., Tanimura, R., and Kamiya, Y. (1982) *Chemistry Lett.* 789-792.
20. Harman, L.S., Carver, D.K., Schreiber, J., and Mason, R.P. (1986) *J. Biol. Chem.* 261, 1642-1648.
21. Stock, B.H., Schreiber, J., Guenat, C., Mason, R.P., Bend, J.R., and Eling, T.E. (1986) *J. Biol. Chem.* 261, 15915-15922.
22. Dalal, N.S., Millar, J.M., Jagadeesh, M.S., and Seehra, M.S. (1981) *J. Chem. Phys.* 74, 1916-23.

Cytotoxicity and Spectroscopic Investigations of Organic Free Radicals in Fresh and Stale Coal Dusts

N.S. Dalal¹, B. Jafari¹ and V. Vallyathan²

¹ Department of Chemistry, West Virginia University

² National Institute for Occupational Safety and Health, Morgantown, WV

Electron spin resonance measurements have now been completed on the decay kinetics of the organic free radicals formed on crushing or grinding of a well characterized anthracite coal. The free radicals exhibit a complex decay pattern for the first few hours after the grinding, and a smooth decay thereafter. Parallel hemolysis studies indicate a half-life of the decrease in the cytotoxicity of the fresh dust to be about half-a-day. The cytotoxicity of the freshly-made dust decreases on addition of superoxide dismutase, catalase and sodium benzoate. The hemolysis rate is lower for the dust stored in buffers as compared to air. A chemical model will be presented to accommodate the cytotoxicity and spectroscopic data, and their implications to pneumoconiosis.

Oc
ica c
or a
cosi
ter f
deve
nod
velo
seve
othe
set a
the
grar
spac
rato
In
ctio
gest
volv
Lun
ind
fror
diti
perc
rele
resu
part
resu
alve
prol
thes
(7,
In
very
velc
pul
the
east
silic
resp
ca.
acu
cha
silic
san
and
in v
she
fres

Generation of Free Radicals from Freshly Fractured Silica Dust: Potential Role in Acute Silica-Induced Lung Injury

V. Vallyathan¹, X. Shi¹, N.S. Dalal², W. Irr¹ and V. Castranova¹

¹Division of Respiratory Disease Studies, National Institute for Occupational Safety and Health, Morgantown, WV

²Department of Chemistry, West Virginia University

Introduction

Occupational exposure to crystalline silica can be associated with either chronic or acute pulmonary disease. Chronic silicosis becomes manifest 20 to 40 years after first exposure and is characterized by development of concentric hyalinized nodular lesions in the lung with the development of dyspnea over a period of several decades. Acute silicosis, on the other hand, is manifested by a rapid onset after exposure and is characterized by the accumulation of an amorphous granular lipoprotein exudate in the air-spaces and rapid development of respiratory disability within a few years (1-3).

Information is growing concerning the etiology of chronic silicosis. Studies suggest that several mechanisms may be involved in the development of fibrosis. Lung injury may result from silica-induced release of lysosomal enzymes from alveolar macrophages (4, 5). In addition, silica-induced activation of superoxide anion and hydrogen peroxide release from alveolar macrophages may result in oxidant-induced damage to lung parenchyma (6). Silica exposure can also result in the release of mediators from alveolar macrophages which enhance the proliferation of fibroblasts and the synthesis of collagen by these pneumocytes (7, 8).

In comparison with chronic silicosis, very little is known concerning the development of acute silicosis. Because the pulmonary responses to silica differ in the chronic and acute presentation of disease, it does not seem likely that acute silicosis can be explained simply as the response of the lung to high levels of silica. We propose that at least part of the acute response is due to some unique characteristic of the dust inhaled. Acute silicosis is commonly associated with sandblasting, rock drilling, tunnelling, and silica mill operations, i.e., operations in which silica particles are crushed or sheared (9). Therefore, it is possible that freshly sheared silica may have surface

SUMMARY Data presented here indicate that freshly fractured silica exhibits surface characteristics and biologic reactivity distinct from aged silica, and on this basis we propose that these surface features may lead to enhanced manifestations of lung injury. Grinding of silica produces $\sim 10^{16}$ Si and Si-O (silicon-based) radicals per gram of dust on the particulate surface which are characterized by an electron spin resonance (ESR) spectrum centered around $g = 2.0018$. These silicon-based radicals react with aqueous media to produce OH radicals, which are demonstrable using a DMPO spin trap. The concentration of silicon-based radicals in silica decreases with aging in air and exhibits a half-life of ~ 30 h, whereas its ability to generate OH radicals in aqueous solution decreases with a half-life of ~ 20 h. However, on storage in aqueous media, the concentration of silicon-based radicals and the dust's ability to generate OH radicals decrease significantly within a few minutes. Freshly ground silica is also more biologically reactive than aged silica, because freshly crushed silica activates a greater respiratory burst in alveolar macrophages than aged silica, i.e., storage of ground dust in air decreases silica-induced superoxide anion secretion, hydrogen peroxide release, and NBT reduction by 25%, 68%, and 43%, respectively. Furthermore, compared to aged silica, freshly ground silica exhibits a greater cytotoxic effect on cellular membrane integrity, i.e., a 1.5-fold increase in LDH release from macrophages, a 36-fold increase in hemolytic activity, and a three-fold increase in the ability to induce lipid peroxidation. Because acute silicosis is frequently associated with occupations in which freshly fractured crystalline silica of respirable size is generated, the present study suggests that fracture-generated silicon-based radicals may play a significant role in the pathogenesis of this disease.

AM REV RESPIR DIS 1988; 138:1273-1279

properties that make it more reactive with lung tissue than aged silica, and that it is this unique reactivity of freshly sheared silica that leads to manifestation of acute pulmonary disease.

Earlier studies have suggested that freshly fractured silica may exhibit surface reactivity not found in aged silica. Hochstrasser and Antinini (10) reported that silicon-based radicals could be generated upon cleavage of a quartz crystal under ultra-high vacuum (10^{-10} mm Hg). Karmanova and colleagues (11) reported release of singlet oxygen from silica dust upon heating, whereas Kolbanev and associates (12) reported generation of H_2O_2 from the reaction of freshly ground silica with water. In addition, Marasas and Harington (13) reported that silica exhibits oxidant properties that may be related to its pathogenicity. However, to date, a systematic evaluation of the generation of silicon-based radicals as a result of shearing or grinding under ambient air which mimics occupational conditions, as well as the decay of these surface radicals and its relevance to biologic reactivity, has not been conducted.

The objective of this study was to

evaluate whether freshly ground silica was more surface reactive and/or cytotoxic than aged silica. First, the generation of short-lived silicon-based radicals on freshly ground silica and possible release of oxygenated radical species was evaluated using electron spin resonance (ESR) techniques. Secondly, the reactivity of freshly ground silica was monitored by comparing its ability to activate a respiratory burst in alveolar macrophages to that of aged silica. Lastly, cytotoxicity of fresh versus aged silica dust was compared by measuring their effects on red blood cell hemolysis, LDH release from alveolar macrophages, and lipid peroxidation.

Methods

Reagents

Horse heart ferricytochrome c, N-2-hydroxyethyl piperazine-N-2-ethane sulfonic acid (HEPES), horseradish peroxidase (Type IX), scopoletin, superoxide dismutase (SOD), catalase, cis-9-cis-12-octadecadienoic acid (linoleic acid), sodium benzoate, sodium dodecyl sulfate, diethylenetriaminepentaacetic acid (DETAPAC), dimethyl sulfoxide (DMSO), ethylenediaminetetraacetic acid (EDTA), and

D-mannitol were obtained from Sigma Chemical Company, St. Louis, Missouri. The 5,5-dimethyl-1-pyrroline-1-oxide (DMPO), 1,3-dimethyl-2-thiourea (DMTU), and 1,1,3,3-tetramethoxypropane were obtained from Aldrich Chemical Company, Milwaukee, Wisconsin, and 1-butanol was obtained from Fisher Scientific Company, Pittsburgh, Pennsylvania.

Preparation of Silica

Crystalline silica (0.2 to 5.0 μm in diameter) was obtained from the Generic Respirable Dust Technology Center, Pennsylvania State University, State College, Pennsylvania. Silica was ground in an agate mortar with a pestle for 30 min and sieved through a 20-micron mesh filter before use. Representative samples of the ground silica were subjected to X-ray spectrometric analysis to confirm that the silica samples were mineralogically pure and contained no detectable trace elemental impurities. For measurement of decay of ESR signal or biologic effects, samples of a single stock of ground silica were taken at various times after grinding to assure uniformity of shearing and particle size.

Measurement of Electron Spin Resonance (ESR)

ESR spectra were obtained at X-band (~ 9.7 GHz) using a Bruker ER 200D ESR spectrometer at the Chemistry Department of West Virginia University. For accurate measurements of the g values and hyperfine splittings, the magnetic field was calibrated with a self-tracking NMR Gaussmeter (Bruker Model ER035M) and the microwave frequency measured with a Hewlett-Packard (Model 5340A) frequency counter. All the measurements were made at room temperature. Typical spectrometer settings are given in the figure legends.

Isolation of Alveolar Macrophages

Alveolar macrophages were harvested from male pathogen-free Sprague-Dawley rats by bronchopulmonary lavage using a calcium- and magnesium-free Hank's balanced salt solution (14). Macrophages from ten 8-ml lavages were sedimented by centrifugation at 500 g for 5 min at 2° C and suspended in HEPES-buffered medium containing 140 mM NaCl, 5 mM KCl, 10 mM HEPES, 1 mM CaCl_2 , and 5 mM glucose (pH 7.4). Cell viability counts were made using the trypan blue dye exclusion procedure (15). Microscopic estimates of purity indicated that 90 to 95% of the lavaged cells were alveolar macrophages.

Activation of Alveolar Macrophages

Silica-induced activation of the respiratory burst in alveolar macrophages was monitored by measuring superoxide and hydrogen peroxide release. Superoxide anion release was monitored by measuring the superoxide-dependent (SOD inhibitable) reduction of

cytochrome *c* spectrophotometrically at 550 nm using a Gilford Spectrophotometer (Model 300-N) (16). Briefly, alveolar macrophages (2×10^6 cells) were added to 2 ml of HEPES-buffered medium containing 0.12 mM cytochrome *c* either in the absence or presence of silica (1 mg/ml). At zero or 30 min, parallel cell suspensions were centrifuged at 2,000 g for 1 min and the absorbance of the supernatant was measured. Superoxide release was proportional to the difference between the absorbance values at 30 and zero min. Absorbance values were converted to nmoles of cytochrome *c* reduced using an extinction coefficient of $21 \text{ mM}^{-1}\text{cm}^{-1}$.

Hydrogen peroxide release was monitored by measuring the change in fluorescence of scopoletin in the presence of horseradish peroxidase (17). Fluorescence was monitored at an excitation wavelength of 350 nm and an emission wavelength of 460 nm using a Perkin-Elmer Fluorescence Spectrophotometer (Model MPG-36) equipped with a stirrer and temperature controlled at 37° C. Briefly, alveolar macrophages (5×10^6 cells) were added to 3 ml of HEPES-buffered medium containing 2.4 μM scopoletin and 6.6 units of horseradish peroxidase either in the absence or presence of silica (1 mg/ml). The decrease in fluorescence was converted to nanomoles of hydrogen peroxide released, using a standard curve constructed by adding known quantities of hydrogen peroxide to the assay cuvette.

Reduction of nitro blue tetrazolium (NBT) to formazan was also monitored to measure respiratory burst activity in alveolar macrophages, using a histochemical technique (18).

Measurement of Cytotoxicity

The cytotoxic potential of fresh or aged silica was monitored by determining the effects of these dusts on cellular membrane integrity, i.e., hemolysis of red blood cells and release of cytosolic LDH from alveolar macrophages, as well as the ability of silica to induce lipid peroxidation. Hemolytic activity of freshly ground or aged silica was measured in a 2% suspension of sheep erythrocytes as the amount of hemoglobin released after incubation in the presence or absence of silica (10 mg/ml for 1 h at 37° C). After treatment, the suspension was centrifuged and the absorbance of the supernates read at 540 nm using a Gilford Spectrophotometer (Model 300-N). Percentage of hemoglobin released was calculated as the ratio of the absorbance value for the supernatant sample from silica-treated red blood cells to that from cells lysed with 0.5% Triton X-100.

The effects of freshly ground or aged silica on membrane integrity were also monitored by measuring cytosolic lactate dehydrogenase (LDH) release from alveolar macrophages. Alveolar macrophages (2×10^6) were incubated for different time intervals in a shaking

water bath at 37° C in the presence or absence of silica (1 mg/ml). After incubation, cell suspensions were centrifuged and LDH released from the macrophages was estimated in the supernate (19). The reaction mixture in a total volume of 3 ml contained phosphate buffer (pH 7.4), 0.1 ml of enzyme supernatant, 0.07 mg/ml NADPH, and 0.0007 M sodium pyruvate. The reaction was initiated by the addition of sodium pyruvate to preincubated reaction mixture. LDH secretion was expressed as percent total enzyme released by Triton X-100 lysis of cells. One unit of LDH activity equals the amount of enzyme that catalyzes the reduction of a μmole of reduced nicotinamide adenine dinucleotide in 1 min at 37° C as measured spectrophotometrically by a decrease in absorbance at 340 nm.

Peroxidation of the polyunsaturated lipid linoleic acid (*cis*-9-*cis*-12-octadecadienoic acid) by freshly ground or aged silica was monitored using a fluorescence method (20) with some modifications. The reaction mixture in a total volume of 0.5 ml contained freshly ground or aged silica and 20 μl of 0.52 mM linoleic acid emulsion in 95% ethanol in HEPES buffer (pH 7.4) without calcium and glucose. After 1 h of incubation in a shaking water bath at 37° C, the reaction was terminated by the addition and mixing of 0.5 ml of 3% sodium dodecyl sulfate followed by 2.0 ml of 0.1 N HCl, 0.3 ml 10% phosphotungstic acid, and 1.0 ml 0.7% 2-thiobarbituric acid, respectively. The mixture was then heated for 30 min at 95 to 100° C, and the thiobarbituric acid reactive substance formed was extracted with 5 ml 1-butanol after cooling. The test tubes were then centrifuged at 3,000 rpm for 1 min, and the fluorescence of the butanol layer was measured at 515 nm excitation and 555 nm emission using a Perkin-Elmer fluorospectrophotometer (Model MPG-36). Malondialdehyde standards were prepared from 1,1,3,3-tetramethoxypropane, and the malondialdehyde produced was calculated from the standard graph.

Effect of Scavengers

SOD, catalase, sodium benzoate, mannitol, DMSO, and DMTU were added to the cytotoxicity assays of hemolysis, H_2O_2 release, and lipid peroxidation in different concentrations to evaluate the most effective dose response. SOD and catalase were added to the test in final concentrations of 85, 170, and 340 units/ml and 312, 625, and 1250 units/ml, respectively. Sodium benzoate, DMSO, and DMTU were added to the test bioassays in 0.05, 0.1, and 0.5 mM, and 0.1 M final concentrations. All the scavengers were added immediately prior to the addition of test silica and evaluated with positive and negative controls. In few experiments, SOD and catalase were denatured by placing in a boiling water bath for 3 min and then used in the test.

Statistical Analysis

Data presented are means \pm standard deviations except where indicated. Measurements concerning the time-dependent decay of silicon-based radicals by ESR or loss of biologic activity were made on the same preparation of ground silica by a one-way analysis of variance. In other experiments, comparisons of data were made by a two-tailed Student's *t* test. In all data comparisons, a probability value of less than 0.05 was considered significant.

Results

The presence of reactive free radical sites on the surface of silica particles was monitored using ESR spectroscopy. No ESR signal was observed with unground crystalline silica particles. However, upon grinding of these silica particles in air, an ESR spectrum centered around $g = 2.0015 \pm 0.0003$ was observed (figure 1A). Such a signal is characteristic of silicon-based radicals (Si-O \cdot and \cdot Si), the so-called E-center (10, 21). Comparing the peak-to-peak height of the ESR signal from freshly ground silica to that of diphenyl picrylhydrazyl (DPPH), a standard of known radical concentration, we estimate that approximately 10^{18} silicon-based radicals were generated per gram of silica after 30 min of grinding in air. As discussed elsewhere (22), these radi-

als are localized on the dust surface and the decay in air was noted by the decrease in signal height, 1pp, with a half-life of about 30 h in air (figure 1B) and an approximate half-life of few minutes in PBS buffer (data not shown). It should be noted that the ESR signal of freshly ground silica decreased in air by about 80% after approximately first-order kinetics. However, 20% of the ESR signal was detectable even after 4 wk of storage in air.

ESR data also suggest that freshly ground silica can react with water to release short-lived, oxygenated free radicals. The generation of such radicals was monitored by ESR after the addition of a spin trap, DMPO, to an aqueous suspension of freshly ground silica. The ESR signal observed from freshly ground silica in aqueous solution in the presence of DMPO is shown in figure 2A. The ESR spectrum was centered around $g = 2.0059 \pm 0.0003$ and exhibited a 1:2:2:1

quartet pattern with a splitting of 14.9 G, quite characteristic of a DMPO-OH adduct (23-26). Therefore, the results indicate OH radicals can be produced during the reaction of freshly ground silica in an aqueous environment.

In order to verify further the presence of the OH radicals, 30% ethanol was added as a secondary OH radical trap (27). Under these conditions, the intensity of the DMPO-OH adduct signal decreased because ethanol served as a scavenger for the OH radicals (figure 2B). The reaction of OH radicals with ethanol results in the production of ethanoly radicals that in turn react with DMPO to give the spin adduct, DMPO-CHOCH $_2$. The characteristic ESR signal of this DMPO-CHOCH $_2$ adduct was observed as indicated by arrows that became the dominant peaks in excess ethanol (figures 2B and 2C). DETAPAC or EDTA, metal chelators, had little effect on the DMPO-

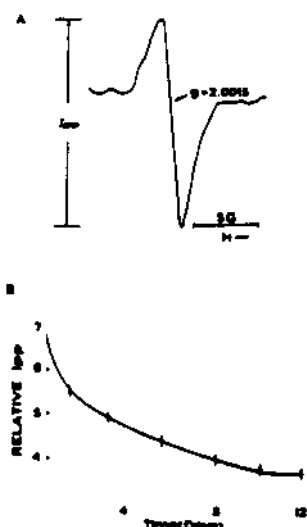


Fig. 1. A. A typical ESR spectrum of silicon-based radicals in silica dust ground in air for 30 min. The signal height, 1pp, is proportional to the radical concentration. B. A plot of the silicon-based radical concentration as a function of storage time in air. The spectrometer settings were: receiver gain, 3.2×10^4 ; modulation amplitude, 2 G; scan time, 100 s; field, $3,470 \pm 50$ G.

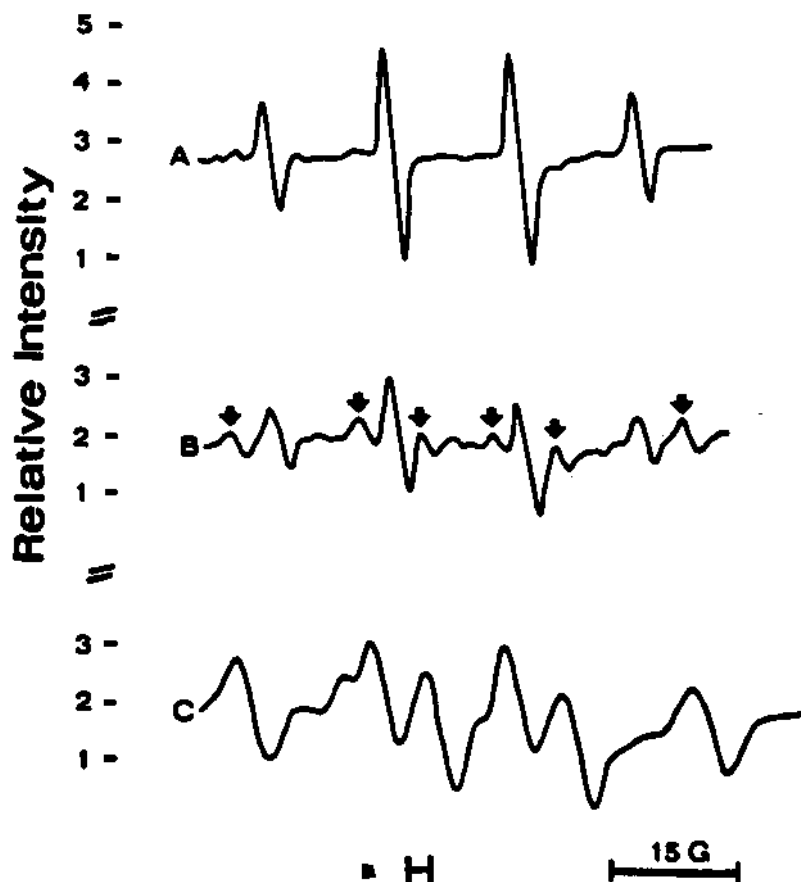


Fig. 2. ESR spectra observed from freshly ground silica in aqueous solution in the presence of either a spin trap, 100 mM DMPO (A), or 400 mM DMPO plus an OH radical scavenger, 30% ethanol (B). The arrows in (B) indicate signals from trapped ethanoly radicals. Figure 2C shows the spectrum in 95% ethanol where the peaks marked by arrows in (B) become dominant. The spectrometer settings were: receiver gain, 5×10^4 ; modulation amplitude, 2 G; scan time, 100 s; field, $3,480 \pm 75$ G. Normally, no background ESR signal was detectable in samples of DMPO without silica. If a signal was detectable with DMPO alone, this stock was discarded and new DMPO stock was used.

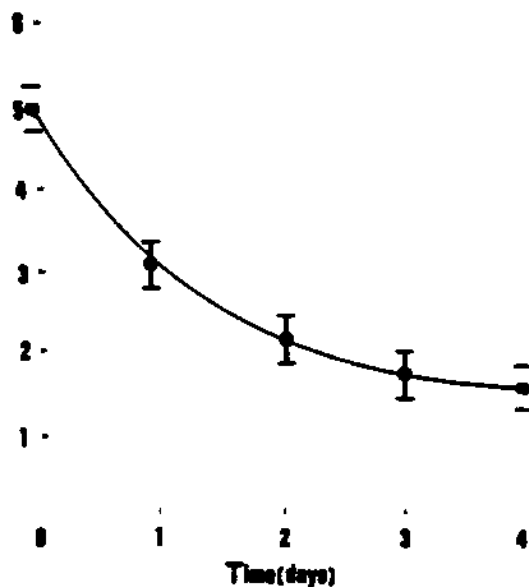


Fig. 3. ESR intensity of the DMPO-OH adduct as a function of the freshness of ground silica. Dust samples for ESR measurements were taken from the same stock of ground silica stored in air at various times after crushing. The concentration of DMPO was 100 mM in aqueous solution. Spectrometer settings were the same as those given in figure 2.

OH signal (data not shown). This suggests that OH radicals are generated directly from the reaction of silicon-based adicals with water (see DISCUSSION).

The ability of silica to react with water and generate OH radicals decreased with time after crushing, as shown by the decrease in the intensity of the DMPO-OH adduct ESR signal as a function of time after grinding and storage of silica in air (figure 3). The half-time for this decay was approximately 20 h.

In order to determine if freshly ground silica was a more potent stimulant of the respiratory burst in alveolar macrophages, superoxide anion release, hydrogen peroxide secretion, and NBT reduction were monitored after *in vitro* exposure of alveolar macrophages to either freshly crushed or aged silica. Freshly crushed silica activated alveolar macrophages to a greater extent than did silica after storage, i.e., silica-induced superoxide release decreased by 16% and 27% after storage of silica in phosphate buffer for 24 or 96 h, respectively (figure 4), whereas silica-induced hydrogen peroxide secretion decreased by 65% after 24 h of storage (figure 5). Furthermore, NBT staining was $69 \pm 11\%$ with freshly ground silica compared to $39 \pm 8\%$ after 48 h of storage. The half-time for the decrease in the ability of ground silica to activate alveolar macrophages was approximately 22 h, which was comparable with half-life for the production of the OH radicals from freshly ground silica (figure 3).

The next series of experiments com-

pared the cytotoxicity of freshly crushed silica with that of aged silica dust. The results indicate that freshly ground silica exhibited a greater effect on membrane integrity than did silica dust after storage. Indeed, compared to aged silica, freshly ground silica was significantly more potent in inducing hemolysis of red

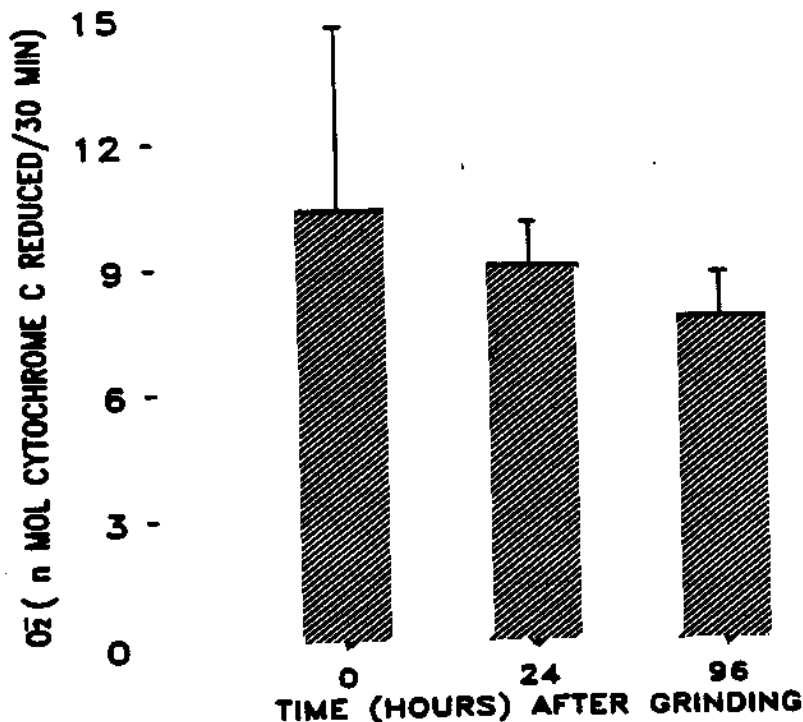


Fig. 4. The effect of freshly ground or aged silica on superoxide anion secretion from alveolar macrophages. Superoxide secretion was measured spectrophotometrically by monitoring the reduction of cytochrome c. The data presented are the means \pm SD of five experiments.

blood cells (figure 6). The half-time for decay of the hemolytic potential of crushed silica was approximately 10 h. Although there was a tendency for the silica-induced release of cytosolic enzyme LDH to decline as silica aged, the differences were minimal (figure 7) compared to hemolytic changes.

Cytotoxicity of freshly ground and aged silica was also determined by monitoring the ability of these dusts to induce peroxidation of lipids (table 1). It is evident from the data presented that freshly ground silica induced lipid peroxidation in a dose-dependent fashion. This is clearly evident for dust freshly ground (zero to 5 min). The ability of ground silica to peroxidize lipids decreased with storage at all doses, i.e., the rate of silica-induced lipid peroxidation declined markedly over the first 48 h after grinding and remained relatively constant thereafter.

Effects of scavengers on the prevention of silica-induced cytotoxicity are presented in table 2. Addition of exogenous SOD and catalase inhibited the cytotoxicity of freshly ground silica in various bioassays at different levels. The results indicate that in bioassays of hemolysis, SOD, catalase, and sodium benzoate provided a partial protection, whereas DMSO, DMTU, and mannitol were totally noneffective in preventing

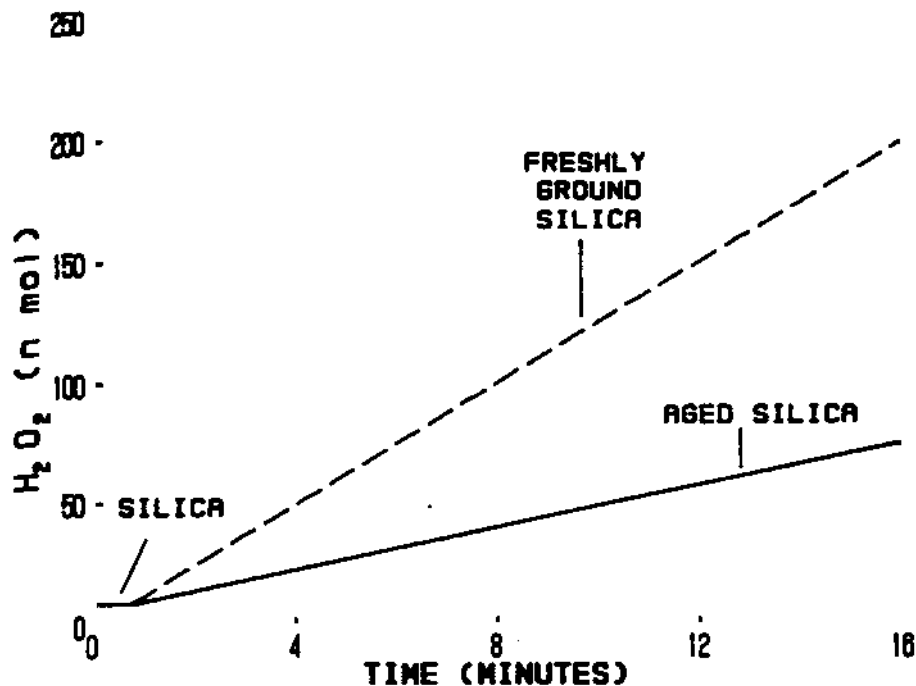


Fig. 5. The effect of freshly ground or aged silica on the secretion of hydrogen peroxide from alveolar macrophages. Hydrogen peroxide secretion was measured fluorometrically by monitoring the oxidation of scopoletin in the presence of horseradish peroxidase.

Fig. 6. Hemolytic potential of freshly ground or aged silica (stored in phosphate buffer). Hemolysis of red blood cells was measured spectrophotometrically and expressed as the percent lysis compared to that with 0.5% Triton X-100. The data presented are the means \pm SD of a minimum of four experiments. Asterisk indicates values significantly different than time zero at $p < 0.05$.

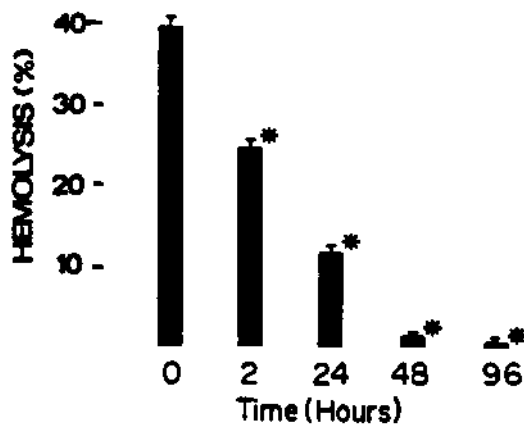
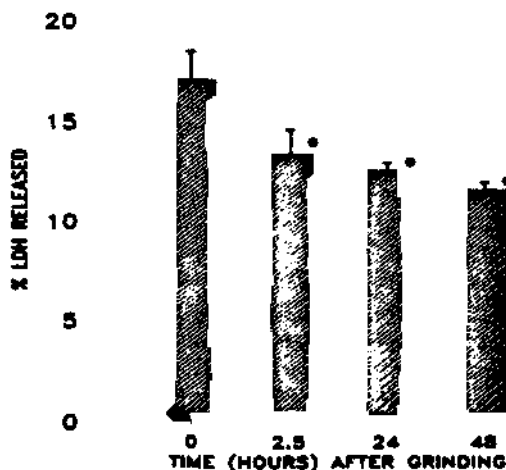


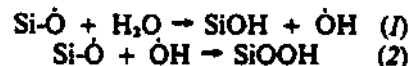
Fig. 7. Release of cytosolic lactate dehydrogenase, LDH, from alveolar macrophages exposed to either freshly ground or aged silica. LDH release was measured by the method of Wroblewski and LaDue (19). The data presented are the means \pm SD of seven experiments. Asterisk indicates values significantly different than time zero at $p < 0.05$.



hemolysis. Among the various scavengers, catalase provided the maximal protective effect in hemolysis. On the other hand, in bioassays of lipid peroxidation and H₂O₂ release, many hydroxyl radical scavengers such as DMSO, DMTU, mannitol, sodium benzoate, and catalase provided a significant inhibitory effect in one or both the bioassays. Catalase provided a complete abrogation of fresh silica-induced secretion of H₂O₂, even at an enzyme concentration of 312 units/ml, whereas it was effective in preventing lipid peroxidation to a 52 \pm 11% level only at a higher concentration (1,250 units/ml). DMTU and sodium benzoate were less effective in preventing H₂O₂ release. A potential for DMTU and sodium benzoate to react with H₂O₂ could not be ruled out.

Discussion

Our results provide evidence that mechanical crushing of crystalline silica for 30 min in air at room temperature produces a significant concentration ($\sim 10^{16}$ radicals/g of silica) of silicon-based radicals and that these radicals decay with time. Although the generation of silicon-based radicals upon cleavage of silicon crystals under ultra-high vacuum (10^{-10} mm Hg) has been reported earlier (10), recent studies from our laboratories and by Fubini (28) have shown the generation of free radicals from silica crushed in air. This report further indicates that these silicon-based radicals exhibit a half-life in the order of 30 h in air and have the ability to generate OH radicals in aqueous medium, making freshly ground silica biologically more reactive than aged silica. Our data also demonstrate that even after 4 wk of storage in air after grinding, as much as 20% of the original ESR signal remained detectable. This suggests the existence of at least two modes for the decay of the silicon-based radicals, i.e., a fast decay with an "average" half-life of about 30 h and a much slower decay with a much longer half-life. The decay mechanism is probably related to their reactions with a variety of chemical species in the atmosphere, including trace amounts of water vapor. We propose the following reaction sequence:



Equation (1) indicates that the silicon-based radicals could react with water in biologic solutions to generate OH radicals. Results shown in figure 2 confirmed

THE RESPIRABLE DUST CENTER

TABLE 1

EFFECT OF GRINDING CRYSTALLINE SILICA ON THE RATE OF LIPID PEROXIDATION AND THE TIME-DEPENDENT LOSS OF LIPID PEROXIDATION POTENTIAL ON STORAGE IN AIR*

Silica (mg/ml)	Malondialdehyde Formation (μ mol)			
	Time After Grinding			
	0-5 min	24 h	48 h	96 h
1.25	6.71 \pm 0.70	4.72 \pm 0.55 ($p < 0.03$)	1.95 \pm 0.45 ($p < 0.01$)	2.03 \pm 0.49 ($p < 0.01$)
2.5	6.48 \pm 0.11	4.58 \pm 0.36 ($p < 0.01$)	1.66 \pm 0.26 ($p < 0.01$)	1.43 \pm 0.14 ($p < 0.01$)
5.0	7.50 \pm 0.63	4.34 \pm 0.32 ($p < 0.01$)	1.96 \pm 0.26 ($p < 0.01$)	1.54 \pm 0.36 ($p < 0.01$)

* Data presented are the means \pm SD of a minimum of four sets of experiments in duplicate. p values given are for differences compared to 0-5 min after grinding silica. Each experimental set used the same stock of freshly ground silica at various times after grinding.

TABLE 2

COMPARATIVE EFFECT OF SCAVENGERS IN THE PREVENTION OF CYTOTOXICITY INDUCED BY FRESHLY FRACTURED SILICA*

Scavenger	Percent Decrease in Comparison to Controls*		
	Hemolysis	H ₂ O ₂ Release	Lipid Peroxidation
SOD, 340 units/ml	30 \pm 8	21 \pm 1	49 \pm 23
Catalase, 1,250 units/ml	80 \pm 16	100 \pm 0	52 \pm 11
Sodium benzoate, 0.1 M	31 \pm 10	26 \pm 2	75 \pm 8
DMSO, 0.1 M	1 \pm 0.5	100 \pm 0	100 \pm 0
DMTU, 0.1 M	3 \pm 2	37 \pm 5	100 \pm 0
Mannitol, 0.1 M	1 \pm 0	100 \pm 0	100 \pm 0

* Data presented are the means \pm SD of a minimum of two experiments in each assay.

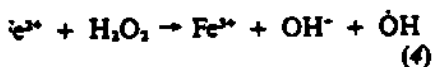
† Assays were carried out in the presence of 10, 1, and 5 mg/ml for hemolysis, H₂O₂ release, and lipid peroxidation, respectively.

formation of OH radicals when freshly crushed silica was suspended in aqueous solution. Because OH radicals are highly reactive toward biologic tissue (21, 30), the generation of such radicals from fresh dust could have important implications regarding the effects of inhaled silica.

We note that SiOOH could be formed during the decay of silicon-based radicals (equation 2) and that SiOOH could be hydrolyzed to produce H₂O₂ according to the following reaction (12):



This H₂O₂ could react with Fe²⁺ possibly present as a trace impurity in aqueous solution or on the silica particles themselves to generate OH radicals by the Fenton reaction as follows:



Our results show that DETAPAC, a strong metal chelator, had little effect on the DMPO-OH adduct ESR signal generated by freshly crushed silica in aqueous solution, i.e., there was little or no variation in the g value or the split-

ting pattern of the signal, with less than a 20% decrease in signal intensity even at an extremely high (3 mM) concentration of chelator. Because an iron-DETAPAC complex is unable to catalyze OH radical formation by equation 4 (24-27), these results indicate that the OH radicals detected were generated directly from the reaction of silicon-based radicals with water possibly according to reaction:



This hypothesis is supported by our finding that addition of catalytic amounts of catalase, which disproportionates H₂O₂ and O₂⁻, suppressed the formation of OH from freshly ground silica.

Other investigators have shown that silica could peroxidize the lipids in biologic membranes (31-33). Our investigation confirms these results and, in addition, indicates that the ability of silica to peroxidize lipids was enhanced by grinding of silica (table 1). The parallelism of the time dependence of lipid peroxidation with decay behavior of the OH radical produced by freshly ground silica (figure 3) leads us to propose that this enhanced

ability may be related to the generation of OH radicals by the reaction of freshly ground silica with water. Because lipid peroxidation has been proposed as a mechanism for cellular damage (34-37), it is possible that some of the harmful effects of silica on membrane integrity, such as hemolysis (figure 6) and LDH release (figure 7), could be mediated by this mechanism.

Data presented in this study indicate that freshly ground silica is more biologically reactive than aged silica, i.e., freshly crushed silica induces a greater respiratory burst in alveolar macrophages (figures 4 and 5) and greater cytotoxicity (figures 6 and 7, table 1). The generation of silicon-based radicals on the silica surface and the formation of OH radicals in solution may partially explain the enhanced reactivity of freshly fractured silica. Another possibility is that silanol (SiOH) groups on the fractured surface are formed by the hydrolysis of silicon-based radicals (equation 1) and that these groups increase the interaction between dust and chemical sites on the cell membrane. The presence of the surface silanol groups has been verified by infrared spectroscopy (38). Cell membranes contain several sites, i.e., oxygen or nitrogen groups that have electron pairs that can form hydrogen bonds with silanols. For example, bonding between a secondary amide and silanol has been reported (39). The formation of such hydrogen bonds may bring the silica particle and cell membrane closer together and, thus, provide more favorable conditions for the initiation of lipid peroxidation or activation of the cell surface.

It should be noted that the silicon-based radicals generated by grinding (figure 1) and the resultant OH radicals formed in water (figure 3) decayed over the course of days. Although the reactivity (figures 4 and 5) and cytotoxicity (figures 6 and 7, table 1) of freshly ground silica also decreased with time, a substantial potency remained even after 4 days. In addition, silica dust aged for years still retained the ability to stimulate alveolar macrophages (40), decrease membrane integrity (33, 41), and cause lipid peroxidation (31-33). Therefore, silicon-based reactive oxygen species can only partly explain the biologic reactivity of silica. Indeed, we have found that superoxide dismutase, catalase, and sodium benzoate were only partially effective in decreasing lysis, in contrast to a significant or complete abrogation of H₂O₂ release and lipid peroxidation by several hydroxyl scavengers (table 2). It is in-

teresting
scavenger
tive eff
release
zoate,
rate th
oxidati
hydrox
lation
ation a
our hy
is biol
freshly
to new
as well
generate
These
levels
ed fro
to fresh
idant
the de

In c
that re
contain
with a
OH
ration
arly gro
aged si
induce
ropha
therefo
icals o
tion o
cant r
initiat
a chain
be par
esis of
fresh
rock d
mill o

We wou
lia Ma
assista
assista

1. Zisi
Rev Re
2. Par
ed. Bos
3. Kle

interesting to note that all the potent OH scavengers provided a significant protective effect in lipid peroxidation and H₂O₂ release except for DMTU, sodium benzoate, and SOD. This ability to ameliorate the fresh silica-induced lipid peroxidation and H₂O₂ release by several hydroxyl scavengers provides direct correlation between the hydroxyl radical generation and cellular injury. Therefore, it is our hypothesis that although aged silica is biologically reactive and cytotoxic, freshly fractured silica is more potent due to newly generated silicon-based radicals as well as the propagation of other oxygenated radicals in aqueous environment. These reactive radicals plus the enhanced levels of reactive forms of oxygen secreted from alveolar macrophages exposed to freshly crushed silica may result in oxidant loads that exceed the capacity of the defense mechanisms of lung tissue.

In conclusion, this study documents that respirable-size freshly ground silica contains silicon-based radicals that react with aqueous environments to produce OH radicals. The free-radical concentration and the biologic reactivity of freshly ground silica are higher than those of aged silica as measured by ESR and silica-induced O₂ and H₂O₂ release from macrophages and by lipid peroxidation. We, therefore, propose that silicon-based radicals on silica and the resultant generation of OH radicals may play a significant role in cell membrane damage by initiation of lipid peroxidation through a chain reaction. This mechanism should be particularly relevant to the pathogenesis of acute silicosis where inhalation of fresh silica occurs, as in sandblasting, rock drilling, tunnelling, and silica flour mill operations.

Acknowledgment

We would like to thank Myhanh Nguyen, Julia Martin, and Daniel Davies for technical assistance, and Lunette Utter for secretarial assistance.

References

1. Ziskind M, Jones RN, Weill H. Silicosis. *Am Rev Respir Dis* 1976; 113:643-65.
2. Parkes WR. Occupational lung disorders. 2nd ed. Boston, MA: Butterworths, 1982.
3. Kleinerman J, Merchant JA. In: Baum GL,

Wolinsky E, eds. Textbook of pulmonary diseases. 3rd ed. Boston, MA: Little Brown and Co., 1983.

4. Heppleston AG. Silicotic fibrogenesis: a concept of pulmonary fibrosis. *Ann Occup Hyg* 1982; 26:449-62.
5. Davis GS. The pathogenesis of silicosis. *Chest* 1986; 89:166-69s.
6. Weiss SJ, LoBuglio AF. Biology of disease: phagocyte-generated oxygen metabolites and cellular injury. *Lab Invest* 1982; 47:5-18.
7. Heppleston AG, Styles JA. Activity of a macrophage factor in collagen formation by silica. *Nature* 1967; 214:521-2.
8. Bitterman PB, Rennard SI, Hunninghake GW, Crystal RG. Human alveolar macrophage growth factor for fibroblasts: regulation and partial characterization. *J Clin Invest* 1982; 70:806-22.
9. Banks DE. Acute silicosis. In: Merchant JA, ed. Occupational respiratory diseases. Washington, DC: U.S. Department of Health, Publication No. 86-102, U.S. Government Printing Office, 1986; 239-41.
10. Hochstrasser G, Antinini JF. Surface states of pristine silica surfaces. *Surface Sci* 1972; 644-64.
11. Karmanova EV, Myasnikov IA, Zayalov SA. Mechanism of the emission of singlet oxygen molecules from a disordered quartz surface. *Zhurnal Fizicheskoi Khimii* 1984; 58:1958-61.
12. Kolbanev IV, Berestskaia IV, Buryagin PY. Mechanochemistry of quartz surface. *Kinetika i Kataliz* 1980; 21:1154-8.
13. Marasas LW, Harington JS. Some oxidative and hydroxylative action of quartz: their possible relationship to the development of silicosis. *Nature* 1960; 188:1173-4.
14. Myrvia QN, Evans DG. Metabolic and immunologic activities of alveolar macrophages. *Arch Environ Health* 1967; 14:92-6.
15. Phillips HJ. Dye exclusion tests for cell viability. In: Kruse PR, Patterson MD, eds. Tissue culture methods and applications. New York: Academic Press, 1973; 406-8.
16. Sweeney JD, Castranova V, Bowman L, Miles PR. Factors which affect superoxide anion release from rat alveolar macrophages. *Exp Lung Res* 1981; 2:85-96.
17. Van Scott MR, Miles PR, Castranova V. Direct measurement of hydrogen peroxide release from rat alveolar macrophages: artifactual effect of horseradish peroxidase. *Exp Lung Res* 1984; 6: 103-14.
18. Murray HW, Cohn ZA. Macrophage oxygen-dependent anti-microbial activity. III. Enhanced oxidative metabolism as an expression of macrophage activation. *J Exp Med* 1980; 152:1956-60.
19. Wroblewski F, LaDue JS. Lactic dehydrogenase activity in blood. *Proc Soc Exp Biol Med* 1955; 90:210-4.
20. Fraga CG, Leibovitz BE, Tappel AL. Halogenated compounds as inducers of lipid peroxidation in tissue slices. *J Free Rad Biol Med* 1987; 3:119-23.
21. Bolis V, Fubini B, Venturello G. Surface characterization of various silica. *J Thermal Anal* 1983; 28:249-57.
22. Dalal NS, Suryan MM, Jafari B, Shi X, Vallyathan V, Green FHY. Electron spin resonance de-

tection of reactive free radicals in fresh coal dust and quartz dust and its implications to pneumoconiosis and silicosis. In: Frantz RL, Ramani RV, eds. Proceedings of International Symposium on Respirable Dust in the Mineral Industries. University Park, PA: The Pennsylvania State University, 1988; 24-9.

23. Weitzman SA, Gracetta P. Asbestos catalyzes hydroxyl and superoxide radical generation from hydrogen peroxide. *Arch Biochem Biophys* 1984; 228:373-6.
24. Finkelstein E, Rosen GM, Rauckman EJ. Spin trapping of superoxide and hydroxyl radical: practical aspects. *Arch Biochem Biophys* 1980; 200:1-6.
25. Rosen GN, Freeman BA. Detection of superoxide generated by endothelial cells. *Proc Natl Acad Sci USA* 1984; 81:7269-73.
26. Bannister JV, Bannister WH. Production of oxygen-centered radicals by neutrophils and macrophages as studied by electron spin resonance (ESR). *Environ Health Perspect* 1985; 37:37-43.
27. Oberley LW. The spin trapping of superoxide and hydroxyl radicals. In: Oberley LW, ed. Superoxide dismutase. Boca Raton, FL: CRC Press, 1982; 2:70-4.
28. Fubini B. The surface chemistry of crushed quartz dust in relation to its pathogenicity. In: *Org Chem Acta* 1987; 138:193-7.
29. Halliwell B. Oxidants and human disease: some new concepts. *FASEB J* 1987; 1:358-64.
30. Halliwell B, Gutteridge JMC. The importance of free radicals and catalytic metal ions in human disease. *Mol Aspects Med* 1985; 8:189-93.
31. Gabor S, Anca Z. Effect of silica on lipid peroxidation in the red cells. *Int Arch Arbeitsmed* 1974; 32:327-32.
32. Gabor S, Anca Z, Zugravu E. *In vitro* action of quartz on alveolar macrophage lipid peroxides. *Arch Environ Health* 1975; 30:499-501.
33. Singh VS, Rahman Q. Interrelationship between hemolysis and lipid peroxidation of human erythrocytes induced by silicic acid and silicate dusts. *J Appl Toxicol* 1987; 7:91-6.
34. Chan PC, Peller DG, Kesner L. Copper (II)-catalyzed lipid peroxidation in liposomes and erythrocyte membranes. *Lipids* 1982; 17:331-7.
35. Tappel AL. Lipid peroxidation damage to cell components. *Fed Proc Fed Am Soc Exp Biol* 1972; 32:1870-4.
36. McKay PB. Physiological significance of lipid peroxidation. *Fed Proc Fed Am Soc Exp Biol* 1981; 40:173.
37. Compurti M. Lipid peroxidation and cellular damage in toxic liver injury. *Lab Invest* 1985; 53: 599-623.
38. Tsuchiya I. Infrared spectroscopic study of hydroxyl groups on silica surfaces. *J Phys Chem* 1982; 86:4107-12.
39. Sumerton J, Hoening S, Butler C, Chvapil M. The mechanism of hemolysis by silica and its bearing on silicosis. *Exp Mol Pathol* 1977; 26:113-28.
40. Castranova V, Pailles WH, Li C. Effects of silica exposure on alveolar macrophages (AM): action of tetrandrine. *The Toxicologist* 1988; 8:199.
41. Wallace WE Jr, Vallyathan V, Keane MJ, Robinson V. *In vitro* biologic toxicity of native and surface-modified silica and kaolin. *J Toxicol Environ Health* 1985; 16:415-24.

Detection of Hydroxyl Radical Formation in Aqueous Suspensions of Fresh Silica Dust and Its Implication to Lipid Peroxidation in Silicosis

X. Shi¹, N.S. Dalal¹ and V. Vallaythan²

¹Department of Chemistry, West Virginia University

²Division of Respiratory Disease Studies, National Institute for Occupational Safety and Health, Morgantown, WV

Cellular damage induced by silica dust is known to be associated with increased fragility and destabilization or destruction of the cell membranes. The mechanism by which silica dust effects biological membranes is still unknown. Using the ESR spin-trap methodology, we find that hydroxyl radicals are generated in aqueous suspensions of freshly ground silica. The amount of the radicals generated depends on the extent of grinding and "freshness" of the dust. Using linoleic acid as a model lipid, we show that the silica dust causes lipid peroxidation via $\cdot\text{OH}$, O_2^- , or linoleic acid related radicals as intermediates. Catalase and superoxide dismutase inhibit the formation of these radicals. The results suggest that free radicals associated with freshly ground silica and the related lipid peroxidation of the membranes may be the starting point of the silicotic processes.

INTRODUCTION

Despite considerable effort over the years, the mechanism by which the quartz particles exert their toxic action on cells and the process(es) by which these actions progress to fibrosis are still not fully understood (1,2). It is generally thought, nevertheless, that the interaction of the quartz particles with the cell membranes is the starting point of the silicotic process (3). We felt that the mechanism of the membrane damage by quartz might involve oxygenated free radicals because (a) a suspension of quartz particles in contact with alveolar macrophages has been reported (4,5) to initiate an enhancement of lipid peroxidation, defined broadly as the oxidative deterioration of polyunsaturated components of lipids, and (b) hydroxyl ($\cdot\text{OH}$) radicals are known to be capable of peroxidation by abstracting hydrogen atoms from cell-membrane lipids (6) and initiating lipid peroxidation in lysosomal membranes (7). Moreover it is known that exposure of cell membranes, fatty acids and unsaturated food oils to ionizing radiation, which generates $\cdot\text{OH}$ radicals, causes rapid peroxidation (6). Earlier studies of the aqueous chemistry of quartz suspensions have reported detection of H_2O_2 (8), implicating the formation of $\cdot\text{OH}$ radicals as transient species, but, we are not aware of any report of the detection of $\cdot\text{OH}$ radicals in quartz suspensions and this provided the motivation for the present undertaking. Since it is known that, because of their high reactivity (hence short life time) in aqueous media, the $\cdot\text{OH}$

radicals cannot be detected via electron spin resonance (ESR) directly (9,10), we have used ESR combined with the spin-trap methodology (9) for studying the $\cdot\text{OH}$ formation.

MATERIALS AND METHODOLOGY

Crystalline silica with particle sizes of 0.2 to 2.5 μm was obtained from the Generic Respirable Dust Technology Center, Pennsylvania State University, University Park, Pennsylvania. Particles in the range of smaller than 25 microns were produced by hand grinding in air, using an agate mortar and pestle because of the structural similarity of agate to that of quartz. Also a rather mixed particle size, rather than a specific range, was employed, with a view to roughly approximate the random particle-size distribution in the mining atmosphere. ESR spectra were obtained at X-band (9.7 GHz) using a Bruker ER 200D ESR spectrometer. For accurate measurements of the g-values and hyperfine splittings, the magnetic field was calibrated with a self-tracking NMR gaussmeter (Bruker, model ER035M) and the microwave frequency was measured with a frequency counter (Hewlett-Packard, Model 5340A). 5,5-dimethyl-1-pyrroline-1-oxide (DMPO) was purchased from Aldrich and used without further purification, since very weak or no ESR signals were obtained from the purchased sample when used by itself. If necessary the background signals were subtracted from those related to quartz by using an Aspect 2000 microcomputer.

RESULTS

Some typical results of the ESR spin-trapping studies are shown in Fig. 1. We found that a 0.1 M aqueous solution of the spin-trap DMPO alone, with unground particles or with TiO_2 powder did not give a detectable ESR spectrum. TiO_2 was used as a control because it is known not to be fibrogenic (11) and has a structure resembling quartz (SiO_2). However, when quartz was ground in a 0.1 M DMPO (aqueous) solution or when ground quartz particles were mixed with 0.1 M DMPO (aqueous) solution, an ESR spectrum ($g = 2.0059$), consisting of a 1:2:2:1 quartet pattern with a splitting of 14.9 G, was observed (Fig. 1a). Based on earlier work (9, 12,13), this spectrum was considered to be due to the DMPO-OH adduct.

Two further tests were made to identify the spectrum. First, the Fenton reaction ($\text{Fe}^{2+} + \text{H}_2\text{O}_2 \rightarrow \text{Fe}^{3+} + \cdot\text{OH} + \text{OH}^-$) (14), known to produce $\cdot\text{OH}$ radicals, was used as a standard. The ESR spin-adduct spectrum obtained by mixing 0.085 M H_2O_2 , 0.0165 M FeSO_4 and 0.1 M DMPO was the same as that of Fig. 1a (obtained with ground quartz), thus attesting to the formation of the $\cdot\text{OH}$ radical in the quartz suspension.

As a second, confirmatory, test of the $\cdot\text{OH}$ radical formation, spin-trap ESR experiments were performed in which ethanol was added as a secondary trap. It has been shown (10,15) that in the presence of ethanol, the intensity of the DMPO-OH signal decreases, because ethanol scavenges some of the $\cdot\text{OH}$ radicals to form the ethanoly radical (12) which react with DMPO to give the spin-adduct DMPO-CHOHCH₃. The ESR spectrum of the spin-adduct DMPO-CHOHCH₃ was indeed

THE RESPIRABLE DUST CENTER

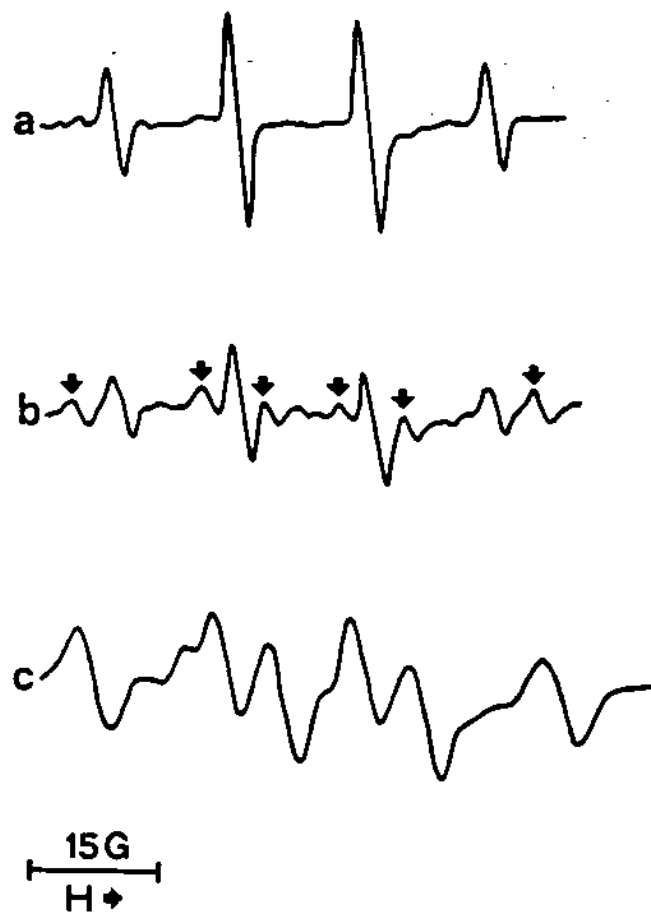


Fig. 1 ESR spectra recorded 2 minutes after mixing 100 mM DMPO aqueous solution with (a) freshly ground quartz particles; (b) same as (a) but with 30% ethanol added; (c) same as (a) but with excess ethanol. Receiver gain, 5×10^5 ; modulation amplitude, 2 G; scan time, 100 seconds; field, 3460 ± 75 G.

observed as indicated by arrows in Fig. 1b (for 30% ethanol) and more clearly in Fig. 1c, obtained in the presence of excess ethanol, thus confirming the $\cdot\text{OH}$ radical formation in the quartz suspension.

The intensity of the $\cdot\text{OH}$ radical adduct signal increases with the amount of grinding (Table I), thus showing that the $\cdot\text{OH}$ radical generation is related to some surface property of the freshly made dust, most likely the silicon-oxygen radical sites known to form on grinding (16-21). Additional spin-trap measurements as a function of the time of "aging" of the dust after grinding showed that freshly generated quartz dust produces more $\cdot\text{OH}$ radicals than that which had been stored in air after grinding (Table II). In order to characterize the kinetics of the dust's aging on its ability to generate $\cdot\text{OH}$ radicals, attempts were made to determine whether the reaction was of the first order (a straight line plot for $\log(\text{con.})$ vs. time) or second order (straight line plot for $(\text{con.})^{-1}$ vs. time). The analysis indicated the kinetics to be neither first nor second order but of a more complex nature. Thus while it was not possible to define a unique half-life for the decrease in the $\cdot\text{OH}$

Table I

Dependence of the ESR intensity of the DMPO-OH adduct (i.e. ·OH production) on size (grinding times) of quartz particles.

Grinding times (minutes)	Relative ESR intensity
0.0	0.0
0.5	0.3 ± 0.3
1.0	1.1 ± 0.6
2.0	2.3 ± 0.7
4.0	3.4 ± 0.8
10.0	5.1 ± 1.2

Table II

Dependence of the ESR intensity of the DMPO-OH adduct (i.e. ·OH production) on the "aging" of quartz dust.

Time after grinding	Relative ESR intensity
5 minutes	5.2 ± 0.8
1 day	3.2 ± 0.8
2 days	1.9 ± 0.7
3 days	1.7 ± 0.8
4 days	1.3 ± 0.7

radical producing potential of the quartz dust on storage after grinding, we note that, on the average, freshly ground quartz dust loses its ·OH-generating capacity to about 50% in approximately 1 day.

DISCUSSION

It is clear that the breakage of quartz crystals implies the homolysis of Si-O-Si bonds and the generation of silicon-based radicals ($\equiv\text{Si}\cdot$, $\equiv\text{SiO}\cdot$, $\equiv\text{SiOO}\cdot$) (8, 16-21). We have indeed verified that Si· and SiO·-type of radicals are produced by grinding in air, and that the radicals decay as a function of time when the dust is stored in air after grinding (17), with a half-life of about one and a half day. Earlier workers (16) have reported that the crushing of quartz under vacuum produces SiO·-type radicals whose concentration decreases drastically on exposure to atmosphere with a half-life of about 30 hours.

Following Kalbanov et al. (8), we suggest that the ·OH radical production might involve the following steps (8):



Kalbanev et al. have also suggested (8) that the hydrolysis of SiOOH could produce H₂O₂, according to reaction (c):



The yield of H₂O₂, depending on the pH and the temperature of hydrolysis, was reported to be as high as 10¹⁸ molecules/g quartz particles (8), enough to be measured by the standard method of wet analytical chemistry, the MnO₄⁻ reduction:



We verified the reducing activity of our quartz particle suspension with respect to KMnO₄, although the H₂O₂ yield was measured to be about an order of magnitude smaller for our samples than those of Kalbanev et al. (8). Thus experiments were carried out to examine whether the ·OH radical formation was through the Fenton reaction (14), the Fe²⁺ possibly being a trace impurity. The experiments consisted of spin-trap measurements in which diethylenetriaminepentaacetic acid (DETAPAC) (0.03 - 3.0 mM) was used as a strong metal-ion chelate. It is known that the iron-DETAPAC complex formation stops the ·OH generation from H₂O₂ (9). On adding DETAPAC the ·OH radical-related ESR signals showed no variation in either the g value or the observed splitting pattern but only a small (-20 %) decrease in intensity even at the high DETAPAC (3 mM) levels. This result, together with the dependence of the ·OH radical concentration on time and surface freshness, suggests that the Fenton-type mechanism is not a major contributor to the ·OH radical generation in our quartz suspensions.

After this work was essentially complete (17-20), two significant reports have appeared. In the first, Fubini et al. (21) have reported the formation of Si·, SiO·, and SiO₂· radicals on quartz particles ground in air, without contact with water. They suggest a possible role of these radicals (or some other surface property) in the mechanism of quartz-induced fibrosis. Our ESR results on the silicon-based radicals (18, 19) agree with Fubini's (21). We further show that the concentration of the Silicon-based radicals is time dependent (17) and that their reaction with aqueous media generates (perhaps) an even more potent species (18-20), the ·OH radicals. The second paper, by Gulumian and Van Wyk (22), reported the detection of ·OH formation in aqueous suspension of glass and quartz fibres in the presence of H₂O₂, and the scavenging of the generated ·OH radicals by the prophylactic agent (polymer) polyvinylpyridine N-oxide (PVPNO). They suggest that the therapeutic efficacy of PVPNO in silicosis might be related to its scavenging effects on ·OH radicals. Our work shows that the grinding process itself causes the quartz surface to be a source of ·OH radicals in aqueous media and that this activity decreases with the aging of the dusts (19,20). This higher toxicity of fresh dust must be taken into consideration in the future *in vitro* or *in vivo* laboratory (e.g., animal exposure) studies of quartz and related mineral dusts.

DETECTION OF HYDROXYL RADICALS

REFERENCE

1. Reiser K.M., Last J.A.: Silicosis and Fibrogenesis: Fact and Artifact. Toxicology 13:15-72 (1979).
2. Singh S.V., Rahman Q. 1987. Interrelationship between Hemolysis and Lipid Peroxidation of Human Erythrocytes Induced by Silicic Acid and Silicate Dusts. J. Appl. Toxicol. 12:91-96 (1987).
3. Parazzi E., Secchi G.C., Pernis B., Vigliani E.: Cytotoxic Action of Silica Dusts on Macrophages in Vitro. Arch. Environ. Health 17:850-859 (1968).
4. Gabor S., Anca Z., Zugravu E.: In Vitro Action of Quartz on Alveolar Macrophage Lipid Peroxides. Arch. Environ. Health 30:499-501 (1975).
5. Koike S., Kuno Y., Morita H.: The Effects of Silica on Lipid Peroxidation, and the Production of Superoxide Radicals by Phagocytizing Rabbit Macrophages. Japanese J. Hygiene 37:510-515 (1982).
6. Halliwell B., Gutteridge J.M.C.: Lipid Peroxidation: A Radical Chain Reaction. In Free Radicals in Biology and Medicine (1985) pp.159. The University Press (Belfast) Ltd. Northern Ireland.
7. Fong K.L., McCay P.B., Poyer J.L., Keel B.B., Misra H.: Evidence That Peroxidation of Lysosomal Membranes Is Initiated by Hydroxyl Free Radicals Produced during Flavine Enzyme Activity. J. Biol. Phys. 248:7792-7797 (1973).
8. Kalbanev I.V., Berestetskaya I.V., Butyagin P.U.: Mechanochemistry of Quartz Surface. Kinetika i Kataliz 21:1154-1158 (1980).
9. Finkelstein E., Rosen G.M., Rauckman E.J.: Spin Trapping of Superoxide and Hydroxyl Radical: Practical Aspects. Arch. Biochem. Biophys. 200:1-16 (1980).
10. Oberley L.W.: The Spin Trapping of Superoxide and Hydroxyl Radicals. In Superoxide Dismutase 2:70-74 (1982). The CRC Press, Boca Raton, Florida.
11. Gormley I.P., Kowolik M.J., Cullen R.T.: The Chemiluminescent Response of Human Phagocytic Cells to Mineral Dusts. Br. J. Exp. Path. 66:409-416 (1985).
12. Bannister J.V., Bannister W.H.: Production of Oxygen-Centered Radicals by Neutrophils and Macrophages as Studied by Electron Spin Resonance (ESR). Environ. Health Persp. 64:37-43 (1985).
13. Rosen G.M., Freeman B.A.: Detection of Superoxide Generated by Endothelial Cells. Proc. Natl. Acad. Sci. USA 81:7269-7273 (1984).
14. Halliwell B., Gutteridge, J.M.C.: Oxygen Toxicity, Oxygen Radical, Transition Metals and Disease. Biochem. J. 219:1-14 (1984).
15. Weitzman S.A., Graceffa P.: Asbestos Catalyzes Hydroxyl and Superoxide Radical Generation. Arch. Biochem. Biophys. 228:373-376 (1984).
16. Hochstrasser G., Antonini J.F.: Surface States of Pristine Silica Surfaces. Surface Sci. 32:644-664 (1972).
17. Dalal N.S., Suryan M.M., Jafari B., Shi X., Vallyathan V., Green F.H.Y.: Electron Spin Resonance Detection of Reactive Free Radicals in Fresh Coal Dust and Quartz Dust and Its Implications to Pneumoconiosis and Silicosis. Proc. Int. Symp. on Respir. Dusts in the Mineral Ind. Pennsylvania State University, State College, Pennsylvania, USA (1986) (in press).

THE RESPIRABLE DUST CENTER

18. Vallyathan V., Shi X., Dalal N.S., Irr W.: Role of Reactive Oxygen Radicals in Silica Cytotoxicity. 4th Int. Cong. on Oxygen Radicals (abstract). p. 98, La Jolla, California, USA (1987).
19. Shi X., Dalal N.S., Vallyathan V.: ESR Evidence for the Hydroxyl Radical Formation in Aqueous Suspension of Quartz Particles and Its Possible Significance to Lipid Peroxidation in Silicosis. J. Toxicol. Environ. Health. (1988) (in press).
20. Vallyathan V., Shi X., Dalal N.S. Irr W., Castranova V.: Generation of Free Radicals from Freshly Fractured Silica Dust: Potential Role in Acute Silica-Induced Lung Injury. Am. Rev. Respir. Dis. 1988 (in press).
21. Fubini B., Bolis V., Giamello E.: The Surface Chemistry of Crushed Quartz Dust in Relation to Its Pathogenicity. Inorg. Chim. Acta. 138: 193-197 (1987).
22. Gulumian M., Van Wyk A.: Free Radical Scavenging Properties of Polyvinylpyridine N-oxide: A Possible Mechanism for Its Action in Pneumoconiosis. Med. Lav. 78:124-128 (1987).

Suppression of Inhaled Particle Cytotoxicity by Pulmonary Surfactant and Re-toxicification by Phospholipase: Distinguishing Properties of Quartz and Kaolin

W.E. Wallace, Jr., M.J. Keane, V. Vallyathan, P. Hathaway, E.D. Regad, V. Castranova, and F.H.Y. Green

West Virginia University and Appalachian Laboratory for Occupational Safety and Health, Division of Respiratory Disease Studies, National Institute for Occupational Safety and Health

Abstract—Inhaled particle contact with pulmonary surfactant in the hypophase lining pulmonary alveoli was modelled *in vitro* by exposing two respirable sized dusts, kaolin and silica quartz, to lecithin, a major component of pulmonary surfactant, emulsified in physiological saline. Lecithin adsorbs to the dusts upon incubation at 37°C and suppresses their cytotoxicity as measured by pulmonary macrophage and erythrocyte assays, suggesting that pulmonary surfactant provides a defence system against prompt cell membrane lysis by inhaled dusts. Subsequent pulmonary macrophage phagocytosis and lysosomal enzyme digestion of the coated dusts was modelled *in vitro* by incubation with phospholipase A₂ for one hour. With increasing lipase activity, silica haemolytic potential was restored to native silica levels. Kaolin was retoxified to levels far in excess of native kaolin haemolytic potential. Elution, thin layer chromatography and phosphate assay of treated dusts indicate that most lecithin on silica is digested to lysolecithin and desorbed, silica retoxification being due to surface and adherent lysolecithin effects. Most lecithin on kaolin is not digested in the same time; that which is, results in adherent lysolecithin which is responsible for the kaolin retoxification. Digestion with phospholipases A₂ and C together produces only weakly retoxified kaolin. Results suggest that surface adsorption properties which control the adherence of prophylactic surfactant distinguish the pathogenic potentials of quartz, kaolin and mixed dust.

INTRODUCTION

ERYTHROCYTE HAEMOLYSIS and pulmonary macrophage enzyme release assays show quantitatively comparable high cytotoxicities for both silica quartz and kaolin respirable sized dusts (BROWN, *et al.*, 1980; DANIEL and LE BOUFFANT, 1980.) This contrasts with the strong potential for respirable quartz dust to induce pulmonary fibrosis and the much more limited potential of kaolin dust to do the same (MORGAN and SEATON, 1975).

In an attempt to understand this anomalous situation, assays were performed on quartz and kaolin dusts incubated with dipalmitoyl lecithin emulsified in physiological saline, to simulate the initial contact of a respired dust with the pulmonary alveolar hypophase. The ability of kaolin dust to adsorb dipalmitoyl lecithin from physiological saline has been quantified (WALLACE, *et al.*, 1975). Such lecithin treatment suppresses

the cytotoxicity of both silica and kaolin to background levels (WALLACE, *et al.*, 1984).

Surfactant coated de-toxified dusts should then be phagocytised by pulmonary macrophages, incorporated into a macrophage secondary lysosome and exposed to hydrolytic lysosomal enzymes. Among these is phospholipase A₂, which hydrolyses diacyl lecithin to lysolecithin. This was modelled by incubating lecithin treated dusts with phospholipase A₂ *in vitro* to determine if the enzyme can digest the dust-adsorbed lecithin, and if the retoxification differs between the two dusts in a manner which might distinguish their pathogenicity.

MATERIALS AND METHODS

The silica used was at least 98.5% pure as determined by X-ray energy spectrometric analysis and was alpha quartz as determined by X-ray diffraction. Its N₂ adsorption specific surface area was 3.97 m²/g. The kaolin used was at least 96% pure, contained no crystalline silica, and had a specific surface area of 13.25 m²/g.

L- α -dipalmitoyl glycerophosphoryl choline (lecithin) (DPL) was ultrasonically dispersed in 0.165 M NaCl saline to produce an emulsion of 10 mg DPL per ml saline. Dry silica or kaolin dusts were mixed into a concentration of 7.5 mg dust per ml emulsion. Mixtures were incubated for one hour at 37°C in a shaking water bath, centrifuged for ten minutes at 990 xg, and the dusts resuspended in calcium and magnesium free phosphate buffered 0.165 M NaCl saline (PBS). This washing procedure was repeated to remove unadsorbed lecithin, the lecithin coated dusts being suspended finally in PBS.

Aliquots of native or lecithin-treated dusts in PBS with 2.0 mM CaCl₂ were incubated with Phospholipase A₂ (PLA₂), obtained from *Crotalus adamanteus* venom, at 37°C for one hour. The concentrations used covered a range of activities from that needed to digest from one-tenth to 1000 \times the amount of kaolin-adsorbed lecithin had the digestion been for a homogeneous phase. 'Phospholipase activity' is given in terms of 'activity equivalents' which are equal to 0.0817 units of phospholipase. Following digestion, the samples were centrifuged and the dusts resuspended in PBS containing 2.0 mM EDTA to stop the enzymatic digestion. This washing procedure was repeated, with the dusts suspended in PBS alone. All procedures were done under sterile conditions.

Suspensions of 2% by volume sheep erythrocytes and 1.0 mg native or treated dust per ml PBS were incubated in a shaking water bath at 37°C for one or two hours, as indicated, to assay the dusts' haemolytic potential (HARRINGTON, *et al.*, 1971). Samples were then centrifuged at 990 xg and the optical density for haemoglobin read at 540 μ m on a spectrophotometer. Haemolysis assays were also performed using kaolin incubated with L- α -lecithin, β palmitoyl (lysolecithin) using the lecithin treatment procedure.

Macrophages lavaged from male Sprague Dawley rats were mixed with native or treated dusts to produce concentrations of 2 \times 10⁶ cells per ml and one mg dust per ml. These were incubated for two hours at 37°C in a shaking water bath. Released enzyme activities were determined for lactate dehydrogenase (LDH) (REEVES and FIMIGNARI, 1963), beta-glucuronidase (B-GLUC) (LOCKART and KENNEDY, 1976), and beta-N-acetyl glucosaminidase (B-NAG) (SELLINGER, *et al.*, 1960). Percentages of enzymes released were calculated relative to Triton X-100 lysed samples.

KAOLIN AND SILICA QUARTZ

Parallel samples of dusts were eluted with methanol/chloroform solvent (2:1 vol/vol) following their lecithin and phospholipase treatments. The eluted material was quantitated for lecithin and for lysolecithin by wet phosphate assay of thin layer chromatograph separated materials (BARTLETT, 1959).

Adsorption by silica and by kaolin of lecithin from physiological saline emulsion at 37°C was measured over a range of final (unadsorbed) supernatant concentrations of 0.02 to 10.0 nanomoles per ml emulsion, as quantitated by wet phosphate assay.

RESULTS

Native quartz and kaolin dusts produce comparable high haemolysis cytotoxic response (Fig. 1). On a surface area basis the two dusts were also comparable with haemolytic strengths of 22.6% for kaolin and 24.4% for silica per square decimeter dust surface area in the dispersion.

Lecithin treatment of dusts suppressed their haemolytic strengths to background levels (Fig. 1). This is due principally to lecithin interaction with the dust rather than with the cells (WALLACE, *et al.*, 1985). Lecithin treatment also suppresses the cytotoxicity of both silica and kaolin for pulmonary macrophages (Fig. 2). The kaolin and silica used in this study had specific adsorptions of around 150 mg lecithin/gram kaolin and 50 mg lecithin/gram silica over the supernatant concentrations of interest (Fig. 3).

Incubation of lecithin-treated quartz with PLA₂ results in increasing retoxification of the silica with PLA₂ activity, up to native quartz haemolytic potential (Fig. 4). Data are fitted by non-linear regression to a first order kinetics curve. Incubation of quartz with PLA₂ (alone) in physiological saline produces dusts of comparable cytotoxicities to native silica. Incubation of lecithin-treated kaolin with PLA₂ results in increasing retoxification of the kaolin with PLA₂ activity (Fig. 5). However, unlike the quartz, kaolin retoxifies to an anomalously high level, well above (of the order of twice) the

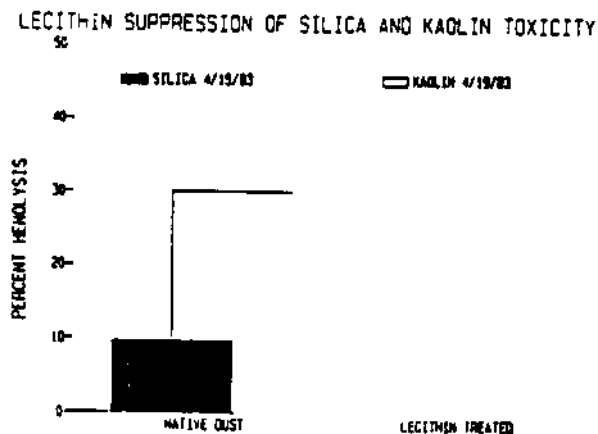


FIG. 1. Silica and kaolin haemolytic strength. Percent haemolysis of sheep erythrocytes induced by incubation for one hour with 1 mg/ml of native or lecithin-treated kaolin or silica.

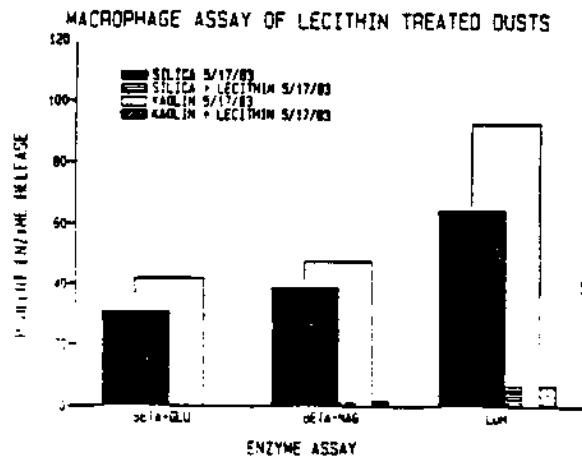


FIG. 2. Macrophage assay of lecithin-treated dusts. Release of beta-glucuronidase, beta-n-acetylglucosaminidase, and lactate dehydrogenase from rat pulmonary macrophage induced by two hour incubation with 1mg/ml of native or lecithin-treated kaolin or silica.

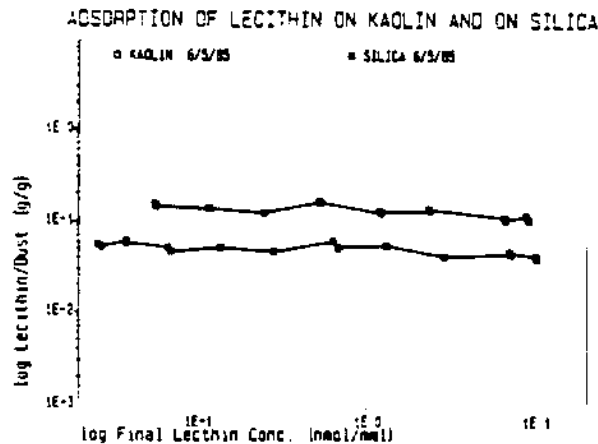


FIG. 3. Adsorption of lecithin on kaolin and on silica. Adsorption isotherm data for mass lecithin adsorbed per mass of kaolin or silica versus concentration of lecithin remaining in the supernatant.

cytotoxicity of native untreated kaolin. Incubation of kaolin with lysolecithin alone dispersed in physiological saline reproduces this high cytotoxicity (Fig. 5). Incubation of kaolin with PLA₂ alone in physiological saline produces dust of comparable cytotoxicities to native kaolin.

After PLA₂ digestion a high percentage of adsorbed lecithin is retained on the kaolin surface (Fig. 6). A significant amount of lysolecithin produced by the lecithin digestion is also associated with the lecithin-kaolin complex. A much smaller fraction of the initially adsorbed lecithin remains on the silica as lecithin or lysolecithin following PLA₂ digestion. Haemolysis assays of parallel samples are shown in Fig. 7.

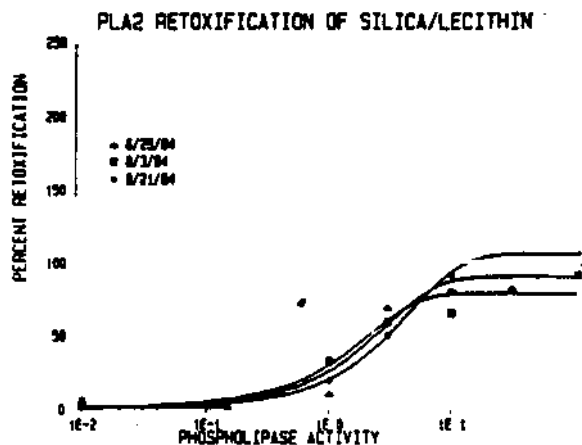


FIG. 4. PLA₂ retoxification of silica/lecithin. Erythrocyte haemolysis induced by two hour incubation with silica treated with lecithin for one hour, and then with differing amounts of phospholipase A₂ for one hour. Ordinate values are expressed as percent of the haemolysis induced by untreated silica. Abscissa values are the number of activity equivalents of phospholipase A₂ applied. Haemolysis by dusts treated with lecithin only is shown at the smallest activity value.

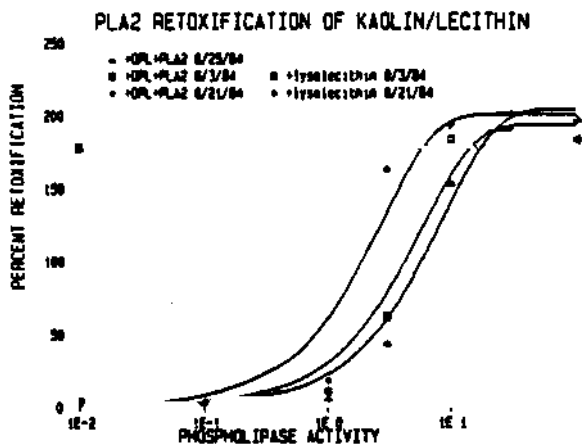


FIG. 5. PLA₂ retoxification of kaolin/lecithin. Erythrocyte haemolysis induced by kaolin treated with lecithin for one hour and then with differing amounts of phospholipase A₂ for one hour, and haemolysis by kaolin treated with lysolecithin only.

COMMENT

A major component of pulmonary surfactant, dipalmitoyl lecithin, can adsorb to quartz and to kaolin and suppress their cytotoxicity. This is consistent with lipidosis associated with large pulmonary dust burdens. Subsequent treatment with phospholipase A₂, a known component of pulmonary macrophage lysosomal enzyme, restores haemolytic ability to both treated dusts. However, this restoration differs quantitatively and qualitatively between the two dusts. This may be a basis for their differing pathogenicities.

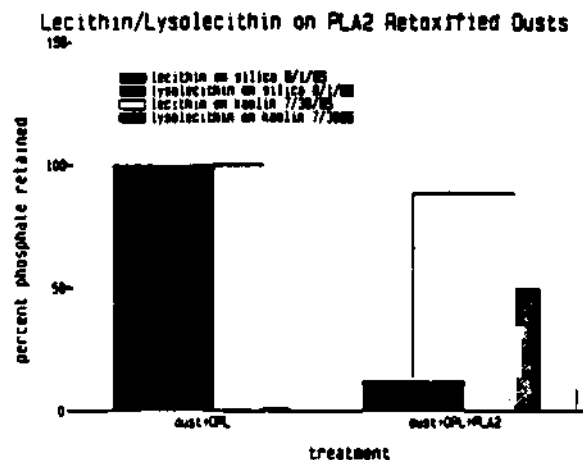


FIG. 6. Lecithin/lysolecithin on PLA₂ retoxified dusts. Lecithin and lysolecithin eluted by organic solvent from silica or kaolin treated with lecithin or treated first with lecithin and then with 1000 activity equivalents of phospholipase A₂. Ordinate values are percent of the lecithin eluted from lecithin-treated dusts.

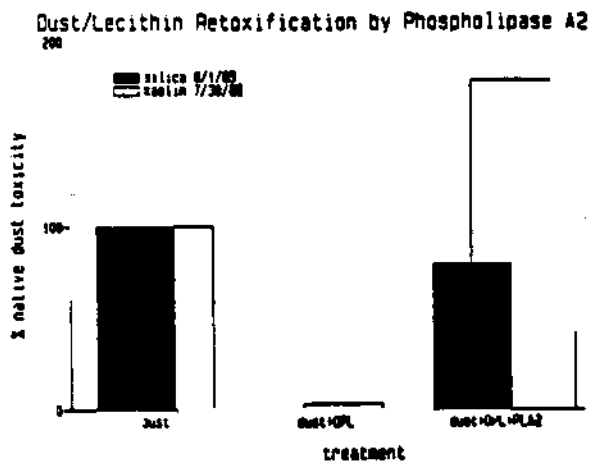


FIG. 7. Dust/lecithin retoxification by phospholipase A₂. Erythrocyte haemolysis induced by the dusts assayed for lecithin/lysolecithin shown in Figure 6.

Retoxification data indicate that the quartz surface is functionally bared by the digestive action of the PLA₂. Retention of most lecithin by kaolin after PLA₂ treatment indicates that kaolin is not functionally bared of lecithin for the short digestion times used here. The presence of lysolecithin on PLA₂ treated kaolin-lecithin and the simulation of kaolin retoxification by kaolin-lysolecithin indicate that kaolin retoxification is due to adherent lysolecithin.

The lysolecithin-based retoxification of kaolin would seem to be a bioassay result contrary to the differences in pathogenicity of the dusts. One must ask: in the normal course of digesting bacteria or other lipid-containing material, is the produced

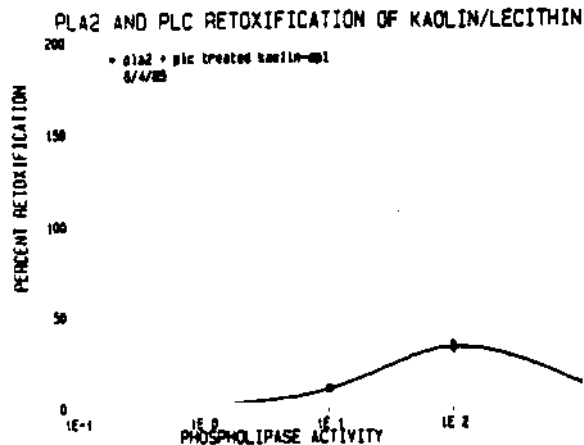


FIG. 8. PLA₂ and PLC retoxification of kaolin/lecithin. Erythrocyte haemolysis induced by kaolin treated with lecithin and then with phospholipase A₂ and phospholipase C together in equal activity equivalents.

lysolecithin further digested by lysosomal lysophospholipase enzymes? Or is the interior of the phagolysosome immune to lysis by lysolecithin? Figure 8 shows the cytotoxicity of kaolin which first has been incubated with lecithin, then retoxified by incubation with PLA₂ and PLC together for one hour. Data are fitted to a first order kinetics model of lecithin conversion to lytic lysolecithin by PLA₂ and subsequent lysolecithin conversion by PLC to non-lytic phosphoryl choline and glycerol palmitate.

The mineral surface properties responsible for these differences in retoxification could involve different strengths of sorption or conformations of the adsorbed lecithin. Kaolin is a mineral of layered alumina octahedra and silica tetrahedra. Alumina catalyses the hydrolysis of lecithin in organic solvent (RENKONEN, 1962); this does not occur for lecithin dispersion in saline. Surface properties would be expected to be more important to disease pathogenesis than the bulk non-biologically available mineral content of an inhaled particle. Occlusion or surface contamination of quartz by alumino-silicate or other coatings in mixed dust atmospheres should affect the biological activity expected of a respirable dust of a given silica concentration, by affecting the retention of surfactant during clearance *in vivo*. And the effectiveness of additive prophylactic agents for quartz-bearing dusts might be affected by their ability to be retained under the action of pulmonary surfactant solubilization and lysosomal enzyme digestion. Tests using lavaged surfactant with isolated lysosomal enzyme in longer term macrophage incubations should determine if such simple initial events in the interaction of mineral dusts with the lung are determinants of the potential for dust-induced pulmonary fibrosis.

Acknowledgements—We thank Dr. Larry Clyde Headley of the U.S. Department of Energy-Morgantown Energy Technology Center for providing specific surface area measurements and particle size distribution measurements and for productive discussions; Jerry L. Clere for particle classification; and Nikki Snider for typing the manuscript.

REFERENCES

- BARTLETT, G.R. (1959) Phosphorus Assay in Column Chromatography. *Biolog. Chem.* 234, 466-468.
- BROWN, R.C., CHAMBERLAIN, M., DAVIES, R., MORGAN, D.M.C., POOLEY, F.D. and RICHARDS, T. (1980) A comparison of 4 *In Vitro* Systems Applied to 21 Dusts. In: *The In Vitro Effects of Mineral Dusts*, (Ed. BROWN, R.G., GORMLEY, I.R., CHAMBERLAIN, M. and DAVIES, R.) Academic Press, London, pp. 47-52.
- DANIEL, H. and LE BOUFFANT, L. (1980) Study of a Quantitative Scale for Assessing the Cytotoxicity of Mineral Dusts. In: *The In Vitro Effects of Mineral Dusts* (Ed. BROWN, R.C., GORMLEY, I.R., CHAMBERLAIN, M. and DAVIES, R.) Academic Press, London, pp. 33-39.
- HARINGTON, J., MILLER, K. and MACNAB, G. (1971) Hemolysis by Asbestos. *Env. Res.* 4, 95-117.
- LOCKART, V.G. and KENNEDY, R.E. (1976) Alterations in Rabbit Alveolar Macrophages As a Result of Traumatic Shock. *Lab. Invest.* 35, 501-506.
- MORGAN, W.K.C. and SEATON, A. (1975) *Occupational Lung Diseases*. W.B. Saunders, Philadelphia.
- REEVES, W.J. and FIMIGNARI, G.M. (1963) An Improved Procedure for the Preparation of Crystalline Lactic Dehydrogenase from Hog Heart. *Biolog. Chem.* 238, 3853-3858.
- RENKONEN, O. (1962) Breakdown of Lecithin on Aluminium Oxide Columns. *Lipid Res.* 3, 181-183.
- SELLINGER, O.Z., BEUFAY, H., JACQUES, P., DOYAN, A. and DEDUVE, C. (1960) The Intracellular Distribution of (Beta)-N-Acetylglucosaminidase and of (Beta)-Galactosidase in Rat Livers. *Biochem. J.* 74, 450-456.
- WALLACE, W.E., JR., HEADLEY, L.C. and WEBER, K.C. (1975) Dipalmitoyl Lecithin Surfactant Adsorption by Kaolin Dust *In Vitro*. *J. Coll. Interf. Sci.* 51, 535-537.
- WALLACE, W.E., KEANE, M.J., VALLYATHAN, V., ONG, T-M and CASTRANOVA, V. (1984) Pulmonary Surfactant Interaction With Respirable Dust. In: *Generic Mineral Technology Center—Coal Mine Dust Conference Proceedings*, (Edited by PENG, S.), pp. 180-187. Available from National Technical Information Service, Report #PB86 169380/AS.
- WALLACE, W.E., VALLYATHAN, V., KEANE, M.J. and ROBINSON, V. (1985) *In Vitro* Biologic Toxicity of Native and Surface-Modified Silica and Kaolin. *J. Tox. and Environ. H.* 16, 415-424.

Oxygenated Radical Formation by Fresh Quartz Dust in a Cell-Free Aqueous Medium and Its Inhibition by Scavengers

N.S. Dalal¹, X. Shi¹, and V. Vallyathan²

¹ Department of Chemistry, West Virginia University

² National Institute for Occupational Safety and Health

Abstract: Using ESR spin trapping methodology, evidence was obtained that fresh quartz dust in a cell-free aqueous medium generated hydroxyl and possibly superoxide radicals. The hydroxyl radical generation potential decreases on storing of fresh quartz dust in ambient air and on the addition of either catalase, superoxide dismutase, desferoxamine, or DMSO. The role of quartz related radicals in the biochemical mechanism of acute silicosis is suggested from these findings.

Introduction

This report summarizes our electron spin resonance (ESR) detection of oxygenated radical formation by freshly crushed quartz particles in a cell-free aqueous medium, and its inhibition by radical scavengers. This study was undertaken with to elucidate the primary biochemical mechanism involved in the development of silicosis (Farber, 1983; Reiser and Last, 1979; Silicosis and Silicate Disease Committee, 1988). In particular the mechanism by which the quartz particles exert their toxic action on cells and the process(es) by which these actions progress to fibrogenesis are still not well understood (Farber, 1983; Reiser and Last, 1979;). It is generally believed that the action of quartz particles on the cell membrane is the starting point of the silicotic process (Farber, 1983; Parazzi et al., 1968). Thus the surface characteristics of the quartz particles have been the subject of several recent studies (Bolis et al., 1983; Dalal et al., 1986; Fubini et al., 1987). Recently, We reported that mechanical crushing of quartz under normal atmosphere generates free radicals which decay with time, and that these free radicals are associated with a higher cytotoxicity of fresh quartz dust as compared to aged dust from the same stock (Dalal et al., 1986; Vallyathan et al., 1988). The formation of Si· and SiO⁻-type of radicals from quartz particles crushed under atmospheric conditions has also been reported by Fubini et al. (1987). In addition, Gulumian and van Wyk (1987) have reported that quartz particles react with hydrogen peroxide (H₂O₂) to generates hydroxyl radicals (·OH) and suggested that this process might contribute to

quartz's pathogenicity. However, these authors did not report the effects of metal chelators, so it was not clear as to whether the detected $\cdot\text{OH}$ radicals simply resulted from the Fenton reaction involving exogenous metal ion contaminants. Earlier, Marasas and Harington (1960) reported that quartz particles could function as an oxidant in a number of *in vitro* oxidations, including the hydroxylations of proline and lysine. They postulated that silica dusts, on reacting with water, could release H_2O_2 which might have the potential to react with various biological constituents and thus cause tissue damage. In fact, Gabor and coworkers (Gabor and Anca, 1974; Gabor et al., 1975) suggested that the cytotoxicity of quartz particles might be associated with the generation of some factor or factors possessing the properties of a free radicals capable of promoting the peroxidative chain cleavage of polyunsaturated fatty acid moieties of the phospholipids in the cell membrane. More recently Weitzman and Graceffa (1984) reported that asbestos is able to catalyze the generation of $\cdot\text{OH}$ radicals from H_2O_2 . Their later work indicated that lipid peroxidation may be one of the mechanism by which asbestos produces tissue injury (Weitzman and Weitberg, 1985). This is significant because $\cdot\text{OH}$ radicals are capable of causing peroxidation by abstracting hydrogen atoms from cell-membrane lipids and initiating lipid peroxidation in lysosomal membrane (Fong et al., 1973). In fact, the formation of oxygenated species in reactions involving quartz was suspected since Kolbanev et al. (1980) reported the detection of H_2O_2 in the reaction of fresh quartz particle with aqueous medium. The present work was thus undertaken to detect the anticipated formation of some oxygenated radical species by reactions of quartz in a cell-free media and its inhibition by radical scavengers. Because of the reactive nature of the oxygenated radicals and their short half-lives, ESR spin trapping methodology (Buettner, 1984) was employed in the present studies, as in the studies using asbestos (Weitman and Graceffa, 1984) and quartz with H_2O_2 (Gulumian and van Wyk, 1987). The results show that $\cdot\text{OH}$ and possibly O_2^- radicals are formed by fresh quartz dust in cell-free aqueous medium and their formation can be inhibited by the dust as it ages or by radical scavengers. Some preliminary results have been reported recently (Shi et al., 1988).

Materials and Methods

ESR spectra were obtained at X-band (-9.7 GHz) using a Bruker ER 200D ESR spectrometer, employing a self-tracking NMR gaussmeter and a microwave

OXYGENATED RADICALS AND QUARTZ

frequency counter. An ASPECT 2000 computer was used for data acquisition, analysis, and for ESR spectral simulations to obtain the splitting constants. Crystalline silica with particle sizes ranging from 0.2 to 2.5 μm was obtained from the Generic Respirable Dust Technology Center, Pennsylvania State University, University Park, PA. Particles in the range of smaller than 25 microns were produced by hand grinding in air, with an agate mortar and pestle because of the structural similarity of agate to that of quartz. Also, a rather mixed particle size rather than a specific range, was employed, to roughly approximate the random particle-size distribution in the mining atmosphere. 5,5-dimethyl-1-pyrroline-N-oxide (DMPO) was used as a spin trap for the $\cdot\text{OH}$ radicals. The DMPO was purchased from Aldrich, Milwaukee, WI and used without further purification, because very weak or no $\cdot\text{OH}$ radical signal was obtained from the purchased sample when used by itself. Superoxide dismutase (SOD) and catalase were obtained from Sigma, St. Louis, MO. Dimethyl sulfoxide (DMSO) was obtained from Fisher Scientific Company, Pittsburgh, PA. All experiments were performed at room temperature (22°C).

Results and Discussions

Figure 1 shows some typical results of the ESR spin trapping measurements. A 0.1 M aqueous solution of the spin trap DMPO with as received (unground) quartz particles did not give a detectable ESR spectrum (Figure 1a). When the quartz particles were crushed in a 0.1 M DMPO aqueous solution or when fresh quartz particles were mixed with 0.1 M DMPO aqueous solution, an ESR spectrum ($g = 2.0059$), consisting of a 1:2:2:1 quartet pattern with splittings of $a_N = a_H = 14.9$ G, was observed (Figure 1b). Based on the splitting constants and 1:2:2:1 lineshape this spectrum was assigned to the DMPO-OH adduct (Buettner, 1984). As supporting evidence for the $\cdot\text{OH}$ radical formation, ESR spin trapping measurements were made in which 30% ethanol was added as a secondary trap (Buettner, 1984). It has been shown (Buettner, 1984; Shi et al., 1988) that in presence of ethanol, the intensity of the DMPO-OH spin-adduct signal decreases because ethanol scavenges some of the $\cdot\text{OH}$ radicals to form the ethanoyl radicals. The signals from the DMPO-trapped ethanoyl radicals are indicated by arrows in Figure 1b. The measured splitting constants, $a_N = 15.8$ G and $a_H = 22.8$ G, for these signals are indeed typical of those of the DMPO-CHOHCH₃ adducts (Buettner, 1984), thus supporting the $\cdot\text{OH}$ radical formation in the quartz particle aqueous suspension, without any added H₂O₂.

An important observation was that the concentration of the $\cdot\text{OH}$ radicals, as

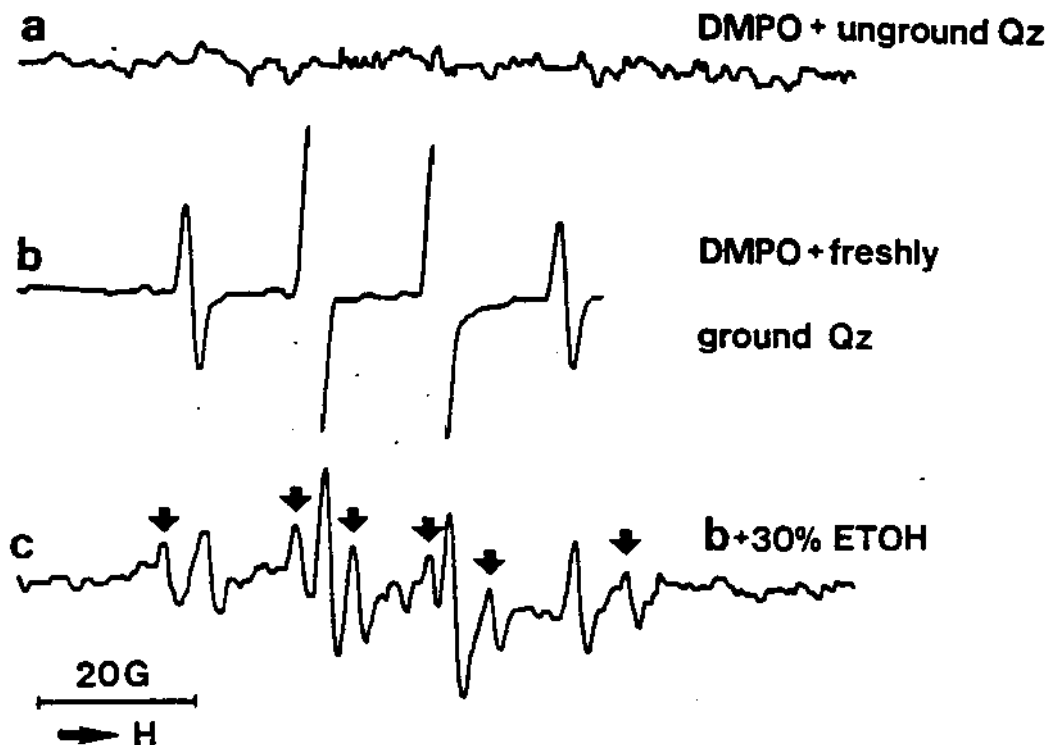


Figure 1. ESR spectra recorded 2 minutes after mixing a 100 mM DMPO aqueous solution with (a) unground quartz; (b) freshly ground quartz particles; (c) same as (b) but with 30% ethanol added. The arrows show the signals from the DMPO-ethanolyl radical adduct, attesting to the $\cdot\text{OH}$ radical formation.

measured by the peak-to-peak height of ESR spin trapping adduct signal, which increased with time of grinding (Figure 2). This showed that the $\cdot\text{OH}$ radical formation is related to some surface property of the fresh quartz particles (Kolbanev et al., 1980). The likely active sites may be the silicon-based radicals ($\text{Si}\cdot$ and $\text{SiO}\cdot$) formed after grinding (Bolis et al., 1983; Dalal et al., 1986; Fubini et al., 1987; Vallyathan et al., 1988). Additional spin trapping experiments show that the ability of the fresh quartz dust to generate $\cdot\text{OH}$ radicals decreases with the aging of the dust in air (Figure 3). It was found that, on an average, freshly ground quartz particles, when kept in air, lose their $\cdot\text{OH}$ -generating capacity by about 50% in approximately a day.

To detect the possible formation of the O_2^- radicals in the fresh quartz particle suspension, SOD (50 ug/ml) and catalase (5000 units/ml) were added individually into the reaction medium. As noted in Figure 4b, SOD reduced the $\cdot\text{OH}$ radical formation to about 65%, indicating that O_2^- radicals may be involved in the mechanism of $\cdot\text{OH}$ radical formation (Weitzman and Graceffa,

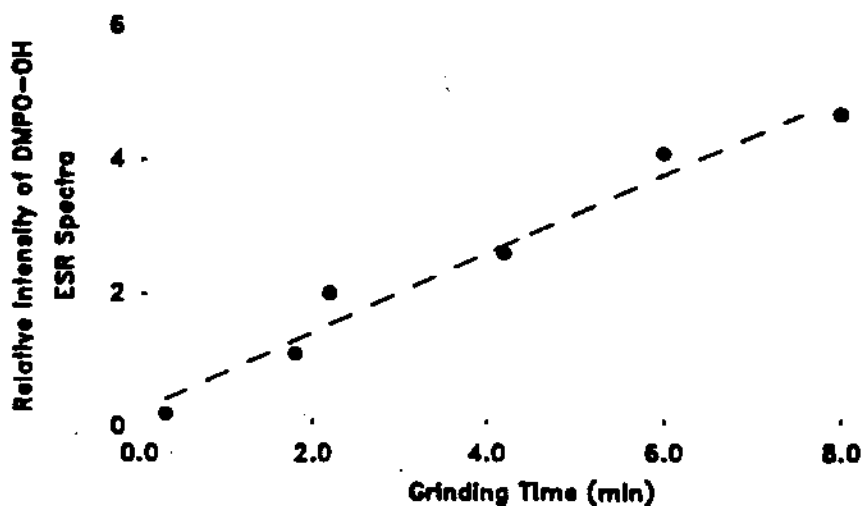


Figure 2. Dependence of the ESR intensity of the DMPO-OH adduct (i.e. $\cdot\text{OH}$ radical production) on grinding time (i.e. surface) of quartz particles).

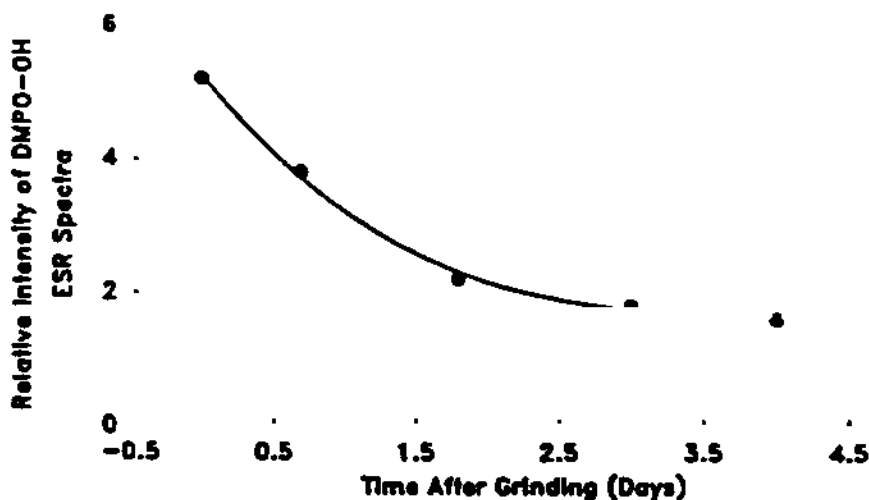


Figure 3. Dependence of the ESR intensity of the DMPO-OH on the aging of the quartz particles.

1984). Catalase, however, completely suppressed the $\cdot\text{OH}$ formation (Figure 4c), indicating that H_2O_2 plays an important role in the $\cdot\text{OH}$ radical formation as reported earlier (Vallyathan et al., 1988). The generation and detection of H_2O_2 was reported with wet analytical chemistry, the KMnO_4 reduction (Kolbanov et al., 1980). Using the same methodology, we did confirm the reducing activity of fresh quartz particle suspension with respect to KMnO_4 , although the H_2O_2 yield was measured to be an order of a magnitude smaller for our sample. Further experiments showed that DMSO, commonly used radical

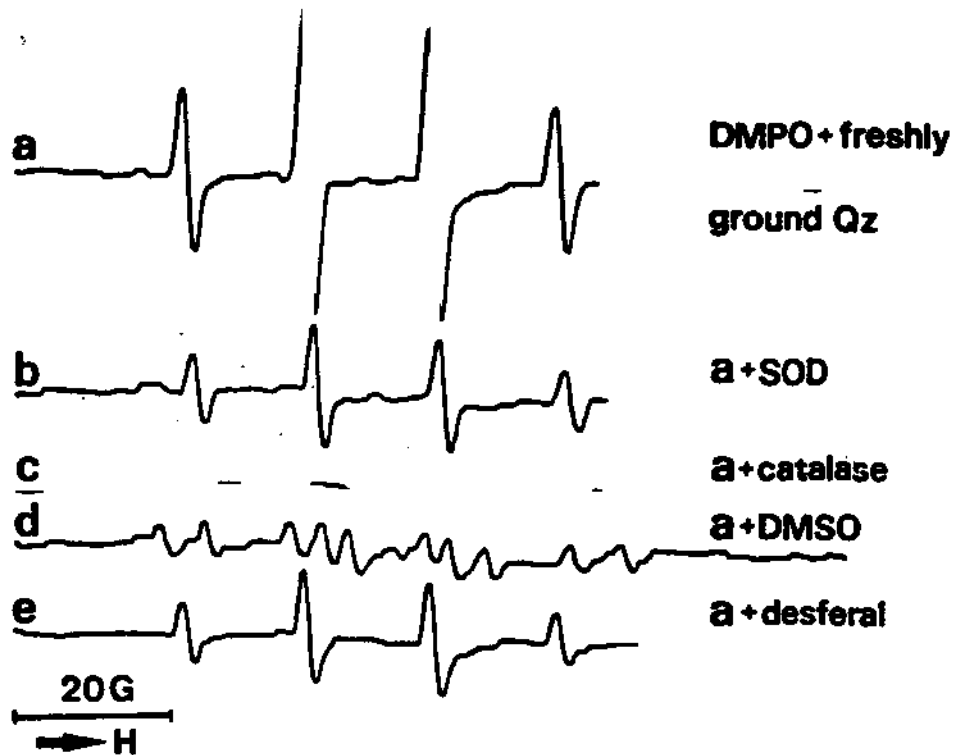


Figure 4. ESR spectra recorded 2 minutes after mixing 100 mM DMPO with (a) fresh quartz particles; (b) same as (a) but with SOD (50 ug/ml); (c) same as (a) but with catalase (5000 units/ml); (d) same as a but with DMSO (25%); (e) same as (a) but with desferal (1 mM).

scavenger (Britigan et al., 1986), suppresses the $\cdot\text{OH}$ radical formation by more than 70% (Figure 4d). We noted that addition of desferal (1 mM) reduced the $\cdot\text{OH}$ radical formation by more than 80%. Thus the Fenton reaction, $\text{Fe}^{2+} + \text{H}_2\text{O}_2 \longrightarrow \text{Fe}^{3+} + \cdot\text{OH} + \text{OH}^-$, may play some role in the $\cdot\text{OH}$ radical formation (Morehouse and Mason, 1988). The Fe^{2+} may be present as a trace impurity or impregnated in the chemical structure of quartz dust.

The above results lead us to suggest the following model of the initial events in the reaction of the quartz dust with a cell membrane. The free radicals ($\text{Si}\cdot$ and $\text{SiO}\cdot$) on the surface of silica dusts and their associated oxygenated radicals ($\cdot\text{OH}$, O_2^- , and H_2O_2) are involved in the interaction of cell membrane with quartz dust. The results of this interaction would be the release of reactive oxygenated species (H_2O_2 , O_2^- , $\cdot\text{OH}$, $\text{R}\cdot$, and $\text{RO}\cdot$). These reactive oxygenated species would further react with the cell membrane leading to additional release of these species and to lipid peroxidation (Fantone and Ward, 1982). As to the sites of the reactions between the cell membranes and

the quartz dust, we noted that the reaction of quartz particles with H_2O produces silanol (SiOH) groups on the particle surface, as detected by infrared spectroscopy (Tsuchiya, 1982). These silanol groups could form hydrogen bonds with the nitrogen or oxygen atomic sites on the cell membrane. This is supported by the report of a weak (hydrogen) bond formation between a secondary amide (peptide) of proteins and silanol moieties (Summerton et al., 1977). Such hydrogen bonding could bring the silica surface and cell membrane close enough to provide a favorable environment for the initiation of lipid peroxidation by the silicon-based radicals and their associated oxygenated radicals.

Conclusions

The present ESR spin trapping experiments show that freshly generated, micron-size quartz particles have an ability to generate the $\cdot OH$ and possibly the O_2^- radicals in a cell free media. Moreover, the ability of such particles to generate these oxygenated radicals decreases with aging of the particles. This result implies that fresh quartz particles should be more fibrogenic than the stale dust (Dalal et al., 1986; Shi et al., 1988; Vallyathan et al., 1988). Indeed, we have reported recently that fresh quartz dust activates a greater respiratory burst in alveolar macrophages than aged dust and that fresh dust exhibits a 50% greater ability for inducing lipid peroxidation (Vallyathan et al., 1987; Vallyathan et al., 1988). We hypothesize that silicon-based radicals and their associated oxygenated radicals may be involved in the initiation of the lipid peroxidation of the cell membrane which results in cell death (Vallyathan et al., 1988).

References

- Bolis V, Fubini B, Venturello G (1983) Surface characterization of various silica: a tentative correlation between the energies of absorption sites and the different biological activities. *J Thermal Anal* 28:249-257.
- Britigan BE, Rosen GM, Thompson BY, Chai Y, Cohen MS (1986) Do human neutrophils make hydroxyl radicals? *J Biol Chem* 261:17026-17032.
- Buettner GR (1984) The spin trapping of superoxide and hydroxyl radicals. In: *Superoxide Dismutase*, vol. 2, ed., Oberly LW, pp. 63-81. CRC press, Boca Raton, Florida.
- Dalal NS, Suryan MM, Jafari B, Shi X, Vallyathan V, Green FHY (1986) Electron spin resonance detection of reactive free radicals in fresh coal dust and quartz dust and its implications to pneumoconiosis and silicosis. In: *Respirable Dust in the Mineral Industries: Health Effects*,

- Characterization, and Control* (Frantz R.L., and Ramani R.V., eds.), P. 25-29. American Conference of Governmental Industrial Hygienists (ACGIH) Publication, ISBN 0-936712-76-7.
- Fantone JC, Ward PA (1982) Role of oxygen-derived free radicals and metabolites in leukocyte-dependent inflammatory reactions. *Am Assoc Pathol* 107:397-418.
- Farber JL (1983) How do mineral dusts cause lung injury? *Lad Invest* 49:379-390.
- Fong KL, McCay PB, Poyer JL, Keel BB, Misra H (1973) Evidence that peroxidation of lysosomal membranes is initiated by hydroxyl free radicals produced during flavine enzyme activity. *J Biol Chem* 248:7792-7797.
- Fubini B, Bolis V, Giamello E (1987) The surface chemistry of crushed quartz dust in relation to its pathogenicity. *Inorg Chim Acta* 138:193-197.
- Gabor S, Anca Z (1974) Effect of silica on lipid peroxidation in the red cells. *Int Arch Arbeitsmed* 32:553-558.
- Gabor S, Anca Z, Zugravu E (1975) *In vitro* action of quartz on alveolar macrophage lipid peroxides. *Arch Environ Health* 30:499-501.
- Gulumian M, van Wyk A (1987) Free radical scavenging properties of polyvinyl-pyridine-N-oxide: a possible mechanism for its action in pneumoconiosis. *Med Lav* 78:124-128.
- Kalbanev IV, Berestetskaya IV, Butyagin PU (1980) Mechanochemistry of quartz surface. *Kinet Katal* 21:1154-1158.
- Marasas LW, Harington JS (1960) Some oxidative and hydroxylative actions of quartz: their possible relationship to the development of silicosis. *Nature* 188:1173-1174.
- Morehouse KM, Mason RP (1988) The transition metal-mediated formation of the hydroxyl free radical during the reduction of molecular oxygen by ferredoxin-ferredoxin: NADP⁺ oxidoreductase. *J Biol Chem* 263:1204-1211.
- Parazzi E, Secchi GC, Pernis B, Vigliani E (1968) Cytotoxic action of silica dusts on macrophages *in vitro*. *Arch Environ Health* 17:850-859.
- Reiser KM, Last JA (1979) Silicosis and fibrogenesis: fact and artifact. *Toxicology* 13:51-72.
- Shi X, Dalal NS, Vallyathan V (1988) ESR evidence for the hydroxyl radical formation in aqueous suspension of quartz particles and its possible significance to lipid peroxidation in silicosis. *J Toxicol Environ Health* 25:237-245.
- Silicosis and Silicate Disease Committee (1988) Diseases associated with exposure to silica and nonfibrous silicate minerals. *Arch Pathol Lab Med* 112:673-720.
- Summerton J, Hoenig S, Butler C, Chvapil M (1977) The mechanism of hemolysis by silica and its bearing on silicosis. *Exp Mol Pathol* 26:113-128.
- Tsuchiya I (1982) Infrared spectroscopic study of hydroxyl groups on silica surface. *J Phys Chem* 86:4107-4112.
- Vallyathan V, Shi X, Dalal NS, Irr W (1987) Role of reactive oxygen radicals in silica toxicity. 4th International Congress on Oxygen Radicals (extended abstract), pp. 98-99, La Jolla, California.
- Vallyathan V, Shi X, Dalal NS, Irr W, Castranova V (1988) Generation of free radicals from freshly fractured silica dust: potential role in acute silica-induced lung injury. *Am Rev Respir Dis* 138:1213-1219.
- Weitzman SA, Graceffa P (1984) Asbestos catalyzes hydroxyl and superoxide radical generation. *Arch Biochem Biophys* 228:373-376.
- Weitzman SA, Weitberg AB (1985) Asbestos-catalyzed lipid peroxidation and its inhibition by desferrioxamine. *Biochem J* 225:259-262.

Mineral Surface-Specific Differences in the Adsorption and Enzymatic Removal of Surfactant and Their Correlation with Cytotoxicity

W.E. Wallace^{1,2}, M.J. Keane¹, P.S. Mike¹, C.A. Hill² and V. Vallyathan²

¹ West Virginia University

² Division of Respiratory Disease Studies, National Institute for Occupational Safety and Health, Morgantown, WV

INTRODUCTION

Respirable quartz dust and a kaolin clay dust have been found to be of comparable cytotoxic potential in vitro on a specific surface area basis (Wallace, et al, 1985), despite the distinctly different potentials of quartz and clay for causing pneumoconiosis or pulmonary fibrosis (Sheers, 1984). A respired particle depositing in a respiratory bronchiole or alveolus will contact a pulmonary surfactant hypophase, of which a primary component is diacyl glycerophosphorylcholine, or diacyl lecithin (DPL) (Clements, et al, 1970). Several studies have found that adsorption of such surfactant suppresses in vitro cytotoxic effects of quartz dust (Marks, 1957). Subsequent phagocytosis and digestion by a macrophage may remove the coating, restoring cytotoxic potential and initiating disease processes (Iler, 1979). Adsorption of dipalmitoyl lecithin (DPL) from emulsion in physiologic saline by respirable sized quartz dust and kaolin dusts, and consequent diminution of the dusts' hemolytic and macrophage cytotoxic potential have been reported (Wallace, et al, 1985). This report presents additional data on the cell-free in vitro phospholipase A2 enzymatic digestion of dipalmitoyl lecithin adsorbed on a quartz and a kaolin respirable sized dust (Wallace, et al, 1988) to investigate mineral specific differences in the rates of digestion and of consequent restoration of dust membranolytic potential.

MATERIALS AND METHODS

Respirable crystalline alpha quartz used was eighty percent smaller than 5 micrometer aerodynamic diameter with a nitrogen adsorption specific surface area of $3.97 \text{ m}^2/\text{g}$. Respirable kaolin dust was ninety percent smaller than 5 micrometer diameter and had a specific surface area of $13.25 \text{ m}^2/\text{g}$.

L-alpha-dipalmitoyl glycerophosphorylcholine (lecithin) (DPL) obtained commercially was ultrasonically emulsified into 0.165 M NaCl. Phospholipase A_2 (PLA₂) enzyme obtained commercially from porcine pancreas was dissolved in 0.165 M saline at a pH between 6.5 and 7.0, with 2.0 mM calcium chloride. Quartz and kaolin dusts were incubated with DPL in physiologic saline emulsion for 1 hr at 37°C at a ratio of 100 mg DPL/g quartz and 200 mg DPL/g kaolin. After incubation, the dusts were washed twice in phosphate buffered saline (PBS), and the DPL-coated dusts finally suspended at a concentration of 2 mg dust/ml PBS. Parallel sets of dusts were used for hemolysis and for phosphate assay of residual adsorbed lecithin and lysolecithin. Saline dilution of lecithin stock emulsion was used for tests which measured the suppression of dust hemolytic potential as a function of adsorbed DPL.

Incubations of DPL-coated dusts with enzymes, carried out for periods of 2, 20, 44, and 72 hours, were started sequentially so that all assays for an experiment were performed at the same time. Following incubation with enzyme, samples were resuspended twice in PBS containing 2.0 mM ethylene diamine triacetic acid (EDTA) to stop the enzymatic digestion. Samples for assay of hemolytic potential were resuspended in PBS.

Hemolytic potential of native dusts, dust plus the maximum value of PLA₂ applied, dusts incubated with DPL/saline emulsion, and DPL-coated dust subsequently incubated with PLA₂, were measured by the method of Harington, et al. (1971). Sheep erythrocytes were washed six times in PBS and prepared as a 4% by volume suspension in PBS. These suspensions were mixed with equal volumes of dust in PBS suspension to result in 2% by volume erythrocyte suspensions with dust concentration of 1 mg/ml. The mixtures were incubated at 37°C for 1 hour. After incubation the optical density of the supernatant at 540 nm wavelength was determined to measure hemoglobin release. Samples for phosphate determinations were vacuum-dried at room temperature, and then eluted with chloroform/methanol (2/1 by volume). Amounts of phospholipid adsorbed to

MINERAL-SPECIFIC DIFFERENCES

dust samples were quantitated as lecithin or lysolecithin (L-alpha-lecithin, beta palmitoyl). Aliquots were separated by thin layer chromatography, and the bands for lecithin and lysolecithin quantitated for phosphate by the method of Bartlett (1959).

RESULTS

Incubation of these quartz and kaolin dusts with increasing amounts of DPL results in neutralization of hemolytic potential between 15 and 20 mg DPL adsorbed per gram quartz, and between 75 to 85 mg DPL/g for kaolin (Keane et al, 1988). This quartz adsorbs about 60 mg DPL/g dust and this kaolin adsorbs about 150 mg/g dust at high lecithin dispersion concentrations. But saline washing removes all but a constant specific adsorption amount retained for each dust. For a series of 24 such measurements the residual adsorbed value for this quartz was 16.5 mg DPL/g quartz, and a series of 12 tests gave the value of 83.0 mg DPL/g kaolin. Using the nitrogen adsorption specific surface areas for these dusts, these lecithin retention values are 5.7 micromoles DPL/square meter of quartz surface, and 8.5 micromoles DPL/m² of kaolin surface.

The digestive removal of DPL from quartz and kaolin is shown in Figure 1. for applied specific activities of 0.82 units PLA2 per micromole DPL on quartz, and 0.96 units PLA2 per micromole DPL on kaolin. Data were taken in three separate experiments with triplicate points for each; standard deviations shown are for the nine values at each time point. Parallel measurements show that most of the produced lysolecithin remains adsorbed on both dusts at the 2 hour time point, with a significant amount still retained on the quartz at 20 hours. It is gone from both dusts at 44 hours. Figure 2 shows the resultant hemolytic potential of the treated dusts.

Digestive removal of DPL when the specific activity applied to quartz is decreased to 0.082 units PLA2 per micromole adsorbed DPL, and when the specific activity applied to kaolin is increased to 2.9 units PLA2 per micromole kaolin-adsorbed DPL is shown in Figure 3. Parallel measurements show the hemolytic potentials for the two dusts track each other from approximately 30% native dust level at 2 hrs digestion to about 50% native dust level at 72 hrs digestion.

In our thin layer chromatographic separation of DPL and lysolecithin we note a band running at the solvent front which is visible after heating but not after staining for phosphate. Two sets of experiments using C-14 radiolabel on the palmitic acid moiety of DPL have found about 50% of the digestion-produced fatty acid stays associated with quartz at the 2 hour time point, and about 70% with the kaolin.

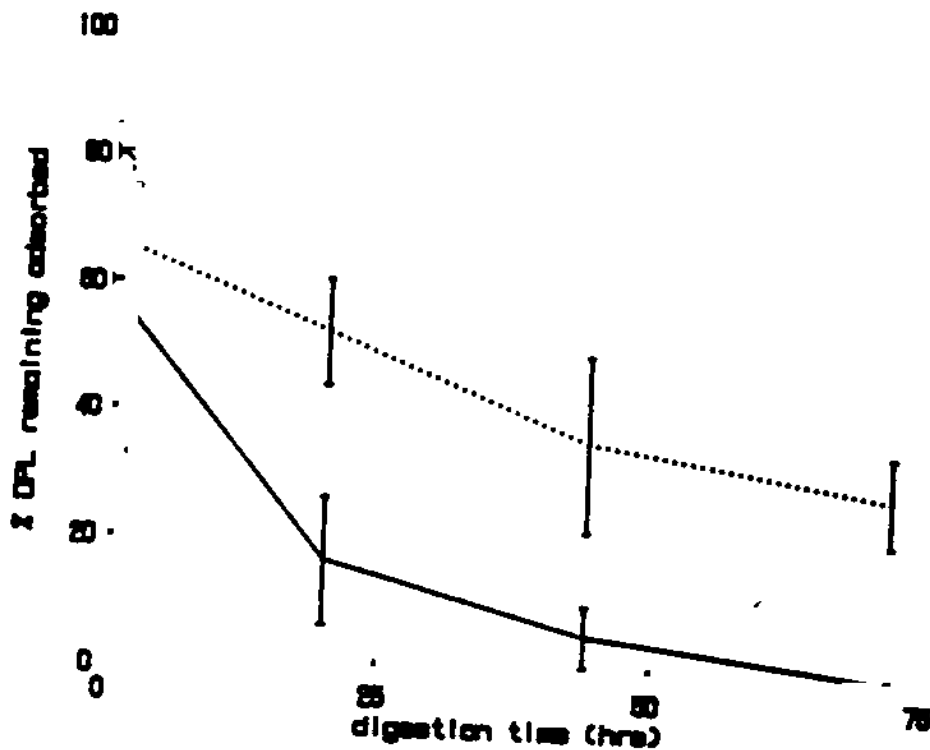


Figure 1. Digestive removal of dipalmitoyl lecithin from quartz (solid line) and from kaolin (dashed line) for applied phospholipase A2 specific activities of 0.82 and 0.96 units per micromole adsorbed lecithin on quartz and kaolin, respectively.

Limited infrared spectroscopic examinations were made of kaolin incubated with critical amounts of DPL in saline, then dried under mild conditions, and analyzed in potassium bromide pellets by grating IR spectroscopy. Contrasting the spectra of kaolin, of DPL, and of DPL adsorbed to kaolin indicates suppression of the broad DPL band in the region of the 3400 cm^{-1} for DPL adsorbed on kaolin. This band is assigned to the hydrated acidic phosphate group of DPL. Subsequent FTIR examination has indicated this band suppression occurs for DPL on kaolin but not significantly for DPL on quartz, while a weak band attributed to the trimethylamine of DPL is diminished for both dusts (Keane, et al, 1988).

DISCUSSION

The quartz and kaolin used in this work are comparably hemolytic on a surface area basis. The amounts of DPL needed to fully suppress the hemolytic potentials of the dusts is about equal to the amounts of DPL retained on the dusts after mild saline rinsing. The ratio of these critical amounts of DPL for kaolin to quartz is about equal to 1.5 times the ratio of their nitrogen

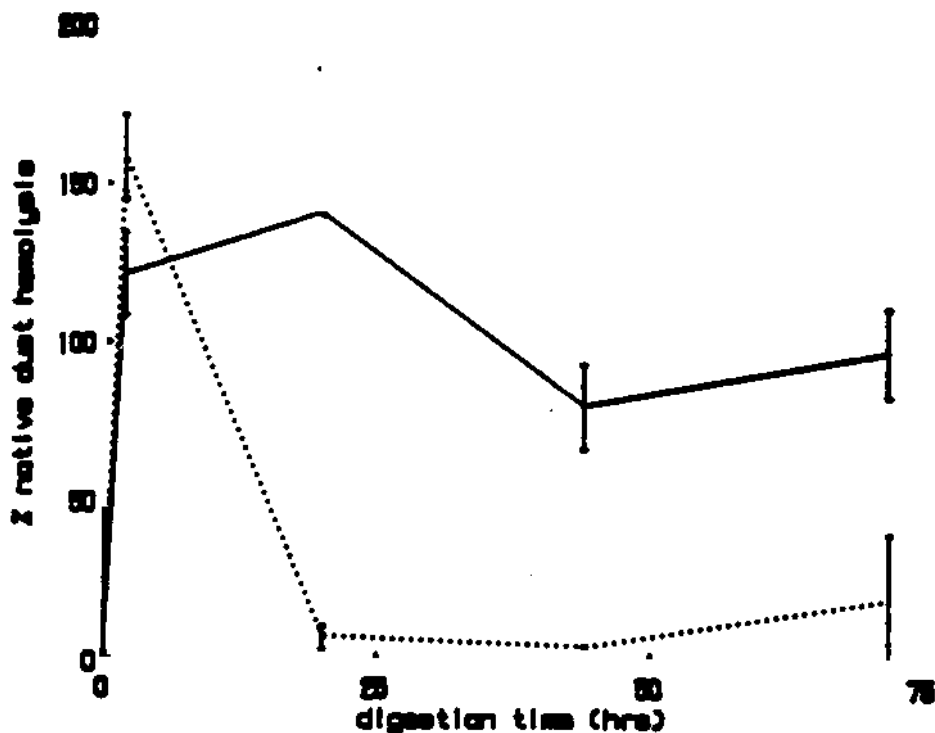


Figure 2. Hemolytic potential of lecithin coated quartz (solid line) and kaolin (dashed line), expressed as percent of native dust potential, following the digestion by PLA2 shown in Figure 1.

adsorption specific surface areas. The critical DPL values are about half the amounts of DPL adsorbed before rinsing. They are a factor of two or more greater than estimates of amounts needed for monolayer coverage using the nitrogen adsorption surface areas and information on molecular size or on water-air interfacial surface spreading of DPL. This is consistent with a picture of the stable DPL coating being a monolayer coverage of the dust surface by DPL molecules oriented with their zwitterionic head groups toward the dust surface, and backed by a second layer, with palmitate tails of the two layers in association and with ionic phosphorylcholine heads of the second layer pointed outward into the surrounding aqueous media. Such an arrangement

would permit ionic interaction of acidic or basic dust surface sites with the zwitterionic DPL phosphorylcholine head group, while minimizing contact of hydrophobic acyl groups with the surrounding aqueous medium.

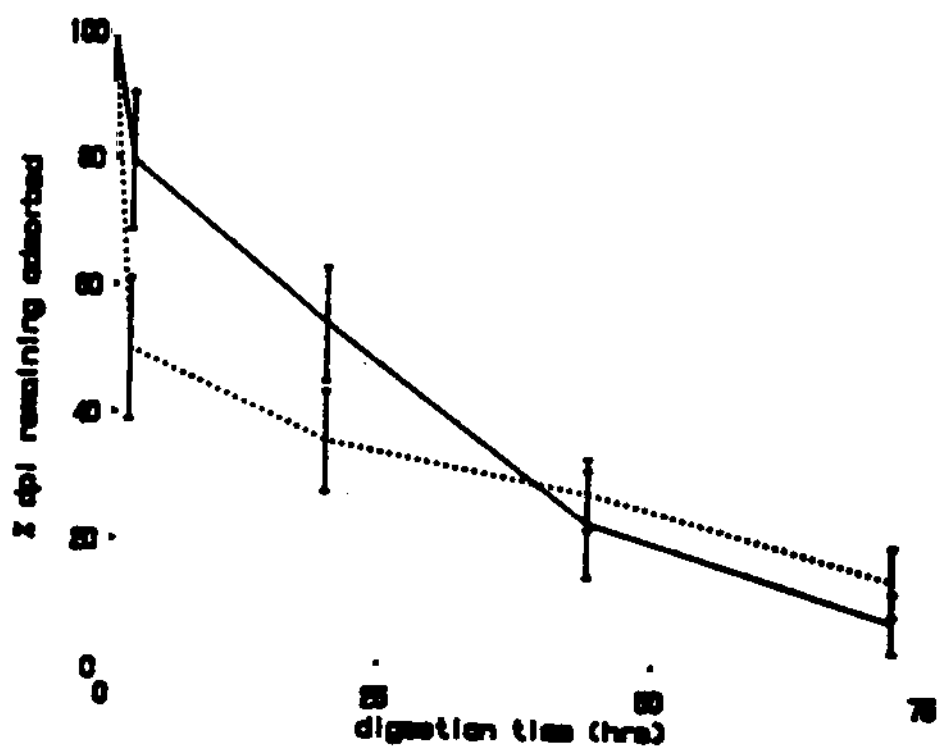


Figure 3. Digestive removal of dipalmitoyl lecithin from quartz (solid line) and from kaolin (dashed line) for applied phospholipase A2 specific activities of 0.082 and 2.9 units per micromole adsorbed lecithin on quartz and kaolin, respectively.

Application of phospholipase A2 to DPL coated dusts results in digestion and eventual removal of DPL and its phosphate-bearing products of digestion. The produced and initially adherent lysolecithin is itself a membranolytic agent. This correlates with exaggerated levels of hemolytic potential seen for all samples at the two hour time point. As the DPL is digested from the dust surface the lysolecithin may be lost by dissolution into the surrounding water, or it may be subject to further enzymatic hydrolytic attack. Non-phosphate fatty acids are also present as measured at the two hour time point. Thus, the hemolytic potential at any time is due to a mixture of effects: direct potential of mineral surface partially bared of lecithin, modified by further suppression of that surface potential by adsorbed palmitic acid product, and modified by additional lytic activity of adsorbed lysolecithin product.

For the applied specific PLA2 activities of about 1 unit per micromole of adsorbed DPL, the quartz is fully stripped in three days, while kaolin retains about 30% to 40% of the DPL. This specific enzyme activity level is an order of magnitude estimate of the total lysosomal phospholipase activity which a single cell contains (Hostetler, et al, 1982) in ratio to the critical DPL coating for a 1 micrometer diameter quartz particle. After initial rapid decrease in adsorbed DPL in the first two hours of digestion, there is a slower rate of digestion over the three day period. This longer time behavior may represent digestive removal of the mineral- surface bound layer of DPL, and therefore be most significant for the restoration of dust surface membranolytic potential. This is indicated by Figures 1. and 2., in which quartz hemolytic potential is fully restored with no contribution from lysolecithin, while kaolin is still significantly suppressed at two and three days digestion. Figure 3. shows that a 30- fold increase in applied enzymatic activity is needed to restore the surface potential of kaolin at the same rate as quartz. This suggests a greater hindrance to enzymatic hydrolysis of DPL bound to kaolin. This is consistent with the spectroscopic indication of association of the DPL-phosphate moiety with kaolin. PLA2 induced hydrolysis of DPL occurs at the glycerol carbonyl ester linkage of the palmitic acid residue adjacent to the phosphate of DPL. This phosphate is acidic, and therefore more likely to associate with basic aluminol groups on the kaolin surface rather than acidic silanol groups on the kaolin or quartz surface. The positively charged trimethylamine head group of DPL may associate with the silanol groups of either dust. A model which suggests itself is that outer adsorbed bilayer DPL molecules are readily enzymatically digested from both dusts; while for the inner, dust surface associated DPL, a clay surface basic aluminol group interaction with the DPL acidic phosphate group results in greater hindrance for PLA2 digestion of kaolin- in contrast to quartz-adsorbed lecithin. This is a much simplified model of cellular phagolysosomal digestion which additionally involves phospholipase C, acidic pH media, and membrane bound enzymes. To determine if such mineral specific differences occur in phagolysosomal digestion within a pulmonary macrophage, and to determine if such dust-specific differences fall on either side of characteristic clearance times for respired particles from the scinar region of the lung, requires data from a more representative digestion system. We are attempting measurements of radiolabelled surfactant digestion from phagocytized dusts and measurement of associated cytotoxic response.

REFERENCES

Bartlett GR (1959) "Phosphorous Assay in Column Chromatography". J. Biolog. Chem. 234:466.

Clements JA, Nellenbogen J, Trahan HJ (1970) "Pulmonary Surfactant and Evolution of the Lungs". Science 169:603.

Harrington J, Miller K, Macnab G (1971) "Hemolysis by Asbestos". Environ. Res. 4:95-117.

Hostetler KY, Yazaki PJ, van den Bosch H "Purification of Lysosomal Phospholipase A. Evidence for Multiple Isoenzymes in Rat Liver". J. Biol. Chem. 257:13367-73.

Iler RK (1979) "The Chemistry of Silica". John Wiley & Sons. ISBN 0-471-02404-X.

Keane MJ, Wallace WE, Seehra M, et al (1988) "Respirable Particulate Surface Interactions with the Lecithin Component of Pulmonary Surfactant". In: Proceedings - VII International Pneumoconiosis Conference; International Labor Organization. In Press.

Marks J (1957) "The Neutralization of Silica Toxicity in vitro". Br. J. Ind. Med. 14:81.

Sheers G (1964) "Prevalence of Pneumoconiosis in Cornish Kaolin Workers". Br. J. Ind. Med. 21:218.

Wallace WE, Vallyathan V, Keane MJ, Robinson V (1985) "In vitro Biologic Toxicity of Native and Surface-Modified Silica and Kaolin". J. Toxicol. Environ. Health 16:415-424.

Wallace WE, Keane MJ, Hill CA, et al (1988) "The Effect of Lecithin Surfactant and Phospholipase Enzyme Treatment on Some Cytotoxic Properties of Respirable Quartz and Kaolin Dusts". In: Respirable Dusts in the Mineral Industries (Frantz RL, and Ramini RV, eds.) pp.154-166. American Congress of Governmental Industrial Hygienists Monograph. ISBN 0-936712-76-7.

ABSTRACT: Respirable quartz and kaolin dusts are comparably cytotoxic to pulmonary macrophage and membranolytic *in vitro*. When incubated in dipalmitoyl glycerophosphorylcholine (lecithin) dispersed in physiologic saline, a component of pulmonary surfactant, the lytic potential of both dusts is suppressed. Subsequent incubation with phospholipase A2 enzyme at applied activity of one unit per micromole of adsorbed lecithin, a simplified model of cellular phagolysosomal digestive processes, fully restores quartz hemolytic potential in three days, while one quarter of kaolin potential is restored. A 30- fold increase in applied activity is necessary to digest lecithin coating from kaolin at the same rate the coating is digested from quartz. Lecithin phosphate interaction with kaolin aluminol groups, indicated by IR spectra, are discussed as bases for the mineral- specific digestion rate differences.

ESR Evidence for the Hydroxyl Radical Formation in Aqueous Suspension of Quartz Particles and Its Possible Significance to Lipid Peroxidation in Silicosis

N.S. Dalal¹, X. Shi¹ and V. Vallyathan²

¹Department of Chemistry, West Virginia University

²Division of Respirable Disease Studies, National Institute for Occupational Safety and Health, Morgantown, WV

Electron spin resonance (ESR) spectrum of the hydroxyl (\cdot OH) radical spin adduct with the spin trap 5,5-dimethyl-1-pyrroline-N-oxide has been obtained in suspensions of freshly ground quartz particles. The concentration of the spin adduct (and hence of the \cdot OH radicals) increases with the amount of grinding. The dust's potential for the generation of the \cdot OH radicals is maximum when fresh (i.e., immediately after grinding) and decreases to 50% in about a day on storage in air. Studies involving metal chelates indicate that the \cdot OH radical formation involves mainly the silica surface and H_2O rather than the Fenton reaction. The results suggest that hydroxyl radical reaction(s) could be important in the lipid peroxidation and fibrogenicity by quartz dust, particularly in acute silicosis.

INTRODUCTION

In this paper we report on our electron spin resonance (ESR) detection of the formation of hydroxyl (\cdot OH) radicals in aqueous suspensions of freshly crushed quartz particles. This work was undertaken with a view to find possible clues to the role of free radicals in the pathogenesis of quartz-induced fibrogenicity, commonly known as silicosis. We noted that while silicosis is one of the major health hazards in coal and mineral industries, the mechanism by which the quartz particles exert their toxic action on cells and the process(es) by which these actions progress to fibrogenesis are still poorly understood (Reiser and Last, 1979; Singh and Rahman, 1987). It is generally thought, nevertheless, that the action of quartz particles on the biolog-

This research has been supported by the Department of the Interior's Mineral Institute program administered by the Bureau of Mines through the Generic Mineral Technology Center for Respirable Dust under grant G1135142.

Requests for reprints should be sent to Dr. N. S. Dalal, Department of Chemistry, West Virginia University, Morgantown, West Virginia 26506.

ical membranes is the starting point of the silicotic process (Parazzi et al., 1968). A possible clue to the mechanism of the membrane damage by quartz particles, in terms of the role of oxygenated free radicals, is suggested by the following observations. A suspension of quartz particles in contact with alveolar macrophages has been reported (Gabor et al., 1975; Koike et al., 1982) to initiate an enhancement of lipid peroxidation, defined broadly as the oxidative deterioration of polyunsaturated components of lipids. Hydroxyl ($\cdot\text{OH}$) radicals are known to be capable of peroxidation by abstracting hydrogen atoms from cell-membrane lipids (Halliwell and Gutteridge, 1985) and of initiating lipid peroxidation in lysosomal membranes (Fong et al., 1973). Along other lines, it is known that exposure of cell membranes, fatty acids, and unsaturated food oils to ionizing radiation, which generates $\cdot\text{OH}$ radicals, causes rapid peroxidation (Halliwell and Gutteridge, 1985). Thus $\cdot\text{OH}$ radicals (and also other oxygenated species such as O_2^- , $^1\text{O}_2$, and H_2O_2) might be expected to play a role in the toxicity of quartz. Earlier studies of the aqueous chemistry of quartz suspensions have reported detection of H_2O_2 (Kalbanev et al., 1980), implicating the formation of $\cdot\text{OH}$ radicals as transient species. However, we are not aware of any report of the detection of $\cdot\text{OH}$ radicals in quartz reactions, and thus the present study was undertaken. Since it is known that, because of their high reactivity (hence short lifetime) in aqueous media, the $\cdot\text{OH}$ radicals cannot be detected via ESR directly (Finkelstein et al., 1980; Buettner, 1982), we have used ESR combined with the spin-trap methodology (Finkelstein et al., 1980) for studying the $\cdot\text{OH}$ formation. The results show that $\cdot\text{OH}$ radicals are indeed formed in aqueous suspensions of freshly ground quartz, thus pointing to a possible new clue to the cytotoxicity of freshly formed quartz particles and thereby to silica fibrogenicity.

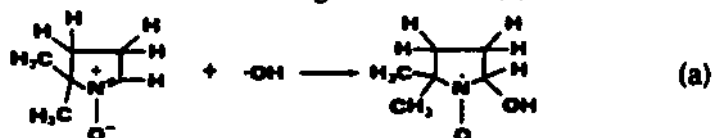
MATERIALS AND METHODOLOGY

Crystalline silica with particle sizes of 0.2–2.5 μm was obtained from the Generic Respirable Dust Technology Center, Pennsylvania State University, University Park, Pa. Particles in the range of smaller than 25 μm were produced by hand grinding in air, using an agate mortar and pestle because of the structural similarity of agate to that of quartz. Also, a rather mixed particle size, rather than a specific range, was employed, with a view to roughly approximate the random particle-size distribution in the mining atmosphere. ESR spectra were obtained at X-band (~ 9.7 GHz) using a Bruker ER 200D ESR spectrometer. For accurate measurements of the g values and hyperfine splittings, the magnetic field was calibrated with a self-tracking NMR gaussmeter (Bruker, model ER035M) and the microwave frequency was measured with a frequency counter (Hewlett-Packard, model 5340A). The micro-

wave power and magnetic field modulation amplitude were adjusted to obtain optimum ESR signal resolution and intensity; the values used are listed in the figure captions. 5,5-Dimethyl-1-pyrroline-*N*-oxide (DMPO) was used as a spin trap for the $\cdot\text{OH}$ radicals. The DMPO was purchased from Aldrich Chemical Company, Milwaukee, Wis., and used without further purification, since very weak or no $\cdot\text{OH}$ radical signal was obtained from the purchased sample when used by itself. An Aspect 2000 computer was used for data acquisition and analysis and for ESR spectral simulations. Different concentrations of DMPO aqueous solutions were made by adding distilled water and frozen until used.

RESULTS

Some typical results of the ESR spin-trapping studies are shown in Fig. 1. As may be noted from this figure, a 0.1 *M* aqueous solution of the spin trap DMPO alone (Fig. 1a), with TiO_2 powder (Fig. 1b), or with unground quartz (Fig. 1c), did not give a detectable ESR spectrum. TiO_2 was used as a control because it is known not to be fibrogenic (Gormley et al. 1985) and has a structure resembling quartz (SiO_2). However, when quartz was ground in a 0.1 *M* DMPO aqueous solution or when ground quartz particles were mixed with 0.1 *M* DMPO aqueous solution, an ESR spectrum ($g = 2.0059$), consisting of a 1:2:2:1 quartet pattern with a splitting of 14.9 G, was observed (Fig. 1d-g, Fig. 2b). Based on earlier work (Bannister and Bannister, 1985; Finkelstein et al., 1980; Rosen and Freeman, 1984), this spectrum appeared to be that due to the DMPO-OH adduct according to reaction (a).



Two further tests were made to identify the spectrum. First, the Fenton reaction ($\text{Fe}^{2+} + \text{H}_2\text{O}_2 \rightarrow \text{Fe}^{3+} + \cdot\text{OH} + \text{OH}^-$) (Halliwell and Gutteridge, 1984), known to produce $\cdot\text{OH}$ radicals, was used as an additional standard for the $\cdot\text{OH}$ identification. The ESR spin-adduct spectrum obtained by mixing 0.085 *M* H_2O_2 , 0.0165 *M* FeSO_4 , and 0.1 *M* DMPO (Fig. 2a) was the same as that of Fig. 2b (obtained with ground quartz), thus attesting to the formation of the $\cdot\text{OH}$ radicals in the quartz suspension. A pH variation study over the range of 4-10 or DMPO concentration over 10^{-3} to 10^{-1} *M* showed no measurable change in either the g factor or the observed splitting pattern.

As a second, confirmatory, test of the $\cdot\text{OH}$ radical formation, spin-trap ESR experiments were performed in which ethanol was added as a secondary trap. It has been shown (Buettner, 1982; Weitzman and Gra-

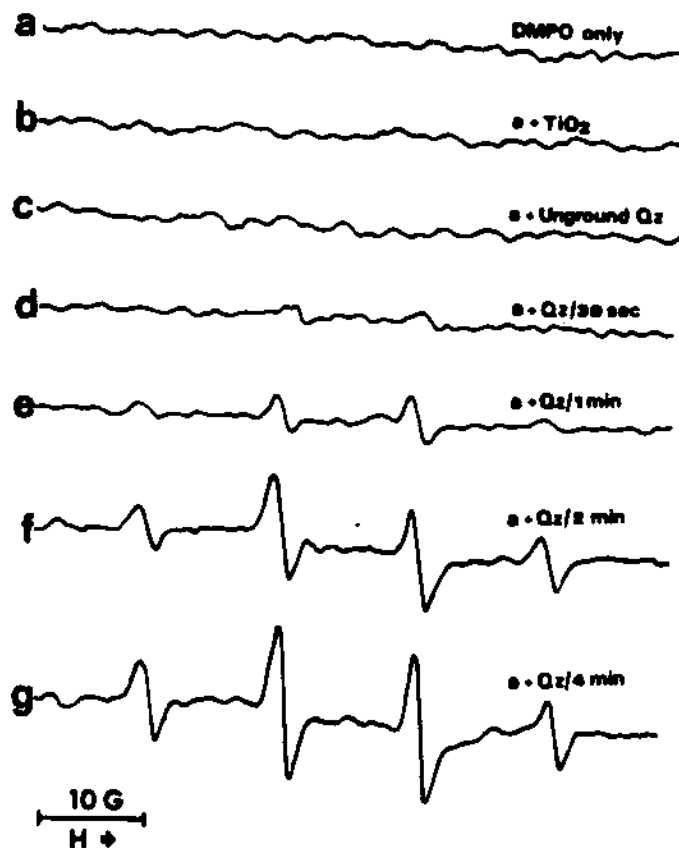
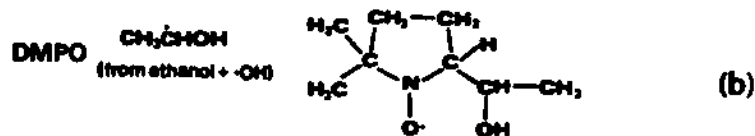


FIGURE 1. ESR spectra recorded 2 min after mixing 100 mM DMPO aqueous solution with (a) distilled water, (b) TiO_2 powder, (c) unground quartz, (d) freshly ground quartz particles, grinding time 0.5 min; (e), (f), and (g) correspond to grinding times of 1, 2, and 4 min, respectively. Receiver gain, 5×10^6 ; modulation amplitude, 2 G; scan time, 100 s; field, 3460 ± 75 G.

ceffa, 1984) that in the presence of ethanol, the intensity of the DMPO-OH signal decreases, because ethanol scavenges some of the $\cdot\text{OH}$ radicals to form the ethanoyl radicals (Buettner, 1982), which react with DMPO to give the spin adduct DMPO-CHOHCH₃, as shown below:



The ESR spectrum of the spin adduct DMPO-CHOHCH₃ was indeed observed, as indicated by arrows in Fig. 2c (for 30% ethanol) and more clearly in Fig. 2d, obtained in the presence of excess ethanol, thus con-

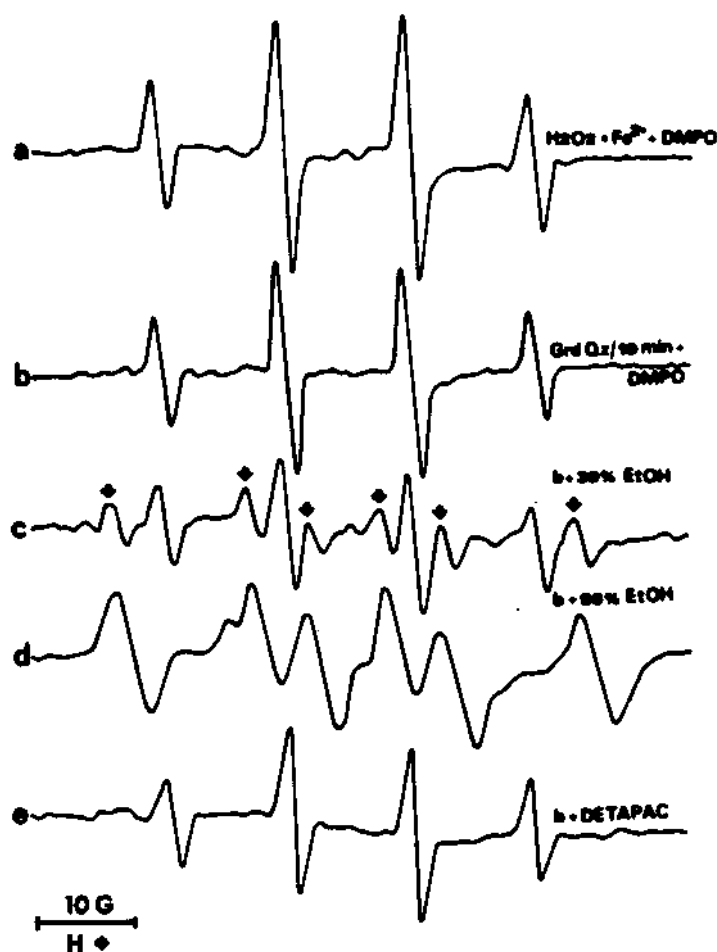


FIGURE 2. ESR spectra recorded 2 mins after mixing 100 mM DMPO with (a) H_2O_2 , 85 mM and FeSO_4 , 16.5 mM; (b) freshly ground quartz particles, grinding time 10 min; (c) same as (b), but with 30% ethanol added; (d) same as (b) but with excess ethanol; (e) same as (b) but with 1 mM DETAPAC added. Receiver gain, 5×10^6 ; modulation amplitude, 2 G; scan time, 100 s; field, 3460 ± 75 G.

firming the $\cdot\text{OH}$ radical formation (Buettner, 1982) in the original (i.e., quartz suspension) system.

An important observation was that the intensity of the $\cdot\text{OH}$ radical adduct signal increased with the amount of grinding (Fig. 1d–g, Fig. 2b), thus showing that the $\cdot\text{OH}$ radical generation is related to some surface property of the freshly made dust, most likely the silicon-oxygen radical sites known to form on grinding (Hochstrasser and Antonini, 1972; Dalal et al., 1986). Additional spin-trap measurements as a function of time of "aging" of the dust after grinding (Fig. 3) showed

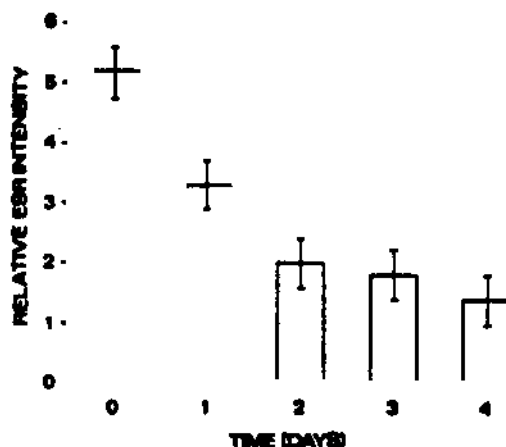


FIGURE 3. Dependence of the ESR intensity of the DMPO-OH adduct on the "aging" of quartz dust, i.e., the time of storage in air after grinding. The concentration of DMPO used was 100 mM. The \cdot OH radical formation is seen to decrease by 50% in about a day.

that freshly generated quartz particles produced more \cdot OH radicals than particles that had been stored in air after grinding. Thus the surface reactivity of the quartz particles for producing the \cdot OH radicals decreases with the time of storage in air. In order to characterize the kinetics of the dust's aging on its ability to generate the \cdot OH radicals, attempts were made to determine whether the reaction was of the first order [a straight line plot for $\log(\text{conc.})$ versus time] or second order [straight line plot for $(\text{conc.})^{-1}$ versus time]. The analysis indicated the kinetics to be neither first nor second order but of a more complex nature. Thus while it was not possible to define a unique half-life for the decrease in the (\cdot OH radical-producing) potential of the quartz dust on storage after grinding, we note that, on the average, freshly ground quartz dust loses its \cdot OH-generating capacity to about 50% in approximately 1 d (~ 24 h). This time scale should be kept in view in laboratory studies of the toxicity of quartz dust.

DISCUSSION

The spin-trap ESR spectra shown in Fig. 1d-g and Fig. 2b-e demonstrate that \cdot OH radicals are generated by the reaction of freshly broken quartz particles with aqueous solutions. While the exact mechanism of the \cdot OH radical production is not yet understood, it is clear that the breakage of quartz crystals implies the homolysis of Si-O-Si bonds and the generation of silicon-based radicals ($=\text{Si}\cdot$, $=\text{SiO}\cdot$, $=\text{SiOO}\cdot$) (Hochstrasser and Antonini, 1972; Kalbanev et al., 1980). We have indeed verified that the $\text{SiO}\cdot$ type of radicals is produced by grinding in air, and that the radicals decay as function of time when the dust is

In conclusion, our ESR spin trapping studies show that $\cdot\text{OH}$ radicals are generated by freshly ground quartz particles in aqueous media. The $\cdot\text{OH}$ production increases with the surface area generated on grinding, but decreases with the "aging" of the dust after grinding. The mechanism of the $\cdot\text{OH}$ production seems to be the reaction of the newly generated silica surface with water, rather than trace minerals. The implication of these results to fibrogenicity is that the quartz particles may damage the cell membrane through lipid peroxidation via the free radical chain mechanism initiated by the $\cdot\text{OH}$ radical, thus suggesting a possible new clue to the biochemical mechanism of pneumoconiosis, in particular of acute silicosis. More recent studies in our laboratory have shown that fresh quartz dust indeed causes a higher degree of lipid peroxidation, and that this lipid peroxidation can be suppressed by radical scavengers (V. Vallyathan, X. Shi, N. S. Dalal, W. Irr, and V. Castranova, 1987, unpublished results).

REFERENCES

- Bannister, J. V., and Bannister, W. H. 1985. Production of oxygen-centered radicals by neutrophils and macrophages as studied by electron spin resonance (ESR). *Environ. Health Perspect.* 64:37-43.
- Buettner, G. R. 1982. The spin trapping of superoxide and hydroxyl radicals. In *Superoxide Dismutase*, vol. 2, ed. L. W. Oberly, pp. 63-81. Boca Raton, Fla.: CRC Press.
- Dalal, N. S., Suryan, M. M., Jafari, B., Shi, X., Vallyathan, V., and Green, F. H. Y. 1986. Electron spin resonance detection of reactive free radicals in fresh coal dust and quartz dust and its implications to pneumoconiosis and silicosis. In *Proc. Int. Symp. Respir. Dusts in the Mineral Ind.* Pennsylvania State University, University Park, Pa., pp. 25-29.
- Durrant, P. J. 1970. Sub-group IV N. Carbon, silicon, germanium, tin and lead. In *Introduction to Advanced Inorganic Chemistry*, pp. 633-644. New York: Wiley.
- Finkelstein, E., Rosen, G. M., and Rauckman, E. J. 1980. Spin trapping of superoxide and hydroxyl radical: Practical aspects. *Arch. Biochem. Biophys.* 200:1-16.
- Fong, K. L., McCay, P. B., Poyer, J. L., Keel, B. B., and Misra, H. 1973. Evidence that peroxidation of lysosomal membranes is initiated by hydroxyl free radicals produced during flavine enzyme activity. *J. Biol. Phys.* 248:7792-7797.
- Gabor, S., Anca, Z., and Zugravu, E. 1975. In vitro action of quartz on alveolar macrophage lipid peroxides. *Arch. Environ. Health* 30:499-501.
- Gormley, I. P., Kowolik, M. J., and Cullen, R. T. 1985. The chemiluminescent response of human phagocytic cells to mineral dusts. *Br. J. Exp. Pathol.* 66:409-416.
- Halliwell, B., and Gutteridge, J. M. C. 1984. Oxygen toxicity, oxygen radical, transition metals and disease. *Biochem. J.* 219:1-14.
- Halliwell, B., and Gutteridge, J. M. C. 1985. Lipid peroxidation: A radical chain reaction. In *Free Radicals in Biology and Medicine*, pp. 159. Belfast: The University Press (Belfast) Ltd.
- Hochstrasser, G., and Antonini, J. F. 1972. Surface states of pristine silica surfaces. *Surface Sci.* 32:644-664.
- Kalbanev, I. V., Berestetskaya, I. V., and Butyagin, P. U. 1980. Mechanochemistry of quartz surface. *Kinet. Katal.* 21:1154-1158.
- Kolke, S., Kuno, Y., and Morita, H. 1982. The effects of silica on lipid peroxidation, and the production of superoxide radicals by phagocytizing rabbit macrophages. *Jpn. J. Hyg.* 37:510-515.

OH RADICALS FROM FRESH QUARTZ DUST

- Parazzi, E., Secchi, G. C., Pernis, B., and Vigliani, E. 1968. Cytotoxic action of silica dusts on macrophages in vitro. *Arch. Environ. Health* 17:850-859.
- Reiser, K. M., and Last, J. A. 1979. Silicosis and fibrogenesis: Fact and artifact. *Toxicology* 13:15-72.
- Rosen, G. M., and Freeman, B. A. 1984. Detection of superoxide generated by endothelial cells. *Proc. Natl. Acad. Sci. USA* 81:7269-7273.
- Singh, S. V., and Rahman, Q. 1987. Interrelationship between hemolysis and lipid peroxidation of human erythrocytes induced by silicic acid and silicate dusts. *J. Appl. Toxicol.* 12:91-96.
- Weitzman, S. A., and Graceffa, P. 1984. Asbestos catalyzes hydroxyl and superoxide radical generation. *Arch. Biochem. Biophys.* 228:373-376.

Do Silicon-Based Radicals Play a Role in Quartz-Induced Hemolysis and Fibrogenicity?

N.S. Dalal¹, X. Shi¹ and V. Vallyathan²

¹Department of Chemistry, West Virginia University

²Division of Respirable Disease Studies, National Institute for Occupational Safety and Health, Morgantown, WV

Correlated spectroscopic and cytotoxicity measurements were made on newly crushed silica to find whether the fracture-induced, silicon related (Si-O· or Si· type) free radicals play a direct role in the mechanism of hemolysis by silica particles. The free radical content of the silica particles was controlled through the radical decay, thermal annealing, and boiling processes, and was followed with electron spin resonance spectroscopy. Portions of the same sample were evaluated for their hemolytic potential, employing sheep erythrocyte and optical absorption techniques. The results indicate little, if any, correlation between the amount of the silicon-based radicals and the hemolytic potential of the fresh dusts, but these or related radical sites might be contributors to silica cytotoxicity and fibrogenicity via peroxidative pathways.

INTRODUCTION

In an earlier communication (1) from our laboratory it was reported that mechanical crushing of coal and quartz under normal air atmosphere generates free radicals on the particle surfaces, and that these radicals decay with time, hence pointing to a higher toxicity of fresh dusts in relationship to pneumoconiosis and silicosis. More recently Fubini et al. (2) have also reported the detection by electron spin resonance (ESR) of the formation of SiO· and Si·-type of radicals from quartz particles crushed under atmospheric conditions. In agreement with earlier ESR studies on single crystals of quartz crushed under high vacuum ($\sim 10^{-10}$ torr) (3) and subsequent exposure to air (3), and to other gases (4), these radicals were identified (2) as being formed by the homolytic cleavage of the Si-O-Si bonds and the reactions of the Si· and SiO· radical with atmosphere. Fubini et al. (2) also suggested that these radicals might be involved in the mechanism of the fibrotic action by silica, either by transforming the particle surface into a selective oxidating agent or as an initiator of a sequence of reactions leading to fibrosis. Earlier Gabor and Anca (5) had reported that lipid peroxidation caused by free radicals on the silica surface might be involved in the red blood cell membrane damage. Thus far, however, no parallel cytotoxicity, fibrogenicity, and free radical studies on a given quartz dust sample have been reported, except for some earlier work from our laboratory (1,6,7). We now present more recent results obtained from parallel cytotoxicity, fibrogenicity, and free radical

measurements on a freshly made quartz dust. The dust's free radical content was measured using ESR spectroscopy while its cytotoxicity potential was estimated via hemolysis. Hemolysis was employed as the toxicity test because it is a widely used method for estimating the potential of a dust for disrupting the cell membrane (8). The fibrotic potential was followed by measuring the dust-induced lipid peroxidation, using linoleic acid as a model lipid. As discussed below, the results obtained suggest new clues to the mechanism of the quartz-related cytotoxicity and fibrogenicity.

MATERIALS AND METHODS

(a) Reagents

Crystalline quartz particles with a size range of 0.2-2.5 μm were obtained from the Generic Respirable Dust Technology Center, Pennsylvania State University, University Park, Pennsylvania. These particles were crushed in air to obtain quartz dust samples with particle sizes smaller than 20 microns. We chose to work with a dust with mixed particle sizes, rather than a specific range, as an effort to simulate the mining atmosphere. An agate mortar-pestle arrangement was used for the crushing and grinding because of the close similarity of the structure of agate to that of quartz. Diethylenetriaminepentaacetic acid (DETAPAC) were purchased from Sigma. All other chemicals were purchased from Fisher or Aldrich.

(b) Hemolysis Experiments

Hemolytic activity of silica was measured, following an established procedure (9), as the amount of hemoglobin released from a 2% suspension of sheep erythrocytes after incubation with 10 mg of silica dust for one hour at 37°C. The hemoglobin release was estimated via the absorbance at 540 nm using a Giorford spectrophotometer. The procedure was calibrated by substituting the silica dust by a phosphate buffer solution as a negative control (background) and 0.5% Triton-X-100 as a positive control (100% hemolysis). The percentage of hemolysis was calculated as follows:

$$\% \text{ Hemolysis} = (I_{\text{silica}} - I_{\text{neg}}) / (I_{\text{pos}} - I_{\text{neg}})$$

where I_{silica} is the absorbance after incubation with the silica dust, while I_{neg} and I_{pos} are those with buffer only and 0.5% Triton-X-100, respectively.

(c) Lipid Peroxidation Measurements

Peroxidation of the polyunsaturated lipid linoleic acid (cis-9-cis-12-octadecadienoic acid) by freshly ground or aged silica was monitored using a fluorescence method (10) with minor modifications. The reaction mixture in a total volume of 0.5 ml contained freshly ground or aged silica and 20 μl of 0.52 mM linoleic acid emulsion in 95% ethanol in HEPES buffer (pH 7.4) with calcium and glucose. The mixture was heated for one hour in a shaking water bath at 37°C. This procedure was followed by the addition and mixing of 0.5 ml of 3% sodium dodecyl sulfate and then of 2.0 ml 0.1 N HCl, 0.3 ml 10%

phosphotungstic acid and 1.0 ml 0.7% 2-thiobarbituric acid. The mixture was then heated for 30 min at 95-100°C and the reactive substance formed was extracted with 5 ml 1-butanol after cooling. The extraction was then centrifuged at 3000 rpm for one minute and the fluorescence of the butanol layer was measured using a 515 nm excitation and 555 nm emission, with a Perkin-Elmer fluorospectrophotometer (Model MPG-36). Malondialdehyde standards were prepared from 1,1,3,3,-tetramethoxypropane to obtain a calibration curve, which was used for calculating the amounts of malondialdehyde produced.

(d) ESR Measurements

ESR spectroscopy was used for identifying the crushing-induced silicon-oxygen radicals, and to follow their concentration as described elsewhere (1,6,7). The ESR measurements were made with a Bruker ER 200D spectrometer operating at X-band (~9.5 GHz) frequencies, and 100 kHz magnetic field modulation. The magnetic field was calibrated with a self-tracking NMR gaussmeter (Bruker, model ER035M). The microwave frequency was measured with a Hewlett-Packard, Model 5340A, digital frequency counter. All ESR measurements were made at room temperature.

RESULTS AND DISCUSSION

Fig. 1 shows a typical, room temperature, ESR spectrum of freshly ground quartz particles. The spectrum is not identical but similar to those reported earlier for the measurements made at room temperature and ambient air environment (1,2). Here we focused on the major species, characterized by $g = 2.0015$, and assigned to a combination of silicon-oxygen radicals (1,2). To correlate the radical content with hemolysis, it was necessary to control the radical concentration. The first method used for this was thermal annealing. Thus the free radical concentration was measured via ESR (at room temperature) after thermal annealing from 50° to 800°C for 30 minutes at each temperature. Fig. 2 shows the change in the radical

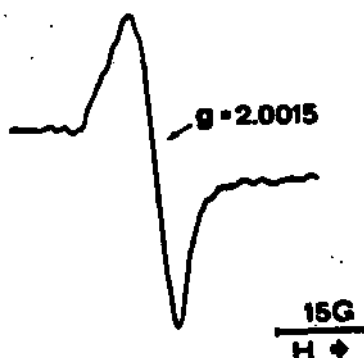


Fig. 1. A typical, room temperature, ESR spectrum of freshly ground quartz particles.

concentration on thermal treatment (Plot A) and the corresponding hemolysis measurements (Plot B). The data for the samples heated above 300°C show that while the free radical content decreases sharply with the heat treatment above 300°C, the hemolytic potential remains virtually unchanged for heating up to 550°C, and starts to decrease on further heating only. It, thus, follows that there is little, if any, direct correlation between the concentration of the free radicals and the hemolytic potential of the dust samples.

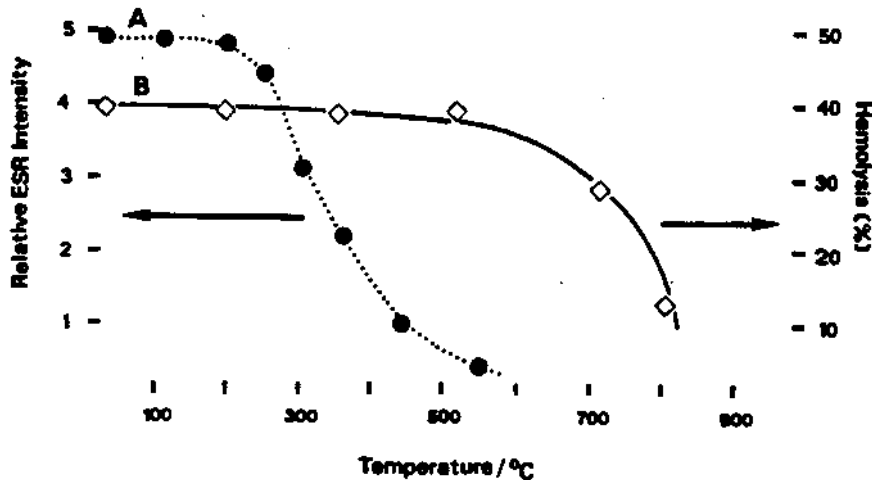


Fig. 2. The effect of heating on the ESR intensity of the grinding-induced silicon-oxygen radicals, plot A (●), and silica-induced hemolysis by the same samples, plot B (◇).

Second, measurements of both the radical concentration and the hemolytic potential were made at several time intervals after the dust preparation. Fig. 3 shows the time dependence of the free radical concentration on storing the dust in air after grinding (Plot A) and the hemolysis induced by the same sample (Plot B). It is seen that while the radical concentration decreases with a half-life of about one and a half day, in agreement with our earlier studies (1,6,7), the hemolytic potential does not change noticeably over at least two weeks, again showing that the grinding-induced radicals on the quartz particles do not play any direct role in the mechanism of the hemolysis by quartz particles.

As the third method for controlling the radical concentration, some freshly ground quartz particles were boiled in a phosphate buffer for about 30 minutes. ESR measurements on these samples showed that their radical concentration decreased to about 10%, while their hemolytic activity decreased to almost zero. In order to find if this decrease was related to the silicon-oxygen radicals, experiments were conducted as an attempt to restore the hemolytic activity. It was found that while an exposure to a phosphate buffer or a KMnO_4

solution (a strong oxidant) did not restore the hemolytic activity, the addition of DETAPAC, a strong metal chelate, to the incubation medium restored the activity to about 60%. Thus, the boiling-induced reduction in the silica's hemolytic potential cannot be attributed to the loss of the radicals on boiling, since it is unlikely that the addition of DETAPAC could restore the silicon-oxygen radicals. These results seem to indicate that the attachment of metal ions to the particle surfaces causes the loss in the hemolytic activity by quenching certain reactive (surface) sites. This conclusion is not unprecedented since earlier hemolysis studies (8) have shown that the presence of metal ions such as Al^{3+} causes a significant decrease in the quartz dust's hemolytic potential. We indeed confirmed that addition of Al^{3+} , Cu^{2+} , or Fe^{2+} ions, at about 1.0 mM concentration, to the incubation medium results in the loss of the hemolytic activity. The new result obtained here is that the subsequent addition of DETAPAC restores it, implying that the metal ions were only loosely bonded to the silica surface.

The above results are consistent with an earlier suggestion (8) that surface silanol ($SiOH$) groups play a key role in the mechanism of hemolysis by quartz particles. Metal ions are expected to be bonded via the surface silanol ($SiOH$) groups by replacing the H^+ ions, thus reducing the number of silanol groups responsible for red blood cell membrane damage (8). Infrared studies on heated silica-gel (11) and silica surfaces (12) demonstrated that silanol groups are formed on the silica surface, and that these moieties are annealed only if silica is heated to higher than $700^{\circ}C$ (11, 13). Since the present work shows that the hemolytic activity of silica decreases markedly on heating to $700^{\circ}C$ (Fig. 2), the role of the silanol groups in the hemolysis by silica seems fairly well established. This finding is consistent with an earlier report (8) of the reduction in the silica toxicity by Al^{3+} and polyvinyl-pyridine-N-oxide (PVPNO).

For obtaining further clues to the mechanism of silica's fibrogenicity, we investigated the possible relationship between silicon-oxygen radicals on fresh dust particles and the dust's lipid peroxidation potential by parallel measurements of the time dependence of radical content by ESR and of the silica-induced lipid peroxidation using linoleic acid as a model lipid (10). Fig. 4 shows the time dependence of the lipid peroxidation. It is seen that the ability of freshly ground silica to peroxidize a lipid decreases on storage, since the rate of silica-induced lipid peroxidation declined markedly over the first 48 hours after grinding and remained fairly constant thereafter. The similarity of the time dependence of the lipid peroxidation (Fig. 4) with the decay behavior of the silicon-oxygen radicals (Fig. 3, plot A) indicates that these radicals might be directly or indirectly involved in the silica-induced lipid peroxidation, which may result in a progressive degeneration of the membrane structure and eventual loss of membrane activity (14).

In conclusion, this work shows that the fracture-induced silicon-oxygen radicals are not directly involved in the mechanism of the erythrocyte hemolysis by quartz. This is consistent with earlier reports which suggest that dust-induced hemolysis and lipid

ROLE OF SILICON-OXYGEN RADICALS

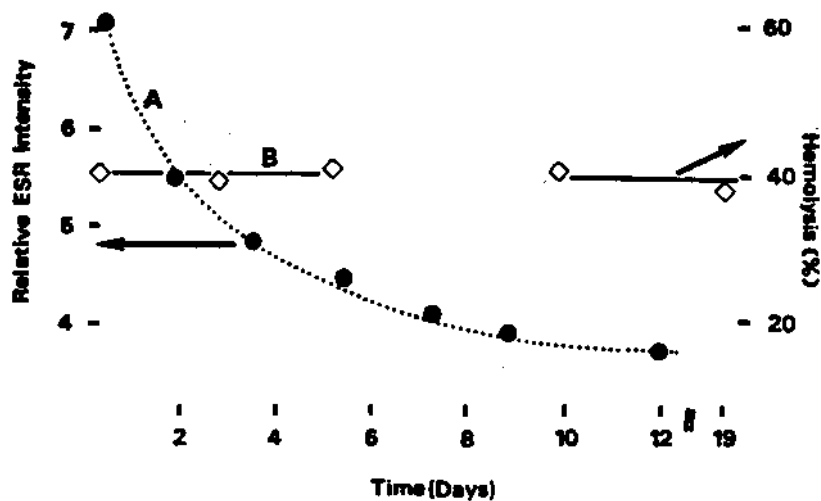


Fig. 3. Time dependence of the ESR intensity of the silicon-oxygen radicals, plot A (●), on storing in air, and the hemolysis, plot B (◇), by the same sample.

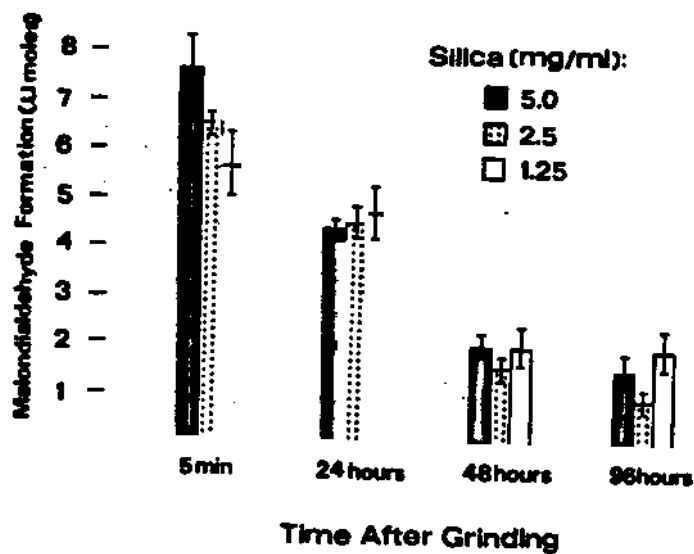


Fig. 4. Effect of "aging" of the quartz dust on the rate of peroxidation of linoleic acid..

peroxidation proceed via independent mechanisms (15,16). Thus the hypothesis (5) that lipid peroxidation caused by free radicals on the silica surface might be directly involved in the erythrocyte membrane damage does not seem likely. However, these radicals might be directly or indirectly involved in an oxidative-type chain reaction leading to macrophage membrane perturbation through lipid peroxidation and eventual fibrosis as noted earlier (2,6,7). It is interesting to note that fibrotic action, as a result of failed phagocytosis, was suggested to be due to the perturbation of macrophage membrane and the consequent release of a macrophage fibrotic factor (17). Recent ESR studies have shown that silica particles release $\cdot\text{OH}$ radicals in the presence of exogenous H_2O_2 (18) and even without it (7), and that the amount of the $\cdot\text{OH}$ radicals formed decreases with the "aging" of the quartz dust (6,7). Thus it is suggested that the $\cdot\text{OH}$ radical related mechanism of fibrogenesis by silica might be a fruitful new approach to understanding the pathogenesis of the silica-induced lung injury.

REFERENCES

1. Dalal N.S., Suryan M.M., Jafari B., Shi X., Vallyathan V., Green F.H.Y.: Electron Spin Resonance Detection of Reactive Free Radicals in Fresh Coal Dust and Quartz Dusts and Its Implications to Pneumoconiosis and Silicosis. Proc. Int. Symp. on Respirable Dusts in the Mineral Industries Pennsylvania State University, University Park, PA, USA. p. 24-29 (1986).
2. Fubini B., Bolis V., Glamello E.: The Surface Chemistry of Crushed Quartz Dust in Relation to Its Pathogenicity. Inorg. Chim. Acta 138:193-197 (1987).
3. Hochstrasser G., Antonini J.F.: Surface States of Pristine Silica Surface. Surface Sci. 32:644-664 (1972).
4. Radtsig V.A., Khalif V.A.: Investigation of Gas Chemisorption Processes on the Surface of Finely Divided Quartz by ESR Spectroscopy and Microcalorimetry. Kinet. Katal. 20:705-713 (1979).
5. Gabor S., Anca Z.: Effect of Silica on Lipid Peroxidation in the Red Cells. Int. Arch. Arbeitsmed. 32:327-332 (1974).
6. Vallyathan V., Shi X., Dalal N.S., Irr W., Castranova V.: Silicon-Oxygen Radicals and Their Role In Acute Silicosis (Abstract). Am. Rev. Respir. Dis. 137(Suppl.):404 (1988).
7. (a) Dalal N.S., Shi X., Vallyathan V.: Detection of Hydroxyl Radicals in Aqueous Suspensions of Fresh Silica Dust and Its Implication to Lipid Peroxidation in Silicosis. Paper presented at this conference (abstract No. 266).
(b) Shi, X., Dalal, N.S., Vallyathan, V.: ESR Evidence for the Hydroxyl Radical Formation in Aqueous Suspension of Quartz Particles and Its Possible Significance to Lipid Peroxidation in Silicosis. J. Toxicol. Environ. Health. 25:000-000 (1988) (in press).
8. Nolan R.P., Langer A.M., Harington J.S., Oster G., Selikoff I.J.: Quartz Hemolysis as Related to Its Surface Functionalities. Environ. Res. 26:503-520 (1981).
9. Harington J.S., Miller K., McNab G.: Hemolysis by Asbestos. Environ. Res. 4:95-117 (1971).
10. Fraga C.G., Leibovitz B.Z., Tappel A.C.: Halogenated Compounds as

- Inducers of Lipid Peroxidation in Tissue Slices. *J. Free Radical Biol. and Med.* 3:119-123 (1987).
11. Peri J.B.: Infrared Study of OH and NH₂ groups on the Surface of a Dry Silica Aereogel. *J. Phys. Chem.* 70:2937-2945 (1966).
 12. Tsuchiya I.: Infrared Spectroscopic Study of Hydroxyl Groups on Silica Surfaces. *J. Phys. Chem.* 82:4107-4112 (1982).
 13. Raask E., Schilling C.J.: Research Finding on the Toxicity of Quartz Particles Relevant to Pulverized Fuel Ash. *Ann. Occup. Hyg.* 23:147-157 (1980).
 14. Girotti A.W.: Mechanism of Lipid Peroxidation. *J. Free Radical Biol. Med.* 1:87-95 (1985).
 15. Kilroe-Smith T.A.: Peroxidative Action of Quartz in Relation to Membrane Lysis. *Environ. Res.* 7:110-116 (1974).
 16. Singh S.V., Rahman Q.: Interrelationship between Hemolysis and Lipid Peroxidation of Human Erythrocytes Induced by Silicic Acid and Silicate dusts. *J. Appl. Toxicol.* 12:91-96 (1987).
 17. Pernis B., Virginia E.C.: The Role of Macrophages and Immunocytes in the Pathogenesis of Pulmonary Diseases due to mineral Dusts. *Am. J. Ind. Med.* 3:133 (1982).
 18. Gulumian M., Wyk A.V.: Free Radical Scavenging Properties of Polyvinylpyridine N-Oxide: A Possible Mechanism for Its Action in Pneumoconiosis. *Med. Lav.* 78:124-128 (1987).

Respirable Particulate Surface Interactions with the Lecithin Component of Pulmonary Surfactant

M.J. Keane¹, W.E. Wallace^{1,2}, M.S. Seehra², C.A. Hill²,
P.S. Raghootama² and P. Mike²

¹West Virginia University

²Division of Respirable Disease Studies, National Institute for Occupational Safety and Health, Morgantown, WV

ABSTRACT

Dipalmitoyl glycerophosphorylcholine (lecithin) dispersed in physiologic saline, a model of the primary component of pulmonary surfactant, is adsorbed by respirable quartz and aluminosilicate dusts. Dust cytotoxicity as measured by erythrocyte hemolysis and pulmonary macrophage enzyme release is suppressed by this adsorption. The degree of suppression of hemolytic potential versus specific adsorption of lecithin from dispersion in saline by respirable quartz, kaolin, and alumina dusts are compared with dusts' BET specific surface areas to interpret the prophylactic effect of lecithin adsorption. Dust hemolytic potential versus media pH are presented. Fourier transform infrared spectroscopy and photoacoustic spectroscopy of lecithin on quartz and of lecithin on kaolin are presented and reviewed with results of studies of the time course of removal of lecithin adsorbed on mineral surfaces by digestion by phospholipase enzyme. Results are discussed in terms of a model of prompt neutralization of respired mineral dusts by pulmonary surfactant, and a gradual re-toxification by digestive processes acting on the adsorbed prophylactic surfactant coating following phagocytosis.

Introduction

Quartz dust of respirable size is well known to cause fibrotic lung disease, but numerous questions persist in the understanding of the initiation and progression of this disease. Our approach concentrates on physical and chemical aspects of mineral dusts early-on in their interactions with living organisms, and we have chosen simplified models to investigate that interaction.

In the alveolar spaces of the lung, tissue is coated with a surface-active material (pulmonary surfactant), which, among other functions, mechanically stabilizes the lung from collapse by reducing the surface tension of water in the alveolar sacs.(1) This surfactant is also the material that is first contacted by a mineral particle that is transported to an alveolus and is impacted there. This surfactant material has been studied extensively. The primary components are known to be proteins (about 11% in dog lavage fluid), and phospholipids (about 88%).(2) Phosphatidyl cholines constitute roughly 80% of the phospholipid fraction; about 70% of the phosphatidyl choline fraction is dipalmitoyl lecithin (DPL).(2) Respirable aluminosilicate particles are capable of adsorbing dipalmitoyl lecithin from dispersion in physiologic saline, a model for a possible initial event occurring upon deposition of a particle in a pulmonary alveolus.(3)

As may be seen from Figure 1, the DPL molecule has several fixed charges at neutral pH; a positive charge on the trimethyl amine (choline) moiety, and a negative charge on the phosphate group. Also evident are the two fatty acid residues of palmitic acid, which are bonded through ester linkages to the glycerol segment of the molecule. The fatty acid moieties of phosphatidyl

DIPALMITOYL LECITHIN (DPL)

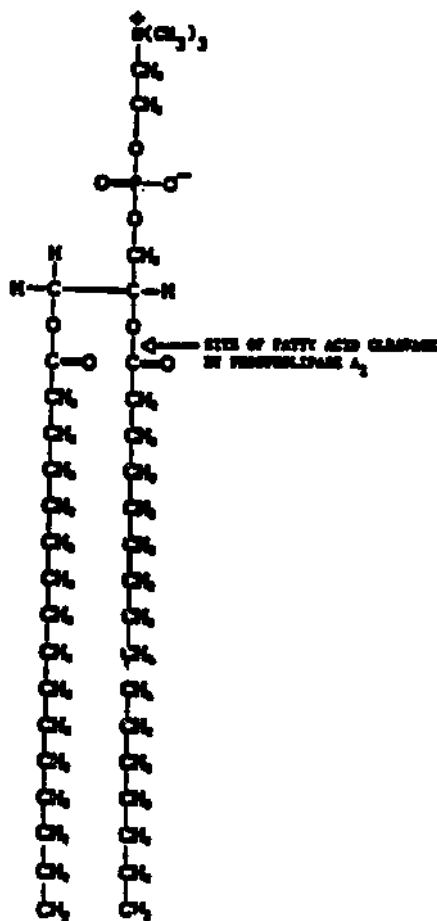


Figure 1: Structural Formula of Phosphatidyl Choline Molecule

choline make the molecule insoluble in aqueous solutions under normal conditions, but a colloidal unit of aggregated molecules called a micelle is usually formed spontaneously above a certain minimum concentration. Small micellar vesicles are generally formed in the laboratory by using ultrasonic agitation or by solvent evaporation methods.

Our simplified system uses dispersions of DPL in physiological saline as a surrogate pulmonary surfactant, and we have used quartz, a crystalline, fibrogenic dust, and kaolin, an aluminosilicate clay that is not generally considered fibrogenic.(4-10) The approach has been to use *in vitro* cytotoxicity assays (sheep erythrocyte hemolysis and lysosomal enzyme release from pulmonary macrophages) to examine the effects of the surrogate surfactant on mineral dust cytotoxicity.(11)

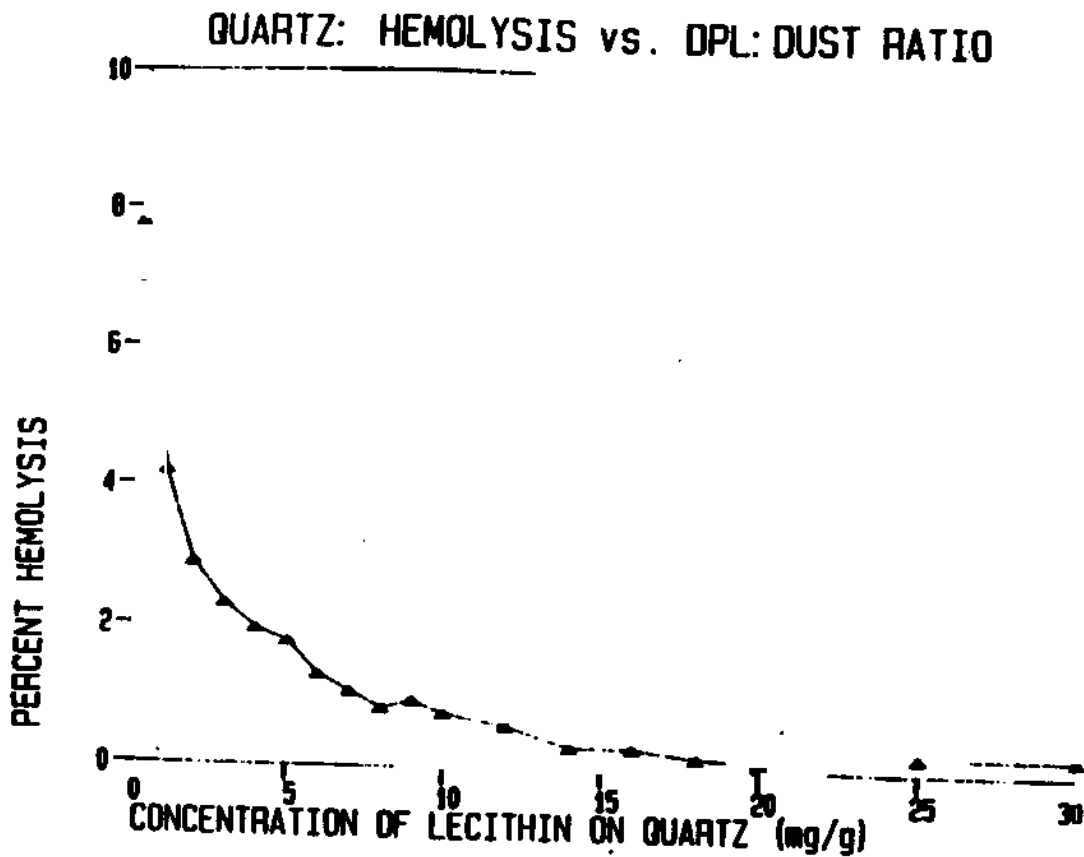


Figure 2: Percent Hemolysis vs. DPL: Quartz Ratio

The first results of the *in vitro* system were that DPL above a certain concentration virtually eliminates cytotoxicity of both dusts;(11) curves of cytotoxicity vs. DPL to dust ratios are shown in Figures 2 and 3. The effect has also been demonstrated with other materials, such as serum proteins and alveolar washings.(12,13) The effect was seen in both cytotoxicity assays, and a dose-response pattern is observed for both dusts.(11) The two untreated dusts are about comparable in cytotoxicity on a BET specific surface basis; the quartz is about 4 m²/g for the less than 5 micron size, and the kaolin is about 13 m²/g for the same size fraction.(11)

While this finding is significant, it is surely not the *in vivo* situation. Quartz is certainly fibrogenic in normal individuals, at least after extended periods. Some of the prevailing theories on silicosis have been recently reviewed; (14) our next approach was to reexamine the current hypotheses on the initiation of fibrosis, and modify them if necessary. Our working hypothesis is shown in Figure 4.

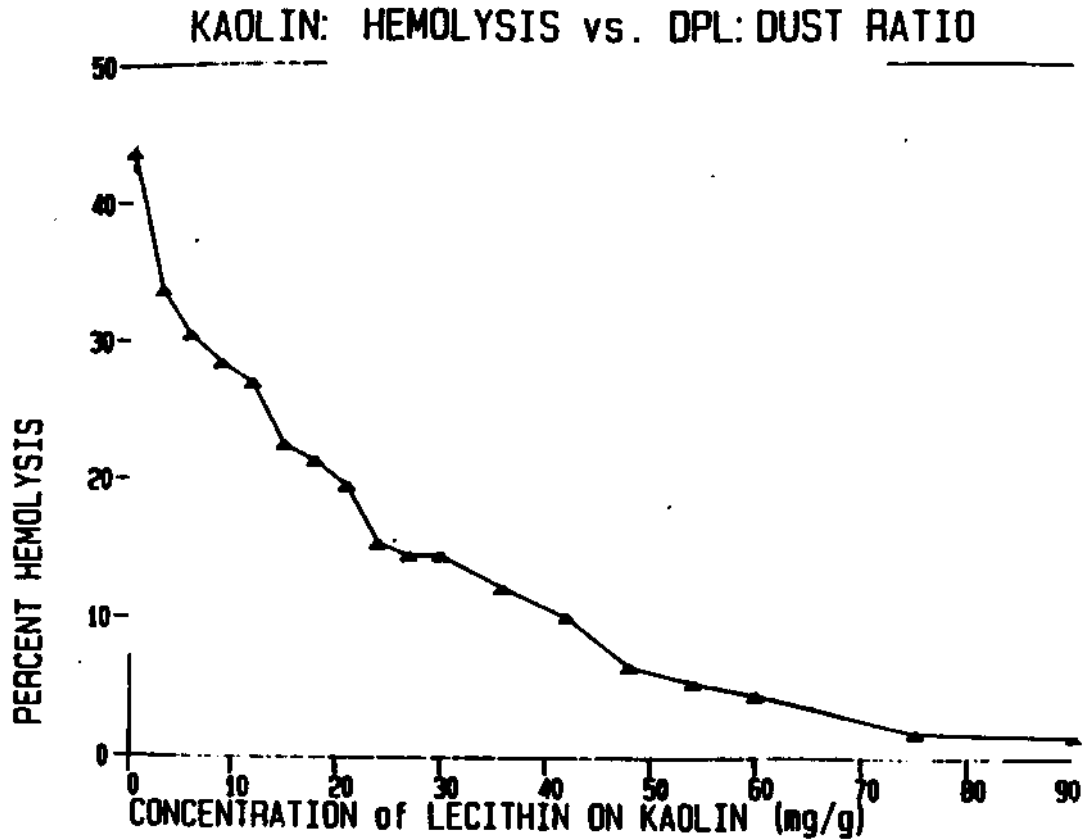


Figure 3: Percent Hemolysis vs. DPL: Kaolin Ratio

HYPOTHESIS: EVENTS OF SILICOSIS INITIATION

1. INHALATION OF SILICA PARTICLES TO ALVEOLAR REGION
2. CONTACT WITH AND SUBSEQUENT COATING OF PARTICLE WITH SURFACTANT
3. PHAGOCYTOSIS OF COATED PARTICLE BY ALVEOLAR MACROPHAGE
4. FORMATION OF PHAGOLYSOSOME IN THE MACROPHAGE
5. HYDROLYSIS OF SURFACTANT BY LYSOSOMAL ENZYMES
6. RETOXIFICATION OF DUST
7. DEATH OR DAMAGE OF MACROPHAGE/ RELEASE OF SIGNAL SUBSTANCE TO FIBROBLASTS
8. PROLIFERATION OF FIBROBLASTS AND COLLAGEN SYNTHESIS
9. FIBROSIS

Figure 4: Working Hypothesis for Silicosis Initiation

Our principal efforts were directed toward item 5, the degradation of surfactant coating on dusts by pulmonary macrophages. We have been using a cell-free in vitro model to characterize enzymatic digestion of dipalmitoyl lecithin adsorbed on mineral dusts, while developing cellular in vitro methods to measure digestion of labelled dipalmitoyl lecithin from phagocytized respirable dusts. In particular, we sought to determine if such adsorption could occur, and if there are mineral specific differences in the rate of such digestion. Our artificial "lysosome" contained the enzyme phospholipase A₂, derived from porcine pancreas, to simulate the phospholipase enzymes found in vivo.(15) These enzymes have been identified in many cells, and we have isolated and concentrated phospholipase A activity from rat liver cell lysosomes, but not at sufficient activity levels to allow large scale laboratory use.(15) The use of commercially prepared enzyme of known activity, rather than a cell culture or in vivo system, allows the elimination of numerous uncontrollable variables, so that attention can be focussed on differences between dusts.(16-18) Our laboratory protocol is shown in Figure 5.

LABORATORY PROTOCOL

1. PREPARE DPL DISPERSION IN SALINE WITH ULTRASONIC AGITATION
2. DUST COATED WITH DPL FOR 1 HOUR AT 37 DEGREES C
3. EXCESS DPL RINSED FROM DUST
4. INCUBATE DUST WITH PHOSPHOLIPASE A2 FOR 2 TO 72 HOURS
5. DUST RINSED WITH EDTA BUFFER TO INACTIVATE ENZYME (TWICE)
6. DUST RESUSPENDED IN BUFFER/CYTOTOXICITY ASSAY
7. LIPIDS EXTRACTED FROM REST OF DUST WITH SOLVENT
8. LIPIDS SEPARATED BY THIN LAYER CHROMATOGRAPHY
9. LIPIDS RECOVERED AND QUANTIFIED BY PHOSPHORUS ASSAY

Figure 5: Laboratory Protocol for In Vitro Cell Free System

Results and Discussion:

When the coated dusts are treated with the phospholipase A₂, several things are evident (Figures 6 and 7). For both dusts, for a short period of time, toxicity in the hemolysis assay may exceed that of the untreated dusts. The Figures indicate that this is invariably the case at the 2 hour point. Subsequent assay of lipids indicate that the hydrolysis product lysophosphatidyl choline (lysolecithin) is retained on the dusts. This product results when the fatty acid ester linked to the center carbon of the glycerol chain is hydrolyzed to a free fatty acid, leaving an hydroxyl group; this substance is also highly lytic to cell plasma membranes, thus explaining the exaggerated cytotoxicity. As time progresses, less lysolecithin is found to be associated with the dusts, as seen in Figures 8 and 9.

The most significant finding is that the quartz toxicity returns to essentially its untreated value, even with fairly low enzyme levels relative to the kaolin. Analysis of the retained lipids confirms that the dust is almost free of adsorbed DPL or other lipids, as seen in Figure 10.

INTERACTION OF DUST AND LIVING ORGANISM

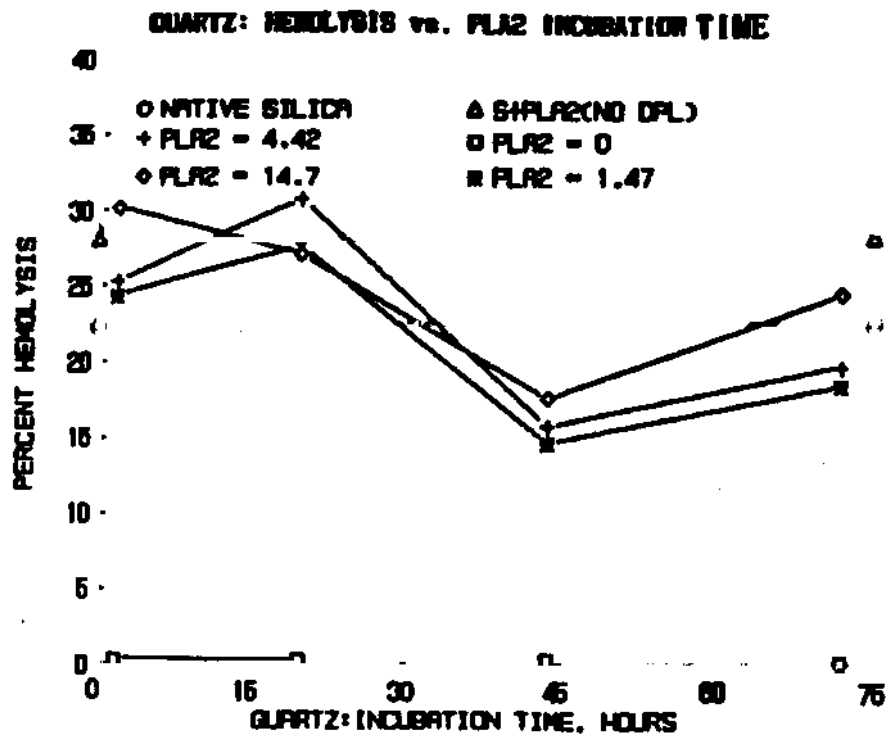


Figure 6: Hemolysis vs. Time for DPL-Coated Quartz Treated with Phospholipase A₂

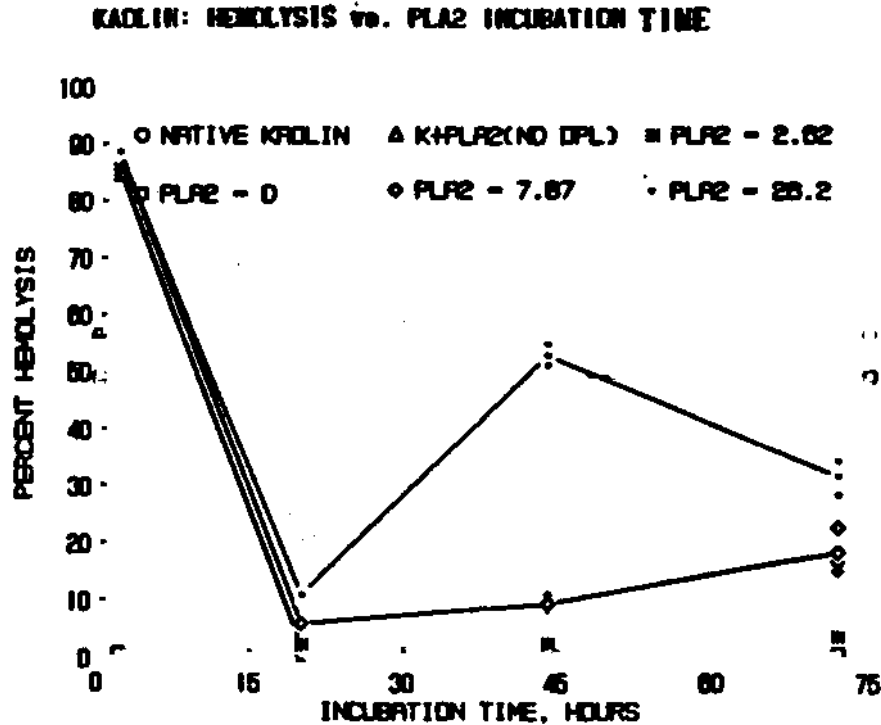


Figure 7: Hemolysis vs. Time for DPL-coated Kaolin Treated with Phospholipase A₂

LYSOLECITHIN REMAINING ON QUARTZ AFTER PLA₂ INCUBATION

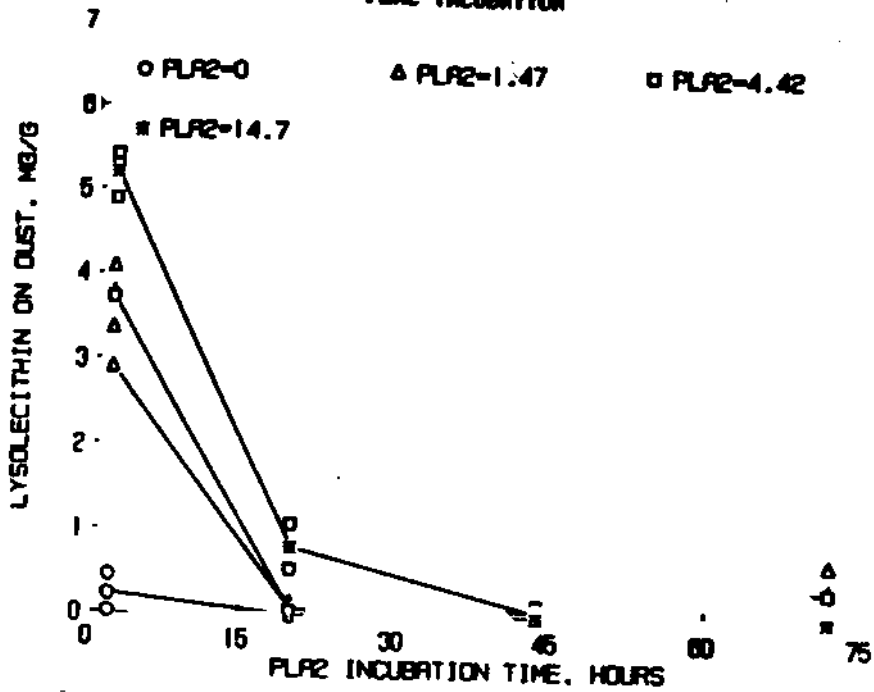


Figure 8: Lysolecithin Retained on Quartz after PLA₂ Incubation vs. Time

LYSOLECITHIN REMAINING ON KAOLIN AFTER PLA₂ INCUBATION

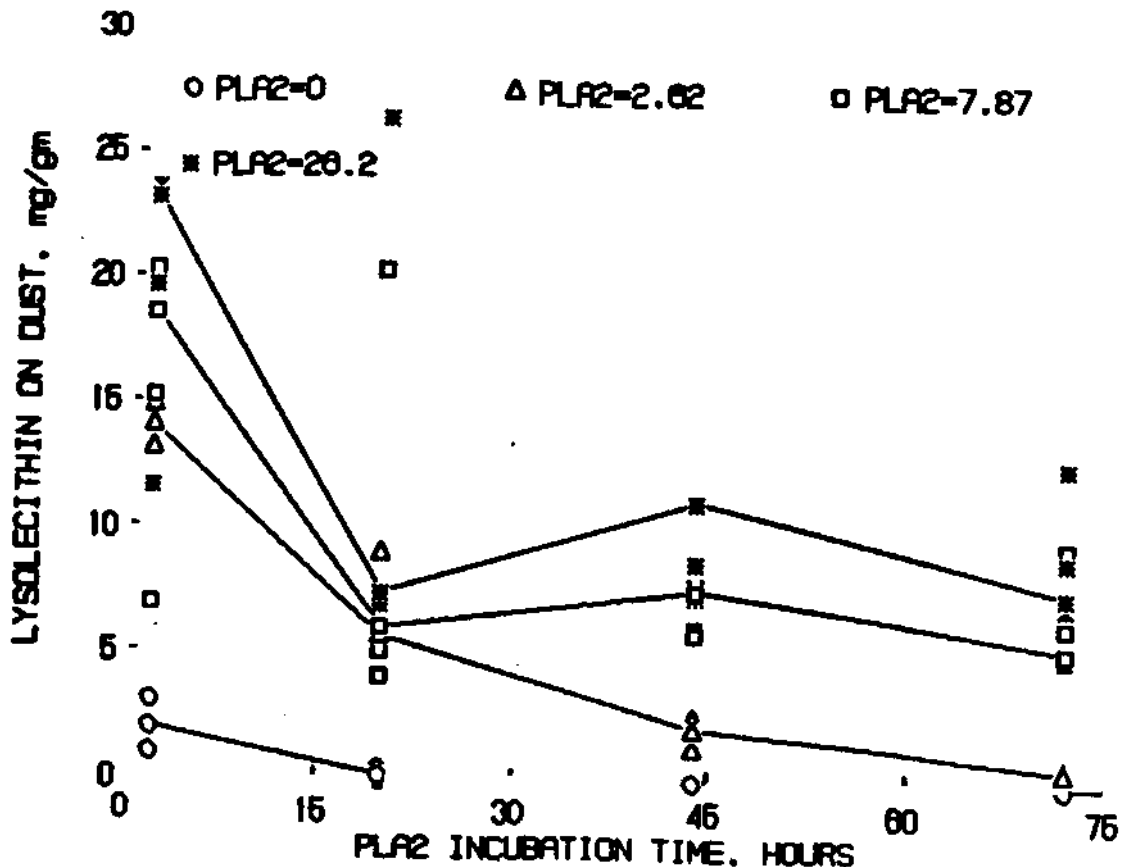


Figure 9: Lysolecithin Retained on Kaolin after PLA₂ Incubation vs. Time

INTERACTION OF DUST AND LIVING ORGANISM

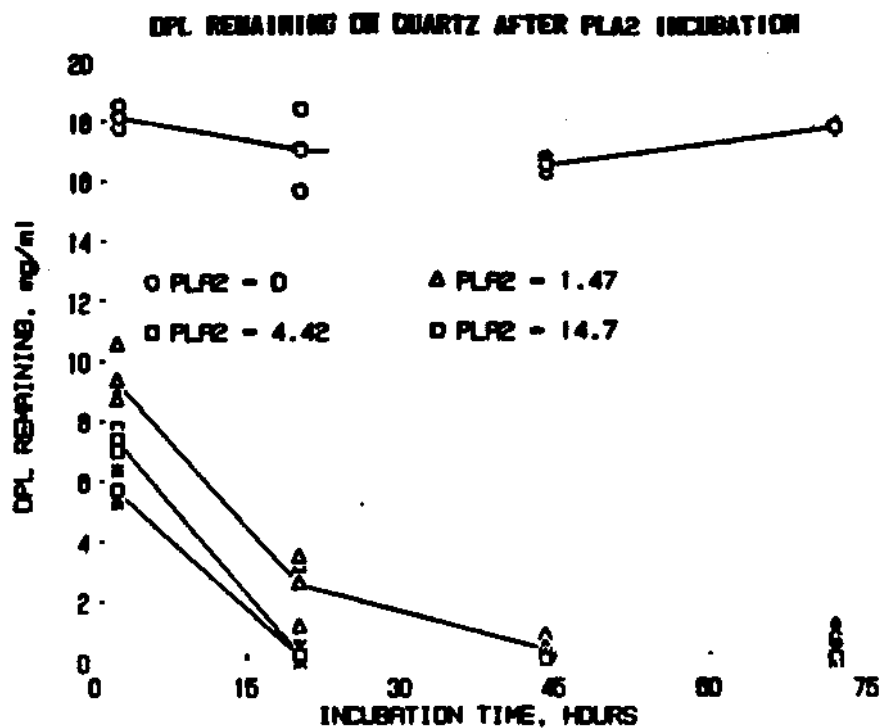


Figure 10: DPL Retained on Quartz after PLA₂ Incubation vs. Time

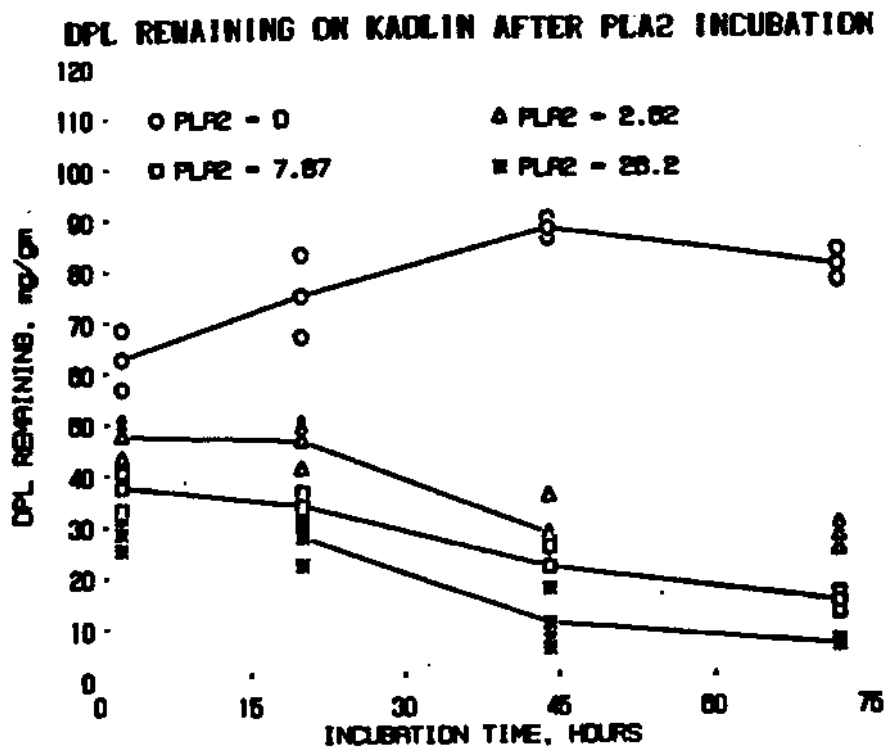


Figure 11: DPL retained on Kaolin after PLA₂ Incubation vs. Time

The situation for kaolin is quite different; toxicity is not restored except at quite high activity levels, and lipids are retained on the surface to a much greater extent, as seen in figure 11.

The results up to this point raise an important question: what is the basis for a difference in retoxification of quartz and kaolin dusts? We have looked at several methods to try to clarify this difference, although the case is by no means closed.

In general, enzymatic digestion of substrate molecules is quite dependent on molecular conformation. Because quartz and kaolin surface structure and functional groups differ significantly, we are investigating the possibility that conformational differences between lecithin adsorbed to quartz and to kaolin surfaces might provide differing degrees of steric hindrance to digestive removal, with resultant differences in rates of restoration of surface cytotoxic potential.

To examine this hypothesis, we used Fourier Transform Infrared Spectrophotometry at the West Virginia University Physics Department to look at the spectra of DPL on both quartz and kaolin, and compared the spectral features to the pure DPL spectrum. The DPL-coated quartz and DPL spectra are shown in Figure 12. Samples were prepared as wet films of DPL or coated dusts on a KBr pellet substrate. In the DPL treated quartz, the 3024 cm^{-1} trimethyl amine band disappears, but the 3400 cm^{-1} band associated with

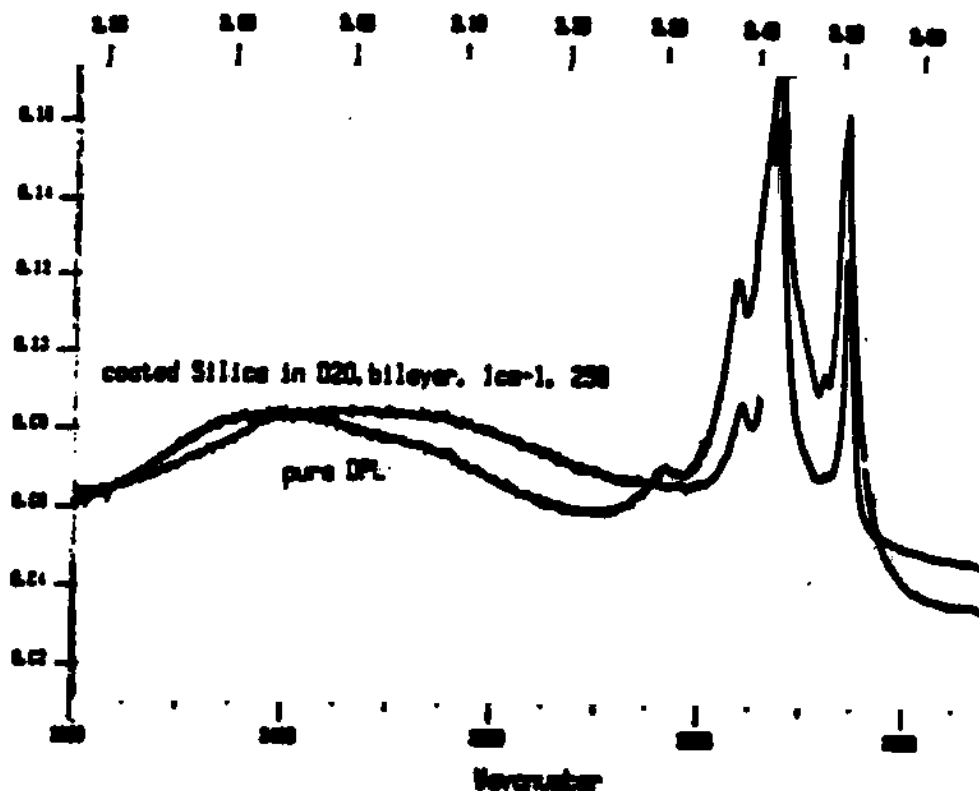


Figure 12 FTIR spectra of DPL-Coated Quartz and DPL only, 2750-3400 cm^{-1}

P-O-NOH is not suppressed. For the kaolin, shown in Figure 13, the 3400cm^{-1} group has virtually disappeared, and the trimethyl amine band is suppressed and shifted. The evidence here is strongly suggestive of a quartz-trimethylamine association, and a kaolin-phosphate association. There also exists the possibility of a kaolin-trimethyl amine association, but the evidence is not as strong. The use of dry or moist samples for IR spectroscopy limits extrapolation of these results to dusts immersed in aqueous media. But the data suggest an association of the phosphate moiety of lecithin with basic aluminol groups on the alumina octahedra portions of the kaolin surface, and a consequent hindrance of enzymatic hydrolysis of the nearby glycerol-to-fatty acid ester.

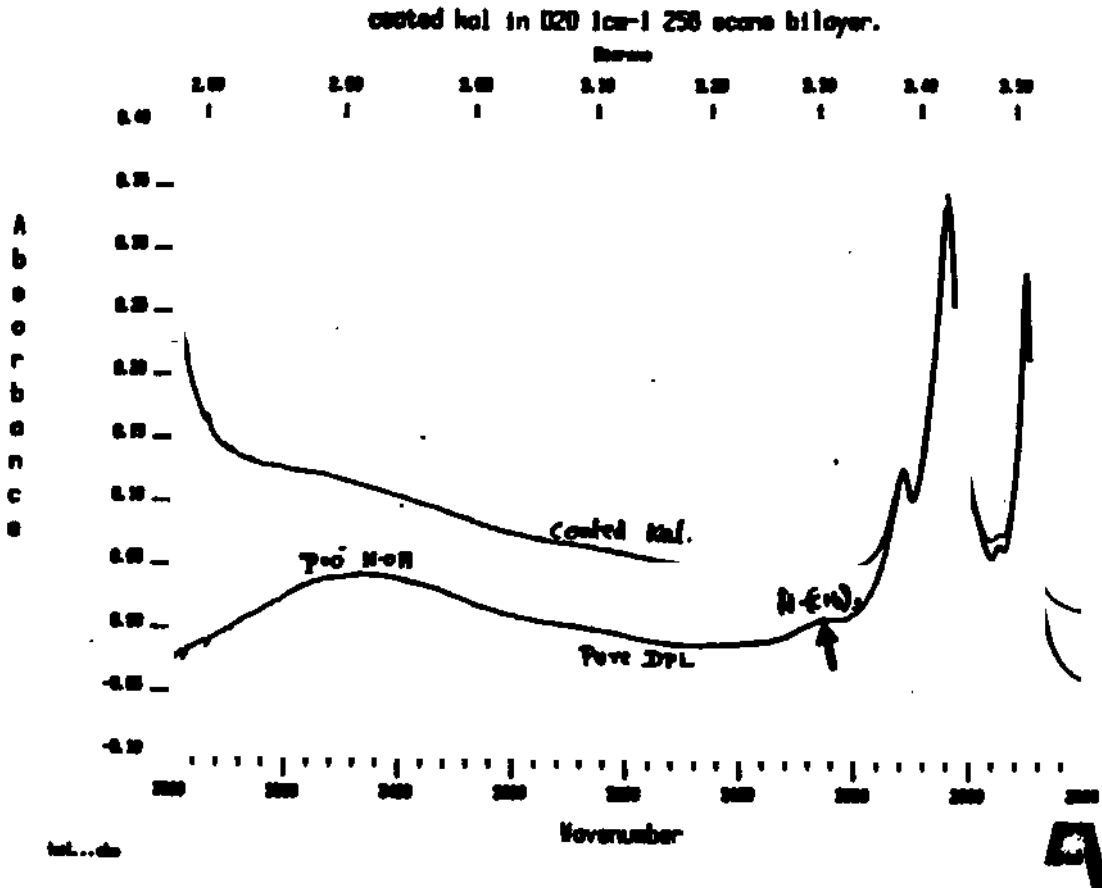


Figure 13 FTIR spectra of Dpl-coated Kaolin and DPL only. $2800-3600\text{ cm}^{-1}$

To consider quartz and kaolin surface functions involved in direct lysis of erythrocyte membrane, in the absence of surfactant coating, we also performed some limited experiments to determine whether pH significantly affected dust cytotoxicity in the hemolysis assay. Quartz would be expected to show only acidic characteristics, due to surface silanol groups, while kaolin may have acidic silanol surface groups, as well as weakly acidic and weakly basic aluminol surface groups. An experimental problem arises here, however: the red blood cells are subject to hemolysis when a hydrogen ion, or other ion, gradient is present across the membrane. We tried to see whether the external osmolarity could be increased to offset this gradient, and the results are shown in Figure 14. The method seemed reasonable down to pH 5, so all blood suspensions were adjusted to 400 mOsm for the pH dependence experiments.

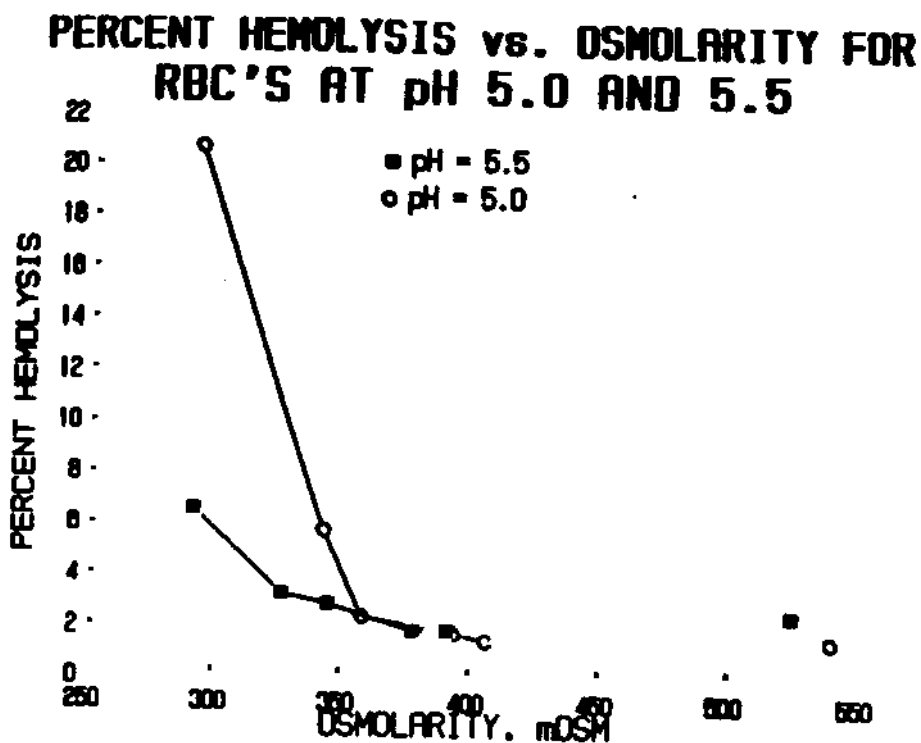


Figure 14: Percent Hemolysis vs. Osmolarity at pH 5 and pH 5.5

Figure 15 shows the dependence of hemolysis on pH. For both quartz and kaolin, the slope is positive between pH 5 and 7, suggesting that a charge dependent mechanism is involved with hemolysis for both dusts. The acidic character of both dusts suggests an acid-base interaction of the minerals with the trimethyl amine group of membrane lecithin. Interpretation of these results on the pH dependence of the lytic potential of uncoated dusts are compromised by questions of the effect of pH on the lytic fragility of the membrane itself.

An overall research hypothesis which presents itself is that native quartz and aluminosilicate dusts can damage cellular membrane by direct interaction with dissociated mineral surface acidic silanol groups; that adsorption of the lecithin portion of pulmonary surfactant masks and thereby passivates these mineral surfaces; that phospholipase enzymatic digestion of lecithin coated dusts following their phagocytosis can remove the protective surfactant coating and restore cytotoxic potential of dusts within the phagocytic cell; and that the rate of this restoration may be affected by conformational differences between lecithin adsorbed to acidic silanol groups on quartz and to acidic silanol and basic aluminol groups on kaolin.

Conclusions

The surface toxicity both of quartz and kaolin dusts is eliminated in short-term cytotoxicity assays by coating the dusts with SPL.

Lecithin treated quartz is readily retoxified by phospholipase A₂ in a cell-free *in vitro* system, and is relatively free of retained phospholipids.

INTERACTION OF DUST AND LIVING ORGANISM

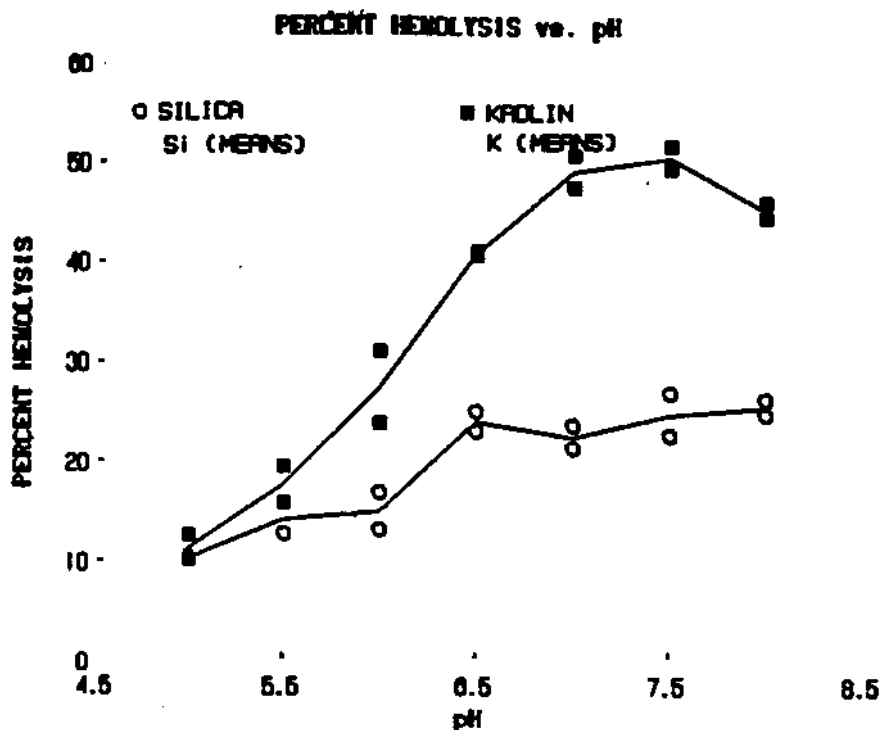


Figure 15: Percent Hemolysis vs. pH for Silica and Kaolin @ 400 mM

DPL treated kaolin is not readily retoxified at comparable enzyme levels, and retains both DPL and phospholipid degradation products.

The pH dependence suggests that both quartz and kaolin have acidic surface groups that are involved in hemolysis, and also may associate with the positively charged trimethylamine group of DPL.

FTIR spectra suggest that kaolin probably interacts with the phosphate group of DPL, and both quartz and kaolin probably interact with the trimethyl amine group. Thus, there may be a surface chemistry effect in the differing rates of hydrolysis by phospholipase A₂.

ACKNOWLEDGEMENT

This research has been supported by the Department of the Interior's Mineral Institute Program administered by the Bureau of Mines through the Generic Mineral Technology Center for Respirable Dust under Grant number G1135142.

References

- (1) King, R.J.: Pulmonary Surfactant. *J. Applied Physiology* 53:1-8 (1982).
- (2) King, R.J., Clements, J.A.: Surface Active Materials From Dog Lung. II. Composition and Physiological Correlations. *American Journal Of Physiology*. 223:715-726 (1972).
- (3) Wallace, W.E., Headley, L.C., Weber, K.C.: Dipalmitoyl Lecithin Surfactant Adsorption by Kaolin Dust *in vitro*. *J. Colloid and Interface Science* 51:535-537 (1975).

THE RESPIRABLE DUST CENTER

- (4) Hamilton, A., Hardy, H.: Industrial Toxicology, Littleton, MA (1982). P.448.
- (5) Parkes, W.: Occupational Lung Disorders Boston, MA (1982).
- (6) Hunter, D.: The Diseases of Occupations, 6th ed., London (1978)p.992.
- (7) Shears, G.: Prevalence of Pneumoconiosis in Cornish Kaolin Workers. Br. J. Ind. Med. 21:218-225.
- (8) Warraki, S., Herant, Y.: Pneumoconiosis in China-Clay Workers. Br. J. Ind. Med. 20:226-230.
- (9) Lynch, K., Mc Iver, P.: Pneumoconiosis from Exposure to Kaolin Dust: Kaolinosis. Am. J. Path. 30:1117-1122 (1954)
- (10) Lapeas, D., Gale, P., Kennedy, T., Rawlings, W., Dietrich, P.: Kaolin Pneumoconiosis. Radiologic, Pathologic, and Mineralogic Findings. Am. Rev. Resp. Dis. 130:282-288.
- (11) Wallace, W., Vallyathan, V., Keane, M., Robinson, V.: In Vitro Biologic Toxicity of Native and Surface Modified Silica and Kaolin Dusts. J. Tox. Env. Health 16:415-424.
- (12) Allison, A., Harington, J., Birbeck, M.: An Examination of the Cytotoxic Effects of Silica on Macrophages. J. Exp. Med. 124:141-154 (1966).
- (13) Emerson, R., Davis, G.: Effect of Alveolar Lining material-coated Silica on Rat Alveolar Macrophages. Env. Health Perspect. 51:81-84.
- (14) Bowden, D. Macrophages, Dust, and Pulmonary Diseases. Exp. Lung Research 12:89-107 (1987).
- (15) DeHaas, G., Postema, E., Nieuwenhuizen, W., VanDeenen, L.: Purification and Properties of Phospholipase A from Porcine Pancreas. Biochim. Biophys. Acta 159:103-117 (1968).
- (16) Wallace, W.E., Keane, M.J., Vallyathan, V., Ong, T-M., Castranova, V.: Pulmonary Surfactant Interaction with Respirable Dust. Proceedings: Generic Mineral Technology Center for Respirable Dust, Coal Mine Dust Conference, pp. 180-187. S.Peng, Ed. (1984). Report No. BP86 169380/AS. National Technical Information Service, Springfield, VA (1986).
- (17) Wallace, W.E., Keane, M.J., Vallyathan, V., Hathaway, P., Regad, E.D., Castranova, V., Green, F.H.Y: Suppression of Inhaled Particle Cytotoxicity by Pulmonary Surfactant and Re-Toxicification by Phospholipase; Distinguishing Properties of Quartz and Kaolin. Proceedings: British Occupational Health Society, Inhaled Particles Conference, 1985, in press.
- (18) Wallace, W.E., Keane, M.J., Hill, C.A., Vallyathan, V., Saus, F., Castranova, V. Bates, D.: The Effect of Lecithin Surfactant and Phospholipase Enzyme Treatment on Some Cytotoxic Properties of Respirable Quartz and Kaolin Dusts. Proceedings: Respirable Dust in the Mineral Industries: Health Effects, Characterization, and Control. pp. 154-166. Frantz, R.L., and Ramani, R.V., Eds.; (1986). American Conference of Governmental Industrial Hygienists (ACGIH) monograph (1988); ISBN 0-936712-76-7.

T
mea
on
sol
mos
was
the
T
the
and
sam
min
T
amo
sub
was
to
spe

Mineral Dust and Diesel Exhaust Aerosol Measurements in Underground Metal/Nonmetal Mines

B.K. Cantrell¹, and K.L. Rubow²

¹U.S. Bureau of Mines, Twin Cities Research Center, Minneapolis, MN

²Mechanical Engineering Department, University of Minnesota

Two source apportionment techniques have been applied by the Bureau of Mines to aerosol measurements in diesel equipped underground noncoal mines. The first technique is based on size selective sampling and the premise that the diesel exhaust fraction of the aerosol is predominately sub-micron in size while the mineral dust fraction of the aerosol is mostly super-micron in size. The second technique, Chemical Mass Balance (CMB) modeling, was used to referee the analysis of diesel and mineral dust aerosol concentrations with the size selective method.

The size distribution data were modeled using a log-normal regression to parameterize the sub- and super-micron fractions of the sampled aerosol and to estimate the mineral and diesel contributions to each. For the mines visited, analysis of the size selective samples yielded an average value for the fraction of the fine aerosol attributable to mineral dust of 3 pct.

The CMB analysis, applied to both fractions of the respirable mine aerosol, yielded the amount contributed to each by the diesel and dust aerosol sources. Less than 5 pct of the sub-micron fraction was mineral dust, however, as much as 20 pct of the diesel aerosol was found in the super-micron fraction requiring a correction of the sub-micron fraction to account for the missing diesel mass. More accurate measurement will require a carbon specific analysis of the aerosol.

Measurement of Coal Dust and Diesel Exhaust Aerosols in Underground Mines

K.L. Rubow and V.A. Marple

Particle Technology Laboratory, Mechanical Engineering
Department, University of Minnesota

Diesel exhaust and mineral dust concentrations have been measured for aerosols generated in the laboratory and as found in five underground coal mines- 3 utilizing diesel-powered hallowage equipment and two electric-powered equipment. Two source apportionment techniques have been applied to differentiate between the mineral dust and diesel exhaust aerosol concentrations. The first technique, using a microorifice uniform deposit impactor (MOUDI) for size selective sampling, is based on modeling aerosol size and the premise that the diesel exhaust portion of the aerosol is predominately submicrometer and the mineral dust portion is mostly greater than one micrometer in size. The second technique, Chemical Mass Balance (CMB) modeling, was used to referee the analysis of diesel exhaust and mineral dust aerosol concentrations from the size selective sampling results.

The MOUDI size distribution data were modeled to obtain parameters describing the fine and coarse fractions of the sampled aerosol and to estimate the contributions to each mode from both mineral dust and diesel exhaust aerosol sources. The results showed the size distribution of the mixed aerosols exhibited two definite modes with the minimum between the modes occurring at 0.8 μm . For the diesel equipped mines, this analysis yielded an average value for the fraction of the fine aerosol attributable to mineral dust of 1 pct. Less than 5 pct of the coal mine diesel aerosol was found in the coarse size fraction. CMB analysis confirms the original premise for using aerosol size to separate diesel exhaust and mineral dust aerosol during sampling.

Ex
of
Pa

V. B
Part
Dep

A
min
of a
in th
mine
cles
high
field
then
cle
a cer
part
then
the
deter
silic
The
ical
agree
was

Experimental and Theoretical Measurement of the Aerodynamic Diameter of Irregular Shaped Particles

V. Marple , K. Rubow and Z. Zhiqun
Particle Technology Laboratory, Mechanical Engineering
Department, University of Minnesota

A theoretical technique has been developed and verified experimentally for determining the aerodynamic diameter of irregular shaped particles. The aerodynamic diameter of a particle is a very important property in determining where that particle deposits in the respiratory tract. Many instruments, such as impactors and cyclones, will determine the aerodynamic size distributions of aerosol particles but few analyze the particles individually. The theoretical approach of our technique is to solve, by use of high speed computers, the three dimensional Navier-Stokes equations to obtain the flow field around an irregular shaped particle of any contour. The computer program will then determine the drag on the particle, and thus the aerodynamic diameter of the particle can be calculated. The experimental approach has been to pass the particles through a centrifuge and collect the particles upon a collection foil. The position of a particle on the foil is an indication of its aerodynamic diameter. These particles were then shadowed in two orthogonal directions and inspected under an SEM. The top view of the particle in the SEM plus the views of the two orthogonal shadows allows one to determine the three dimensional shape of the particle. Studies have been performed on silica, coal and talc particles with aerodynamic diameters in the 1 to 4 μm size range. The three dimensional shape, as is determined from SEM analysis, was used in the theoretical computer program and the results compared. It was found that in most cases the agreement between the experimentally and theoretically determined aerodynamic diameters was within 5%.

Some Observations on Particulates Collected in Diesel and Non-Diesel Underground Coal Mines

J. M. Mutmansky and L. Xu
Department of Mineral Engineering, The
Pennsylvania State University

ABSTRACT

This paper outlines the results obtained when sampling twenty underground coal mine sections, each in a different mine. The sampling effort was oriented toward a detailed characterization of coal mine dusts and thus eight-stage Anderson Model 298 impactors were used as the primary collection instrument. This instrument allowed a rather detailed size distribution for each of the particulates sampled. Because four of the mines used diesel outby equipment and/or diesel shuttle cars at the face, it is possible to make some comparisons on the particulate distributions in diesel versus non-diesel mines.

One of the more interesting results is the pattern that exists in mines that contain only diesels used for outby utility haulage. Particulates in these mines seem to be consistently heavy in the fine size ranges, perhaps being of significant concern to the industry. While no definite conclusions can be achieved from the limited data collected in this study, the data indicates that more detailed study of particulates in diesel mines is needed so that some idea of the particulate loadings in diesel mines can be achieved.

SAMPLING AND ANALYSIS

INTRODUCTION

The subject of particulate emissions from underground diesel equipment is currently a very important topic as health concerns and regulation of diesel particulate emissions have emerged and created new environmental problems for mine operators. The amount of particulate matter originating from diesels has not been extensively measured and problems with differentiating coal and mineral dust from diesel particulates make existing data questionable. However, it is important to make an assessment of the problem to prepare to solve it.

It is known that particulates from diesels are solid aerosols formed in the combustion process in diesel engines. Technically, this places the particles in the category of fumes. It is also known that about 90% of diesel particles are less than 1 μm in aerodynamic diameter. This information comes from Khatri and Johnson (1979) and represents data collected in tests where no mineral dust could be a factor in the measurements. To measure the diesel component of a coal/diesel particulate mixture, Johnson et al. (1982) have developed procedures for utilizing laser Raman spectroscopy. The determination of diesel content in a coal/diesel mixture is a difficult one due to the chemical similarity of the two organic materials. However, laser Raman spectroscopy, which is often used for identification of organic materials, has potential if the Raman spectra for the two materials are different and unique. The study concluded that an

accuracy of $\pm 6\%$ could be achieved for mixtures containing up to 55% diesel particulate. The method is relatively complex and would need additional development for routine application.

Other researchers have made an attempt at measuring the amount of diesel particulates that exist in the coal mine environment when diesels are employed. McCawley and Cocalis (1986) have discussed measurements of particulates collected where diesels were used in coal mine sections. Their work utilized multi-stage impactors plus cyclones and single-stage impactors designed to separate submicron particles. The results indicated submicron particle mass concentrations of 0.22 to 0.60 mg/m^3 in an Illinois mine and of 0.10 to 0.77 mg/m^3 in a Utah mine. This paper made no attempt at analysis of what proportion of the particles were of diesel origin.

Another paper of importance here is that authored by Cantrell (1987). His work was oriented toward the chemical mass balance process by assessing the proportions of the mine aerosol collected that originated from the coal seam, the rock dust, the diesel fuel combustion process and the lubricating oil fumes emanating from hot engine surfaces. Using the aerosols collected from a diesel mine and a statistical source apportionment procedure based upon neutron activation analysis of the elemental makeup of the aerosols and sources, the study indicated that 75% of the minus 0.7 μm aerosol was originating from the diesel fuel combustion. This study was an important step in the direction of source

identification but it has some limitations. First, it is based upon work previously performed on atmospheric aerosols. In this application, pollutant sources (power plants, chemical plants, etc.) are characterized by sampling their emitted material and an attempt is made to apportion the material collected in a sampler. In the mine diesel study, however, the diesel fuel and lubricating oil were characterized rather than the aerosols emitted. This may possibly affect the precision of the results. Second, there was no easy method of cross-checking the results.

A very recent paper (Rubow, Cantrell and Marple, 1988) has revealed additional information on field experiments where the chemical mass balance approach was used to estimate the diesel content of submicron coal mine particulate matter. Using a multi-stage, uniform-deposit impactor and chemical mass balance procedures to determine the proportion of diesel matter, the authors show that a size cut at $0.8 \mu\text{m}$ offers the least error. Again, however, the quantitative analysis depends entirely upon the chemical mass balance procedure. The method was changed for this study by characterizing the diesel tailpipe emissions but it is not clear how much this will improve the precision of the chemical mass balance procedure.

This paper will not provide an answer to the question of how much of the submicron aerosol in diesel coal mines is of diesel origin. However, it will provide additional data on submicron concentrations in underground coal mines. It is based upon a dust

sampling program that was conducted in twenty underground coal mine sections, each section located in a different mine.

Eight-stage Anderson Model 298 impactors were used as the primary collection instruments. This instrument allows a rather detailed size distribution for each of the particulates sampled. Because four of the mines used diesel outby equipment and/or diesel shuttle cars at the face, it is possible to make some comparisons on the particulate distributions in diesel versus non-diesel mines.

SAMPLING PROCEDURE

Preparation for Sampling

Our research was specifically oriented toward the determination of coal mine dust characteristics over its entire size range. As a result, we considered a number of gravimetric dust samplers. Most of the gravimetric dust collection devices that can be utilized in a mine environment can be classified as either single- or multi-stage samplers. Personal dust samplers that collect compliance dust samples and single-stage impactors that simulate the characteristic curve of the human lung belong in the former category. Because these samplers normally collect dust on filters, the dust must be separated from the collection filter and dispersed in a gaseous or liquid suspension medium to obtain size distributions. During these preparation procedures, important information about the agglomeration and deagglomeration is likely to be lost. Furthermore, the sizing in the different

SAMPLING AND ANALYSIS

size analyzers may not be based on the aerodynamic diameter. To avoid problems of this type, it was decided to utilize multi-stage cascade impactors for respirable coal mine dust collection in our research.

In choosing a multi-stage impactor for use in an underground coal mine, a number of different requirements must be met. First, the impactor must be powered by a permissible pump. This more or less limits the samplers to those that can utilize the standard 2 l/min permissible pumps now available on the market. Second, the sampler must be relatively compact, rugged enough for underground use, and able to be transported underground without special handling. There are only a few multi-stage impactors that can meet these requirements. We chose the Sierra Model 298 Marple personal cascade impactor now marketed by Anderson Samplers, Inc. (Rubow et al., 1985). This multi-stage sampler was designed to be used on a personal basis and hence is rather compact. As shown in Figure 1, the sampler has been combined with a DuPont Model P2500A pump to form a manageable package for use underground.

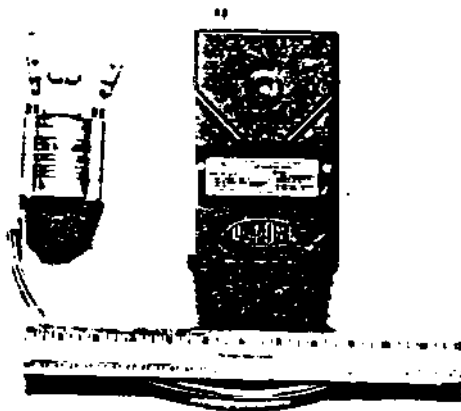


Figure 1. Sierra Model 298 multi-stage impactor and DuPont Model P2500A constant-flow pump.

The Sierra Model 298 consists of eight stages and a backup filter. It is shown in its disassembled form in Figure 2. The dust-laden air enters the instrument at the top and passes through a series of progressively smaller jets. At each stage, there is a collection substrate of mylar or stainless steel on which particles are impacted according to their aerodynamic diameters. The cut points range from 0.6 to 21 μm for this impactor. A 34-mm

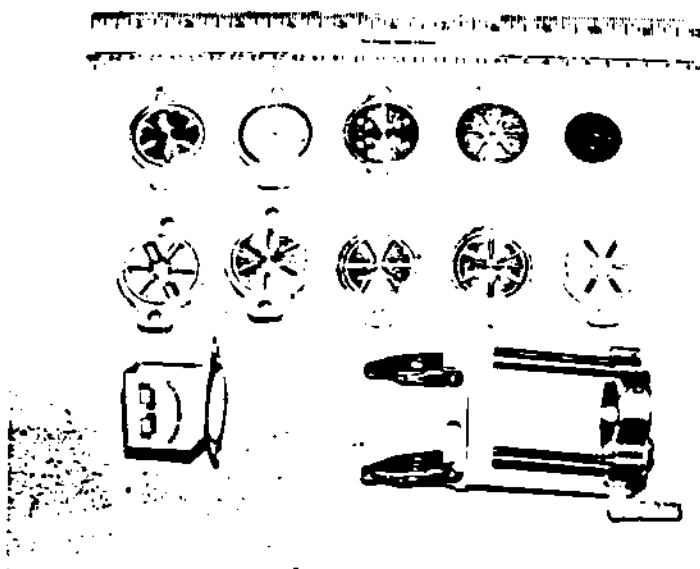


Figure 2. Disassembled Sierra Model 298 multi-stage impactor.

PVC backup filter with a five-micron pore size is used to gather the dust that is not impacted on the mylar substrates. A grease or other collection medium is normally used on the substrates to provide a more efficient collection process. It should be noted that we used mylar substrates in all of our research.

To provide accurate estimates of the mass of dust on each of the substrates, a microbalance capable of determining the masses of the substrates plus dust to a precision of 1 μg was used. To insure that moisture did not affect the mass determinations, the

SAMPLING AND ANALYSIS

substrates were greased and placed in a desiccation chamber overnight before the final mass determinations were performed. The PVC filters were handled in an identical manner except that no collection grease was applied. To overcome the effects of any static charges that might build up on the surface of the mylar substrates, a small polonium 210 radiation source was located in the weighing chamber. The substrates were passed over the source before weighing to remove the static charges.

A series of tests was then run in our Elpram Systems aerosol test chamber (Marple and Rubow, 1983) to select a proper collection grease for the impactor substrates and to determine proper sampling times. The test work concluded in the choice of petroleum jelly as our collection grease and in the determination of the variable sampling time dependent on dust mass concentration to collect proper loadings on our substrates. More details on this test work is available in Lee and Mutmanský (1986).

Sampling Procedure

The primary objective of this research study is to collect coal mine airborne dust at various locations in continuous miner development openings for characterization purposes and to identify sources in the mine that contribute to the various characteristics. As a result, the sampling plan was designed to allow sampling at various points throughout the section with samplers located from outby the section in the intake airway to four breakthroughs downwind of the last dust source in each return airway. A typical sampling plan for a continuous miner section employing a double-split ventilation plan is shown in Figure 3. Obviously, the plan for sampling in each mine section will differ, depending

on the section layout, the equipment utilization and the ventilation plan.

In reporting results in this paper, we will concentrate on three sampler locations. We designated the intake to the section (sampling location #1 in Figure 3) as the IN location, the intake to the continuous miner (sampling location #2 in Figure 3) as the CI location and the return from the continuous miner (sampling location #3 in Figure 3) as the CR location. The data quoted in this paper will be entirely from these three locations. The individual samplers used here were not always used in exactly the same fashion due to section differences. The IN sampler was normally hung at the centroid of the intake cross section. The CR sampler was hung from the roof with the sampler at the

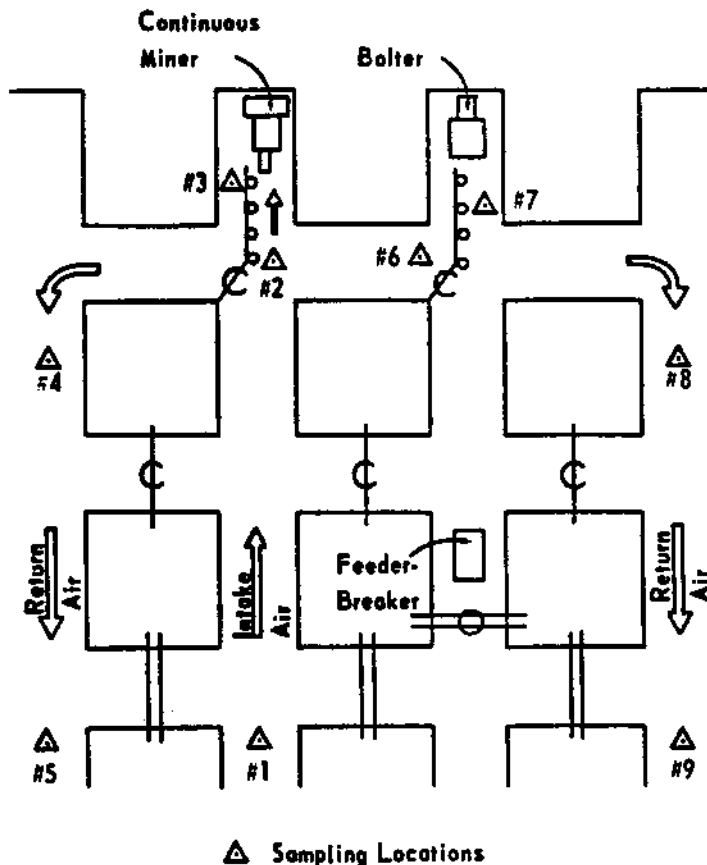


Figure 3. Typical sampling locations for a continuous miner development section using line brattice and a double-split ventilation plan.

SAMPLING AND ANALYSIS

centroid of the area behind the brattice. In mines using ventilation tubing, the sampler was hung near the end of the tubing in the dust cloud caused by the miner.

The CI sampler was located in the face intake but typically could not be located at the airway centroid because of the shuttle cars. Instead, it was typically hung from a roof bolt near the left or right side of the opening where it would not hinder the section operating crew.

The sampling times in these three locations were variable with the amount of sampling time being inversely proportional to the dust concentrations measured periodically with a mini - RAM. Typically, the IN samplers were operated for most of the shift (typically 5 to 6 hours), the CI samplers were operated for several hours or several cuts, and the CR samplers were operated for one cut (generally about 30 to 45 minutes). The samplers were moved when the continuous miner was moved so that their positions were kept constant relative to the continuous miner. The IN sampler was not normally moved and the CR samplers were normally operated for only one cut; thus these samplers were not normally affected by moves. However, the CI sampler normally made several moves during its sampling period. Also, the samplers were shut off during rock dusting to help eliminate rock dust from the samples.

The sampling procedures were applied in twenty different mines in the states of Pennsylvania, West Virginia, Ohio, Kentucky, Illinois, Colorado and Utah. Eighteen of the mines employed continuous miners; the anthracite mines used the breast-and-pillar method employing explosives for coal breakage.

Thus, eighteen of the mines should allow for valid comparisons. Of these eighteen, fourteen were all-electric mines, three employed diesels for outby utility vehicles and one mine employed two diesel shuttle cars as well as diesel outby equipment. While activity at the face was similar in the eighteen continuous miner sections, intake activity varied significantly with some intakes being heavily used for supply purposes and others being associated with little or no activity.

Finally, it should be mentioned that the dust samples were not compliance samples taken to insure that dust regulations were being met. The samplers collect total dust samples and were located in some positions (behind the brattice, for example) where extremely high dust concentrations are found. The dust concentrations reported are therefore not representative of the respirable dust concentrations in the atmosphere of the miner. This point should be noted by those using this data.

SAMPLING RESULTS

Because the multi-stage impactors provide information on eight cut sizes of the mine aerosols, it is possible to look at the results and make some conclusions concerning the nature of the particulates in diesel versus non-diesel mines. A general summary of results in the eighteen continuous miner sections is shown in Table 1. All mines are identified by letter only as anonymity was guaranteed by the investigators. A number of data values have been left out of the table. Several of the mass concentrations were omitted from the CI and CR columns because they were not considered to be valid and numerous mass concentrations for the IN sampler were omitted because they contained insufficient

SAMPLING AND ANALYSIS

Table 1
Particulate Sampling Results for Eighteen Coal Mine Sections
Utilizing Continuous Miners

Mine	Diesel Use	Mass Concentration (mg/m ³)						CR	Face Air Quantity (cfm)	Coal Type	
		<0.6 μm	IN	Total	<0.6 μm	<1.0 μm	Total				<1.0 μm
A	None			0.010	0.026	2.120	0.008	0.085	21,990	11,300	Med. & High-Vol. Bituminous
B	"	0.008	0.014	0.105	0.140	5.310	0.076	0.105	8,360	23,100	"
C	"						0.029	0.544	86,690		"
D	"	0.041	0.089	0.002	0.075	0.780	0.041	0.090	8,090	54,500	Low Vol. Bituminous
E	"			0.042	0.069	3.260	0.017	0.214	43,920	10,100	Med. & High-Vol. Bituminous
F	"			0.004	0.053	5.616	0.200	0.370	25,135	21,700	Vol. Bituminous
I	"			0.067	0.124	3.235	0.467	1.090	34,016	17,000	"
J	"						0.021	0.039	0,726	26,500	"
K	"			0.028	0.077	14.730				6,500	"
L	"			0.059	0.064	1.459	0.169	0.860	35,757	16,100	Low-Vol. Bituminous
M	"			0.007	0.056	0.431	0.146	0.669	29,545	19,900	"
N	"			0.017	0.035	2.723	0.062	0.390	4,577	21,100	Med. & High-Vol. Bituminous
O	"						0.117	0.221	8,970	15,100	"
P	"			0.100	0.196	1.823	0.124	0.402	6,944	20,500	"
Q	Outby	0.262	0.281	0.509	0.280	0.800	0.400	0.733	9,955	41,300	Subbituminous
R	Outby/Face	0.201	0.234	3.173	3.591	6.135	2.943	3.417	21,682	45,000	"
S	Outby	0.211	0.266	0.625	0.200	1.702	0.809	1.167	47,607	51,200	Med. & High-Vol. Bituminous
T	Outby	0.133	0.184	0.377	0.323	0.658	0.457	0.518	11,789	25,900	"

Note: (1) Mines C and N were anthracite mines; data not considered to be comparable.
 (2) Missing data values were either unavailable or not considered to be valid.

Table 2
Average Mass Concentrations and Ranges of Percent
of Mass for Diesel Versus Non-Diesel Mines

Type of Mine	Average Mass Concentration (mg/m ³)			Percentage of Mass (Range)								
	IN <1.0 μm	CI <1.0 μm	CR <1.0 μm	IN <0.6 μm	CI <0.6 μm	CR <0.6 μm						
Non-Diesel	0.02 ^a	0.05 ^a	0.04	0.09	0.11	0.39	2.2-7.9 ^a	3.8-17 ^a	0.07-5.5 ^a	0.52 ^a -13 ^a	0.03-2.9 ^a	0.38-8.5 ^a
Diesel (Outby Vehicles Only)	0.20 ^b	0.24 ^b	0.23 ^b	0.27 ^b	0.56 ^b	0.81 ^b	34-51 ^b	43-55 ^b	9.5-32 ^b	12-49 ^b	1.7-4.0 ^b	2.5-7.4 ^b
Diesel (Outby and/or Face Vehicles)	0.20 ^c	0.24 ^c	0.97 ^c	1.09 ^c	1.15 ^c	1.46 ^c	34-54 ^c	43-63 ^c	9.5-52 ^c	12-58 ^c	1.7-14 ^c	2.5-16 ^c

a - based on only 2 observations
b - based on only 3 observations
c - based on only 4 observations

SAMPLING AND ANALYSIS

particulate quantities to be measured with acceptable precision.

A study of the data patterns in Table 1 and Table 2 shows that the mass concentrations in the $< 0.6 \mu\text{m}$ and $< 1.0 \mu\text{m}$ ranges are higher for diesel mines than in non-diesel mines. This is in general agreement with measurements made by other researchers. In intake (IN) airways, for example, an average of 0.05 mg/m^3 is $< 1.0 \mu\text{m}$ in non-diesel mines while an average of 0.24 mg/m^3 is $< 1.0 \mu\text{m}$ in diesel mines. For the CI location (intake to the continuous miner) an average of 0.09 mg/m^3 of the particulate matter is $< 1.0 \mu\text{m}$ in non-diesel mines while an average of 0.27 mg/m^3 is $< 1.0 \mu\text{m}$ in diesel mines using outby diesel vehicles only and an average of 1.09 mg/m^3 is $< 1.0 \mu\text{m}$ in diesel mines using outby and/or face diesel vehicles. This may be the most meaningful data because the CI location is close to the location normally sampled for compliance purposes.

In the return airway of the continuous miner (CR location), the average mass concentration of submicron particles is 0.39 mg/m^3 for non-diesel mines, 0.81 mg/m^3 for mines using outby vehicles only and 1.46 mg/m^3 for mines using outby and/or face diesel vehicles. It should be noted that the mass concentrations for mine R, where both outby and face vehicles were used, are quite high. These values may be abnormally high due to adverse grade and bottom conditions and thus any averages calculated using the data may be affected. Caution should be exercised therefore in drawing conclusions from the mine R data.

Perhaps a more meaningful way of looking at the data would be to study some of the mass distribution curves for the particulate matter. Figures 4 and 5 show the mass distribution at the IN

location for the non-diesel mines B and D. They tend to show a single distinct mode at about 3.5 μm . Figures 6 and 7 show a different distribution for mines S and R in which diesels are used. These distributions show a distinct mode in the area below 0.6 μm and a less peaked mode at around 2-5 μm . We must assume (because of the intake location) that most of the mass below 0.6 μm in size was of diesel origin due to outby vehicles operating in the intake airways.

A look at some typical distribution curves for the CI location is also of interest. Figures 8 and 9 provide the mass distributions for mines B and E, indicating a much coarser average particle size (probably due to vehicles kicking up dust) with only small percentages of material in the submicron range. Figures 10 and 11 show the CI distribution data for two of the diesel mine sections (from mines Q and R). Here, the distribution of the particle mass indicates a high percentage of submicron material

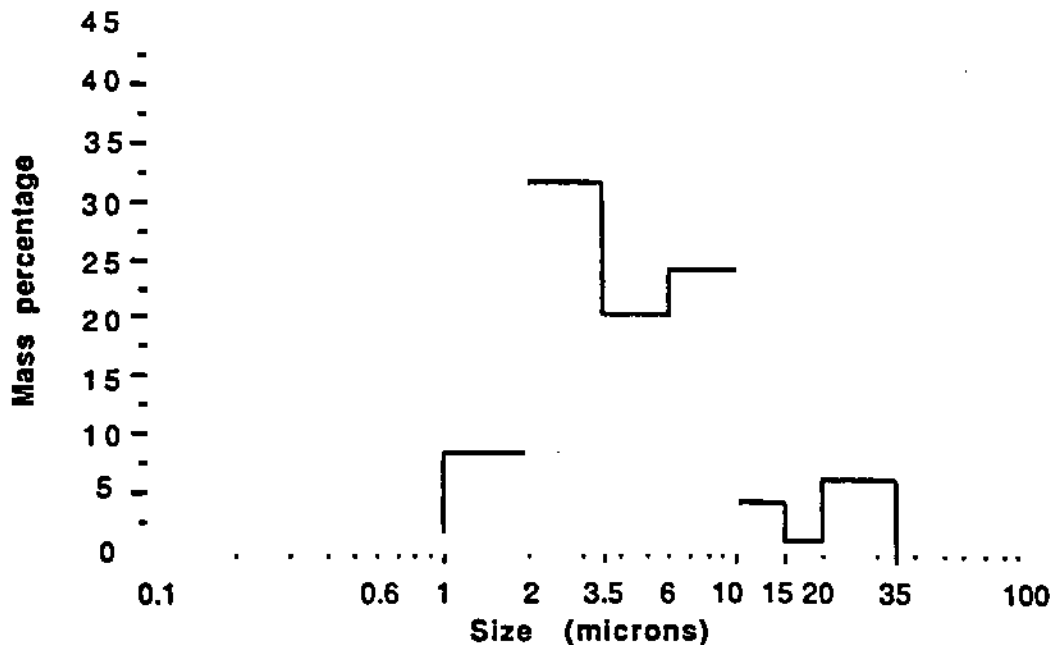


Figure 4. Particulate mass distribution at the IN location in mine B.

SAMPLING AND ANALYSIS

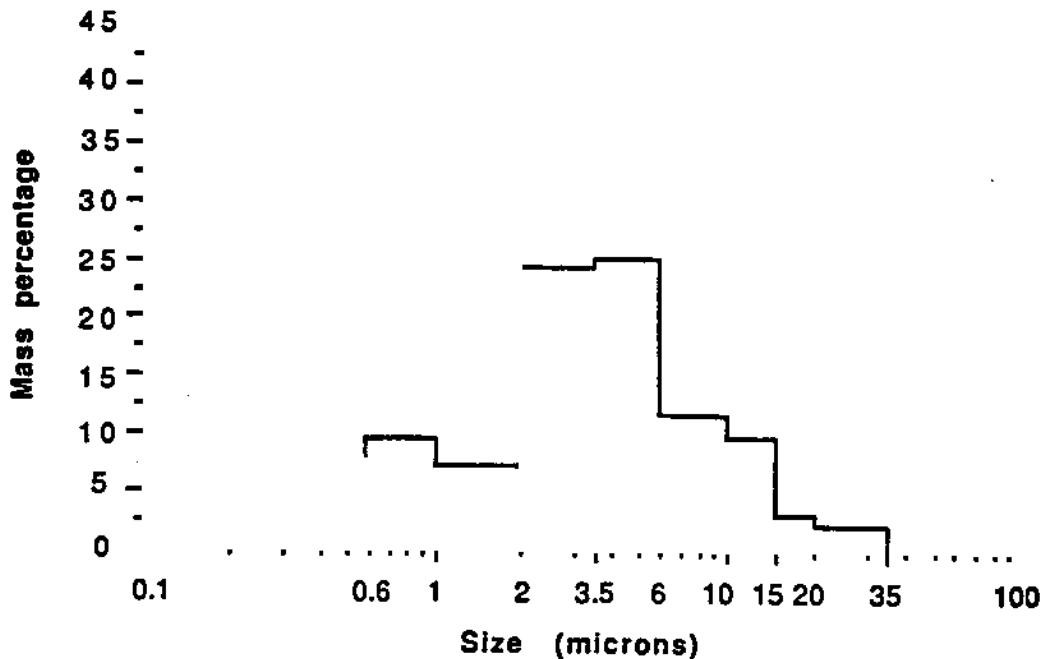


Figure 5. Particulate mass distribution at the IN location in mine D.

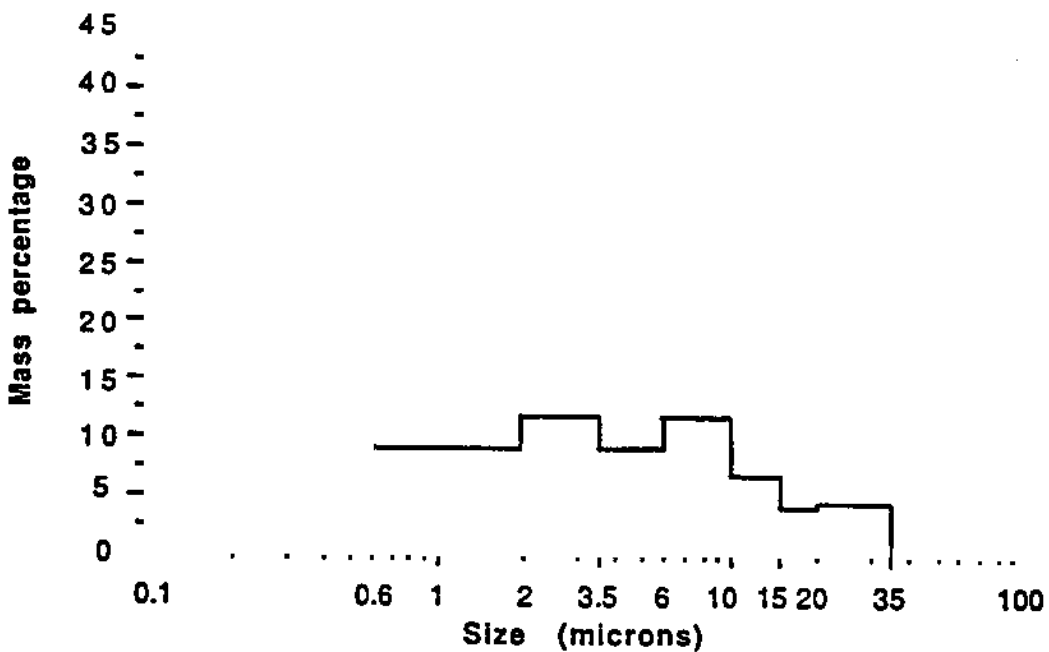


Figure 6. Particulate mass distribution at the IN location in mine S.

THE RESPIRABLE DUST CENTER

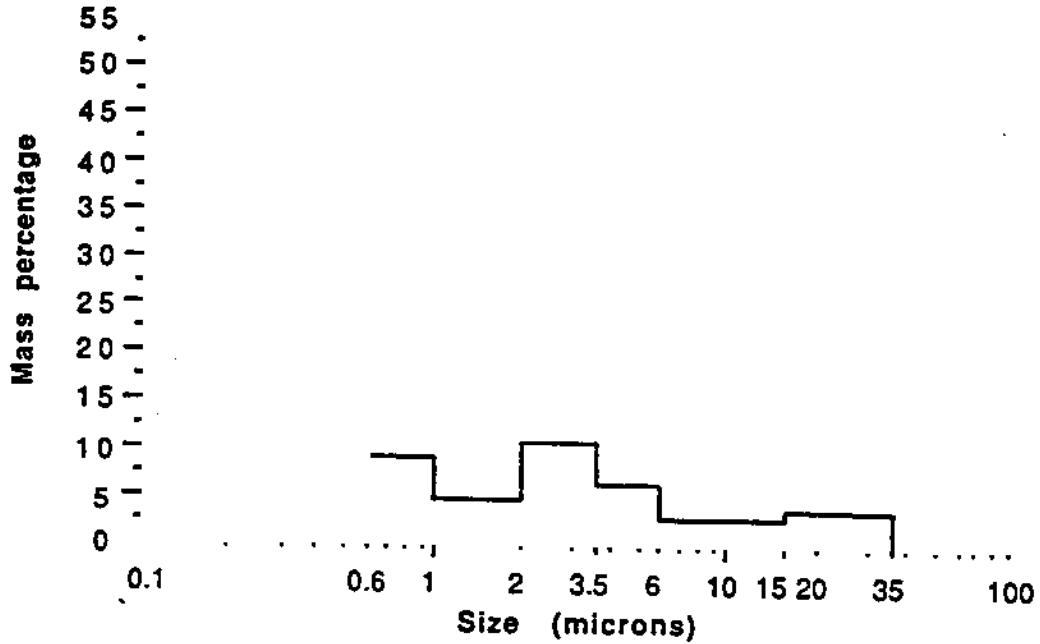


Figure 7. Particulate mass distribution at the IN location in mine R.

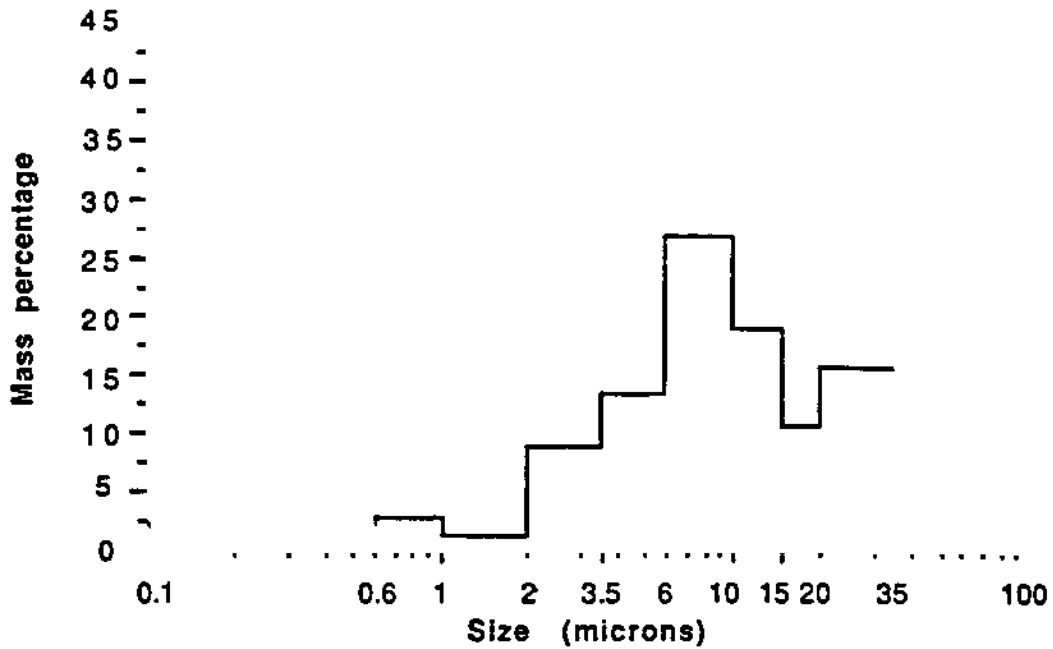


Figure 8. Particulate mass distribution at the CI location in mine B.

SAMPLING AND ANALYSIS

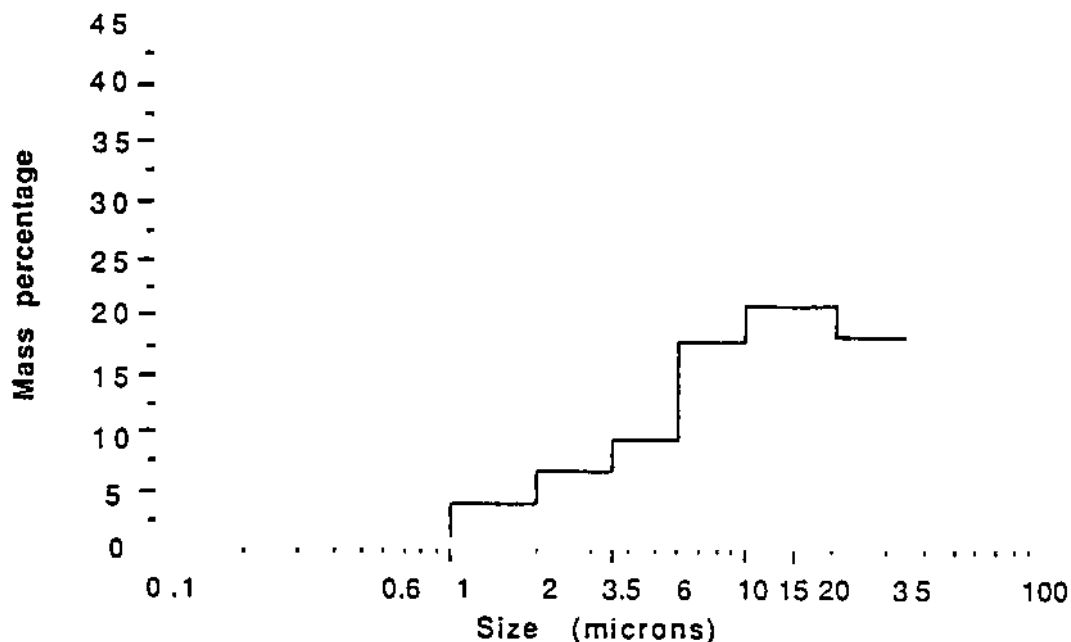


Figure 9. Particulate mass distribution at the CI location in mine E.

with most of the submicron mass being in the $< 0.6 \mu\text{m}$ range. It must be assumed that most of the material in the $< 0.6 \mu\text{m}$ range is of diesel origin as the range of percentage of $< 0.6 \mu\text{m}$ material in non-diesel mines is shown in Table 2 for the CI location to be 0.07% to 5.5%.

A similar pattern of distributions occurs for the CR location. However, the amount of dust from the continuous miner in this location tends to reduce the overall percentage of diesel particulate matter. Figures 12 and 13 show the mass distributions for non-diesel mines B and E at the CR location. They indicate a large amount of dust in the coarser ranges, obviously a result of the miner operation. The distributions also show a small percentage of submicron dust. The distribution for diesel mines Q and R are shown in Figures 14 and 15. In these two distributions,

THE RESPIRABLE DUST CENTER

the mode occurs in the 6-10 μm range but a significant percentage of material occurs in the submicron range.

An overall analysis of the data would tend to support the fact that a rather large proportion of submicron particles in diesel mines is due to diesel material. However, no side-by-side experiments were conducted in which diesel versus all-electric equipment could be compared to determine the coal and mineral dust contribution to the overall submicron particulates. One rather surprising result in the data is the concentration of submicron particulate matter in the intakes of mines using diesels only for outby utility vehicles. These mines show an average submicron mass concentration of 0.24 mg/m^3 . These mass loadings varied from 43% to 55% of the total mass concentration of particulate matter. This may represent a problem if it is proven that this material is of diesel origin. However, there was no attempt to measure the diesel content of this material in this study.

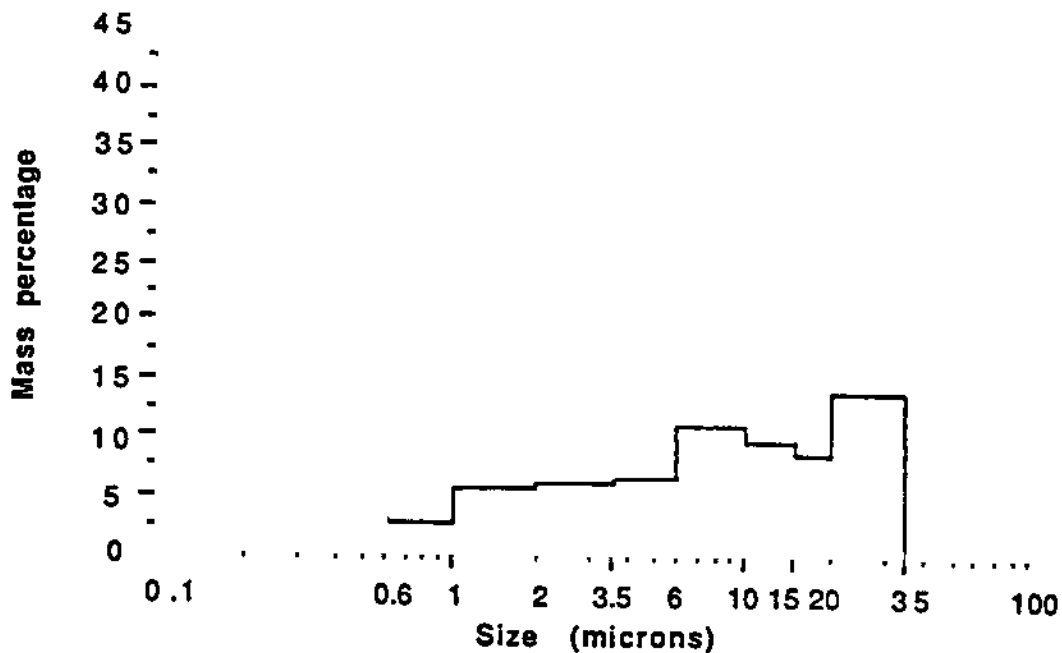


Figure 10. Particulate mass distribution at the CI location in mine Q.

SAMPLING AND ANALYSIS

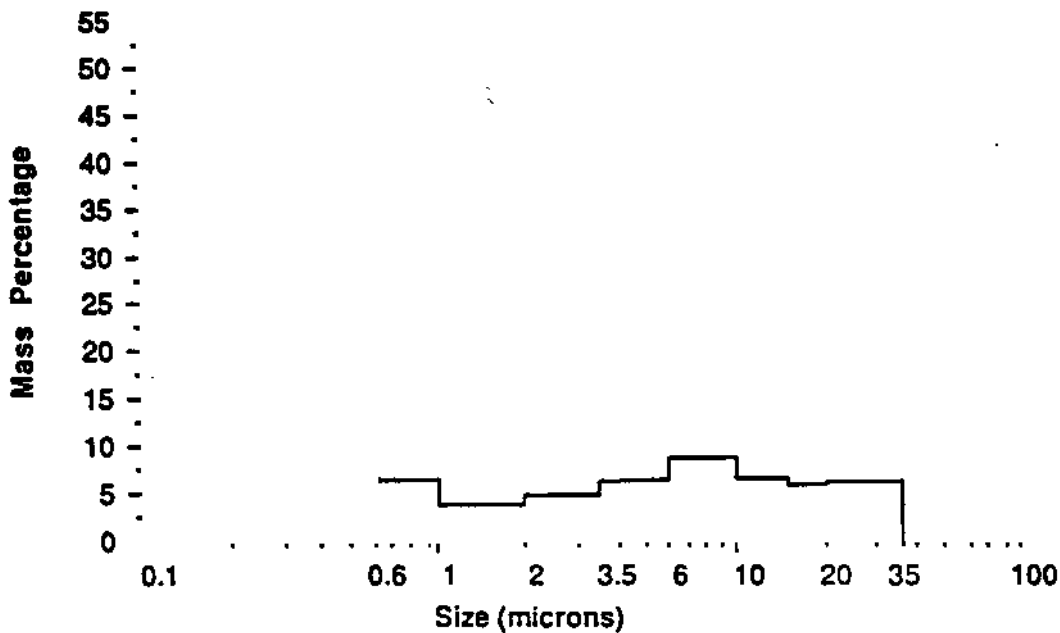


Figure 11. Particulate mass distribution at the CI location in mine R.

The particulates generated by diesel outby vehicles are perhaps due to the size of the particulate matter. Because the particle emissions of a diesel engine are 90% in the submicron range (Khatri and Johnson, 1979), outby vehicles represent a significant problem if it is shown that diesel particles are hazardous. This can be shown by the use of Stokes' law which is given as follows:

$$V = \frac{(\rho - \rho') d^2 g}{18 \mu}$$

where:

- V = terminal settling velocity, cm/s
- ρ = solid density, g/cm³
- ρ' = fluid density, g/cm³
- d = particle diameter, cm
- g = acceleration of gravity, 980 cm/s²
- μ = viscosity of the fluid, g/cm·s

While this equation is not normally applied to a turbulent, moving air mass, the settling velocity is indicative of how readily

THE RESPIRABLE DUST CENTER

particles will settle out of the mine air. For example, at a air density of 0.00122 g/cm^3 and an air viscosity of $181 \text{ g/cm}\cdot\text{s}$, a diesel particle of $1.0 \text{ }\mu\text{m}$ aerodynamic diameter and an assumed density of 0.83 g/cm^3 will fall at a velocity of only 0.0025 cm/s . If the

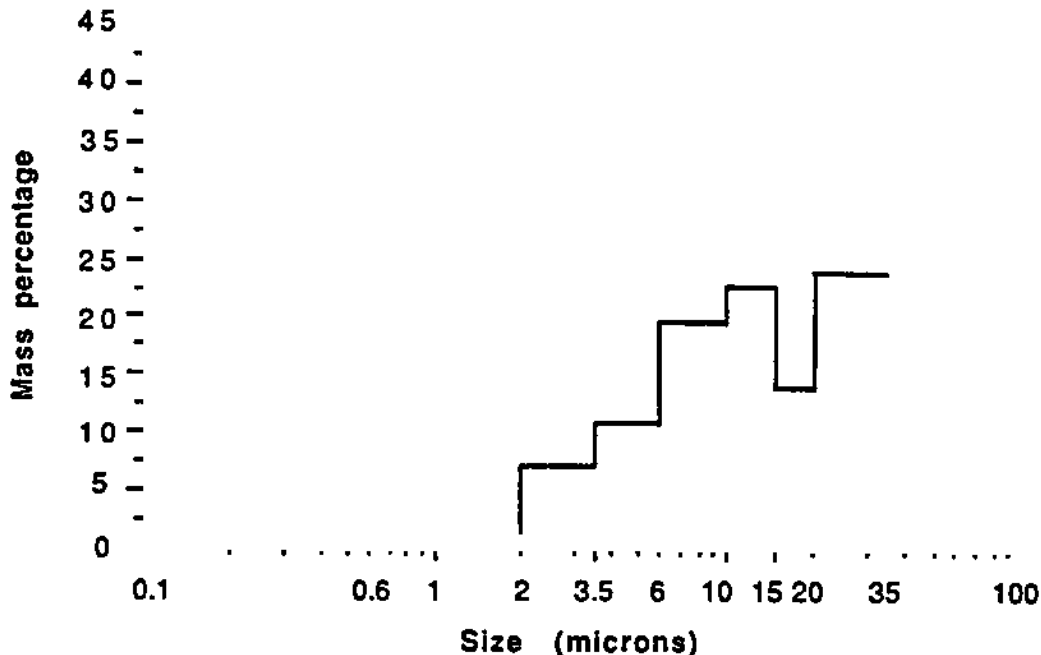


Figure 12. Particulate mass distribution at the CR location in mine B.

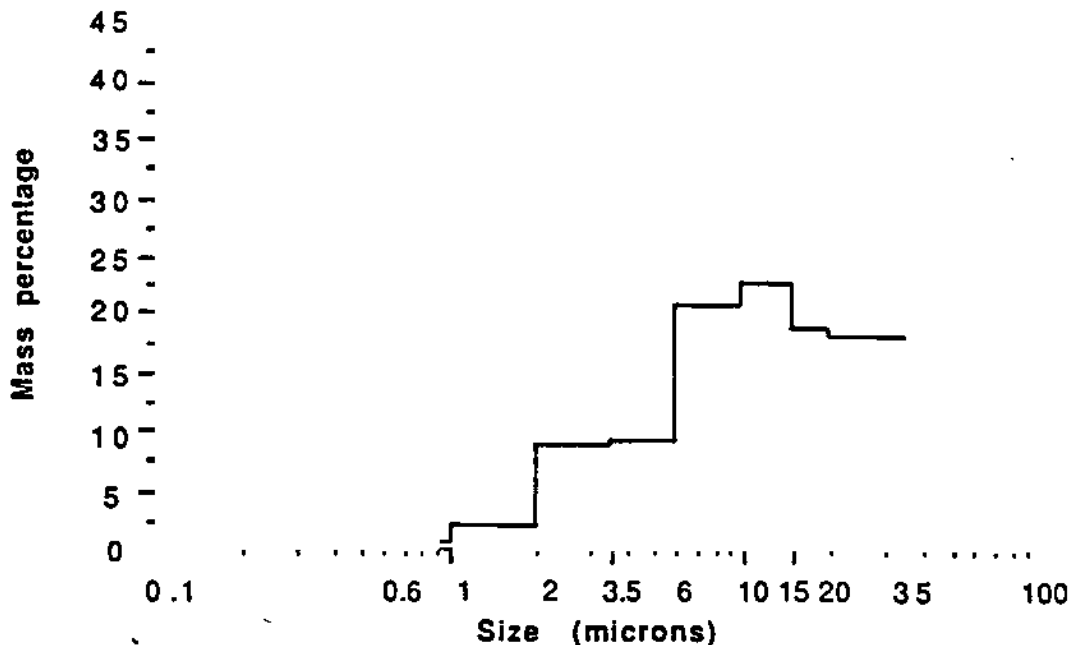


Figure 13. Particulate mass distribution at the CR location in mine E.

SAMPLING AND ANALYSIS

particle is emitted at a height of 2 m, it would then take about 1300 minutes to fall to the mine floor. However, the velocity of air in the mine would normally be 30 to 400 m/min, insuring that most particles of less than a micron in diameter generated in the intake air stream would be carried through the entire mine and out the mine exhaust before settling out of the air stream. This tends to make outby vehicles almost as important in particulate generation as equivalent equipment operated in the section.

OBSERVATIONS

The research outlined here was oriented toward study of dusts in coal mine sections. By chance rather than plan, four of the mines visited used outby and/or face vehicles in their operating plan. This allowed some comparisons to be made on diesel versus non-diesel mines. Because of the small numbers of mines sampled with diesel equipment and the absence of the capability for separating diesel from coal and mineral articles, definitive conclusions cannot be made. However, the following general observations seem to apply:

- (1) The mass concentrations and size distributions in diesel and non-diesel mines found in this study are in general agreement with those of other authors on the topic.
- (2) The mine particulates in non-diesel mines showed a definite trend to have only one mode with that mode varying in particle size from 2-10 microns depending on location in the mining section.
- (3) Mine particulates in diesel mines all seemed to possess two distinct modes with the second mode occurring somewhere below 0.6 μm in particle size.
- (4) The proportion of diesel particulates in the submicron size range is impossible to determine from the data obtained. However, general scrutiny of the data would lead one to conclude that most of the submicron material in the diesel mines is of diesel origin.

THE RESPIRABLE DUST CENTER

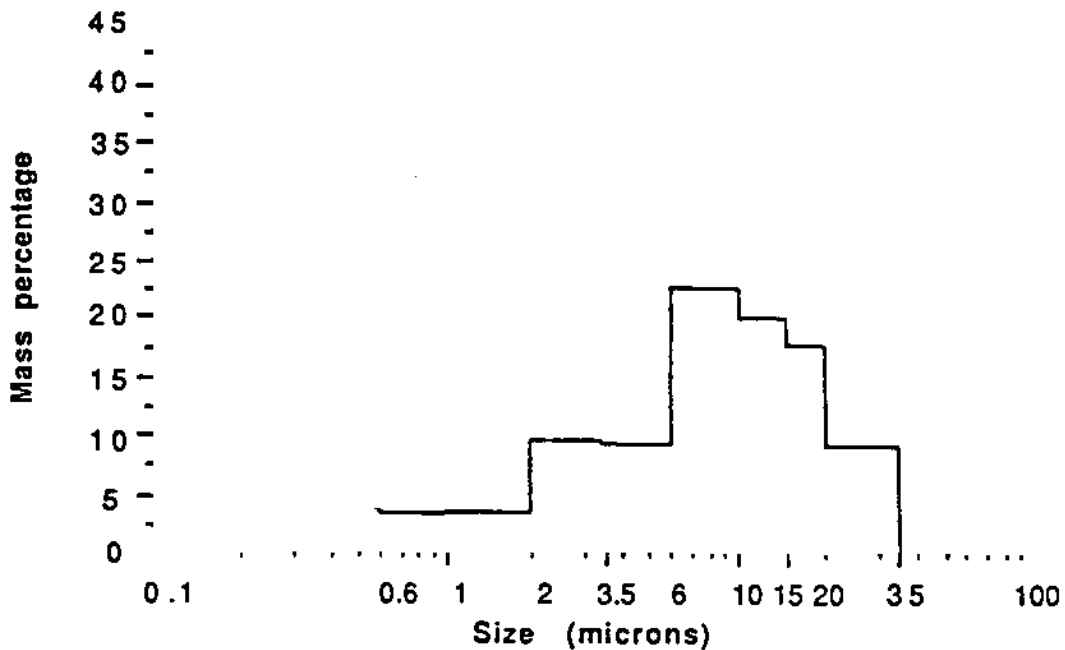


Figure 14. Particulate mass distribution at the CR location in mine Q.

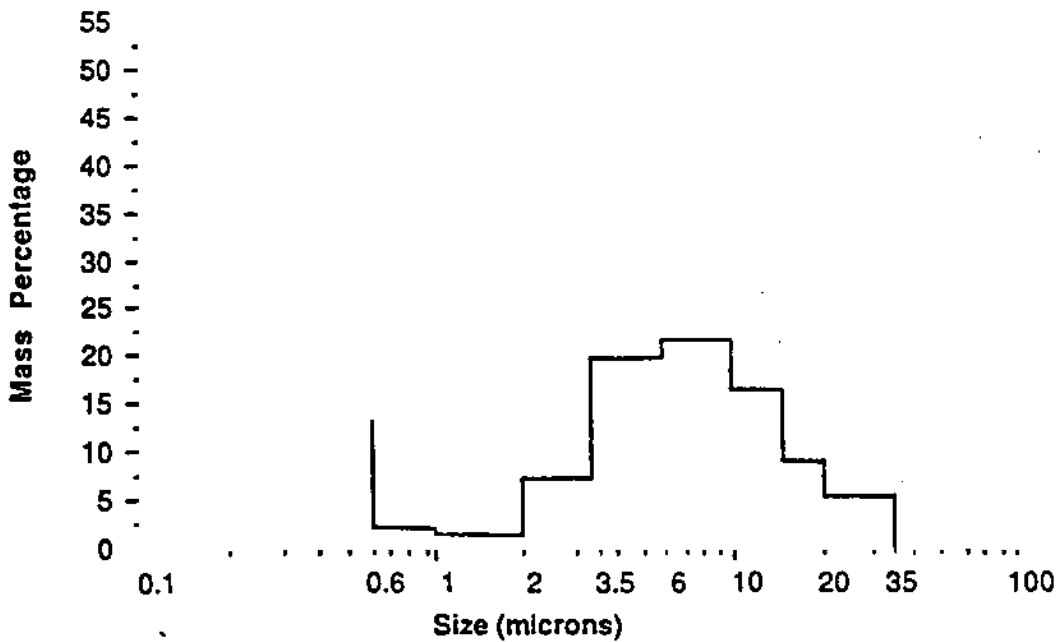


Figure 15. Particulate mass distribution at the CR location in mine R.

SAMPLING AND ANALYSIS

The absence of a method for differentiating between diesel and other particulate matter on impactor substrates is a serious limitation in this type of study. The samples in the CI location in non-diesel mines showed submicron mass readings of up to about 0.2 mg/m^3 while samples in the CR location in non-diesel mines showed mass concentrations of up to 1.09 mg/m^3 . The existence of this level of dust in the submicron range would make a size-selective particulate measuring procedure inaccurate in some mines. The overall results indicate that a size-selective sampler with a cut size of $0.8 \text{ }\mu\text{m}$ would, in general, give a good reading with deteriorating accuracy as more fine-size coal dusts are generated in the working section.

The use of any method for determining the percentage of diesel particulate in a coal/diesel particulate mixture is a difficult process. Both the Raman spectroscopic method and the chemical mass balance (source apportionment) method have been applied to the process. To avoid the many problems associated with complicated analysis procedures of determining the proportion of diesel matter in a coal mine particulate, a size selective method has also been proposed. The size-selective impactor method is simple and easy to apply but cannot differentiate between coal and diesel particles.

Before any diesel exposure measuring technique is adopted, additional research is necessary. Neither the analysis techniques, which are relatively complicated, nor the size-selective method has been sufficiently proven as yet. Before such a procedure is adopted, studies proving the validity of the measurement cross-checked by both

THE RESPIRABLE DUST CENTER

the Raman spectroscopy and the chemical mass balance methods would be necessary. Other analysis methods, if not too complicated, would be welcome as the method of determining diesel particulates in mines should be both accurate and easy to apply.

ACKNOWLEDGEMENT

This research has been supported by the Department of the Interior's Mineral Institute program administered by the Bureau of Mines through the Generic Mineral Technology Center for Respirable Dust grant number G1135142.

REFERENCES

- Cantrell, B.K., "Source Apportionment Analysis Applied to Mine Dust Aerosols: Coal Dust and Diesel Emissions Aerosol Measurements," Proceedings, Third Mine Ventilation Symposium, Society of Mining Engineers, Littleton, Colorado, 1987, pp. 495-501.
- Johnson, J.H. et al., "Monitoring and Control of Mine Air Diesel Pollutants: Tailpipe Emissions Measurements, Aftertreatment Device Evaluation and Quantification of Diesel and Coal Fractions of Particulate Matter With Raman Spectroscopy," Final Report, U.S. Bureau of Mines Contract J0199125, Michigan Technological University, November 1982.
- Khatri, N.J. and J.H. Johnson, "Physical Size Distribution of Diesel Particulate Matter and the Study of the Coagulation Process," Technical Paper 780788, Society of Automotive Engineers Off-Highway Vehicle Meeting, Milwaukee, September 1978.
- Lee, C. and J.M. Mutmanský, "A Strategy for Coal Mine Respirable Dust Sampling Using Multi-Stage Impactors for Characterization Purposes," Engineering Health and Safety in Coal Mining, Society of Mining Engineers, Littleton, CO, 1986, pp. 202-215.
- Marple, V.A., and Rubow, K.L., "An Aerosol Chamber for Instrument Evaluation and Calibration," American Industrial Hygiene Association Journal, Vol. 44, No. 5, May 1983, pp. 361-367.
- McCawley, M. and J. Cocalis, "Diesel Particulate Measurement Techniques for Use With Ventilation Control Strategies in Underground Coal Mines," Annals of the American Conference of Governmental Industrial Hygienists, Volume 14, Cincinnati, 1986, pp. 271-281.

SAMPLING AND ANALYSIS

Rubow, K.L., et al., "A Personal Cascade Impactor: Design, Evaluation and Calibration," Publication No. 469, Particle Technology Lab, University of Minnesota, Minneapolis, April 1985.

Rubow, K.L., B.K. Cantrell and V.A. Marple, "Measurement of Coal Dust and Diesel Exhaust Aerosols in Underground Mines," VII International Conference on the Pneumoconiosis, Pittsburgh, August 1988.

Effect of Thermal Treatment on the Surface Characteristics and Hemolytic Activity of Respirable Size Silica Particles

B.L. Razzaboni¹, P. Bolsaitis¹, W.E. Wallace^{2,3} and M.J. Keane²

¹Energy Laboratory, Massachusetts Institute of Technology, Cambridge, MA

²Division of Respirable Disease Studies, National Institute for Occupational Safety and Health, Morgantown, WV

³West Virginia University

Thermal treatment of respirable size silica dust samples results in marked changes in their hemolytic activity. These changes can be correlated with changes in the characteristics of the particle surface as measured by infrared spectra, zeta potentials, and specific surface area. Silica samples from various sources (Min-U-Sil, fumed silica, and a NIOSH standard sample) were heated or calcined at temperatures ranging from 100-1095C. The hemolytic activity of the crystalline materials decreased after thermal treatment. The behavior of the fumed material was found to be more complex. Material of very large surface area (small particle size) exhibits an initial increase in hemolytic activity upon calcination. This result confirms other experimental observations pointing to a particle size of maximum toxicity. The changes in hemolytic activity can be related to infrared spectra and zeta potentials of the materials. The absorption band in the 3200-4000 cm^{-1} frequency region of the fumed material disappears upon heat treatment while a sharp, characteristic band at 3750 cm^{-1} increases in intensity. Zeta potential measurements conducted in the pH range of 2.0-10.5 exhibit a unique change in zeta potential v.s. pH profile with heat treatment. These findings indicate that the removal of active surface silanol groups by calcination results in reduced cytotoxicity, as measured by a hemolysis test.

Alteration of Respirable Quartz Particle Cytotoxicity by Thermal Treatment in Aqueous Media

C.A. Hill¹, W.E. Wallace^{1,2}, M. J. Keane², S.J. Page³ and P. Bolsaitis⁴

¹West Virginia University

²Division of Respirable Disease Studies, National Institute for Occupational Safety and Health, Morgantown, WV

³U.S. Department of Interior, Bureau of Mines

⁴Energy Laboratory, Massachusetts Institute of Technology

ABSTRACT

Boiling respirable quartz dust in water for 10 to 40 minutes decreases the cytotoxicity for both erythrocyte hemolytic potential and pulmonary macrophage release of lactate dehydrogenase in vitro. The potential is reduced to near zero in the boiling concentration range of 1 to 10 mg quartz per ml water in boiling times of 20 to 40 minutes. Below this range the detoxification occurs over a longer boiling time. Above this range the hemolytic potential remaining after 40 minutes of boiling approaches native quartz potential with increasing concentration up to 30 mg quartz per ml water. Replacing the media with fresh at the midpoint of boiling results in full detoxification through 20 mg per ml. Pre-boiling the medium with quartz or silica gel reduces the effect of subsequently boiling test samples. Detoxification persists after mild drying at 110 C for 8 hours, and persists after three days of resuspension in water at room temperature. Additional data on persistence of the effect, on the use of acidic and basic media treatment, and on surface analyses are presented, with a discussion of a working hypothesis and research needs.

Introduction:

Research underway to determine interactions of quartz and other mineral dust surfaces with pulmonary fluids and alveolar macrophages in culture led to the observation that when dusts were autoclaved in aqueous suspension, their cytotoxic effects on macrophages were suppressed, in some cases fully and even after several days incubation with the cells. This finding was in direct contradiction to earlier results from both short term macrophage lysosomal enzyme release assays, as well as longer term cytotoxicity assays from macrophages in culture; in those studies, dusts were steam autoclaved at 121 °C with no liquid water but with steam present.(1,2) However detoxification under boiling conditions has been reported in other research.(3) It was decided to use the hemolysis assay to further investigate these findings, because of its sensitivity, simplicity and cost.

Results and Discussion:

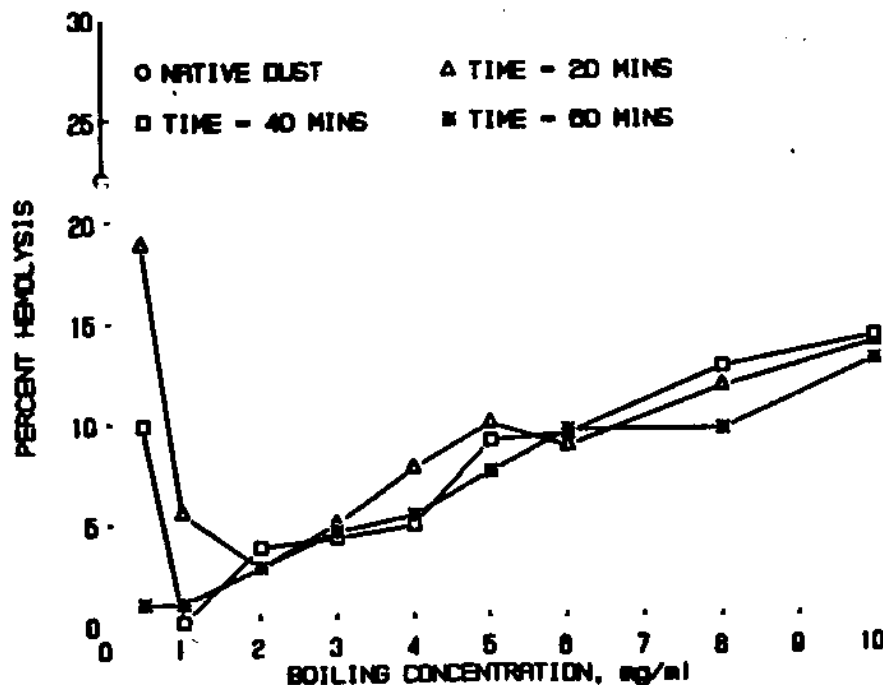
Respirable quartz dust used in this study was taken from a stock of crystalline silica, Min-U-Sil, obtained from Pennsylvania Sand Glass Corporation, fractionated in air with a particle classifier. The small size

fraction retained for use was 80% less than 5 micrometer particle diameter, with an area equivalent median diameter of 1.24 micrometers as estimated by automated image analysis. The silica was at least 98.5 mass percent silica as determined by X-ray energy spectrometric analysis; and the crystalline form was alpha-quartz as determined by X-ray diffraction. It's specific surface area was 3.97 square meters per gram as determined by nitrogen adsorption isotherm methods. (1)

To measure the erythrocyte hemolytic potential of treated and untreated dusts we use the method of Marington et al, (4) with minor modification. (1) Briefly, dusts suspended in buffer are mixed with an equal volume of 4% sheep red blood cells, and incubated 60 min. at 37°C with periodic mixing. Next the cells are spun down, and the absorbance of the released hemoglobin from any lysed cells read at 540 nm. Absorbance values are compared to positive controls (100% lysed cells) and negative controls (cells in buffer only).

Initial experiments involved bringing deionized water to a boil, adding the dry dust (12 mg), vortexing, and boiling for periods up to 60 min., without stirring. This was done in flint glass tubes for samples with dust concentrations of greater than 1 mg/ml, and in polycarbonate tubes for lower concentrations. After the boiling period was completed, sample tubes were spun down for 60 sec., the supernatant discarded, and the dust resuspended in phosphate buffered saline (PBS) and run in the hemolysis assay. Results indicated that the toxicity was reduced almost to zero at 1 mg/ml, and increased in a roughly linear fashion to approximately full (native dust) toxicity at 20 mg/ml dust concentration during boiling. (Figure 1).

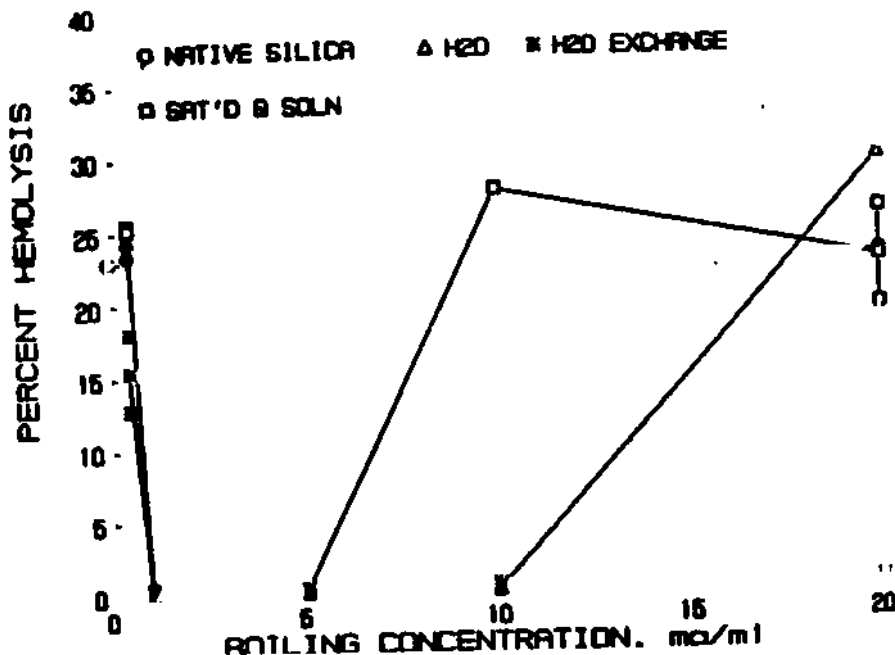
SILICA CYTOTOXICITY WITH BOILING



ALTERATION BY THERMAL TREATMENT

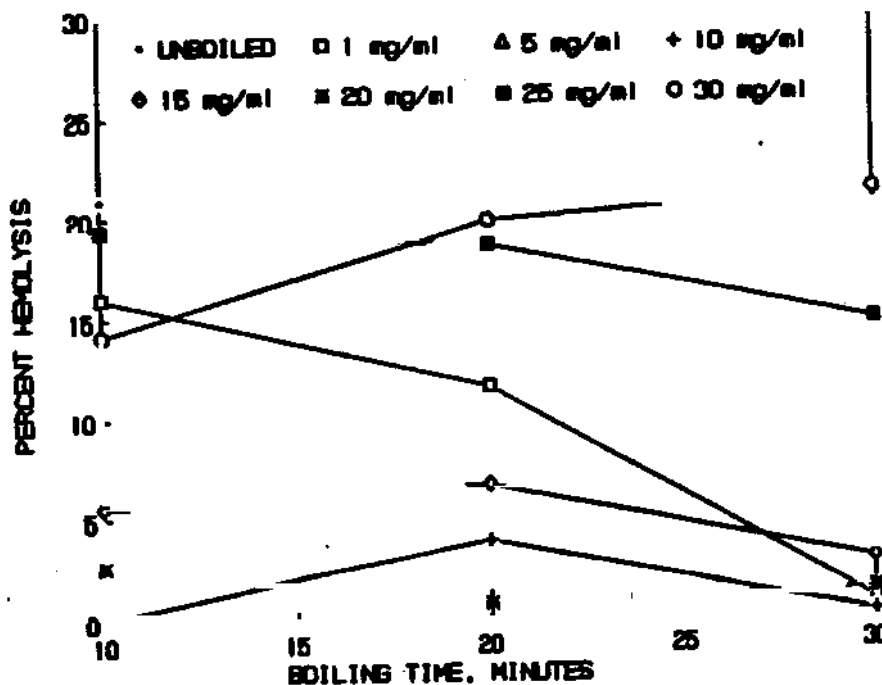
When individual magnetic stirrers were used in each sample, results were similar, except the toxicity was reduced to virtually zero at concentrations to 10 mg/ml, and then increased in a linear fashion. Samples were also boiled for half the specified times, centrifuged, the medium changed to fresh water, and boiling continued for the rest of the period. The toxicity was reduced to very low levels through the highest concentration tested. (Figure 2) As also shown, pre-boiling the water with a separate quartz sample before using the still hot supernatant to boil the test sample, somewhat diminished the detoxification phenomenon. We observed this diminution also in the case of pre-boiling the water with silica gel.

QUARTZ BOILED 40° IN VARIOUS SOLUTIONS



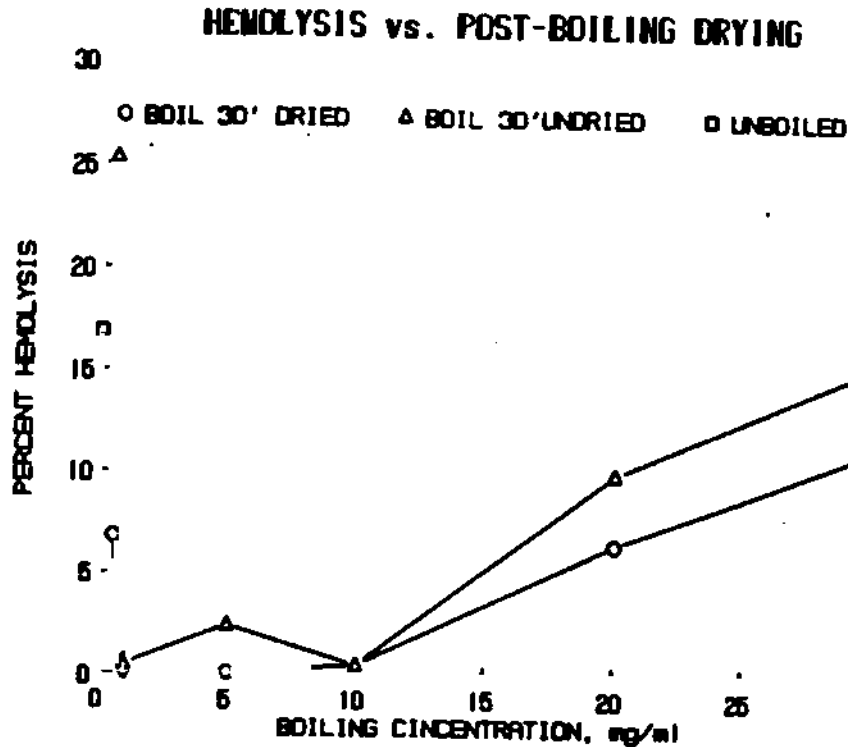
Experiments involving various boiling times showed a weak dependence of detoxification with time, except at 1 mg/ml, where detoxification progressed with boiling time. (Figure 3)

HEMOLYSIS vs. BOILING TIME



THE RESPIRABLE DUST CENTER

Limited tests of the persistence of the detoxification have been made and are continuing. One question was whether or not the passivation effect was due to some gel or other coating which might not withstand drying and resuspension. Samples were vacuum dried after boiling, and assayed the following day. Fully detoxified samples remained the same, and partially detoxified samples had slightly less toxicity after drying than replicate samples promptly assayed. (Figure 4) Fully detoxified samples boiled at 1 and 10 mg/ml which



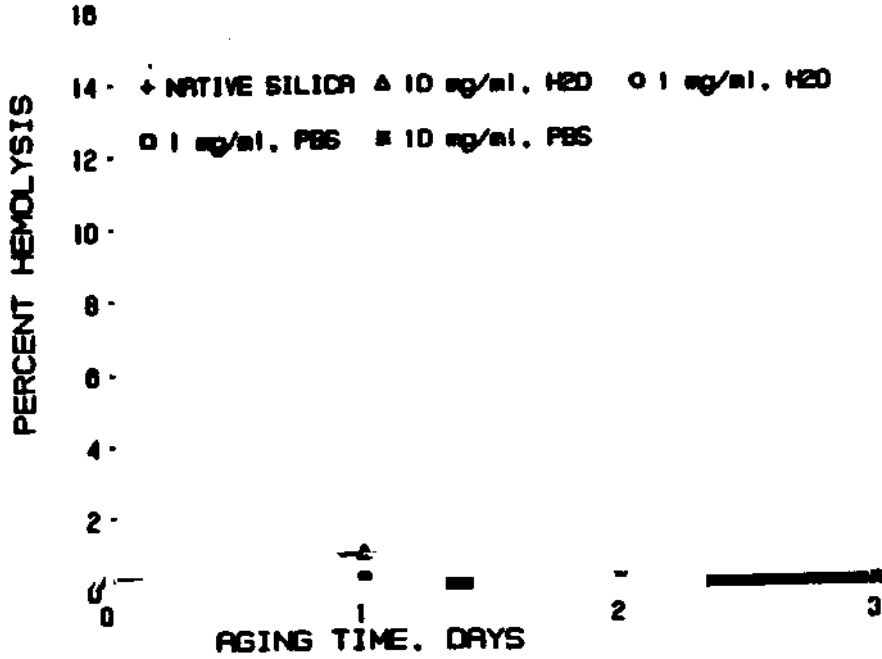
were decanted and placed in fresh distilled water or PBS did not retoxify over a 3 day period. (figure 5) Other samples were left standing after boiling in the supernatant from the boiling water at room temperature. Fully detoxified samples boiled at 1 mg/ml remained at zero toxicity after 4 days. Samples at higher concentrations showed some increase with time; the sample boiled at 10 mg/ml was essentially fully retoxified. (Figure 6)

Certain samples in the assay yielded consistently anomalous results, and were difficult to reconcile with any simple physical model; specifically, samples boiled at 0.5 mg/ml were not detoxified. The only experimental difference in these samples was that they were boiled in plastic (polycarbonate) centrifuge tubes, since glass tubes were not available in an appropriate size. When quartz was boiled in flint glass, polycarbonate, and Tefzel tubes, only partial detoxification was seen. When boiled in polycarbonate tubes using water that had been boiled only in polycarbonate, no detoxification was seen at any concentration. (Figure 7)

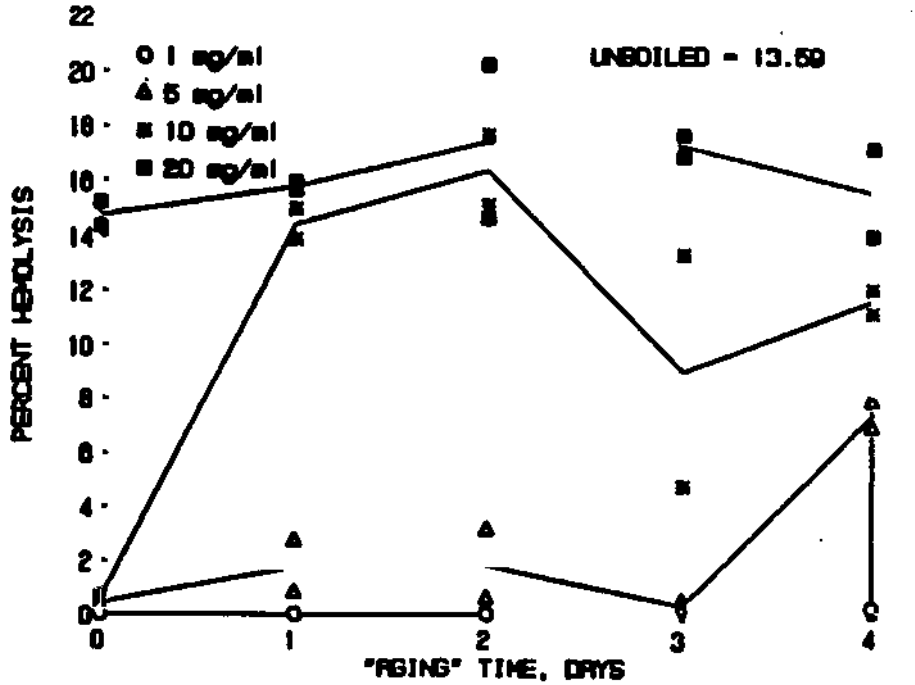
Since the effect seemed clearly to be an effect of the glass containers, additional experiments were done to clarify the finding. Quartz dusts were boiled in water in polycarbonate tubes with varying amounts of 3 mm soda-lime glass beads. (Figure 8) There is a roughly proportional dependence of detoxification on the number of glass beads, and thus the glass surface area

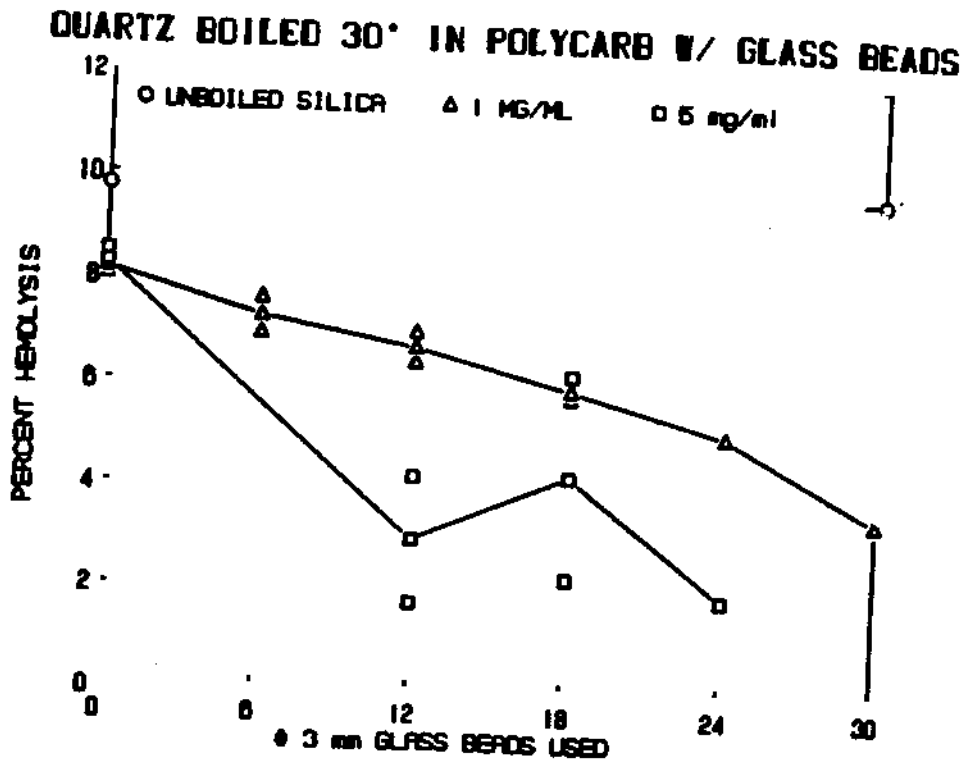
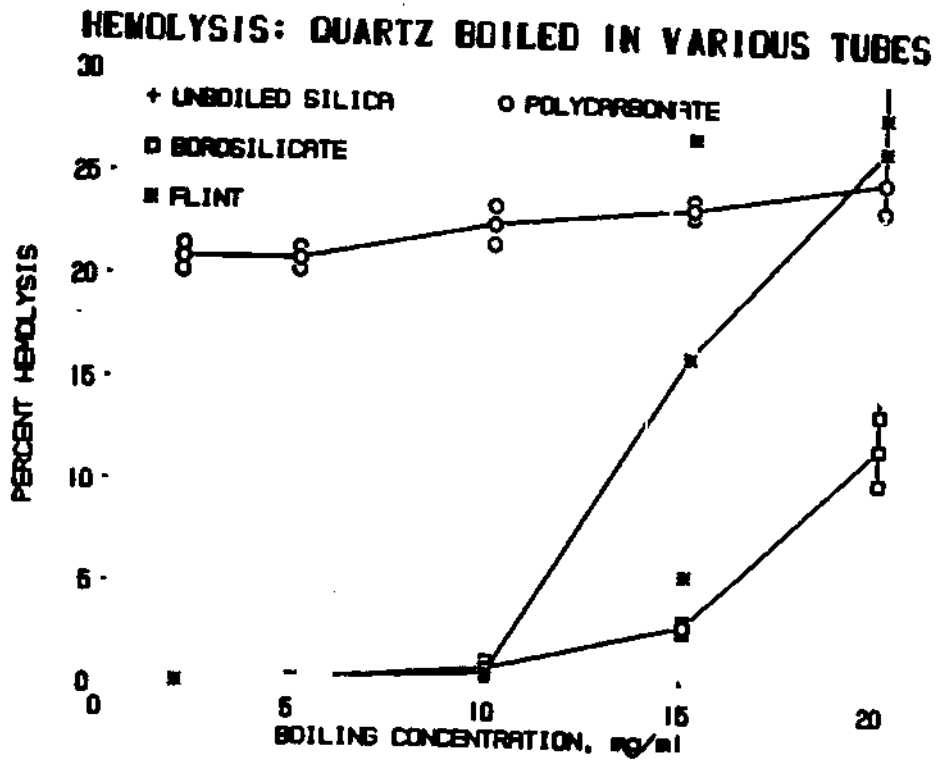
ALTERATION BY THERMAL TREATMENT

QUARTZ AGED IN H₂O AND PBS



HEMOLYSIS vs. TIME IN SUPERNATANT AFTER BOILING

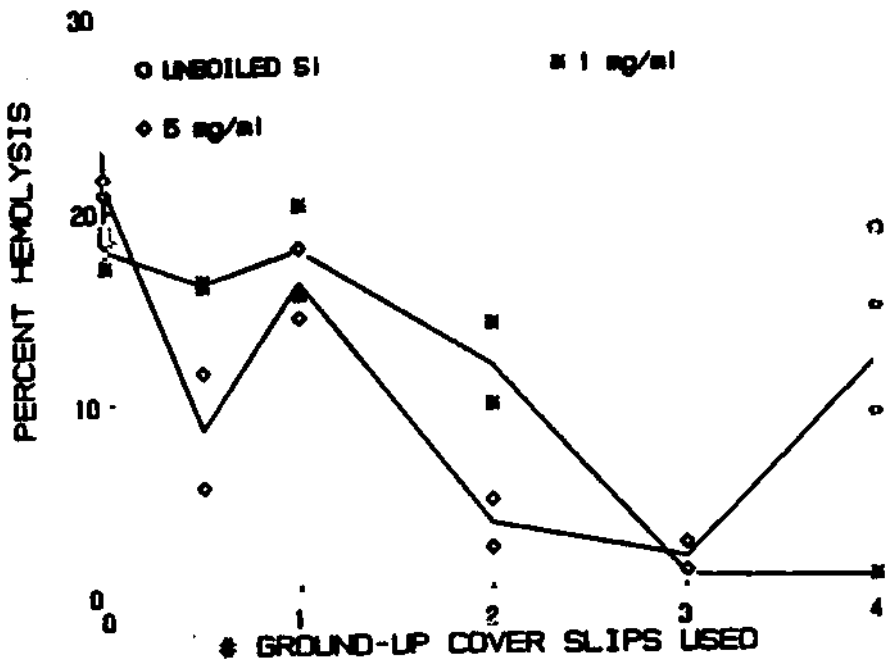




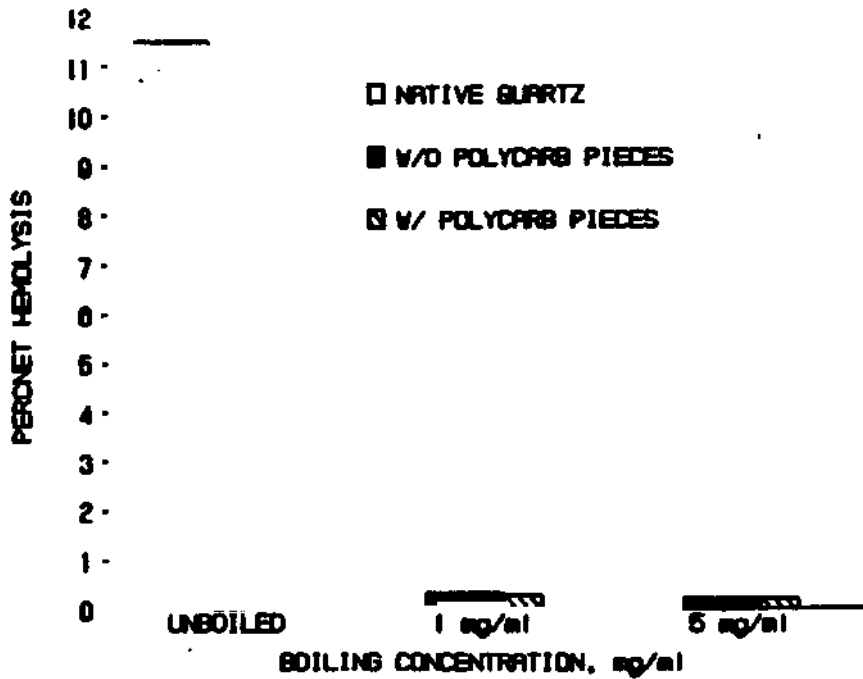
present. The effect was investigated also by using shards of glass cover slips in polycarbonate tubes during boiling. In general detoxification occurs with increasing glass content, but with a lessening of the effect seen at the highest glass content level. (Figure 9) The converse of this hypothesis, that polycarbonate somehow suppressed the detoxification of quartz, was tested by boiling quartz in flint glass tubes with polycarbonate pieces in suspension; no significant effect of the polycarbonate was seen. (Figure 10)

ALTERATION BY THERMAL TREATMENT

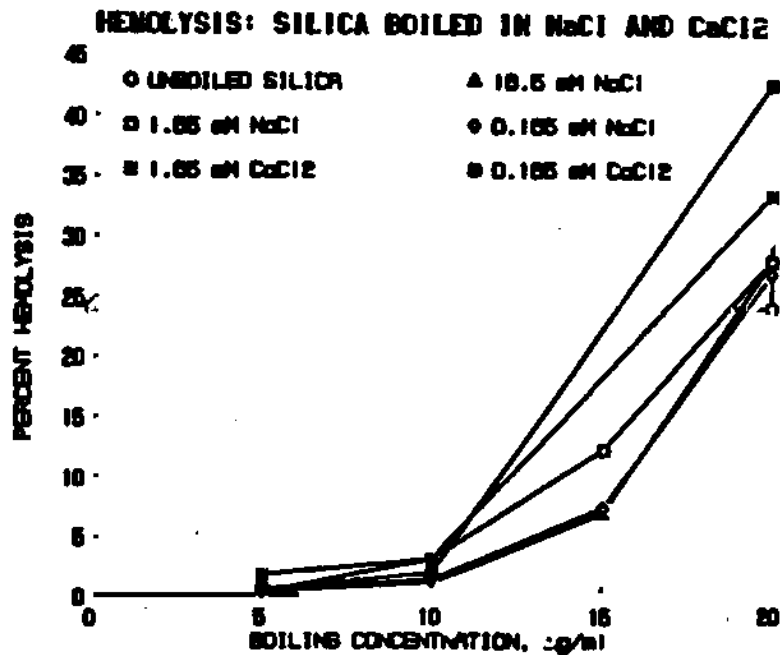
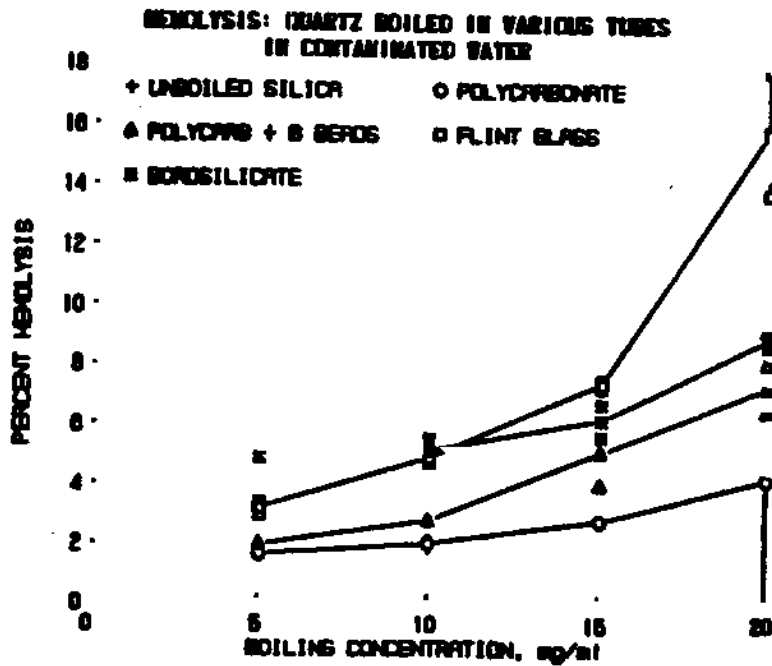
QUARTZ BOILED 30' IN POLYCARB V/ GLASS PIECES



HEMOLYSIS OF QUARTZ BOILED IN FLINT GLASS WITH AND WITHOUT POLYCARBONATE PIECES



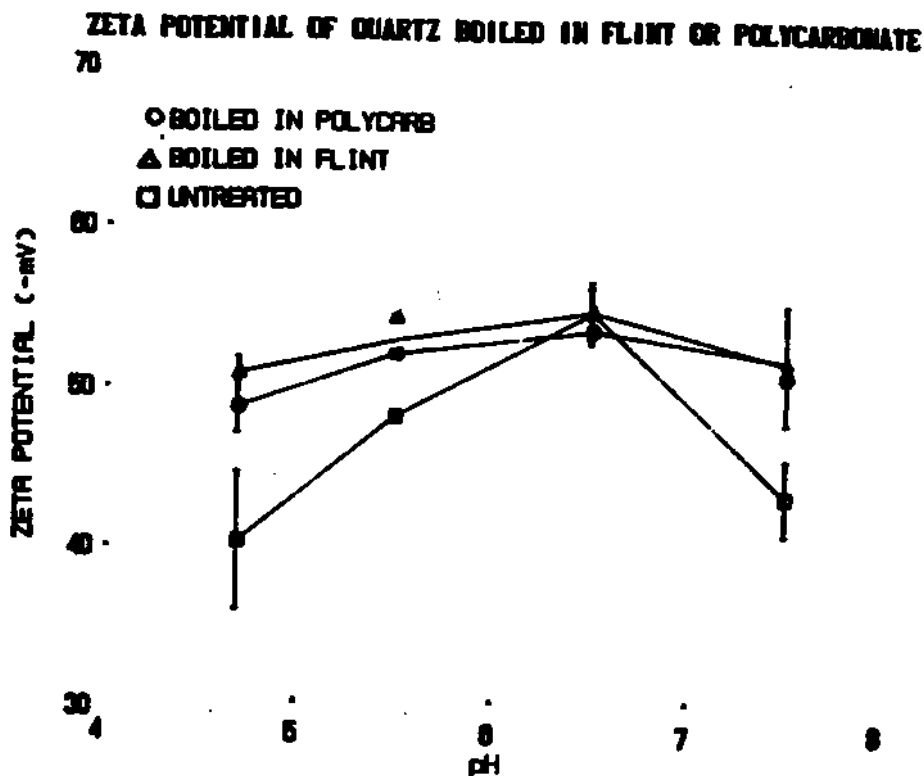
An additional anomalous result occurred when there was a failure in the reverse osmosis water purification cartridge in our laboratory building distilled water system, resulting in a higher impurity level than that present in tap water. Toxicity was partially suppressed in all samples, even those boiled in polycarbonate; but detoxification was not complete for any treatment, even using flint glass tubes. (Figure 11) When the water system was restored to proper operation, the results agreed with previous findings. In a limited investigation of this, quartz samples were boiled with sodium and calcium chloride solutions of several different concentrations; the effects were weak, slightly lessening the detoxification. (Figure 12)

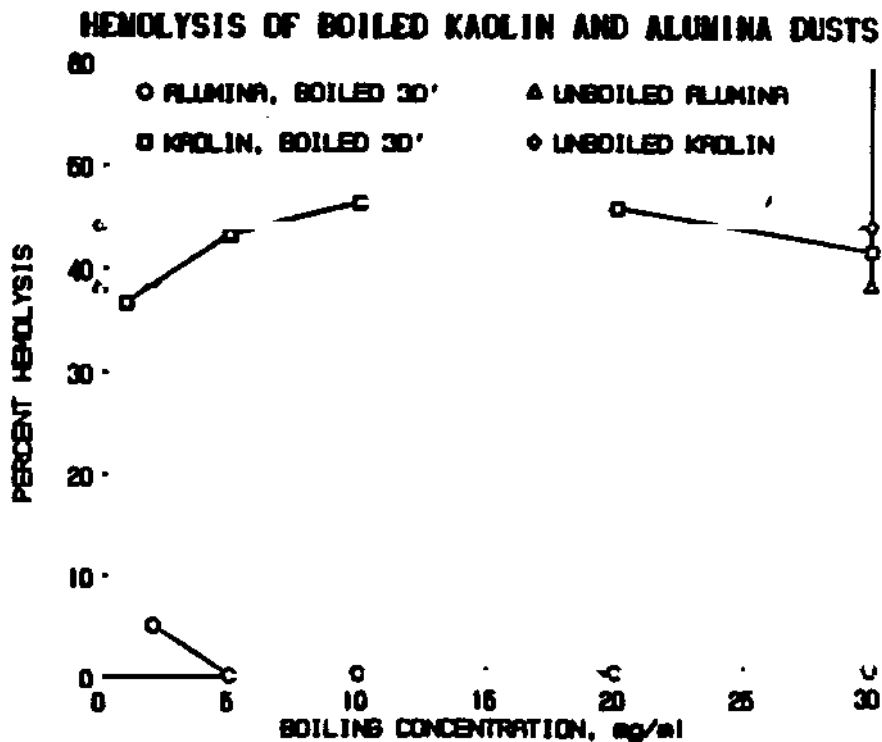


ALTERATION BY THERMAL TREATMENT

Initial zeta potential measurements have been made on samples of unboiled quartz and on quartz boiled at 5 mg/ml in flint glass and in polycarbonate tubes. The zeta potentials for unboiled quartz and for quartz boiled in polycarbonate are essentially identical, while the samples boiled in flint glass show a less negative zeta potential. (Figure 13)

The boiling treatment was also applied to kaolin and alumina dusts. The kaolin dust, previously described (1), was unaffected. A commercially obtained respirable sized alumina expressed hemolytic potential in its untreated state, and was detoxified upon boiling. (Figure 14) The untreated and treated alumina samples were subsequently analyzed by photoelectron spectroscopy, courtesy of the U.S. Department of Energy, Morgantown Energy Technology Center. The intention was to determine if the elemental composition of the alumina surface showed substantial levels of silicon in addition to aluminum after treatment. Results of the test showed, however, that the surface of the untreated alumina itself had a silicon-to-aluminum elemental ratio of about 4-to-1. This was reduced to about 1-to-1 after boiling. Studies using other dusts including asbestiform materials are ongoing.





Conclusions:

At this point, several conclusions may be stated, and a partial working hypothesis formulated, namely:

-Quartz boiled in flint glass for times greater than ten minutes at concentrations between 1 and 10 mg/ml is partially to fully detoxified in the hemolysis assay.

-The effect is strongly concentration dependent between 10 and 30 mg/ml

-If a change is made to fresh boiling water midway in the process, then full detoxification occurs across the entire concentration range.

-The effect is present only in samples boiled in glass tubes, flint or borosilicate having been tested thus far; plastic tubes do not show the effect.

-The effect is only moderately time-dependent, tests having been limited to boiling times of 10 minutes or more thus far; at most concentrations the effect seems nearly complete at 10-15 minutes.

-The effect seems to persist on mild drying (overnight vacuum drying).

-Fully detoxified samples appear to show little or no cytotoxicity after soaking at room temperature in the supernatant from boiling for periods up to 4 days; partially detoxified samples show an increase with time.

-The detoxification shows some proportionality to available surface area of glass present during boiling.

-There is some indication that pre-boiling water with silica partly diminishes the detoxification effect for subsequently boiled quartz.

Further investigation is needed to more fully clarify the mechanism of quartz detoxification, but a partial hypothesis can be stated:

Boiling water releases a soluble or partially soluble factor, possibly silicic acid or sodium and/or calcium silicates or hydroxides, which, in monomeric or polymeric form, react or are physically adsorbed on the quartz surface, which fully or partially detoxify the mineral surfaces, as shown in in vitro cellular toxicity assays.

There is a significant amount of discussion in the literature concerning the dissolution of silica in water. Molt and King found that all sizes of quartz particles behave as if a soluble fraction of silica is leached from their surface, and that surface leached at pH 9 will rapidly adsorb the dissolved silica species.(5) Baumann measured the uptake of silicic acid by quartz from aqueous solution prepared by mixing silica gel in water.(6) In general, various silicates, including vitreous glass and quartz, are reported to have slight solubilities in aqueous media. The values found for quartz are on the order of one magnitude lower than the values obtained for glass under the same test conditions.(7) Iler states that the ability of quartz surface to hold water of hydration even after outgassing at 100C, in contrast to the behavior of amorphous silica, suggests a powerful hydrogen bonding capacity of the quartz surface silanol groups. He suggests this may be related to the peculiar power of quartz to adsorb multilayers of silicic acid as noted by Baumann.(8) This seems to favor a hypothesis that some soluble form of silica dissolves from both quartz particles and the glass container; that the "silicic acid" or a polymerized derivative re-adsorbs to the quartz; and this masks or otherwise passivates the quartz surface. Tests using pre-saturated medium raise the possibility that the quartz surface must undergo a desorption step or some conditioning before or in conjunction with adsorption of passivating species.

Suggested strategies for clarifying this would include radiolabel experiments to distinguish the source of surface silica groups after boiling treatment, and to determine if native quartz surface groups are exchanged with the medium in the passivation process; further investigation of the effect of treatment on the zeta potential of quartz; and the attempted use of surface spectroscopy methods, such as diffuse reflectance Fourier transform infrared spectrophotometry to identify surface structural changes following treatment. If acid-base reactions are involved, the pH dependence of detoxification should be looked at in detail.

The prime question raised here is under what moderate treatment conditions will quartz be surface modified so that it becomes biologically inert for cytotoxicity in cellular assays or for fibrogenicity in vivo. That is, what physical and chemical conditions are necessary and sufficient to passivate the quartz surface? This study has identified some parameters involved: the process proceeds in aqueous solution; glass surface must be present; there is a concentration dependence; details of the boiling procedure can significantly affect the results.

Another question is whether the passivation effect persists. The effect should be monitored in long term experiments involving physical and/or chemical methods, as well as in vitro assays, and possibly in vivo bioassays to determine the long term persistence in air and in physiological fluids.

The last question is whether this phenomenon is a feasible basis for prevention strategies. One major unknown here is the long term persistence of the effect under in vivo conditions.

In any event, the possibility exists for de-toxification of quartz by relatively mild treatment conditions. Seemingly innocuous preparation procedures used in biological assays of quartz could produce respirable dust surface property changes which are not readily detected by chemical or physical analysis, but which can confound interpretation of bioassay results. The possibility for such should be recognized in research protocols.

References:

- (1) Wallace, W.E., Vallyathan, V., Keane, M., Robinson, V.: In Vitro Biologic Toxicity of native and Surface Modified Silica and Kaolin Dusts. J. Tox. Env. Health 16:415-424 (1986).
- (2) Wallace, W.E., Keane, M.J., Hill, C.A., Vallyathan, V. Saus, F., Castranova, V., Bates, D.: The Effect of Lecithin Surfactant and Phospholipase Enzyme Treatment on Some Cytotoxic Properties of Respirable Quartz and Kaolin Dusts. Proceedings: Respirable Dust in the Mineral Industries: Health Effects, Characterization, and Control. pp.154-166. Frantz, S.L., and Essani, R.V., Eds.;(1986). American Conference of Governmental Industrial Hygienists (ACGIH) publication (1988); ISBN 0-936712-76-7.
- (3) Personal communication; Dr. Klaus Rebeck, Bergbau-Forschung BmbH, Essen.
- (4) Harrington, J.S., Miller, K., Macnab, G.: Hemolysis by Asbestos. Environ. Res. 4:95-117 (1971).
- (5) Holt, P.F., King, D.T.: Solubility of Silica. Nature 175:514-515 (1955).
- (6) Baumann, H.: Adsorption von Kieselsaure an Quartz. Naturwissenschaften 53: 177-178 (1966).
- (7) Iler, R.K.: The Chemistry of Silica. John Wiley and Sons. ISBN 0-471-02404-X. p.37 (1979).
- (8) Iler, R.K.: The Chemistry of Silica. John Wiley and Sons. ISBN 0-471-02404-X. p.641 (1979).

Acknowledgments:

The authors gratefully acknowledge the support of the U.S. Bureau of Mines under Interagency Agreement H0358030, and also gratefully acknowledge support by Grant # G1135142 of the Department of Interior's Mineral Institute Program administered by the U.S. Bureau of Mines through the Generic Mineral Technology Center for Respirable Dust.

IV
INTERACTION OF
DUST AND LUNGS

1
b
r
s
f
I
S
E
R
V
I
C
E
I
E
C

Factors that May Influence Interactions Between Mineral Dusts and Lung Cells

G.L. Barlett and J.D. Barry

Milton S. Hershey Medical Center, The Pennsylvania State University,
Hershey, Pa.

Supernatant media of dust-exposed pulmonary alveolar macrophages (PAMs) were inactive in assays for both Interleukin-1 and fibroblast growth factors (FGF). We have begun to evaluate several factors that may interfere with dust-PAM interactions.

To determine the effect of sterilization on the activity of dusts, PAMs were exposed to autoclaved dust, heat-sterilized dust or to dust that had not been heated. Supernatants from the first two groups were inactive in the FGF assay, but supernatant from PAMs exposed to unheated dusts stimulated growth of lung fibroblasts.

Recent data have revealed that freshly crushed mineral dusts possess labile free radicals that are absent in dust that has been stored for more than a few days. Suspensions were prepared of a "stale" sample of anthracite dust 867 and of a freshly ground sample of the same dust. These suspensions were instilled intratracheally into guinea pigs under general anesthesia. Two, five or eight days later, PAMs were collected from the lungs by bronchoalveolar lavage, and the cells were counted. At two and five days after instillation, all lavage suspensions contained 70 to 85% PAMs, of which 5 to 18% contained phagocytized dust particles. On day eight there were again 80-84% PAMs in all suspensions, but in the presence of "fresh" dust, 48% of PAMs had phagocytized particles in comparison to 16% in the presence of "stale" dust. A similar experiment was performed in short-term cell culture. During 24 hours, >95% of PAMs phagocytized dust particles, whether or not the dust was "stale" or "fresh". Our studies are being extended to determine the effect of (1) removing surface oil contaminants by organic extraction and (2) suspending dusts without surfactant.

Effect of Coal Dust on Mucin Production by the Rat Trachea

V.P. Bhavanandan

Department of Biological Chemistry, The Milton S. Hershey Medical Center, The Pennsylvania State University, Hershey, Pa.

The mucus secreted in the respiratory tract provides the first barrier against inhaled particulate and gaseous toxicants. Trachea removed from pathogen-free rats were maintained as organ cultures and used to study the effects of coal dust exposure on the synthesis of mucin. The high molecular weight isotopically labeled (^3H -glucosamine, ^{14}C -leucine or ^{35}S -sulfate) mucin could be purified by gel filtration, treatment with testicular hyaluronidase, ion exchange chromatography, delipidation and CsBr density gradient centrifugation. To examine effect of coal dust on mucin production, groups of explant cultures were exposed to media containing coal dust at 100 μg per ml every 2 days for 2 weeks while control cultures were treated with media without dust. Analysis of the spent culture media showed that treatment with dust markedly decreased the production of non-dialysable glycoproteins as well as hyaluronidase-resistant acid-precipitable fraction consisting mainly of mucin. Since the synthesis of protein was not affected to the same extent the decrease in mucin production is not entirely due to cell death. In separate experiments rats were subjected to *in vivo* coal dust exposure in inhalation chambers and tracheae of these and control rats were removed for explant cultures. The incorporation of precursor isotopes into mucin by these explant cultures are being examined. (Supported by U.S. Bureau of Mines through the Generic Mineral Technology Center for Respirable Dust under grant G1135142, project 4210).

Acoustic Impedance Method for Detecting Lung Dysfunction

J. Sneckenberger and T. Whitmoyer

West Virginia University

ABSTRACT

The acoustic impedances of seven rat lungs were measured at frequencies between 100 and 6400 Hz. Rats were divided into two groups: a silica exposed group (N=3) and a control group (N=4). The silica exposed group was injected intratracheally with silica solution. Three of the control group were intratracheally injected with saline. Between four and six weeks after the injections, all lungs were excised and degassed. Lungs were suspended in a pressure chamber, with the trachea canula attached to the end of a tapered impedance tube. The lungs were subjected to transpulmonary pressures between -30 cm H₂O and 6 cm H₂O to simulate deflation and inflation. With transpulmonary pressure being held constant, the impedance tube was excited with random noise. A dual channel analyzer calculated $H_{12}(f)$, the transfer function between the two microphones. This function was used to calculate the lung's impedance at that pressure. The impedance magnitude spectra of both groups typically had peaks at 2000, 3500, and 5500 Hz. Statistically significant differences (90% confidence level or greater) between the two groups occur at the 3500 Hz peak at transpulmonary pressures of 20, 8, 6, 4, and 2 cm of H₂O. This fact seems to confirm that this method can detect lung disease. Further research will indicate whether this method will be able to detect the onset of coal worker's pneumoconiosis.

INTRODUCTION

One of the first studies of impedance of the human lung were conducted by DuBois et al.[2] using the forced oscillation technique. This technique, however, was limited to frequencies below 30 Hz. Further studies by Van Den Berg [6] revealed that the lung reflected higher frequency sounds (100-10,000 Hz), instead of behaving as an anechoic termination. This discovery has lead to several studies of the acoustical properties of both human and animal lungs at high frequencies [3,4,5].

Ishizaka et al.[4] measured the input impedances of laryngectomized human subjects using a two microphone technique. This study reported peaks in the impedance magnitude at 640, 1400, and 2100 Hz. Fredberg et al.[3] used a transient forced oscillation technique to measure the input impedance of excised canine lungs for frequencies up to 10,000 Hz. Jayaraman and Frazer [5] used a two microphone technique in combination with transmission matrix

theory to study changes in the acoustic impedance of excised rat lungs during deflation and inflation.

This study's focus is to determine the differences in the acoustic impedance of excised silicotic and healthy rat lungs. Seven Long Evans Hooded rats, weighing between 200 and 250 g, were divided into two groups. The silica-exposed group (N=3) were intratracheally injected with a silica-saline solution to induce silicosis. Three rats of the control group (N=4) were given a sham exposure of saline. During a period four to six weeks after injection, all lungs were excised and degassed.

METHODS

Figure 1 displays a block diagram of the impedance tube facility used in this study. An excised lung is attached to the end of a tapered tube within a plexyglass pressure chamber. Random noise, produced by a Bruel and Kjaer 2032 dual channel analyzer, is amplified and introduced into the tube via a side-mounted speaker driver (University, type ID-30C-8). The standing waves thus formed in the impedance tube are measured by two Bruel and Kjaer 4136 pressure microphones mounted 2.3 cm apart in a plexiglass cylinder. The signals of these microphones are the inputs to the dual channel analyzer, which calculates the transfer function between the two microphones, H_{12} , and its inverse Fourier transform, $h(t)$. Following Jayaraman and Frazer's example [5], exponential weighting is applied to $h(t)$ and transmission matrix theory applied to the resulting transfer function to yield the input impedance of the excised lung.

The plexiglass chamber's pressure is controlled by a variable speed pump to produce transpulmonary pressures between 30 and -6 cm of H_2O . The difference between chamber pressure and atmospheric pressure is monitored by a water manometer. A lung is first inflated to 30 cm of H_2O , then deflated to -6 cm of H_2O , pausing at several pressures for impedance measurements. Once fully deflated, the lung is inflated to 30 cm of H_2O , again stopping at various pressures for measurements.

RESULTS

The average magnitude spectra of the silica and control groups are presented in Figures 2, 3, and 4 for transpulmonary pressures of 30, 8, and 2 cm of H_2O , respectively.

DISCUSSION

The impedance magnitude spectra of all rats have been computed for transpulmonary pressures of 30, 20, 10, 8, 6, 4, 2, 0, and -2 cm of H_2O . Typical rats in both groups had peaks at 2000, 3500,

MEASUREMENT OF ACOUSTIC IMPEDANCE

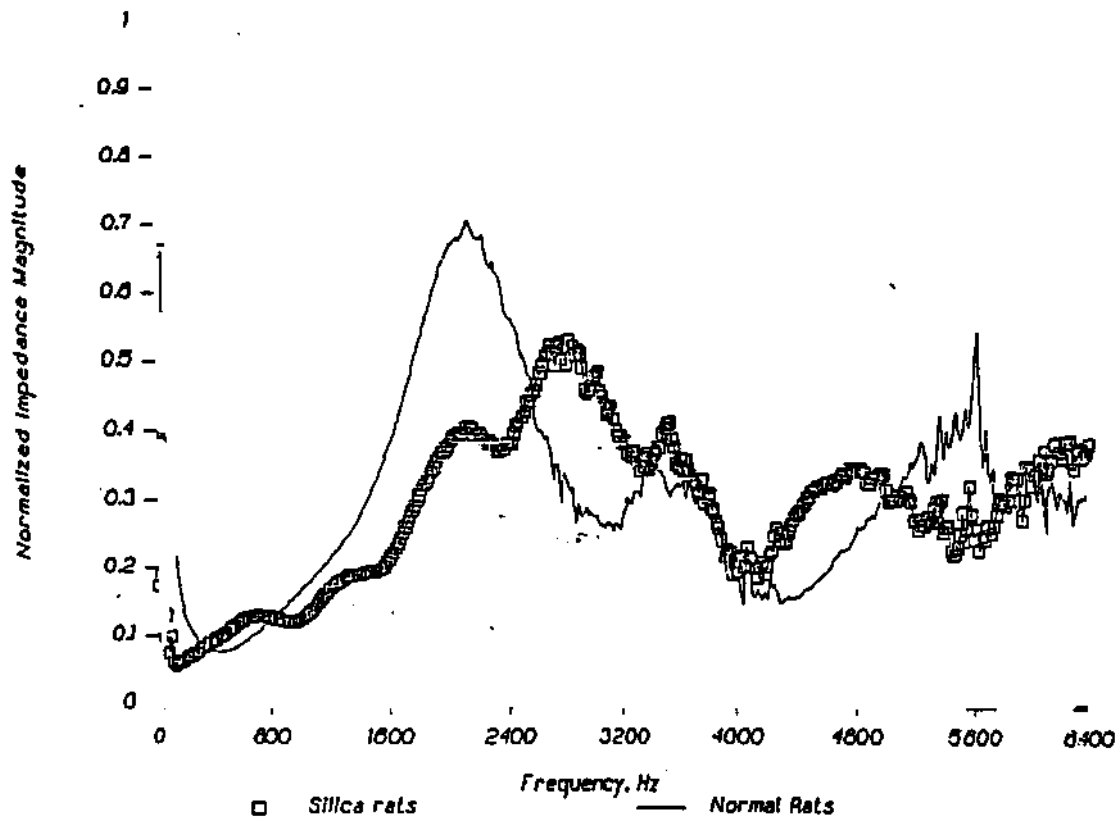


Figure 2. Comparison of average impedance spectra of silica and control groups. Deflation 30 cm H₂O.

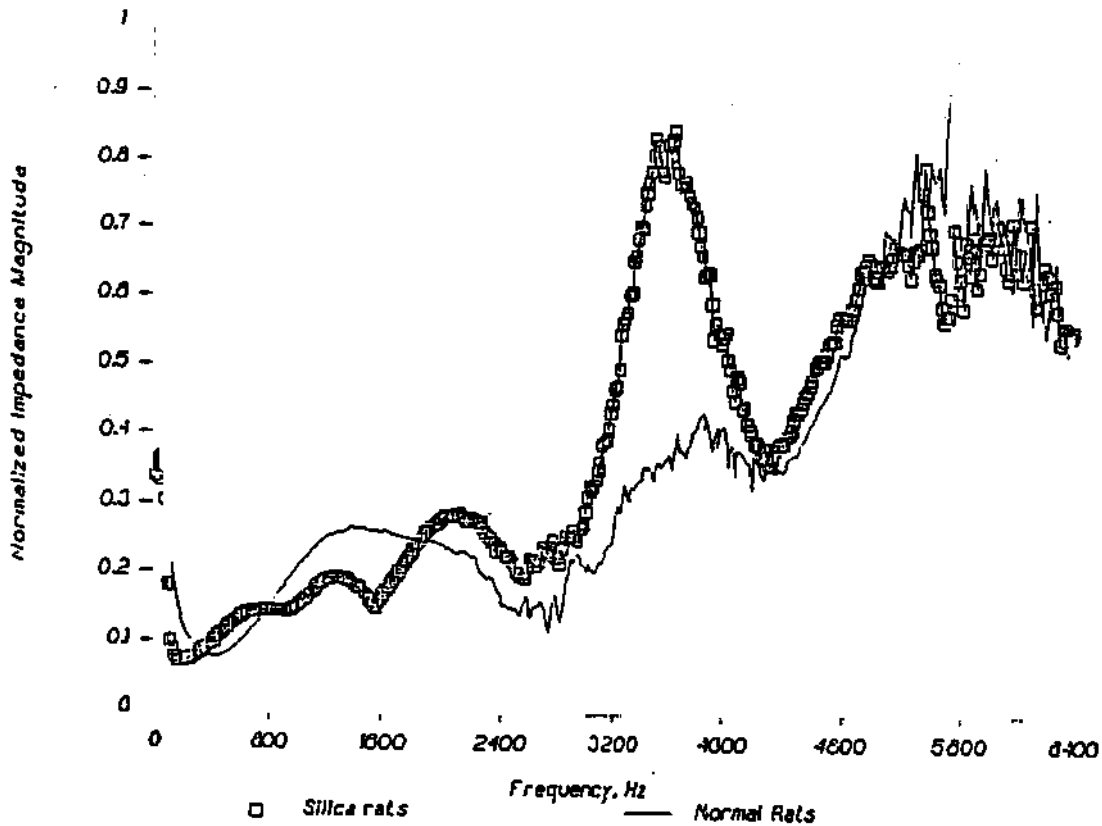


Figure 3. Comparison of average impedance spectra of silica and control groups. Deflation 8 cm H₂O.

and 5500 Hz. The placement of these peaks compare favorably with the study of Jayaraman and Frazer [5], with the exception that in this study, no peak occurred at 600 Hz.

Significant differences between the silica and control groups occurred at the peak at 3500 Hz. T-tests performed on the peak magnitudes at this frequency showed that the silica group had significantly higher impedance (90% confidence level) at transpulmonary pressures of 20 and 8 cm of H₂O during deflation. The silica group also had significantly higher impedance (98% confidence level) at 3500 Hz at pressures of 6 and 4 cm of H₂O during deflation. These findings show that changes in the mechanical properties of lung tissue and the closure of airways occurred at higher pressures in the silica group than with the control group. This finding agrees with the work of Chvalova et al. [1] which found that the pressure-volume curve of silicotic rats was shifted to higher pressures compared to normal rat lungs.

CONCLUSIONS

The above findings indicate that silicosis in rat lungs can be detected by measuring the lung input impedance. The key indicator thus far is the impedance magnitude of the peak at about 3500 Hz. Further studies will determine the effectiveness of the method in detecting the development of lung diseases and if the measurement of acoustic impedance can be an effective clinical tool for the treatment of lung diseases.

ACKNOWLEDGMENTS

The authors wish to thank the Division of Respiratory Disease Studies, NIOSH, Morgantown, WV for the use of their facilities during this study. This research has been supported by the Department of the Interior's Mineral Institute program administered by the Bureau of Mines through the Generic Mineral Technology Center for Respirable Dust under grant number G1135142.

REFERENCES

1. Chvalova, M., Kuncova, J., Havrankova, J., and Palecek, F.: Regulation of Respiration in Experimental Silicosis. *Physiol. Bohemoslov.* 23:539-547 (1974).
2. DuEois, A.E., Brody, D.H., Lewis, D.H., and Burgess, B.F.: Oscillation Mechanics of Lungs and Chest in Man. *J. Appl. Physiol.* 8:587-594 (1956).
3. Fredberg, J.J., Sidell, R.S., Wohl, M.E., and DeJong, R.G.: Canine Pulmonary Input Impedance Measured by Transient Forced Oscillations. *J. Biomech. Eng.* 100:67-71 (1978).

MEASUREMENT OF ACOUSTIC IMPEDANCE

4. Ishizaka, K., Matsudaira, M., and Kaneko, T. : Input Acoustic Impedance Measurement of the Subglottal System. J. Acoust. Soc. Am. 60:190-197 (1976).
5. Jayaraman, K. and Frazer, D. : Broadband Acoustical Impedance of Excised Rat Lungs at Transpulmonary Pressures between -5 cm and 30 cm of H O. Fall Conference of the American Physiological Society, New Orleans, LA, 1986.
6. Van Den Berg, J.W.: An Electrical Analogue of the Trachea, Lungs, and Tissues. Acta. Physiol. Pharmacol. Neerl. 9:361-385 (1960).

Bronchoalveolar Lavage in Subjects Exposed to Occupational Dusts

G. Goodman, N.L. Lapp, V. Castranova, W.H. Pailes and D. Lewis
 West Virginia University Hospital and
 Division of Respiratory Disease Studies, National Institute for Occupational
 Safety and Health, Morgantown, WV

We performed bronchoscopy with bronchoalveolar lavage (BAL) in 8 control subjects with no exposure to occupational dusts, 8 healthy power plant workers exposed to mixed dusts (primarily fly ash), 1 healthy coal miner and 1 rock driller with acute silicosis. All subjects were non-smoking males. We analyzed lavage effluents for total numbers of alveolar macrophages, lymphocytes and neutrophils and monitored chemiluminescence at rest (REST CL) and after stimulation with $3 \times 10^{-6}M$ phorbol-12-myristate-13-acetate (PMA CL) or 2 mg/ml zymosan (ZYM CL). The data are as follows:

	CONTROLS (mean \pm SEM)	FLY ASH (mean \pm SEM)	COAL DUST	ACUTE SILICOSIS
# ALVEOLAR MACS $\times 10^6$	7.4 \pm 1.2	14.1 \pm 2.1*	4.0	9.8
# LYMPHOCYTES $\times 10^6$	4.5 \pm 0.8	8.4 \pm 1.1*	4.6	65.6*
# NEUTROPHILS $\times 10^6$	2.9 \pm 0.7	7.3 \pm 2.5*	3.1	30.3*
REST CL TOTAL COUNTS $\times 10^6$	27.0 \pm 6.0	38.9 \pm 6.0	65.8	144.6*
PMA CL TOTAL COUNTS $\times 10^6$	68.2 \pm 22.6	83.0 \pm 10.7	64.5	250.2*
ZYM CL TOTAL COUNTS $\times 10^6$	41.4 \pm 12.4	84.0 \pm 8.4*	47.4	509.0*

*significantly greater than control at $p < 0.05$

The data indicate altered alveolar cell populations and phagocytotic activity in asymptomatic occupationally exposed subjects. Similar, more extreme changes were seen in the subject with acute silicosis.

Microcomputer Control of Particle Concentrations in a Cotton Dust Exposure System

T. B. Whitmoyer¹, J.E. Sneckenberger¹, D.G. Fraser²,
V.A. Robinson², A. Giza² and D.S. DeLong²

¹Department of Mechanical and Aerospace Engineering,
West Virginia University

²Physiology Laboratory, Investigations Branch, National Institute for
Occupational Safety and Health, Morgantown, WV

ABSTRACT

A cotton dust animal exposure system has been modified to incorporate a microcomputer feedback loop to monitor particle concentrations. The loop's major components are a miniature real-time aerosol monitor (miniram) to estimate concentrations and a microcomputer to read the miniram's data and to control a stepper motor that adjusts the amount of dilutant air mixing with respirable cotton dust. Ninety minute trials of this system indicate that the standard deviation of particle concentrations is within 0.68 mg/m³ of the average concentration, insuring a near constant concentration of respirable dust throughout the exposure.

INTRODUCTION

Previous Work

Weyel *et al.* (1984) have determined that respirable cotton dust can be shaken from bulk cotton samples using acoustical energy. The particle generator designed to utilize this fact operates like a commercially available sonic sifter, but on a much larger scale.

While this generator successfully resuspended trapped respirable cotton dust, the generator output concentration decreased exponentially with time. This disadvantage was solved by Frazer *et al.* (1986) by operating the generator with a sinusoidal voltage near the minimum resonance frequency of the generator. This adjustment enabled the generator to produce respirable cotton dust for six hours or longer.

Frazer *et al.* (1987) utilized the modified acoustical generator to produce a cotton dust animal exposure system. The cotton dust concentrations were estimated by a miniram, a light scattering aerosol monitor. The system operator used the miniram values to adjust the system's parameters to maintain the desired concentration level.

Purpose

The objective of this study was to introduce a computerized feedback loop to the operator controlled cotton dust animal exposure system. The miniram's estimates were analyzed by a microcomputer to determine what adjustments in the flow of dilutant air were necessary to maintain the desired cotton dust concentration. These modifications were intended to improve system performance and ease the system operator's work burden.

METHODS

Exposure System with Operator Feedback

The operator feedback exposure system is fully described by Frazer *et al.* (1987). Air entering the exposure system is conditioned by a water seal air compressor, a HEPA and charcoal filter, and a flow-temperature-humidity controller. Cotton dust resuspended by acoustical energy is carried toward the exposure chamber by conditioned air entering at the generator's base and exiting from its top. Nonrespirable cotton dust particles are removed in a settling tank. The respirable cotton dust is

THE RESPIRABLE DUST CENTER

diluted with conditioned air to achieve the desired particle concentration.

The cotton dust aerosol is passed through a miniature real-time aerosol monitor (miniram), which uses light scattering to estimate the particle concentration. The miniram's output is recorded on a printer for permanent record. The dilutant air flow is adjusted by the operator according to the miniram's measurements. The aerosol leaving the exposure chamber. A portion of the aerosol is removed from the exposure chamber by a constant flow pump. The cotton dust is removed from this sample by a PCV filter. The remaining aerosol is passed through a HEPA filter and exhausted.

Computerized Feedback Subsystem

The operator feedback loop is replaced by a microcomputer controlled feedback loop. The miniram's digital output is received by a microcomputer (IBM XT) via an RS-232 serial connection. The miniram estimates particle concentrations every ten seconds. Each measurement is compared with the concentration setpoint indicated by the operator. If the current concentration is above the setpoint, the microcomputer opens the dilutant air valve. If the concentration is below the setpoint, the dilutant air valve is closed. The amount of opening or closing depends upon the distance to the setpoint.

The dilutant air valve is activated by a pancake type, four-phase, bidirectional stepper motor (Copal Electronics 076197). The shaft of the stepper motor is connected to the input pinion of a 7.5 to 1 gear reduction system to compensate for the stepper motor's 0.035 N-m driving torque. The output of the gear reduction is mated to the dilutant air valve by a machined adapter.

The stepper motor is controlled by the microcomputer using a stepper motor driver (Alpha Products model ST-143) and a bus adapter (Alpha Products model AR-133). These products allow the stepper motor to be activated using BASICA's OUT instruction.

The number of steps the stepper motor turns is linearly proportional to the difference between the miniram reading and the setpoint. If the miniram reading is within five percent of the setpoint, the stepper motor is not moved. The number of steps the motor moves is limited to prevent system instability. The selection of this limit is discussed in more detail in the following section.

The block diagram of the computerized feedback animal exposure system is presented in Figure 1. The components of the computerized feedback subsystem are indicated by darkened lines.

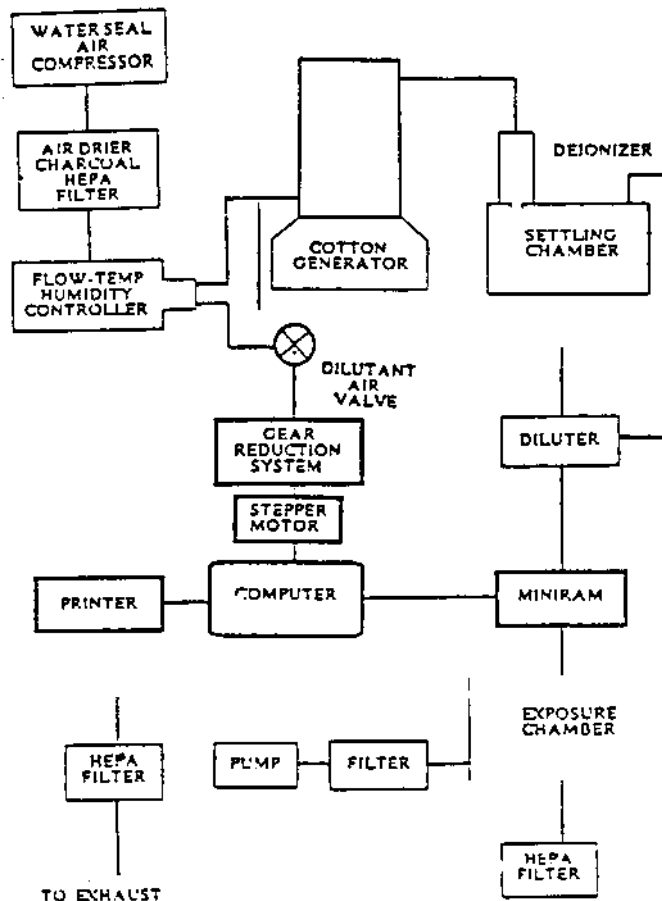


Figure 1. Block diagram of cotton dust animal exposure system with microcomputer feedback. Feedback subsystem drawn with emphasized lines.

RESULTS AND DISCUSSION

Feedback Stability

The stability of the microcomputer controlled feedback system depends on the maximum stepper motor movement allowed during each adjustment of the dilutant air. Since adjustments are made every ten seconds, the feedback loop overreacts to large differences between the setpoint and measured concentrations. If the stepper motor movements are small enough, the particle concentrations converge to the setpoint. Several trials indicate the the critical stepper motor movement per adjustment to be between six and seven steps (one step equals 7.5 degrees). At six steps maximum per adjustment, the particle concentration converge, while seven steps or greater per adjustment leads to large oscillations in the particle concentrations.

MONITORING PARTICLE CONCENTRATION

Gravimetric Analysis

The performance of the microcomputer controlled animal exposure system was evaluated by measuring the amount of cotton dust trapped in the PVC filters. Two trials of the system were made: one with a setpoint of 10.0 mg/m^3 , the other with a setpoint of 35.0 mg/m^3 . Each trial lasted 90 minutes, with the PVC filters being changed every 30 minutes. The average particle concentration determined by gravimetric sampling and the average miniram measurement for each test are displayed in Table 1. Additional tests were conducted to measure the system's performance over longer periods of time. Figure 2 shows the miniram's output for a 15.0 mg/m^3 setpoint during a six hour trial. Figure 3 shows the gravimetric results for several long term tests at various setpoints.

Comparison of Operator and Microcomputer Control

The performance of the operator controlled system with a setpoint of 35.0 mg/m^3 were reported by Frazer et al. (1987). The average particle concentration was $34.5 \pm 1.5 \text{ mg/m}^3$ for a six hour exposure. The microcomputer controlled system yielded an average of $33.7 \pm 0.3 \text{ mg/m}^3$ for a 90 minute exposure. The average miniram output for the same 90 minute period was 34.8 mg/m^3 . This fact indicates that the discrepancy between the exposure's setpoint and the calculated concentration is due to inaccuracies in the miniram's estimation of particle concentration. The standard deviation of the concentrations indicate that the microcomputer controlled system yields more consistent concentrations. Since the system suspending the cotton dust is the same for both forms of control, the average and standard deviation of cotton dust concentrations of the microcomputer system does not change significantly if the trial time is increased from 90 minutes to six hours. In any case, the microcomputer-controlled system required far less attention than the operator-controlled system.

CONCLUSION

In summary, a microcomputer controlled feedback subsystem has been incorporated into a cotton dust animal exposure system. The resulting combination yielded a system producing more consistent concentration levels and requiring less supervision than the operator feedback system that it replaced. In addition, the microcomputer controlled system was able to maintain a given setpoint for six hours without operator interference. While this study focused on cotton dust, the exposure system should work equally well with other respirable dusts, such as silica or coal dust.

a)		
TIME (min)	CONCENTRATION FROM GRAVIMETRICS (mg/m^3)	AVERAGE MINIRAM CONCENTRATION (mg/m^3)
0 to 30	9.87	10.7
30 to 60	8.27	10.2
60 to 90	8.66	10.1

b)		
TIME (min)	CONCENTRATION FROM GRAVIMETRICS (mg/m^3)	AVERAGE MINIRAM CONCENTRATION (mg/m^3)
0 to 30	33.7	34.6
30 to 60	33.3	34.9
60 to 90	34.0	35.0

Table 1. Results of 90 minute trial
 a) Setpoint = 10.0 mg/m^3 .
 Gravimetric Average = $8.93 \pm 0.68 \text{ mg/m}^3$.
 b) Setpoint = 35.0 mg/m^3 .
 Gravimetric Average = $33.7 \pm 0.30 \text{ mg/m}^3$.

TYPICAL MINIRAM CONCENTRATION READINGS

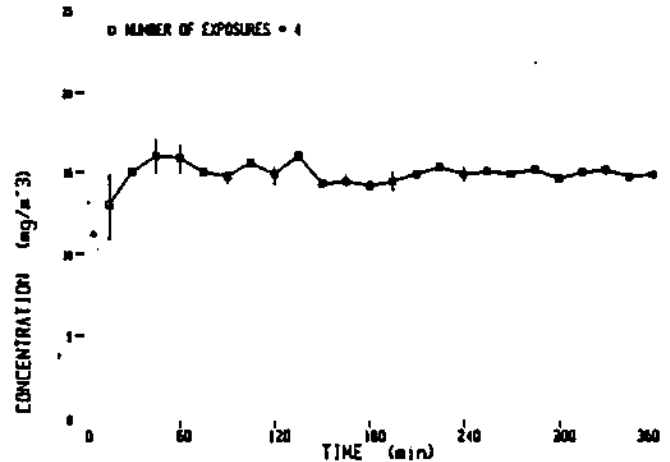


Figure 2. Miniram output for a six hour trial with a setpoint of 15.0 mg/m^3 .

GRAVIMETRIC CONCENTRATION DATA

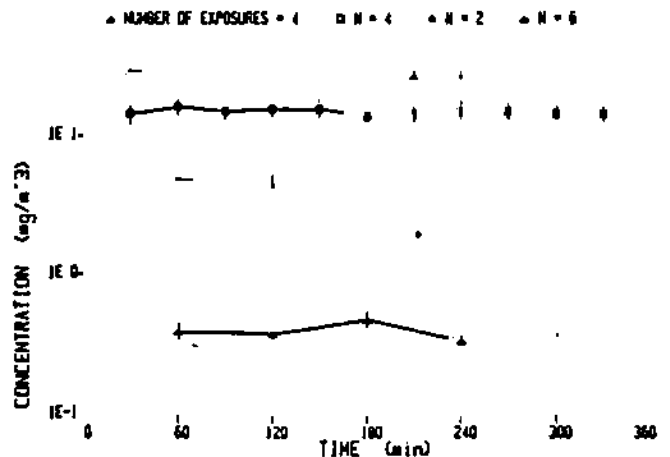


Figure 3. Gravimetric results for extended trials with setpoints of 30.0 , 15.0 , 5.0 , and 0.5 mg/m^3 .

THE RESPIRABLE DUST CENTER

ACKNOWLEDGMENTS

The authors wish to thank the Division of Respiratory Disease Studies, NIOSH, Morgantown, WV for the use of their facilities during this study and Jeffrey Carpenter and Vinay Sandhir for their assistance in performing the initial trials. This study was conducted as part of "Development of New Early Detection Methods for Black Lung. Task A: Tracheal Acoustic Impedance of Lung Air Passages". This research has been supported by the Department of the Interior's Mineral Institute program administered by the Bureau of Mines through the Generic Mineral Technology Center for Respirable Dust under grant number G1135142.

REFERENCES

Frazer, D. G., Robinson, V. A., Jayaraman, K., Weber, K. C., DeLong, D. S., Glance, C., 1986, "Improved Operating Parameters for the Pitt-3 Aerosol Generator During Resuspension of Respirable Cotton Dust," Proceedings of the Tenth Cotton Dust Respiration Conference. R. R. Jacobs and P. J. Wakelyn, eds., National Cotton Council, Memphis, TN, pp. 122-125.

Frazer, D. G., Robinson, V. A., DeLong, D. S., Rose, D., Tucker, J., Weber, K. C., Olenchock, S. A., Jayaraman, K., 1987, "A System for Exposing Laboratory Animals to Cotton Dust Aerosol That Is Stabilized with Feedback Control," Proceedings of the Eleventh Cotton Dust Respiration Conference, R. R. Jacobs and P. J. Wakelyn, eds., National Cotton Council, Memphis, TN, pp 74-78.

Weyel, D. A., Ellakkani, M., Alarie, Y., Karol, M., 1984, "An Aerosol Generator for the Resuspension of Cotton Dust," Toxicology and Applied Pharmacology, Vol. 76, pp. 544-547.

Effects of Platelet Activating Factor on Various Physiological Parameters of Neutrophils, Alveolar Macrophages, and Alveolar Type II Cells

K. Van Dyke¹, J. Rabovsky², D.J. Judy², W.H. Pailles², M. McPeck², N.A. Sapola² and V. Castranova^{2,3}

¹Department of Pharmacology and Toxicology, West Virginia University

²Department of Physiology, West Virginia University

³Division of Respiratory Disease Studies, National Institute for Occupational Safety and Health, Morgantown, WV

Platelet activating factor (PAF) can be released from pneumocytes following exposure to occupational dust (Am. Rev. Respir. Dis. 135:83, 1987). In addition, PAF has been shown to induce pulmonary inflammation, edema, and bronchoconstriction (Hosp. Prac. 19, 67, 1983). This investigation reports the effects of PAF on the properties of three types of cells found in the lung. PAF (1-10 μ M, $K_{1/2}$ = 2.5 μ M) caused depolarization of neutrophils as well as generation of chemiluminescence and secretion of hydrogen peroxide. These responses were dependent on the presence of extracellular sodium. However, PAF did not alter oxygen consumption of neutrophils. Although PAF (10 μ M) caused depolarization of alveolar macrophages, no stimulation of chemiluminescence, superoxide secretion, or oxygen consumption was observed. However, PAF (10 μ M) did potentiate chemiluminescence and superoxide secretion in response to zymosan (2 mg/ml) by 55% and 36%, respectively. In addition, PAF (10-90 μ M) caused aggregation of alveolar macrophages. PAF (2-10 μ M) also caused depolarization of type II cells, but did not affect membrane integrity or oxygen consumption. However, PAF (10-18 μ M) enhanced the activities of two distinct forms of cytochrome P-450 in type II cells and caused aggregation of type II cells at PAF doses above 18 μ M. These data indicate that PAF can affect the secretory activity of pulmonary phagocytes and the ability of type II cells to detoxify foreign compounds (Bureau of Mines Grant - G1175142).

INTRODUCTION

Platelet activating factor (PAF) is a glycerophospholipid (1-O-alkyl-2-acetyl-sn-glycerol-3-phosphoryl choline) which has been shown to mediate a broad range of biological activities (1-3). Its pulmonary actions include contraction of pulmonary tissue (4), secretion of leukotrienes from leukocytes (5), airway constriction (6), pulmonary edema (7), and enhanced migration of neutrophils into the airspaces of the lungs (8,9).

PAF can be released from several different cell types, such as, basophils, neutrophils and alveolar macrophages, in response to a variety of particulates or membrane stimulants which include zymosan, calcium ionophore, phorbol esters, chemotactic agents, and endotoxin (10-13). Therefore, PAF may play an important role in the development of pneumoconioses by mediating pulmonary responses of lung cells to a variety of occupational dusts. To investigate this possibility, we determined the effects of PAF on several physiological parameters of neutrophils, alveolar macrophages, and alveolar type II epithelial cells.

METHODS

Isolation of Cells

Neutrophils were isolated from human blood by dextran settling and centrifugal elutriation (14). Isolated neutrophils (93% pure) were resuspended in HEPES-buffered medium (145 mM NaCl, 5 mM KCl, 10 mM HEPES, 5 mM glucose, and 1 mM CaCl₂; pH = 7.4). Cell number and volume were determined with an electronic cell counter equipped with a sizing attachment.

Rat alveolar macrophages were obtained by pulmonary lavage with Ca²⁺, Mg²⁺-free Hanks balanced salts solution (15). Alveolar macrophages (94% pure) were resuspended in HEPES-buffered medium, counted, and sized electronically.

Rat alveolar type II cells were isolated by enzymatic digestion for 35 minutes at 37° C with 40 μ/ml type I elastase and 0.1% collagenase and purified by centrifugal elutriation (16,17). Type II cells (92% pure) were resuspended in HEPES-buffered medium for measurement of membrane potential, oxygen consumption, and trypan blue exclusion. Type II pneumocytes were resuspended in 0.1 M NaCl plus 0.05 M HEPES (pH = 7.8) to measure cytochrome P450-dependent activities and aggregation. Cell size and number were determined electronically.

Measurement of Transmembrane Potential

Membrane potential of isolated cells in suspension was measured using a fluorescent probe, Di-S-C₃ (5), as described previously for neutrophils (14), alveolar macrophages (18), and type II cells (19). Fluorescence was monitored at excitation and emission wavelengths of 622 and 665 nm, respectively. An increase in the fluorescence emission from the cell suspension indicated membrane depolarization.

Measurement of Respiratory Burst Activity

Release of reactive forms of oxygen by phagocytic cells was determined at 37°C by measuring the generation of chemiluminescence, secretion of hydrogen peroxide, or release of superoxide anion. Chemiluminescence from neutrophils (1 x 10⁶ cells/5 ml of HEPES-buffered medium) was measured in the presence of 1 x 10⁻⁸M luminol using a liquid scintillation counter operated in the out-of-coincidence mode (20). Chemiluminescence from alveolar macrophages (3 x 10⁶ cells/0.5 ml of HEPES-buffered medium) was measured in the presence of 1 x 10⁻⁵ M luminol using a Berthold 9505 Luminometer.

Hydrogen peroxide release from neutrophils or alveolar macrophages (1 X 10⁷ cells/2.5 ml or 4 X 10⁶ cells/3 ml, respectively) in HEPES-buffered medium containing 2.5 μM scopoletin, and 40 μg/ml horseradish peroxidase (type IX) was monitored fluorometrically at an excitation wavelength of 350 nm and an emission wavelength of 460 nm (21,22).

Superoxide anion secretion from neutrophils or alveolar macrophages (1 X 10⁷ cells/2.5 ml or 4.5 X 10⁶ cells/6 ml, respectively) in HEPES-buffered medium was monitored spectrophotometrically at 550 nm as the reduction of 0.12 mM cytochrome C (21,15).

PLATELET ACTIVATING FACTOR

Measurement of Cellular Viability

Oxygen consumption was measured at 37°C with an oxygraph equipped with a Clark electrode. Type II cells (10^7 cells), neutrophils (6.5×10^6 cells), or alveolar macrophages (5×10^6 cells) were suspended in 1.7 ml of HEPES-buffered medium for these measurements (16, 21, 23).

Membrane integrity was determined by measuring the exclusion of trypan blue dye under light microscopy (24).

Functional Measurements with Type II Cells

Cytochrome P450-dependent ethoxyphenoxazone dealkylase (EtOPhase) (EC 1.14.14.1) activity of type II cells was monitored at 36°C in a direct kinetic assay based upon the formation of a fluorescent product, resorufin, measured at an excitation wavelength of 530 nm and an emission wavelength of 585 nm (17). NADPH was maintained at 0.5 mM by a glucose-6-phosphate dehydrogenase generating system.

Aggregation of type II cells was monitored at 37°C using a Lumi Aggregometer. Increased aggregation was measured as increased light transmission.

Type II cells used for measurement of cytochrome P450 and aggregation were isolated from rats metabolically induced by pretreatment with 8-naphthoflavone. For these assays, cells were suspended in 0.1 M NaCl and 0.05 M HEPES (pH = 7.8).

Statistical Analysis

Data are expressed as means \pm standard errors of n experiments conducted with cells obtained from different preparations. Data were analyzed by a Student's t test with significance set at $p < 0.05$.

RESULTS

Platelet activating factor can initiate a wide variety of pulmonary responses (1,4-9). However, details concerning the cellular mechanisms responsible for the activities of PAF are not fully defined. Therefore, this investigation characterized the actions of PAF on three types of lung cells, i.e., two types of pulmonary phagocytes (neutrophils and alveolar macrophages) and alveolar type II epithelial cells.

The effects of PAF on pulmonary phagocytes are summarized in Table I. PAF was a direct stimulant of neutrophils in vitro. PAF induced substantial depolarization of the plasma membrane which was rapid (peaking within 15 sec after addition of PAF) and transient (returning to the resting level within 2 min). The effect of PAF on the membrane potential (E_m) of neutrophils was dose-dependent, exhibiting a $K_{1/2}$ value of 2.5 μ M. This PAF-induced depolarization was sodium-dependent, i.e., removal of extracellular sodium eliminated the effect. PAF (10 μ M) was also a potent activator of neutrophils, i.e., it induced significant generation of chemiluminescence and release of hydrogen peroxide. As was the case for membrane depolarization, stimulation of the secretory activity of neutrophils by PAF was dependent on extracellular sodium. In contrast to the above responses, in vitro treatment of

neutrophils with PAF (10 μ M) resulted in only a small increase in superoxide anion release and no significant elevation of oxygen consumption.

As with neutrophils, *in vitro* treatment of alveolar macrophages with PAF (12 μ M) resulted in membrane depolarization. This response was rapid (peaking within 40 sec) and prolonged (not returning to resting Em). In contrast to neutrophils, *in vitro* treatment of alveolar macrophages with PAF (12 μ M) did not activate the respiratory burst in these cells, i.e., there was little or no PAF-induced increase in chemiluminescence, hydrogen peroxide release, superoxide secretion, or oxygen consumption (Table I). However, PAF(12 μ M) did potentiate activation of alveolar macrophages by zymosan (2 mg/ml), i.e., PAF increases zymosan-stimulated superoxide release by 36% (Figure 1) and zymosan-induced chemiluminescence by 55% (Figure 2).

The *in vitro* effects of PAF on isolated type II cells were also characterized. At levels of 12 μ M or below, PAF did not affect membrane integrity or oxygen consumption, i.e., trypan blue exclusion was $81 \pm 2\%$ before and $82 \pm 1\%$ after PAF treatment while oxygen consumption levels were 0.23 ± 0.04 and 0.19 ± 0.03 nmoles O_2 /min/ 10^6 cells, respectively. However, PAF (12 μ M) did cause

SUPEROXIDE ANION SECRETION BY ALVEOLAR MACROPHAGES

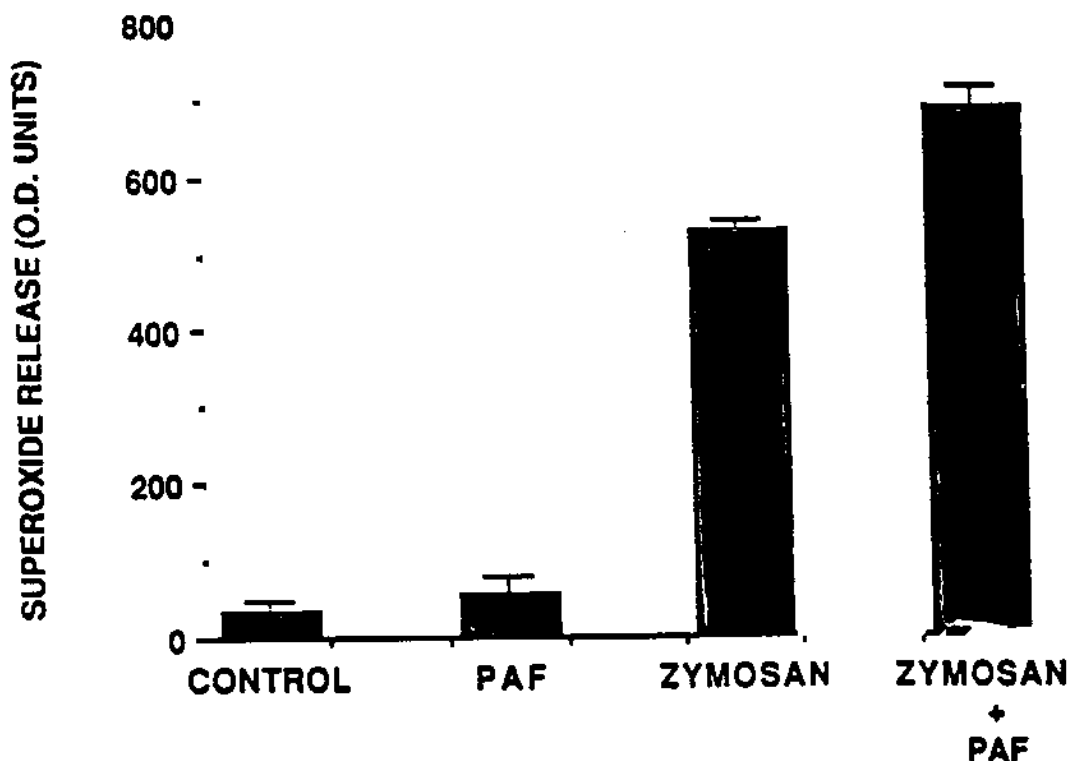


Figure 1. Effects of PAF on superoxide anion release from rat alveolar macrophages. Superoxide secretion at 37°C was monitored spectrophotometrically by measuring the reduction of cytochrome c over 30 minutes at a wavelength of 550 nm. Cells (4.5×10^6 cells/6 ml) were treated *in vitro* with 12 μ M PAF and/or 2 mg/ml zymosan. Values are means \pm standard errors of four different preparations.

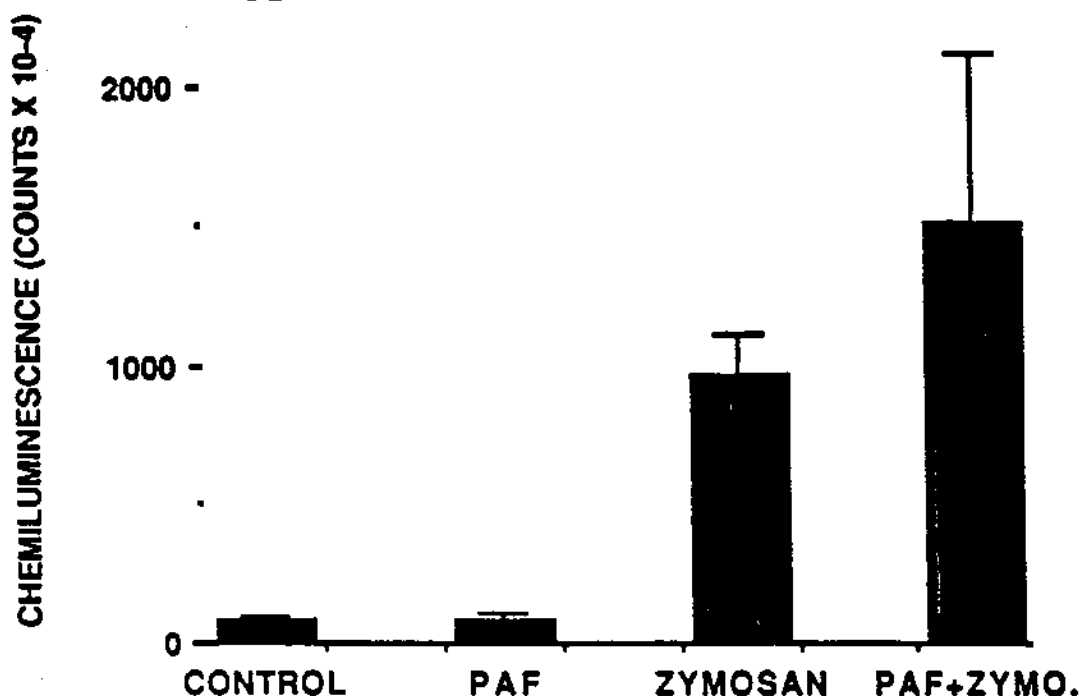
EFFECTS OF PAF AND/OR ZYMOSAN ON CL
GENERATED FROM ALVEOLAR MACROPHAGES

Figure 2. Effects of PAF on chemiluminescence generated from rat alveolar macrophages. Chemiluminescence was measured for 10 minutes at 37°C in the presence of 10⁻⁵M luminol. Cells (3X10⁶ cells/0.5 ml) were preincubated at 37°C in the presence or absence of 12 μM PAF for 15 minutes prior to addition of 2 mg/ml zymosan and measurement of chemiluminescence. Values are means ± standard errors of three different preparations.

depolarization of type II cells which was rapid (peaking within 1 min) and prolonged. This depolarization exhibited dependence on extracellular sodium. PAF also enhanced the activity of cytochrome P450-dependent ethoxyphenoxazone dealkylase (EtOPhase). A maximum stimulation of 2.5 fold was noted at 10 μM PAF (Figure 3). Such activation was demonstrated in intact cells but not in sonicated preparations (Table 2) or microsomes. The decline in P450 activity at higher levels of PAF may be due in part to PAF-induced aggregation of type II cells which was significant at PAF levels above 18 μM (Figure 4).

DISCUSSION

Neutrophils are blood phagocytes which are recruited into the pulmonary air spaces following inhalation of foreign substances, such as, bacteria, virus, or dusts (25). Alveolar macrophages are free lung phagocytes located on the surface of the small airways and the alveoli (26). Upon exposure to microorganisms or occupational dust these phagocytes exhibit a respiratory burst releasing reactive oxygen species, such as, superoxide anion, hydrogen peroxide, and hydroxyl radicals (27-29). Evidence indicates that dust exposure may cause hyperactivation of these phagocytes. The resultant secretion of reactive products may result in inflammation, cellular damage, and in extreme cases fibrosis or emphysema (30,31).

THE RESPIRABLE DUST CENTER

In this investigation we evaluated the ability of platelet activating factor (a potentially important mediator of pneumoconioses) to activate phagocytes. The data indicate that PAF depolarizes neutrophils by increasing membrane permeability to sodium. Such depolarization may trigger secretory activity in neutrophils (20). Indeed, PAF does activate neutrophils to secrete hydrogen peroxide and generate chemiluminescence (Table I). However, activation of the respiratory burst is incomplete in neutrophils since PAF does not stimulate oxygen consumption and elevates superoxide release only slightly.

Although PAF depolarizes alveolar macrophages, it does not directly activate a respiratory burst (Table I). However, PAF treatment does prime the cells to be more responsive to subsequent exposure to particles (Figures 1 and 2). Since PAF may be released following dust exposure, the potentiating action of PAF could have important consequences in escalating the cycle of inflammation and tissue damage seen in certain occupational lung diseases.

Cytochrome P450-dependent monooxygenases are responsible for the metabolism of organic chemicals in pulmonary tissue (32). We have shown that within the lung high levels of P450-dependent activities are found in alveolar type II cells (17). Recent studies have suggested that endogenous factors released from phagocytes may depress P450-dependent activity in hepatocytes (33-35). Since PAF is released from phagocytes (10-13), we tested its effect on P450-dependent activity of type II cells. In contrast to the hepatic system, PAF (a phagocyte-derived mediator) enhances P450-dependent activity of alveolar type II cells (Figure 3). This effect seems to be mediated through the cell membrane, since PAF fails to activate P450 in sonicated cells or microsomes (Table II). It is possible that PAF may alter membrane structures which translate into increased P450 activity. Action of PAF at the plasma membrane is supported by our evidence of PAF-induced changes in membrane permeability to ions and membrane potential. In addition, higher concentrations of PAF alter the membrane surface of type II cell sufficiently to cause aggregation (Figure 4).

In conclusion, PAF may be released from phagocytes following occupational exposures. This PAF would be inflammatory by directly activating neutrophils and potentiating the response of macrophages to particulates. In addition, xenobiotic metabolism by alveolar type II cells would be enhanced affecting the detoxication and/or activation of foreign compounds. The role which these cellular changes play in pneumoconioses remains to be defined.

This research has been supported by the Department of the Interior's Mineral Institute Program administered by the United States Bureau of Mines through the Generic Mineral Technology Center for Respirable Dust under grant number G1175142.

PLATELET ACTIVATING FACTOR

TABLE I

Effects of Platelet Activating Factor on Phagocytes

<u>Cell Types</u>	<u>Em</u>	<u>Oxygen Consumption</u>	<u>Superoxide Release</u>	<u>Chemiluminescence</u>	<u>Hydrogen Peroxide Release</u>
Neutrophils	transient depolarization	0	+	+++	+++
Alveolar Macrophages	prolonged depolarization	0	0	0	0

Maximal responses of neutrophils and alveolar macrophages after *in vitro* exposure to 10 μ M or 12 μ M PAF, respectively. The relative magnitude of enhancement is signified by +. No response is signified by 0. Data for each assay are taken from four separate experiments.

TABLE II

Effect of Sonication on the Responsiveness of Alveolar Type II Cell Cytochrome P450-Dependent Activity to Platelet Activating Factor

<u>Additive^b</u>	<u>P450-Dependent Activity^a Cells</u>	<u>Sonicate^c</u>
None	16.6 \pm 3.4	38.7 \pm 5.6
BSA-HEPES	16.2 \pm 2.4	38.6 \pm 11.0
PAF (19 μ M)	34.0 \pm 6.4	34.2 \pm 4.9

a) Specific activity expressed as pmoles resorufin formed/min/mg protein. Protein determined by the procedure of Lowry et al. (25). Data are means \pm standard errors of two experiments.

b) Additive: None - 0.1M NaCl, 0.5 mM NADPH, and 0.05M HEPES (pH = 7.8); BSA-HEPES - 10 μ l of 0.5% BSA in 0.01M HEPES (pH = 7.8) added to the above solution; PAF - 10 μ l of PAF in 0.5% BSA and 0.01M HEPES (pH = 7.8) added.

c) Disrupted type II cells were obtained by pulse sonication (0.33 sec on, 0.67 sec off) of the cell suspension for 30 seconds at 3 Watts at 2°C.

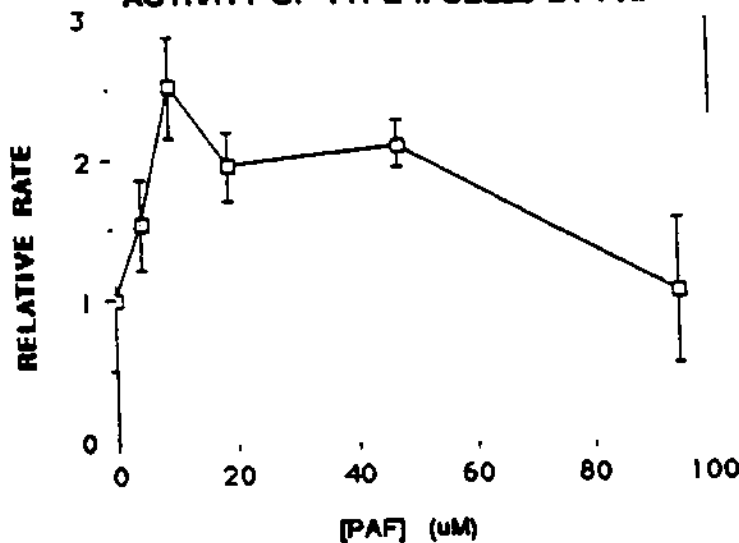
STIMULATION OF CYTOCHROME P450 DEPENDENT
ACTIVITY OF TYPE II CELLS BY PAF

Figure 3. Effect of PAF on cytochrome P450-dependent EtOPhase activity in rat alveolar type II cells. Type II cells were obtained from β -naphthoflavone-treated rats. Cells ($1.6\text{--}2.5 \times 10^6/\text{ml}$) were suspended in 0.1M NaCl , 0.5 mM NADPH , and 0.05 M HEPES ($\text{pH} = 7.8$) at 36°C , a fluorescence baseline established, and the reaction initiated with $2.5\text{ }\mu\text{M EtOPh}$. In the absence of PAF, EtOPhase activity of 3 separate preparations of type II cell was 1.06 , 1.38 , and 0.50 pmoles resorufin formed/min/ 10^6 cells, respectively. Data after addition of PAF are rates relative to these controls (means \pm standard errors).

PAF-INDUCED AGGREGATION OF TYPE II CELLS

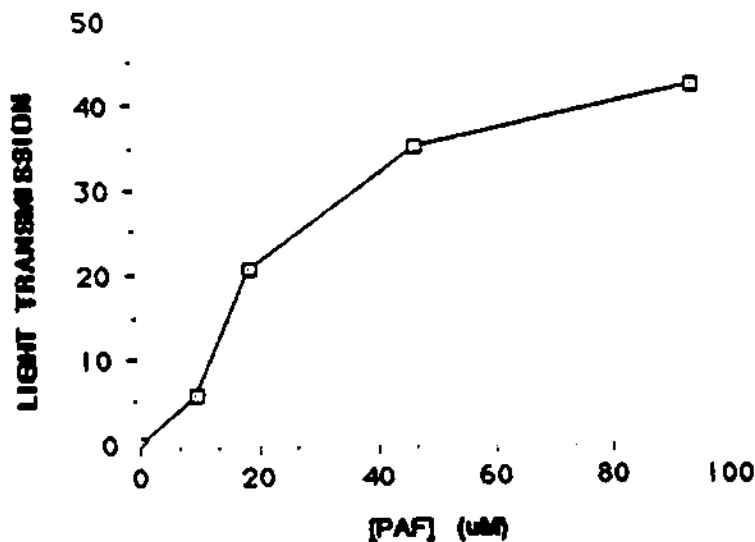


Figure 4. Effect of PAF on aggregation of rat alveolar type II cells. Type II cells were obtained from β -naphthoflavone-treated rats. Cells ($2.5\text{--}2.7 \times 10^6$ cells/ml) were suspended in 0.1M NaCl and 0.05M HEPES ($\text{pH} = 7.8$) at 37°C and aggregation monitored as light transmission. Data are means of two experiments.

PLATELET ACTIVATING FACTOR

REFERENCES

1. Barquet. P., Rola-Pleszczynski. M.: Platelet-Activating Factor and Cellular Immune Responses. *Immunol. Today* 8:345-352 (1987).
2. Benveniste. J., Tence. M., Varenne. P., Bidault. J., Boullat. C., Polonsky. J.: Platelet Activating Factor. *Comptes Rendus hebdomadaire de l'Académie des Sciences Paris* 289D:1037-1040 (1979).
3. Demopoulos. C.A., Pinckard. R.M., Hanahan. D.J.: Platelet Activating Factor. *J. Biol. Chem.* 254:9355-9358 (1979).
4. Stimler. W.P., D'Flaherty. J.T.: Spasmogenic Properties of Platelet-Activating Factor: Evidence for a Direct Mechanism in the Contractile Response of Pulmonary Tissue. *Am. J. Pathol.* 113:75-84 (1983).
5. Lin. A.H., Morton. D.R., Gorman. R.R.: Acetyl Glyceryl Ether Phosphorylcholine Stimulates Leukotriene B₄ Synthesis in Human Polymorphonuclear Leukocytes. *J. Clin. Invest.* 70:1058-1065 (1982).
6. Cuss. F.M., Dixon. C.M.S., Burnes. P.J.: Effects of Inhaled Platelet Activating Factor on Pulmonary Function and Bronchial Responsiveness in Man. *Lancet* ii:189-192 (1986).
7. Pinckard. R.M., Halonen. M., Pulmer. J.D., Butler. C., Shaw. J.O., Henson. P.M.: Intravascular Aggregation and Pulmonary Sequestration of Platelets during IgE-Induced Systemic Anaphylaxis in the Rabbit: Abrogation of Lethal Anaphylactic Shock by Platelet Depletion. *J. Immunol.* 119:2185-2191 (1977).
8. Humphrey. D.M., Hanahan. D.: Induction of Leukocyte Infiltrates in Rabbit Skin by Acetyl Glyceryl Ether Phosphorylcholine. *Lab. Invest.* 47:227-234 (1982).
9. Czarnetzki. B.M., Benveniste. J.: Effect of 1-O-Octadecyl-2-O-Acetyl-sn-Glycerol-3-Phosphocholine (PAF-Acether) on Leukocytes. I. Analysis of the In Vitro Migration of Human Neutrophils. *Chem. Phys. Lipids* 29:317-326 (1981).
10. Benveniste. J., Henson. P.M., Cochrane. C.G.: Leukocyte-Dependent Histamine Release from Rabbit Platelets. *J. Exp. Med.* 136:1356-1377 (1972).
11. Betz. S.J., Henson. P.M.: Production and Release of Platelet-Activating Factor (PAF): Dissociation from Degranulation and Superoxide Production in Human Neutrophils. *J. Immunol.* 125:2756-2763 (1980).
12. Arnoux. B., Duval. B.: Release of Platelet-Activating Factor (PAF-Acether) from Alveolar Macrophages by the Calcium Ionophore A23187 and Phagocytosis. *Eur. J. Clin. Invest.* 10:437-441 (1980).
13. Rylander. R., Beijer. L.: Inhalation of Endotoxin Stimulates Alveolar Macrophage Production of Platelet-Activating Factor. *Am. Rev. Respir. Dis.* 135:83-86 (1987).
14. Jones. G.S., Van Dyke. K., Castranova. V.: Purification of Human Granulocytes by Centrifugal Elutriation and Measurement of Transmembrane Potential. *J. Cell. Physiol.* 104:425-431 (1980).
15. Sweeney. T., Castranova. V., Bowman. L., Miles. P.R.: Factors which Affect Superoxide Anion Release from Rat Alveolar Macrophages. *Exp. Lung Res.* 2:85-96 (1981).
16. Jones. G.S., Miles. P.R., Lantz. R.C., Hinton. D.E., Castranova. V.: Ionic Content and Regulation of Cellular Volume in Rat Alveolar Type II Cells. *J. Appl. Physiol.: Respirat. Environ. Exercise Physiol.* 53:258-266 (1982).
17. Rabovsky. J., Judy. D.J., Sapola. N.A., Pailles. W.H., McPeak. M., Castranova. V.: Cytochrome P450-Dependent Alkoxyphenoxazone Dealkylase Activity in Rat Alveolar Type II Cells: Effect of Pretreatment with 8-Naphthoflavone. *Cell Biochem. Funct.* in press.

THE RESPIRABLE DUST CENTER

18. Castranova. V., Bowman. L., Miles. P.R.: Transmembrane Potential and Ionic Content of Rat Alveolar Macrophages. *J. Cell. Physiol.* 101:471-480 (1979).
19. Castranova. V., Jones. G.S., Miles. P.R.: Transmembrane Potential of Isolated Rat Alveolar Type II Cells. *J. Appl. Physiol.: Respirat. Environ. Exercise Physiol.* 54:1511-1517 (1983).
20. Jones. G.S., Van Dyke. K., Castranova. V.: Transmembrane Potential Changes Associated with Superoxide Release from Human Granulocytes. *J. Cell. Physiol.* 106:75-83 (1981).
21. Van Dyke. K., Matamoros. M., Van Dyke. C.J., Castranova. V.: Calcium Ionophore-Stimulated Chemiluminescence (CL) from Human Granulocytes: Evidence that A23187-Induced Chemiluminescence Originates from Arachidonic Acid Metabolism. *Microchem. J.* 28:568-579 (1983).
22. Van Scott. M.R., Miles. P.R., Castranova. V. Direct Measurement of Hydrogen Peroxide Release from Rat Alveolar Macrophages: Artfactual Effect of Horseradish Peroxidase. *Exp. Lung Res.* 6:103-114 (1984).
23. Castranova. V., Bowman. L., Miles. P.R., Reasor. M.J.: Toxicity of Metal Ions to Alveolar Macrophages. *Am. J. Indus. Med.* 1:349-357 (1980).
24. Castranova. V., Bowman. L., Wright. J.R., Colby. H., Miles. P.R.: Toxicity of Metallic Ions in the Lung: Effects on Alveolar Macrophages and Alveolar Type II Cells. *J. Tox. Environ. Health* 13:845-856 (1984).
25. Lowry. O.H., Rosebrough. N.J., Farr. A.L., Randall. R.J.: Protein Measurements with the Folin Phenol Reagent. *J. Biol. Chem.* 193:265-275 (1951).
26. Castranova. V., Robinson. V.A., Tucker. J.H., Schwegler. D., Rose. D.A., DeLong. D.S., Frazer. D.G.: Time Course of Cotton Dust in Guinea Pigs and Rats. In: Proc 11th Cotton Dust Res Conf. R.R. Jacobs and P.J. Wakelyn (eds). Nat. Cotton Council, Memphis, TN, pp 79-83 (1987).
27. Weibel. E.R.: Morphological Basis of Alveolar-Capillary Gas Exchange. *Physiol. Rev.* 53:419-495 (1973).
28. DeChatelet. L.R.: Initiation of a Respiratory Burst in Human Polymorphonuclear Neutrophils: A Critical Review. *Res J. Reticuloendothel. Soc.* 24:73-83 (1978).
29. Johnston. R.B.: Oxygen Metabolism and the Microbicidal Activity of Macrophages. *Fed. Proc. Fed. Am. Soc. Exp. Biol.* 37:2759-2764 (1978).
30. Weiss. S.J., LoBuglio. A.F.: Biology of Disease: Phagocyte Generated Oxygen Metabolites and Cellular Injury. *Lab Invest.* 47:5-18 (1982).
31. Halliwell. B.: Oxidants and Human Disease: Some New Concepts. *FASEB. J.* 1:358-364 (1987).
32. Minchin. R.F., Boyd. M.R.: Localization of Metabolic Activation and Deactivation Systems in the Lung: Significance of the Pulmonary Toxicity of Xenobiotics. *Ann. Rev. Pharmacol Toxicol.* 23:217-238 (1983).
33. Peterson. T.C., Williams. C.M.: Depression of Peripheral Blood Monocytes Aryl Hydrocarbon Hydroxylase Activity in Patients with Liver Disease: Possible Involvement of Macrophage Factors. *Hepatology* 7:333-337 (1987).
34. Williams. J.F.: Induction of Tolerance in Mice and Rats to the Effect of Endotoxin to Decrease the Hepatic Microsomal Mixed-Function Oxidase System. Evidence for a Possible Macrophage-Derived Factor in the Endotoxin Effect. *Inter. J. Immunopharmac.* 7:501-509 (1985).
35. Woolles. W.R., Munson. A.E.: The Effects of Stimulants and Depressants of Reticuloendothelial Activity on Drug Metabolism. *J. Retic. Soc.* 9:108-119 (1971).

Use of a Sensitive Electro-Optical Method to Quantify Superoxide Release from Single PAM Exposed to Dusts In Vitro or In Vivo: Some Current Experimental and Model Results

E.V. Clento, K.A. DiGregorio and R.C. Lantz
Departments of Chemistry and Anatomy, West Virginia University

This laboratory has developed a sensitive electro-optical method to quantify the initial rate (R) and total amount (MAX) of superoxide (SO) produced by single pulmonary alveolar macrophages (PAM). The method uses a microscope to visualize PAM in culture, and to videorecord the images during the time the cells produce SO. MAX and R are calculated from measurement of temporal changes in optical density in the images due to precipitated diformazan formed by the reaction of SO, produced by each PAM, with nitroblue tetrazolium present in the culture medium. To date, values of R and MAX, measured due to adherence of PAM to the dish, have been compared to values obtained when quartz, coal mine dust (CMD), and kaolin were added to the medium (in vitro). R and MAX have also been calculated for PAM lavaged from animals exposed to quartz and CMD in the WVU Inhalation Facility. Presently, experiments are being done using serum which permits PAM to be restimulated by different dusts to help establish a dose-response effect, and a means to study the effects of lung surfactant on modifying the toxicity of inhaled dusts. Long term, this methodology should provide useful insight into establishing the role SO plays in the phagocytosis of inhaled dusts and bacteria, in PAM dysfunction, and in lung diseases such as pneumoconioses. Supported by the Department of the Interior's Mineral Institute Program administered by the Bureau of Mines through the Generic Mineral Technology Center for Respirable Dust (G1135142).

A Kinetic Model of Superoxide Production from Single Pulmonary Alveolar Macrophages

E.V. Cilento, K.A. DiGregorio and R.C. Lantz

Departments of Chemistry and Anatomy, West Virginia University

A kinetic model was developed to describe the production of superoxide (O_2^-) by single pulmonary alveolar macrophages (PAM). Model predictions were compared to experimental results obtained from single rat PAM. The O_2^- was quantified by measuring the reduction of nitroblue tetrazolium (NBT)² to a diformazan precipitate (NBTH₂) from video-recorded images of individual cells. The kinetic model considered three reactions: (1) the production of extracellular O_2^- from the reduction of oxygen by NADPH oxidase using intracellular NADPH as the substrate, (2) the subsequent dismutation of O_2^- to form H_2O_2 , and (3) the reaction of O_2^- and NBT. NBT specificity for O_2^- was analyzed by comparing results in the presence and absence of superoxide dismutase (SOD) which catalyzes the dismutation of O_2^- to H_2O_2 . Measured PAM heterogeneity was accounted for by varying the concentration of intracellular NADPH, its rate of depletion, and the concentration of intracellular NADPH oxidase in the kinetic model. Model predictions compared favorably with experimental results except when SOD was present. This discrepancy may be due to diffusional limitations since NBT is a relatively small molecule (818 MW) compared to SOD (34000 MW). In addition, the cell surface is both ruffled and negatively charged, which may introduce steric hindrances and/or electrostatic effects since SOD is also negatively charged.

ACKNOWLEDGEMENTS

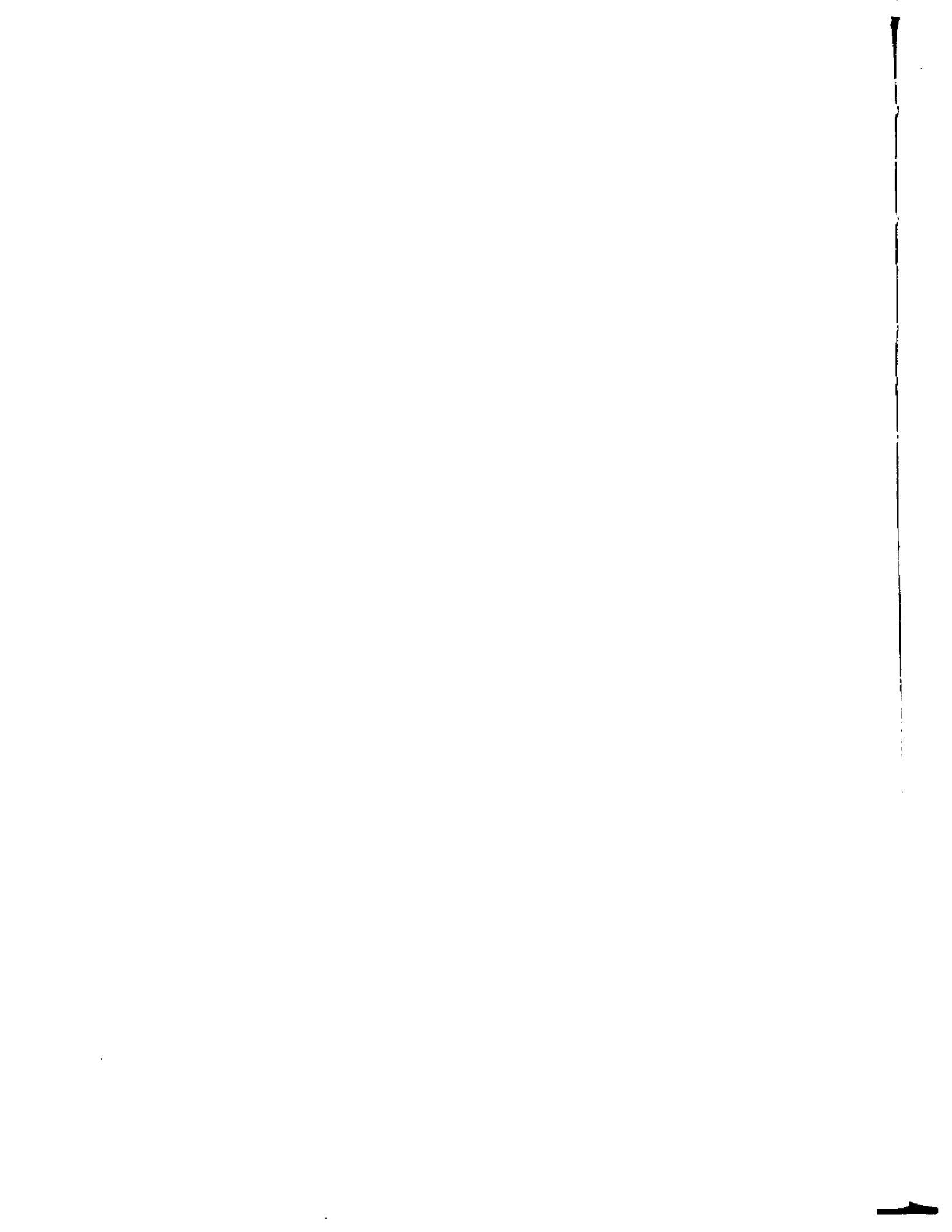
This research has been supported by the Department of the Interior's Mineral Institute program administered by the Bureau of Mines through the Generic Mineral Technology Center for Respirable Dust under grant number G1135142.

Effects of Serum on Superoxide Release from Single Pulmonary Alveolar Macrophages

K.A. Digregorio, E.V. Cilento, and R.C. Lantz
Departments of chemical Engineering and Anatomy,
West Virginia University, Morgantown, WV

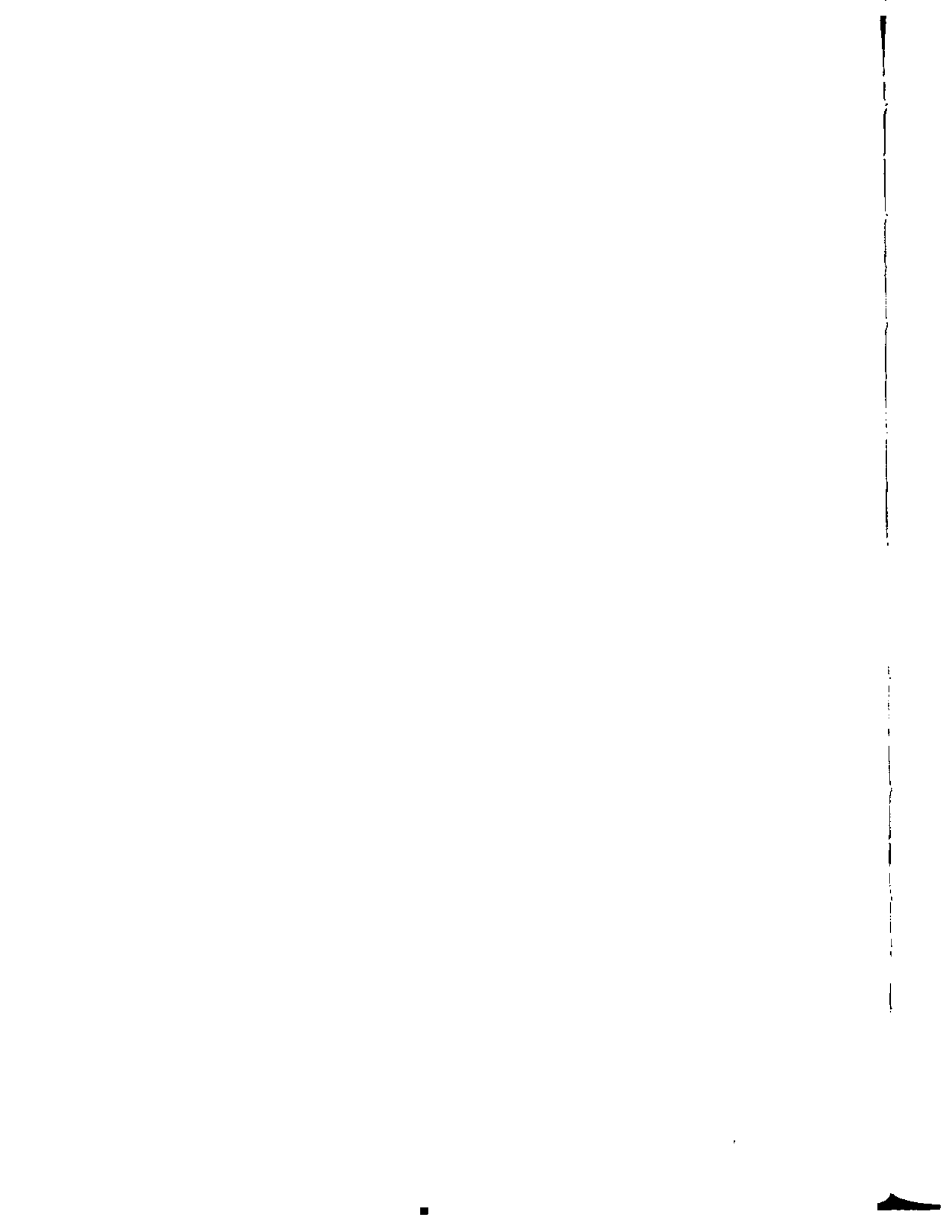
Pulmonary inflammation is accompanied by increased microvascular permeability and leakage of plasma into alveolar spaces. Serum has been shown to affect superoxide (O_2^-) production from pulmonary alveolar macrophages (PAM) in vitro, and in some cases serum has been shown to be necessary for stimulation of PAM. An electro-optical method was used to measure O_2^- production from single PAM by measuring the reduction of nitroblue tetrazolium (NBT) to a diformazan precipitate (NBTH₂) from videorecorded images of individual cells. PAM were stimulated by their initial attachment to culture dishes independent of serum. The addition of 2% serum to the culture medium increased NBTH₂ production during attachment, whereas concentrations of 5 and 10% serum had no additional effect. In contrast, PAM incubated for 2 hrs could not be stimulated by phorbol myristate acetate (PMA) or zymosan particles to produce O_2^- unless serum was present during the incubation and/or stimulation; however, NBTH₂ production was similar in all cases of serum addition. Also, serum alone did not stimulate adherent PAM indicating that serum is necessary but not sufficient for stimulation of attached PAM. These results suggest that changes in microcirculatory permeability may have a pronounced effect on superoxide production by PAM and that serum may help regulate or condition these cells during inflammation of the lung. (Supported by USBOM G1135142.)

Submitted December 1987, for presentation at Microcirculatory Society Meetings. [WV09-9]



V

**RELATIONSHIP OF MINE
ENVIRONMENT, GEOLOGY AND
SEAM CHARACTERISTICS TO DUST
GENERATION AND MOBILITY**



An Analysis of the Mass-Size Distribution of Airborne Coal Mine Dust in Continuous Miner Sections

C. Lee¹ and J. Mutnansky²

¹ University of Korea

² Department of Mineral Engineering,
The Pennsylvania State University

Abstract

The size distribution of coal mine dust is one of its most important characteristics because the particle size is known to govern the region of deposition of dust within the human respiratory tract. In addition, dust characteristics, particle settling rate, transportability of the dust and the efficiency of dust control measures are all affected by the particle size. As a result, particle size distribution of the airborne dust in a coal mine is a fundamental property that impacts on the health of underground workers.

This paper deals with some basic findings on the size distribution of coal mine dust based upon the results of data collection in six underground coal mines using continuous miners. All airborne dust sampling was performed on development sections using eight stage cascade impactors and permissible 2.0 l/min pumps. Samplers locations were fixed in the sections with respect to the continuous miner and roofbolter or with respect to the intake and return airways. Sampling times varied from 45 minutes to 6 hours, depending upon the dust concentration.

The first topic of analysis was the test to determine whether the commonly used lognormal distribution is valid when applied to airborne coal mine dust. Secondly, the conventional method of representing the distribution using two parameters, the geometric mean and the geometric standard deviation, is questioned. Since almost all size data were found to show some degree of bimodality, the two parameter lognormal distribution may not represent the total airborne coal mine dust size, quite adequately. Bimodal lognormal distribution was tested to be a good approximation in the case with two modes in the size distribution.

The final topic discussed in this paper is the locational variation of the airborne dust size distributions within the continuous mining section. The size distributions varied considerably at the different sampling locations with the continuous miner and roofbolter producing the coarser distributions. Fine size modes in the range of 2 to 4 μ m including mostly respirable dust particles were present in almost all samples. Second dust generating sources such as the shuttle car movement were found to be major causes of high respirable dust concentrations in some cases.

THE RESPIRABLE DUST CENTER

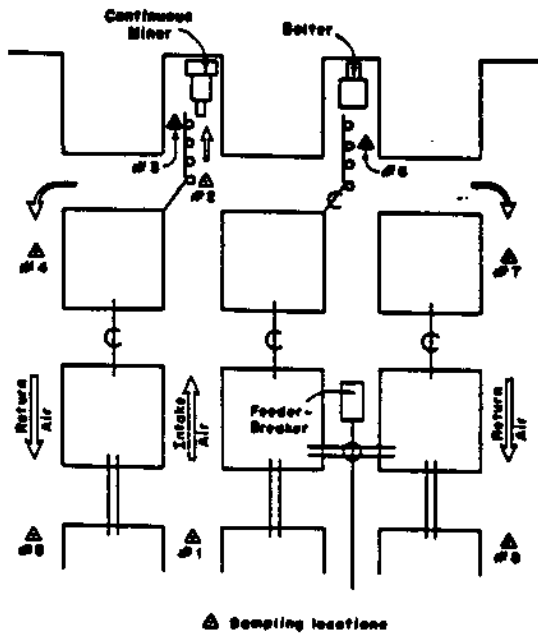
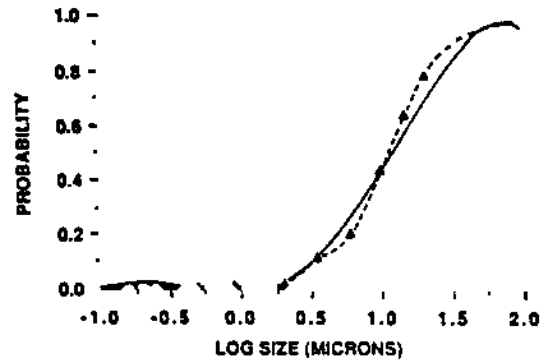
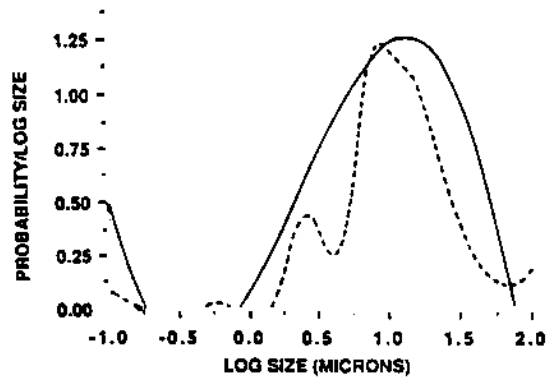


Fig. 1. Sampling locations for a continuous miner development section using line brattices

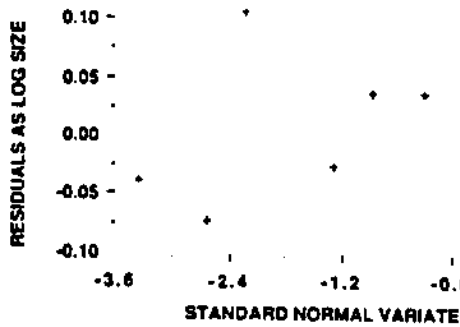


a. Cumulative mass size distributions.

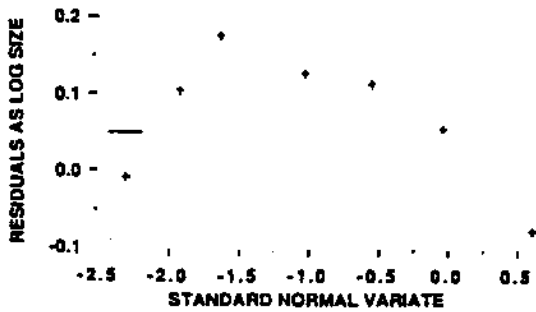


b. Mass size frequency distributions.

Fig. 2. Cumulative mass size distributions approximated by Chebychev approximation function (solid line) and Cubic-Spline interpolation (dotted line) and their corresponding frequency distributions



a. Random variation of the residuals.



b. Curvilinear variation of the residuals.

Fig. 3. Residual analysis for the lognormality test.

Table 1. Size distributions of the two dust samples from roofbolter operations

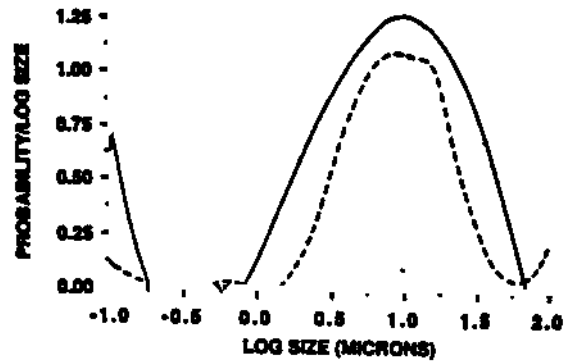
Cut size (μm)	Finer than	
	Sample A (%)	Sample B (%)
21	84.84	86.95
15	70.83	83.74
10	52.21	80.53
6	28.95	59.55
3.5	10.21	31.19
2.0	2.05	5.48
0.9	1.23	2.46
0.5	0.94	0.95

ANALYSIS OF DUST IN CONTINUOUS MINER SECTIONS

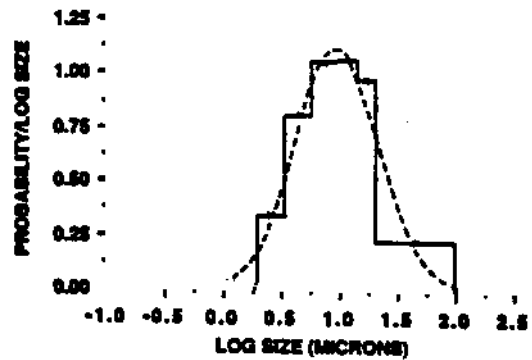
Table 2. Results of the size analyses of the two dust samples from roofbolter operations

Results	Sample A	Sample B
Residual Analysis	Linear	Curvilinear
Empirical Distribution		
Modal Values (μm)		
1. Chebychev Approximation	M 1 = 10.96	M 1 = 4.37
2. Spline Interpolation	M 1 = 7.94	M 1 = 3.12
	M 2 = 15.49	M 2 = 19.50
Lognormal Distribution		
1. Unimodal	GM = 9.91	GM = 4.22
	GS = 2.29	GS = 1.95
	$s'_{mod} = 0.02$	$s'_{mod} = 0.21$
2. Bimodal	GM1 = 5.02	GM1 = 4.24
	GS1 = 1.68	GS1 = 1.82
	% 1 = 0.35	% 1 = 0.86
	GM2 = 14.40	GM2 = 30.31
	GS2 = 1.89	GS2 = 1.41
	$s'_{mod} = 0.01$	$s'_{mod} = 0.06$

- Notes: (1) M denotes the modal value.
 (2) GM and GS denote the geometric mean and standard deviation, respectively.
 (3) Subscripts 1 and 2 denote the first and second modes, respectively.
 (4) %1 denotes the mass percentage of the first mode.
 (5) The unit of the geometric mean is micron.

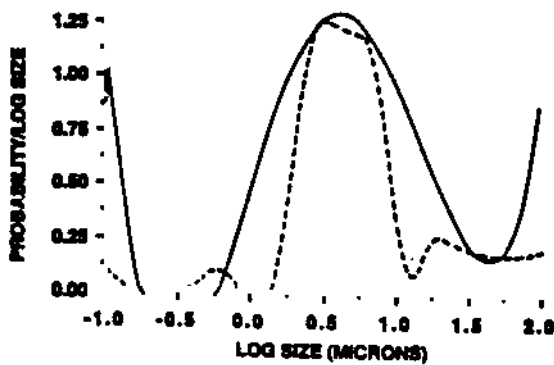


a. Empirical frequency distributions.

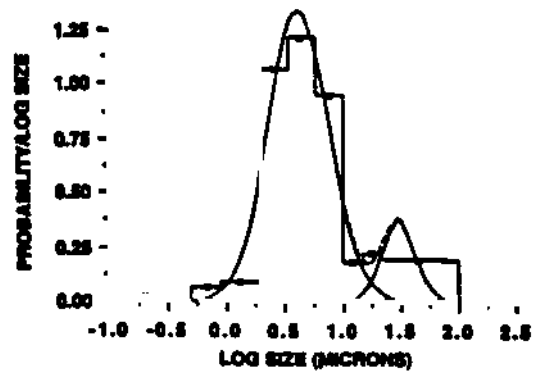


b. Lognormal frequency distributions.

Fig. 4. Empirical and lognormal distributions of sample A



a. Empirical frequency distributions.



b. Lognormal frequency distributions.

Fig. 5. Empirical and lognormal distributions of sample B

참 고 문 헌

- 1) Heyder, J., Gebhart, J., and W. Stahlhofen, 1980, Inhalation of Aerosols : Particle Deposition and Retention : Ch. 3 in Generation of Aerosols, K. Willeke, Ed., Ann Arbor Science, Ann Arbor, MI.
- 2) Jayaraman, N. I., Schroeder, W. E., and F. N. Kissel, 1986, Studies of Dust Knockdown by Water Sprays Using a Full - Scale Model Mine Entry : Society of Mining Engineers of AIME, Transactions, Vol.278, pp. 1875-1882.
- 3) Grigal, D., Ufken, G., Sandstedt, J., Blom, M., Johnson, D., 1982, Development of Improved Scrubbers for Coal Mine Applications : Final Report, U. S. Bureau of Mines Contract No. H 0199055 Donaldson Co. Inc.
- 4) Burkhart, J. E., McCawley, M. A., and R. W. Wheeler, 1983, Particle Size Distributions in Underground Coal Mines : A paper presented at American Industrial Hygiene Association Conference, Philadelphia, PA.
- 5) Lee, C., and J. M. Mutmanky, 1986, A Strategy for Coal Mine Respirable Dust Sampling Using Multi - Stage Impactors for Characterization Purpose : Proceedings of the Symposium on Engineering Health and Safety in Coal Mining; A. W. Khair, Ed., Society of Mining Engineers of AIME, Littleton, Co.
- 6) Deepak, A., and G. P. Box, 1982, Representation of Aerosol Size Distribution Data by Analytical Methods : Atmospheric Aerosols : Their Formation, Optical Properties and Effects. A. Deepak, Ed., Spectrum Press, Hampton, VA.
- 7) Whitby, K. T., 1974, Modeling of Multimodal Aerosol Distributions : Proceedings of the 1974 Conference on Aerosols in Nature, Medicine and Technology, Vorderhinderland, FRG.
- 8) Sinclair, A. J., 1976, Application of Probability Paper in Mineral Exploration : Special Volume No.4, Association of Exploration Geochemists, Amsterdam, Netherlands.
- 9) Coenen, W., 1966, Staub, Vol. 26(Title and particulars of reference unavailable).
- 10) Knutson, E. O., and P. J. Lioy, 1983, Measurement and Presentation of Aerosol Size Distributions : Air Sampling Instruments for Evaluation of Atmospheric Contaminants, American Conference of Governmental Industrial Hygienists, Cincinnati, OH., pp. G.1- G.12.
- 11) Willeke, K., Whitby, K. T., Clark, W. E. and V. A. Marple, 1974, Size Distribution of Denver Aerosols - A Comparison of Two Sites Atmospheric Environment, Vol.8, pp. 609-633

A
C
L

C.J
Dep
The

Th
seve
non-
cord
the
of t
Al
leve
ical
With
cate
the
dust
mine
from

A Comparative Analysis of the Elemental Composition of Mining-Generated and Laboratory-Generated Coal Mine Dust

C.J. Johnson and C.J. Bise
Department of Mineral Engineering,
The Pennsylvania State University

The occurrence of Coal Worker's Pneumoconiosis (CWP) has been potentially linked with several characteristics of coal such as rank, volatility, percent content of ash and non-coal components, quartz content, and the presence of several trace elements. According to the National Research Council, numerous epidemiological studies indicate that the incidence of CWP varies significantly with the composition and/or the concentration of the coal mine dust.

Although advances in dust suppression techniques have markedly reduced respirable dust levels in underground coal mines, the National Research Council has concluded that chemical characteristics of respirable dust from different coal seams should be studied. With this objective in mind, research has been conducted in underground coal mines located in the eastern and midwestern United States, and in the laboratory to characterize the elemental composition of mining-generated airborne dust and laboratory-generated dust derived from samples taken from these mines. The goal of the research is to determine if a relationship exists between mining-generated and laboratory-generated dust from the same mine. Results of this research will be presented.

Seeking the "Rank Factor" in CWP Incidence: The Potential Role of Respirable Dust Particle Purity

R. L. Grayson, R. Andre, and T. Simonyi
West Virginia University,
Morgantown, WV

Results from research directed at determining the reason(s) for the "rank factor" in correlations between coal workers' pneumoconiosis incidence and coal seam of employment are presented. Using compliance dust samples collected from two longwall panels operating in coal seams of widely different rank, respirable particles were identified by mineral species under manual scanning electron microscope (SEM) energy dispersive x-ray (EDX) analysis and then further characterized by their physical diameter, general shape, and periphery angularity. Size fractional, mineralogical variations are presented.

Of primary significance, the percentage of mineral particles from the higher rank coal seam that were uncontaminated by non-stoichiometric elements for a specific mineral species was twice that of those in the lower rank seam. The relationship held for each mineral species, including quartz. This fact may form the basis for the "rank factor" known to exist as well as provide a reason for the contradictory role of quartz and other minerals in previous CWP studies.

An important subsequent research priority is now focusing on determining the percentage of all respirable dust particles that are minerals versus single-phase organic or multi-phase organic-inorganic complexes. This effort will be accomplished using automated SEM-EDX. The mineral purity factor will be developed further, but additional emphasis will be focused on determining the extent of inorganic inclusions in organic particles.

Mineral Content Variability of Coal Mine Dust by Coal Seam, Sampling Location, and Particle Size

T.J. Stobbe, H. Kim, and R.W. Plummer
Department of Industrial Engineering,
West Virginia University

The probability of developing coal workers' pneumoconiosis (CWP) varies among miners in different geographic areas, coal seams, and jobs. Many studies have revealed the correlation between mineral content and the frequency and severity of CWP development still remains controversial. Furthermore, the mineral content and its variability in different areas is unknown.

Since mineral content is expected to vary from location to location within a mine, between mines, between coal seams, and over time, this information will be valuable in understanding the variations in CWP incidence, as well as in establishing the appropriate kinds of dust to use in toxicological research programs studying CWP.

Size-selective airborne dust samples were collected using 4-stage cassette impactors at 9 different locations in each of five coal seams. These coal seams were the Upper Freeport, Pittsburgh, Kittaning, Coal Burg, and Pocahontas. Mineralogical analyses were done by a x-ray powder diffraction photographic technique.

Common minerals found in coal mine dust were illite, calcite, kaolinite, quartz, siderite, dolomite, gypsum, anhydrite, and pyrite. The distribution of minerals in inter- and intra location samples will be reported. Early results on the mineral content show wide variations between locations in a mine and between coal seams, and small, but significant, variations between particle sizes.

INTRODUCTION

In spite of its long history of incidence, and the large amount of research conducted on it, coal workers' pneumoconiosis (CWP) is still prevalent among coal miners and needs further research to develop effective preventive and remedial measures. Although the dose-response relationship between simple CWP and coal mine dust has been established (1), the causal agent(s) and the mechanism(s) involved in the progression of simple to complicated CWP are not yet defined. Many plausible hypotheses have been made to explain the mechanisms involved in the disease progression, however, none of them is satisfactory. In addition, the source of variation in occurrence of CWP among miners in different geographic areas (2), rank of coal seam (3,4), and job (5) remain unsolved.

As a result, more epidemiological and medical efforts have been directed toward identifying the causal agent(s) by investigating the physical and chemical properties of coal mine dust. Among the

THE RESPIRABLE DUST CENTER

many factors investigated, the mineralogical composition has received attention because past epidemiological and post-mortem lung tissue studies have shown some correlation with the prevalence and severity of CWP and the quantity and type of minerals found in the coal mine dust. (6 - 8) Such findings have inspired many toxicological studies designed to assess toxicity of coal minerals in vivo and in vitro. These investigations have reported toxicity of coal minerals although contradictory toxicological results on the toxicity of each mineral by itself and in combination have been reported. (9 - 12)

Although these studies have provided us useful medical and toxicological information of coal minerals, some of them should be interpreted cautiously because the experimental settings used may not be comparable to actual mine situations. Furthermore, the studies provided little or no information about the "dust" used (i.e., dust size, mineral content, etc.). A recent review of one hundred toxicological studies and experiments designed to assess the health effects of exposure to coal and coal related minerals (13) revealed that, in many cases (43 %), the geographic location where the test substance was obtained was not reported. Rarely was a specific seam or mine identified. The review also disclosed that many studies (67 %) did not list how the test substance was obtained or created. Among those preparation methods reported, grinding or crushing of bulk coal samples was the main preparation technique used (22 %). It was followed by collecting airborne mine dust at the coal face or in the return airway. Compounding the interpretation problem is the fact that the mineral composition of the dust was not incorporated for assessing dust toxicity in the majority of studies. In addition, most studies concentrated on evaluating the toxicity of a limited number of minerals and were not designed to assess the interaction of those minerals found in coal mine dust.

It is clear that toxicological studies designed to evaluate the effect of coal mine dust with different mineral combinations and concentrations are currently lacking because the mineral content as well as variability of coal mine dust has not been defined. Therefore, the purpose of this research was to identify the mineral matter contained in coal mine dust, to establish the variability of each mineral, and to find those factors that affect mineral content changes so that the results can be used as the basis of dust selection in toxicological research.

EXPERIMENTAL PROCEDURE

Sampling Location

Details of the sampling methodology have been reported previously. (14, 15) Thus, only a brief summary is provided here. Six working sections from five mines, one section from each of four mines and two sections in one mine, located in the Appalachian bituminous coal field were investigated. In each mine, dust samples were collected at nine different locations on a continuous mining section. These locations include: the intake

ANALYSIS OF DUST IN CONTINUOUS MINER SECTIONS

airway, the dinner hole, immediately before and after the continuous miner, immediately before and after the roofbolter, the feeder, the haulageway, and the return airway. These locations were selected such that the researchers could monitor the contribution of mining activities to the changes observed in the mineral content of the dust in the mine air as it moves from the intake side of the face to the return side. These locations are illustrated in Figure 1.

Sampling Equipment

Dust samples were collected using 4-stage cassette impactors. They were designed and constructed using a modification of an original design described by Jones et al. (16) Figure 2 shows the exploded view of the cassette impactor. Aluminum foil was used as the collection substrate for stages 1 to 4 and a standard 37 mm, 5 um pore size, polyvinyl chloride (PVC) membrane filter was used for the last stage. The aluminum substrates were brush coated with a mixture of Apiezon L grease and toluene to reduce particle bounce. Sampling was done at a flow rate of 5 liters per minute (LPM) to improve dust collection efficiency by increasing the Reynolds number (Re). The flow rate was maintained with three MSA Model G air sampling pumps connected with tubing and Y-connectors

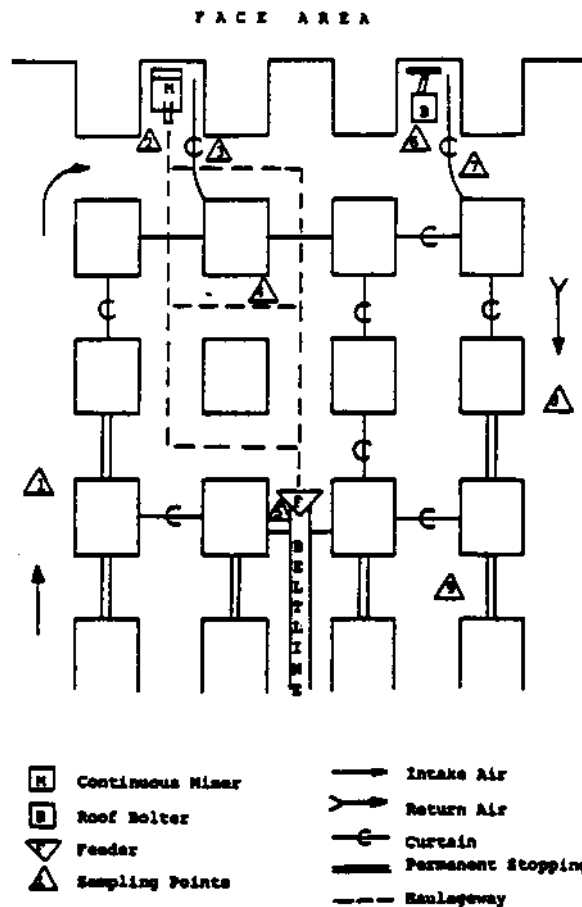


Figure 1. A Typical Continuous Mining Section Layout and the Sampling Locations Selected for the Study

THE RESPIRABLE DUST CENTER

to a pre-calibrated precision rotameter. Figure 2 also shows the in-mine dust sampling equipment arrangement.

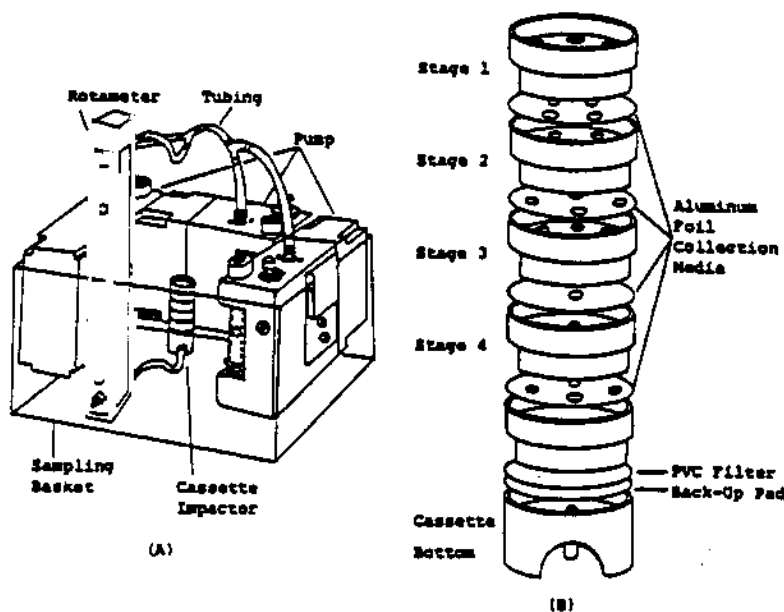


Figure 2. (A) Assembled in-mine Sampling Arrangement
Showing the Pumps, Tubing, and Impactor

(B) Exploded View of the Cassette Impactor

Analysis

The analytical method used for the characterization of the mineral content of the dust samples was X-ray diffraction powder photography. The X-ray machine used was a Norelco X-ray generator type 12045/3 manufactured by North American Philips Electronic Instruments. The camera used was a Debye-Scherrer geometry camera of 114.6 mm diameter. The diffraction pattern was recorded on Kodak diagnostic, direct exposure DEF 329, GBX-2 film. Dust samples were mounted onto a thin glass spline mounted in wax on a copper stud. The sample to be X-rayed was placed into the camera which was then mounted on the X-ray generator. The aligned, rotating sample was exposed to copper Ka radiation monochromated with an Ni filter for 5 hours. The X-ray unit was operated at a voltage of 35 kilo-volts at 20 milliamperes. Each mineral was identified from the location of its diffraction line by comparing the film spectrum with the spectral data reported in the American Society of Testing Materials (ASTM) Powder Data File. Semi-quantitative estimation of the minerals present in the dust sample was accomplished by measuring the intensity of the diffraction lines and using weighting factors to compensate for the differences in the diffraction intensity of individual minerals. In this procedure, the intensity of each mineral was

ANALYSIS OF DUST IN CONTINUOUS MINER SECTIONS

measured from the developed X-ray films using a micro-photodensitometer. The height of each peak was measured after the estimated background which occurs primarily because of the grease and the organic coal dust matrix was subtracted. The raw intensities were then multiplied by weighting factors determined by Renton. (17) Mineral percentages were then calculated using the sum of weighted intensities as the denominator.

RESULTS AND DISCUSSION

Mineral matter here is defined as the inorganic and discrete mineral grains. In this study, only those minerals commonly found with relatively high abundance ($> 0.1\%$) were analyzed.

The minerals identified in the airborne coal mine dust samples were calcite, illite, kaolinite, quartz, siderite, dolomite, gypsum, anhydrite, and pyrite. The term illite describes an illite dominated mixed layered clay. The distribution of each mineral is depicted in Figure 3. Among these minerals, illite was the most dominant consisting of $43\% \pm 22\%$ of the mineral matter found in the samples collected. The other major mineral was calcite which amounted to $28\% \pm 24\%$ of the sample material. Similarly, kaolinite accounted for $9\% \pm 8\%$ of the sampled material, while quartz accounted for $4\% \pm 4\%$. For these four minerals, the coefficient of variation (CV) ranged from 0.5 to 1.0. This is indicative of the very high variability found in the mineral content of coal mine dust. Other minor minerals, with

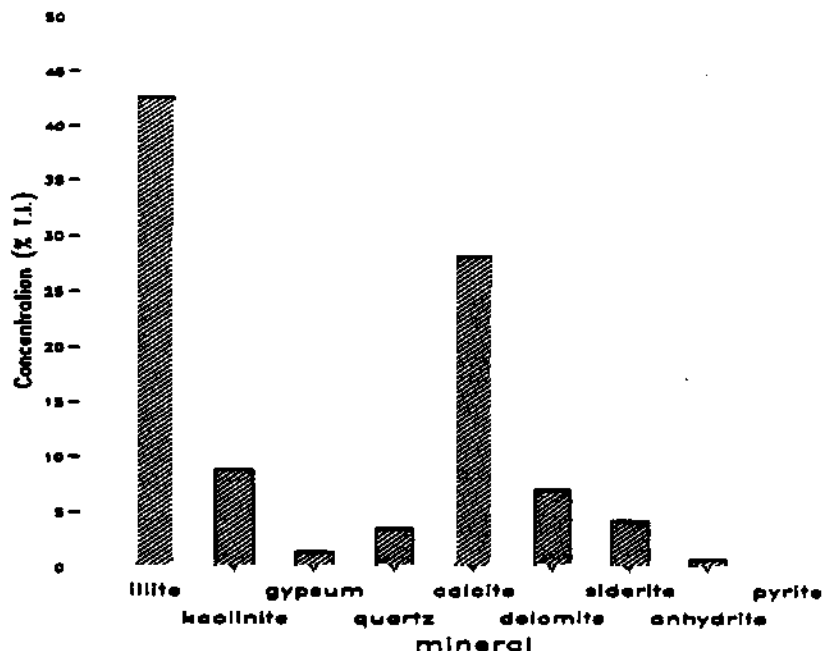


Figure 3. Overall Mineral Content Distribution of the Appalachian Bituminous Coal Field

THE RESPIRABLE DUST CENTER

concentrations ranging from 1 to 10 %, included dolomite, siderite, and gypsum. The CVs for these minerals ranged from .68 to 1.47. Trace minerals with less than 1 % concentration were anhydrite and pyrite.

In order to find factors affecting mineral content changes, the data were analyzed by a two-level nested-crossed analysis of variance (ANOVA). Subsequently, differences in mean values were evaluated using the Duncan's Multiple range Test. The ANOVA revealed that the coal seam factor was the cause of significant changes in mineral content for almost all minerals in the coal mine dust sampled in the region. Two exceptions were gypsum and siderite. A statistically significant high percentage of illite was found in the Coalburg seam while the lowest concentration was found in the Pittsburgh seam. Distribution patterns similar to that of illite were also observed for kaolinite and quartz. The distribution pattern for calcite, however, was almost opposite the patterns observed for the silicate minerals. Calcite content was the highest in the Pittsburgh seam while the lowest concentration was found in the Pocahontas and the Coalburg seams. In the case of such minerals as dolomite, anhydrite, and pyrite, they were more coal seam specific. The Pocahontas seam contained a significantly high (about 4 to 7 times) percentage of dolomite while more anhydrite was found in the Coalburg seam. Reportable amounts of pyrite were found only in the Upper-Freeport and the Pocahontas seams. The distribution of mineral content by coal seam is provided in Figure 4.

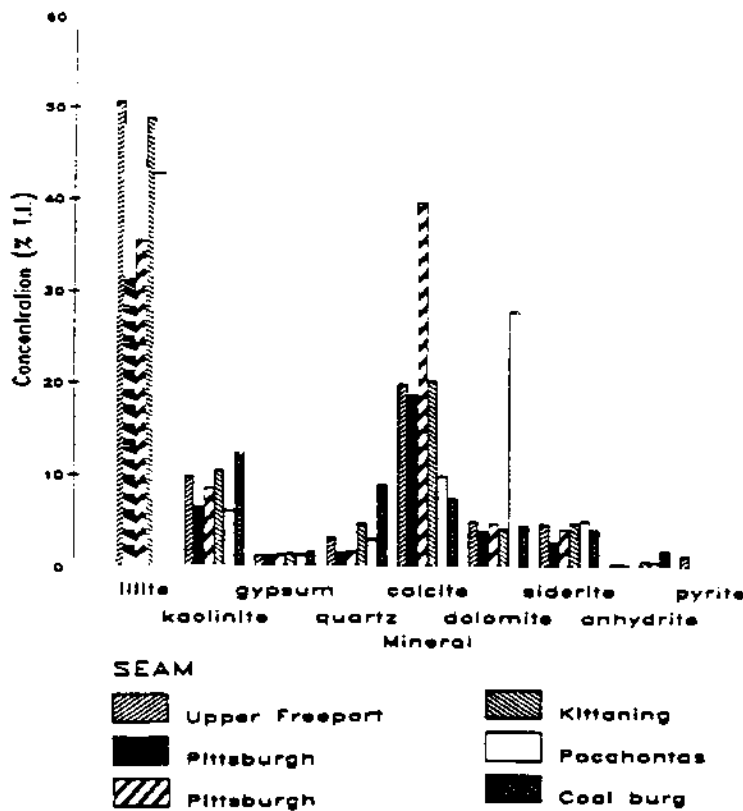


Figure 4. Mineral Content Distribution by Coal Seam

ANALYSIS OF DUST IN CONTINUOUS MINER SECTIONS

The working sections within a mine did not cause significant mineral content changes. No statistically significant changes in mineral content were observed between two working sections within a mine located in the Pittsburgh seam for all minerals except calcite. Similarly, the overall effect of sampling location on mineral content was not statistically significant. Although no statistically significant difference was found, some trends were observed. The distribution of mineral content by sampling location is illustrated in Figure 5. High percentages of illite, kaolinite,

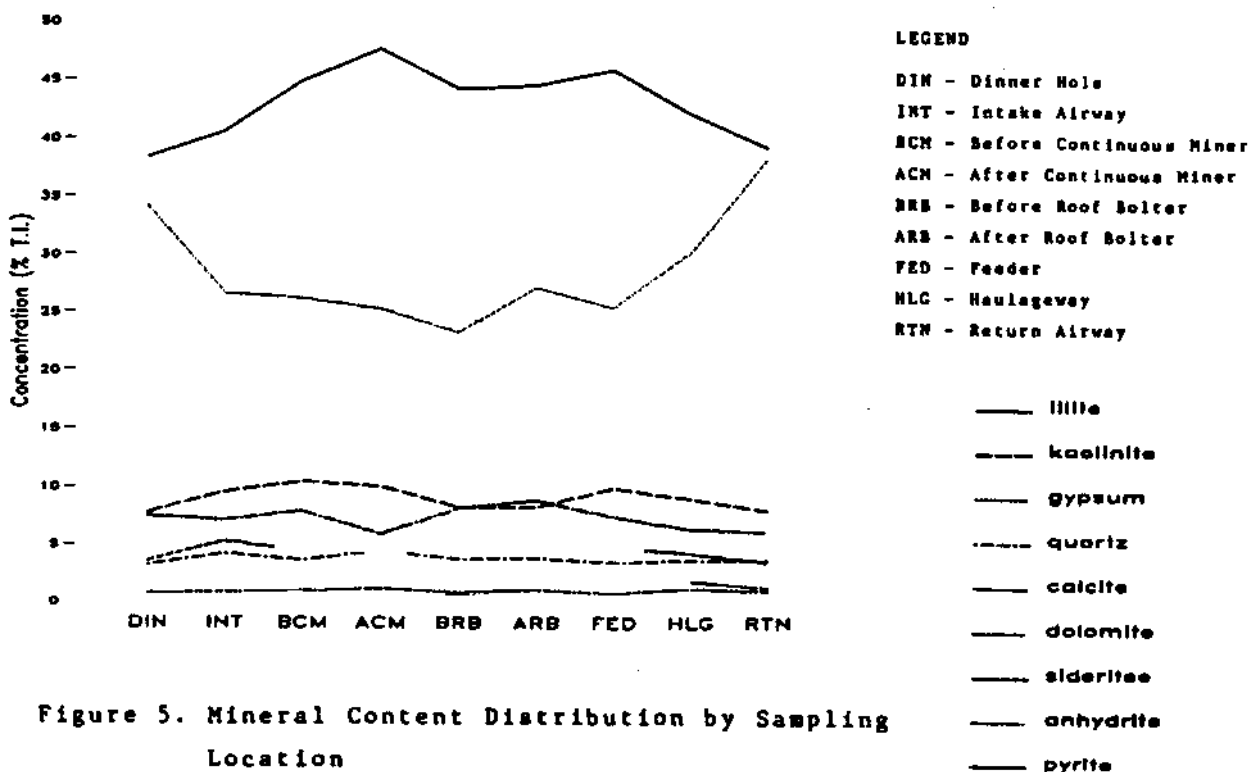


Figure 5. Mineral Content Distribution by Sampling Location

and quartz in the samples collected near the continuous miner were observed while their concentrations were low in the samples collected in the return airway. Illite and kaolinite percentages were also relatively high in the feeder area. These results suggest that coal cutting and dumping liberates those minerals contained in coal. Their concentration then decreases as they gradually mix with other minerals as the mine air travels to the return airway. Quartz and siderite were relatively rich in the intake air samples while dolomite was found in the samples from near the roofbolter. Calcite content was the lowest in the coal producing area and the highest in the samples from the return air followed by the samples from the dinner hole. No particular patterns were observed for gypsum, anhydrite, and pyrite.

The distribution of mineral content by particle size is provided in Figure 6. The results of the ANOVA showed significant size effects on the mineral content for all minerals except kaolinite

THE RESPIRABLE DUST CENTER

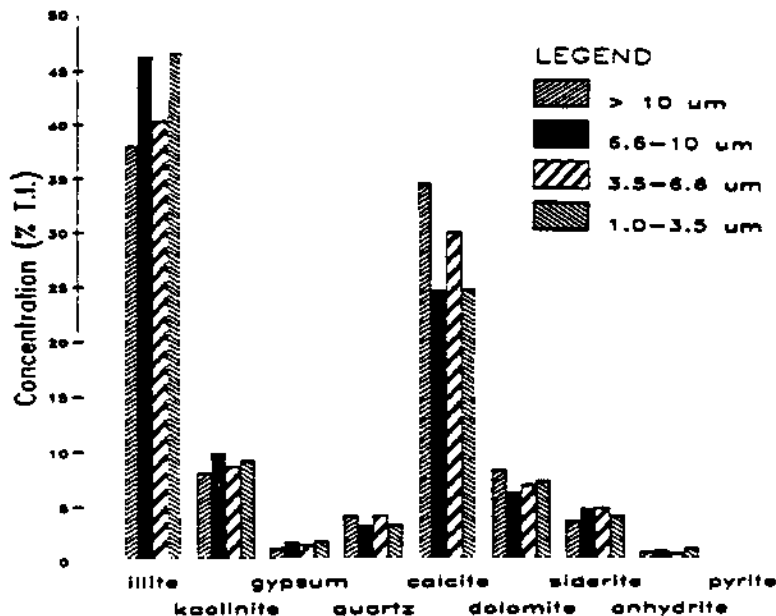


Figure 6. Mineral Content Distribution
by Particle Size

and pyrite. Subsequent analysis showed that the illite concentration was the highest in the size range of 1 to 3.5 μm followed by the size range of 6.6 to 10 μm . The pattern for gypsum was similar to that of illite. For calcite, the trend was exactly opposite of the illite pattern. The highest concentration was found at the top stage (over 10 μm) followed by the third stage (3.5 to 6.6 μm). The pattern for quartz was similar to that of calcite although the highest concentration was observed on the third stage. Dolomite content was the highest on the top stage while no statistically significant difference in mineral content was found among the rest of the stages. The trend for siderite was exactly opposite of that of dolomite. Although some patterns of mineral content change as a function of particle size were observed, no general relationship was established.

CONCLUSIONS

This research identified nine common minerals associated with coal mine dust in samples collected on continuous mining section in the Appalachian Bituminous coal field. Among these minerals, illite and calcite followed by kaolinite and quartz are the dominant minerals. The relative abundance of all minerals except siderite and gypsum, however, is coal seam specific. This indicates the existence of coal seam variability. Also, mineral content was affected by particle size although no general relationship was established. The influence of sampling location upon changes in mineral content proved to be minimal. Likewise, no statistically significant difference was found between two working sections within a mine. However, significant variations in particle size distribution and respirable dust concentration were observed between sampling locations.

ANALYSIS OF DUST IN CONTINUOUS MINER SECTIONS

The results of this research clearly indicate that mineral content is highly variable and dependent upon coal seam and particle size. Therefore, it is clear that much of the previous medical and toxicological research on coal mine dust and CWP, which failed to consider, evaluate, and report the size specific mineral content of the administered dust can supply only limited information about the causal relationship between CWP and coal mine dust. This has left significant gaps in our knowledge of CWP causation and is at least to some degree, responsible for the conflicting results obtained by some of the past research. Thus, it is imperative that future research of this kind should carefully consider the physical and chemical nature of the "dust" used, and report in detail on the "dust" source, preparation method, and nature. This will allow appropriate interpretations to be drawn from the results, and subsequent research can be based upon it.

REFERENCES

1. Jacobsen, M., Rae, S., Walton, W.H., and Rogan, J.M.: The Relation Between Pneumoconiosis and Dust-Exposure in British Coal Mines. Inhaled Particles III, Ed. by W.H. Walton, pp 903-919. The Gresham Press, Old Woking, Surrey, England (1971).
2. Morgan, W.K.C., Burgess, D.B., Jacobson, G., O'Brien, R.J., Pendergrass, E.P., Reger, R.B., And Shoub, E.P.: The Prevalence of Coal Workers' Pneumoconiosis in U.S. Coal Miners. Arch. Env. Health. 7: No.4:221-226 (1973).
3. Dessauer, P., Baier, E.J., Crawford, G.M., and Beatty, J.A.: Development of Patterns of Coal Workers' Pneumoconiosis in Pennsylvania and Its Association with Respiratory Impairment. Ann. N.Y. Acad. Sci. 200:220-251 (1972).
4. McBride, W.E., Pendergrass, E.P., and Lieben, J.: Pneumoconiosis Study of Pennsylvania Anthracite Miners. J. Occup. Med. 8:365-376 (1966).
5. Lainhart, W.S., and Morgan, W.K.C.: Extent and Distribution of Respiratory Effects. Pulmonary Reactions to Coal Dust pp 29-56. Academic Press, New York (1971).
6. Walton, W.H., Dodgson, J., Hadden, G.G., and Jacobson, M.: The Effect of Quartz and Other Non-Coal Dusts in Coal Workers' Pneumoconiosis. Inhaled Particles IV Ed. by W.H. Walton, pp 669 - 690. Pergamon Press, Oxford (1977).
7. Spink, R., and Nagelschmidt, G.: Dust and Fibrosis in the Lungs of Coal Workers from the Wigan Area of Lancashire. Brit. J. Ind. Med. 20:118-123 (1963).
8. Davis, J.M.G., Ottery, J., and Anne LeRoux: The Effects of Quartz and Other Non-Coal Dusts in Coal Workers' Pneumoconiosis. Inhaled Particles IV, Ed. by W.H. Walton, pp 691-702. Pergamon Press, Oxford (1977).

THE RESPIRABLE DUST CENTER

9. Hilscher, W., Parov, E., Grover, R., and Molik, B.: Investigations into the Specific Harmfulness of Respirable Coal Mine Dusts. Part II. Determination of Fibrogenity of 50 Dust from Ruhr and Saar Coal Mines by the Quantitative Lymph Node Test. Essen, FRG, Verl. Glueckauf, Silikosebericht Nordrhein-Westfalen 13:265-270 (1981).
10. Martin, J.C., Daniel, H., and Le Bouffant, L.: Short and Long-Term Experimental Study of the Toxicity of Coal Mine Dust and Some of Its Constituents. Inhaled Particles IV, Ed. by W.H. Walton, pp 361-370. Pergamon Press, Oxford (1977).
11. Le Bouffant, L., Daniel, H., and Martin, J.C.: Die Rolle des Quarzes bei der Bildung Pneumokoniotischer Lasionen beim Steinkohlen-Bergarbeiter. Schriftenreihe Arbeitshygiene und Arbeitsmedizin Nr.19 der EGKS, Katalog-Nr. CE-22-77-411-DE-C, Luxembourg (1977).
12. Reisner, M.T.R.: Results of Epidemiological Studies of Pneumoconiosis in West German Coal Miners. Inhaled Particles III Ed. by W.H.Walton, pp 921- 929. Unwin Bros., Old Woking, Surrey (1971).
13. Stobbe, T.J., Kadrichu, N. and Daughy, R.: Research Parameter Summary: Medical/Toxicological Dust Toxicity Research (in press) Occupational Health and Safety Engineering, West Virginia University (1988).
14. Stobbe, T.J., Plummer, R.W., Kim, H. and Dower, J.H.: Characterzation of Coal Mine Dust. International Conference on the Health of Miners. Ann.Am.Conf.Gov.Ind.Hyg. 14:689-696 (1986).
15. Kim, H., Stobbe, T.J. and Plummer, R.W.: Particle Size Specific Mineralogy of Airborne Coal Mine Dust. Proceedings of The 10th Korea Symposium on Science and Technology pp 1697-1703. Seoul, Korea (1987).
16. Jones, W., Jankovic, J., and Baron, P.:Design, Construction, and Evaluation of a Multi-Stage "Cassette" Impactor. Am. Ind. Hyg. Assoc.J. 44(b):409-418 (1983).
17. Renton, J.J.: Use of Weighted X-Ray Diffraction Data for Semi-Quantitative Estimation of Minerals in Low Temperature Ashes of Bituminuous Coal and in Shales. U.S.Department of Energy. METC/CR-7915 (1979).

Measurement of Airborne Diesel Particulate in a Coal Mine Using Laser Raman Spectroscopy

B.D. Cornilsen, J.H. Johnson, P.L. Loyselle, and D.H. Carlson
Michigan Technological University,
Houghton, Michigan

In-mine airborne particulate samples have been successfully collected and the relative amounts of diesel and coal determined using the Laser Raman Quantitative Analysis (LRQA) method. This method allows analysis of filters which have been collected by a method similar to that used to determine the airborne respirable dust concentration in US underground coal mines. Samples were taken near the feeder-breaker, on haulage vehicles, and in the returns. Sampling methodologies were developed for coal-only and diesel-only particulate reference samples with sufficient filter loading for the LRQA method. A statistical analysis of reproducibility has been carried out. Samples have been collected simultaneously at two locations using the LRQA and the size-selective sampling methods. Good agreement between the two methods has been found.

INTRODUCTION

The goal of this research has been to develop the Laser Raman Quantitative Analysis (LRQA) method to measure the composition of respirable particulate, i.e. the fractions of coal and of diesel particulate, in the mine ambient air. In earlier Bureau of Mines sponsored research, we successfully demonstrated that the LRQA method could be used to measure the fraction of Diesel Particulate Matter (DPM) in coal/diesel particulate mixtures which were prepared in the laboratory.(1) The immediate objective was to test and refine this LRQA method on samples collected in a diesel underground coal mine.

Specific objectives required to meet this goal include:

- 1) Develop in-mine sample collection methods which will insure sufficient particulate loading on filters for LRQA.
- 2) Develop methodology for in-mine collection of reference samples ("coal-only" and "diesel-only" filters) which are required for quantitative LRQA.
- 3) Analyze precision and accuracy of the LRQA method.
- 4) Compare composition measurements with another analytical method, i.e. the University of Minnesota/Bureau of Mines size-selective sampling Micro-Orifice Uniform Deposit Impactor (MOUDI) method.

An advantage of the LRQA method is that it allows analysis of filters which have been collected by a method similar to that used to determine the respirable dust concentration in US underground coal mines. No new sampling instruments and techniques are required. Transfer of sample from collection substrate to analysis substrate is not necessary. Furthermore, other analyses can be made on the same sample since the technique is nondestructive.

The health effects of diesel exhaust, especially particulate, are a concern in the underground workplace. The constituents of DPM include insoluble carbonaceous particle

THE RESPIRABLE DUST CENTER

agglomerates, adsorbed or condensed soluble organic compounds, trace metals, and low level sulfates. Many of the organic compounds are mutagenic and some are known carcinogens.(2,3)

Measurements made in underground mines with diesel equipment have shown that DPM may contribute as much as 60 % of the 2.0 mg/m³ respirable coal mine dust standard.(4) While coal dust has been an important health concern for a number of years, the concern about DPM is more recent.(5)

Measurement of pollutant concentrations is prerequisite to engineering control of the airborne particulate and gaseous pollutants to which a miner is exposed in a diesel underground coal mine. At the present time, there is no fully-proven quantitative analysis method which can distinguish between diesel and coal particulate.

EXPERIMENTAL

The mine air particulate samples were collected in a manner similar to that used for gravimetric respirable dust sampling in underground coal mines. Respirable dust was sampled using a personal sampler which draws mine air at 2 L/min through a 10 mm nylon preseparator and then through a filter at 2 L/min. Diesel/coal samples were collected in triplicate (collection times varied from 2.95 to 7.27 hr). Smaller Gelman A/E glass fiber particulate collection filters (25 mm filters instead of the normal 37 mm diameter) were used to assure filter loadings close to 0.10 mg/cm² and preferably 0.15 mg/cm². This 0.1 mg/cm² nominal level was determined by LRQA of various filter loadings above and below this level in previous studies. Only 8% of the samples fell below 0.07 mg/cm² with the majority falling in the 0.1 to 0.4 mg/cm² range (72%). Three locations were sampled for the diesel/coal mixtures each day: near the feeder-breaker, in the return, and on the ram car within 2 feet of the operator (as designated in Figure 1).

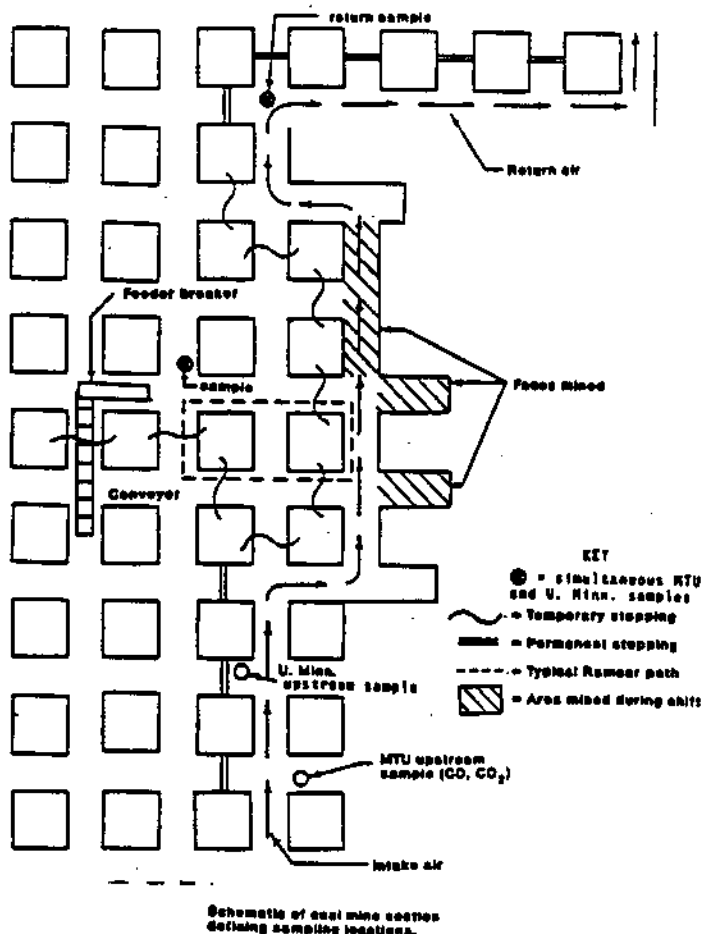


Figure 1. Schematic of coal mine section defining sampling locations.

LASER RAMAN QUANTITATIVE ANALYSIS

As part of a systematic approach to monitoring diesel emissions for control of mine air quality, we also measure ambient air pollutants and CO₂ concentrations.(6) This approach, developed at Michigan Technological University (MTU), provides a means to relate air quality measurements to engineering controls. The CO₂ concentration, which is related to the fuel consumption and airflow per unit of diesel power used, is related to the DPM fraction. A typical value of 13 mg/m³/ %CO₂, determined from previous sampling in a number of metal mines, was used to calculate this CO₂-derived DPM value. The DPM concentration estimated using the % CO₂ does not compare well with LRQA values; % CO₂ -is expected to be a rough indicator only.

Four "diesel-only" tailpipe particulate matter samples were collected from each of 3 Ram Cars using the portable Emissions Measurement Apparatus (EMA). The EMA, developed at MTU, is illustrated in Figure 2.(1) The EMA is a tailpipe apparatus designed to instantaneously and dynamically dilute the exhaust to a dilution ratio of about 20:1. A 63 mm diameter Pallflex T60A20 filter was used to collect particulate (ca. 1.5 min sampling time).

"Coal-only" particulate reference samples were taken daily for 4 days next to the continuous miner (CM) scrubber (Figure 3). The collection procedure was similar to that used for the diesel/coal mixture samples. With the high dust concentrations between the cutter and scrubber, respirable coal dust can be collected in 15 minutes or less.

After weighing to determine the respirable dust concentration, the filter is mounted on a sample spinner and analyzed by LRQA. No transfer of the particulate to a different filter is required. Samples are rotated to prevent decomposition in the laser beam.(1) The schematic in Figure 4 depicts the LRQA instrumentation.

The LRQA spectral scan procedures have been designed to test for sampling inconsistencies which might arise from sample decomposition in the laser beam. Four spectra are collected, a pair at each of two different radii on the spinning filter. The individual spectra are designated as "1x spectra." The sum of the two spectra at one radius is designated as a "2x spectrum." Any decomposition in the laser beam will be apparent upon comparison of two 1x spectra. Comparison of two 2x spectra will indicate radial inhomogeneity. This procedure also allowed detection of radial sampling inhomogeneities on a filter which are caused by particle size segregation. The sum of all four 1x spectra is designated as a "4x spectrum," and is representative of a given filter.

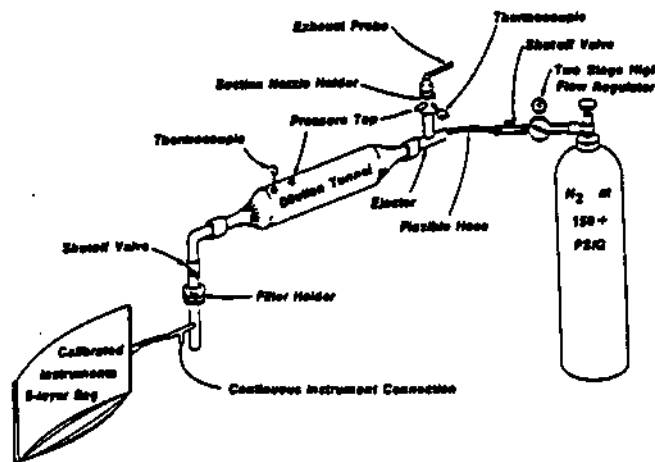


Figure 2. Schematic of Emissions Measurement Apparatus (EMA-2) which is used to collect diesel-only tailpipe samples.

THE RESPIRABLE DUST CENTER

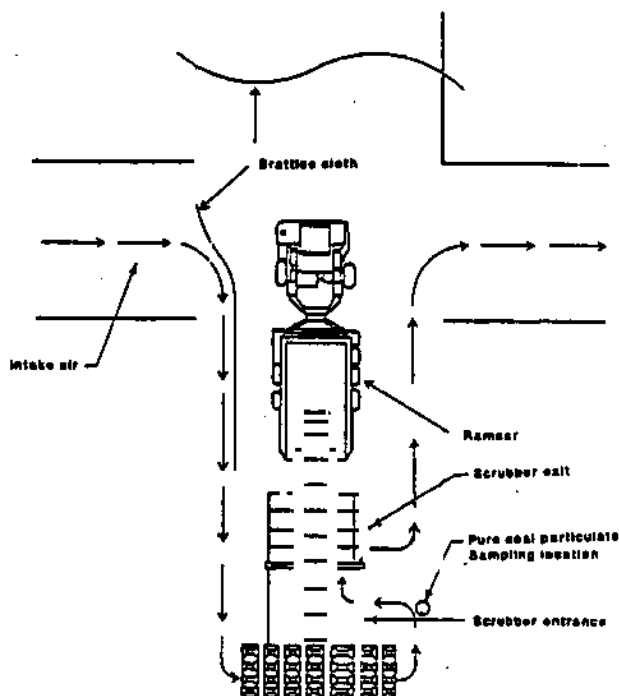


Figure 3. Illustration showing location of coal-only particulate sample collection.

LRQA samples have been collected simultaneously with the size-selective sampling method being developed at the Twin Cities Research Center (TCRC) and the University of Minnesota.(4,7) The latter samples were collected by University of Minnesota personnel. MOUDI samplers, used for this purpose, separate the particles into size fractions on the basis of their aerodynamic diameters and densities.(7) This side by side collection allows direct comparison of the fractions of diesel and coal in the mine air measured by the two methods. All samples were collected during one week of underground air sampling during August, 1987, in the Kerr McGee Galatia Mine.

RESULTS AND DISCUSSION

Coal-only and Diesel-only Measurements and Use

A well defined relationship (equation 1) exists between the diesel/coal composition (y) and the intensity ratio (M) of two bands in the Raman spectrum of a mixture.(1) Figure 5 graphically depicts this relationship. Raman spectra of coal-only and diesel-only samples are shown in Figure 6.

$$1/y = (g'/g) ((r'-M)/(M-r)) + 1 \quad (1)$$

y is the percent diesel particulate matter, %DPM, in a coal/DPM mixture. g represents the coal-only intensity and g' represents the DPM-only intensity. The slope in equation 1, g'/g , is the intensity ratio of the two samples and must be obtained when the two components are identically aligned. The coal-only intensity ratio (r) and the DPM-only ratio (r') must be determined to allow quantitative analysis of the mixtures.

The ratio for coal-only filters (r) was determined for 6 filters which were collected on three different days. The 1x, 2x and 4x spectra demonstrate good reproducibility. This consistency shows that the samples are not decomposing in the laser beam. The mean and standard deviation (SDEV) for the coal-only samples are 0.522 and 0.022, respectively (C.V.=4.3%). This precision is comparable to that expected theoretically for these scan times.(1) The overall accuracy of mixture composition analysis depends on precise measurement of the coal-only intensity ratio (r) and the DPM-only ratio (r').

LASER RAMAN QUANTITATIVE ANALYSIS

Spectral ratios have been determined for four DPM-only filters (after-scrubber), collected from two different ram cars. A mean r' value has been calculated by averaging the ratios measured for the four filters (a pair collected from each ram car). Reproducibilities for these are reasonable with an average r' of 0.958 and with a SDEV of 0.089 (C.V.= 9.3%).

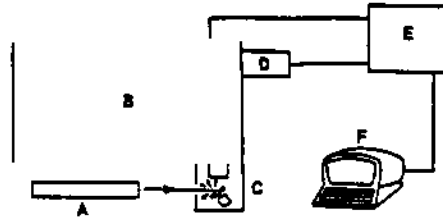


Figure 4. Schematic diagram of Raman instrumentation used to collect coal/diesel particulate spectra.

- A) Argon-ion laser
- B) Spectrometer (double monochromator)
- C) Sample chamber with spinning sample holder
- D) Photomultiplier tube
- E) Interface between spectrometer and computer
- F) Computer used to control spectrometer and to analyze spectra

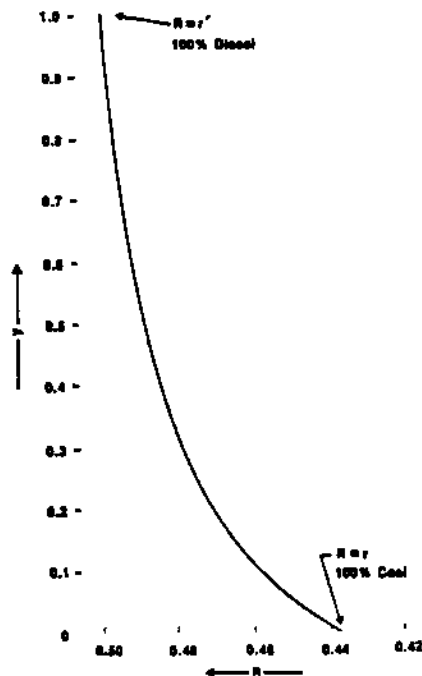


Figure 5. A graphical representation of the dependence of composition, i.e. %DPM (y), upon the experimental intensity ratio (R).

THE RESPIRABLE DUST CENTER

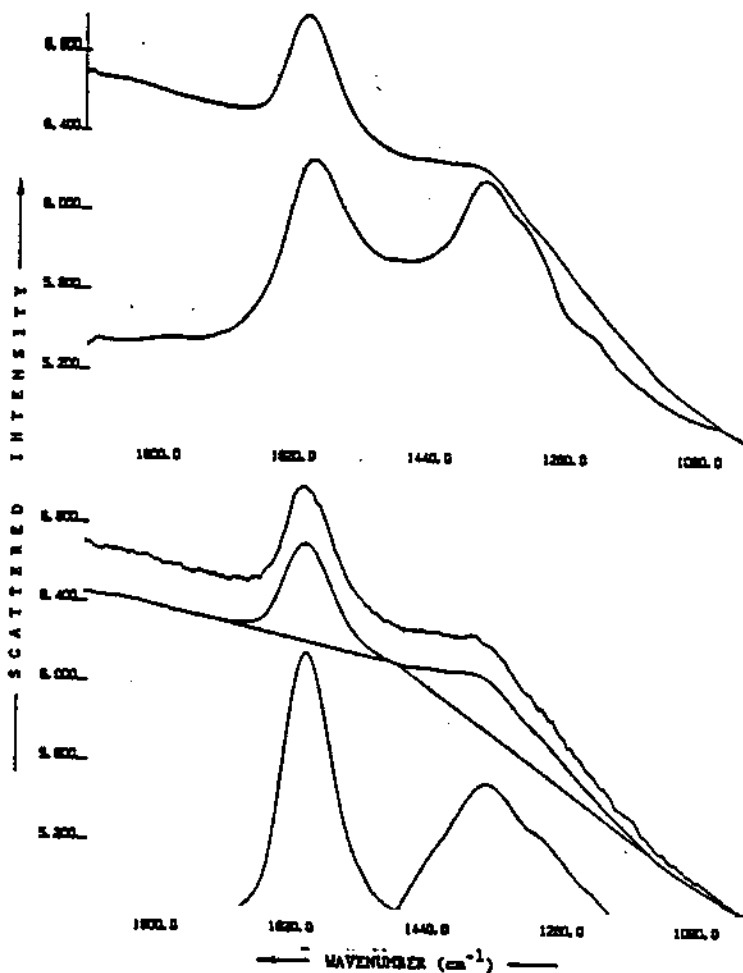


Figure 6. Raman spectra of coal-only and DPM-only filters (top), and baseline subtraction procedure for measurement of the intensity ratio (bottom).

Spectral Analysis and Reproducibility

The calculated %DPM values are analyzed statistically to demonstrate spectral reproducibility for a triplicate set of filters. Table I summarizes the %DPM values for one set of diesel/coal mixture filters collected at the feeder-breaker. The %DPM for each filter in column B of Table I are each an arithmetic mean of four 1x spectra. Column C gives the corresponding standard deviations. At the bottom of this table the overall arithmetic mean and standard deviation for the 12 spectra are given. Column D presents the %DPM measured on the summed (4x) spectra, with the mean and standard deviation for the set of three at the bottom. Note that the standard deviation for the 4x spectra is smaller than for the 1x spectra because of the increased S/N ratio in each summed spectrum. The inter-filter mean composition is 64.9% DPM.

The intra-filter reproducibility is measured by the standard deviation of the %DPM (in column C of Table I) for each filter. The 4x %DPM for each filter (column D) must be consistent with the 1x average (column B), and they are in each case. These results indicate that the samples have not changed during the time of measurement in the laser beam. Table I also compares %DPM values for 2x spectra (each a sum of two 1x spectra) collected at two different radii (columns F and G). This comparison shows whether or not the sample is radially homogeneous.

LASER RAMAN QUANTITATIVE ANALYSIS

The inter-filter reproducibility is demonstrated by the standard deviation for the three filters (bottom of Table I, column C). In particular, the values in column D provide a measure of the inter-sample precision which can be attained for three filters collected simultaneously. The SDEV of 3.0% DPM demonstrates the high precision attainable. It is comparable to the uncertainty predicted theoretically upon consideration of standard counting statistics and the count time per data point. SDEV values that are higher than this will be found when real sampling differences occur.

Composition Measurements at the Feeder Breaker, Ram Car, and Returns

Table II summarizes the DPM compositions at the various mine locations. While we have observed some inconsistencies for some filters, DPM compositions between 60 and 83% (SDEV < 10.5) have been measured with good precision. Samples with compositions outside this range exhibit inconsistencies among the multiple 1x spectra. Their origin is under further study.

In some filters the compositions measured at the two different radial positions differ substantially, as indicated by a t-test on the difference of the means (see Table II). Table III presents an example calculation. The null hypothesis that the two sets of data are equal can be rejected at the 95 % confidence level if the t-value is greater than 2.9. We can reject the null hypothesis since the observed t-value is 6.4. This result indicates that the compositions measured at these two radii are statistically different. The inner radius has a higher coal content.

Five out of eleven of the filter sets listed in Table II show significant differences between the means for the 2x spectra at the inner and outer radii. These results indicate inhomogeneous deposition which changes the measured coal/diesel ratio. Visual observation also reveals the inhomogeneous particulate deposition on some filters. Therefore steps must be taken to insure uniform deposition.

Segregation by particle size can cause such inhomogeneity, with the larger particle size coal particulate concentrated toward the center. This natural tendency for nonuniform deposition of particulate on the filter surface has been observed with asbestos fiber collection. Size-selective sampling research has indicated that coal dust tends to exhibit a particle size distribution above +0.7 micrometer with diesel particulate below 0.7 micrometer.(4,7) Improved uniformity of particulate deposition has been achieved for asbestos fiber collection by using a cassette with a cylindrical "extension cowl". It should be pointed out that the observation of radial inhomogeneity demonstrates the sensitivity of the LRQA technique.

Table I.

Statistical Analysis of %DPM for a Triplicate Set of Filters Collected at the Feeder-Breaker (on 8/10/87)

Column:	B	C	D	F	G
	% DPM for four 1x spectra		% DPM for one 4x spectrum	% DPM for the 2x spectra	
Filter	Mean	SDEV		Inner	Outer
3393	60.4	9.3	65.9	55.6	70.9
4730	61.9	8.7	67.6	62.5	68.9
6337	<u>67.7</u>	<u>8.4</u>	<u>61.7</u>	<u>57.1</u>	<u>65.9</u>
Values for twelve 1x spectra:	63.3	8.8	Values for three 2x spectra, mean:	58.4	68.6
Values for three 4x spectra:	64.9	3.0	and SDEV:	3.6	2.5

THE RESPIRABLE DUST CENTER

Table II.

Summary of %DPM and Statistical Results to Determine if Inner Radius and Outer Radius Analyses Differ.

Sample Location	Date taken	No.*	% DPM		C.V. %	Calc. t	t at 0.05	Inhomogeneous at 95% conf.	% DPM*** est. from CO ₂ conc.
			Mean**	SDEV**					
Feeder	8/10	3	64.9	3.0	4.6	3.8	2.9	yes	ND
	8/11	2	65.1	10.5	16.1	5.9	6.3	-	ND
	8/12	3	47.4	16.4	34.6	7.1	6.3	yes	68.8
	8/13	2	47.9	30.3	63.1	3.6	6.3	-	93.6
Ram Car	8/11	3	48.4	13.4	27.8	6.4	2.9	yes	47.2
	8/12	2	68.2	6.3	9.2	8.1	6.3	yes	65.1
	8/13	2	70.0	10.0	14.2	2.0	6.3	-	54.8
Return	8/10	2	77.9	0.6	0.7	2.0	6.3	-	78.9
	8/11	3	83.1	7.5	9.1	2.7	2.9	-	57.7
	8/12	2	82.4	7.9	9.6	3.0	6.3	-	49.9
	8/13	3	60.7	11.1	18.2	4.1	2.9	yes	59.7

* Number of samples analyzed per set.
 ** Mean and standard deviation for two or three 4x scans.
 *** %DPM estimated from CO₂ concentration in mine.

Table III.

Statistical Analysis of %DPM for a Triplicate Set of Filters with Radial Inhomogeneity; Ram Car (8/11/87)

Column:	B	C	D	F	G	H
	% DPM for four 1x scans		% DPM for one 4x scan	% DPM for two 2x scans		Delta
Filter	Mean	SDEV	Mean	Inner	Outer	F-G
2022	68.0	14.1	63.2	39.4	72.7	33.3
2431	51.8	30.3	45.1	20.8	75.6	54.8
6541	20.2	30.8	16.9	00.0	56.8	56.8
Total number of spectra analyzed:	12		3	3	3	3
Mean:	46.7		48.4	20.1	68.4	48.3
SDEV:		31.5	13.4	19.7	10.2	13.0
t :						6.4

Comparison of Compositions as Measured by Different Methods

For two of three simultaneously collected samples there is excellent agreement between the MOUDI and the LRQA results (see 8/12 and 8/13 results in Table IV). The MOUDI gives %DPM values of 46.2% and 47.4%, while the LRQA gives values of 62.1% and 60.7% DPM. For these two pairs, the overall time spans for collection were comparable and no sampling irregularities occurred. It is important to note that the Raman triplicate filters are collected at the same time and for the whole period (ca. 5 to 6 hr.), whereas the MOUDI samples are collected in sequence. Each MOUDI filter is collected over a 1 to 2.5 hr period. Thus the arithmetic mean %DPM values calculated by the two methods may differ because of the differences in times sampled. For the third measurement (on 8/11), the two methods do not exhibit such agreement. The mean values differ by 25%. During the last hour of sample collection on 8/11, the dust from the mine face did not pass by the samplers. This occurred when the continuous miner broke through the mine face into the adjacent drift, drastically changing the air flow pattern.

LASER RAMAN QUANTITATIVE ANALYSIS

Table IV.
Comparison of Compositions Measured by LRQA with those Measured by MOUDI and those Estimated from %CO₂

Date/ Location	Sample No.	start	TIME stop	diff.	%DPM Est. from CO ₂ conc.	%DPM	MOUDI		LRQA	
							Mean	SDEV	Mean	SDEV
8/11/87 Return	GNA-1	10:19	11:19	60 min.*	47.1	47.1	57.9	14.84		
	GNA-2	11:41	12:41	60 min.+	51.7	51.7	57.9	14.84		
	GNA-3	13:01	14:01	60 min.**	74.8	74.8				
8/12/87 Feeder	20	8:20	14:00	5.76hr.	56.7	77.8			83.1	7.5
	21	"	"	"	57.2	79.7				
	22	"	"	"	59.2	91.7				
8/13/87 Return	GNA-4	8:38	11:08	150 min.**	51.7	51.7	46.2	7.78		
	GNA-5	11:29	13:59	150 min.**	40.7	40.7	46.2	7.78		
	30	8:35	13:45	5.17 hr.	59.5	40.9			47.4	16.4
	31	"	"	"	78.1	35.2				
	32	"	"	"		66.0				
8/13/87 Return	GNA-6	9:45	11:45	120 min.*	64.9	64.9	62.1	4.03		
	GNA-7	12:00	12:49	158 min.*	59.2	59.2	62.1	4.03		
		15:34	17:23							
	44	9:36**	17:15	4.87h	53.4	55.3			60.7	11.1
	45	"	"	"	60.0	55.3				
	47	"	"	"	65.7	73.4				

+ some mining, moving mine roof bolting
 ++ dust from face not passing samplers
 * mining
 ** hauling
 *** pump off 12:51-15:38

THE RESPIRABLE DUST CENTER

The S/N ratio based upon the counting statistics for the scan time used in this study indicates that precision is not limited by the scan time. (A longer scan time will, of course, improve the S/N ratio.) Radial inhomogeneity reduces inter-filter reproducibility. Empirical variables can be controlled to improve precision. These are being optimized in our continuing work.

CONCLUSIONS

The LRQA method has been tested and refined on samples collected in a diesel underground coal mine. The amounts of DPM found at the feeder-breaker, on the ram car or at the returns, are in the range from 37 to 83 % DPM. Total respirable DPM ranges from 0.18 to 1.61 mg/m³ (Table 5). Sampling reproducibility (precision) has been confirmed by statistical analysis of results for triplicate filters. Standard deviations below ± 10 % DPM are attainable. This precision is that expected for the scan conditions used. Reproducibility can be improved with longer scan times.

Composition measurements for samples collected simultaneously and analyzed by the LRQA and size-selective methods have been compared. The %DPM values obtained for this limited set of samples at two locations are in reasonable agreement. Two out of three %DPM comparisons agree very well, the third does not.

Table V.

Summary of LRQA %DPM, Total Respirable Dust, and Airborne Diesel Particulate Matter

Sample Location	Date Taken	No.**	LRQA % DPM Mean*	Total Respirable Dust, mg/m ³	DPM mg/m ³
Feeder	8/10	3	65.1	0.915	0.596
	8/11	2	65.1	0.582	0.379
	8/12	2	47.4	0.596	0.283
	8/13	2	47.9	0.373	0.179
Ram Car	8/11	3	48.4	1.523	0.737
	8/12	2	68.2	1.158	0.790
	8/13	2	70.0	1.074	0.752
Return	8/10	2	77.9	1.073	0.836
	8/11	3	83.1	1.690	1.404
	8/12	2	82.4	1.957	1.613
	8/13	3	60.7	0.987	0.599

* Mean for two or three 4x scans.

** Number of samples analyzed per set.

Sampling objectives were attained which make quantitative Raman analysis possible. First, in-mine collection methods have been shown to provide satisfactory particulate loading on filters. Secondly, methods to provide the diesel-only and coal-only reference samples were developed.

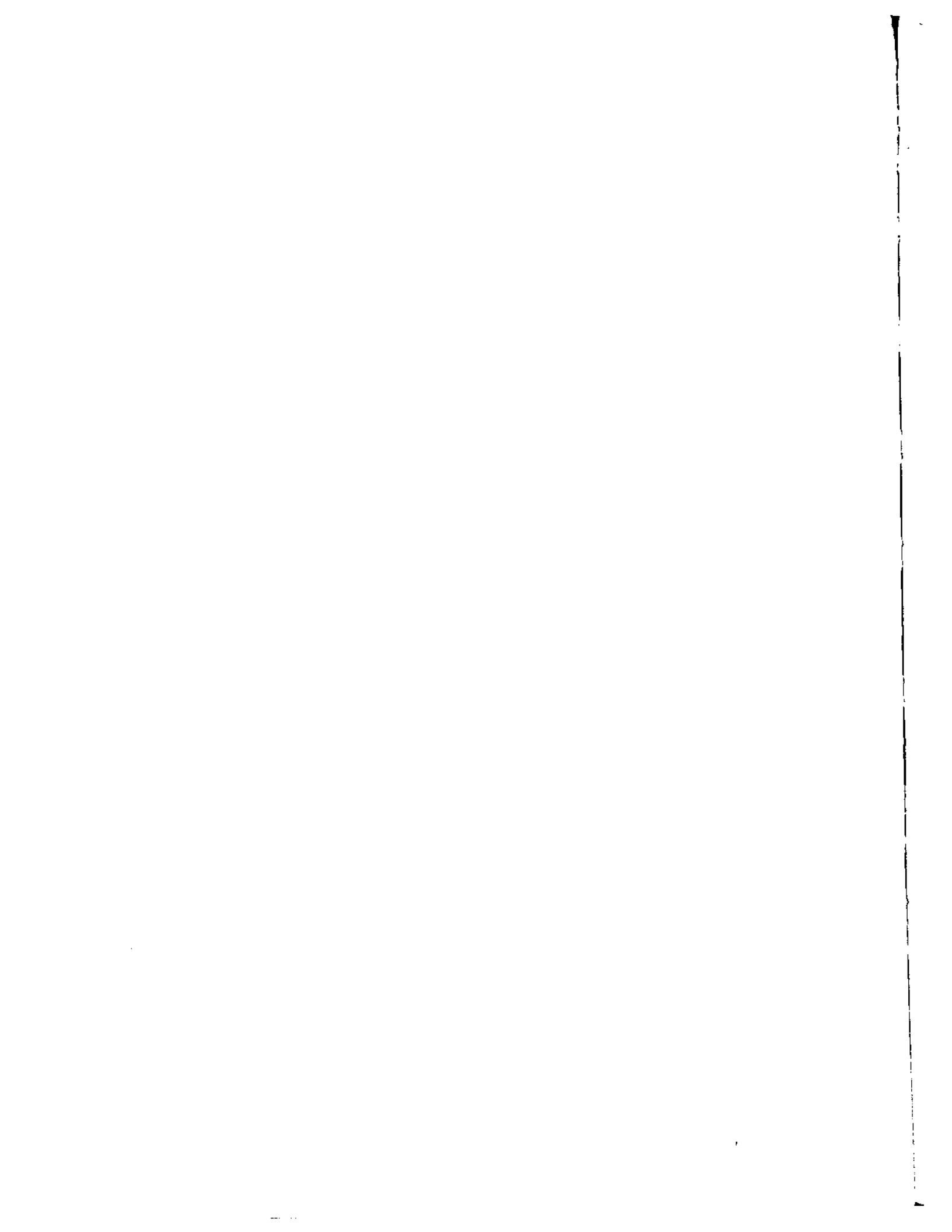
We have demonstrated that sample homogeneity on the filter surface can be confirmed by scanning at two different radii. Filter "extension cowls" are expected to remove radial inhomogeneities, and these will be tested in up-coming work.

These results indicate the importance of DPM-monitoring techniques. Optimization of the LRQA procedures will allow increased precision and accuracy. Further comparison of the size-selective and the LRQA methods is needed. Improved monitoring methods that are able to quantify the diesel and coal fractions are prerequisite to the development of adequate control technology.

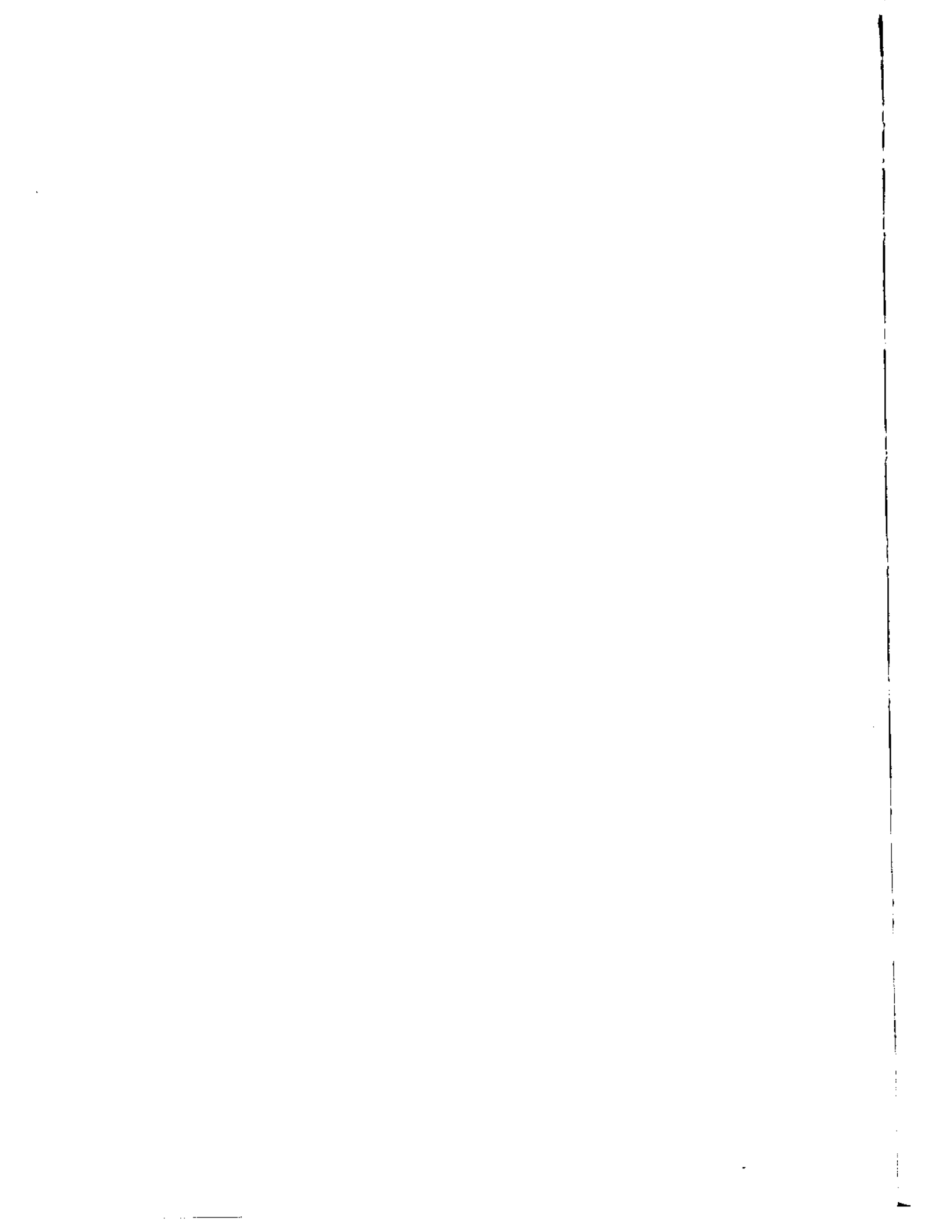
LASER RAMAN QUANTITATIVE ANALYSIS

REFERENCES

1. Johnson, J.H., Carlson, D.H., Osborne, M.D., Reinbold, E.O., Cornilsen, B.C., and Lorprayoon, V.: Monitoring and Control of Mine Air Diesel Pollutants: Tailpipe Emissions Measurements, Aftertreatment Device Evaluation and Quantification of Diesel and Coal Fractions of Particulate Matter by Raman Spectroscopy. Annual Report to the United States Department of Interior, Bureau of Mines for Contract No. JO199125, Michigan Technological University, Houghton, Michigan 49931 (November 15, 1982).
2. Dainty, E.D., Mitchell, E.W., and Schuakenberg, Jr., G.H.: Objectives and Achievements of a "Organization Three-Government Collaborative Program on Diesel Emissions Reduction Research and Development" Heavy-Duty Diesel Emission Control: A Review of Technology. CIM Special Volume 36 (1986).
3. French, I.W. and Mildon, M.A.: Health Implications of Exposure of Underground Mine Workers to Diesel Exhaust Emissions - An Update. 607 pp. CANMET, Energy, Mines and Resources, Canada, Contract No. Oust.82-00121 (April 1984).
4. Cantrell, B.K., Zeller, H.W., Williams, K.L. and Cocalis, J.: Monitoring and Measurement of In-Mine Aerosol Diesel Emissions. pp 18-40. USBM IC 9141 (1987).
5. Miner, G. M., Chairman: Report of the Mine Safety and Health Administration Advisory Committee on Standards and Regulations for Diesel-Powered Equipment in Underground Coal Mines. Report to the Secretary of Labor, U. S. Department of Labor, MSHA (July, 1988).
6. Johnson, J.H., Carlson, D.H., and Renders, C.F.: Summary of Results of Diesel Mine Vehicle Emissions Control Research in MTU Mine Air Quality Laboratory. Final Report to U.S. Department of Interior, Bureau of Mines for Contract JO145007, Michigan Technological University, Houghton, Michigan 49931 (February 15, 1987).
7. Cantrell, B.K.: Source Apportionment Analysis Applied to Mine Dust Aerosols: Coal Dust and Diesel Emissions Aerosol Measurement. Third U.S. Mine Ventilation Symposium, Penn State Univ. (Oct. 12-14, 1987).



IV
COORDINATION



Air Quality in Mines: Progress and Prospects of Legal Control

R.V. Ramani
Department of Mineral Engineering,
The Pennsylvania State University

ABSTRACT

Exposure to respirable contaminants in mine atmospheres has long posed a serious hazard to miners. The control of these hazards, some of which can have sudden and catastrophic effects and some others, slow and long enduring consequences, has been a major concern for labor, management and government alike. This concern has manifested itself in four primary mechanisms of control -- (1) regulatory control through minimum standard setting by the passage of mine health and safety laws, (2) engineering control through design and operation of mines according to the best recommended practices, (3) medical control through periodic physical examinations, wearing personal protection devices, etc., and (4) legal and social control through workmen's compensation laws for occupation related health deterioration.

The respirable contaminants in mine atmospheres are toxic and explosive gases, toxic and explosive dusts, diesel exhaust particulates, radon progeny, etc. Perhaps the most important of all these and the most widely occurring in mine atmospheres is respirable dust, an inevitable product of fragmentation, a unit operation fundamental to all mining operations. In fact, the most serious health hazard for workers in the mining and minerals processing industries is still the exposure to respirable dust, and solutions to the problem of respirable dust disease remain to be found.

The 1969 Coal Mine Health and Safety Act and its provisions for the respirable dust standards in underground coal mines are briefly reviewed. An overview of the research accomplishments in meeting the standards is presented. The current state of knowledge on the effectiveness of the standards and the new and emerging problems are discussed. A brief summary of the research programs of the Generic Technology Center on Respirable Dust is presented.

In general, underground mines are becoming increasingly safe. The mine atmospheric environment is definitely improving

* Professor and Head, Department of Mineral Engineering, The Pennsylvania State University, University Park, PA

for the better. Significant progress has been made in lowering the dust levels in mines. It is generally agreed that mines are less dusty today than they were a decade ago. However, as long as the risks of occupation-related diseases are not completely eliminated, vigilance can hardly be relaxed, and the search for engineering solutions must be intensified.

BACKGROUND

Prior to 1969, the U.S. Federal government was extremely reluctant to intrude into areas of mine health and safety, particularly the enforcement of standards, which were viewed primarily as a state responsibility. The concern for health and safety of the Nation's miners, however, was longstanding. As early as 1865, a bill was introduced in Congress to create a Federal Mining Bureau. In July 1910, an act of Congress established a Bureau of Mines in the Department of the Interior. The Bureau of Mines Organic Act, P.L. 1910, states that the Bureau shall conduct ". . . diligent investigation of methods of mining, especially in relation to the safety of mines, and the appliances best adapted to prevent accidents, the possible improvements of conditions under which mining operations are carried on . . ." but this Act contained a specific denial of "any right or authority in connection with the inspection or suspension of mining" (Committee on Human Resources, 1978). As a result, inspection and enforcement were left to the states and state laws reflected the nature and extent of mining in the states. For example, Pennsylvania's regulations date back to 1869, and the Illinois law dates back to 1872. Furthermore, enactment of significant health and safety legislation at both the federal and state levels has closely followed major mine disasters. Changes in the federal government's responsibility for mine safety have developed through a series of legislative actions in 1865, 1910, 1941, 1946, 1947 and 1952, culminating with the passage of the Federal Metal and Non-Metallic Mine Safety Act of 1966 (the 1966 Metal Act), the Federal Coal Mine Health and Safety Act of 1969 (the 1969 Coal Act), and the Federal Mine Safety and

Health Amendments Act of 1977 (the 1977 Mine Act).

The 1969 Coal Act represents a significant piece of legislation in the annals of mine health and safety. In passing this Act, Congress declared that "the first priority and concern of all in the coal mining industry must be the health and safety of its most precious resource - the miner." According to Congress, the purpose of the Act is "to establish interim mandatory health and safety standards . . . to protect the health and safety of the Nation's coal miners." In Title I, the 1969 Act had provisions for mandatory inspections, investigations, closure orders, penalties, etc. (U.S. Congress, 1969). In setting mandatory health standards in Title II, Congress stated that the purpose is "to provide to the greatest extent possible, that the working conditions in each underground coal mine are sufficiently free of respirable dust concentrations in the mine atmosphere to permit each miner the opportunity to work underground during the period of his entire adult working life without incurring any disability from pneumoconiosis or any other occupation-related disease during or at the end of such period." In Title III, the Congress states its purpose is "to provide for the immediate application of mandatory safety standards developed on the basis of experience and advances in technology and to prevent newly created hazards resulting from new technology in coal mining." The Congress directed the Secretary to "immediately initiate studies, investigations, and research to further upgrade such standards and to develop and promulgate new and improved standards promptly that will provide increased protection to the miners." In Title IV, the Congress considered the plight of miners suffering from pneumoconiosis arising out of employment in underground coal mines and provided for the payment of Black Lung benefits. In Title V, the Congress identified the need for studies, research, experiments and demonstrations and appropriated funds to carry out these directives. These studies were to encompass scientific, engineering and medical aspects. Among the specific areas mentioned include research and studies to:

1. improve working conditions and practices in coal mines, and to prevent accidents and occupational diseases originating in the coal-mining industry;
2. develop new or improved means and methods of reducing concentrations of respirable dust in the mine atmosphere of active workings of the coal mine;
3. develop epidemiological information to (a) identify and define positive factors involved in occupational diseases of miners, (b) provide information on the incidence and prevalence of pneumoconiosis and other respiratory ailments

of miners, and (c) improve mandatory health standards;

4. develop techniques for the prevention and control of occupational diseases of miners, including tests for hypersusceptibility and early detection;
5. evaluate the effect on bodily impairment and occupational disability of miners afflicted with an occupational disease; and
6. study the relationship between coal mine environments and occupational diseases of miners.

Within eight short years of the enactment of the 1969 Coal Act, Congress passed the 1977 Mine Safety Act by combining the health and safety programs of the 1966 Metal Act and 1969 Coal Act into one Act, and transferring the responsibility for enforcement of the provisions to the Department of Labor (from the Department of the Interior). Furthermore, new provisions were enacted to provide mandatory health and safety training to new miners and refresher training to all miners. The 1977 Mine Act is purported to have adopted the stronger features of the Occupational Health and Safety Act of 1970, perhaps the most significant piece of legislation in reference to workmen's occupational health and safety in the U.S. history. It is nearly two decades since the enactment of the 1969 Coal Act. This Act and the regulations thereunder defined in great specificity many standards for healthful and safe operation of a mine. However, this paper is concerned with only the respirable dust standards in underground coal mines. It is the purpose of this presentation to outline the rationale of the standards, discuss the results achieved to date, and examine both the success and the emerging new issues.

DUST STANDARDS

One of the major objectives of the 1969 Coal Act was the prevention of Coal Worker's Pneumoconiosis (CWP). In establishing, for the first time, dust standards for the Nation's coal mines, Congress considered the risks of exposure to high dust levels (Committee on Education and Labor, 1970). According to a report submitted to Congress by the Department of the Interior on the causation of pneumoconiosis, it was indicated that the probability of developing simple pneumoconiosis decreases with decreasing dust concentrations. According to this report, "at 7.0 mg/m³, the rate of simple pneumoconiosis per 1000 miners, after 35 years exposure would be 380 (36 percent); at 4.5 mg/m³, the expected rate would be 150 (15 percent); at 3.0 mg/m³, the expected rate would be 50 (5 percent); and at 2.0 mg/m³, the expected rate would be 20 (2 percent)." The probability of developing progressive massive fibrosis (complicated pneumoconiosis) also decreases with reduced

AIR QUALITY IN MINES

exposure. For example, "at 7.0 mg/m^3 , the rate per 1000 miners, after 35 years exposure would be 130 (13 percent), at 4.5 mg/m^3 , the expected rate would be 40 (4 percent), and at 3.0 mg/m^3 , the expected rate would be 20 (2 percent)." These probabilities were based on British medical data on dose-response relationships extrapolated to various dust concentrations.

The 1969 Act states that "each operator shall continually maintain the average concentration of respirable dust in the mine atmosphere during each shift to which each active miner is exposed at or below 3.0 mg/m^3 of air. Effective three years after the enactment of the Act, each operator shall continually maintain the average concentration of respirable dust . . . at or below 2 mg/m^3 of air." Obviously, it was the intent of Congress to ensure that the risks of contracting pneumoconiosis disease during 35 years of working life were minimized or eliminated. The Act also called for a reduced dust standard formula to be established if the concentration of respirable dust in the mine atmosphere of any working place contained more than 5 percent quartz.

The significance of these quantitative provisions and their impacts on the coal mining industry were obvious. A U.S. Bureau of Mines survey of 29 mines in the 1968-69 period had found average dust concentrations in excess of 6 mg/m^3 of air (Shepich, 1983). Clearly, a concerted effort by government and industry had to be mounted to bring mines into compliance. There, however, were several questions as the feasibility of achieving them, the economic burden that will be placed on the underground coal mining industry, and the adequacy of the standards themselves.

COAL MINE DUST RESEARCH

The passage of the 1969 Coal Act made available to the U.S. Bureau of Mines significant increases in funds for health and safety research. In fact, prior to 1969, the average Bureau budget for health and safety research was less than \$2 million per year. In 1970, this was increased to just under \$11 million and, by 1972, health and safety research funds were increased to over \$30 million. After the enactment of the 1977 Mine Act, there was an additional increase in health and safety research funds. The total amount in 1978 was over \$50 million. A significant fraction of these funds were spent in research directed at improving coal mine health and safety. Coal mine dust research was initiated by the Bureau in several directions including information collection and transfer; instrumentation for, and sampling of coal mine dust; chemical and physical properties of coal mine dust; suppression of respirable coal mine dust;

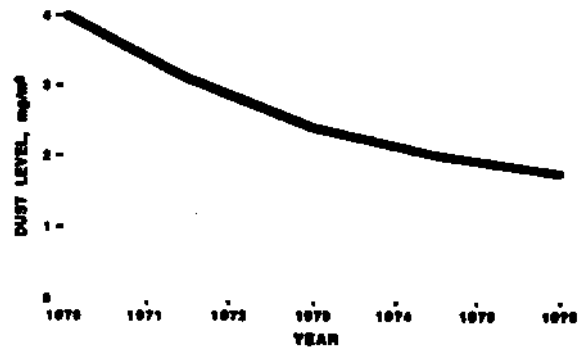


Figure 1. CONTINUOUS MINER DUST CONTROL

control of respirable coal mine dust; machine design to reduce coal dust production; and collection of respirable and mine dust. Significant research and development efforts were also expended by the coal companies to bring operations under compliance and by the late 1970's, it was clear that the vast majority of underground coal mining working sections were in compliance with the mandatory dust standards. Continuous mining sections were brought into meeting the standards with the application of improved spray systems, scrubbers and better face ventilation plans (Figure 1). Longwall mining systems initially posed severe problems. Even here application of improved spray systems resulted in more compliance (Figures 2 and 3). A committee of the National Academy of Sciences (1980) noted that the diligent application of existing technology resulted in procedures and practices which allowed to meet the 2 mg/m^3 standard. The committee, however, concluded that "further significant progress requires a new approach. In the future, research . . . should be directed more toward obtaining fundamental understanding of the origin, transport and characteristics of respirable coal mine dust" (National Academy of Sciences, 1980). The dust control research led to methods to reduce the generation of dust during cutting, suppress and minimize the entrainment of generated dust, extract and collect the airborne dust, prevent the dispersion of dust to work locations, dilute the airborne dust concentrations and to

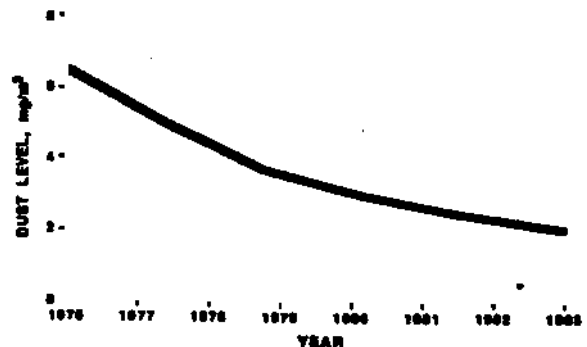


Figure 2. LONGWALL FACE DUST CONTROL

remove dust from work areas (Niewiadowski, 1983). The objective to reduce worker exposure to high concentrations of dust resulted in, as far as practicable, keeping the worker away from dust or the dust away from the worker, even if necessary by curtailing production operations.

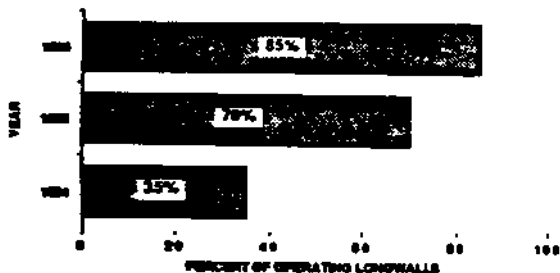


Figure 3. COMPLIANCE WITH LONGWALL FACE DUST STANDARDS

NATIONAL COAL STUDY AND OTHER FINDINGS

The adequacy of the 2 mg/m³ respirable dust standard is one key assumption which will determine the prevalence of pneumoconiosis among coal miners in the future. As has already been stated, Congress based the dust standards on British research and extrapolation of that data to U.S. conditions. A more recent update of the British study by Hurlay et al. (1982) concludes that, "on average, the new incidence risks estimated from a long-term study of 2600 miners are similar to, but marginally higher than, those reported 10 years ago based on different observations. We consider these average risks a reasonable guide to what is likely to be experienced generally in a survivor population. Nevertheless, extreme colliery-related differences occur for reasons we do not understand. No clearcut overall effect of quartz was found, though some men reacted unfavorably over relatively short (10-year) periods to dust with a relatively high quartz content." In the U.S., much of the findings on the prevalence of CWP and other mining related lung diseases in recent years come from the National Coal Study (NCS) administered by NIOSH. This study began in 1969 and initially involved the examination of over 9000 miners at 31 mines, distributed nationwide. By 1984, three surveys were conducted. According to Attfield (1984), the results derived from the U.S. miners do not indicate that the British models are inappropriate for U.S. conditions. Specifically, "Results from the National Coal Study support the view that the U.S. mining environment is similar to that of the British. As a consequence it appears that the current Federal standard will drastically reduce the level of CWP, both simple and complicated." The current prevalence of Category 1 and 2 cases are 9.1% and 9%, respectively. The projected

prevalences, respectively, are 9% and 2%. There is reason to believe that the dust standards are having beneficial outcomes. Whether all pneumoconiosis will be eliminated is a question that remains to be answered. A fourth round of the NCS has been in progress since 1984 and results from this study are expected later this year.

Examination of the Black Lung benefit payments under the 1969 Coal Act reveals that the number of new claims per year now average between 400 and 500, costing an additional \$60 to \$70 million per year. This compensation program is funded by a charge on every ton of coal. At the present time, the charge is \$1.10 per ton of underground mined coal and \$0.55 per ton of surface mined coal. The cumulative annual benefits paid out of this fund, thus far, totals over \$22 billion. The number of claims processed in 1987 under this fund totalled nearly 300,000, and the amount expended nearly \$1.8 billion (Figure 4).



Figure 4. TOTAL COMPENSATION FOR BLACK LUNG BENEFITS

Yet another factor that has become significant in recent years is the quartz concentration in the airborne respirable coal mine dust. While there was little or no indication of the severity of the problem in 1980, prior to 1976 no sections were identified requiring the application of a reduced standard. By 1983, the number of such sections had increased to nearly 2,500 affecting as much as 15,000 to 20,000 workers. The number of sections to be affected in the future were estimated to be in excess of 5,000 and the number of workforce affected, one-third of the entire underground coal mine workforce (Jankowski, Nesbit and Kissell, 1984). More recent estimates of the number of work locations to be affected is even much higher (Figure 5). In summary, while all indications are positive that the dust standards are working, there still remains occurrences of CWP among coal workers, and new problems are becoming apparent as the ability to measure and characterize dust increases.

The National Academy of Sciences Study (1980), proposed a significant increase in dust research considering the impact on society of mine workers' pneumoconiosis and the magnitude of the research and development effort needed to bridge the information gaps identified by

AIR QUALITY IN MINES

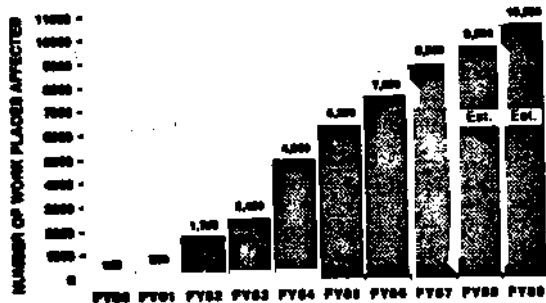


Figure 1. NUMBER OF WORK PLACES UNDER REDUCED STANDARDS FOR QUARTZ DUST

the MAS study group. It is within this context that a comprehensive program designed to permit an accelerated attack on the fundamental research problems for the control of respirable dust in mines was initiated in 1983 in the Generic Mineral Technology Center for Respirable Dust. The Center was funded by the U.S. Bureau of Mines under the Mineral Institutes Program.

The primary goal of the Center is to reduce the incidence and severity of respirable dust disease through researching and advancing the fundamental understanding of all aspects of respirable dust associated with mining and milling and the interaction of dust and lungs. The Dust Center's research program explores the health and safety concerns of respirable dust with the objective of refining existing strategies and developing new respirable dust control techniques that are consistent with the fundamental dust-lung interaction processes that lead to mine worker disability. The work concentrates on (1) control of dust generation; (2) dilution, dispersion and collection in mine airways; (3) characterization of dust particles; (4) interaction of dust and lungs; and (5) relationship of mine environment, geology and seam characteristics to dust generation and mobility. The fundamental aspects of this work are applicable to the control of respirable dust problems in both hard rock mines and coal mines and to other dusts such as diesel-generated soot. These concerted efforts by scientists, engineers, biomedical and medical researchers attempt to answer such questions as the effect of trace elements, fresh dust vs. stale dust, and the responses of individuals to dust inhalation.

REMARKS

There is little doubt the underground mine air in U.S. coal mines has become cleaner. Also, at the present time, in U.S. coal mines, there is a greater opportunity to escape, and lesser possibility of total mine involvement, in the event of a disaster. These achievements involved considerable cost

to government, industry and the general public (Consolidation Coal Co., 1980). There has been significant increases in capital investment for health and safety equipment as well as in operating costs due to changes in work procedures and practices. However, as the recent data point out, there are a number of questions yet remaining to be answered, particularly with regard to the complete healthful quality of the mine atmospheric environment. As the ability to monitor, analyze and characterize the mine atmospheric environment increases, these questions as well as new questions will continue to be raised.

The major success of the 1969 Coal Mine Act rests on such strong foundations as methane concentrations control, dust control, intrinsic safety and explosion proof enclosures, minimum air quantity and quality standards, escapeway provisions and miner training. These requirements drastically impacted mine ventilation planning, engineering and practice leading to both greater expectation and fulfillment of safe working conditions. The Act recognized the need for increased scientific, engineering, biomedical and medical research and studies not only to support the new legislation but also for the development of new equipment and methods. A systems approach to the eradication of CWP was prescribed through increased health and safety standards, medical examinations, inspections and development of more effective engineering controls.

A word of caution, however, is in order. Mining conditions and work place environment can be improved only through a better understanding of the cause and effect, dose-response relationships. The experience world over is that engineering controls and a knowledgeable workforce are the most effective preventive measures from occupation-related health and safety hazards. Legal controls cannot solve problems of health and safety if they are not supported by extensive research findings, feasible engineering designs and practices and excellent professional judgement. Otherwise, they will just be no more than statements of good intent and may even frustrate professional progress towards safer work environment. In fact, the search and development of engineering solutions to the emerging problems along with enlightened legislation are the only realistic avenues to the complete elimination of the health and safety hazards in the mine atmospheric environment.

ACKNOWLEDGEMENTS

The author wishes to acknowledge with thanks the assistance received from the U.S. Bureau of Mines, the National Institute for Occupational Safety and Health, and the U.S. Department of Labor during the preparation of this paper.

REFERENCES

- Attfield, M. D., 1984. Recent Results on Forthcoming Studies in the Epidemiology of Coal Worker's Pneumoconiosis in Underground Mines, Coal Mine Dust Conference, Generic Technology Center on Respirable Dust, West Virginia University, pp. 156-162.
- Committee on Education and Labor, 1970. Legislative History of the Federal Coal Mine Health and Safety Act, U.S. Government Printing Office, Washington, DC, pp. 14-17.
- Committee on Human Resources, 1978. Legislative History of the Federal Mine Safety and Health Act of 1977, U.S. Government Printing Office, Washington, DC, pp. 589-591.
- Consolidation Coal Co., 1980. Cost/Benefit Analysis of Deep Mine Federal Safety Legislation and Enforcement, Pittsburgh, PA, 167 pp.
- Harley, J. F., Burns, J., Copland, L., Dodgson, J. and Jacobsen, M., 1982. Coalworker's Simple Pneumoconiosis and Exposure to Dust in 10 British Coal Mines, British Journal of Medicine, Vol. 39, pp. 120-127.
- Jankowski, R. A., Nesbit, R. E. and Kissell, F. N., 1984. Concepts for Controlling Quartz Dust Exposures of Coal Mine Workers, Coal Mine Dust Conference, Generic Technology Center on Respirable Dust, West Virginia University, pp. 126-136.
- National Academy of Sciences, 1980. Measurement and Control of Respirable Dust, NMAS-363, Washington, DC, pp. 1-18.
- Niewiadomski, G. W., 1983. Improving Dust Control Technology, Proc. Symp. on Control of Respirable Coal Mine Dust, Mine Safety and Health Administration, Washington, DC, pp. 41-71.
- Shepich, T. J., 1983. Welcome Remarks, Proceedings of the Symposium on Control of Respirable Coal Mine Dust, Mine Safety and Health Administration, Washington, DC, pp. 3-6.
- U.S. Congress, 1969. Federal Coal Mine Health and Safety Act, 1969, 91st Congress, PL 91-173, 63 pp.

INDEX

THE CUMULATIVE AUTHOR INDEX

Authors are sorted alphabetically. Papers by the same author are sorted in decreasing chronological order which puts the more recent papers first.

Authors' names appear in standardized form, that is, last names and initials. This is not necessarily the way the name appears on the paper.

THE CUMULATIVE SUBJECT INDEX

Every entry in the CUMULATIVE SUBJECT INDEX contains the following information:

- 1) Last name of the first listed author with the number of authors in parenthesis if the article had multiple authors.
- 2) A short descriptive phrase, generally the title of the paper.
- 3) The year in which the paper was published or presented.
- 4) The location of the paper in The Respirable Dust Center publication volume.

1

2

3

4

GENERIC MINERAL TECHNOLOGY CENTER FOR RESPIRABLE DUST

CUMULATIVE AUTHORS INDEX
1984-1988

- Ananth, G. Vol. 5, 244-248
Andre, R. A. Vol. 8, 244; Vol. 5, 319-327
Aplan, F. F. Vol. 6, 94-105; Vol. 5, 123-128; Vol. 5, 129-138
Austin, F. F. Vol. 8, 73-83
- Barry, J. D. Vol. 8, 211
Bartlett, G. L. Vol. 8, 211; Vol. 5, 274-281
Bates, D. Vol. 5, 261-273
Begley, R. D. Vol. 4, 9-55
Bhaskar, R. Vol. 8, 31-45; Vol. 8, 46; Vol. 8, 47-54 Vol. 5, 55-60; Vol. 5, 61-71;
Vol. 4, 109-118; Vol. 3, 25-31
Bhavanandan, V. P. Vol. 8, 212; Vol. 6, 170
Bieniawski, Z. T. Vol. 8, 3-19; Vol. 8, 20-27; Vol. 6, 3-17; Vol. 5, 3-10;
Vol. 5, 11-17
Bise, C. J. Vol. 8, 243; Vol. 4, 155-157; Vol. 3, 85-90
Bolsaitis, P. Vol. 8, 196; Vol. 8, 197-208
- Caldow, R. Vol. 6, 152
Cantrell, B. Vol. 6, 152
Carlson, D. H. Vol. 8, 255-265
Castranova, V. Vol. 8, 99-105; Vol. 8, 113-120; Vol. 8, 218; Vol. 8, 223-232;
Vol. 6, 157-162; Vol. 5, 261-273; Vol. 4, 121-139; Vol. 3, 53-60
Chander, S. Vol. 6, 76-93; Vol. 6, 94-105; Vol. 6, 106-122; Vol. 5, 123-128
Cheng, L. Vol. 6, 123-133
Chiang, H. S. Vol. 5, 72-81; Vol. 5, 95-108; Vol. 5, 129-138; Vol. 5, 139-147;
Vol. 3, 32-34
Cilento, E. V. Vol. 8, 233; Vol. 8, 234; Vol. 8, 235; Vol. 6, 163-169; Vol. 5, 257-260;
Vol. 3, 63-67
Cornilsen, B. C. Vol. 8, 255-265
- Dalal, N. S. Vol. 8, 84-91; Vol. 8, 92-97; Vol. 8, 98; Vol. 8, 99-105; Vol. 8, 106-112;
Vol. 8, 121-128; Vol. 8, 137-145; Vol. 8, 146-153; Vol. 6, 134-137; Vol. 6, 138-140;
Vol. 5, 194-199; Vol. 5, 200-202
DeLong, D.S. Vol. 8, 219-222
Demers, L. M. Vol. 5, 282-288
DeVilder, W. M. Vol. 4, 56-63
DiGregorio, K. A. Vol. 8, 233; Vol. 8, 234; Vol. 8, 235; Vol. 6, 163-169;
Vol. 5, 257-260; Vol. 3, 63-67
Dower, J. M. Vol. 5, 352-358
Dubbs, S. B. Vol. 6, 170
Dumm, T. F. Vol. 8, 73-83; Vol. 6, 59-65; Vol. 6, 66-75; Vol. 5, 148-154;
Vol. 5, 155-185; Vol. 5, 186-193
- Edelson, R. E. Vol. 5, 282-288
- Fang, C. P. Vol. 6, 151; Vol. 6, 153
Fissan, H. J. Vol. 5, 244-248
Frantz, R. L. Vol. 5, 361-365
Frazer, D.G. Vol. 8, 219-222

THE RESPIRABLE DUST CENTER

- Giza, A.** Vol. 8, 219-222
Goodman, G. Vol. 8, 218
Grayson, R. L. Vol. 8, 244; Vol. 5, 319-327; Vol. 5, 328-345; Vol. 3, 35-42;
Vol. 3, 91-94
Green, F. H. Y. Vol. 8, 113-120; Vol. 5, 200-202; Vol. 4, 121-139
- Hathaway, P.** Vol. 8, 113-120; Vol. 4, 121-139
Hering, S. Vol. 5, 224-243
Hill, C. A. Vol. 8, 129-136; Vol. 8, 154-166; Vol. 8, 197-208; Vol. 6, 141-148;
Vol. 5, 261-273
Hinton, D. Vol. 5, 289-293; Vol. 4, 157-163
Hogg, R. Vol. 8, 57-72; Vol. 6, 59-65; Vol. 6, 66-75; Vol. 6, 76-93; Vol. 5, 148-154;
Vol. 5, 155-185; Vol. 5, 186-193
- Irr, W.** Vol. 8, 99-105
- Jafari, B.** Vol. 8, 98; Vol. 6, 134-137; Vol. 5, 194-199; Vol. 5, 200-202
Johnson, J. H. Vol. 8, 255-265
Johnson, C. J. Vol. 8, 243
Jones, W. G. Vol. 5, 346-351
Judy, D. J. Vol. 8, 223-232
Jung, S. Vol. 6, 18-32
- Keane, M. J.** Vol. 8, 113-120; Vol. 8, 129-136; Vol. 8, 154-166; Vol. 8, 196;
Vol. 8, 197-208; Vol. 6, 141-148; Vol. 5, 261-273; Vol. 4, 121-139;
Vol. 4, 140-149; Vol. 3, 53-60
Khair, A. W. Vol. 6, 18-32; Vol. 5, 18-41; Vol. 5, 42-52; Vol. 4, 3-8; Vol. 4, 9-55;
Vol. 4, 56-63; Vol. 4, 64-91; Vol. 4, 92-106; Vol. 3, 3-10; Vol. 3, 11-22
Kim, H. Vol. 8, 245-254; Vol. 5, 346-351; Vol. 5, 352-358
Kittleson, D.B. Vol. 6, 153
Koka, V. R. Vol. 8, 73-83
- Lantz, R. C.** Vol. 8, 233; Vol. 8, 234; Vol. 8, 235; Vol. 6, 163-169; Vol. 5, 257-260;
Vol. 4, 157-163; Vol. 3, 63-67
Lapp, N. L. Vol. 8, 218
Lee, C. Vol. 8, 239-242; Vol. 6, 173-182; Vol. 5, 295-305; Vol. 5, 306-318; Vol. 3, 71-84
Lewis, D. Vol. 8, 218
Loyselle, P. L. Vol. 8, 255-265
Lui, B. Y. H. Vol. 5, 113-120
Luo, Y. Vol. 5, 95-108
- Marple, V. A.** Vol. 8, 168; Vol. 8, 169; Vol. 6, 149; Vol. 6, 150; Vol. 6, 153;
Vol. 5, 109-112; Vol. 5, 204-223; Vol. 5, 224-243; Vol. 5, 244-248;
Vol. 3, 45-52
McCawley, D. Vol. 4, 157-163
McPeck, M. Vol. 8, 223-232
Meloy, T. P. Vol. 5, 249-250; Vol. 5, 251-254
Mike, P. S. Vol. 8, 129-136; Vol. 8, 154-166; Vol. 8, 197-208
Mohal, B. R. Vol. 6, 94-105; Vol. 6, 106-122; Vol. 5, 123-128; Vol. 5, 129-138;
Vol. 5, 139-147
Moore, M. P. Vol. 3, 85-90
Mutmansky, J. M. Vol. 8, 47-54; Vol. 8, 170-195; Vol. 8, 239-242; Vol. 6, 173-182;
Vol. 6, 183-191; Vol. 5, 295-305; Vol. 5, 306-318; Vol. 4, 155-157; Vol. 3, 71-84

INDEX

Olson, K. Vol. 6, 152
Ong, T. M. Vol. 3, 53-60
Organiscak, J. Vol. 8, 47-54

Page, S. J. Vol. 8, 197-208
Palles, W. H. Vol. 8, 218; Vol. 8, 223-232
Pederson, A. B. Vol. 5, 274-281
Peng, S. S. Vol. 5, 72-81; Vol. 5, 95-108; Vol. 5, 328-345; Vol. 3, 32-34; Vol. 3, 35-42;
 Vol. 3, 91-94
Pisano, F. Vol. 4, 157-163
Phummer, R. W. Vol. 8, 245-254; Vol. 5, 346-351; Vol. 5, 352-358
Prasad, K. V. K. Vol. 6, 35-49
Pui, D. Y. H. Vol. 6, 152

Qin, J. Vol. 8, 47-54

Rabovsky, J. Vol. 8, 223-232
Raghoottama, P. S. Vol. 8, 154-166; Vol. 6, 123-133
Ramani, R. V. Vol. 8, 31-45; Vol. 8, 46; Vol. 8, 47-54; Vol. 8, 269-274; Vol. 6, 35-49;
 Vol. 6, 50-56; Vol. 5, 55-60; Vol. 5, 61-71; Vol. 5, 361-365; Vol. 4, 109-118;
 Vol. 3, 25-31
Razzaboni, B. L. Vol. 8, 196; Vol. 8, 197-208
Reddy, N. P. Vol. 5, 18-41; Vol. 5, 42-52; Vol. 4, 64-91
Regad, E. D. Vol. 8, 113-120; Vol. 4, 121-139
Robinson, V. Vol. 8, 219-222; Vol. 4, 140-149
Rose, M. Vol. 5, 282-288
Rubow, K. L. Vol. 8, 167; Vol. 8, 168; Vol. 8, 169; Vol. 6, 149; Vol. 6, 150;
 Vol. 6, 153; Vol. 5, 109-112; Vol. 5, 204-223; Vol. 5, 244-248; Vol. 3, 45-52

Sapola, N.A. Vol. 8, 223-232
Saus, F. Vol. 5, 261-273
Seehra, M.S. Vol. 8, 154-166; Vol. 6, 123-133
Shi, X. Vol. 8, 84-91; Vol. 8, 92-97; Vol. 8, 99-105; Vol. 8, 106-112; Vol. 8, 121-128;
 Vol. 8, 137-145; Vol. 8, 146-153; Vol. 6, 138-140; Vol. 5, 194-199
Simonyi, T. Vol. 8, 244; Vol. 5, 319-327
Sneckenberger, J. Vol. 8, 213-217; Vol. 8, 219-222
Stanley, C. Vol. 5, 289-293; Vol. 4, 157-163
Stobbe, T. J. Vol. 8, 245-254; Vol. 5, 346-351; Vol. 5, 352-358
Sun, G. C. Vol. 3, 32-34
Superdock, D. T. Vol. 5, 282-288
Suryan, B. Vol. 6, 134-137; Vol. 5, 194-199

Thompson, S. D. Vol. 5, 82-94
Trass, O. Vol. 8, 73-83
Tsai, C. J. Vol. 6, 152

Ueng, T. H. Vol. 5, 82-94

Vallyathan, V. Vol. 8, 84-91; Vol. 8, 99-105; Vol. 8, 113-120; Vol. 8, 121-128;
 Vol. 8, 129-136; Vol. 8, 137-145; Vol. 8, 146-153; Vol. 8, 154-166; Vol. 8, 197-208;
 Vol. 6, 134-137; Vol. 6, 138-140; Vol. 5, 200-202; Vol. 5, 261-273; Vol. 4, 121-139;
 Vol. 4, 140-149; Vol. 3, 53-60
VanDyke, K. Vol. 8, 223-232

THE RESPIRABLE DUST CENTER

Wallace, W. E. Vol. 8, 113-120; Vol. 8, 129-136; Vol. 8, 196; Vol. 8, 197-208;
Vol. 6, 141-148; Vol. 5, 261-273; Vol. 4, 121-139; Vol. 4, 140-149; Vol. 3, 53-60
Wang, Y. J. Vol. 5, 82-94
Whitmoyer, B. Vol. 8, 219-222

Xu, L. Vol. 8, 170-195

Zhigun, Z. Vol. 8, 169; Vol. 5, 113-120

Zipf, Jr., R. K. Vol. 8, 3-19; Vol. 8, 20-27; Vol. 6, 3-17; Vol. 5, 3-10; Vol. 5, 11-17

GENERIC MINERAL TECHNOLOGY CENTER FOR RESPIRABLE DUST

CUMULATIVE SUBJECT INDEX 1984-1988

CONTROL OF DUST AND PARTICULATE MATTER GENERATION

- Begley, Richard D.** (2) Coal fracture analysis using two simultaneous wedge indentors and laser holographic interferometry. 1985, Vol. 4, 56-63.
- Khair, A. Wahab** (2) An analysis of respirable dust generation by continuous miner. 1986, Vol. 5, 18-41.
- Khair, A. Wahab** (2) Characterization of coal breakage as a function of operating parameters. 1986, Vol. 5, 42-52.
- Khair, A. Wahab** Characterizing fracture types in rock/coal subjected to quasi-static indentation using acoustic emission technique. 1985, Vol. 4, 3-8.
- Khair, A. Wahab** (2) Correlation of fragment size distribution and fracture surface in coal cutting under various conditions. 1985, Vol. 4, 9-57.
- Khair, A. Wahab** Design and fabrication of a rotary cutting simulator. 1984, Vol. 3, 3-10.
- Khair, A. Wahab** (2) Identification of fracture in coal by AE in dynamic test. 1987, Vol. 6, 18-32.
- Khair, A. Wahab** (2) Mechanisms of respirable dust generation by continuous miner. 1985, Vol. 4, 92-106.
- Khair, A. Wahab** Study of fracture mechanisms in coal subjected to various types of surface tractions using holographic interferometry. 1984, Vol. 3, 11-22.
- Zipf, Jr., R. Karl** (2) Development of a mixed mode testing system for geological materials. 1987, Vol. 6, 3-17.
- Zipf, Jr., R. Karl** (2) Estimating the crush zone size under a cutting tool. 1988, Vol. 8, 3-19.
- Zipf, Jr., R. Karl** (2) Fracture mode and loading rate influences on the formation of respirable size fragments on new fracture surfaces. 1986, Vol. 5, 11-17.
- Zipf, Jr., R. Karl** (2) Microscopic studies of fractures generated under mixed mode loading. 1988, Vol. 8, 20-27.
- Zipf, Jr., R. Karl** (2) Mixed mode testing for fracture toughness of coal based on critical - energy - density. 1986, Vol. 5, 3-10.

DILUTION, DISPERSION, AND COLLECTION OF DUST

- Bhaskar, R.** (2) Behavior of dust clouds in mine airways. 1985, Vol. 4, 109-118.
- Bhaskar, R.** (2) Comparison of the performance of impactors and gravimetric dust samplers. 1987, Vol. 6, 50-56.

- Bhaskar, R.** (2) Dust flows in mine airways: a comparison of experimental results and mathematical predictions, 1988, Vol. 8, 31-39.
- Bhaskar, R.** (2) Experimental studies of dust dispersion in mine airways, 1986, Vol. 5, 55-60; Vol. 6, 40-45.
- Bhaskar, R.** (3) Experimental studies on dust dispersion in mine airways, 1988, Vol. 8, 40-45.
- Chiang, H. S.** (3) Size distribution of the airborne dust in longwall coal faces, 1986, Vol. 5, 95-108.
- Chiang, H. S.** (4) Some factors influencing the airborne dust distribution in longwall face area, 1984, Vol. 3, 32-34.
- Grayson, Robert L.** (2) Analysis of an airborne dust study made for a southwestern Pennsylvania underground bituminous coal mine, 1984, Vol. 3, 35-42.
- Marple, V. A.** (3) Numerical technique for calculating the equivalent aerodynamic diameter of particles, 1986, Vol. 5, 113-120.
- Peng, S. S.** (2) Air velocity distribution measurements on four mechanized longwall coal faces, 1986, Vol. 5, 72-81.
- Ramani, R. V.** (2) Application of knowledge based systems in mining engineering, 1987, Vol. 6, 35-49.
- Ramani, R. V.** (2) Dust transport in mine airways, 1984, Vol. 3, 25-31.
- Ramani, R. V.** (5) On the relationship between quartz in the coal seam and quartz in the airborne respirable coal dust, 1988, Vol. 8, 47-54.
- Ramani, R. V.** (2) On the transport of airborne dust in mine airways, 1988, Vol. 8, 46.
- Ramani, R. V.** (2) Theoretical and experimental studies on dust transport in mine airways, 1986, Vol. 5, 61-71.
- Rubow, K. L.** (2) Application of a particle dispersion system for obtaining the size distribution of particles collected on filter samples, 1986, Vol. 5, 109-112.
- Rubow, K. L.** (2) Measurement of coal dust and diesel exhaust aerosols in underground mines, 1988, Vol. 8, 168.
- Ueng, T. H.** (3) Simulations on dust dispersion for a coal mine face using a scale model, 1986, Vol. 5, 82-94.

CHARACTERIZATION OF DUST PARTICLES

- Austin, L. G.** (4) A rapid method of determination of changes in shape of comminuted particles using a laser diffractometer, 1988, Vol. 8, 73-75.
- Bolsaitis, P.** (4) Effect of thermal treatment on the surface characterizations and hemolytic activity of respirable size silica particles, 1988, Vol. 8, 196.
- Cantrell, B. K.** (2) Mineral dust and diesel exhaust aerosol measurements in underground metal/nonmetal mines, 1988, Vol. 8, 167.

INDEX

- Chander, S.** (3) Wetting behavior of coal in the presence of some nonionic surfactants, 1986, Vol. 5, 129-138.
- Chander, S.** (3) Wetting characteristics of particles and their significance in dust abatement, 1986, Vol. 5, 123-128.
- Dalal, N. S.** (2) Cytotoxicity and spectroscopic investigations of organic free radicals in fresh and stale coal dusts, 1988, Vol. 8, 98.
- Dalal, N. S.** (2) Do silicon-based radicals play a role in quartz-induced hemolysis and fibrogenicity, 1988, Vol. 8, 146-153.
- Dalal, N. S.** (2) Detection of hydroxyl radical formation in aqueous suspensions of fresh silica dust and its implication to lipid peroxidation in silicosis, 1988, Vol. 7, 106-112.
- Dalal, N. S.** (3) Oxygenated radical formation by fresh quartz dust in a cell-free aqueous medium and its inhibition by scavengers, 1988, Vol. 8, 121-128.
- Dalal, N. S.** (4) Electron spin resonance detection of reactive free radicals in fresh coal dust and quartz dust and its implications to pneumoconiosis and silicosis, 1986, Vol. 5, 194-199.
- Dalal, N. S.** (3) Potential role of silicon-oxygen radicals in acute lung injury, 1988, Vol. 8, 84-91.
- Dumm, T. F.** (2) A procedure for extensive characterization of coal mine dust collected using a modified personal sampler, 1986, Vol. 5, 186-193.
- Dumm, T. F.** (2) Distribution of sulfur and ash in ultrafine coal, 1987, Vol. 6, 66-75.
- Dumm, T. F.** (2) Estimation of particle size distributions using pipet-withdrawal centrifuges, 1986, Vol. 5, 148-154.
- Dumm, T. F.** (2) Particle size distribution of airborne dust, 1987, Vol. 6, 59-65.
- Dumm, T. F.** (2) Standard respirable dusts, 1986, Vol. 5, 155-185.
- Dumm, T. F.** (2) Washability of ultrafine coal, 1988, Vol. 8, 76-83.
- Hering, Susanne** (2) Low-pressure and micro-orifice impactors for cascade impactor sampling and data analysis, 1986, Vol. 5, 224-243.
- Hill, C. A.** (5) Alternation of respirable quartz particle cytotoxicity by thermal treatment in aqueous media, 1988, Vol. 8, 197-208.
- Hogg, R.** Characterization problems in comminution, 1988, Vol. 8, 57-72.
- Hogg, R.** (2) Surface characterization for coal processing, 1987, Vol. 6, 76-93.
- Jafari, B.** (3) Detection of organic free radicals in coal-dust exposed lung tissue and correlations with their histopathological parameters, 1986, Vol. 5, 200-202.
- Keane, M. J.** (6) Respirable particulate surface interactions with the lecithin component of pulmonary surfactant, 1988, Vol. 8, 154-166.
- Marple, V. A.** (2) An impactor with respirable penetration characteristics and size distribution capabilities, 1987, Vol. 6, 150.

THE RESPIRABLE DUST CENTER

- Marple Virgil A.** (3) Experimental and theoretical measurement of the aerodynamic diameter of irregular shaped particles, 1988, Vol. 8, 169.
- Marple, Virgil A.** (2) Instrumentation for the measurement of respirable coal mine dust, 1984, Vol. 3, 45-52.
- Marple, Virgil A.** (2) Low pressure and micro-orifice impactor, 1986, Vol. 5, 224-243.
- Marple, Virgil A.** (4) Micro-orifice uniform deposit impactor, 1986, Vol. 5, 244-248.
- Marple, Virgil A.** (2) Theory and design guidelines for cascade impactor sampling and data analysis, 1986, Vol. 5, 204-223.
- Meloy, Thomas P.** A hypothesis on the possible contribution of coal cleats to CWP, 1986, Vol. 5, 249-250.
- Meloy, Thomas P.** A working hypothesis on how silica and silica surface may cause silicosis and CWP, 1986, Vol. 5, 251-254.
- Mohal, B. R.** (2) A new technique to determine wettability of powders-inhibition time measurements, 1986, Vol. 5, 139-147.
- Mohal, B. R.** (2) Surfactant adsorption and wetting behavior of freshly ground and aged coal, 1987, Vol. 6, 106-122.
- Mutmansky, J. M.** (2) Some observations on particulates collected in diesel and non-diesel underground coal mines, 1988, Vol. 8, 170-195.
- Rubow, K. L.** (2) A method for resuspending particles deposited on filters, 1987, Vol. 6, 149.
- Rubow, K. L.** (4) Measuring the size distribution of diesel exhaust and mine dust aerosol mixtures with the micro-orifice uniform deposit impactor, 1987, Vol. 6, 153.
- Seehra, M.** (3) Photoacoustic spectroscopy of quartz, 1987, Vol. 6, 123-133.
- Shi, X.** (2) ESR evidence for the hydroxyl radical formation in aqueous suspension of quartz particles and its possible significance to lipid peroxidation in silicosis, 1988, Vol. 8, 137-145.
- Shi, X.** (2) On the mechanism of the chromate reduction by glutathione: ESR evidence for the glutathionyl radical and an isolable Cr(V) intermediate, 1988, Vol. 8, 92-97.
- Tsai, C. J.** (5) Fragment size distribution from simple fracture of coal and rock, 1987, Vol. 6, 152.
- Vallyathan, V.** (5) Generation of free radicals from freshly fractured silica dust: potential role in acute silica-induced lung injury, 1988, Vol. 8, 99-105.
- Vallyathan, V.** (4) Role of reactive oxygen radicals in silica cytotoxicity, 1987, Vol. 6, 138-140.
- Wallace, Jr., W. E.** (4) In vitro biologic toxicity of native and surface-modified silica and kaolin, 1985, Vol. 4, 140-149.
- Wallace, Jr., W. E.** (5) Mutagenicity of diesel exhaust particles and oil shale particles dispersed in lecithin surfactant, 1987, Vol. 6, 141-148.

INDEX

Wallace, Jr., W. E. (5) Pulmonary surfactant interaction with respirable dust, 1984, Vol. 3, 53-60.

Wallace, Jr., W. E. (7) Suppression of inhaled particle cytotoxicity by pulmonary surfactants and re-toxication by phospholipase--distinguishing properties of quartz and kaolin, 1985, Vol. 4, 121-139.

INTERACTION OF DUST AND LUNGS

Bartlett, G. L. (2) Effects of coal dusts and alveolar macrophages and growth of lung fibroblasts, 1986, Vol. 5, 274-281.

Bartlett, G. L. (2) Factors that may influence interactions between mineral dusts and lung cells, 1988, Vol. 8, 211.

Bhavanandan, V. P. Effect of coal dust on mucin production by the rat trachea, 1988, Vol. 8, 212.

Bhavanandan, V. P. (2) Mucins secreted by rat tracheal explants in culture, characterization and influence of dust, 1987, Vol. 6, 164-166.

Cilento, E. V. (3) Measurement of superoxide release from single pulmonary alveolar macrophages, 1987, Vol. 6, 157-163.

Cilento, E. V. (3) Use of sensitive electro-optical method to quantify superoxide release from single PAM exposed to dusts in vitro or in vivo: some current experimental and model results, 1988, Vol. 8, 233.

Demers, Lawrence M. (4) The effects of coal mine dust particles on the metabolism of arachidonic acid by pulmonary alveolar macrophages, 1986, Vol. 5, 282-288.

DiGregorio, K. A. (3) A kinetic model of superoxide production from single pulmonary alveolar macrophages, 1988, Vol. 8, 234.

DiGregorio, K. A. (3) Effects of serum on superoxide release from single pulmonary alveolar macrophages, 1988, Vol. 8, 235.

DiGregorio, K. A. (3) Superoxide release from single pulmonary alveolar macrophages, 1987, Vol. 6, 257-260.

DiGregorio, K. A. The development of an electro-optical technique to measure superoxide release from pulmonary alveolar macrophages exposed to coal dusts, 1984, Vol. 3, 63-67.

Lantz, R. Clarke (3) Development of alternations in the lung induced by inhaled silica: a morphometric study, 1986, Vol. 5, 289-292.

Lapp, N. L. (5) Bronchoalveolar lavage in subjects exposed to occupational dusts, 1988, Vol. 8, 218.

Pisano, F. (5) Evaluation of the size distribution of large aerosols in an animal exposure chamber, 1984, Vol. 4, 153-159.

Sneckenberger, J. (2) Acoustic impedance method for detecting lung dysfunction, 1988, Vol. 8, 213-217.

VanDyke, K. (2) Detection of receptor and synthesis antagonists of platelet activating factor in human blood and neutrophils using liminol-dependent chemiluminescence, 1987, Vol. 6, 151-156.

THE RESPIRABLE DUST CENTER

- VanDyke, K.** (7) Effects of platelet activating factor on various physiological parameters of neutrophils, alveolar macrophages, and alveolar type II cells, 1988, Vol. 8, 223-232.
- Wallace, W. E.** (5) Mineral surface-specific differences in the adsorption and enzymatic removal of surfactant and their correlation with cytotoxicity, 1988, Vol. 8, 129-136.
- Wallace, W. E.** (7) Suppression of inhaled particle cytotoxicity by pulmonary surfactant and re-toxication by phospholipase: distinguishing properties of quartz and kaolin, 1988, Vol. 8, 113-120.
- Wallace, W. E.** (7) The effect of lecithin surfactant and phospholipase enzyme treatment on some cytotoxic properties of respirable quartz and kaolin dusts, 1986, Vol. 5, 261-273.
- Whitmoyer, T. B.** (6) Microcomputer control of particle concentrations in a cotton dust exposure system, 1988, Vol. 8, 219-222.

RELATIONSHIP OF MINE ENVIRONMENT, GEOLOGY AND SEAM CHARACTERISTICS TO DUST GENERATION AND MOBILITY

- Andre, R. A.** (3) Variation in mineral and elemental composition of respirable coal mine dusts by worker locations and coal seams, 1986, Vol. 5, 319-327.
- Bise, Christopher** (2) Coal mine respirable dust, 1985, Vol. 4, 163-165.
- Cornilsen, B. C.** (4) Measurement of airborne diesel particulate in a coal mine using laser raman spectroscopy, 1988, Vol. 8, 255-265.
- Grayson, R. L.** (2) Characterization of respirable dust on a longwall panel, 1986, Vol. 5, 328-345.
- Grayson, R. L.** (2) Correlation of respirable dust mass concentration with worker positions, 1984, Vol. 3, 91-94.
- Johnson, C. J.** (2) A comparative analysis of the elemental composition of mining-generated and laboratory-generated coal mine dust, 1988, Vol. 8, 243.
- Grayson, R. L.** (3) Seeking the "rank factor" in CWP incidence: the potential role of respirable dust particle purity, 1988, Vol. 8, 244.
- Lee, Changwoo** (2) A strategy for coal mine respirable dust sampling using multi-stage impactors for characterization purposes, 1986, Vol. 5, 295-305.
- Lee, Changwoo** (2) An analysis of the mass-size distribution of airborne coal mine dust in continuous miner sections, 1988, Vol. 8, 239-242.
- Lee, Changwoo** (2) Application of the size and elemental characteristics of airborne coal mine dust for dust source identification, 1987, Vol. 6, 173-182.
- Lee, Changwoo** (2) Statistical analysis of the elemental characteristics of airborne coal mine dust, 1986, Vol. 5, 306-318.
- Moore, Michael P.** (2) The relationship between the hardgrove grindability index and the potential for respirable dust generation, 1984, Vol. 3, 85-90.

INDEX

- Mutmansky, Jan M.** An analysis of coal and geological variables related to coal workers' pneumoconiosis, 1984, Vol. 3, 71-84.
- Mutmansky, Jan M.** Worldwide coal mine dust research, 1987, Vol. 6, 183-191.
- Stobbe, Terrence J.** (4) A methodology for determining the mineral content and particle size distribution of airborne coal mine dust, 1986, Vol. 5, 346-351.
- Stobbe, Terrence J.** (4) Characterization of coal mine dust, 1986, Vol. 5, 352-358.
- Stobbe, Terrence J.** (3) Mineral content variability of coal mine dust by coal seam, sampling location, and particle size, 1988, Vol. 8, 245-254.

COORDINATION

- Frantz, Robert L.** (2) A review of the programs and activities of the Generic Mineral Technology Center for Respirable Dust, 1986, Vol. 5, 361-365.
- Ramani, R. V.** Air quality in mines: progress and prospects of legal control, 1988, Vol. 8, 269-274.